Modelling and identification of physical linear networks

Modelling and identification of physical linear networks

Lizan Kivits

Modelling and identification of physical linear networks

PROEFSCHRIFT

ter verkrijging van de graad van doctor aan de Technische Universiteit Eindhoven, op gezag van de rector magnificus prof.dr. S.K. Lenaerts, voor een commissie aangewezen door het College voor Promoties, in het openbaar te verdedigen op donderdag 22 februari 2024 om 13:30 uur

door

Elizabeth Martina Maria Kivits

geboren te Roggel

Dit proefschrift is goedgekeurd door de promotoren en de samenstelling van de promotiecommissie is als volgt:

voorzitter:	prof.dr.ir. A.B. Smolders	
promotoren:	prof.dr.ir. P.M.J. Van den Hof	
	prof.dr. S. Weiland	
leden:	prof.dr.ir. T.A.E. Oomen	
	prof.dr.ir. B. De Moor	(Katholieke Universiteit Leuven)
	em.prof.dr.ir. J. Schoukens	(Vrije Universiteit Brussel)
	prof.dr. M. Enqvist	(Linköping University)
adviseur:	dr.ir. M. van Berkel	(Dutch Institute for Fundamental Energy Research)

Het onderzoek dat in dit proefschrift wordt beschreven is uitgevoerd in overeenstemming met de TU/e Gedragscode Wetenschapsbeoefening.

Modelling and identification of physical linear networks

Lizan Kivits

This project has received funding from the European Research Council (ERC), Advanced Research Grant SYSDYNET, under the European Union's Horizon 2020 research and innovation programme (Grant Agreement No. 694504).

This dissertation has been completed in fulfillment of the requirements of the Dutch Institute of Systems and Control (DISC) for graduate study.

E.M.M. Kivits. *Modelling and identification of physical linear networks*. Ph.D. thesis, Eindhoven University of Technology, 2024.

A catalogue record is available from the Eindhoven University of Technology Library. ISBN: 978-90-386-5931-2.

This thesis was typeset using LaTeX.
Reproduction by ADC Nederland, 's-Hertogenbosch, The Netherlands.

Summary

Networks are essential parts of our natural and physical world. They are everywhere around us and have penetrated deeply into our contemporary society. Physical linear networks consist of interconnected systems that exist in the natural and physical world. Some examples of these networks are: interactions in ecological systems; industrial process plants that manufacture chemicals; pipelines for transporting liquid or gas over long distances; manufacturing and testing integrated circuits and printed circuit board assemblys (PCBAs); and robots communicating with each other. In recent decades, vast technological developments have led to larger and more complex systems and thus, it has become more valuable to study dynamic networks and understand their behaviour. This is conducted by exploiting the laws of nature and by utilising experimental data to build a mathematical model. In this thesis, we pursue the objective of: *Developing model structures and identification tools for parameter estimation in physical linear networks*.

In this thesis, we focus on linear physical networks that are characterised by symmetric diffusive couplings. A diffusive coupling is a relationship between manifest signals that is based on sharing information instead of a predefined direction of information flow. This type of interconnection is more natural for physical networks, while input-output relations are more natural for digital systems, such as controllers. The ultimate goal is to solve identification problems for physical networks, such as topology detection and the identification of all dynamics or only a selection of dynamics that are present in the network. Before going into network identification (Part II), a suitable network model is being determined (Part I). Physical linear networks are often connected to digital systems, such as controllers, leading to mixed dynamic networks, which are studied as well (Part III).

Part I focuses on finding an appropriate model structure for describing physical linear networks. In Chapter 2, we examine numerous existing model structures and we explore whether one of them is appropriate for modelling physical linear dynamic networks for identification purposes. A model structure is suitable for this aim if it is able to incorporate both the characteristic properties of physical

linear systems as well as the network interconnection structure. We discuss these aspects and various properties, including the generality of the model structures and relations between the model structures. Based on this, the three most promising model structures are selected for further investigation.

In Chapters 3 and 4, these model structures are further studied and graphical aspects receive significant attention. We study the level on which networks can graphically be represented and how to move from one level to another by including or excluding topological information. This leads to an extension of the concept of immersion to a single-path and a multi-path version. We find mappings between the interaction-oriented model focusing on subsystems (often used in control) and the module representation focusing on signals (often used in identification). This directly connects these network models to each other and therefore, also the network control and identification fields. In addition, we develop an extended version of the module representation by allowing for self-loops and multiple-input multiple-output (MIMO) modules. This module dynamic network is capable of describing state-space systems, such that a state-space form and a module representation can always be converted into each other without losing any information.

None of the existing model structures that we examine is sufficiently suitable for modelling physical linear dynamic networks for identification purposes, because none of them is able to incorporate both the characteristic properties of physical linear systems and the network topology. Therefore, in Chapter 5, we develop a new model structure that meets the aforementioned specifications. This diffusively coupled linear network model is developed in a polynomial framework and possesses the specific structural properties that the polynomial matrix describing the internal network dynamics is symmetric (reflecting the symmetric nature of the linear diffusive couplings) and nonmonic. These structural properties have to be accounted for in the identification procedure.

Now that the network model is decided on, we proceed with the identification of physical linear networks, to which Part II is dedicated. First, we gather relevant identification tools from the literature in Chapter 6. Then, in Chapter 7, the (undirected) diffusively coupled linear network model is translated into the (directed) module representation, to which network identification tools from the literature are applied. In this way, the identification of all dynamics in the network or a selection of dynamics is possible. However, in this framework, the structural properties of physical linear networks lead to too strict identifiability conditions and expensive experiments. Therefore, it is more attractive to preserve the polynomial representation and develop identification tools for this network model structure.

This is exactly what Chapter 8 is devoted to: developing identification tools for the diffusively coupled linear network model. By combining the ideas and tools for the identification of polynomial models and dynamic network identification,

we develop identification tools, results, and algorithms for the identification of all dynamics (and the topology) for structured polynomial models. The conditions for identifiability, and consequently for consistent identification, are rather simple compared to the ones we derived in Chapter 7 for the module framework. The experimental condition reduces to a single excitation signal in the case that all manifest node signals are measured. The simplicity of the conditions is entirely due to the structural conditions that can maximally be exploited in the polynomial framework. We solve the resulting nonconvex optimisation problem with a multistep algorithm that leads to consistent results.

In Chapter 9, we consider the identification of a subnetwork. The experimental setting is again very simple due to the characteristic properties of physical linear networks. For the identification, only the node signals of the subnetwork and their neighbour node signals are required and all other node signals can be discarded. This means that subnetwork identification can be solved really locally in the network. The identification procedure consists of identifying the immersed network (in which only the required node signals are described) from which the dynamics of the subnetwork are obtained.

In the previously mentioned identification results, it is assumed that all node signals can be measured, leading to the requirement of a single excitation signal. In Chapter 10, the experimental conditions are relaxed by considering the situation in which not all node signals can be measured. Analysing the uniqueness of the network description leads to a flexible instrumentation scheme for identifiability. For identifiability of the complete network, it is sufficient that each node signal is equipped with either a sensor or an actuator and that one node signal has a colocated sensor-actuator pair.

After deriving all these identification results for physical linear networks, we concentrate on physical linear networks that also include directed dynamics, such as digital controllers, in Part III and Chapter 11. Adding directed interconnections to (undirected) physical linear networks destroys the symmetry property of the network model. This is accounted for in the identification procedure by adapting the identifiability conditions and the identification procedure. Suggestions for algorithms are presented and the implementation is saved for the future.

Finally, Chapter 12 concludes the thesis. It contains an overview of the main findings and their implications, which lead to answers to the research questions of this theses. Subsequently, a general conclusion is given regarding the main research objective. In this respect, the newly developed network model for the identification of physical linear networks is described and the developed identification tools are summarised. Lastly, suggestions for future research are given.

Contents

List of figures

List of tables

List of symbols

General: Variables

ξ	Indeterminate variable
s	Complex Laplace variable
t	Time variable
z	Complex frequency variable

General: Sets, spaces, and fields

$\mathbb{N}$	Set of natural numbers
$\mathbb{Z}$	Set of integer numbers
$\mathbb{R}$	Set of real numbers
$\mathbb{R}_+$	Set of positive real numbers
$\mathbb{C}$	Set of complex numbers
$\mathbb{R}^{x\times y}[\xi]$	Field of polynomial functions of dimension $x \times y$
$\mathbb{R}^{x\times y}(\xi)$	Field of rational functions of dimension $x \times y$
$C^\infty(\mathbb{R}^x, \mathbb{R}^y)$	Set of infinitely differentiable functions from $\mathbb{R}^x$ to $\mathbb{R}^y$

General: Polynomial and matrix notation

$A(\xi)$	Polynomial matrix
$a(\xi)$	Polynomial scalar
A	Constant matrix

a	Constant scalar
a	Physical component
$a_{jk}(\xi)$	The (j,k)th polynomial element of the polynomial matrix $A(\xi)$
A_ℓ	The ℓth matrix of the polynomial matrix $A(\xi)$
$a_{jk,\ell}$	The (j,k)th element of the matrix A_ℓ, that is, the ℓth coefficient of the polynomial $a_{jk}(\xi)$
$A_{\mathcal{J}\bullet}(\xi)$	All jth rows of $A(\xi)$ for which $j \in \mathcal{J}$

General: Operators

$\frac{d}{dt}x(t)$	Derivative of $x(t)$ with respect to time
$\dot{x}(t)$	Derivative of $x(t)$ with respect to time
p	Differential operator meaning $px(t) = \frac{d}{dt}x(t)$
q	Forward shift operator meaning $qx(t) = x(t+1)$
q^{-1}	Backward shift operator meaning $q^{-1}x(t) = x(t-1)$
$A \succ 0$	A is positive definite
$A \succeq 0$	A is positive semi-definite
A^{-1}	Inverse of matrix A
$A^\top$	Transpose of matrix A
$A^{-\top}$	Transpose of the inverse of matrix A
A^*	Complex conjugate transpose of matrix A
A^{-*}	Complex conjugate transpose of the inverse of matrix A
adj	Adjugate
det	Determinant
diag(A)	Diagonal matrix with diagonal elements equal to the vector A or to the diagonal of matrix A
dim	Dimensions
gcd(a, A)	Greatest common divisor of scalar a and all scalar elements of matrix A
rank	Rank
rowsum	Column vector with elements equal to the sum of the elements of the corresponding row

arg	Argument of
min	Minimum
$\int$	Integral
$\prod$	Product
$\sum$	Summation
$\lvert \cdot \rvert$	Absolute value
$\lVert \cdot \rVert^2$	Euclidean vector norm
$\mathbb{E}\{\cdot\}$	Expectation operator
$\bar{\mathbb{E}}\{\cdot\}$	$\bar{\mathbb{E}}\{\cdot\} := \lim_{N\to\infty} \frac{1}{N} \sum_{t=1}^{N} \mathbb{E}\{\cdot\}$
$\mathcal{F}\{\cdot\}$	Fourier transform
$\mathcal{L}\{\cdot\}$	Laplace transform
$\Re(\cdot)$	Real part
$\lambda(\cdot)$	Eigenvalue

General: Probability

$P(\cdot)$	Probability
$P(\cdot\|\cdot)$	Conditional probability
$Pa(\cdot)$	Parents, that is the preceding variables

General: Graphs

G	Graph
$A(\cdot)$	Adjacency matrix
$D_{in}(\cdot)$	In-degree matrix
$D_{out}(\cdot)$	Out-degree matrix
$L_{in}(\cdot)$	In-degree Laplacian matrix
$L_{out}(\cdot)$	Out-degree Laplacian matrix

Networks: Signals

$e(t)$	White noise signals

$\hat{e}(t)$	Innovation signals
$r(t)$	External excitation signals
$s(t)$	Sensor noise signals
$v(t)$	Disturbance signals
$w(t)$	Internal node signals
$y(t)$	Measured output signals
$z(t)$	Data signals ($w(t)$ and $r(t)$)
$\kappa(t)$	External signals ($e(t)$ and $r(t)$)

Networks: Numbers and matrices

c	Number of measured output signals $y_c(t)$
K	Number of external excitation signals $r_k(t)$
L	Number of internal node signals $w_i(t)$
N	Number of data points
I	Identity matrix
Λ	Covariance matrix

Networks: Polynomial matrices

$A(\xi)$	Network dynamics (symmetric structure)
$B(\xi)$	Input dynamics
$C(\xi)$	Output dynamics
$P(\xi)$	Dynamics between internal node signals (hollow and symmetric structure)
$Q(\xi)$	Dynamics connected to the internal node signals (diagonal structure)
$U(\xi)$	Unimodular matrix
$X(\xi)$	Dynamics connecting the internal node signals to the ground (diagonal structure)
$Y(\xi)$	Dynamics between internal node signals (Laplacian structure)
$\Upsilon(\xi)$	Network dynamics in mixed network

Networks: Rational matrices

$F(q)$	Noise model
$G(q)$	Network dynamics (hollow structure)
$H(q)$	Noise model
$R(q)$	Input dynamics
$T_{yx}(q)$	Transfer function from $x(t)$ to $y(t)$
$W(q)$	Predictor filter

Networks: Spectra

$\Phi_{ab}(\omega)$	Cross power spectral density of vector signals $a(t)$ and $b(t)$
$\Phi_a(\omega)$	Auto power spectral density of vector signal $a(t)$

Networks: Sets of signals and matrices

$\mathcal{N}_j$	Set of indices of internal node signals that are neighbours of the internal node signals $w_j(t)$
$\mathcal{J}$	Set of indices of internal node signals that are part of the target subnetwork
$\mathcal{D}$	Set of indices of internal node signals that are neighbours of the target subnetwork
$\mathcal{Y}$	Set of indices of internal node signals that will be preserved in the network
$\mathcal{Z}$	Set of indices of internal node signals that will be eliminated (immersed) from the network
$\mathcal{B}$	Set of binary, diagonal polynomial matrices
$\mathcal{F}$	Set of monic, stable, and stably invertible rational matrices
$\mathcal{H}$	Set of monic, stable, and stably invertible rational matrices
$\mathcal{P}$	Set of hollow and symmetric polynomial matrices
$\mathcal{Q}$	Set of diagonal polynomial matrices

Models: Energy-based model

e	Effort variable
f	Flow variable
p	Generalised momentum variable
q	Generalised displacement variable
s	Supply rate
C	Capacitance
E	Energy
L	Inductance
R	Resistance
P	Power
$H(\xi)$	Hamiltonian function
$S(\xi)$	Storage function
$\mathcal{B}$	Set of behaviours
$\mathcal{D}$	Dirac structure
$\mathcal{E}$	Effort space
$\mathcal{F}$	Flow space
$\mathbb{T}$	Time space
$\mathbb{W}$	Signal space

Models: State-space model

$r(t)$	Input signals
$x(t)$	State signals
A	State matrix
B	Input matrix

Models: Interaction-oriented model

$s(t)$	Internal signals
$u(t)$	Input signals

$v(t)$	Disturnbance signals
$y(t)$	Output signals
$z(t)$	Internal signals
Σ_j	jth subsystem
$C(q)$	Transfer function matrix with output dynamics
$D(q)$	Transfer function matrix with direct feedthrough dynamics
$L(q)$	Transfer function matrix with interaction dynamics
$T(q)$	Transfer function matrix with subsystem dynamics
$T^{yx}(q)$	Transfer function from $x(t)$ to $y(t)$

Models: Network structure sets

r_{ccs}	'Set' of a particular complete computational structure
$\mathcal{R}_{sub}$	Set of all realisations of a given complete computational structure in the subsystem structure
$\mathcal{R}_{sig}$	Set of all realisations of a given complete computational structure in the signal structure
$\mathcal{R}_{ms}$	Set of all realisations of a given complete computational structure in the manifest structure

Identification: Parameters

θ	Parameter vector
θ^0	True parameter vector
θ^n	Parameter vector of nth order approximation model
$\hat{\theta}_N$	Estimated parameter vector
Θ	Parameter space
ϑ	Parameter vector
η	Parameter vector of nth order model
Π	Parameter space
ζ	Parameter vector of nth order model
λ	Langrange multipliers

Identification: General

α	Constant scalar scaling factor
γ	Vector for linear parameter constraints $\Gamma\theta = \gamma$
Γ	Matrix for linear parameter constraints $\Gamma\theta = \gamma$
$\hat{y}(t\|t-1)$	One-step-ahead predictor
$\varepsilon(t)$	Prediction error
$\varphi(t)$	Regressor
D	Diagonal matrix
P	Permutation matrix
R	Remainder matrix
M	Model
$M(\cdot)$	Parameterised model
$\mathcal{M}$	Model set
$\mathcal{S}$	Data generating system
$P(\cdot)$	Covariance matrix
$Q(\cdot)$	Regression matrix
$T(\cdot)$	Correction matrix
$V(\cdot)$	Cost function
$W(\cdot)$	Weigting matrix
Z^N	Data set with signals $z(t)$

Identification: Mixed networks

$\bar{\wedge}_i$	Number of parameterised entries in the ith row of $G_m^\infty(\eta)$
$\wedge_i$	Number of parameterised entries in the ith row of $G_m(q,\eta)$
$\bar{\vee}_i$	Number of parameterised entries in the ith row of $R_m^\infty(\eta)$
$\vee_i$	Number of parameterised entries in the ith row of $\begin{bmatrix} R_m(q,\eta) & H_m(q,\eta) \end{bmatrix}$
$\bar{\bigwedge}_i$	Permutation matrix
$\bigwedge_i$	Permutation matrix
$\bar{\bigvee}_i$	Permutation matrix
$\bigvee_i$	Permutation matrix

List of abbreviations

ARMAX	Autoregressive-moving average with exogeneous input
ARX	Autoregressive with exogeneous input
BIBO	Bounded-input bounded-output
BJ	Box-Jenkins
FEM	Finite element method
FIR	Finite impulse response
LMFD	Left matrix-fraction description
LPM	Local polynomial method
LTI	Linear time-invariant
MFD	Matrix-fraction description
MIMO	Multiple-input multiple-output
MISO	Multiple-input single-output
ODE	Ordinary differential equation
OE	Output error
PCBA	Printed circuit board assembly
PMU	Phasor measurement unit
RLC	Resistor-inductor-capacitor
RMFD	Right matrix-fraction description
RMSE	Relative mean squared error
SD	Standard deviation
SISO	Single-input single-output

SLS	Sequential least squares
SS	State-space
WNSF	Weighted null-space fitting

1 | Introduction

Nowadays, systems become more complex and more systems become interconnected. In addition, more precise descriptions of systems and networks are required. In system identification, or data-driven modelling, mathematical system representations are determined from data. The techniques for open-loop and closed-loop identification have been extended to directed dynamic networks, where signals of interest are connected through directed dynamic modules with an input-output structure. However, physical networks consist of interconnected physical subsystems that share information. These networks do not possess any predefined directions of information flow. On the other hand, identification methods for physical systems do not incorporate the interconnection structure of networks. In this thesis, we develop model structures and identification tools for parameter estimation in physical linear networks. A modelling framework is set up for identification in physical networks, while incorporating the physical characteristics and interconnection structure. This research includes various aspects, such as determining a proper modelling framework; finding conditions under which identification leads to unique results; identifying the complete dynamics of the network, with known or unknown interconnection structure; identifying local dynamics in the network; designing the experiment; developing algorithms; and including directed links. This introductory chapter presents physical network models in a broad sense. The main motivation and challenges are presented and it concludes with the objectives of each of the subsequent chapters.

1.1 Systems

Science is the 'knowledge about the structure and behaviour of the natural and physical world, based on facts that you can prove, for example, by experiments' (Oxford University Press, 2023). This means that science helps us to understand

the extremely complicated world. The knowledge of science can, for example, be used to predict what the future will bring us and even to influence upcoming events. The ultimate goal of science would be to achieve a complete understanding of the enormous complexity of the natural and physical world, preferably by the simplest general principles.

How to improve our understanding of the world? To improve our understanding of the world, we need to expand our knowledge by contributing to science. This can be achieved by studying the properties of a *system*. A system is 'a group of things that work together in a particular way or for a particular purpose' (Oxford University Press, 2023). So, the system is the object or the collection of objects that we want to study. Everything excluded from the system is called the *environment* and represents 'the conditions in which someone/something exists' (Oxford University Press, 2023). If this system is 'always active, changing, or making progress', we refer to it as being *dynamic* and otherwise it is *static* (Oxford University Press, 2023). In particular, we will consider *dynamic systems* as systems whose state varies over time and depends on the past. In other words, dynamic systems have a memory, while static systems are memoryless and contain instantaneous relationships between quantities.

Example 1.1 (Throwing a dice). *The outcome of throwing a dice is a static system, with the outcome of the last throw as its state. The state only depends on the outcome of the current throw and does not depend on the outcomes of the previous throws, because each throw is independent. At each throw, the chance of a specific outcome is the same, no matter what the outcomes of the previous throws were (hence, it has no memory).*

Example 1.2 (Conductor). *A conductor (or resistor) is a static system, because its resistance (R) describes a proportional relationship between the voltage drop (V) and the current flow (I) through the conductor by Ohm's law ($V = IR$). Even though the voltage drop and current flow may vary over time, their ratio remains the same at all times. At each time instant, the current flow can be determined from the resistance and the voltage drop (and vice versa), without using any observation from the past.*

Example 1.3 (Throwing a dice). *The total sum of the outcomes of throwing a dice is a dynamic system, with the total sum of the outcomes of all throws as its state. The state depends on the outcome of the current throw and on the outcomes of all previous throws. The state remembers the sum of all outcomes (hence, it has a memory) and adds the new outcome to it.*

Example 1.4 (Inductor). *An inductor (or coil) is a dynamic system, because it stores energy in a magnetic field when electric current flows through it. Storing energy in the buffer is a kind of memory of the inductor. The current flow generates a magnetic field with a magnetic flux that is proportional to the inductance. Any change in current flow creates a change in magnetic flux, which induces a voltage across the inductor. By Faraday's law of induction, this induced voltage is proportional to the (negative) rate of change of the current flow. In other words, the induced voltage is time-dependent on the current flow.*

Example 1.5 (Ecological system). *An ecological system, consisting of multiple animal species that are in a predator-prey relationship, is a dynamic system. The number of animals of a specific species depends on the birth and death rates of that species and also on the number of animals of the other species over time. If there are many predators, the prey will be eaten (resulting in less prey and food shortage for the predators, so they will die out) and if there are few predators, the prey can reproduce (resulting in more prey and food surplus for the predators, so they will reproduce).*

How to study a system? We can study a system by performing experiments on it and by using the experimental data to answer questions about the system's properties. Experiments are performed by applying some input to the system, the system will react to that and respond with an output. In this way, we can investigate how the system responds to different input signals and study the input-output behaviour of the system. In many systems, there are multiple options for choosing the input and output signals. For example, for the conductor in Example 1.2, a voltage can be the input signal with the current flow as the output signal or the other way around. Choosing different input and output signals results in different reactions of the system. The reaction from voltage to current is the exact opposite/inverse of the reaction from current to voltage. Therefore, the input-output behaviour of a system is dependent on the choice of input and output signals and thus, on the experiment that is performed on the system.

How does a system behave? In the natural and physical world, systems just exist. They can be seen as systems that share signals with each other, while they do not consist of signal flows or cause-effect relationships. Therefore, these systems are considered just like that: the way they are present in the world. These so-called *physical system* 'acts according to the laws of nature or what is likely' (Oxford University Press, 2023). Hence, their behaviour is independent of the experiment that is performed on it and therefore, also studied without labelling any signals as 'input' and 'output' or as 'cause' and 'effect' (Polderman and Willems, 1998;

Willems, 2007, 2010). This is further discussed in Section 1.7.

1.2 Networks

What has changed? Scientists have been studying all kinds of systems for many centuries. These systems have become larger and more complex with the tremendous technological developments of the last decades. Nowadays, many systems consist of several coupled subsystems that work together. Instead of considering a single system, it becomes more natural and more valuable to also consider the interactions with other systems. Think, for example, about communicating cars in the automotive industry, electrical and mechanical devices including ever-smaller chips with ever-more components, more extensive and more complex manufacturing systems, and the sewage system and power grid. In addition, detailed information is included to a greater extent to improve the understanding of the system. This happens, for example, in biological and medical processes, in which an increasing amount of influencing factors are incorporated; and in ecological systems , as in Example 1.5, in which an increasing number of species and environmental factors get included.

Another development that took place over the past few years is that sensors have been improved. They have become cheaper, more accurate, and more versatile, making data acquisition more easy. As a result, many different types of signals can be measured within a single system. The relations among those signals can also be seen as subsystems that describe the interaction between the signals.

What is a network? These large systems, or *systems of systems*, are called *networks*: 'groups of things that are connected to each other' (Oxford University Press, 2023). With a *dynamic network*, we mean a system that consists of interconnected dynamic subsystems. That is, a dynamic network is a system of dynamic systems. In particular, a physical network is a dynamic network with subsystems that share information through their interconnections rather than having inputs and outputs or directed cause-effect relationships. The interconnection structure of the network is referred to as the *topology* of the network.

Example 1.6 (Maps). *Maps, such as flight maps and road maps, are static networks that display graphs of travel paths and their intersection points. These graphs give an overview of all possible travel options and are useful for making a travel route.*

Example 1.7 (Phylogenies and pedigrees). *Phylogenies and pedigrees are one of the oldest networks that exist. They display the genetic relations among groups of organisms and individuals, respectively (Morrison, 2016). Phylogenies help in understanding how species evolve over time and pedigrees do the same for individual genetic information.*

Example 1.8 (Digestive system). *The digestive system in human bodies is a dynamic network as it consists of several organs (with time-dependent behaviour) that interact with each other. Each organ can be seen as a separate system that is connected to other organs to form the complete digestive system.*

Example 1.9 (Electric circuit). *An electric circuit consisting of interconnected (voltage or current) sources, resistors, capacitors, and inductors is a (linear) physical network. These networks can be analysed using, for example, Kirchhoff's voltage law, Kirchhoff's current law, and Ohm's law. The interesting signals are typically the voltage drop and current flow across the components.*

1.3 Models

How to study a system? As discussed before, we can study a system by performing experiments on it. However, it is not always possible to perform these experiments, for example, because it is too expensive, too dangerous, or because the system still has to be designed. Instead of using the actual system, we can create a *model*: 'an object that is a copy of the system' or 'a simple description, especially a mathematical one, of a group of complex systems or processes, used for understanding or explaining how something works' (Oxford University Press, 2023). Once we have created the model, it can be used to study the properties of the system without using the actual system itself. According to Ljung and Glad (1994), that is really what science is about: 'Constructing models for a slice of reality and studying their properties'.

What kind of models do exist? Models do exist in many forms; for example, consider the following ones (Ljung and Glad, 1994; Ljung, 1999): In our daily lives, we use *mental models* at the back of our heads to make all kinds of predictions and decisions. Based on the experience we have gained throughout our lives, we have all kinds of expectations for what will happen if we do or say something.

Physical models are used to imitate a system and are visible or touchable, such as a design, scale model, prototype, mould, and template. Every day, we use *verbal models* to explain or describe something with words. Similar, we use *graphical models* to illustrate or characterise something with visuals, such as figures or pictures. In science, we use *mathematical models* to explain or describe relationships among quantities with mathematical (and analytical) relations, such as equations. Sometimes *software models*, such as digital computer programmes, are used to capture the behaviour of a system. The graphical and mathematical models are the ones that will be considered further.

What information is in the model? The model needs to contain only the aspects of the system that are essential for answering our questions. That means that the system's information that is captured by the model thus depends on the purpose of our study: on what we want to achieve. In addition, only the system's information that is observed from the outside world can be captured by the model. A model can never capture all the information. Even though the model might be a very good representation of the system, it is never an exact copy of the true system. We should always keep this in mind when we are using models to learn to understand the world.

What are the building blocks of a model? When building a model of a system, one has to set the *boundaries* of the system: one has to decide on what is captured by the model and what is considered to be the environment. The system interacts with the environment across the boundaries. The environment can excite the system through known signals, which are referred to as *external excitation signals*, and the system can be subject to unknown signals from the environment, which are referred to as *disturbance signals*. Furthermore, the environment can observe some *signals of interest* from the system.

What is the purpose of a model? A model is used to study a system. So, what can we actually learn about the system? First of all, building the model gives insight into the system, as formulating the mathematical relations helps to *understand* the behaviour of the system. Once the model is available, it can be analysed and used for several purposes. A model can be used to *estimate* quantities that cannot be measured in the system. A model can also be used to make *predictions* about future outcomes and to see what is likely to happen. Sometimes these predictions are made based on *simulations*. Then many experiments are performed on the model to see how it responds. Simulations can provide much information on the behaviour of the system. Using the model, we can *monitor* the behaviour of the system by comparing the behaviour of the model and the system. If the (predicted) outcome of the model is different from the actual outcome of the system, this new information can be used to improve the model. However, this difference can also indicate that the system itself has changed, for example,

because a component or interconnection has been broken. In this way, the model can be used for *fault detection*. The next step would be to *diagnose* the underlying cause of the faults. A model can also be created for systems that do not exist yet. The purpose of the model is then to *design the system* such that it shows the desired behaviour. In a similar way, the behaviour of an already existing system can be improved by, for example, *(re)designing* specific components in the system. The system can also be influenced by the environment in order to control its behaviour, where *control* is 'the power to influence a process or a course of events' (Oxford University Press, 2023). Then the purpose of the model is to *design the controller*, such that the controlled system (the system and the controller together) shows the desired behaviour.

Example 1.10 (Prediction). *In weather forecasting, a mathematical model is used to describe the behaviour of the atmosphere and the exchanges with its environment, the Earth and space. The purpose of this model is to predict the behaviour of the atmosphere and thus predict the weather (i.e. atmospheric state at a specific point in time and geographic location) (Coiffier, 2011).*

Example 1.11 (Fault detection and diagnostics). *In medical diagnostics, a patient's health is examined by taking several tests. These tests can be performed through questionnaires, scans, medical imaging, and tests on samples gathered from the patient's body. Any deviation from what is expected indicates a symptom or a 'fault'. A doctor or medical specialist can look for the cause of the symptoms, which leads to the diagnosis of an underlying disease or condition.*

Example 1.12 (Control). *In automotive industry, adaptive cruise control can continuously adjust the speed of a vehicle while maintaining a safe distance from the preceding car. It adjusts the throttle position to accelerate and decelerate in order to maintain the desired cruise speed (selected by the driver) and safety distance (preset by the manufacturer) (Nice, 2021).*

How to build a mathematical model? A mathematical model can, for example, be obtained by one of the following two approaches: In the first method, the model is derived by utilising the scientific knowledge that is available in the literature and the experience of experts. The laws of nature and other principles are exploited to capture the behaviour of the system. Therefore, this principle-based method is referred to as *first-principles modelling*. In the second method, the model is constructed by utilising the observations of the system. The experimental data are

the driving force behind the model. Therefore, this data-based method is referred to as *data-driven modelling*.

How informative is the model? The insight the model gives into the behaviour of the system can be of different levels. Some models are clearly interpretable in terms of their behaviour and predictions and the relations among different quantities. These models are referred to as *white box models*, because everything is crystal clear. Other models are not interpretable at all. As one is completely in the dark about the interpretation of the model, these models are referred to as *black box models*. Of course, there are also models that are partially interpretable and they are referred to as *grey box models* for obvious reasons.

How accurate is the model? Once the model has been built, it is interesting to know how well it captures the behaviour of the system. In order to investigate how precise and reliable our model is, the behaviour of the model and the system can be compared. The differences can be evaluated using various validation tools. As mentioned before, the model can never be an exact copy of the system and contain all the information. Therefore, every model is only valid in a limited range of conditions. Sometimes, this domain is large enough to capture all the interesting behaviour, but sometimes the range of conditions limits the domain of where the model is an accurate representation of the system. We should always be aware of this limited range and possibly limit the range of operation of the system.

1.4 Modelling of physical linear networks

1.4.1 Modelling

What is the purpose of a network model? Similar to a general model, a network model is used to study a network. So, similar purposes hold for network models, such as understanding, estimation, prediction, simulation, monitoring, fault detection, diagnosing, system (re)designing, and controller designing. As networks are more comprehensive than general systems, these objectives are also broader. The objectives can be formulated for the complete network, for only a single system, for a subset of systems, and/or for (a part of) the interconnection structure. These additional considerations make studying networks different and more extensive than studying single systems.

How to model a network? After setting the boundaries of the network, the network itself can be modelled. Basically, there are three approaches for modelling a network. First of all, one can consider the network to be a *single system*. Then all behaviour in the network is merged. In this way, the complete internal structure

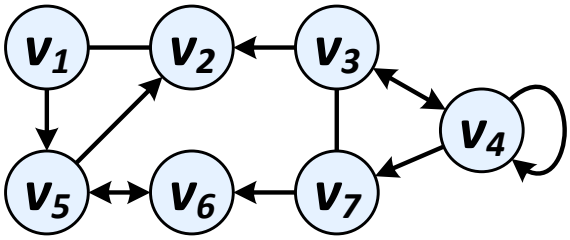

Figure 1.1: Graph with vertices v_i and directed edges (lines with a single arrow), bi-directed edges (lines with two arrows), and undirected edges (lines without arrows).

of the network disappears and all existing modelling techniques can simply be applied. A second method for modelling a network is by selecting the interesting signals of the network and relating them to each other. In this way, a network is viewed as an *interconnection of signals*. There are numerous ways of relating the interesting signals to each other and therefore, many interpretations of the topology. The topology together with the relations among the signals contain the full information of the network. A third technique for modelling a network is by viewing it as an *interconnection of subsystems*. Then each subsystem can be modelled individually and the relations among the subsystems can be modelled by analysing the interconnections (Willems, 2007, 2010). The models of the subsystems and interconnections together describe the complete network. In this way, the internal structure of the network remains present in the network model. Both the second and third methods require more extensive modelling procedures than the first method.

How to represent a network model? As just discussed, networks can be seen as signals or subsystems that are interconnected with each other. The interconnection structure makes a crucial difference with single systems. Therefore, network models consist of two parts: a graphical representation and a mathematical representation of the network model.

A *graphical network model*, or *graph*, is a visualisation of the interconnection structure of the dynamic network. It consists of vertices that are interconnected through edges. Figure 1.1 shows an example of graph. There are roughly two options for making a graph of a dynamic network: the dynamic subsystems are placed at the vertices, while the edges represent the information or signals that are shared between the subsystems; or the signals of interests are placed at the vertices and the edges represent the dynamics that relate them. Depending on what the edges mean, they can either be directed (pointing from one vertex to another one), bi-directed (pointing from one vertex to another one and back), or

undirected (connecting two vertices without specific directions), as illustrated in Figure 1.1.

A *mathematical network model* describes the behaviour of a dynamic network with mathematical relations. It captures the dynamics of the subsystems and their interconnections. These mathematical relations can, for example, be given by functional dependencies, differential equations, difference equations, or transfer functions.

What network models are available? It is conceivable that networks occur in numerous research areas. All these networks represent a diversity of processes with their own objectives. They have different priorities in terms of what is important and therefore, they are also differently modelled. As a result, various network models are available in the literature. The choice of the network model, of course, influences its graphical and mathematical representation. An extensive discussion on network models is presented in Chapter 2. Here we provide a brief overview of the broad range of linear time-invariant (LTI) network models.

1.4.2 State-of-the-art network models

Physical systems are often modelled by using first-principles modelling by using the laws of nature (Young and Freedman, 2012). Energy is an important physical quantity and therefore, there exist many energy-based models, such as bond-graph models, (multi)port models, and Hamiltonian models (Paynter, 1961; van der Schaft and Jeltsema, 2014). The characteristic symmetry property of many linear physical components is very clear in first-order and second-order diffusively coupled models (Jones, 1985; Ren et al., 2005; Cheng et al., 2017). Many of these models lead to polynomial descriptions.

Example 1.13 (Mechanical system). *A mechanical mass-spring-damper system, or the rotational analogy, is modelled by first-principles modelling by using the constitutive laws of the components and Newton's second law or Euler's second law (Young and Freedman, 2012).*

Example 1.14 (Electrical circuit). *An electrical resistor-inductor-capacitor (RLC) circuit is modelled by first-principles modelling by using the constitutive laws of the components and Kirchhoff's laws (Balabanian and Bickart, 1969).*

Single system models can be used to model complete networks, if the network is viewed as a single system. The polynomial models of Ljung (1999) and Hannan

and Deistler (2012) are very popular for modelling systems for identification purposes. System identification of these models is therefore extensively studied (Ljung, 1999). Second-order (vector) differential equations are often used to model physical systems (Ljung and Glad, 1994; Young and Freedman, 2012). For identification purposes, this model is often rewritten in a state-space form (De Angelis et al., 2002; Lopes dos Santos et al., 2015). State-space models themselves are also commonly used for modelling (and identification of) physical systems (Mesbahi and Egerstedt, 2010; Verhaegen and Verdult, 2012).

Interconnections of signals can be modelled in numerous ways. In *probabilistic models*, each vertex represents a single time instant from a time series of a random (or stochastic) variable and the edges represent the conditional dependencies among the stochastic variables. The complete graph shows the joint distributions, for example, as in the (dynamic) Bayesian network (Koller and Friedman, 2009; Sucar, 2021). Closely related are *structural equation models*, which have vertices representing a single time instant from a time series of a variable and edges representing the functional dependencies among the vertex variables (Pearl, 2000). In *vector autoregressive models*, the vertices represent (time series of) variables and the edges represent the causal relations among them (Tsay, 2013). *Transfer function models* also have vertices that represent (time series of) variables, but now the edges represent transfer function relations among the vertex variables. Some examples are the dynamical structure function (Gonçalves et al., 2007), the module representation (Van den Hof et al., 2013), and networks with Wiener filters (Materassi and Innocenti, 2010). *State-space models* have their states as vertices and the first-order relations between them at the edges.

Interconnections of subsystems can also be modelled in various ways. The subsystems at the vertices can be modelled by any modelling approach for dynamic systems (Lunze, 1992). The edges represent the input and output signals coming from and going to other subsystems. An alternative way of modelling the subsystems is through the *behavioural approach* (Willems, 2007, 2010). Then the edges represent signals or quantities that are shared among the subsystems. Hence, this method does not make use of input-output structures in the subsystems.

Different levels of topology can be incorporated into the network model. One can be very precise and include all the structural (and dynamical) details in the network model. On the other hand, one can be very loose and exclude all topological information and describe the complete network by a single system. In between these two extremes are the models that interconnect signals or subsystems. Research has been done on similarities and differences between these network representations at different levels of detail (Yeung et al., 2010, 2011a; Chetty and Warnick, 2015; Warnick, 2015).

Which dynamic network model to use for identification? Sometimes, state-

space models are used for the identification of dynamic networks (Verhaegen and Verdult, 2012). However, most often, transfer function models are used for the identification of dynamic networks and the most popular one is probably the *module representation* (Van den Hof et al., 2013). The module representation is a generalisation of the classical closed-loop system. In the graphical network model, the (measurable) signals of interest are located in the vertices and the dynamics that relates these signals is captured in so-called *modules* in the edges. The modules are black boxes that mathematically describe the dynamics through transfer functions. These modules can be seen as subsystems, like the plant and controller in a closed-loop system. The edges represent information flow and therefore, they are directed. The vertices are summation points that sum all incoming signals together to create the signal of interest, which can often be measured and is referred to as the *node signal*.

1.5 Identification of physical linear networks

1.5.1 System identification

What is system identification? System identification deals with data-driven modelling problems in dynamical systems. This means 'building mathematical models of dynamical systems based on observed data from the system' (Ljung, 1999). For reaching this objective, three basic ingredients are necessary: a data set, a model set, and a selection criterion or algorithm (Eykhoff, 1974; Ljung, 1999; Pintelon and Schoukens, 2012). To acquire an accurate model, the data need to contain sufficient information, the model set needs to be chosen so that it contains the system, and a proper selection criterion has to be chosen. The validity of the obtained model is tested using a validation criterion.

The *data set* contains the signals obtained from the experiment that is performed on the system. These data signals can have several properties that are important for the subsequent choices. These aspects include the type of excitation signals (e.g. periodic, random); considerations on the disturbance and noise signals that might be present; the type of data signals (e.g. deterministic, stochastic); the behaviour of the data signals in between the samples that are taken (e.g. zero-order hold, band-limited); discrete-time or continuous-time data; and time-domain or frequency-domain data.

The *model set* contains a description of the models that are considered during identification. Partially, the structure of the models depends on the data. However, there is much freedom in making various choices about the model structure. Some options are: the level of detail; white/grey/black box; parametric or nonparametric;

linear or nonlinear; time-invariant or time-varying; input-output structure or not; and linear-in-the-parameters or nonlinear-in-the-parameters.

The *identification criterion* or *algorithm* selects the best possible model from the candidate models in the model set. The identification criterion depends on the data set and the model set. There exist time-domain and frequency-domain identification methods for both discrete-time and continuous-time data, such as subspace identification methods, prediction error methods, and Bayesian approaches.

The *validation criterion* is used to check whether the selected model properly describes the data. These tests are often based on the residuals: the part of the data that is not captured by the model. To judge the accuracy of the model, the covariance between the residuals and the past inputs and the correlation among the residuals themselves can be evaluated. For physical systems, the physical interpretation and feasibility of the estimated parameter values also need to be considered.

For studying the accuracy of the identification methods, the measures of bias, variance, and mean-squared-error of the parameters are frequently used. This study is performed by identifying systems for which the coefficients are known, after which the identified parameters are compared with the true (known) coefficients.

1.5.2 State-of-the-art network identification

What to identify of a dynamic network? As dynamic networks are more comprehensive than general systems, there are multiple questions regarding identification that can be raised. These identification problems can roughly be divided into three main categories.

Topology identification or *topology detection* concerns the identification of the interconnection structure of the network. As stated before, the interconnection structure is what makes dynamic networks different from general systems and reveals the relations among the subsystems. For topology detection, the network dynamics is frequently unknown. Several methods have been developed for estimating the interconnection structure of a network (Mantegna, 1999; Timme, 2007; Materassi and Innocenti, 2010; Shahrampour and Preciado, 2015; Shi et al., 2019; Dimovska and Materassi, 2021; van Waarde et al., 2021). Information on the global network structure is present in the spectral properties of the network (Mauroy and Hendrickx, 2017).

Full network identification holds the identification of the dynamics of the complete network. As mentioned before, the complete network can be identified by

considering it to be a single system. Then, traditional identification approaches can be applied, such as the ones presented by Ljung (1999); Markovsky et al. (2006); Pintelon and Schoukens (2012); Verhaegen and Verdult (2012). However, then the network structure is not incorporated. Some methods use an additional step to retrieve the network structure from the identified complete network. For state-space models, these methods use, for example, matrix transformations (Friswell et al., 1999; Lopes dos Santos et al., 2015) or eigenvalue decompositions (Fritzen, 1986; De Angelis et al., 2002; Mukhopadhyay et al., 2016). For transfer function models, the topology and dynamic modules can be retrieved through matrix transformations (Gonçalves and Warnick, 2008; Yuan et al., 2011) or optimisation steps (Fonken et al., 2020) that lead to consistent and asymptotically efficient results. Other identification approaches directly incorporate the known topology in the estimation procedure (Risuleo et al., 2017; Weerts et al., 2018c). Furthermore, methods that identify both the topology and the dynamics of the complete network have been developed (Chiuso and Pillonetto, 2012; Hayden et al., 2014).

Local network identification concerns the identification of the dynamics of a small part of the network, such as a *subnetwork* or *single dynamics* (sometimes referred to as a *single module*). As dynamic networks consist of many interconnected subsystems, it is natural that only a small part of the network might be of interest. The target dynamics can be identified from an unstructured complete network through an indirect method (Gevers et al., 2018; Hendrickx et al., 2019; Bazanella et al., 2019). However, identifying the complete network dynamics seems to be excessive and a waste of energy and cost. Another way to obtain local dynamics is by blocking the target dynamics and performing a local experiment, as is often done in, for example, in-circuit testing (General Radio, 1984). However, it is not always desired or possible to block the target dynamics. Therefore, local identification methods have been developed that operate on the complete network (Van den Hof et al., 2013; Haber and Verhaegen, 2014; Linder and Enqvist, 2017; Ramaswamy et al., 2019; Materassi and Salapaka, 2020; Ramaswamy and Van den Hof, 2021; Jahandari and Materassi, 2022a).

Additional identification aspects that have been investigated with regard to the above three main identification problems are the following:

Data informativity considers the information that is present in the experimental data, which should be sufficient for obtaining a solution to the posed identification problem. For dynamic networks, this often leads to spectral conditions on internal or external signals (Gevers and Bazanella, 2015; Gevers et al., 2018). Data informativity has also been studied further for specific identification methods (Van den Hof and Ramaswamy, 2020; Bombois et al., 2023; Van den Hof et al., 2023).

Network identifiability considers the uniqueness of the solution to one of

the main network identification problems described above. For this, a unique representation of the network is necessary (Bottegal et al., 2018; Weerts et al., 2020). If multiple solutions are available, it is unclear which one corresponds to the true system. This makes it difficult to interpret the results. A distinction is made between *global network identifiability* (the ability to distinguish between *all* models in the model set) (Weerts et al., 2018b), *generic network identifiability* (the ability to distinguish between *almost all* models in the model set) (Hendrickx et al., 2019; Bazanella et al., 2019), and *generic local identifiability* (Legat and Hendrickx, 2020) (the ability to distinguish between *all* models in a *neighbourhood* in the model set). Network identifiability has been studied for full network identification (Adebayo et al., 2012; Hayden et al., 2016, 2017; van Waarde et al., 2018; Weerts et al., 2018b; van Waarde et al., 2020) and local network identification (Hendrickx et al., 2019; Bazanella et al., 2019; Shi et al., 2023).

Scalable algorithms are necessary for solving identification problems in large networks. The optimisation problems that are formulated for solving the identification problems are often nonlinear-in-the-parameters, which are difficult to solve, especially for large networks. Therefore, simple algorithms with relatively short computation times are required, such that they can easily be applied to large networks. Kernel-based methods can be used to decrease the computation time by decreasing the number of parameters (Pillonetto et al., 2014) and they can also be applied to identification in dynamic networks (Chiuso and Pillonetto, 2012; Risuleo et al., 2017; Everitt et al., 2018; Ramaswamy et al., 2018). Methods for improving the numerical calculations are discussed by Ljung (1999) and include convex recursive algorithms. More recent developments are tailored to dynamic networks and consist of multiple convex (least-squares) steps that can lead to consistent and asymptotically efficient results (Weerts et al., 2018a; Galrinho et al., 2019; Dankers, 2019; Fang et al., 2021; Fonken et al., 2022).

Experiment design includes the allocation of excitation actuators and the positioning of measurement sensors. The excitation and measurement signals need to be selected in such a way that the identification objective can be achieved (Gevers and Bazanella, 2015; Bazanella et al., 2017; Cheng et al., 2022, 2023). This also leads to the question of how to deal with unmeasured signals in a network. Typically, this is done by removing the unmeasured signals from the representation through a Gaussian elimination procedure, such as Kron reduction in electrical circuits (Kron, 1949; Dörfler and Bullo, 2013; Dörfler et al., 2018) and immersion (Dankers et al., 2016) or abstraction (Woodbury et al., 2017; Woodbury and Warnick, 2019; Weerts et al., 2020) in dynamic networks. Another topic for experiment design is the design of the excitation signals themselves. These signals should be rich enough to induce informative experimental data, which is also related to data informativity (Mareels, 1984).

Software has been developed to make system identification theory accessible and easy to use. A system identification toolbox has been developed for dynamic system modelling, time-series analysis, and forecasting (Ljung, 1999; The Mathworks, Inc., 2021). A software implementation for system identification of dynamic systems in the behavioural approach has been developed accompanied by Markovsky et al. (2006). In addition, a frequency domain system identification toolbox for MATLAB has been developed to support Pintelon and Schoukens (2012). For data-driven modelling in dynamic networks, a MATLAB app and toolbox are under development (SYSDYNET, 2023).

Other objectives in identification of dynamic networks are: considering known dynamics (Dreef et al., 2022), confounding variables (Dankers et al., 2016, 2017; Ramaswamy and Van den Hof, 2021), rank-reduced noise (Weerts et al., 2018c; Gevers et al., 2019), and sensor noise (Dankers et al., 2015) in the network models; monitoring, fault detection, and fault diagnostics (General Radio, 1984; Mishra and de Callafon, 2020; Dankers et al., 2021); validation of (especially local) identification results; and controller design (Lunze, 1992; Steentjes et al., 2021).

1.6 Practical applications

1.6.1 Pipelines

Pipelines are used for transporting liquid or gas over long distances. Think, for example, of oil distribution or the sewage system. Leaks in these systems can be caused by material failure, ground movement, corrosion, or external influences. Leaks can be harmful to the environment and endanger safety and health. The pipelines are monitored to restrain the impact of leaks, for example, by acoustic measurements with fibre optic sensors, where light pulses are sent down the cable and the reflected light is measured. The response changes if the pipeline is deformed or broken. Thus, damage to the pipelines can be detected by monitoring the acoustic response and detecting faults in the reflected light (Dankers et al., 2021).

Many sensors show faulty responses due to a single leak. Even though damage can be detected, it remains impossible to find the exact location of the defect. To locate the damaged pipe, the interconnection structure of the pipeline system has to be incorporated into the model. The resulting network model contains dynamic modules that depend on each other, because they (partially) describe the same physics of the pipe. Due to the input-output structure of the dynamic modules, the wave propagating from left to right is separately described from the wave propagating from right to left, while, actually, they pass through exactly the same

part of the pipe. The physical (and symmetric) characteristics of the pipelines need to avoid single dynamics occurring in multiple dynamic modules. Therefore, physical network models are useful for locating defects in addition to detecting faults.

1.6.2 Electric power networks

Electric power networks transmit and distribute power from power plants to individual customers. The network needs to be robust to variability and uncertainty in power supply and demand, which lead to fluctuations in voltage and frequency and therefore in admittance. Due to the current developments in renewable energy and energy storage, these fluctuations are increasing. For the reliability of the network, it is key to detect abrupt changes in the line admittance as quickly as possible. Synchronised phasor measurement units (PMUs) are used for real-time monitoring of three-phase voltage and currents, from which the three-phase line admittance can be estimated (Mishra and de Callafon, 2020).

Abrupt changes in admittance can only be detected through real-time monitoring. This asks for fast calculations, which can be performed by using simple algorithms (such as, for example, least squares) and small amounts of signals and parameters. If fewer signals are required, then less equipment is required, which also saves money that can be invested otherwise. Physical linear network models are necessary for incorporating the physical characteristics of the electrical power network in the most extensive way. This will lead to a minimum number of required parameters and measurement signals, resulting in short time intervals in which the admittance can be estimated. As changes in the admittance can be detected relative quickly, the reliability of the electric power network is high.

1.6.3 Smart grid

The smart grid is crucial for a smart and carbon-neutral society. This modern power network contains more and more new equipment related to renewable energy sources, energy storage, and control, which lack effective state awareness and maintenance protocols. The increasing diversity of devices also leads to larger power fluctuations. The more complex and intelligent operation conditions ask for higher requirements on safety and reliability, also on the long term. In addition, the desire for a carbon-neutral society leads to new operation requirements to reduce emissions during planning, operation, and maintenance (Li et al., 2023).

Slow and low-reliable methods are the current standard for fault detection. Often, fault detection and diagnostics are even done by employees going step-by-

step through manuals. Autonomous real-time measurements, fast calculations, and accurate assessments are necessary to detect faults in due time. This can be achieved through real-time data-driven identification and accurate parameter prediction. To this end, identification tools for physical linear network models that describe the smart grid on different levels of detail have to be utilised to detect, locate, and diagnose faults in a short time.

1.6.4 Printed circuit boards

Printed circuit board assemblys (PCBAs) are the objects that result from placing components on a printed circuit board. To validate the production procedure and check whether there are any defects or faults, an in-circuit test procedure is followed. During this test, each connection or component is checked separately by attaching external measurement equipment to the PCBA and performing component-wise experiments. A fault is detected when an experiment gives different results than expected. A fault can have several causes, such as a broken link, a shortcut, a wrong component, or parasitic effects (additional components or connections that should not be present) (Meijer, 2021).

Component-wise testing takes many experiments and is therefore time-consuming and costly. The testing procedure can be improved by creating single tests that are capable of validating multiple components and interconnections. These tests should check the presence and absence of links, the values of the placed components, and the presence of parasitic effects. To create these intelligent tests, the topological information and the characteristics of the physical components need to be incorporated. Therefore, physical network models are necessary for efficient in-circuit testing of PCBAs.

1.6.5 Wafer scanners

Wafer scanners manufacture integrated circuits. These machines are becoming more complex and operate under highly advanced conditions to increase the production, accuracy, and functionality of the chips. They are composed of many (physically) interconnected subsystems. Component malfunctions, such as loosened bolts, broken screws, and cable shortcuts, lead to changes in dynamics. A single fault results in performance degradation throughout the whole machine, which makes it difficult to locate the cause of the problem. The problem is often solved by employees going step-by-step through manuals, which is a time-consuming approach. During the search and repair of the malfunction, the machine is inoperable, causing a discontinuation of chip production. Nimble fault detection

and diagnostics are necessary to reduce these expensive downtimes. Especially rare errors take much time and are sometimes not identified at all. As they occur so seldom, only few data are available to gain knowledge on these errors (Nikitas, 2023).

Knowledge on (rare) errors can be gained by creating a digital twin. This model should be capable of simulating realistic, accurate, and faulty machine operation. By simulating faults in the digital twin, the distribution of performance degradation throughout the machine can be monitored. Analysing the generated data gives insight into what kind of changes in the data are caused by which faults. This leads to better fault detection and diagnostics techniques. The digital twin should generate realistic data on both a properly working machine and a faulty machine. Currently, the subsystems are described using finte-element-method (FEM) models with high accuracy (Nikitas, 2023), while the models of the interconnections lack accuracy. Physical networks can be used to precisely model the physical interconnections between the subsystems.

1.7 Problem statement

1.7.1 Boundaries

By now, it is clear that *systems, and in particular dynamic networks*, are everywhere around us and thus occur in many research areas. In this work, we will restrict to a particular class of dynamic networks, namely physical networks. As mentioned before, physical systems are characterised by the fact that they 'act according to the laws of nature or what is likely'. To be more precise, physical systems and physical networks are defined by Willems (2007) as follows:

Definition 1.15 (Physical system (Willems, 2007)). *A* physical system *is a system whose behaviour is described by relations between system variables.*

Definition 1.16 (Physical network (Willems, 2007)). *A* physical network *is a network consisting of interacting physical systems (as defined in Definition 1.15). These physical systems are interconnected by sharing variables among subsystems.*

In other words, *no predefined input-output structure* is present in physical systems and an interconnection of physical systems implies that these systems share information (or system variables). There is no predefined signal flow or cause-effect relationship in physical networks. The physical systems define mappings

from time to outcomes. The collection of all possible outcomes is the behaviour of the system. In line with this, a physical system is defined as follows:

Definition 1.17 (Physical system (Willems, 1986a)). *A physical system is defined as the triplet*

$$\Sigma = (\mathbb{T}, \mathbb{W}, \mathcal{B}), \tag{1.1}$$

with

1. $\mathbb{T} \subseteq \mathbb{R}$ *the* time space.
2. $\mathbb{W} \subseteq \mathbb{R}^{\mathtt{w}}$ *the* signal space*, with* $\mathtt{w} \in \mathbb{N}$ *the dimension of the trajectories* $w(t)$.
3. $\mathcal{B} \subseteq \mathbb{W}^{\mathbb{T}}$ *the* behaviour*, with* $\mathbb{W}^{\mathbb{T}}$ *the collection of all maps from* $\mathbb{T}$ *to* $\mathbb{W}$.

Linearity and time invariance are natural characteristics of many laws used in science and engineering. Typically, systems are designed to operate in the LTI region. Consider for example a resistor, which describes a linear and static relation between the current flow and the voltage drop through Ohm's law, see Example 1.2. For very large changes in the current flow, this relation might change and become nonlinear. Typically, the electrical circuit is designed so that the resistor's behaviour can be described well with Ohm's law. Therefore, we restrict ourselves to LTI systems and networks. *Linearity* means that superposition and scaling of trajectories result in allowed trajectories, that is, for two trajectories $w_1(t) \in \mathcal{B}$ and $w_2(t) \in \mathcal{B}$ and for all scalars $\alpha, \beta \in \mathbb{R}$, the trajectory $\alpha w_1(t) + \beta w_2(t) \in \mathcal{B}$. *Time invariance* means that time shifting trajectories results in allowed trajectories, that is, for trajectory $w(t) \in \mathcal{B}$ and time $t_1 \in \mathbb{T}$, the trajectory $w(t + t_1) \in \mathcal{B}$. The behaviour of physical LTI systems (1.1) can be described by linear constant-coefficient ordinary differential equations (ODEs).

Definition 1.18 (Physical LTI systems (Willems, 1986a; Polderman and Willems, 1998)). *The behaviour* $\mathcal{B}$ *of a physical system as defined in Definition 1.17 that has LTI behaviour and with* $\mathtt{p} \leq \mathtt{w}$ *can be described by an ODE as*

$$\mathcal{B} = \{w(t) \in C^{\infty}(\mathbb{R}, \mathbb{R}^{\mathtt{w}}) |\ R(\frac{d}{dt})w(t) = 0\} \tag{1.2}$$

with $t \in \mathbb{T}$ *indicating the time,* $C^{\infty}(\mathbb{R}, \mathbb{R}^{\mathtt{w}})$ *the set of infinitely differentiable functions from* $\mathbb{R}$ *to* $\mathbb{R}^{\mathtt{w}}$*, and* $R(\xi) \in \mathbb{R}^{\mathtt{p} \times \mathtt{w}}[\xi]$.

The *ODE* in (1.2) describes the behaviour of the trajectories $w(t) \in \mathcal{B}$ without an explicit input-output mapping. The coefficients of the polynomial matrix

$R(\xi)$ depend on the physics and so, the ODE can be seen as a function that restricts the trajectories to legitimate behaviour. The behaviour can be subject to disturbances, which act as inputs to the trajectories. To include these disturbances in the behaviour, the signal space is extended to include the trajectories of the disturbances.

Definition 1.19 (Physical LTI systems with disturbances (Polderman and Willems, 1998)). *A physical system, as described in Definition 1.18, that is subject to disturbances $v(t)$ is defined by the triplet $\Sigma_v = (\mathbb{T}, \mathbb{W}_v, \mathcal{B}_v)$ with*

1. *Signal space $\mathbb{W}_v := \mathbb{W} \cup \mathbb{V} \subseteq \mathbb{R}^{\mathtt{w}+\mathtt{v}}$, with $\mathtt{v} \in \mathbb{N}$ the dimension of the trajectories $v(t)$.*
2. *Behaviour $\mathcal{B}_v \subseteq \mathbb{W}_v^{\mathbb{T}}$.*

and can be described by an ODE as

$$\mathcal{B}_v = \{w(t) \in C^\infty(\mathbb{R}, \mathbb{R}^{\mathtt{w}}), v(t) \in C^\infty(\mathbb{R}, \mathbb{R}^{\mathtt{v}}) |\ R(\frac{d}{dt})w(t) = v(t)\}. \quad (1.3)$$

Physical networks as defined by Definition 1.16 are interconnections of physical systems and therefore, physical LTI networks can also be represented by the ODE in (1.3). This particular model can be seen as a basis for many other models describing physical linear networks. In order to identify these networks, the identification setting is limited by the following choices:

The *data set* is considered to contain time-domain data. The interconnections in the network are assumed to be deterministic in the sense that they are either present or absent. We do not consider switching interconnections or connections that are only present with a certain probability. On the other hand, the input signals can be stochastic signals, meaning that the network is subject to unknown disturbances.

The *model set* is limited to LTI models. Although many physical laws are not LTI by nature, we typically design systems and subsystems to operate in an LTI region, as mentioned before. These models describe the network behaviour through mathematical relations and use parameters to capture the dynamics. We do not limit our research to a particular model structure. In fact, finding the proper model structure is part of the research.

The *identification criterion* is chosen to be a quadratic and possibly weighted function of the prediction error. We chose prediction error over simulation error, because it is easer to optimise and less computational intense (Aguirre et al.,

2010); a rigorous theoretical analysis on the error bounds is available, where stability of the error is guaranteed; and measured data gives more information on the dynamics than estimated signals. Networks can consist of many signals and therefore, computational simplicity is important. Hence, we restrict ourselves to prediction error identification methods.

1.7.2 Open problem

The identification objective is either the dynamics of the full physical linear network or the dynamics of a part of a physical linear network. This dynamics is described by parameters that are directly related to the physical components in the network. The objective is thus to estimate these parameters. Identifying the interconnection structure between the subsystems is of minor interest. However, for full network identification, the topology does not have to be known in advance and moreover, it can be identified simultaneously. That is, if the dynamics of an interconnection is determined to be zero, it implicitly means that the interconnection is absent. Nevertheless, this work is mostly concerned with identification questions regarding network dynamics.

What is the current situation? For the identification of physical networks, there are essentially two approaches available in the literature. The first one considers the network as a single physical system and the second one considers the network as a dynamic network. As discussed in Section 1.5.2, several modelling and identification techniques are available in the literature. The most relevant models for the identification of physical linear networks are state-space models, dynamic network models, and behavioural models.

State-space models can be used to model physical networks either directly or by transforming second-order (vector) differential equations into state-space forms. The state-space model is identified using a subspace identification method. Sometimes, the parameters related to the interesting physical components can directly be extracted from the identified state-space model, but often there is an additional step needed to obtain these parameters in the second-order vector differential equations.

Are there performance guarantees? For subspace identification methods, there are no guarantees on statistical accuracy and disturbances acting on the systems are not considered (except for white noise on the measured signals). Therefore, it is unclear how well these methods perform, especially for networks that are subject to unknown disturbance signals. In addition, the question is whether the network topology can be incorporated into these methods and how to do this.

Dynamic network models, such as the module representation, explicitly exploit the topology of the network. There is much literature on the identification of dynamic networks, especially for this module representation. If physical networks can be modelled by the module representation, all the identification tools that are available for dynamic networks can be applied to the identification of physical networks.

Has it the correct structure? The module representation is a generalisation of the open-loop and closed-loop systems and therefore consists of directed information flows among input-output subsystems. However, physical networks do not possess any input-output structure. Therefore, the question is whether physical networks can be modelled with an input-output structure for identification purposes and what the consequences are for doing so.

The behavioural approach is the modelling approach that lies closest to the nature of physical systems and networks. Physical networks can be modelled by modelling the subsystems and the interconnections separately, and therefore, the topology can be represented in the model.

Is there identification theory available? Although there exist some literature on system identification in the behavioural approach, to our best knowledge, there is no literature available on the identification of networks in this setting. Therefore, it remains challenging to incorporate the network topology into the identification procedure and to oversee the consequences.

1.7.3 Research objective

What is the main problem? The physical linear network models need to consider disturbance signals and the topology needs to be taken into account, especially for local identification problems. The problem with state-space models is that the influence of disturbance signals is unclear and the topology is hidden in the model structure. However, it is possible to include these aspects in dynamic network models. The problem with dynamic network models is that it is unknown whether the noninput-output structure of the subsystems can be modelled. In the natural and physical world, there are only physical systems, which do not possess a predefined input-output structure. The behavioural approach is suitable for modelling these physical networks, but in this setting, there is a lack of identification tools for networks. Then again, it is unclear how to incorporate the topology into the identification procedure. This raises the question of whether one of the above approaches is attractive for accurately identifying some (or all) dynamics in physical linear networks or whether it would be better to take an alternative approach with a new model structure.

What is the main objective? Once the model structure is determined, the identification procedure for estimating the network dynamics can be investigated. As mentioned, the focus of this research will be on the dynamics of the full network or of a part of the network. The topology is of minor interest and might be detected implicitly during the identification procedure. Summarising this leads to the objective of this research.

> **Research objective.** *Develop model structures and identification tools for parameter estimation in physical linear networks.*

This research objective consists of four concepts, which are elaborated on here.

Physical linear networks are the networks that are considered in this work. They are physical networks, as defined in Definition 1.16, that are restricted to having only linear dynamics. This dynamics represents the behaviour of the physical components that are present in the network.

Model structures need to be developed to describe the physical linear networks in a way that is appropriate for identification purposes. This means that the model structures should capture the specific characteristics of physical components, incorporate the topology of the network, and account for disturbance signals that can process through the network.

Parameter estimation is used to select the best model from the model structure. The parameters represent the physical components in the network model and therefore, parameter estimation leads to the values of the physical elements in the network. In this work, we either aim for all parameters describing all dynamics in the network or for a subset of parameters, which only describe a subset of the network dynamics.

Identification tools have to be developed to perform the parameter estimation. Next to algorithms and software implementations to execute the parameter estimation, additional tools need to be developed to arrive at these results. These include methods to modify the network description, conditions under which network models can uniquely be determined, and conditions under which the parameter estimation can be performed. This leads to guidelines for the experimental setup, restrictions on the network model, and assumptions on the disturbance signals.

The process of achieving this research objective comprises several topics. These topics lead to the subquestions of this research, which are presented next.

1.8 Subquestions

1.8.1 Model structure

The model set is one of the three main objects that are necessary for system identification, as explained in Section 1.5.1. It describes the candidate models that will be considered during identification. The set of candidate models is parameterised as a model structure. There are many model structures available in the literature, but it is unclear whether any of them is suitable for identification in physical linear networks. We can already reveal that this is not the case, which means that an appropriate model structure needs to be developed. This leads to the first question.

> **Research question 1.** *What model structure to use for identification of physical linear networks?*

*The model structure*that we are looking for should be such that it allows for capturing the specific characteristics of the physical components that are present in the network. In addition, the topology of the network should be incorporated and the model structure should account for disturbance signals that can process through the network. The approach to determining a desired model structure consists of several steps. First, the physical linear network model is viewed as an interconnection of physical components, where the physical components and interconnections will be described by the laws of nature. This modelling procedure is similar to the method of *tearing, zooming, and linking* (Willems, 2007). Second, all relations are combined to describe the signals of interest in terms of other signals that are present in the network, similar to the approach of the module representation (Van den Hof et al., 2013). This will lead to a (new) network model for physical linear networks that includes both the dynamics and the topology of the network in such a way that it accommodates the properties of the physical components.

1.8.2 Network identifiability

Identification is the process of selecting the model from the model set that best explains the experimental data. In order to make this selection, the best model must be unique. In other words, there must be only one model in the model set that explains the data best. For physical networks, this uniqueness is particularly significant, because the model parameters are directly related to the coefficients of the physical components that are present in the network. Furthermore, the

experimental data consist of external excitation signals and internal measured network signals. In a network, there are plenty of options for selecting these signals. The excitation locations and measurement signals need to be selected so that identification can be performed. This leads to the second research question.

> **Research question 2.** *Under what conditions are physical linear network models identifiable?*

An identifiability problem is the problem of distinguishing network models in a network model set. The approach to deriving identifiability conditions for identification of the complete network dynamics is based on finding a network model that uniquely describes the data. This is done by investigating the uniqueness of matrix-fraction descriptions (MFDs), which describe a transfer function matrix in terms of a numerator and denominator polynomial matrix. The resulting conditions restrict the model structure so that the uniqueness of the network model can be guaranteed. This includes the selection of measured internal signals and the allocation of external excitation signals. Prior knowledge on network dynamics, network topology, and the presence of excitation signals (and measurable signals) restricts the model structure and therefore facilitates identifiability. In the situation where only some local dynamics needs to be identified (i.e. only a subnetwork), then only that particular part of the network needs to be identifiable. This leads to more relaxed conditions.

All (relevant) node signals are assumed to be measurable in the initial situation. The identifiability results are dual for networks in which external excitation signals are present at all (relevant) node signals. However, it is not always possible to measure all relevant node signals and it is doubtful whether it is possible to allocate external excitation signals at any desired location. Therefore, networks with a selected set of actuators and sensors are considered. The identifiability analysis follows the same path as the one for networks with full measurement (i.e. networks in which all node signals are measurable) and for networks with full excitation (i.e. networks in which all node signals are excited).

1.8.3 Full network identification

An identification criterion or algorithm is necessary for estimating the parameters. This is the next ingredient in the identification procedure, once the network model is guaranteed to be unique within the model set. There are several identification methods available in the literature. We have to investigate which identification procedure is suitable for the physical linear networks described by the developed

model structure. Further, algorithms need to be developed to perform the optimisation in the identification methods. This leads to the third question.

Research question 3. *How to identify a full physical linear network?*

Full identification refers to the identification of both the dynamics and the topology of the network. The approach to identifying the full physical linear network is based on the prediction error identification method, for which conditions for consistency (and minimum variance) will be derived. These conditions include conditions for identifiability of the network dynamics and restrictions on the experimental data. The optimisation problem resulting from the prediction error identification method will be nonconvex, because the prediction error is nonlinear in the parameters. The larger the network, the more parameters are present in the model and therefore, the more tuning nobs are available for adjusting the solution. This makes it more likely to arrive at local optima, while the computation time is also high. To make the identification algorithm suitable for large networks and to reach the global optimum, a multistep convex algorithm will be developed based on the weighted null-space fitting (WNSF) algorithm (Galrinho et al., 2019). This algorithm also allows for incorporating prior knowledge on the dynamics or topology of the network.

1.8.4 Subnetwork identification

Identifying a subnetwork is another objective, next to identifying all network dynamics and the topology. Especially for large networks, it is imaginable that only a small part of the network is of interest or that insufficient information is available to identify the full network. The larger the network, the more relevant it becomes to consider this. This leads to the fourth question.

Research question 4. *How to identify specific components in a physical linear network?*

In subnetwork identification, the consideration of the part of the network that is outside the target subnetwork is an additional aspect that plays a crucial role. This includes the problem of dealing with unmeasurable signals. In the module representation, unmeasured signals are eliminated through immersion (Dankers et al., 2016). For physical linear networks, a similar mechanism will be developed that, at the same time, accounts for the characteristic properties of physical components. Similar to the identification of the full network, conditions for consistency will be derived and a multistep convex algorithm has to be developed for performing

the identification. Again, incorporating prior knowledge on the dynamics and topology of the network is supported by the algorithm. However, the topology in the neighbourhood of the target dynamics is required to enable the identification. The remaining topological information is not necessary for identification.

1.8.5 Directed interconnections

Controllers often influence physical linear systems or networks in practice. A digital controller is an example of a nonphysical element that has a predefined input-output structure and therefore, has properties that are different from the physical components in the network. Therefore, physical networks with digital controllers lead to networks with different characteristics. In addition, nonsymmetric components, such as diodes or one-way check valves, can be present in the network. Hence, it is of substantial value to manage directed dynamics in the network model and the identification procedure. This leads to the final question.

Research question 5. *How to account for directed dynamics in physical linear networks?*

Directed dynamics can be present in physical networks in several ways. For example, the network may contain just some additional directed links, or there may also be some additional node signals that are only influenced by directed dynamics. This leads to mixed linear dynamic networks that contain both directed and undirected interconnections. The directed dynamics can be unknown, but may also be known, for example, when they represent a controller. Incorporating known dynamics into the identification procedure facilitates the identification. As directed dynamics have different properties than physical components, including directed dynamics in the network model will destroy the structure. This has consequences for the identification procedure and changes, for example, the identifiability conditions. All identification tools that have been developed will be analysed again to discover the consequences due to the directed dynamics. Adjustments to the identification tools will be made to make them suitable for handling directed dynamics.

1.9 Overview

1.9.1 Introduction

The remaining part of the thesis consists of three parts.

Part I concerns the modelling of physical linear networks and therefore, this part is completely dedicated to Research question 1. In this part of the thesis, we search for a suitable model structure of physical linear networks for identification purposes.

Part II is devoted to the identification of physical linear networks by studying Research question 2-4. In this part of the thesis, we explain which conditions have to be satisfied for identifiability, how a full physical linear network can be identified, and how a subnetwork can be identified.

Part III contains the extension of physical linear networks to mixed linear dynamic networks. Research question 5 is explored in this part, which means that we investigate the consequences of including directed dynamics in the modelling and identification of physical linear networks.

1.9.2 Part I: Modelling of physical linear networks

Chapter 2: Linear dynamic network models

Physical linear networks and their characteristic properties are discussed. Numerous dynamic models for systems and networks are presented. These models are compared on several aspects that are important for the identification of dynamic networks. The most promising dynamic network models are selected for further research. This chapter contributes to the answer to Research question 1.

Chapter 3: Graphical structures of linear dynamic networks

Graphical representations of linear dynamic networks are analysed and four main graphical structures are discussed. Networks can be described at different levels of detail by including or excluding structural and dynamic information. The relations between these representations are analysed, including a comparison between the module representation and the interaction-oriented model. This chapter contributes to the answer to Research question 1.

Chapter 4: Representations of linear dynamic networks

Various representations of dynamic networks are studied. The relations between state-space models and module representations of dynamic networks are investigated, leading to a dynamic network model that can capture both representations. Modelling tools are developed for analysing this network model. These tools

allow for zooming in on and zooming out of the network model and including and excluding structural information. With this, a network can be described at different levels of detail, as discussed in Chapter 2. This chapter contributes to the answer to Research question 1.

This chapter is a slightly extended version of

> E.M.M. Kivits and P.M.J. Van den Hof. On representations of linear dynamic networks. *IFAC-PapersOnLine*, 51(15):838–843, 2018. Proceedings of the 18th IFAC Symposium on System Identification (SYSID).

Chapter 5: Diffusively coupled linear network models

A diffusively coupled linear network model is introduced to describe physical linear networks. This network model possesses several interesting equivalent representations, which are analysed. Their relationships, advantages, and disadvantages are discussed. The use of this network model to describe networks from different physical domains is illustrated and the analogies among them are clarified. In addition, the application of this newly developed network model to other types of networks than physical networks is elaborated on. This chapter contributes to the answer to Research question 1.

1.9.3 Part II: Identification of physical linear networks

Chapter 6: Linear dynamic network identification tools

Identification tools from the literature are presented that form the basis for the identification tools for physical linear networks that will be developed in the remainder of the thesis. Polynomial models and their properties are provided, because they are relevant for the diffusively coupled network model that has been developed in Chapter 5. In addition, concepts for identification in dynamic networks are specified.

Chapter 7: Identification through a dynamic network approach

A dynamic network approach is applied to identify diffusively coupled linear network models that have been developed in Chapter 5. The network model is translated into the module representation (Van den Hof et al., 2013). The specific properties of the resulting network model are analysed. The identification tools that are available for the module representation lead to conditions and algorithms

for full network identification. Identification tools and an identification set-up for local identification are derived. This chapter contributes to the answer to Research question 3-5.

This chapter is a revised and extended version of

> E.M.M. Kivits and P.M.J. Van den Hof. A dynamic network approach to identification of physical systems. In *Proceedings of the 58th IEEE Conference on Decision and Control (CDC)*, pages 4533–4538, 2019.

Chapter 8: Identification through structured polynomial models

Conditions and a convex algorithm for consistent identification of the complete physical linear network are derived. These physical linear networks are modelled by the diffusively coupled linear network model of Chapter 5. The conditions include conditions for identifiability of the full physical network and conditions for data informativity. The identification is performed in the discrete-time domain by using a prediction error identification method. The algorithm consists of multiple steps of convex optimisations and polynomial matrix manipulations. The main part of the algorithm is similar to the WNSF (Galrinho et al., 2019)), which is adapted to account for the structural characteristics of diffusively coupled linear networks and to incorporate the identifiability constraints. A simulation example is shown to illustrate the algorithm. This chapter contributes to the answers to Research question 2 and 3.

This chapter is equivalent to

> E.M.M. Kivits and P.M.J. Van den Hof. Identification of diffusively coupled linear networks through structured polynomial models. In *IEEE Transactions on Automatic Control*, vol. 68, no. 6, pages 3513-3528, 2023.

Chapter 9: Subnetwork identification

Identification of only a small part of the network is considered here. Due to the specific characteristics of physical components, the objective for this *local identification* is revised for physical linear networks and reformulated into a subnetwork identification problem. A tool for eliminating unmeasured signals from diffusively coupled linear networks is developed based on immersion (Dankers et al., 2016). Conditions for consistent identification of the target dynamics are derived and algorithms are developed for performing the identification. A simulation example illustrates the identification. This chapter contributes to the answers to Research question 2 and 4.

This chapter adds Section 9.9 and 9.10 to the work that is equivalent to

> E.M.M. Kivits and P.M.J. Van den Hof. Local identification in diffusively coupled linear networks. In *Proceedings of the 61st IEEE Conference on Decision and Control (CDC)*, pages 874-879, 2022.

Chapter 10: Identifiability with partial instrumentation

Identifiability conditions are derived for diffusively coupled linear networks in which only a selected set of node signals is measurable and where external excitation signals can only be allocated at specific locations. The identifiability conditions for diffusively coupled networks in which all node signals are measurable are repeated and the dual conditions for the situation in which all node signals are excited are given. Along the same line of reasoning, conditions for the partial instrumentation case are derived. Using a special case, the sufficient conditions on the actuator and sensor locations are illustrated. This chapter contributes to the answers to Research question 2-4.

This chapter adds Remark 10.18 to the work that is equivalent to

> E.M.M. Kivits and P.M.J. Van den Hof. Identifiability of diffusively coupled linear networks with partial instrumentation. *Preprints of the 22nd IFAC World Congress*, 2706-2711, July 2023.

1.9.4 Part III: Extension of physical linear networks

Chapter 11: Mixed linear dynamic networks

Mixed linear dynamic networks with both directed and undirected interconnections are discussed. Two types of mixed networks are modelled in the polynomial framework that is used for describing diffusively coupled linear networks. One of these mixed networks is also modelled in the module representation that is used for describing directed dynamic networks. For all three models, the implications for identification are analysed. This leads to adapted conditions for consistent identification of the complete networks, including identification of the directed dynamics. Suggestions for algorithms are given and the results are discussed. This chapter contributes to the answers to Research question 5.

Chapter 12: Conclusions and future research

Conclusions are drawn by evaluating the main research objective and answering the five research questions. Suggestions for future research are presented, which include the improvement of algorithms, continuous-time identification, and practical applications to monitoring, fault detection, and diagnostics.

Part I

Modelling of physical linear networks

2 | Linear dynamic network models

Systems in the natural and physical world can be described in various ways. There also exist several models for interconnections of these physical systems. Physical linear networks are described in detail and their particular properties are explained. Several mathematical models of linear systems and networks are discussed. The main advantages and shortcomings of the linear dynamic network models for modelling and identification of physical linear dynamic networks are discussed.

2.1 Introduction

Networks can be found in various different research areas, including biology, economy, engineering, physics, and social sciences (Ren et al., 2005; Boccaletti et al., 2006; Mesbahi and Egerstedt, 2010). All these research areas have their own environment with specific conditions and unique issues. This gives rise to research questions that are pertinent to the particular situation. Therefore, each research area has its own unique way of expressing its problem. The choice of model structure to describe or represent these networks is usually aligned with the environment, preconditions, model objectives, and questions. This leads to numerous models for describing linear networks, each of which is tailored to a particular situation.

The overall interest of this research is parameter estimation in networks from the natural and physical world. These physical networks act according to the laws of nature or what is likely. Many physical laws can be approximated well by linear and time-invariant relations and therefore, this work is restricted to linear time-invariant (LTI) models. In addition, many of these laws can be expressed

by systems of ordinary differential equation (ODE), which are therefore used in many mathematical network models. Some examples of these models are state-space models, which are often used in biology and economy (Mesbahi and Egerstedt, 2010; Verhaegen and Verdult, 2012; Bullo, 2022); second-order vector differential equation models, which are often used in mechanics (Ljung and Glad, 1994; Van den Bosch, 2009); and polynomial models, which are often used in an identification setting (Ljung and Glad, 1994; Ljung, 1999).

Networks with uncertain interconnections are modelled by (dynamic) Bayesian networks, which describe joint probabilities over a set of random variables (Koller and Friedman, 2009; Sucar, 2021).

For modelling linear dynamic networks, Wiener filters (Materassi and Innocenti, 2010), the dynamical structure function (Gonçalves et al., 2007), and the module representation (Van den Hof et al., 2013) are popular approaches. Here, signals are interconnected through transfer function relations, the so-called modules of the network. Linear dynamic networks can also be modelled by interconnecting subsystems through an interaction-oriented model (Lunze, 1992).

Energy is a well-studied quantity in physical networks, for example, in energy balances and energy or power exchange. Therefore, there are many energy-based modelling techniques, such as bond-graph models, (multi)port models, and (port-)Hamiltonian models (Paynter, 1961; van der Schaft and Jeltsema, 2014). A more general modelling technique is the behavioural approach, which considers just the interconnections between physical components Willems (2007). This is a modelling technique that lies very close to the natural and physical world.

One might wonder whether users of different network models can learn from each other. Some questions arising in one research area may already be answered in another research area, where they use a different network model. Perhaps it is possible to transform results for one model structure into results for another model structure. Therefore, it is important to know the relations among the network models.

This chapter addresses the questions of which network models are available for the identification of physical linear networks and what the relations between them are. Some mathematical definitions and notation are introduced in Section 2.2. Some general modelling aspects are presented in Section 2.3. Section 2.4 describes a number of network models. The main advantages and shortcomings of the linear network models for modelling and identification of physical linear dynamic networks are discussed in Section 2.5. Finally, Section 2.6 concludes the chapter.

2.2 Mathematical definitions and notation

2.2.1 Variables

Throughout the thesis, consider the following definitions of variables:

Definition 2.1 (Manifest variable (Polderman and Willems, 1998)). *A* manifest variable *is a variable of interest.*

Definition 2.2 (Latent variable (Polderman and Willems, 1998)). *A* latent variable *is a variable that is not manifest.*

The manifest variables are the variables that are modelled and on which the attention is focussed. The latent variables are auxiliary variables that are used to achieve a convenient expression of the model. Remark that each variable is either manifest or latent.

2.2.2 Signals

Signals capture the change of variables over time. A signal can be multidimensional. Multiple signals $w_j(t)$, $j = 1, 2, \ldots, L$ can be captured in a vector as

$$w(t) = \begin{bmatrix} w_1(t) \\ w_2(t) \\ \vdots \\ w_L(t) \end{bmatrix}, \tag{2.1}$$

and $w(t)$ is sometimes referred to as a *vectorised version* of $w_j(t)$, $j = 1, 2, \ldots, L$. Here, $w_j(t)$ can also be a multidimensional signal, but without loss of generality we will restrict our attention in this thesis to scalar-valued signals $w_j(t)$.

2.2.3 Polynomials

A polynomial $a(\xi) \in \mathbb{R}[\xi]$ in indeterminate $\xi \in \mathbb{C}$, consists of elements $a_\ell \in \mathbb{R}$ such that

$$a(\xi) = \sum_{\ell=0}^{n_a} a_\ell \xi^\ell = a_0 + a_1\xi + a_2\xi^2 + \ldots + a_{n_a}\xi^{n_a}. \tag{2.2}$$

A polynomial is called *monicity* if $\lim_{\xi\to\infty} a(\xi) = 1$, that is if $a_0 = 1$.

The indeterminate ξ in (2.2) can be substituted by the differential operator p meaning $pu(t) = \frac{d}{dt}u(t)$, leading to

$$a(p)u(t) = \sum_{\ell=0}^{n_a} a_\ell \frac{d^\ell}{dt^\ell}u(t) = a_0u(t) + a_1\frac{d}{dt}u(t) + a_2\frac{d^2}{dt^2}u(t) + \ldots + a_{n_a}\frac{d^{n_a}}{dt^{n_a}}u(t). \tag{2.3}$$

The indeterminate ξ in (2.2) can be substituted by the backward shift operator q^{-1} meaning $q^{-1}u(t) = u(t-1)$, leading to

$$a(q^{-1})u(t) = \sum_{\ell=0}^{n_a} a_\ell u(t-\ell) = a_0u(t) + a_1u(t-1) + a_2u(t-2) + \ldots + a_{n_a}u(t-n_a). \tag{2.4}$$

The indeterminate ξ in (2.2) can be substituted by the forward shift operator q meaning $qu(t) = u(t+1)$, leading to

$$a(q)u(t) = \sum_{\ell=0}^{n_a} a_\ell u(t+\ell) = a_0u(t) + a_1u(t+1) + a_2u(t+2) + \ldots + a_{n_a}u(t+n_a). \tag{2.5}$$

2.2.4 Polynomial matrices

A polynomial matrix $A(\xi) \in \mathbb{R}^{L\times K}[\xi]$ in indeterminate $\xi \in \mathbb{C}$, consists of matrices $A_\ell \in \mathbb{R}^{L\times K}$ such that

$$A(\xi) = \sum_{\ell=0}^{n_a} A_\ell \xi^\ell, \tag{2.6}$$

and such that

$$A(\xi) = \begin{bmatrix} a_{11}(\xi) & a_{12}(\xi) & \cdots & a_{1K}(\xi) \\ a_{21}(\xi) & a_{22}(\xi) & \ldots & a_{2K}(\xi) \\ \vdots & \vdots & \ddots & \vdots \\ a_{L1}(\xi) & a_{12}(\xi) & \cdots & a_{LK}(\xi) \end{bmatrix}, \tag{2.7}$$

with (j,k)th polynomial elements

$$a_{jk}(\xi) = \sum_{\ell=0}^{n_a} a_{jk,\ell}\xi^\ell, \tag{2.8}$$

with $j = 1, 2, \ldots, L$ and $k = 1, 2, \ldots, K$. Hence, the (j,k)th element of the matrix A_ℓ is denoted by $a_{jk,\ell}$.

Definition 2.3 (Monic (Kailath, 1980)). *A polynomial matrix $A(\xi)$ is called* monic *if $\lim_{\xi\to\infty} A(\xi) = I$, with I the identity matrix, that is if $A_0 = I$, or in other notation, if $a_{jj,0} = 1$ and $a_{jk,0} = 0$ for $j \neq k$.*

2.2.5 Rational functions

A rational function $G(\xi) \in \mathbb{R}(\xi)$ in indeterminate $\xi \in \mathbb{C}$, consists of a numerator and denominator polynomial $n(\xi) \in \mathbb{R}[\xi]$ and $d(\xi) \in \mathbb{R}[\xi]$, respectively, such that

$$G(\xi) = \frac{n(\xi)}{d(\xi)} = \frac{\sum_{\ell=0}^{r_n} n_\ell \xi^\ell}{\sum_{\ell=0}^{r_d} d_\ell \xi^\ell}. \tag{2.9}$$

A rational function applied to a signal is interpreted as

$$G(\xi)u(t) := \sum_{\ell=0}^{\infty} g_\ell \xi^\ell u(t), \tag{2.10}$$

with g_i the analytic part of the Laurent series expansion of the rational function $G(\xi)$ at the point 0.

The indeterminate ξ in (2.10) can be substituted by the differential operator p, leading to

$$G(p)u(t) = \sum_{\ell=0}^{\infty} g_\ell \frac{d^\ell}{dt^\ell} u(t) = g_0 u(t) + g_1 \frac{d}{dt} u(t) + g_2 \frac{d^2}{dt^2} u(t) + \dots \tag{2.11}$$

The indeterminate ξ in (2.10) can be substituted by the backward shift operator q^{-1}, leading to

$$G(q^{-1})u(t) = \sum_{\ell=0}^{\infty} g_\ell u(t-\ell) = g_0 u(t) + g_1 u(t-1) + g_2 u(t-2) + \dots \tag{2.12}$$

The indeterminate ξ in (2.10) can also be substituted by the forward shift operator q. However, we decide to use a different definition for $G(q)$.

Definition 2.4 (Transfer function G(q) (Ljung, 1999)). *The notation $G(q)$ is used as an alias for the rational function $G(q^{-1})$. That is, q is used as an argument of G to indicate the rational function $G(\xi)$ with q^{-1} substituted for ξ. This choice is made to be in formal agreement with the Z-transform and*

Fourier-transform expressions, which are common in linear system theory (Hespanha, 2023) and system identification (Ljung, 1999). Furthermore,

$$G(q) := \sum_{\ell=0}^{\infty} g(\ell) q^{-\ell}, \tag{2.13}$$

with $g(\ell)$ the ℓth sample of the impulse response, is referred to as the transfer function*, even though the notion* transfer function *is strictly speaking reserved for the Z-transform of the impulse response.*

2.2.6 Rational function matrices

A rational function matrix $G(\xi) \in \mathbb{R}^{L\times K}(\xi)$ in indeterminate $\xi \in \mathbb{C}$, consists of matrices $G_\ell \in \mathbb{R}^{L\times K}$ such that

$$G(\xi) = \sum_{\ell=0}^{n_G} G_\ell \xi^\ell, \tag{2.14}$$

and such that

$$G(\xi) = \begin{bmatrix} G_{11}(\xi) & G_{12}(\xi) & \cdots & G_{1K}(\xi) \\ G_{21}(\xi) & G_{22}(\xi) & \dots & G_{2K}(\xi) \\ \vdots & \vdots & \ddots & \vdots \\ G_{L1}(\xi) & G_{12}(\xi) & \cdots & G_{LK}(\xi) \end{bmatrix}, \tag{2.15}$$

with (j,k)th polynomial elements

$$G_{jk}(\xi) = \sum_{\ell=0}^{n_G} g_{jk,\ell} \xi^\ell \tag{2.16}$$

with $j = 1, 2, \dots, L$ and $k = 1, 2, \dots, K$. Hence, the (j,k)th element of the matrix G_ℓ is denoted by $g_{jk,\ell}$.

Definition 2.5 (Proper, strictly proper, monic (Kailath, 1980)). *A rational function matrix $F(\xi)$ is* proper *if $\lim_{\xi\to\infty} F(\xi) = c \in \mathbb{R}^{L\times K}$; it is* strictly proper *if $c = 0$; and* monic *if $K = L$ and c is the identity matrix.*

Definition 2.6 (Stability (Hespanha, 2023)). *Consider a transfer function $G(\xi)$ that describes a linear dynamic system according to the relation $y(t) = G(\xi)u(t)$. The system is (bounded-input bounded-output (BIBO))*

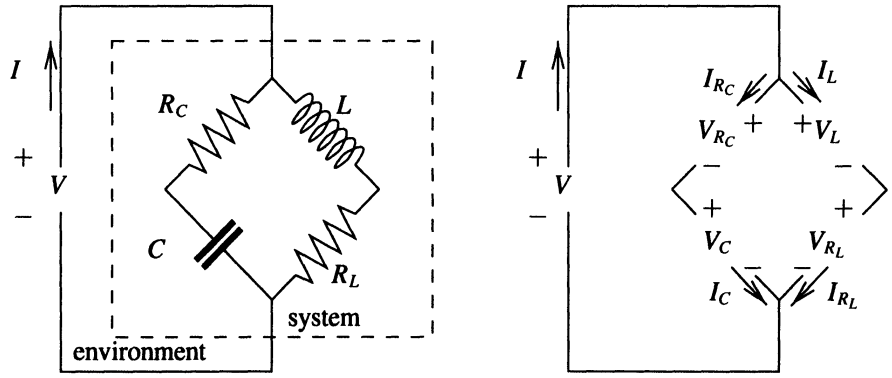

(a) Depiction of the components. (b) Depiction of the signal variables.

Figure 2.1: Electrical circuit with resistors (R_L, R_C), inductor (L), and capacitor (C) and with current flows (I) and voltage drops (V) (Polderman and Willems, 1998).

stable *if a bounded input signal $u(t)$ leads to a bounded output signal $y(t)$.*

Definition 2.7 (Stability continuous-time (Hespanha, 2023)). *In continuous-time, the transfer function matrix $F(s)$ is (BIBO)* stable *if all its poles have strictly negative real part ($|\Re(s)| < 0$) and thus lie in the strict left half plane.*

Definition 2.8 (Stability discrete-time (Hespanha, 2023)). *In discrete-time, the transfer function matrix $F(z)$ is (BIBO)* stable *if all its poles have magnitude strictly smaller than 1 ($|z| < 1$) and thus lie within the unit circle.*

2.3 Physical linear dynamic networks

2.3.1 Electrical circuits

One of the most famous examples of a physical linear network is an electrical circuit. An electrical circuit consisting of resistors, capacitors, and inductors is referred to as an *RLC circuit*. An electrical circuit can be modelled using the constitutive relations, Kirchhoff's current law, and Kirchhoff's voltage law.

Example 2.9 (Electrical circuit (Polderman and Willems, 1998)). *Consider the circuit shown in Figure 2.1, which consists of two resistors (R_L, R_C), an inductor (L), and a capacitor (C). The dynamics of this circuit are modelled with the constitutive relations:*

$$V_{R_C} = R_C I_{R_C}, \qquad V_{R_L} = R_L I_{R_L}, \qquad C\frac{dV_C}{dt} = I_C, \qquad L\frac{dI_L}{dt} = V_L; \tag{2.17}$$

Kirchhoff's current law:

$$I = I_{R_C} + I_L, \qquad I_{R_C} = I_C, \qquad I_L = I_{R_L}, \qquad I_C + I_{R_L} = I; \tag{2.18}$$

and Kirchhoff's voltage law:

$$V = V_{R_C} + V_C, \qquad V = V_L + V_{R_L}, \qquad V_{R_C} + V_C = V_L + V_{R_L}, \tag{2.19}$$

with voltage drops V_x among the components and current flows through the components I_x, $x \in \{R_C, R_L, L, C\}$. To find the relation between the variables of interest V and I, (2.17)*,* (2.18)*, and* (2.19) *need to be combined in a smart way by eliminating the other variables V_{R_C}, I_{R_C}, V_{R_L}, I_{R_L}, V_C, I_C, V_L, and I_L. This results in two cases: either $R_L R_C C \neq L$ (case 1) or $R_L R_C C = L$ (case 2). The behaviour of the variables of interest in cases 1 and 2 is described by*

$$\left(1 + (R_C + R_L)C\frac{d}{dt} + CL\frac{d^2}{dt^2}\right)V = \left(R_L + L\frac{d}{dt}\right)\left(1 + R_C C\frac{d}{dt}\right)I, \tag{2.20a}$$

$$\left(1 + R_L C\frac{d}{dt}\right)V = R_L\left(1 + R_C C\frac{d}{dt}\right)I, \tag{2.20b}$$

respectively[a].

[a] If $R_L R_C C \neq L$ (case 1), the eliminated variables are observable from the variables of interest, otherwise (case 2) not (Polderman and Willems, 1998).

Another electrical circuit with the same topology as the electrical circuit of Example 2.9 may lead to a different mathematical model with a different network complexity (order of the differential equations) depending on the physical components that are present in the interconnections. In addition, Example 2.9 proves that it is possible to eliminate all variables other than the variables of interest.

2.3.2 Kron reduction

There are several ways to eliminate the latent variables. One way is to manipulate (2.17), (2.18), and (2.19) and find smart combinations together with Gaussian elimination to remove the latent variables one by one from the equations. A more structured way to eliminate the latent variables is by *Kron reduction* (Kron, 1949). In this method, the conductance matrix is constructed and its Schur complement is used to eliminate the latent variables in a single step.

Consider an electrical circuit with two vertices, vertex 1 and vertex 2. The electrical circuit can be modelled as

$$\begin{bmatrix} I_1 \\ I_2 \end{bmatrix} = \begin{bmatrix} G_{11} & G_{12} \\ G_{21} & G_{22} \end{bmatrix} \begin{bmatrix} P_1 \\ P_2 \end{bmatrix}, \tag{2.21}$$

with I_x and P_x, $x \in \{1, 2\}$, the current flow that is inserted at vertex x and the electrical potential at vertex x, respectively, and with G_{xy}, $x, y \in \{1, 2\}$, the conductance between I_x and P_y. Gaussian elimination of the electric potential P_2 can be performed by rewriting the second equation in (2.21) as

$$P_2 = G_{22}^{-1} I_2 - G_{22}^{-1} G_{21} P_1, \tag{2.22}$$

and substituting this into the first equation in (2.21) leading to the reduced model

$$I_1 = G_{red} P_1 + Q_{12} I_2, \tag{2.23}$$

with

$$G_{red} = G_{11} - G_{12} G_{22}^{-1} G_{21}, \qquad Q_{12} = G_{12} G_{22}^{-1}, \tag{2.24}$$

with G_{red} the Schur complement of the conductance matrix in (2.21).

Kron reduction is often used in electrical circuits to eliminate so-called internal vertices, which are not subject to any externally inserted current flow. To give a better idea of its value and how it can be applied in electrical circuits, Kron reduction is illustrated by Example 2.10 (Dörfler and Bullo, 2013; Dörfler et al., 2018).

Example 2.10 ($Y - \Delta$ transformation). *Consider the electrical circuit in Figure 2.2a (the Y-circuit). To each vertex i, $i \in \{1, 2, 3, 4\}$, an electrical potential P_i and an inserted current flow I_i is allocated. Now suppose that the objective is to eliminate the latent variables corresponding to the centre vertex, that is P_4 and I_4. Observe that there is no current flow inserted at the centre vertex, so $I_4 = 0$. This results in the electrical circuit in Figure 2.2b (the Δ-circuit). This transformation is referred to as the $Y - \Delta$*

transformation.
A mathematical model of the Y-circuit follows from the constitutive relations

$$P_1 - P_4 = R_1 I_1, \qquad P_2 - P_4 = R_2 I_2, \qquad P_3 - P_4 = R_3 I_3, \tag{2.25}$$

and Kirchhoff's current law

$$I_1 + I_2 + I_3 = 0. \tag{2.26}$$

Using the conductances $G_i = R_i^{-1}$, (2.25) *and* (2.26) *lead to*

$$\begin{bmatrix} I_1 \\ I_2 \\ I_3 \\ 0 \end{bmatrix} = \begin{bmatrix} G_1 & 0 & 0 & -G_1 \\ 0 & G_2 & 0 & -G_2 \\ 0 & 0 & G_3 & -G_3 \\ -G_1 & -G_2 & -G_3 & G_1 + G_2 + G_3 \end{bmatrix} \begin{bmatrix} P_1 \\ P_2 \\ P_3 \\ P_4 \end{bmatrix}. \tag{2.27}$$

The objective is to eliminate the latent variable P_4 *from the model. Using Kron reduction, the reduced conductance matrix becomes*

$$G_{red} = \begin{bmatrix} G_1 & 0 & 0 \\ 0 & G_2 & 0 \\ 0 & 0 & G_3 \end{bmatrix} - \begin{bmatrix} -G_1 \\ -G_2 \\ -G_3 \end{bmatrix} (G_1 + G_2 + G_3)^{-1} \begin{bmatrix} -G_1 & -G_2 & -G_3 \end{bmatrix}, \tag{2.28a}$$

$$= (G_1 + G_2 + G_3)^{-1} \begin{bmatrix} G_1 - G_1 G_1 & -G_1 G_2 & -G_1 G_3 \\ -G_1 G_2 & G_2 - G_2 G_2 & -G_2 G_3 \\ -G_1 G_3 & -G_2 G_3 & G_3 - G_3 G_3 \end{bmatrix}, \tag{2.28b}$$

leading to the reduced model

$$\begin{bmatrix} I_1 \\ I_2 \\ I_3 \end{bmatrix} = G_{red} \begin{bmatrix} P_1 \\ P_2 \\ P_3 \end{bmatrix} + (G_1 + G_2 + G_3)^{-1} \begin{bmatrix} -G_1 \\ -G_2 \\ -G_3 \end{bmatrix} I_4. \tag{2.29}$$

Observe that $I_4 = 0$ *as vertex* 4 *is an internal vertex and does not have an externally inserted current flow. This leads to the model of the* Δ*-circuit*

$$\begin{bmatrix} I_1 \\ I_2 \\ I_3 \end{bmatrix} = (G_1 + G_2 + G_3)^{-1} \begin{bmatrix} G_1 - G_1 G_1 & -G_1 G_2 & -G_1 G_3 \\ -G_1 G_2 & G_2 - G_2 G_2 & -G_2 G_3 \\ -G_1 G_3 & -G_2 G_3 & G_3 - G_3 G_3 \end{bmatrix} \begin{bmatrix} P_1 \\ P_2 \\ P_3 \end{bmatrix}, \tag{2.30}$$

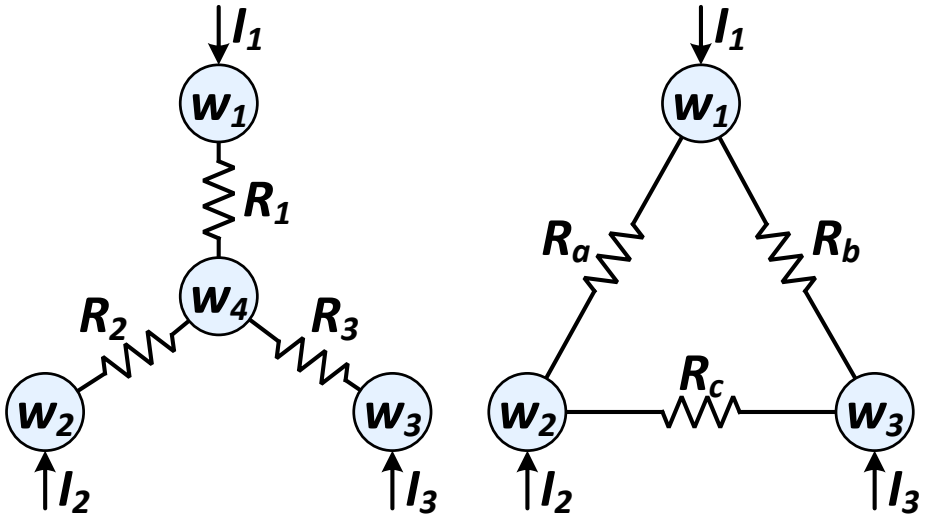

(a) Electrical circuit with four vertices (Y) (b) Electrical circuit with three vertices (Δ)

Figure 2.2: $Y - \Delta$ transformation in an electrical circuit by eliminating the centre vertex as described by Example 2.10.

which describes the resistances

$$R_a = \left[\frac{G_1 G_2}{G_1 + G_2 + G_3}\right]^{-1} = \frac{R_3}{R_1 R_2 + R_1 R_3 + R_2 R_3}, \tag{2.31a}$$

$$R_b = \left[\frac{G_1 G_3}{G_1 + G_2 + G_3}\right]^{-1} = \frac{R_2}{R_1 R_2 + R_1 R_3 + R_2 R_3}, \tag{2.31b}$$

$$R_c = \left[\frac{G_2 G_3}{G_1 + G_2 + G_3}\right]^{-1} = \frac{R_1}{R_1 R_2 + R_1 R_3 + R_2 R_3}. \tag{2.31c}$$

There exist other elimination methods that are similar to Kron reduction. One of these methods is *immersion* for module representations (Dankers et al., 2016), which is described in Section 2.4.8. Another method is the elimination of latent variables for the behavioural approach (Polderman and Willems, 1998).

2.3.3 Diffusive couplings

One particular property of physical linear components is that they are symmetric in the sense that they act exactly the same when they are turned around, i.e. when

the connection points of the component are interchanged. For example, if one of the resistors (R_C, R_L), inductor (L), or capacitor (C) in the RLC circuit of Figure 2.1 is removed and placed backward at the same location in the circuit in such a way that the terminals of the component switch places, the component and the circuit behave exactly the same. Moreover, the symmetric interactions appear in the differential equations as so-called *diffusive couplings*.

Definition 2.11 (Diffusive coupling (Jones, 1985)). *A* diffusive coupling *is an interconnection that depends on the difference of variables.*

For example, a connection with a resistor can be modelled by the constitutive relation

$$P_1 - P_2 = RI, \tag{2.32}$$

where P_1 and P_2 are the electric potential on each side of the resistor with resistance R and with I the current flow through the resistor. The strength of the interconnection, given by the resistance, depends on the difference in electric potential on each side of the resistor. By replacing the voltage drop V_x in (2.17), (2.18), and (2.19) by the difference in electric potential between the connected terminals, the diffusive couplings become clear in the model of the electrical circuit of Example 2.9.

Similar to electrical circuit components, mechanical springs and dampers can also be modelled with diffusive couplings, as the force induced by these mechanical components depends on the difference in position and velocity, respectively. That is, a linear spring and a linear damper can, respectively, be modelled by

$$F = k(x_1 - x_2), \qquad F = b(v_1 - v_2), \tag{2.33}$$

respectively, with force F, where x_1 and x_2 are the positions on each side of the spring with spring constant k, and where v_1 and v_2 are the velocity on each side of the damper with damping constant b.

Diffusive couplings thus appear naturally in physical linear networks. However, they also appear in other types of networks, such as in *consensus networks*. These networks are, among others, used to describe multiagent systems, for example, for cooperative or formation control. The typical objective in consensus networks is to let the agents come to consensus, that is to let them converge to joint behaviour (Ren et al., 2005). In these networks, each vertex i is associated with an agent (or subsystem) with state $x_i(t)$. All vertices (say n) are diffusively coupled with other vertices as

$$\dot{x}_i(t) = -\sum_{j=1, j\neq i}^{n} w_{ij}[x_i(t) - x_j(t)] + \sum_{k=1}^{p} b_{ik}u_k(t), \tag{2.34}$$

with inputs $u_k(t)$ and with w_{ij} and b_{ik} the weight of the edge from vertex j and input k to vertex i, respectively. The dynamics of the complete consensus network is described by the LTI system

$$\dot{x}(t) = -Lx(t) + Bu(t), \tag{2.35}$$

where $L \in \mathbb{R}^{n\times n}$ is the Laplacian matrix of the network, consisting of elements

$$L_{ij} = \begin{cases} -\sum_{k\neq j} w_{kj}, & \text{if } i = j, \\ w_{ij}, & \text{if } i \neq j. \end{cases} \tag{2.36}$$

and $B \in \mathbb{R}^{n\times p}$ is the input matrix, consisting of elements $B_{ik} = b_{ik}$. The Laplacian matrix captures the structure of the diffusive couplings among the agents. If the weight from vertex i to vertex j is the same as the weight from vertex j to vertex i, then $w_{ji} = w_{ij}$ and the Laplacian matrix L is symmetric. Then the network can be depicted by an undirected graph.

In this section, both electrical and mechanical components have been modelled with diffusive couplings. Moreover, a more careful look at (2.32) and (2.33) shows that these equations have the same structure. This analogy holds for many physical systems, such as electrical circuits and mechanical (both translational and rotational) systems, but also hydraulic flow systems, pneumatic flow systems, acoustic systems, thermal systems, mass flow systems, compartment models in pharmacy kinetics, and chemical reactions (Paynter, 1961; Ljung and Glad, 1994; Van den Bosch, 2009; van der Schaft and Jeltsema, 2014). The analogies among physical domains and the transitions between them are further discussed in Section 5.4.

2.4 Dynamic network models

2.4.1 Graphical representation

A network model consists of two parts: a graphical and a mathematical representation. The graphical network model is a visualisation of the interconnection structure of the dynamic network. It is a graph consisting of two main components: the vertices (or nodes) and the edges (or links). One can choose to place the signals of interest in the vertices and interconnect them through edges that represent the influences or dynamics between them. Then the dynamics of the network is thus located in the edges. One can also choose to place subsystems in the vertices and interconnect them through edges that represent the information or signals that are shared between them. Then the dynamics of the network is thus

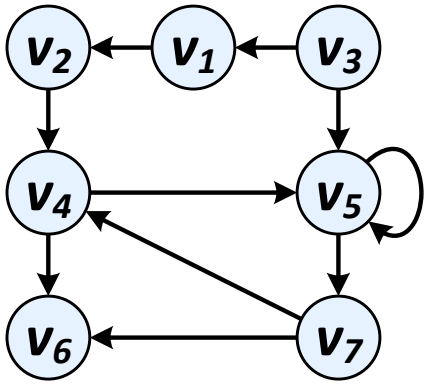

Figure 2.3: Directed graph with vertices v_i and directed edges (arrows).

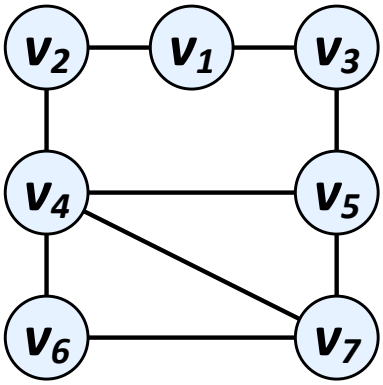

Figure 2.4: Undirected graph with vertices v_i and undirected edges (lines).

located in the vertices. The relations between several graphical representations are investigated in Chapter 3.

Consider the directed graph and undirected graph shown in Figure 2.3 and Figure 2.4, respectively. We will use these graphs to introduce some nomenclature and concepts for graphs, see, for example, Godsil and Royle (2001) and Mesbahi and Egerstedt (2010).

An edge leaving a vertex is an *outgoing edge* and an edge entering a vertex is an *incoming edge*; for example, the edge between v_1 and v_2 is an outgoing edge of v_1 and an incoming edge of v_2. Two vertices that are directly connected to each other are *neighbours*; for example, v_1 and v_2 are neighbours. To be more precise, v_1 is an *in-neighbour* of v_2 and v_2 is an *out-neighbour* of v_1. A vertex with only outgoing edges is a *source*, for example, v_3; a vertex with only incoming edges is a *sink*, for example, v_6; and vertices with both incoming and outgoing edges are *internal vertices*, for example, v_1.

A *path* is a sequence of vertices and outgoing edges; for example, the path (v_1, v_2, v_4). The *length of a path* is the number of edges in a path; for example, the path (v_1, v_2, v_4) has length 2. A *direct path* is a path of length 1; for example, the path (v_1, v_2). There is no direct path between v_1 and v_4, because that path needs to pass through v_2, i.e. the path becomes (v_1, v_2, v_4). Multiple paths are called *vertex disjoint paths* if they do not share any vertices; for example, the paths (v_1, v_2) and (v_3, v_5) are vertex disjoint paths, while the paths (v_1, v_2) and (v_2, v_4) are not vertex disjoint paths. Multiple paths are called *parallel paths* if they start at the same vertex and end at the same vertex; for example, the path (v_7, v_6) is a parallel path to the path (v_7, v_4, v_6). A *loop* is a path that starts and ends at the

same vertex; for example, the path (v_5, v_6, v_4, v_5). A *self-loop* is a loop that is a direct path; for example, the path (v_5, v_5).

A *digraph* is a graph with directed edges, as shown in Figure 2.3. An *undirected graph* is a graph with undirected or bi-directed edges, see Figure 2.4. For undirected graphs, all edges are both incoming and outgoing and hence, all neighbours are both in-neighbours and out-neighbours. Such a network has no sources and sinks, only internal vertices. If there is a path between two vertices, then there also is a path in the opposite direction, implying that if there is a path between two vertices, there also is a loop between those vertices.

The *adjacency matrix* $A(G)$ is a square matrix that encodes the adjacency relations in the graph G by its elements

$$[A(G)]_{ij} = \begin{cases} a_{ij}, & \text{if } (v_j, v_i) \text{ exists} \\ 0, & \text{otherwise,} \end{cases} \tag{2.37}$$

where $a_{ij} \neq 0$ is the weight of the edge (v_j, v_i). If the weight $a_{ij} = 0$, then it coincides with the situation that there is no edge (v_j, v_i).

The *in-degree matrix* $D_{in}(G)$ is a diagonal matrix that encodes the weights of the in-neighbour edges of the vertices by its diagonal elements

$$[D_{in}(G)]_{ii} = \sum_{\{j|(v_j,v_i) \text{ exists}\}} a_{ij}. \tag{2.38}$$

The (in-degree) *Laplacian matrix* $L_{in}(G)$ is defined by

$$L_{in}(G) = D_{in}(G) - A(G). \tag{2.39}$$

By construction, the sum of each row of $L_{in}(G)$ equals zero, that is the vector with all elements equal to 1 lies in the null space of $L_{in}(G)$.

For the graph shown in Figure 2.3, the adjacency matrix, the in-degree matrix, and the (in-degree) Laplacian matrix are, respectively,

$$A(G) = \begin{bmatrix} 0 & 0 & 1 & 0 & 0 & 0 & 0 \\ 1 & 0 & 0 & 0 & 0 & 0 & 0 \\ 0 & 0 & 0 & 0 & 0 & 0 & 0 \\ 0 & 1 & 0 & 0 & 0 & 0 & 1 \\ 0 & 0 & 1 & 1 & 1 & 0 & 0 \\ 0 & 0 & 0 & 1 & 0 & 0 & 1 \\ 0 & 0 & 0 & 0 & 1 & 0 & 0 \end{bmatrix}, \quad D_{in}(G) = \begin{bmatrix} 1 & 0 & 0 & 0 & 0 & 0 & 0 \\ 0 & 1 & 0 & 0 & 0 & 0 & 0 \\ 0 & 0 & 0 & 0 & 0 & 0 & 0 \\ 0 & 0 & 0 & 2 & 0 & 0 & 0 \\ 0 & 0 & 0 & 0 & 3 & 0 & 0 \\ 0 & 0 & 0 & 0 & 0 & 2 & 0 \\ 0 & 0 & 0 & 0 & 0 & 0 & 1 \end{bmatrix}, \tag{2.40}$$

$$L_{in}(G) = \begin{bmatrix} 1 & 0 & -1 & 0 & 0 & 0 & 0 \\ -1 & 1 & 0 & 0 & 0 & 0 & 0 \\ 0 & 0 & 0 & 0 & 0 & 0 & 0 \\ 0 & -1 & 0 & 2 & 0 & 0 & -1 \\ 0 & 0 & -1 & -1 & 2 & 0 & 0 \\ 0 & 0 & 0 & -1 & 0 & 2 & -1 \\ 0 & 0 & 0 & -1 & 0 & 0 & 1 \end{bmatrix}. \tag{2.41}$$

Opposite to the in-degree matrix and in-degree Laplacian matrix are the out-degree matrix and out-degree Laplacian matrix. The *out-degree matrix* $D_{out}(G)$ is a diagonal matrix that encodes the weights of the out-neighbour edges of the vertices by its diagonal elements

$$[D_{out}(G)]_{ii} = \sum_{\{j|(v_i,v_j) \text{ exists}\}} a_{ij}. \tag{2.42}$$

The (out-degree) *Laplacian matrix* $L_{out}(G)$ is defined by

$$L_{out}(G) = D_{out}(G) - A(G). \tag{2.43}$$

By construction, the sum of each column of $L_{out}(G)$ equals zero.

The in-degree versions capture how a vertex is influenced by other vertices, while the out-degree versions capture how a vertex influences other vertices. For undirected graphs, the adjacency matrix is symmetric ($A(G) = A(G)^\top$) and the in-degree matrix is equal to the out-degree matrix ($D_{in}(G) = D_{out}(G)$). Hence, the in-degree and out-degree Laplacian matrices are symmetric ($L_{in}(G) = L_{in}(G)^\top$ and $L_{out}(G) = L_{out}(G)^\top$) and equal ($L_{in}(G) = L_{out}(G)$) and therefore, simply referred to as the Laplacian matrix $L(G)$.

Definition 2.12 (Connected digraph (Mesbahi and Egerstedt, 2010)). *A digraph is*

1. strongly connected *if there exists a directed path between every pair of vertices.*
2. weakly connected *if there exists an undirected path between any pair of vertices.*

To find the undirected paths in a digraph, replace all directed edges by undirected edges. The resulting graph is referred to as the underlying undirected graph.

For undirected graphs, strong connectivity and weak connectivity are equivalent and therefore, simply referred to as connectivity.

Definition 2.13 (Connected graph (Mesbahi and Egerstedt, 2010)). *An undirected graph is* connected *if there exists a path between every pair of vertices.*

The in-degree Laplacian matrix (and especially the one of undirected graphs) has some special properties. For an undirected graph with n vertices, the Laplacian matrix is a symmetric $n \times n$ matrix ($L(G) = L^\top(G)$). The sum of all elements in a single row of the Laplacian matrix is zero and because the Laplacian matrix is symmetric, all elements in a single column add up to zero as well. This holds for each row and each column of the Laplacian matrix. Algebraically, this means that the vector with all elements equal to 1 lies in the kernel of $L(G)$ and the kernel of $L^\top(G)$. The Laplacian matrix $L(G)$ is positive semi-definite with real eigenvalues

$$\lambda_1(L(G)) \leq \lambda_2(L(G)) \leq \cdots \leq \lambda_n(L(G)), \tag{2.44}$$

with $\lambda_1(L(G)) = 0$ (Mesbahi and Egerstedt, 2010). An undirected graph is connected if and only if $\lambda_2(L(G)) > 0$ (Mesbahi and Egerstedt, 2010, Theorem 2.8). Note that if an undirected graph is connected, then $\operatorname{rank}(L(G)) = n - 1$.

A polynomial matrix $L(\xi) \in \mathbb{R}^{M \times K}$ is Laplacian if all its matrices L_i are Laplacian matrices. As a result, $L(\xi)$ itself has a Laplacian structure in the sense that in each row and in each column, the elements add up to zero. That is

$$\sum_{m=1}^{M} \ell_{mk}(\xi) = 0, \qquad \text{and} \qquad \sum_{k=1}^{K} \ell_{mk}(\xi) = 0, \tag{2.45}$$

respectively.

2.4.2 State-space model

In physics and control, state-space models are often used to describe dynamic systems, for example, for the purpose of system analysis or controller design (Mesbahi and Egerstedt, 2010; Verhaegen and Verdult, 2012; Bullo, 2022). State-space models are also used in other research areas, such as biology and economy, for example, to describe brain connectivity (Friston et al., 2014; Prando et al., 2020), gene regulation (Huang et al., 2005), or other biochemical reaction networks (Anderson et al., 2011). In addition, state-space models are used to describe the interaction between subsystems or agents, where each vertex represents a subsystem or agent and the state-space model describes the links between them (Boccaletti et al., 2006; van der Schaft and Maschke, 2013; Haber and Verhaegen, 2014; van Waarde et al., 2018; Cheng and Scherpen, 2021).

State-space representations capture the behaviour of physical systems through inputs, outputs, and state variables that are related to each other through a set of first-order differential equations.

Definition 2.14 (State-space model (Kalman, 1960)). *A state-space model consists of n internal state variables $x_1(t), \ldots, x_n(t)$; p known external excitation signals $u_1(t), \ldots, u_p(t)$; and c measured signals $y_1(t), \ldots, y_c(t)$. The behaviour of the system is described by*

$$\frac{d}{dt}x(t) = Ax(t) + Bu(t), \qquad y(t) = Cx(t) + Du(t), \tag{2.46}$$

with $t \in \mathbb{R}$ indicating the time, with matrices $A \in \mathbb{R}^{n\times n}$, $B \in \mathbb{R}^{n\times p}$, $C \in \mathbb{R}^{c\times n}$, and $D \in \mathbb{R}^{c\times p}$, and where

$$x(t) = \begin{bmatrix} x_1(t) & x_2(t) & \ldots & x_n(t) \end{bmatrix}^\top, \tag{2.47a}$$

$$u(t) = \begin{bmatrix} u_1(t) & u_2(t) & \ldots & u_p(t) \end{bmatrix}^\top, \tag{2.47b}$$

$$y(t) = \begin{bmatrix} y_1(t) & y_2(t) & \ldots & y_c(t) \end{bmatrix}^\top. \tag{2.47c}$$

Graphically, state-space models can be depicted by directed graphs G, where the vertices represent the states of the network and the edges represent the first-order relations between the states. These relations are exactly captured by the state matrix A. That is, A coincides with the adjacency matrix $A(G)$ of the corresponding graph G. Two additional layers can be added: one for the inputs and one for the outputs. The additional edges represent the static relations from the inputs to the states and from the states to the outputs, captured by the input matrix B, output matrix C, and direct feedthrough matrix D.

In state-space models that describe interactions between subsystems or agents, each state variable is related to a subsystem. The directed graphs depicting these networks now have vertices that are directly related to specific subsystems.

Example 2.15 (State-space model of an electrical circuit). *Consider again the electrical circuit in Figure 2.1. This circuit is described in a state-space model as*

$$\begin{bmatrix} \frac{d}{dt}V_C(t) \\ \frac{d}{dt}I_L(t) \end{bmatrix} = \begin{bmatrix} 0 & -\frac{1}{C} \\ \frac{1}{L} & -\frac{R_L+R_C}{L} \end{bmatrix} \begin{bmatrix} V_C(t) \\ I_L(t) \end{bmatrix} + \begin{bmatrix} \frac{1}{C} \\ \frac{R_C}{L} \end{bmatrix} I(t), \tag{2.48a}$$

$$\begin{bmatrix} V(t) \\ V_C(t) \\ V_{R_L}(t) \end{bmatrix} = \begin{bmatrix} 1 & -R_c \\ 1 & 0 \\ 0 & R_L \end{bmatrix} \begin{bmatrix} V_C(t) \\ I_L(t) \end{bmatrix} + \begin{bmatrix} R_C \\ 0 \\ 0 \end{bmatrix} I(t). \tag{2.48b}$$

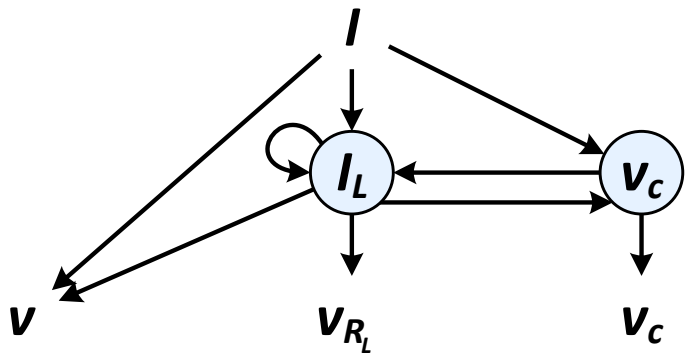

Figure 2.5: State-space model of the electrical circuit of Example 2.15.

Figure 2.5 shows the graphical representation of this state-space model. This figure shows three layers: one with the input, one with the two states, and one with the three outputs. The causal relations between the signals are depicted by the directed graph.

Remark 2.16 (Discrete time). *State-space models can similarly be formulated in discrete time. Then the internal state variables* $x_1(k), \ldots, x_n(k)$*, with time instant* k*, are related to each other through a set of first-order difference equations. This results in a formulation that explains the state variables at the next time instant,* $x(k+1)$*, in terms of the state variables at the current time instant and the external excitation signals* $u(k)$*. The output equation is formulated* mutatis mutandis*.*

2.4.3 Second-order model

Many physical systems can be modelled by second-order vector differential equations (Wittenburg, 1977; Ljung and Glad, 1994; Van den Bosch, 2009). Some well-known examples are mechanical mass-spring-damper systems for modelling multibody dynamics, structure dynamics, or vibration dynamics (Wittenburg, 1977; Fritzen, 1986; De Angelis et al., 2002; Lopes dos Santos et al., 2015), and electrical resistor-inductor-capacitor circuits. These second-order representations capture the behaviour of physical systems through second-order (ordinary vector) differential equations.

Definition 2.17 (Second-order model (Wittenburg, 1977)). *A second-order model consists of n internal variables $x_1(t), \ldots, x_n(t)$; p known external excitation signals $u_1(t), \ldots, u_p(t)$; and c measured signals $y_1(t), \ldots, y_c(t)$. The behaviour of the system is described by*

$$M\frac{d^2}{dt^2}x(t) + D\frac{d}{dt}x(t) + Kx(t) = Fu(t), \qquad y(t) = Cx(t), \tag{2.49}$$

with $t \in \mathbb{R}$ indicating the time, with matrices $M, D, K \in \mathbb{R}^{n\times n}$, $F \in \mathbb{R}^{n\times p}$, and $C \in \mathbb{R}^{c\times n}$, and where

$$x(t) = \begin{bmatrix} x_1(t) & x_2(t) & \ldots & x_n(t) \end{bmatrix}^\top, \tag{2.50a}$$

$$u(t) = \begin{bmatrix} u_1(t) & u_2(t) & \ldots & u_p(t) \end{bmatrix}^\top, \tag{2.50b}$$

$$y(t) = \begin{bmatrix} y_1(t) & y_2(t) & \ldots & y_c(t) \end{bmatrix}^\top. \tag{2.50c}$$

For physical systems, the system matrices M, D, and K are often symmetric and positive semi-definite matrices, due to the symmetric nature of the physical components and the positive value of their coefficients. The internal variables $x_i(t)$ represent generalised displacements or charges and the number of internal variables n is equal to the number of degrees of freedom. A graphical representation of a physical system follows from the interconnections of the physical components. The number of internal variables n is equal to the number of vertices in the network. Moreover, each vertex is directly related to an internal (state) variable. The edges in the undirected graph represent the components between the internal variables, the input, and the ground (or reference), see, for example, (Cheng et al., 2017).

Second-order models are particularly useful for modal analysis of the system, where the natural frequencies (eigenfrequencies), damping factors, and mode shapes are analysed. These quantities are, for example, useful in vibration analysis of mechanical structures (Luş et al., 2003; Lopes dos Santos et al., 2015; Mukhopadhyay et al., 2015).

Example 2.18 (Second-order model of an electrical circuit). *Consider again the electrical circuit in Figure 2.1. This circuit is described by a second-order model as*

$$\begin{bmatrix} 0 & 0 & 0 \\ 0 & C & 0 \\ 0 & 0 & 0 \end{bmatrix} \begin{bmatrix} \frac{d^2}{dt^2}V(t) \\ \frac{d^2}{dt^2}V_C(t) \\ \frac{d^2}{dt^2}V_{R_L}(t) \end{bmatrix} + \begin{bmatrix} \frac{1}{R_C} & -\frac{1}{R_C} & 0 \\ -\frac{1}{R_C} & \frac{1}{R_C} & 0 \\ 0 & 0 & \frac{1}{R_L} \end{bmatrix} \begin{bmatrix} \frac{d}{dt}V(t) \\ \frac{d}{dt}V_C(t) \\ \frac{d}{dt}V_{R_L}(t) \end{bmatrix} +$$

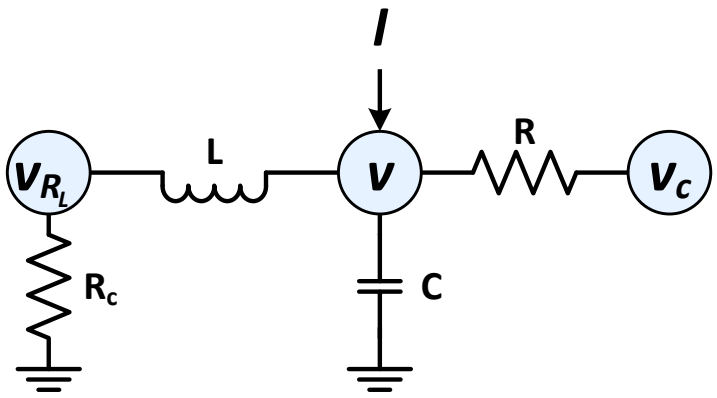

Figure 2.6: Second-order model of the electrical circuit of Example 2.18.

$$\begin{bmatrix} \frac{1}{L} & 0 & -\frac{1}{L} \\ 0 & 0 & 0 \\ -\frac{1}{L} & 0 & \frac{1}{L} \end{bmatrix} \begin{bmatrix} V(t) \\ V_C(t) \\ V_{R_L}(t) \end{bmatrix} = \begin{bmatrix} \frac{d}{dt} \\ 0 \\ 0 \end{bmatrix} I(t). \quad (2.51)$$

Figure 2.6 shows the graphical representation of this second-order model. This figure shows three layers: one with the input, one with the internal variables, and one with the ground. The physical interpretation is clear from the undirected graph.

For the purpose of analysis, control, and in particular identification of physical systems, the second-order model is often translated into a first-order state-space representation (Fritzen, 1986; Friswell et al., 1999; Luş et al., 2003; Ramos et al., 2013; Lopes dos Santos et al., 2015). There are many options for choosing the state vector of the state-space model, all with their own advantages, for example, as the generalised displacement and velocity, or as the modal displacement and velocity (Luş et al., 2003). The most commonly used approach is probably to define the state of the state-space model as $\xi(t) := \begin{bmatrix} x^\top(t) & \frac{d}{dt}x^\top(t) \end{bmatrix}^\top$ leading to the continuous-time state-space model

$$\frac{d}{dt}\xi(t) = \begin{bmatrix} \frac{d}{dt}x(t) \\ \frac{d^2}{dt^2}x(t) \end{bmatrix} = \begin{bmatrix} 0 & I \\ -M^{-1}K & -M^{-1}D \end{bmatrix} \begin{bmatrix} x(t) \\ \frac{d}{dt}x(t) \end{bmatrix} + \begin{bmatrix} 0 \\ M^{-1}F \end{bmatrix} u(t), \quad (2.52)$$

provided that M is invertible. If M is not invertible, then the following system of differential and algebraic equations (DAE) is used:

$$\begin{bmatrix} I & 0 \\ 0 & M \end{bmatrix} \frac{d}{dt}\xi(t) = \begin{bmatrix} 0 & I \\ -K & -D \end{bmatrix} \frac{d}{dt}\xi(t) + \begin{bmatrix} 0 \\ F \end{bmatrix} u(t). \quad (2.53)$$

Remark 2.19 (Discrete time). *Second-order models can similarly be formulated in discrete time. Then the behaviour of the system is captured by second-order vector difference equations. A state-space model of the discrete-time second-order model is formulated* mutatis mutandis.

2.4.4 Polynomial model

Polynomial models are popular representations for describing dynamic systems, especially for identification purposes with prediction error identification methods (Ljung, 1999; Hannan and Deistler, 2012). Therefore, they are typically formulated in discrete time, where the input and output signals are related through polynomials in the time-shift operator.

Definition 2.20 (Polynomial model (Ljung and Glad, 1994)). *A polynomial model consists of p known external excitation signals $u_1(t), \ldots, u_p(t)$; n unknown external noise signals $e_1(t), \ldots, e_n(t)$; and c measured signals $y_1(t), \ldots, y_c(t)$. The behaviour of the system is described by*

$$A(q^{-1})y(t) = F^{-1}(q^{-1})B(q^{-1})u(t) + D^{-1}(q^{-1})C(q^{-1})e(t), \tag{2.54}$$

with $t \in \mathbb{Z}$ the time instant, with delay operator q^{-1} meaning $q^{-1}u(t) = u(t-1)$, with polynomial matrices $A(q^{-1}) \in \mathbb{R}^{c\times c}[q^{-1}]$, $B(q^{-1}) \in \mathbb{R}^{c\times p}[q^{-1}]$, $C(q^{-1}) \in \mathbb{R}^{c\times n}[q^{-1}]$, and $D(q^{-1}), F(q^{-1}) \in \mathbb{R}^{c\times c}[q^{-1}]$, and where

$$u(t) = \begin{bmatrix} u_1(t) & u_2(t) & \ldots & u_p(t) \end{bmatrix}^\top, \tag{2.55a}$$

$$y(t) = \begin{bmatrix} y_1(t) & y_2(t) & \ldots & y_c(t) \end{bmatrix}^\top, \tag{2.55b}$$

$$e(t) = \begin{bmatrix} e_1(t) & e_2(t) & \ldots & e_n(t) \end{bmatrix}^\top. \tag{2.55c}$$

The polynomial matrices $A(q^{-1})$, $D(q^{-1})$, and $F(q^{-1})$ are assumed to satisfy $\det(A_0) \neq 0$, $\det(D_0) \neq 0$, and $\det(F_0) \neq 0$, where $A_0 = lim_{z\to\infty}A(z)$, $D_0 = lim_{z\to\infty}D(z)$ and $F_0 = lim_{z\to\infty}F(z)$. Further, $A^{-1}(q^{-1})F^{-1}(q^{-1})B(q^{-1})$ and $A^{-1}(q^{-1})D^{-1}(q^{-1})C(q^{-1})$ are assumed to be proper transfer function matrices. For uniqueness of the representation, $A(q^{-1})$, $C(q^{-1})$, $D(q^{-1})$, and $F(q^{-1})$ are often assumed to be monic, meaning that $\lim_{z\to\infty} A(z) = I$, $\lim_{z\to\infty} C(z) = I$, $\lim_{z\to\infty} D(z) = I$, and $\lim_{z\to\infty} F(z) = I$.

Some well-known polynomial model structures are the finite impulse response (FIR), the output error (OE), the autoregressive with exogeneous input (ARX), the autoregressive-moving average with exogeneous input (ARMAX), and the

Table 2.1: Simplified polynomial model structures (Ljung and Glad, 1994; Ljung, 1999).

Model structure	Simplification
FIR	$A(q^{-1}) = C(q^{-1}) = D(q^{-1}) = F(q^{-1}) = I$
OE	$A(q^{-1}) = C(q^{-1}) = D(q^{-1}) = I$
ARX	$C(q^{-1}) = D(q^{-1}) = F(q^{-1}) = I$
ARMAX	$D(q^{-1}) = F(q^{-1}) = I$
BJ	$A(q^{-1}) = I$

Box-Jenkins (BJ) model structures. Their exact simplifications of the general polynomial model structure are captured in Table 2.1.

Remark 2.21 (Continuous time). *In continuous time, polynomial models are formulated similarly by relating the input and output signals through polynomials in the differential operator p meaning $pu(t) = \frac{d}{dt}u(t)$.*

Remark 2.22 (Relation with second-order model). *A discrete-time second-order model (the discrete-time version of* (2.49)*) with $C = I$, that is with $y(t) = x(t)$, is equivalent to a polynomial model* (2.54) *with $C(q^{-1}) = 0$ and $D(q^{-1}) = F(q^{-1}) = I$.*

Even though this relation with second-order models exists, there is not really an interpretation in terms of networks (yet) and therefore also no graphical representation. Dynamical networks that are modelled by these polynomial models are considered to be a single system.

Example 2.23 (Polynomial model of an electrical circuit). *Consider again the electrical circuit in Figure 2.1. This circuit is described by a polynomial model as*

$$\begin{bmatrix} \frac{1}{R_C}p + \frac{1}{L} & -\frac{1}{R_C}p & -\frac{1}{L} \\ -\frac{1}{R_C}p & Cp^2 + \frac{1}{R_C}p & 0 \\ -\frac{1}{L} & 0 & \frac{1}{R_L}p + \frac{1}{L} \end{bmatrix} \begin{bmatrix} V(t) \\ V_C(t) \\ V_{R_L}(t) \end{bmatrix} = \begin{bmatrix} p \\ 0 \\ 0 \end{bmatrix} I(t). \tag{2.56}$$

Eliminating the output variables $V_C(t)$ and $V_{R_L}(t)$ leads to (2.20).

Observe that the polynomial model in (2.56) in Example 2.23 is of the form $A(p)y(t) = B(p)u(t)$ and that the diffusive couplings appear in this network

model by symmetry of the polynomial matrix $A(p)$.

2.4.5 Bayesian network

The first version of a Bayesian network was used in genetic pedigrees to describe genetic inheritances (Koller and Friedman, 2009). The model was further developed for describing games of change. A Bayesian network describes joint probabilities over a set of random variables. If the conditional dependencies between the variables change over time, the network is called a dynamic Bayesian network. The information on the probabilistic dependencies is used to draw conclusions on what might be true and on how to act. From an identification perspective, the main objective is to determine the causal dependencies, or topology, between the variables. Nowadays, Bayesian networks are applied in many different fields, for example, in medical diagnostics and decision making; analysis of marketing data; text and speech recognition and language and image processing; modelling and prediction of pollution, epidemics, and weather; fault detection and diagnostics in industrial equipment; and artificial intelligence (Koller and Friedman, 2009; Sucar, 2021).

Definition 2.24 (Bayesian network (Pearl, 2000)). *A Bayesian network consists of L random state variables $x_1, \ldots, x_L$ and conditional dependencies between them. The joint probability distribution is described by*

$$P(x_1, \ldots, x_L) = \prod_{j=1}^{L} P(x_j \,|Pa(x_j)), \tag{2.57}$$

with $P(x)$ the probability of x, with $P(x\,|y)$ the probability of x given y, and with $Pa(x_j)$ the parents of x_j.

Definition 2.25 (Dynamic Bayesian network (Pearl, 2000)). *A dynamic Bayesian network consists of L random state variables $x_1(t), \ldots, x_L(t)$ at time instances $t = 1, \ldots, N$ and conditional dependencies between them. The joint probability distribution is described by*

$$P(\{x_1(t), \ldots, x_L(t)\}_{t=1}^{N}) = \prod_{t=1}^{N} \prod_{j=1}^{L} P(x_j(t) \,|Pa(x_j(t))), \tag{2.58}$$

with $P(x)$ the probability of x, with $P(x\,|y)$ the probability of x given y, and with $Pa(x_j)$ the parents of x_j.

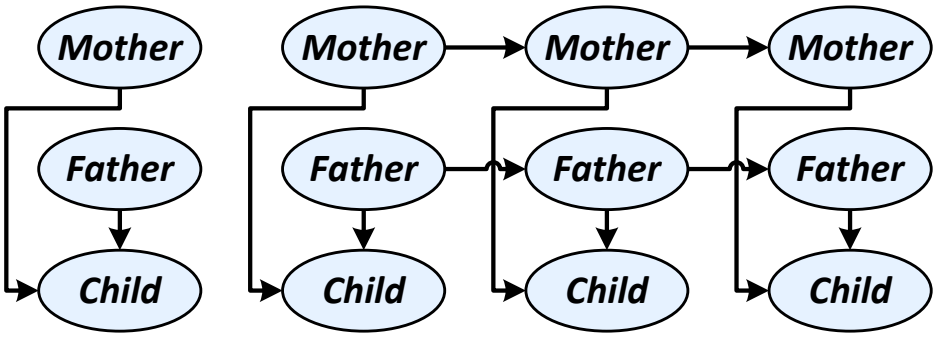

(a) Time slice. (b) Dynamic Bayesian Network unrolled over 3 time steps.

Figure 2.7: Dynamic Bayesian Network for genetic inheritance that changes over time.

Graphically, Bayesian networks are represented by directed acyclic graphs, where the vertices represent the random variables and the edges represent conditional dependencies. Dynamic Bayesian networks are similarly represented as Bayesian networks, but now the vertices represent the random variables at each specific time step.

Example 2.26 (Dynamic Bayesian network of a genetic inheritance). *Consider a disease that is genetically transmissible from the parents to their child. The genetic inheritance can be modelled by a Bayesian network, which can graphically be visualised by the graph in Figure 2.7a.*
Suppose that the probability of genetic transmission changes over time, for example, because the probability depends on the age of the parents. At each time instant, for example, at each year, the genetic inheritance can again be modelled by the Bayesian network in Figure 2.7a. Over time, the probabilities of inheritance of the parents change, but only by a personal factor. The dynamic Bayesian network can graphically be visualised by the graph in Figure 2.7b.

2.4.6 Wiener filter models

Wiener filter descriptions of dynamic networks are typically used to determine the interconnection structure of the signals. They were initially used to reconstruct the topological structure between random signals (Materassi and Innocenti, 2010; Materassi and Salapaka, 2012; Innocenti and Materassi, 2012; Materassi and

Salapaka, 2015) and they can also be used to identify the dynamics of the network (Materassi and Salapaka, 2020; Jahandari and Materassi, 2022a,b; Dimovska and Materassi, 2021). Some typical application domains are neural networks, economy, biology, cognitive sciences, ecology, and geology (Materassi and Salapaka, 2012; Talukdar et al., 2020).

Definition 2.27 (Wiener filter model (Materassi and Innocenti, 2010)). *The dynamic networks that are considered consist of L measured signals $y_1(t), \ldots, y_L(t)$ and p unknown external stochastic excitation signals $e_1(t), \ldots, e_p(t)$. The behaviour of the network is described (in the frequency domain) by*

$$Y(z) = H(z)Y(z) + E(z), \tag{2.59}$$

with complex frequency variable z, and where $Y(z) = \mathcal{Z}\big(y(t)\big)$ and $E(z) = \mathcal{Z}\big(e(t)\big)$, the Z-transform of $y(t)$ and $e(t)$, respectively, and where $H(z)$ is a hollow transfer function matrix and with $z \in \mathbb{C}$ the complex frequency variable.
A Wiener filter model of this network is described by

$$Y(z) = W(z)Y(z), \tag{2.60}$$

where the Wiener filter $W(z)$ is a real-rational transfer function matrix and a fraction of (cross-)power spectral densities:

$$W_{ij}(z) = \frac{\Phi_{y_j,y_i}(z)}{\Phi_{y_j}(z)}. \tag{2.61}$$

As the main interest is to reconstruct the topology of the network, these networks are typically depicted by directed graphs, where the vertices represent the signals ($y_i(t)$) and the edges represent the presence of dynamic transfer functions between them. A nonzero Wiener filter $W_{ij}(z)$ corresponds to the presence of an edge from signal $y_j(t)$ to signal $y_i(t)$.

In general, the Wiener filter (2.61) can be noncausal. The corresponding causal Wiener filter is constructed as

$$W_{ij}^{C}(z) = \left\{ \frac{\Phi_{y_j,y_i}(z)}{\Phi_{y_j}(z)} S(z) \right\}_{C} S^{-1}(z), \tag{2.62}$$

with $S(z)$ the spectral factorisation of $\Phi_{y_j}(e^{i\omega}) = S(e^{i\omega})S^{*}(e^{i\omega})$ and with causal truncation operator $\{W(z)\}_C$ selecting the causal part of $W(z)$.

Remark 2.28 (Continuous time). *Even though the Wiener filter description of dynamic networks is typically formulated in discrete time, it can be formulated similarly in continuous time in terms of the complex Laplace variable s.*

2.4.7 Dynamical structure function

The dynamical structure function has its origin in system biology (Gonçalves et al., 2007). It describes interconnections of LTI systems with partial state observations and with causal dependencies between the observed state variables. The main objective of this research is to reconstruct the structure and dynamics of the network from the input-output transfer function that is obtained from measurement data. Further research involves: including noise (Yuan et al., 2011); identifiability conditions (Adebayo et al., 2012); topology identification (Hayden et al., 2014); identifiability in particular situations (Hayden et al., 2016, 2017); minimal state-space realisations (Yuan et al., 2017); and well-posedness, realisations, and abstractions (Woodbury et al., 2017, 2018)

The networks are considered to be state-space models, with input signals, output signals, measured and unmeasured state variables, and sometimes noise. The unmeasured state variables are eliminated from the representation, leading to the dynamical structure function as formulated by Gonçalves and Warnick (2008).

Definition 2.29 (Dynamical structure function (Gonçalves et al., 2007)). *A dynamical structure function consists of L measured state variables $y_1(t), \ldots, y_L(t)$ and p known external excitation signals $u_1(t), \ldots, u_p(t)$. The behaviour of the network is described by*

$$Y(s) = Q(s)Y(s) + P(s)U(s), \tag{2.63}$$

with

1. *$s \in \mathbb{C}$ the complex Laplace variable.*
2. *$Y(s) = \mathcal{L}\big(y(t)\big)$ and $U(s) = \mathcal{L}\big(u(t)\big)$, the Laplace transform of $y(t)$ and $u(t)$, respectively.*
3. *Strictly proper transfer function matrix $Q(s) \in \mathbb{R}^{L\times L}(s)$ that is hollow, i.e. $Q_{ii}(s) = 0$, $\forall i$.*
4. *Strictly proper transfer function matrix $P(s) \in \mathbb{R}^{L\times p}(s)$.*

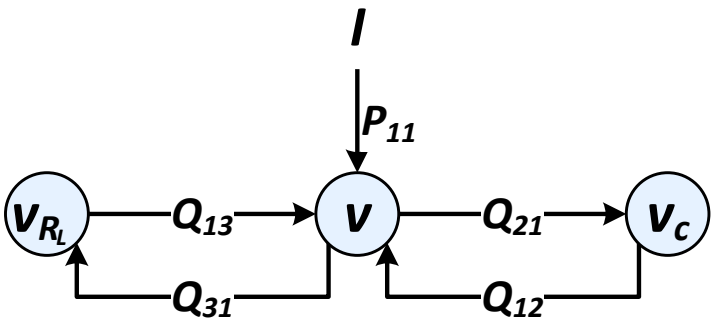

Figure 2.8: Dynamical structure function of the electrical circuit of Example 2.30.

The zero structure of $Q(s)$ describes the internal structure of the network and the zero structure of $P(s)$ describes the control structure.

Example 2.30 (Dynamical structure function of an electrical circuit). *Consider again the electrical circuit in Figure 2.1. This circuit is described by a time-domain dynamical structure function as*

$$\begin{bmatrix} V(t) \\ V_C(t) \\ V_{R_L}(t) \end{bmatrix} = \begin{bmatrix} 0 & \frac{Lp}{R_C+Lp} & \frac{R_C p}{R_C+Lp} \\ \frac{p}{1+CR_C p^2} & 0 & 0 \\ \frac{R_L}{R_L+Lp} & 0 & 0 \end{bmatrix} \begin{bmatrix} V(t) \\ V_C(t) \\ V_{R_L}(t) \end{bmatrix} + \begin{bmatrix} \frac{R_C Lp}{R_C+Lp} \\ 0 \\ 0 \end{bmatrix} I(t), \tag{2.64}$$

with differential operator p meaning $pI(t) = \frac{d}{dt}I(t)$. *Gaussian elimination of the state variables* $V_C(t)$ *and* $V_{R_L}(t)$ *leads to* (2.20).

The graphical representation of the dynamical structure function of Example 2.30 is shown in Figure 2.8. The dynamical structure function is depicted by a directed graph with measured state variables at the vertices and the causal transfer functions $P_{ij}(s)$ and $Q_{ij}(s)$ at the edges.

The unmeasured state variables are hidden in these transfer functions and are therefore referred to as *hidden states*. Moreover, the elimination process in a network can lead to the situation in which multiple transfer functions contain the same unmeasured state variables. This is referred to as *shared hidden states*, because the hidden states are shared among several transfer functions (Warnick, 2015).

Remark 2.31 (Discrete time). *Even though the dynamical structure function is typically formulated in continuous time, it can be formulated similarly in discrete time in terms of the complex frequency variable z.*

2.4.8 Module representation

The module representation is probably the most popular transfer function model that is used for identifying dynamic networks with prediction error identification methods. As it is formulated for prediction error identification purposes, it is formulated in discrete time. The module representation is a generalisation of the classical closed-loop system (Van den Hof et al., 2013). The main objectives in this research are to identify the topology of the network (Materassi and Innocenti, 2010; Chiuso and Pillonetto, 2012; Shi et al., 2019), the complete network dynamics (Weerts et al., 2018c; Fonken et al., 2020), or the dynamics of a subnetwork (Van den Hof et al., 2013; Dankers et al., 2016; Ramaswamy and Van den Hof, 2021). Other research objectives are related to identifiability (Weerts et al., 2018b; Hendrickx et al., 2019; Bazanella et al., 2019; Shi et al., 2023), experiment design (Gevers and Bazanella, 2015; Bazanella et al., 2017) and allocation of excitation signals (Cheng et al., 2022; Dreef et al., 2022), developing scalable algorithms (Everitt et al., 2018; Fonken et al., 2022), control (Steentjes et al., 2021), and applications (Dankers et al., 2021).

In the module representation, a set of interesting signals (node signals) is interconnected through dynamic systems (modules) and possibly driven by known external excitation signals and unknown external disturbance signals (Van den Hof et al., 2013). Sometimes measurement noise is taken into account as well (Dankers et al., 2015).

Definition 2.32 (Module representation (Van den Hof et al., 2013)). *A module representation consists of L internal node signals $w_1(t), \dots, w_L(t)$ interconnected through transfer function modules; K known external excitation signals $r_1(t), \dots r_K(t)$; and L unknown disturbance signals $v_1(t), \dots, v_L(t)$. The behaviour of the node signals $w_j(t)$, $j = 1, \dots, L$, is described by*

$$w_j(t) = \sum_{i \in \mathcal{N}_j} G^0_{ji}(q) w_i(t) + \sum_{k=1}^{K} R^0_{jk}(q) r_k(t) + v_j(t), \tag{2.65}$$

with

1. *$t \in \mathbb{Z}$ the time instant.*

2. *q the shift operator meaning $qw_j(t) = w_j(t+1)$.*
3. *$\mathcal{N}_j$ the set of indices of node signals $w_i(t)$ $i \neq j$ with direct paths to node signals $w_j(t)$ (i.e. $\mathcal{N}_j$ is the set of in-neighbours of $w_j(t)$).*
4. *$G^0_{ji}(q)$ proper rational transfer functions, referred to as modules, with $G^0_{jj}(q) = 0$.*
5. *$R^0_{jk}(q)$ known stable proper rational transfer functions.*

Combining the expressions of all node signals results in the following matrix equation describing the full behaviour of the network:

$$w(t) = G^0(q)w(t) + R^0(q)r(t) + v(t), \tag{2.66}$$

where $G^0(q)$ and $R^0(q)$ consist of elements $[G^0(q)]_{ij} = G^0_{ij}(q)$ and $[R^0(q)]_{ij} = R^0_{ij}(q)$, respectively, and where

$$w(t) = \begin{bmatrix} w_1(t) & w_2(t) & \dots & w_L(t) \end{bmatrix}^\top, \tag{2.67a}$$
$$r(t) = \begin{bmatrix} r_1(t) & r_2(t) & \dots & r_K(t) \end{bmatrix}^\top, \tag{2.67b}$$
$$v(t) = \begin{bmatrix} v_1(t) & v_2(t) & \dots & v_L(t) \end{bmatrix}^\top. \tag{2.67c}$$

The disturbance signals $v(t)$ are modeled as a filtered white noise process such that $v(t) = H^0(q)e(t)$, with $H^0(q)$ a square rational transfer function matrix that is monic, stable, and has a stable inverse; and with $e(t)$ the with noise process with covariance $\Lambda^0 \succ 0$.

The dynamic network is assumed to be stable, meaning that the transfer function matrix $\left(I - G^0(q)\right)^{-1}$ only contains stable transfer function elements. The dynamic network is also assumed to be well-posed, meaning that all principal minors of $\lim_{z\to\infty}\left(I - G^0(z)\right)$ are nonzero.

Remark 2.33 (Continuous time). *Even though the module representation is typically formulated in discrete time, it can be formulated similarly in continuous time in terms of the differential operator p meaning $pw_j(t) = \frac{d}{dt}w_j(t)$.*

The graphical module representation corresponding to Example 2.35 is shown in Figure 2.9. The circles are the vertices, which are summation points leading to the node signals $w(t)$. The boxes in the edges represent the transfer function modules interconnecting the node signals. The arrows represent internal and

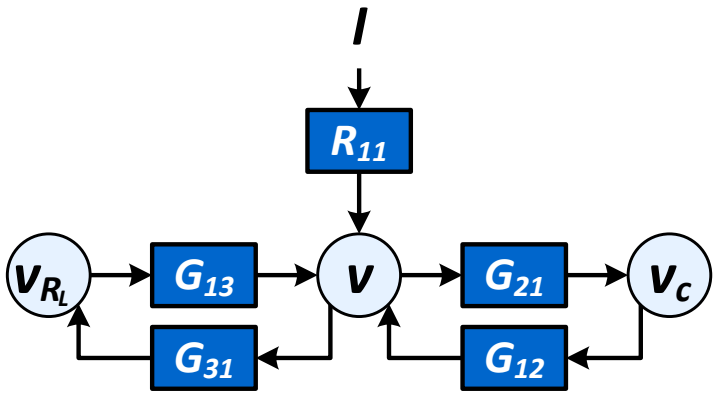

Figure 2.9: Module representation of the electrical circuit of Example 2.35.

external signals and describe a directed information flow. Observe that the module representation of the electrical circuit in Figure 2.1, described by (2.70) and shown in Figure 2.9, is exactly the same as the dynamical structure function of this network, described by (2.64) and shown in Figure 2.8.

Immersion

Immersion is an operation to eliminate node signals from the network representation, whilst preserving the behaviour of the remaining node signals (Dankers et al., 2016). This is, for example, useful for removing unmeasured node signals from the module representation. Then the representation resulting from immersion describes the relations among the measured node signals. Immersion is performed both graphically and mathematically, as illustrated by the following example:

Example 2.34 (Immersion). *Consider the module representation shown in the graph in Figure 2.10a, which consists of three node signals at the vertices and the modules at the edges between them. This module representation is described by*

$$\begin{bmatrix} w_1(t) \\ w_2(t) \\ w_3(t) \end{bmatrix} = \begin{bmatrix} 0 & 0 & G_{31}(q) \\ G_{21}(q) & 0 & 0 \\ 0 & G_{32}(q) & 0 \end{bmatrix} \begin{bmatrix} w_1(t) \\ w_2(t) \\ w_3(t) \end{bmatrix} + \begin{bmatrix} r_1(t) \\ 0 \\ 0 \end{bmatrix}. \tag{2.68}$$

Eliminating $w_2(t)$ from the network is graphically performed by lifting the path through $w_2(t)$; combining the dynamics in this path; and removing $w_2(t)$ from the graph. The resulting module representation is shown in

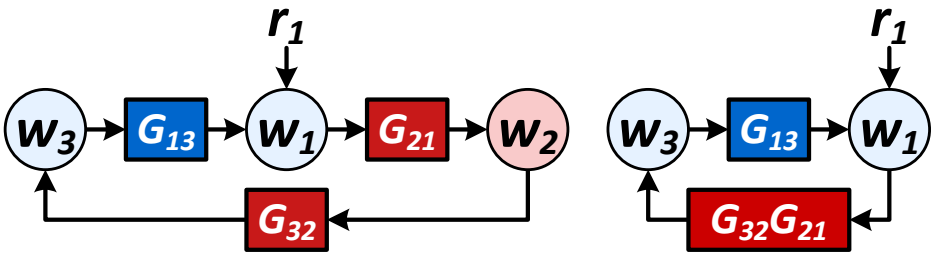

(a) The original module representation. (b) The immersed network.

Figure 2.10: Module representation of the dynamic network of Example 2.34 and the immersed network resulting from eliminating $w_2(t)$ from the network.

Figure 2.10b. Mathematically, $w_2(t)$ is eliminated by selecting the second row of (2.68)*, i.e. $w_2(t) = G_{21}(q)w_1(t)$; substituting it in the other rows of* (2.68)*; and removing $w_2(t)$ from* (2.68)*. The resulting module representation is described by*

$$\begin{bmatrix} w_1(t) \\ w_3(t) \end{bmatrix} = \begin{bmatrix} 0 & G_{31}(q) \\ G_{32}(q)G_{21}(q) & 0 \end{bmatrix} \begin{bmatrix} w_1(t) \\ w_3(t) \end{bmatrix} + \begin{bmatrix} r_1(t) \\ 0 \end{bmatrix}. \tag{2.69}$$

Mathematically, a node signal $w_j(t)$ is removed from the representation by Gaussian elimination. To be precise, the equation describing the behaviour of $w_j(t)$ is used to eliminate $w_j(t)$ from the network. Sometimes, it is also possible to use the equation of other node signals to eliminate $w_j(t)$ from the network. For example, in Example 2.34 the third row of (2.68) can be used to eliminate $w_2(t)$. This procedure is a generalisation of immersion and referred to as *abstraction* (Weerts et al., 2020). Abstraction also results in a representation in which the behaviour of the remaining node signals is preserved. However, then the modules are not guaranteed to be proper.

Example 2.35 (Module representation of an electrical circuit). *Consider again the electrical circuit in Figure 2.1. This circuit is described by a continuous-time module representation as*

$$\begin{bmatrix} V(t) \\ V_C(t) \\ V_{R_L}(t) \end{bmatrix} = \begin{bmatrix} 0 & \frac{Lp}{R_C+Lp} & \frac{R_C p}{R_C+Lp} \\ \frac{p}{1+CR_C p^2} & 0 & 0 \\ \frac{R_L}{R_L+Lp} & 0 & 0 \end{bmatrix} \begin{bmatrix} V(t) \\ V_C(t) \\ V_{R_L}(t) \end{bmatrix} + \begin{bmatrix} \frac{R_C Lp}{R_C+Lp} \\ 0 \\ 0 \end{bmatrix} I(t). \tag{2.70}$$

Immersion of the node signals $V_C(t)$ and $V_{R_L}(t)$ leads to (2.20).

2.4.9 Interaction-oriented model

The interaction-oriented model of Lunze (1992) thanks its name to the explicit description of the interactions between the dynamic subsystems. The interactions are modelled as dynamic relations between signals. The interaction-oriented model contains two types of dynamic elements: subsystems and interconnections. It originates from a perspective of (distributed) control of interconnected dynamical subsystems in which each subsystem is described by a state-space model. It is used in (distributed) control applications of interconnected systems, such as in smart grids, communication networks, and chemical plants (Lunze, 1992; Dullerud and D'Andrea, 2004; Langbort et al., 2004; Steentjes et al., 2021; Bullo, 2022).

In the interaction-oriented model, a set of subsystems interact through dynamic interconnections. The subsystems are connected to the environment with external signals and interconnected with each other through internal signals. In an input-output setting, the subsystems are driven by internal input signals coming from the network and known external excitation signals coming from the environment. It produces measured external output signals leaving the network and internal output signals processing through the network. The interconnection dynamics and the internal signals can be subject to unknown external disturbance signals.

Definition 2.36 (Interaction-oriented model (Lunze, 1992)). *An interaction-oriented model consists of N subsystems $\Sigma_1, \ldots, \Sigma_N$, with m_{u_i} external input signals $u_i(t)$, m_{s_i} internal input signals $s_i(t)$, r_{y_i} external output signals $y_i(t)$, and r_{z_i} internal output signals $z_i(t)$. The behaviour of the ith subsystem Σ_i is described (in state-space form) by*

$$\Sigma_i = \begin{cases} \dot{x}_i(t) = A_i x_i(t) + B_i u_i(t) + E_i s_i(t), & \text{(2.71a)} \\ y_i(t) = C_i x_i(t) + D_i u_i(t) + F_i s_i(t), & \text{(2.71b)} \\ z_i(t) = C_{z_i} x_i(t) + D_{z_i} u_i(t) + F_{z_i} s_i(t), & \text{(2.71c)} \end{cases}$$

with initial condition $x_i(0) = x_{i0}$ and where the behaviour of the interconnections is described by

$$s(t) = L(p)z(t), \tag{2.72}$$

with $t \in \mathbb{R}$ indicating the time, p the differential operator meaning $pz(t) = \frac{d}{dt}z(t)$, and $L(p) \in \mathbb{R}^{M_{si} \times r_{zi}}(p)$.

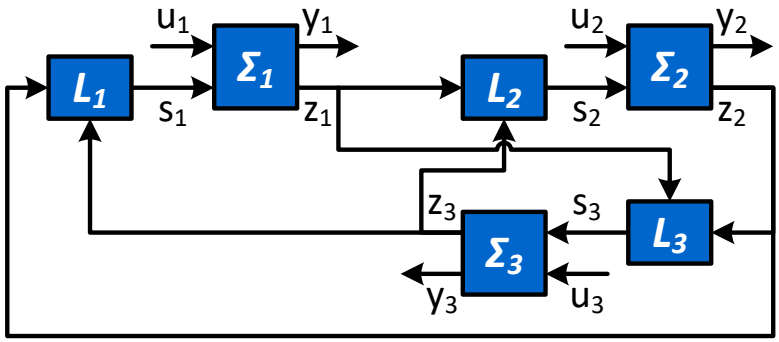

Figure 2.11: Interaction-oriented model with three subsystems Σ_i, $i = 1, 2, 3$, and with L_i the interconnections between them representing the ith row of $L(p)$.

In Definition 2.36, the subsystems Σ_i are described in a state-space form, because this is typically done in literature. However, it is also possible to describe the behaviour of the subsystems using any other modelling technique. Moreover, the dynamics can even be nonlinear. Further, the interconnections can be dynamic, as in Definition 2.36, but can also be static by considering a static $L(p) := L$ in (2.72). The interactions capture the topology of the network, which is described by the zero-structure of $L(p)$.

Graphically, the interaction-oriented model is depicted by a directed graph with vertices representing the subsystems and the interconnections and with edges representing the internal and external signals. The subsystems Σ_i are blocks with two input signals and two output signals, while the interactions $L_{ij}(p)$ are SISO blocks. Sometimes the interactions with a subsystem Σ_i are captured by a single multi-input single-output (MISO) block L_i, representing the ith row of $L(p)$. Figure 2.11 shows an interaction-oriented model with three subsystems Σ_i, $i = 1, 2, 3$ and with the interconnections between them captured by L_i, $i = 1, 2, 3$ representing the ith row of $L(p)$.

Remark 2.37 (Discrete time). *The interaction-oriented model can similarly be formulated in discrete time. Then the dynamics of the subsystems is described by discrete-time state-space models (see Section 2.4.2).*

2.4.10 Behavioural approach

Introduction

All aforementioned model representations are input-output descriptions, which means that preselected output signals are described by preselected input signals (and possibly, initial conditions). This induces a signal flow from the input, through the system, to the output. Allocating the inputs and outputs often depends on the experiment that is being performed. The dynamics between the inputs and outputs depend on the selected input and output signals. This type of modelling leads to a model that depends on the experiment, while the physical system remains the same for any experiment and is thus independent of the experiment. Hence, assigning inputs and outputs to a system is usually a result of the chosen experiment and not a characteristic of the system itself. The chosen experiment can be one out of several, which means that the input-output structure of a system is not unique.

In input-output descriptions of dynamic networks, subsystems are interconnected through couplings of inputs and outputs. That is, the input signal to a subsystem depends on the output signals of some other subsystems and possibly on input signals from the environment. However, physical systems interact with their environment by exchanging matter, energy, or information. For many of these interconnections, it is not clear or obvious which signals serve as inputs or outputs of interconnected subsystems. Physical subsystems in physical networks also interact with each other. The interconnections between subsystems are characterised by variable sharing. A mathematical model of a physical linear network describes simultaneous occurring events, often with unclear cause-effect relations or signal flows.

Exactly because of these reasons, Willems (1986a,b, 1987) came up with the behavioural approach, in which the behaviour of the system is described without assigning inputs and outputs. Only the relations among the variables are described. This model is independent of the chosen experiment. Causal relations can be part of the physics, but are not dictated, while additional input and output signals can be selected after designing the experiment. System properties such as controllability are defined based on the behavioural description of the system alone, without defining inputs and outputs. Therefore, these properties are properties of the system instead of properties of the representation (as in, for example, state-space models).

Dynamical systems

In the behavioural approach, the behaviour of a dynamical system is described by signal trajectories.

Definition 2.38 (Behavioural approach (Willems, 1986a)). *A dynamical system is defined as the triplet*

$$\Sigma = (\mathbb{T}, \mathbb{W}, \mathcal{B}), \tag{2.73}$$

with

1. $\mathbb{T} \subseteq \mathbb{R}$ *the time space.*
2. $\mathbb{W} \subseteq \mathbb{R}^{\mathtt{w}}$ *the signal space, with* $\mathtt{w} \in \mathbb{N}$ *the dimension of the trajectories* $w(t)$.
3. $\mathcal{B} \subseteq \mathbb{W}^{\mathbb{T}}$ *the behaviour, with* $\mathbb{W}^{\mathbb{T}}$ *the collection of all maps from* $\mathbb{T}$ *to* $\mathbb{W}$.

Definition 2.39 (Kernel representation (Willems, 1986a; Polderman and Willems, 1998)). *The behaviour* $\mathcal{B}$ *of a dynamical system with* $\mathtt{p} \leq \mathtt{w}$ *can be described in the kernel representation by*

$$\mathcal{B} = \{w(t) \in C^{\infty}(\mathbb{R}, \mathbb{R}^{\mathtt{w}}) |\ R(\frac{d}{dt})w(t) = 0\} \tag{2.74}$$

with $t \in \mathbb{T}$ *indicating the time,* $C^{\infty}(\mathbb{R}, \mathbb{R}^{\mathtt{w}})$ *the set of infinitely differentiable functions from* $\mathbb{R}$ *to* $\mathbb{R}^{\mathtt{w}}$*, and* $R(\xi) \in \mathbb{R}^{p \times \mathtt{w}}[\xi]$.

If $\mathtt{p} = \mathtt{w}$, the behaviour of (2.74) is autonomous in the sense that no free inputs can be distinguished.

The behavioural approach only describes the trajectories of signals $w(t)$, no input-output mapping. However, there always exists a nonunique partitioning of the signals $w(t)$ into inputs $u(t)$ and outputs $y(t)$. In this input-output partitioning, the input $u(t)$ can be chosen freely and the output $y(t)$ is bounded and completely determined by the past and the input, such that $(u(t), y(t)) = w(t) \in \mathcal{B}$. Even though the partitioning is nonunique, the dimensions of $u(t)$ and $y(t)$ are fixed and thus independent of the partitioning. Moreover, for the kernel representation of the behaviour, the dimension of the output is equal to the rank of $R(\xi)$, that is $\operatorname{rank}(R(\xi)) = \dim(y(t)) = \mathtt{p}$. The partitioning of $w(t)$ into input and output signals leads to an input-output representation.

Definition 2.40 (Input-output representation (Polderman and Willems, 1998)). *The behaviour $\mathcal{B}$ of a dynamical system can be described in the input-output representation by*

$$\mathcal{B} = \{w(t) = \begin{bmatrix} u(t) \\ y(t) \end{bmatrix} \in C^\infty(\mathbb{R}, \mathbb{R}^{\mathtt{w}}) |\ P(\frac{d}{dt})y(t) = Q(\frac{d}{dt})u(t)\} \tag{2.75}$$

with $P(\xi) \in \mathbb{R}^{p\times p}[\xi]$ and $Q(\xi) \in \mathbb{R}^{p\times \mathtt{m}}[\xi]$, with $\mathtt{m} = \mathtt{w} - \mathtt{p}$, with $\det(P(\xi)) \neq 0$ and with $P^{-1}(\xi)Q(\xi)$ a matrix of proper rational functions.

The fact that the transfer function matrix $P^{-1}(\xi)Q(\xi)$ is required to be proper, imposes restrictions on the input-output partitioning of $w(t)$.

Example 2.41 (Behavioural model of a resistor). *The behaviour of a resistor can be described by Ohm's law as*

$$\mathcal{B} = \{(V(t), I(t)) \in \mathbb{R}^2 |\ V(t) = R_s I(t)\}, \tag{2.76}$$

where $V(t)$ is the voltage across the resistor, R_s is the resistance, and $I(t)$ is the current flowing through the resistor. The corresponding kernel representation is given by

$$\underbrace{\begin{bmatrix} -1 & R_s \end{bmatrix}}_{R(\frac{d}{dt})} \begin{bmatrix} V(t) \\ I(t) \end{bmatrix} = 0. \tag{2.77}$$

As $\mathrm{rank}(R(\frac{d}{dt})) = 1$, the resistor can be modelled by an input-output model with one output and thus $2 - 1 = 1$ input. As $R(\frac{d}{dt})$ is static, there is no causal relation between the signals in $w(t)$ and thus no signal is obliged to be an input or an output signal.

The behavioural model of the electrical circuit in Figure 2.1 is given by (2.20) (Polderman and Willems, 1998; Willems, 2007, 2010). This model is in an input-output representation as defined in Definition 2.40.

Networks of interconnected systems

Networks of interconnected systems are modelled by tearing, zooming, and linking (Willems, 2007). In this method, the network is first torn apart into subsystems (modules) with terminals that contain the physical variables that can be shared. Second, each subsystem is modelled separately by zooming into it. Finally, the

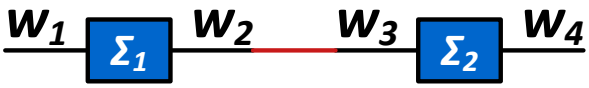

Figure 2.12: Network of two interconnected systems Σ_1 and Σ_2.

subsystems are linked with each other by modelling the relations among the shared variables.

This modelling is similar to the interaction-oriented model explained in Section 2.4.9, with the difference that the interaction-oriented model has subsystems with an input-output structure, while here the subsystems share variables.

In a network of interconnected systems, the behaviour of each system is described by $\Sigma_i = (\mathbb{T}, \mathbb{W}_i, \mathcal{B}_i)$, $i = 1, 2, \ldots$. The interconnection between any two systems Σ_j and Σ_k, denoted by $\Sigma_j \wedge \Sigma_k$, is modelled by any law $L_{jk}\big(w_j(t), w_k(t)\big) = 0$, where $w_i(t) \in \mathcal{B}_i$, $i = j, k$.

Example 2.42 (Two interconnected systems). *Consider a network of two interconnected systems Figure 2.12. Suppose that Σ_1 and Σ_2 are linear dynamic systems of which the behaviour is described by the kernel representations*

$$\begin{bmatrix} R_1(\frac{d}{dt}) & R_2(\frac{d}{dt}) \end{bmatrix} \begin{bmatrix} w_1(t) \\ w_2(t) \end{bmatrix} = 0, \tag{2.78a}$$

$$\begin{bmatrix} Q_1(\frac{d}{dt}) & Q_2(\frac{d}{dt}) \end{bmatrix} \begin{bmatrix} w_3(t) \\ w_4(t) \end{bmatrix} = 0, \tag{2.78b}$$

respectively. Let the interconnection $\Sigma_1 \wedge \Sigma_2$ also be linear and be described by $w_2(t) = w_3(t)$, that is

$$\begin{bmatrix} 1 & -1 \end{bmatrix} \begin{bmatrix} w_2(t) \\ w_3(t) \end{bmatrix} = 0. \tag{2.79}$$

Then the network is described by

$$\begin{bmatrix} R_1(\frac{d}{dt}) & R_2(\frac{d}{dt}) & 0 & 0 \\ 0 & 1 & -1 & 0 \\ 0 & 0 & Q_1(\frac{d}{dt}) & Q_2(\frac{d}{dt}) \end{bmatrix} \begin{bmatrix} w_1(t) \\ w_2(t) \\ w_3(t) \\ w_4(t) \end{bmatrix} = 0, \tag{2.80}$$

which is equivalent to the minimal kernel representation

$$\begin{bmatrix} R_1(\frac{d}{dt}) & R_2(\frac{d}{dt}) & 0 \\ 0 & Q_1(\frac{d}{dt}) & Q_2(\frac{d}{dt}) \end{bmatrix} \begin{bmatrix} w_1(t) \\ w_2(t) \\ w_4(t) \end{bmatrix} = 0, \tag{2.81}$$

where the latent variable $w_3(t)$ has been eliminated.

2.4.11 Bond-graph models

The behavioural model is closely related to energy-based modelling approaches, such as bond-graph models and (multi)port models (Paynter, 1961; Ljung and Glad, 1994; Borutzky, 2010, 2011). These modelling approaches are based on energy preservation and power interconnections. They are generally based on two types of variables, effort e and flow f, whose product equals power. The flow variable is a rate of change of state and the effort variable is an equilibrium-determining variable. Typical flow variables are current flow, (angular) velocity, and flow rate, while typical effort variables are potential, force, torque, and pressure.

Let the linear space $\mathcal{F}$ and the dual space $\mathcal{E} := \mathcal{F}^*$ be the spaces of flows $f \in \mathcal{F}$ and efforts $e \in \mathcal{E}$, respectively. Then the power of the total space is defined by (van der Schaft and Jeltsema, 2014)

$$P =< e|f >= e^\top f, \qquad (f, e) \in \mathcal{F} \times \mathcal{E}. \tag{2.82}$$

Physical components can be classified in multiple ways. In bond-graph and port models, they are typically modelled based on the number of energy transaction forms (Paynter, 1961). Each energy transaction is modelled by a bond or port with a flow and effort variable through which the physical elements are interconnected. These bonds are closely analogous to chemical valency bonds between atoms. One-ports are generalised impedances, such as resistive, capacitive, and inductive components or effort and flow sources. These components have only a single bond and therefore, allow only simple interconnections. Two-ports are generalised transport processes, such as energy transformation, energy transmission, and energy transduction processes. These elements have two bonds and therefore, allow for chain interconnections. Three-ports are generalised modulators, such as energy junctions, power and signal amplifiers or modulators, and power exchangers. These elements have three bonds and therefore, allow for more complex interconnection structures.

Energy junctions are one example of three-port elements (Paynter, 1961). There are two types of ideal energy junctions: effort junctions and flow junctions. Effort junctions (or 1-junctions) are a generalisation of Kirchhoff's loop law (Kirchhoff's voltage law). They are characterised by equal flows at all bonds, resulting in efforts that sum to zero. Flow junctions (or 0-junctions) are a generalisation of Kirchhoff's node law (Kirchhoff's current law). They are characterised

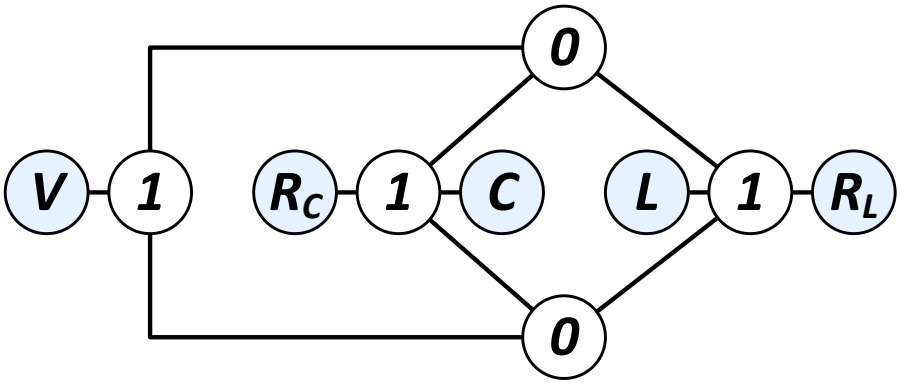

Figure 2.13: Bond-graph model of the electrical circuit of Example 2.43.

by equal efforts at all bonds, resulting in flows that sum to zero. The k-dimensional effort junction and flow junction are, respectively, given by

$$\mathcal{D}_e := \big\{(f,e) \in \mathcal{F} \times \mathcal{E} \mid e_1 = e_2 = \cdots = e_k,\ f_1 + f_2 + \cdots + f_k = 0\big\}, \quad (2.83a)$$

$$\mathcal{D}_f := \big\{(f,e) \in \mathcal{F} \times \mathcal{E} \mid e_1 + e_2 + \cdots + e_k = 0,\ f_1 = f_2 = \cdots = f_k\big\}, \quad (2.83b)$$

where $e = \begin{bmatrix} e_1^\top & e_2^\top & \dots & e_k^\top \end{bmatrix}^\top$ and $f = \begin{bmatrix} f_1^\top & f_2^\top & \dots & f_k^\top \end{bmatrix}^\top$.

Example 2.43 (Bond-graph model of an electrical circuit). *Consider again the electrical circuit in Figure 2.1. This circuit is graphically depicted by the bond-graph model shown in Figure 2.13. This figure shows the interconnection structure of the network and it shows the four components and the voltage source as one-port elements (blue circles), because they have only one connection, and the junctions (white circles) as multiport elements, because they have multiple connections. The 1-junctions represent Kirchhoff's voltage law and the 0-junctions represent Kirchhoff's current law.*

Once the bond-graph model of dynamic networks is drawn using ports, causality can be added. Causality, which depends on environmental conditions, is similar to the direction in which chemical reactions proceed, which depends on ambient conditions. First, the energy exchange of the system with the environment is considered, which can be seen as the experimental setup. Then, the internal causal structure can be chosen by following specific steps. Once causality is added to the bond-graph model, it can be converted into a state-space model. A special form of a state-space model is a Hamiltonian system. Port models that are converted into a Hamiltonian state-space model are referred to as port-Hamiltonian

systems (van der Schaft and Jeltsema, 2014).

2.4.12 Port-Hamiltonian models

Introduction

In Hamiltonian models, physical components are characterised by their energy-consuming behaviour. The physical components are divided into three groups: energy-storing elements, energy-dissipating elements, and energy-routing elements. In port-Hamiltonian models, interconnections are again made through ports with a flow and effort variable attached to them. As the product of flow and effort equals power (2.82), the interconnections ensure power preservation. Port-Hamiltonian models are closely related to the behavioural approach and to bond-graph models. (van der Schaft and Maschke, 2013; van der Schaft and Jeltsema, 2014). Moreover, bond-graph models can also be formulated as port-Hamiltonian systems (Golo et al., 2003).

Dynamical systems

Energy-storing elements save energy for later use. Examples of energy-storing elements are capacitive and inductive components. Energy-dissipating elements, such as resistive components, consume energy. Transformers and constraints are examples of energy-routing elements, which preserve a power balance and redirect the energy. Energy can be supplied to a system by the environment that is connected through external ports.

Using efforts, flows, and power, the *Dirac structure* is defined, which captures the energy-routing elements and provides power conservation between the interconnected ports.

Definition 2.44 (Dirac structure (van der Schaft and Jeltsema, 2014)). *Consider a finite-dimensional linear space $\mathcal{F}$ with $\mathcal{E} = \mathcal{F}^*$. A subspace $\mathcal{D} \subset \mathcal{F} \times \mathcal{E}$ is a* Dirac structure *if*

1. $< e|f >= 0, \forall (f, e) \in \mathcal{D}$ *(power conservation).*
2. $\dim \mathcal{D} = \dim \mathcal{F}$.

Observe that the effort and flow junctions (2.83) are examples of Dirac structures.

In connection with efforts and flows, let us define the bilinear form.

Definition 2.45 (Bilinear form (van der Schaft and Jeltsema, 2014)). *A bilinear form $\ll, \gg$ on the space $\mathcal{F} \times \mathcal{E}$ is defined as*

$$\ll (f_1, e_1), (f_2, e_2) \gg := < e_1 | f_2 > + < e_2 | f_1 >, \tag{2.84}$$

with $(f_1, e_1), (f_2, e_2) \in \mathcal{F} \times \mathcal{E}$.

Using the bilinear form defined in Definition 2.45, the following result on the Dirac structure is formulated:

Proposition 2.46 (Dirac structure (van der Schaft and Jeltsema, 2014)). *A Dirac structure on $\mathcal{F} \times \mathcal{E}$ is a subspace $\mathcal{D} \subset \mathcal{F} \times \mathcal{E}$ such that $D = D^{\perp}$, with $\perp$ the orthogonal companion with respect to the bilinear form $\ll, \gg$.*

The energy stored in an energy-storing element is defined by the space $\mathcal{X}$ and a Hamiltonian function $H(x) : \mathcal{X} \to \mathbb{R}$ that denotes the energy. The power flowing into the energy-storing element is given by

$$\frac{d}{dt} H(x) = < \frac{\partial}{\partial x} H(x), \frac{d}{dt} x(t) > = \frac{\partial^{\top}}{\partial x} H(x) \frac{d}{dt} x(t) = -e_s^{\top} f_s, \tag{2.85}$$

with state $x \in \mathcal{X}$, time $t \in \mathbb{R}$, effort $e_s = \frac{\partial}{\partial x} H(x)$, and flow $f_s = -x$.

An energy-dissipating element is defined by the energy-dissipating relation

$$\mathcal{R} \subset \mathcal{F}_r \times \mathcal{E}_r, \qquad < e_r \mid f_r > = e_r^{\top} f_r \leq 0, \quad \forall (f_r, e_r) \in \mathcal{R}. \tag{2.86}$$

For linear resistive elements, the mapping becomes $f_r = -R e_r$, with matrix $R = R^{\top} \geq 0$.

The interaction with the environment is modelled with external ports with variables (f_p, e_p). This leads to the overall power balance

$$e_s^{\top} f_s + e_r^{\top} f_r + e_p^{\top} f_p = 0, \tag{2.87}$$

that is

$$\frac{d}{dt} H(x) = e_r^{\top} f_r + e_p^{\top} f_p \leq e_p^{\top} f_p. \tag{2.88}$$

This means that the increase of the internally stored energy (represented by the Hamiltonian $H(x)$) is always less than or equal to the externally supplied power.

Figure 2.14 shows the general structure of a port-Hamiltonian system. The energy-storing elements with effort e_S and flow f_S are collected in the blue oval with the label *Storage*, the energy-dissipating elements with effort e_R and flow f_R are collected in the blue oval with the label *Dissipation*, and the energy-routing elements are collected in the blue circle with the label $\mathcal{D}$ representing the Dirac structure. The effort e_P and flow f_P represent the external port connecting the system with the environment.

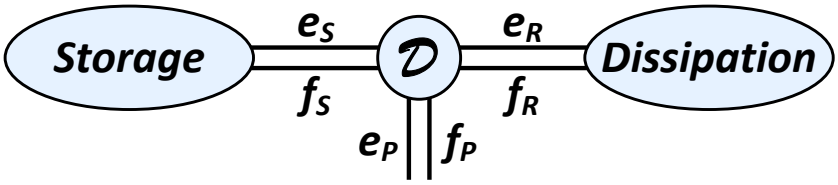

Figure 2.14: Structure of a port-Hamiltonian system (van der Schaft and Jeltsema, 2014).

Networks of interconnected systems

The Dirac structure can be used to describe interconnections of systems. Furthermore, the interconnection of power-conserving elements is again power-conserving, which means that the composite of Dirac structures is again a Dirac structure (van der Schaft and Jeltsema, 2014). This is illustrated by the following example:

Example 2.47 (Two interconnected Dirac structures (van der Schaft and Jeltsema, 2014)). *Consider the interconnection of two Dirac structures as shown in Figure 2.15, where the two Dirac structures $\mathcal{D}_A$ and $\mathcal{D}_B$ shown in the blue circles are interconnected through the empty blue circle. Suppose that the two Dirac structures are described by*

$$\mathcal{D}_A \in \mathcal{F}_1 \times \mathcal{F}_2 \times \mathcal{E}_1 \times \mathcal{E}_2, \tag{2.89a}$$

$$\mathcal{D}_B \in \mathcal{F}_2 \times \mathcal{F}_3 \times \mathcal{E}_2 \times \mathcal{E}_3, \tag{2.89b}$$

with $\mathcal{E}_i = \mathcal{F}_i^*$, $i = 1, 2, 3$. The spaces $\mathcal{F}_2$ and $\mathcal{E}_2$ are the spaces of shared flow and effort variables, respectively. Let

$$(f_1, e_1, f_A, e_A) \in \mathcal{D}_A, \qquad (f_B, e_B, f_3, e_3) \in \mathcal{D}_B, \tag{2.90}$$

where $< e_A | f_A >$ and $< e_B | f_B >$ denote the incoming power in $\mathcal{D}_A$ and $\mathcal{D}_B$, respectively. The interconnection between $\mathcal{D}_A$ and $\mathcal{D}_B$ is constraint by

$$f_A = -f_B \in \mathcal{F}_2, \qquad e_A = e_B \in \mathcal{E}_2, \tag{2.91}$$

leading to the composite Dirac structure

$$\mathcal{D}_A \circ \mathcal{D}_B := \big\{(f_1, e_1, f_3, e_3) \in \mathcal{F}_1 \times \mathcal{E}_1 \times \mathcal{F}_3 \times \mathcal{E}_3 \mid \exists (f_2, e_2) \in \mathcal{F}_2 \times \mathcal{E}_2 \\ \text{s.t. } (f_1, e_1, f_2, e_2) \in \mathcal{D}_A \text{ and } (-f_2, e_2, f_3, e_3) \in \mathcal{D}_B\big\}. \tag{2.92}$$

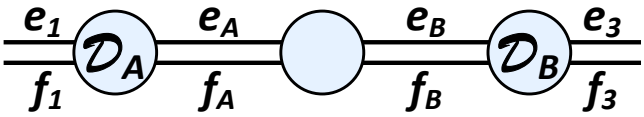

Figure 2.15: The composite Dirac structure $\mathcal{D}_A \circ \mathcal{D}_B$ (van der Schaft and Jeltsema, 2014).

Remark 2.48 (Link with the Behavioural approach). *The difference between energy-based models and the behavioural approach is that the energy-based methods have power transmissions through interconnected ports with effort and flow variables, while in the behavioural approach, the subsystems are interconnected through terminals with any possible quantities, which cannot necessarily be interpreted as energy flow. For example, the* Υ *and* Δ *circuits shown in Figure 2.2 have three terminals, but only a single port.*

2.5 Discussion

2.5.1 Introduction

To describe physical linear networks for identification purposes, a suitable modelling approach needs to be chosen. The candidate linear dynamic (network) models that are presented in Section 2.4 are discussed here to make well-considered and well-motivated decisions on the network model structure.

The focus lies on several modelling aspects that are important for the identification of physical linear networks, which include: incorporating the physical characteristics; representing the topology; including higher-order dynamics; the interaction with the environment; and dealing with unknown disturbances and noise signals. In addition, the availability of identification theory for the candidate models is discussed. Based on these aspects, a comparison is made between the candidate models to see which models are most suitable for the identification of physical linear networks.

2.5.2 Diffusive couplings

Physical components are characterised by diffusive couplings, as has been explained in Section 2.3. For linear components, this leads to symmetric relations

between signals. This characteristic needs to be incorporated into the dynamic network model.

In the behavioural approach, the bond-graph model and port-Hamiltonian models this can easily be done, because their interconnections are based on sharing variables, which do not require input-output descriptions. This is further discussed in Section 5.3. In addition, the behavioural approach is not bound by interconnections through effort and flow pairs. Therefore, the behavioural approach is preferred above port-Hamiltonian models, which are more general than bond-graph models (Golo et al., 2003).

The interaction-oriented model describes subsystems and interconnections with input-output models and therefore, this model is less suitable for describing physical linear dynamic networks.

The symmetric nature of physical components appears in polynomial models through the symmetry of the polynomial matrix $A(q^{-1})$, as illustrated by Example 2.23, and therefore, diffusive couplings can also be incorporated in these models.

In the module representation, the symmetric nature of the linear physical components leads to the situation that coefficients of single components appear in several transfer function modules. This happens because every dynamic module describes an input-output relation from one signal to another, while two interconnected signals both depend on the physical components that are in the interconnection between them. A similar mechanism appears in the Wiener filter model and the dynamical structure function. The shared dynamics in the relations between the signals makes these models less suitable for describing physical linear dynamic networks.

2.5.3 Topology

As this research considers networks, it is necessary that the interconnections can be modelled and that the topology can be incorporated into the network model. In addition, it would be nice if the topology is directly visible in the mathematical network model, because this makes it easy to include *a priori* topological information and draw conclusions on the topology based on the mathematical description of the network.

The module representation is designed for dynamic networks and the topology is clearly visible in the transfer function matrix $G(q)$ describing the dynamics of the network. A zero element in $G(q)$ corresponds to an edge with a zero transfer function between the corresponding signals, which can be interpreted as an absent edge. A similar reasoning holds for the input transfer function matrix $R(q)$ and

the noise model $H(q)$. The same mechanism is present in the dynamical structure function model and the Wiener filter model, where in the latter case a zero filter is interpreted as an absent edge.

In polynomial models of networks, the topology appears in the polynomial matrix $A(q^{-1})$ describing the dynamics of the network. Similar as in the module representation, a zero element in $A(q^{-1})$ can be interpreted as an absent edge between the corresponding signals. A similar mechanism holds for the input dynamics described by $F^{-1}(q^{-1})B(q^{-1})$ and the noise model $D^{-1}(q^{-1})C(q^{-1})$.

The behavioural approach of dynamic network models describes the subsystems and their interactions separately, from which the topology is visible in the graphical network model. In general, these objects are only explicitly described by equations, from which the topology is not immediately visible in the mathematical model. If the dynamic network is described by the kernel representation (2.74), then $R(\frac{d}{dt})$ has the same functionality as $A(q^{-1})$ in the polynomial model and therefore, $R(\xi)$ includes the topology, where again a zero element can be interpreted as an absent edge between the corresponding signals.

The interaction-oriented model also describes the subsystems and their interactions separately. The topology is visible in the interconnection matrix $L(q)$, where a zero element is interpreted as an absent edge between the corresponding subsystems.

Port-Hamiltonian models are able to model the interconnections of systems. The typical strategy is to merge all Dirac structures, causing the topology to get lost in the network model. To avoid this, the Dirac structures should not be merged. Then each system in the network consists of a Dirac structure with a group of storage elements and a group of dissipative elements connected to it. In addition, the Dirac structures should be modelled such that they have multiple ports to the environment, which will be used to connect to other systems and the outside world. Then the topology remains present in the graphical network model, although it remains unclear how the topology is present in the mathematical model.

2.5.4 Higher-order dynamics

State-space models are first-order models and therefore, a special case of second-order models, which are a special case of polynomial models as they can include even higher-order terms. Even though most physical linear systems are naturally described by at most second-order models, some signals may be inaccessible or latent and therefore be eliminated from the network representation. This leads to higher-order network descriptions.

On the other hand, every polynomial model and every second-order model can be written as a state-space model by introducing additional state variables. Rewriting a model into a lower-order model can lead to the reproduction of component coefficients, meaning that a single coefficient of a physical component appears multiple times in the model. This is disadvantageous for identification and moreover, it can vanish the network topology from the representation. Therefore, the polynomial model is preferred over the second-order model and state-space model.

Transfer function representations, such as the Wiener filter model, dynamical structure function, and module representation are suitable for incorporating higher-order dynamics. The interaction-oriented model only includes input-output models between internal and external signals, which can be of any finite order. A similar reasoning holds for the behavioural approach and the interaction-oriented model, where every subsystem and interconnection are characterised by their behaviour or any input-output model, respectively, which can include any finite-order dynamics.

2.5.5 External signals

In general, all models can be extended to include known external input signals, unknown disturbance signals that process through the system or network, and noise that is added to the measured signals. However, in some models, it is more common to include disturbances than in other models. Measurement noise comes only into play when identification is considered.

In the interaction-oriented model, disturbance signals can be added to the subsystems or interactions. The same holds for state-space models and second-order models, although disturbance signals are often not included in the corresponding identification theory. Measurement noise is sometimes taken into account. Polynomial models do include disturbance signals and noise models are included in the identification theory. Therefore, the polynomial model is preferred over the second-order model and state-space model.

The behavioural approach, bond-graph models, and port-Hamiltonian models typically model exact dynamics, which means that disturbance signals are not considered.

Wiener filter models typically only include unknown external excitation signals. Known external signals can be added to the model, but are not included in the available identification theory. On the other hand, the dynamical structure function only includes known external excitation signals and does not consider disturbance signals, also not in the available identification theory.

The module representation includes both known external excitation signals and unknown external disturbance signals. Furthermore, measurement noise can be included in the module representation (Dankers et al., 2015). The module representation is preferred over the Wiener filter model and the dynamical structure function, because it is more general in the sense of incorporating external (disturbance) signals and measurement noise in both the network model as well as in the network identification theory that is available.

2.5.6 Network identification

For state-space models, there exists an extensive identification theory consisting of subspace identification methods (Verhaegen and Verdult, 2012). However, there are no statistical guarantees and the influence of disturbances remains unclear. Second-order models are usually identified by first identifying a state-space model and then translating the first-order state-space model into a second-order model, see, for example, De Angelis et al. (2002).

For polynomial models, there also exists a major identification theory consisting of prediction error identification methods (Ljung, 1999), including algorithms, statistical guarantees, and validation methods.

The Wiener filter model has been developed for topology identification in dynamic networks and it can also be used for identifying the dynamics. The dynamical structure function and the module representation have been developed specifically for identification purposes in dynamic networks. By now, considerable network identification literature has been built, including solutions to various network identification problems, see, for example, (Gonçalves and Warnick, 2008; Materassi and Innocenti, 2010; Van den Hof et al., 2013; Ramaswamy et al., 2019; Jahandari and Materassi, 2022a).

For the behavioural approach and port-Hamiltonian models, there is some identification theory available (Roorda and Heij, 1995; Markovsky et al., 2006). However, this has not been extended to dynamic networks.

2.5.7 Relations between network models

As mentioned, the network models that are developed in the literature, originate from various research domains, all with their own objectives and circumstances. The discussion of the models above raises the question of how theory developed in one domain is connected to other domains. For example, if an identification or control problem is solved for a particular model, can this solution be translated to another model? How to do this and what are the consequences of doing so?

The dynamic Bayesian network model is not fit for modelling physical linear dynamic networks, because it uses probability distributions and conditional dependencies to describe relations between signals, while the relations between signals in physical linear networks are considered to be fixed. However, the dynamic Bayesian network model is useful for topology identification in dynamic networks.

Polynomial models, second-order models, and state-space models can be transformed into each other, which means that the theory for each of these models is also accessible to the other models by transforming the model. This approach is, for example, applied in the identification of second-order models, where first a state-space model is identified, which is then translated into a second-order model. The transformation the other way around, that is, translating the theory instead of the model is more complicated. Reviewing the discussion points in Section 2.5.2-2.5.6, shows that the polynomial model is more general than the state-space model and the second-order model and that the identification theory that is available for polynomial models is more attractive. Therefore, the polynomial model is preferred above the state-space model and the second-order model. In addition, the polynomial model is able to incorporate diffusive couplings, higher-order dynamics, the network topology, and disturbance signals, and therefore, seems suitable for modelling physical linear dynamic networks.

The Wiener filter model, dynamical structure function, and module representation are all developed for directed dynamical network representations and are very much alike, which makes it feasible to translate theory from one model to another. Still, the differences between the Wiener filter model and the other two models are slightly too large to make a complete translation of the theory. For example, both for the Wiener filter model and the module representation there exist (graphical) conditions for identifiability (Jahandari and Materassi, 2022a,b; Ramaswamy and Van den Hof, 2021), which are very much alike and should be related to each other. However, the exact mapping between the results remains unsolved for the time being. The module representation is considered to be the most general one of these network models and therefore, it is preferred over the other two. The module representation is able to incorporate higher-order dynamics, the network topology, and disturbance signals. In addition, extensive literature on dynamic network identification is available. A disadvantage of the module representation is that it is less suitable for describing diffusive couplings.

The interaction-oriented model is as good as the module representation for modelling physical linear dynamic networks, as it has the same modelling advantages and disadvantages. Even though the interaction-oriented model is typically not used for identification purposes, but for (distributed) control (Lunze, 1992). Therefore, there is also less identification theory available in the literature.

The behavioural approach is closely related to bond-graph models and port-Hamiltonian models. The behavioural approach is the most general one and thus, it is preferred above the other two. This modelling approach is able to incorporate diffusive couplings, higher-order dynamics, and the network topology. However, there is little literature on identification in the behavioural setting and especially for dynamic networks.

It is more complicated to relate theory from, for example, polynomial models and the module representation to each other. Especially for dynamic networks, which include topology next to just dynamics. Polynomial models are more suitable for representing undirected interconnections, which occur, for example, in physical networks. Module representations are more suitable for representing directed interconnections, which occur, for example, in digital networks, such as controllers. Often, digital and physical systems are interconnected with each other, for example, when a digital controller is applied to a physical system. Both models are interesting for modelling these mixed networks, which are further studied in Chapter 11.

More research is needed to find the relations between these models and to use this knowledge to draw conclusions on the relations between, for example, identification results. The relations between several (more distinct) network models receive more attention in Chapter 3, 4, 5, and 7. Figure 2.16 shows an overview of the twelve dynamic network models that have been discussed in this chapter. Thin lines show the relations among closely related models. The dynamic network models that are highlighted with bold letters and a thick border are the most general models. The relations that are studied further are indicated with a thick line. The number corresponds to the chapter where the relation is discussed. Graphical models are discussed in Chapter 3.

2.5.8 Conclusion

Higher-order models (such as general polynomial models) can be transformed into lower-order models (such as state-space models) by introducing additional latent variables. The conversion in the opposite direction is performed by eliminating variables. This means that a dynamic system or network can be represented on different levels. This is an interesting phenomenon that needs to be understood better, especially for dynamic networks. The representation of LTI dynamic networks on different structural levels is further studied in Chapter 3 and 4.

From the models that are discussed in Section 2.4, the polynomial model, module representation, interaction-oriented model, and behavioural approach are the most general.

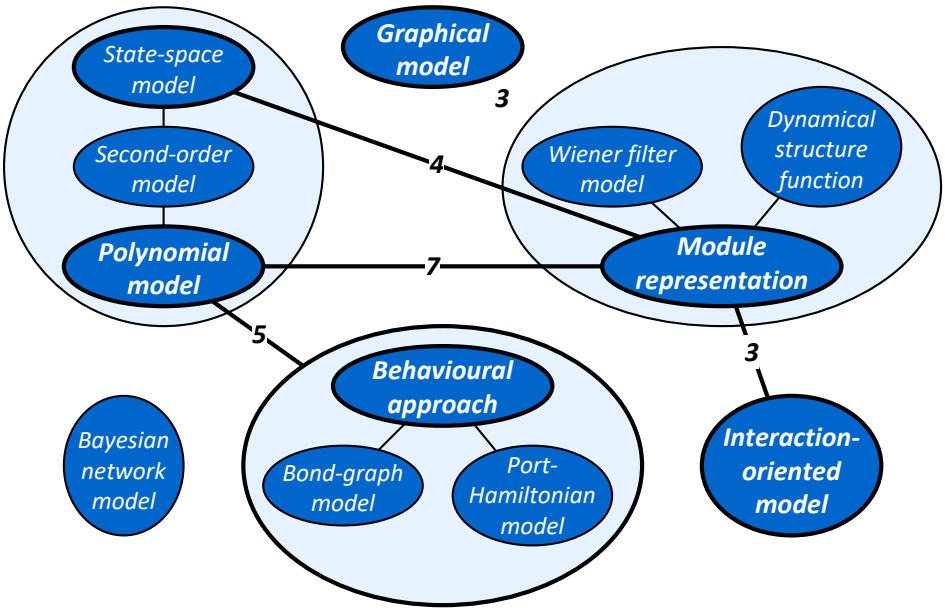

Figure 2.16: Overview of the twelve dynamic network models that have been discussed in Chapter 2. The relations that are studied in subsequent chapters are indicated with thick lines, where the number indicates the chapter.

For the behavioural approach, there is only a little literature on the identification and it is also difficult to connect this modelling approach with other modelling techniques for which there is literature on the identification in dynamical networks, in particular the module representation. Therefore, this modelling technique is not further considered.

This leaves the polynomial model, module representation, and interaction-oriented model as the most attractive ones for modelling and identification of physical linear networks. The interaction-oriented model and the module representation seem to be related to each other. The relation between these models deserves more attention and this is further investigated in Section 3.3.

The polynomial model seems the most attractive for modelling physical systems. However, currently, it is not used in a network setting. So, there is also no network identification literature for the polynomial model, which is extensively available for the module representation. Though, the module representation is less suitable for incorporating diffusive couplings. Further research on identification in these models is needed to determine which model is most suitable for identification in physical linear networks, which is done in Chapter 7.

2.6 Conclusion

Physical linear networks are characterised by linear diffusive couplings, which are interconnections that depend on the difference of variables. Various modelling approaches for describing physical LTI systems and dynamic networks have been presented. Based on several modelling aspects, the polynomial model, module representation, and interaction-oriented model are selected as the most attractive ones for modelling and identification of physical linear networks.

The discussion on the network models raises the question of how theory developed in one domain is connected to other domains. To answer this question, more research is needed on the different network models. This additional research will also support the final decision on which model is most suitable for modelling and identification of physical linear networks. Therefore, the relations between the network models are further investigated in Chapter 3, 4, 5, and 7.

In this chapter, the focus was mainly on the mathematical part of the models. It has been shown that dynamic networks can be represented on different structural levels. This graphical aspect of the network modes is further studied in Chapter 3 and 4. This also gives insight into how the different linear dynamic network models are related to each other.

3 | Graphical structures of linear dynamic networks

Systems in the natural and physical world can be described in various ways. There also exist several models for interconnections of these physical systems. To each of them, a graphical representation is associated that depicts the internal structure of the network. Four structural representations of dynamic networks are discussed and the relations between them are interpreted. Two of them are further studied by comparing two specific network models: the module representation from the network identification domain and the interaction-oriented model from the network control field. It follows that these two network models can be transformed into one another, which connects the network identification domain with the network control field.

3.1 Introduction

Networks can be found in various different research areas, including biology, economy, engineering, physics, and social sciences (Ren et al., 2005; Boccaletti et al., 2006; Mesbahi and Egerstedt, 2010). All these research areas have their own environment with specific conditions and unique issues. This gives rise to research questions that are pertinent to the particular situation. Therefore, each research area has its own unique way of expressing its problem. The choice of model structure to describe or represent these networks is usually aligned with the environment, preconditions, model objectives, and questions. This leads to numerous models for describing linear networks, each of which is tailored to a particular situation.

Every network model consists of two parts: the dynamics characterising the behaviour of the network and the structure representing the topology of the

network. The dynamics is modelled by mathematical relations, for which many models exist. The structure is depicted by a graph and is a property of the network model, not of the network itself. Therefore, every network model has its own graph. All network models have their own aspects of attention and thus, they include different network information. As a result, dynamic networks can be represented on different structural levels, including different topological information.

Four main network structures have been introduced in the literature (Yeung et al., 2010, 2011a; Chetty and Warnick, 2020). The complete computational structure contains the most detailed information on the internal interconnection structure of the network. On the other hand, the manifest structure contains the least topological information. In between these extremes are the signal structure and the subsystem structure, which consider the network as an interconnection of signals or dynamic subsystems, respectively. The differences and similarities between these two structural network representations received much attention (Yeung et al., 2011b; Chetty and Warnick, 2015; Warnick, 2015). Moreover, the signal structure is depicted by a graph with the signals in the vertices and the dynamic relations in the edges, while the subsystem structure is depicted by a graph with the subsystems in the vertices and the signals in the edges.

The interaction-oriented model is a popular network model in the domain of distributed control (Lunze, 1992; Dullerud and D'Andrea, 2004; Langbort et al., 2004; Steentjes et al., 2021; Bullo, 2022). In this model, a dynamic network is viewed as a set of subsystems that interact with each other through possibly dynamic interconnections. Here, the focus is on the subsystems and the interconnections between them and thus, this network model has a subsystem structure.

In data-driven identification of dynamic networks, the module representation is a popular model (Gonçalves and Warnick, 2008; Van den Hof et al., 2013; Hendrickx et al., 2019; Materassi and Salapaka, 2020; van Waarde et al., 2020). A dynamic network consists of signals of interest that are interconnected through dynamic transfer function modules. In this network model, the focus lies on the behaviour of the signals and the relations between them and therefore, this network model has a signal structure.

In this chapter, the four main network structure representations are reviewed and the relations between them are discussed. The connections between the structural representations are important to give insight into how to include or exclude information in the network model and the consequences of this. The relations between graphs with signals in the vertices and dynamics in the edges and graphs with subsystems in the vertices and signals in the edges are studied, as well as the question of how a preference for one of the two different representations

can be judged. The subsystem structure and signal structure are further examined by comparing extended versions of the module representation (Van den Hof et al., 2013) and the interaction-oriented model (Lunze, 1992).

This chapter investigates the graphical representations of linear dynamic networks. The structure of network models can graphically be represented on different levels of detail as explained in Section 3.2. The relation between the module representation and the interaction-oriented model is further investigated in Section 3.3. In Section 3.4 the insights that are gained are discussed, after which Section 3.5 concludes the chapter.

3.2 Different levels of detail

3.2.1 Network structures

Introduction

The graphical part of a network model shows the topology of the network. This representation of the interconnection structure of the network can include different levels of detailed information, which depends on the chosen modelling technique. Four main network structure representations are presented in the literature (Yeung et al., 2010, 2011a,b; Chetty and Warnick, 2015; Warnick, 2015; Chetty and Warnick, 2020). In this section, these network structures are presented in a slightly different way to make the connection with several network models, such as the module representation and the interaction-oriented model. The relations between the network structures are interpreted to gain insight on the advantages and disadvantages of each structural representation.

A dynamic system constrains the behaviour of its *manifest variables* (the variables of interest), possibly through *latent variables* (auxiliary variables) that are internally hidden in the system. A network consists of the interconnection of a number of dynamic subsystems, all with their own manifest variables. The manifest variables of the network are a subset of the set of manifest variables of all the subsystems it contains. This means that some variables that are manifest for the subsystems may be latent for the network.

Complete computational structure

The most precise description of the network includes all the details. It maximally zooms in on the network and includes all manifest and latent network variables

and all relations between them, as described by *atomic systems*. In linear dynamic systems, the behaviour of an atomic system is described by first-order and static relations, otherwise there are additional (latent) variables internal to atomic systems. A network thus consists of atomic subsystems that are interconnected through their manifest variables. This most precise network representation is referred to as the *complete computational structure*.

Definition 3.1 (Complete computational structure (Yeung et al., 2010)). *The* complete computational structure *describes first-order and static relations between manifest and latent variables. It is depicted by a graph with vertices representing the atomic subsystems and with edges corresponding to the manifest and latent variables.*

The complete computational structure is an exact description of the relations between all variables in the network. The internal structure of the network is thus completely described. An example of such a representation for linear time-invariant (LTI) models is a state-space model, where the manifest variables are the input and output variables and the latent (internal) variables are the state variables. The manifest and latent variables are related through static and first-order equations.

Manifest structure

On the other extreme, all internal structure is left out of the representation. This representation maximally zooms out of the network and only includes the behaviour between the manifest variables. Therefore, this network representation is referred to as the *manifest structure*.

Definition 3.2 (Manifest structure (Yeung et al., 2010)). *The* manifest structure *describes the relations between manifest variables. It is depicted by a graph with vertices representing the manifest variables and with edges corresponding to the behaviour of ordered pairs of manifest variables.*

As the manifest structure only contains the relations between the manifest variables, it includes no information on any internal variable or on the internal structure of the network. An example of a manifest structure for LTI models is an input-output relation, such as a transfer function representation, where only the relations from input variables to output variables are described. Therefore, the manifest structure is sometimes referred to as the *input-output structure*.

Subsystem structure

In between the two extreme situations described by the complete computational structure and the manifest structure, there exist many intermediate structures. These intermediate structures represent the network as the interconnection of several distinct subsystems. The subsystems are distinct in the sense that the latent variables of a subsystem are distinct from the latent variables of the other subsystems in the network. The latent variables of a subsystem are hidden in the subsystem and therefore, are referred to as *hidden variables* or *hidden states* (Warnick, 2015). These subsystems consist of one or multiple joint atomic systems and therefore, the subsystems are not restricted to having static or first-order dynamics and can also have higher-order dynamics. In general, these intermediate structures only partially reveal the internal interconnection structure of the network, while the remaining part is hidden in the subsystems. The most interesting intermediate structure is the one that has the highest number of subsystems that are interconnected through the manifest variables of the network. This intermediate representation is referred to as the *subsystem structure*.

Definition 3.3 (Subsystem structure (Yeung et al., 2010)). *The* subsystem structure *describes the relations between manifest variables with the highest number of distinct subsystems. It is depicted by a graph with vertices representing the subsystems and with edges corresponding to the manifest variables.*

If every subsystem is atomic, the subsystem structure is equal to the complete computational structure. If all subsystems are interconnections between pairs of manifest variables, the subsystem structure is equivalent to the manifest structure. Examples of LTI models that have a subsystem structure are the interaction-oriented model (Lunze, 1992), the behavioural model (Willems, 2007), and port-Hamiltonian models (van der Schaft and Maschke, 2013).

Signal structure

The above three structures are very general representations of the network in the sense that a network is viewed as the interconnections of subsystems, while the exact modelling technique that is used to describe the dynamics of the subsystems remains free. Therefore, these structures do not limit themselves to linear or time-invariant behaviour or causal dependencies. The subsystems can be modelled very generally in the behavioural framework as defined in Definition 2.38.

Motivated from a system identification perspective, where the network structure is recovered from data, is a network structure in which the manifest variables

are related through causal dependencies. The manifest variables, or manifest signals, are central to this network structure instead of the (subsystem) dynamics. Therefore, this network representation is referred to as the *signal structure*.

Definition 3.4 (Signal structure (Yeung et al., 2010)). *The* signal structure *describes the network dynamics by causal dependencies among its manifest variables. It is depicted by a graph with vertices representing the manifest variables and with edges corresponding to the causal influences of ordered pairs of manifest variables on each other.*

The causal relations between the manifest variables are sometimes referred to as dynamic *modules*. They include input-output relations to describe the directed information flow of one manifest signal to another. These relations are not restricted to being static or first-order and can also be higher-order. In the latter case, the modules contain latent variables that are hidden in the modules. The modules in the signal structure are allowed to have hidden (latent) variables that are the same among several modules. These variables are said to be *shared* among the modules and therefore, are referred to as *shared hidden variables* or *shared hidden states* (Warnick, 2015). Examples of LTI models that have a signal structure are the polynomial model (Ljung, 1999; Hannan and Deistler, 2012), (dynamic) Bayesian model (Koller and Friedman, 2009), Wiener filter model (Materassi and Innocenti, 2010), dynamical structure function (Gonçalves and Warnick, 2008), and module representation (Van den Hof et al., 2013).

3.2.2 Relations between the network structures

The relations among the four network structures that are presented in Section 3.2.1 are also studied in literature (Yeung et al., 2010, 2011a,b; Chetty and Warnick, 2015; Warnick, 2015; Chetty and Warnick, 2020). These relations are clarified by the following observations.

The complete computational structure includes all structural information in the network model, while the manifest structure excludes all internal structural information from the network model. In between these two extremes are many intermediate frameworks that include some structural information. The most significant intermediate frameworks are the subsystem structure and the signal structure.

Excluding structural information from the model can be seen as zooming out of the network and is performed with abstractions (performed by eliminating variables from the model). In particular, a manifest abstraction from a complete computational structure is, for example, a transfer function representation of a

state-space model, which is known to have a unique result. Including more structural information in the model can be seen as zooming in on the network and is performed with realisations, which are nonunique. In particular, the complete computational structure realisation from a manifest structure is, for example, a state-space realisation of a transfer function model. Hence, the relation between the manifest structure and the complete computational structure is the same as the relation between the transfer function and state-space representation for LTI models, where a transfer function possesses numerous state-space realisations, while every state-space model specifies a unique transfer function.

The complete computational structure is the only structure that contains latent variables. The signal structure, subsystem structure, and manifest structure describe only relations between manifest variables. In an input-output setting, the manifest structure describes closed-loop relations between manifest variables, that is, relations from input variables to output variables. The subsystem structure and the signal structure describe open-loop relations between manifest variables, that is, they also describe the influence that output variables have on each other. Therefore, the subsystem structure and the signal structure contain more structural information than the manifest structure, as the influences of manifest variables on each other are included in the representation.

Both the complete computational structure and the subsystem structure are represented by a graph with vertices that represent dynamics and edges that represent variables. Conversely, both the signal structure and the manifest structure are represented by a graph with vertices that represent variables and edges that represent dynamics. This contradiction is due to the following: The complete computational structure and the subsystem structure represent the internal structure between distinct dynamics, captured by multivariable subsystems (that are atomic in the complete computational structure). The edges are tools to represent the interconnections between these subsystems, which are realised by latent and manifest variables that are shared among subsystems. Hence, the subsystems and the structure between them are the main information to depict. The signal structure and the manifest structure represent the influences between pairs of manifest variables (which are causal relations in the signal structure). The exact relations, which can share dynamics among them, are of less importance. The manifest variables and the (causal) influences between them are the main information to depict.

The subsystem structure follows naturally from block diagrams, where the subsystems have a central role, while the signal structure follows naturally from signal processing, where the signals are in the spotlight. In the subsystem structure, every subsystem is distinct, meaning that each subsystem has latent variables (or hidden variables) that are distinct from the ones from other subsystems in the

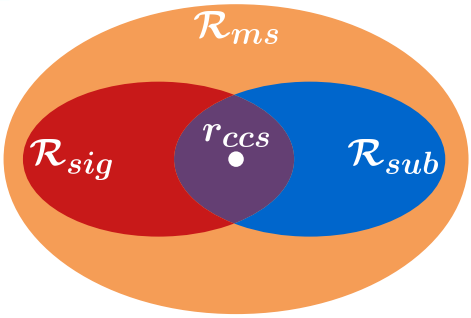

Figure 3.1: The set of all realisations of the signal structure $\mathcal{R}_{sig}$ (red oval), subsystem structure $\mathcal{R}_{sub}$ (blue oval), and manifest structure $\mathcal{R}_{ms}$ (orange oval) of a particular complete computational structure r_{ccs} (white dot).

network. As a result of this, subsystems in the subsystem structure can have multiple inputs and multiple outputs. On the other hand, modules in the signal structure always have a single input and a single output. In accordance with this, the modules in a signal structure can have latent variables that are the same as the ones from other modules. In other words, modules may contain shared hidden variables.

If all modules in a signal structure are independent from each other, which means that they do not have any shared hidden states, then the modules can be seen as independent subsystems and therefore, this signal structure is equivalent to a subsystem structure. On the other hand, if all subsystems in subsystem structure are causal and have a single-input single-output (SISO) structure, which means they describe causal relations from one manifest variable to another, then the subsystems can be seen as modules and therefore, this subsystem structure is equivalent to a signal structure.

Consider a network resulting from a particular interconnection of atomic subsystems. From this complete computational structure r_{ccs}, the corresponding subsystem structure, signal structure, and manifest structure are uniquely obtained. The set of all realisations of this subsystem structure, signal structure, and manifest structure are denoted by $\mathcal{R}_{sub}$, $\mathcal{R}_{sig}$, and $\mathcal{R}_{ms}$ respectively. Then observe that $r_{ccs} \in \mathcal{R}_{sub} \subseteq \mathcal{R}_{ms}$ and $r_{ccs} \in \mathcal{R}_{sig} \subseteq \mathcal{R}_{ms}$, which is illustrated by Figure 3.1. This figure also shows the relation between the subsystem structure and signal structure, which are generally not equivalent and related to each other by $\mathcal{R}_{sub} \nsubseteq \mathcal{R}_{sig}$, $\mathcal{R}_{sig} \nsubseteq \mathcal{R}_{sub}$, and $\mathcal{R}_{sub} \cap \mathcal{R}_{sig} \neq \emptyset$ (Warnick, 2015).

3.2.3 Examples

The relations between the network structures are further clarified by two examples. In the first example, the behaviour of the subsystems is described by the behavioural approach as defined in Definition 2.38. In the second example, a network of interconnected LTI systems is considered, where the behaviour of the subsystems is described by input-output models.

Example 3.5 (Four atomic systems). *Consider four atomic systems A_i of which the behaviour is described by $A_i = (\mathbb{T}, \mathbb{W}_i^1 \times \mathbb{W}_i^2, \mathcal{B}_i)$, $i = 1, 2, 3$ and $A_4 = (\mathbb{T}, \mathbb{W}_4^1 \times \mathbb{W}_4^2 \times \mathbb{W}_4^3, \mathcal{B}_4)$. Consider a network G consisting of these four subsystems interconnected through the relations $w_1^2(t) \equiv w_4^1(t)$, $w_4^2(t) \equiv w_2^1(t)$, and $w_4^3(t) \equiv w_3^1(t)$. Let the manifest variables be $w_1^1(t)$, $w_2^2(t)$, $w_3^1(t)$, and $w_3^2(t)$ and hence, the latent variables are $w_1^2(t)$, $w_2^1(t)$, $w_4^1(t)$, $w_4^2(t)$, and $w_4^3(t)$. The interconnection structure of this network is shown in Figure 3.2a, with the manifest variables in blue and the latent variables in red.*
Make the following observations on this network:

1. *The behaviour of the complete computational structure, shown in Figure 3.2b, is given by $G_{ccs} = (\mathbb{T}, \mathbb{W}_1^1 \times \mathbb{W}_1^2 \times \mathbb{W}_2^1 \times \mathbb{W}_2^2 \times \mathbb{W}_3^1 \times \mathbb{W}_3^2, \mathcal{B}_{ccs})$.*
2. *If A_1 and A_4 are combined in a composite subsystem, the behaviour of this intermediate frame, shown in Figure 3.2c, is given by $G_{subs1} = (\mathbb{T}, \mathbb{W}_1^1 \times \mathbb{W}_2^1 \times \mathbb{W}_2^2 \times \mathbb{W}_3^1 \times \mathbb{W}_3^2, \mathcal{B}_{subs1})$.*
3. *If A_2 and A_4 are combined in a composite subsystem, the behaviour of this intermediate frame, shown in Figure 3.2d, is given by $G_{subs2} = (\mathbb{T}, \mathbb{W}_1^1 \times \mathbb{W}_1^2 \times \mathbb{W}_2^2 \times \mathbb{W}_3^1 \times \mathbb{W}_3^2, \mathcal{B}_{subs2})$.*
4. *The behaviour of the subsystem structure, shown in Figure 3.2e, is given by $G_{sub} = (\mathbb{T}, \mathbb{W}_1^1 \times \mathbb{W}_2^2 \times \mathbb{W}_3^1 \times \mathbb{W}_3^2, \mathcal{B}_{sub})$.*
5. *The behaviour of the manifest structure, shown in Figure 3.2f, is also given by $G_{ms} = G_{sub}$.*

Example 3.5 illustrates several observations that hold in general. Potentially, there exist numerous different intermediate views of the network. The complete computational structure is the intermediate frame that consists of the largest number of subsystems. It includes only atomic subsystems and possibly many latent variables. The subsystem structure is the intermediate frame that consists of

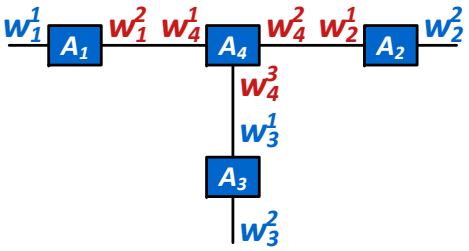

(a) The interconnection structure of the four atomic systems.

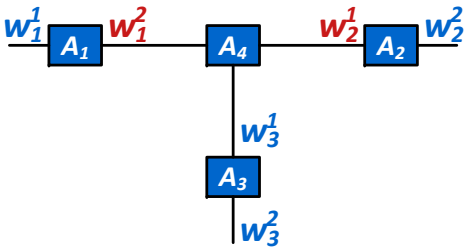

(b) The complete computational structure of G_{ccs}.

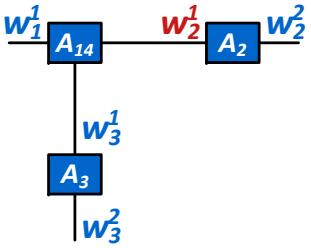

(c) The intermediate structure of G_{subs1}.

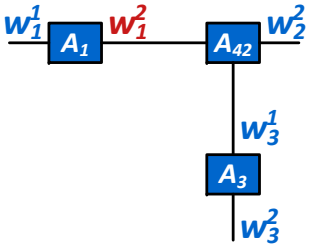

(d) The intermediate structure of G_{subs2}.

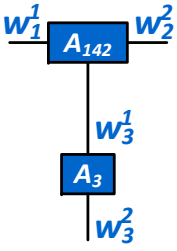

(e) The subsystem structure of G_{sub}.

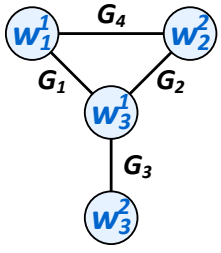

(f) The manifest structure of G_{ms}.

Figure 3.2: Six graphical structures of the network consisting of four atomic systems as described in Example 3.5, with the manifest variables in blue and the latent variables in red.

the largest number of subsystems, while only describing the behaviour between manifest variables. All latent variables are eliminated from the network. If all interconnection variables are manifest variables for the network, then the complete computational structure and the subsystem structure are equal. The difference between the subsystem structure and the manifest structure is that the manifest structure only depicts SISO relations between *pairs* of manifest variables, while the subsystem structure depicts multiple-input multiple-output (MIMO) relations between manifest variables. If all relations between the manifest variables are

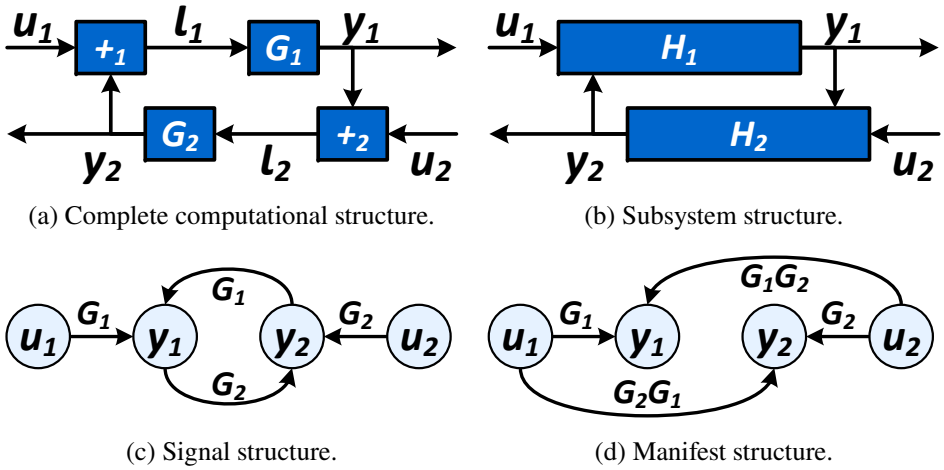

(a) Complete computational structure.

(b) Subsystem structure.

(c) Signal structure.

(d) Manifest structure.

Figure 3.3: The four graphical structures for the feedback system of Example 3.6.

SISO in the subsystem structure, this structure is equivalent to the manifest structure.

Example 3.6 (Feedback interconnection). *Consider a feedback system as shown in Figure 3.3. This network consists of four subsystems, of which* $+_1$ *and* $+_2$ *are algebraic summation equations meaning* $u_1(t) + y_2(t) = \ell_1(t)$ *and* $u_2(t) + y_1(t) = \ell_2(t)$*, respectively, and* G_1 *and* G_2 *are distinct dynamic systems. The manifest signals are the input signals* $u_1(t)$ *and* $u_2(t)$ *and the output signals* $y_1(t)$ *and* $y_2(t)$*. The latent signals are* $\ell_1(t)$ *and* $\ell_2(t)$*.*
Make the following observations on this network:

1. *Figure 3.3a shows the complete computational structure if the two subsystems* G_1 *and* G_2 *are atomic. Otherwise, this figure shows an intermediate frame, where the (distinct) subsystems* G_1 *and* G_2 *contain additional latent variables.*

2. *Figure 3.3b shows the subsystem structure with subsystems* H_i *combining the subsystems* G_i *and* $+_i$*,* $i = 1, 2$*.*

3. *Figure 3.3c shows the signal structure, which depicts the causal dependencies among the manifest variables.*

4. *Figure 3.3d shows the manifest structure, which depicts the input-output structure of the network.*

Example 3.6 illustrates several observations that hold in general. The complete computational structure and the subsystem structure contain only distinct subsystems, while the modules in the signal structure do not have to be distinct. If all modules in the signal structure are distinct, then the signal structure is equivalent to the subsystem structure. If there are no causal dependencies among the output variables, then the signal structure is equal to the manifest structure.

3.2.4 Dynamics in the vertices or in the edges

As mentioned above, the complete computational structure and the subsystem structure are represented by a graph with dynamics in the vertices and variables in the edges, while the signal structure and the manifest structure are represented by a graph with variables in the vertices and dynamics in the edges. Thus, a dynamic network can graphically be represented by a graph with the variables in the vertices and the dynamics in the edges, or by a graph with the variables in the edges and the dynamics in the vertices. The difference between the two graphical representations is a matter of user's choice (for example, based on what deserves the most attention: the dynamics or the variables) and definition: what is a 'vertex' and what is an 'edge'. In addition, it was explained before that under certain conditions, some structures can be equal or equivalent, and with that, a graph with dynamics in the vertices and variables in the edges can be equivalent to a graph with variables in the vertices and dynamics in the edges. This equivalence is further studied here, with a focus on the subsystem structure and the signal structure.

For LTI models, the interaction between subsystems is often static and occurring via a summation of variables. Think, for example, of the feedback system in Example 3.6 or Kirchhoff's current law. Applying this interaction law to the signal structure implies that a vertex is a summation point, where all incoming edges are added together to create the variable corresponding to the vertex. In general, this interaction remains implicit and hidden in the vertices of the signal structure. The module representation (Van den Hof et al., 2013) is such a signal structure that contains summation points in the vertices. It also explicitly depicts the dynamic modules in the edges.

The subsystem structure can be adapted by separating interaction dynamics from subsystem dynamics and allows for these specific latent variables. This is especially convenient when the interaction dynamics is more advanced than a simple summation of variables. Typical subsystem structure models, such as the interaction-oriented model (Lunze, 1992) and the behavioural approach (Willems, 2007), indeed model interactions separately from subsystems. The vertices can be

divided into two sets, one describing the interaction dynamics and one describing the subsystem dynamics.

In this situation, where the interactions take place through summations of variables, the link between the subsystem structure and the signal structure becomes rather easy. This is illustrated by the following examples.

Example 3.7 (Signal structure). *Consider the signal structure depicted in Figure 3.3c. Let the interactions be such that the manifest variable in each vertex is created by adding all incoming variables together, where an incoming variable is created by the dynamics on the corresponding edge multiplied by the manifest variable in the vertex from which the edge leaves. This gives*

$$y_1(t) = G_1 u_1(t) + G_1 y_2(t), \qquad y_2(t) = G_2 u_2(t) + G_2 y_1(t), \tag{3.1}$$

which is visualised in Figure 3.3a. As all dynamics in the edges are distinct, this signal structure is equivalent to the subsystem structure shown in Figure 3.3b, where each subsystem represents a dynamic module.

Example 3.8 (Subsystem structure). *Consider the subsystem structure depicted in Figure 3.3b. Let the dynamic subsystems be such that the two input variables are summed together to create a latent variable that is then applied to the subsystem dynamics to create the output. This gives*

$$y_1(t) = G_1\big(u_1(t) + y_2(t)\big), \qquad y_2(t) = G_2\big(u_2(t) + y_1(t)\big). \tag{3.2}$$

The summation of variables can be separated from the subsystem dynamics, as shown in Figure 3.3a. As the dynamic subsystems have a single input and a single output, this subsystem structure is equivalent to the signal structure shown in Figure 3.3c.

These examples illustrate that in LTI models, the static interactions (for example, summations of variables) can be separated from dynamic interactions and that if the dynamic modules in the signal structure are distinct and the subsystems in a subsystem structure are SISO, then the subsystem structure and the signal structure are equivalent.

3.2.5 Conclusion

In this section, we showed how a dynamic network can graphically be represented at different levels of detail, where the level of detail relates to the amount of structural information that is incorporated in the graph. The different network structures with corresponding graphical representations and the mechanisms of moving from one to another, by including more information in the network model and excluding information from the network model, give the user the opportunity to analyse the network at the desired level of detail.

The relation between the subsystem structure and the signal structure has already been extensively studied in the literature (Yeung et al., 2011a,b; Chetty and Warnick, 2015; Warnick, 2015) and in this section. The relations between intermediate structures, such as the subsystem structure and the signal structure, are further analysed by comparing the module representation and the interaction-oriented model in the following section, Section 3.3. More analysis of the zooming mechanisms is useful and therefore studied in Chapter 4 by analysing the relation between the complete computational structure and the signal structure.

3.3 Module representation and interaction-oriented model

3.3.1 Module representation

Consider the module representation of Van den Hof et al. (2013), as presented in Section 2.4.8, which has a signal structure. The manifest variable, or manifest signals, are located at the vertices (referred to as *nodes*) and therefore, referred to as *node signals*. The causal, dynamic influences in the edges are captured in dynamic *modules*. The node (or vertex) is a summation point, where all signals that enter are summed together to generate the node signal, which is the output signal of the node. The signals entering a node are of three types: known external excitation signals, unknown external disturbance signals, and internal (latent) output signals of dynamic modules (Van den Hof et al., 2013).

To construct an output vector with possibly partial measurements of node signals and subject to measurement noise, a measurement equation is added to the module representation. Communication between the environment and the network takes place through external input signals that enter the network and external output signals that leave the network.

This leads to the following definition of the module representation that will be considered in this chapter.

Definition 3.9 (Module representation). *A module representation consists of L internal node signals $w_1(t), \ldots, w_L(t)$; $K \leq L$ known external excitation signals $r_1(t), \ldots r_K(t)$; L unknown disturbance signals $v_{w_1}(t), \ldots, v_{w_L}(t)$; $c \leq L$ measured output signals $y_1(t), \ldots, y_c(t)$; and c sensor noise signals $v_{y_1}(t), \ldots, v_{y_L}(t)$. The behaviour of the node signals $w_j(t)$, $j = 1, \ldots, L$, and the output signals $y_j(t)$, $j = 1, \ldots, c$ is described by*

$$w_j(t) = \sum_{i \in \mathcal{N}_j} G_{ji}(q) w_i(t) + \sum_{k=1}^{K} R_{jk}(q) r_k(t) + v_{w_j}(t), \tag{3.3a}$$

$$y_j(t) = \sum_{i=1}^{L} C_{ji}(q) w_i(t) + \sum_{k=1}^{K} D_{ji}(q) r_k(t) + v_{y_j}(t), \tag{3.3b}$$

with

1. *q the shift operator meaning $qw_j(t) = w_j(t+1)$.*
2. *$\mathcal{N}_j$ the set of indices of signals $w_i(t)$ $i \neq j$ with direct paths to $w_j(t)$.*
3. *$G_{ji}(q)$ proper rational transfer function modules with $G_{jj}(q) = 0$.*
4. *$R_{jk}(q)$ stable proper rational transfer functions.*
5. *$C_{ji}(q)$ stable proper rational transfer functions.*
6. *$D_{ji}(q)$ stable proper rational transfer functions.*

Combining the expressions of all node signals and output signals results in the following matrix equations describing the full behaviour of the network.

$$w(t) = G(q)w(t) + R(q)r(t) + v_w(t), \tag{3.4a}$$

$$y(t) = C(q)w(t) + D(q)r(t) + v_y(t), \tag{3.4b}$$

where the vectors $w(t)$, $r(t)$, $v_w(t)$, $y(t)$, and $v_y(t)$ consists of elements $w_{j1}(t) = w_j(t)$, $r_{j1}(t) = r_j(t)$, $v_{w_{j1}}(t) = v_{w_j}(t)$, $y_{j1}(t) = y_j(t)$, and $v_{y_{j1}}(t) = v_{y_j}(t)$, respectively, and where $G(q)$, $R(q)$, $C(q)$, and $D(q)$ consist of elements $G_{ij}(q)$, $R_{ij}(q)$, $C_{ij}(q)$, and $D_{ij}(q)$, respectively.

The dynamic network is assumed to be stable, meaning that the transfer function matrix $\big(I - G(q)\big)^{-1}$ only contains stable transfer function elements.

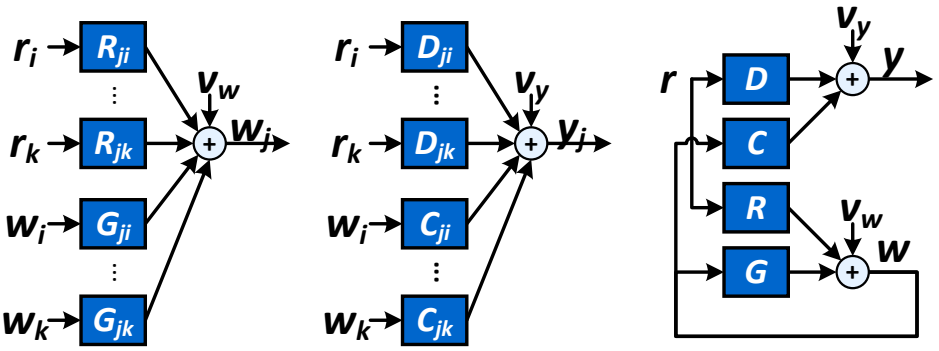

(a) Construction of the node signal $w_j(t)$ in the module representation according to (3.3a).

(b) Construction of the output signal $y_j(t)$ in the module representation according to (3.3b).

(c) Complete module representation as in (3.4) with internal network dynamics $G(q)$.

Figure 3.4: Graphical representations of (parts of) the module representation.

The dynamic network is also assumed to be well-posed, meaning that all principal minors of $\lim_{z\to\infty}\big(I - G(z)\big)$ are nonzero. Often, $R(q)$ and $C(q)$ are diagonal, binary, and known, meaning that they are selection matrices and $D(q) = 0$.

Figure 3.4a shows how a node signal is constructed in the module representation and Figure 3.4b shows how an output signal is constructed in the module representation. Using the mathematical representation of the module representation (3.4), the overall network can graphically be represented as in Figure 3.4c. The transfer function matrix $G(q)$ contains both the dynamics and the interconnection structure of the network. The module representation can be seen as dynamic plant model $G(q)$ with direct feedback and with an output signal created from the node signals and external input signals.

3.3.2 Interaction-oriented model

Consider the interaction-oriented mode of Lunze (1992), as presented in Section 2.4.9, which has a subsystem structure. The behaviour of the subsystems can be described by an input-output model, such as a state-space model or a transfer function matrix. To connect with the module representation, a transfer function matrix is used in this section. To account for disturbances and modelling errors, external disturbance signals are added to the model. Then each subsystem has two input signals: a known external input signal and an internal input signal. Each

subsystem has two output signals: an internal output signal that can be subject to disturbances and an external output signal that can be subject to measurement noise.

The dynamics of the interconnections is also described by any input-output model, which is again a transfer function here. The interconnections have the internal output signals of the subsystems as an input signal and the internal input signals of the subsystems as an output signal, which can be subject to external disturbances as well. The internal signals are not visible from the environment. The communication between the environment and the network takes place through external input signals that enter the network and external output signals that leave the network.

This leads to the following definition of the interaction-oriented model that will be considered in this chapter.

Definition 3.10 (Interaction-oriented model). *An interaction-oriented modell consists of L internal signals $s_1(t), \ldots, s_L(t)$; L internal signals $z_1(t), \ldots, z_L(t)$; $K \leq L$ known external excitation signals $u_1(t), \ldots u_K(t)$; L unknown disturbance signals $v_{s_1}(t), \ldots, v_{s_L}(t)$; L unknown disturbance signals $v_{z_1}(t), \ldots, v_{z_L}(t)$; $c \leq L$ measured output signals $y_1(t), \ldots, y_c(t)$; and c sensor noise signals $v_{y_1}(t), \ldots, v_{y_L}(t)$. The behaviour of the subsystems Σ_j is described by*

$$\Sigma_j = \begin{cases} z_j(t) = T_j^{zs}(q)s_j(t) + T_j^{zu}(q)u_j(t) + v_{z_j}(t), & \text{(3.5a)} \\ y_j(t) = T_j^{ys}(q)s_j(t) + T_j^{yu}(q)u_j(t) + v_{y_j}(t), & \text{(3.5b)} \end{cases}$$

and the behaviour of the jth interconnection is described by

$$s_j(t) = \sum_{i=1}^{L} L_{ji}(q)z_i(t) + v_{s_j}(t), \tag{3.6}$$

with q the shift operator meaning $qw_j(t) = w_j(t+1)$ and with proper rational transfer function matrices $T_j^{zs}(q)$, $T_j^{zu}(q)$, $T_j^{ys}(q)$, $T_j^{yu}(q)$, and $L_{ji}(q)$.

Combining the expressions of all subsystems and interconnections results in the following description of the overall network

$$\begin{bmatrix} z(t) \\ y(t) \end{bmatrix} = \underbrace{\begin{bmatrix} T^{zs}(q) & T^{zu}(q) \\ T^{ys}(q) & T^{yu}(q) \end{bmatrix}}_{T(q)} \begin{bmatrix} s(t) \\ u(t) \end{bmatrix} + \begin{bmatrix} v_z(t) \\ v_y(t) \end{bmatrix}, \tag{3.7}$$

with diagonal $T^{zs}(q)$, $T^{zu}(q)$, $T^{ys}(q)$, and $T^{yu}(q)$, and with network interconnections

$$s(t) = L(q)z(t) + v_s(t), \tag{3.8}$$

where $s(t)$, $u(t)$, $y(t)$, $z(t)$, $v_s(t)$, $v_y(t)$, and $v_z(t)$ consists of elements $s_{j1}(t) = s_j(t)$, $u_{j1}(t) = u_j(t)$, $y_{j1}(t) = y_j(t)$, $z_{j1}(t) = z_j(t)$, $v_{s_{j1}}(t) = v_{s_j}(t)$, $v_{y_{j1}}(t) = v_{y_j}(t)$, and $v_{z_{j1}}(t) = v_{z_j}(t)$, respectively, and where $T^{zs}(q)$, $T^{zu}(q)$, $T^{ys}(q)$, and $T^{yu}(q)$, consists of elements $T^{zs}_{jj}(q) = T^{zs}_j(q)$ and $T^{zs}_{ji}(q) = 0$ for $i \neq j$, $T^{zu}_{jj}(q) = T^{zu}_j(q)$ and $T^{zu}_{ji}(q) = 0$ for $i \neq j$, $T^{ys}_{jj}(q) = T^{ys}_j(q)$ and $T^{ys}_{ji}(q) = 0$ for $i \neq j$, $T^{yu}_{jj}(q) = T^{yu}_j(q)$ and $T^{yu}_{ji}(q) = 0$ for $i \neq j$, respectively, and where $L(q)$ consists of elements $L_{ij}(q)$.

The dynamic network is assumed to be stable, meaning that the transfer function matrix $\left(I - T_{zs}(q)L(q)\right)^{-1}$ only contains stable transfer function elements. The dynamic network is also assumed to be well-posed, meaning that all principal minors of $\lim_{z\to\infty}\left(I - T_{zs}(z)L(z)\right)$ are nonzero. Often, the interconnections described by $L(q)$ are static and only one of the disturbance signals $v_s(t)$ and $v_z(t)$ is taken into account.

Figure 3.5a shows how the signals of a single subsystem are constructed in the interaction-oriented model and Figure 3.5b shows how the signals of an interaction are constructed in the interaction-oriented model. Using the mathematical transfer function representation of the interaction-oriented model (3.7) and (3.8), the overall network can graphically be represented as in Figure 3.5c. The transfer function matrix $T(q)$ contains the dynamics of the subsystems, while $L(q)$ contains the dynamics and structure of the interactions between the subsystems. The interaction-oriented model can be seen as a dynamic plant model $T(q)$ with output feedback $L(q)$.

3.3.3 Mappings between the module representation and the interaction-oriented model

Mappings

In this section, the mapping between the interaction-oriented model and the module representation is studied. Here, a more mathematical approach is taken in comparison with Section 3.2, where network structures are compared, which is stronger based on the interpretation.

Comparing the interaction-oriented model with the module representation leads to the following observations regarding the dynamics that is present in the models. In the interaction-oriented model, the dynamics of the subsystem and

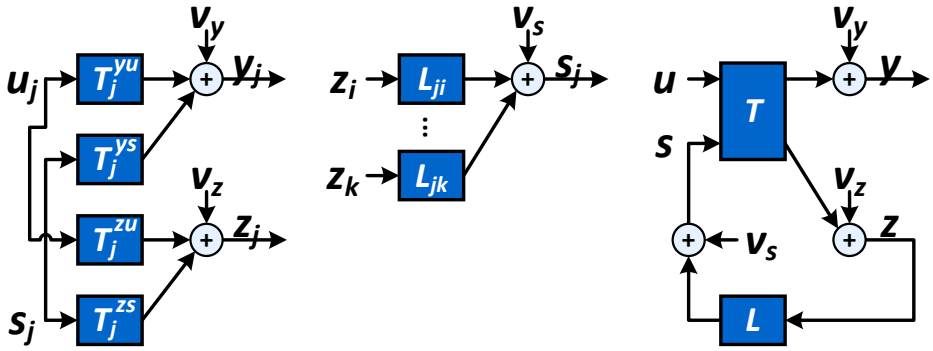

(a) Construction of the output signals of a subsystem in the interaction-oriented model according to (3.5).

(b) Construction of the output signal of an interaction in the interaction-oriented model according to (3.6).

(c) Complete interaction-oriented model as in (3.7) and (3.8) with system dynamics $T(q)$ and interactions $L(q)$.

Figure 3.5: Graphical representations of (parts of) the interaction-oriented model.

the dynamics of the interconnections are separated from each other, while in the module representation, all dynamics is combined in the dynamic modules. In the interaction-oriented model, the four main signals ($s(t)$, $z(t)$, $u(t)$, and $y(t)$) are attributed to the subsystems: each subsystem has an internal and an external input and an internal and an external output signal. In the module representation, on the other hand, the three main signals ($w(t)$, $r(t)$, and $y(t)$) cannot be tightened to a module. For example, the internal signals $w(t)$ can enter multiple modules and the external signals are not even necessarily tight to a single internal signal $w(t)$ (although the latter is often the case in practice).

Furthermore, both models have a single known external excitation signal ($r(t)$ in the module representation and $u(t)$ in the interaction-oriented model) and both models have a single external output signal $y(t)$ with measurement noise $v_y(t)$. These signals have the same interpretation for both models. The module representation has two types of internal signals: $w(t)$, influenced by the disturbance signal $v_w(t)$, and the output signals of the modules, which do not appear in the mathematical representation. The interaction-oriented model also has two internal signals: $s(t)$ and $z(t)$, influenced by disturbance signals $v_s(t)$ and $v_z(t)$, respectively.

Every interaction-oriented model can be mapped into a module representation by equating either one of the internal signals $s(t)$ or $z(t)$ to the internal signal $w(t)$ of the module representation and eliminating the other one from the representation.

In both cases, the dynamics of the interconnections is combined with the dynamic subsystems to create the modules. However, in each cases, this is done differently, leading to different module representations. Hence, there are at least two different module representations for each interaction-oriented model.

On the other hand, splitting the dynamic modules into dynamic subsystems and interconnections is less straightforward. Module representations with $R(q)$, $C(q)$, and $D(q)$ diagonal, can be mapped into an interaction-oriented model by equating the interconnection dynamics of the interaction-oriented model to the dynamic modules in the module representation and capturing the input and output dynamics, described by $R(q)$, $C(q)$, and $D(q)$, by the subsystems. The reason for the requirement of diagonality of $R(q)$, $C(q)$, and $D(q)$ is that the interaction-oriented model only allows for a single external input and output signal in the subsystems, while all dynamic interconnections are between internal signals.

From interaction-oriented model to module representation: eliminating *s(t)*

Eliminating the internal signal $s(t)$ from an interaction-oriented model leads to a module representation.

Proposition 3.11 (Interaction-oriented model to module representation). *An interaction-oriented model described by* (3.5) *and* (3.6) *is equivalent to a module representation* (3.3) *with*

1. *Internal signals* $w_j(t) = z_j(t)$.
2. *Unknown external disturbance signals* $v_{w_j}(t) = T_j^{zs}(q)v_{s_j}(t) + v_{z_j}(t)$.
3. *Known external excitation signals* $r_k(t) = u_j(t)$ *with* $k = j$ *and* $K = L$.
4. *External output signals* $y_j(t) = y_j(t)$.
5. *Unknown measurement noise signals* $v_{y_j}(t) = T_j^{ys}(q)v_{s_j}(t) + v_{y_j}(t)$.
6. *Dynamic modules* $G_{ji}(q) = T_j^{zs}(q)L_{ji}(q)$.
7. *Input dynamics* $R_{jj}(q) = T_j^{zu}(q)$ *and* $R_{ji}(q) = 0$ *for* $i \neq j$.
8. *Output dynamics* $C_{ji}(q) = T_j^{ys}(q)L_{ji}(q)$.
9. *Output dynamics* $D_{jj}(q) = T_j^{yu}(q)$ *and* $D_{ji}(q) = 0$ *for* $i \neq j$..

Proof: Eliminating $s_j(t)$ from the interaction-oriented model by substituting

(3.6) into (3.5) leads to

$$\Sigma_j = \begin{cases} z_j(t) = T_j^{zs}(q) \sum_{i=1}^{L} L_{ji}(q) z_i(t) + T_j^{zu}(q) u_j(t) + T_j^{zs}(q) v_{s_j}(t) + v_{z_j}(t), \\ y_j(t) = T_j^{ys}(q) \sum_{i=1}^{L} L_{ji}(q) z_i(t) + T_j^{yu}(q) u_j(t) + T_j^{ys}(q) v_{s_j}(t) + v_{y_j}(t), \end{cases}$$

which is a module representation (3.3) with 1.-9. ■

Proposition 3.11 shows that the external signals of the interaction-oriented model and the module representation are equal. Every node signal and every output signal is excited by (at most) one known external excitation signal, which is captured by the diagonality of the input transfer function matrix $R(q)$ and the feedthrough output matrix $D(q)$. In addition, if $v_{s_j}(t)$ is absent in the interaction-oriented model, then $v_{w_j}(t) = v_{z_j}(t)$ and $v_{y_j}(t) = v_{y_j}(t)$. This means that $v_{z_j}(t)$ in the interaction-oriented model has the same role as $v_{w_j}(t)$ in the module representation, which also follows naturally from the fact that the node signal in the module representation becomes the remaining internal signal of the interaction-oriented model, that is $w_j(t) = z_j(t)$.

Self-loops are present in the resulting module representation if $L_{jj} \neq 0$, because then $G_{jj}(q) \neq 0$. The transfer function modules have shared hidden dynamics in the sense that some transfer functions have common dynamics that are not explicitly measured. This common dynamics is the following: $G_{ji}(q), \forall j$, have common dynamics $T_j^{zs}(q)$; $C_{ji}(q), \forall j$, have common dynamics $T_j^{ys}(q)$; and $G_{ji}(q)$ and $C_{ji}(q)$ have common dynamics $L_{ji}(q)$. Hence, the interconnection structure from node signal $w_i(t)$ to node signal $w_j(t)$ and to output signal $y_j(t)$ is the same and described by $L_{ji}(q)$. If $v_{s_j}(t)$ is present, then the models of the disturbance signals $v_{w_j}(t)$ and $v_{y_j}(t)$ share dynamics with $G_{ji}(q)$ and $C_{ji}(q)$, respectively. If $T_j^{ys}(q) = T_j^{zs}(q)$ and $T_j^{yu}(q) = T_j^{zu}(q)$, then $y_j(t) = w_j(t) + v_{y_j}(t) - v_{z_j}(t)$.

Figure 3.6 illustrates the transformation from the interaction-oriented model to the module representation by eliminating the internal signals $s_j(t)$. Figure 3.6a shows the interaction-oriented model. First, the interactions $L(q)$ are split into SISO interconnections described by $L_{21}(q)$ and $L_{31}(q)$ and second, the system Σ_1 with dynamics $T_1(q)$ is split into SISO systems, with dynamics described by the transfer functions $T_1^{zs}(q)$, $T_1^{zu}(q)$, $T_1^{ys}(q)$, and $T_1^{yu}(q)$, resulting in Figure 3.6b. Third, the internal signal $s_1(t)$ is eliminated from the network through immersion (Dankers et al., 2016), leading to new SISO dynamic systems, as shown in Figure 3.6c. Finally, the network of Figure 3.6c is related to the module representation (3.4) and the dynamic blocks and the signals are renamed accordingly, resulting in the module representation shown in Figure 3.6d.

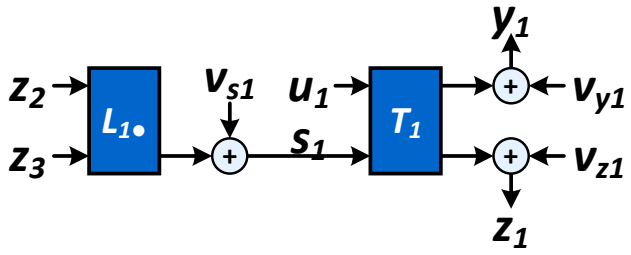

(a) Interaction-oriented model.

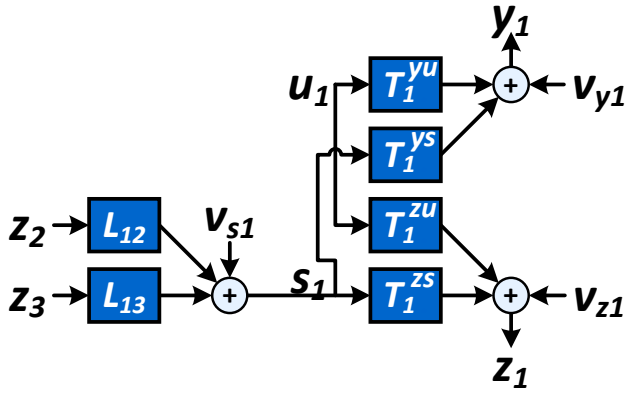

(b) SISO systems and interconnections.

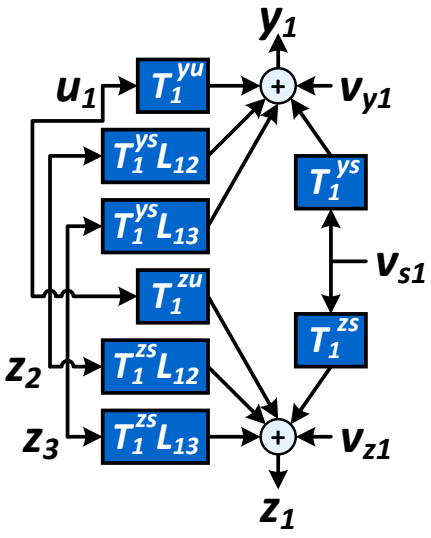

(c) Combined transfer functions.

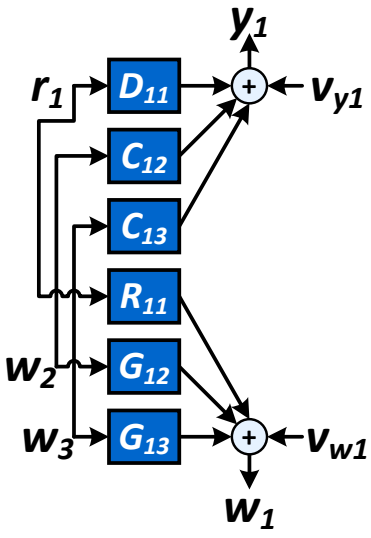

(d) Module representation.

Figure 3.6: Interaction-oriented model transformed into a module representation by eliminating internal variable $s(t)$.

From interaction-oriented model to module representation: eliminating *z(t)*

Eliminating the internal signal $z(t)$ from an interaction-oriented model also leads to a module representation, but a different one than for eliminating the internal signal $s(t)$ from the interaction-oriented model.

Proposition 3.12 (Interaction-oriented model to module representation). *An interaction-oriented model described by* (3.5) *and* (3.6) *is equivalent to a module representation* (3.3) *with*

1. *Internal signals* $w_j(t) = s_j(t)$.
2. *Unknown external disturbance signals* $v_{w_j}(t) = \sum_{i=1}^{L} L_{ji}(q) v_{z_i}(t) + v_{s_j}(t)$.
3. *Known external excitation signals* $r_k(t) = u_j(t)$ *with* $k = j$ *and* $K = L$..
4. *External output signals* $y_j(t) = y_j(t)$.
5. *Unknown measurement noise signals* $v_{y_j}(t) = v_{y_j}(t)$.
6. *Dynamic modules* $G_{ji}(q) = L_{ji}(q) T_i^{zs}(q)$.
7. *Input dynamics* $R_{ji}(q) = L_{ji}(q) T_i^{zu}(q)$.
8. *Output dynamics* $C_{jj}(q) = T_j^{ys}(q)$ *and* $C_{ji}(q) = 0$ *for* $i \neq j$.
9. *Output dynamics* $D_{jj}(q) = T_j^{yu}(q)$.

Proof: Eliminating $z_j(t)$ from the interaction-oriented model by substituting (3.5a) into (3.6) gives

$$\Sigma_j = \begin{cases} s_j(t) = \sum_{i=1}^{L} L_{ji}(q) \left[T_i^{zs}(q) z_i(t) + T_i^{zu}(q) u_i(t) + v_{z_i}(t) \right] + v_{s_j}(t), \\ y_j(t) = T_j^{ys}(q) s_j(t) + T_j^{yu}(q) u_j(t) + v_{y_j}(t), \end{cases}$$

which is a module representation (3.3) with 1.-9. ■

Proposition 3.11 shows that the input and output signals of the interaction-oriented model and the module representation are equal. Every output signal is determined by exactly one node signal and at most one input signal, which is captured by the diagonality of the output transfer function matrix $C(q)$ and the

feedthrough output matrix $D(q)$. In addition, if $v_{z_j}(t)$ is absent in the interaction-oriented model, then $v_{w_j}(t) = v_{s_j}(t)$. This means that $v_{s_j}(t)$ in the interaction-oriented model has the same role as $v_{w_j}(t)$ in the module representation, which also follows naturally from the fact that the node signal in the module representation becomes the remaining internal signal of the interaction-oriented model, that is $w_j(t) = s_j(t)$.

Self-loops are present in the resulting module representation if $L_{jj} \neq 0$, because then $G_{jj}(q) \neq 0$. The transfer function modules have shared hidden dynamics in the sense that some transfer functions have common dynamics that are not explicitly measured. This common dynamics is the following: $G_{ji}(q)$, $\forall i$, have common dynamics $T_i^{zs}(q)$; $R_{ji}(q)$, $\forall i$, have common dynamics $T_i^{zu}(q)$; and $G_{ji}(q)$ and $R_{ji}(q)$ have common dynamics $L_{ji}(q)$, which are also present in the model of the external disturbance $v_{w_j}(t)$ if $v_{z_j}(t)$ is present. Hence, the interconnection structure from input signal $r_i(t)$ and node signal $w_i(t)$ to node signal $w_j(t)$ is the same and described by $L_{ji}(q)$.

Figure 3.7 illustrates the transformation from the interaction-oriented model to the module representation by eliminating the internal signals $z_j(t)$. Figure 3.7a shows the interaction-oriented model. First, the interactions $L(q)$ are split into SISO interconnections described by $L_{12}(q)$ and $L_{13}(q)$ and second, the systems Σ_i, $i = 1, 2, 3$, with dynamics $T_i(q)$, $i = 1, 2, 3$, are split into SISO systems, with dynamics described by the transfer functions $T_i^{zs}(q)$, $T_i^{zu}(q)$, $T_i^{ys}(q)$, and $T_i^{yu}(q)$, $i = 1, 2, 3$, resulting in Figure 3.7b. Third, the internal signals $z_2(t)$ and $z_3(t)$ are eliminated from the network through immersion (Dankers et al., 2016), leading to new SISO dynamic systems, as shown in Figure 3.7c. Finally, the network of Figure 3.7c is related to the module representation (3.4) and the dynamic blocks and the signals are renamed accordingly, resulting in the module representation shown in Figure 3.7d.

From module representation to interaction-oriented model

Consider a module representation with diagonal $R(q)$, $C(q)$, and $D(q)$, that is $R_{ji}(q) = 0$, $C_{ji}(q) = 0$, and $D_{ji}(q) = 0$ for $i \neq j$. Equating the interconnection dynamics $L_{ji}(q)$ of the interaction-oriented model to the dynamic modules $G_{ji}(q)$ in the module representation and capturing the input and output dynamics, described by $R_{jj}(q)$, $C_{jj}(q)$, and $D_{jj}(q)$ by the subsystem Σ_j, leads to an interaction-oriented model.

Proposition 3.13 (Module representation to interaction-oriented model). *A module representation* (3.3) *with* $R(q)$, $C(q)$, *and* $D(q)$ *diagonal is*

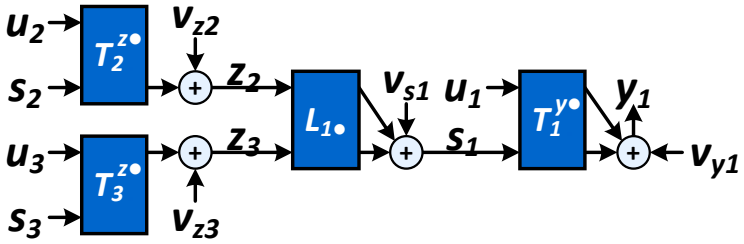

(a) Interaction-oriented model.

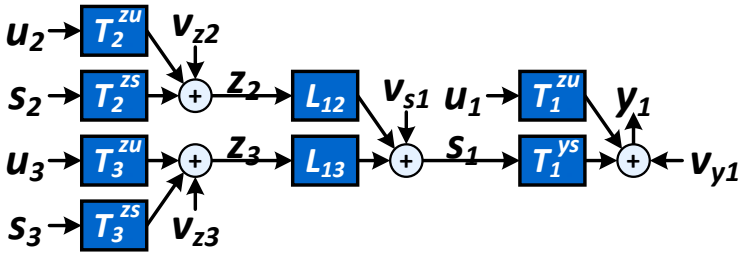

(b) SISO systems and interconnections.

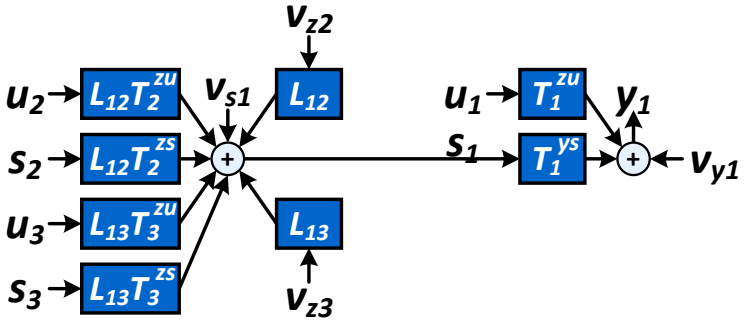

(c) Combined transfer functions.

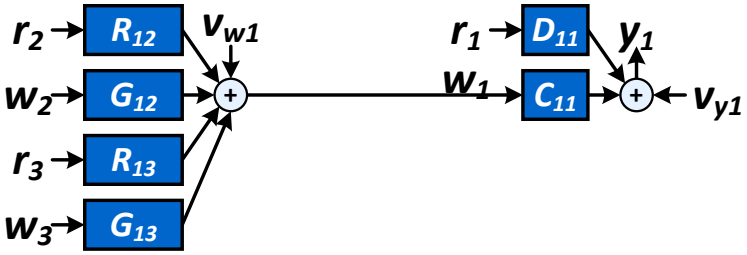

(d) Module representation.

Figure 3.7: Interaction-oriented model transformed into a module representation by eliminating internal variable $z(t)$, where $L_{1\bullet}$ indicates the first row of $L(q)$ and $T_i^{z\bullet}$ and $T_i^{y\bullet}$ indicate the rows of $T_i(q)$ corresponding to z and y, respectively.

equivalent to an interaction-oriented model described by (3.5) *and* (3.6) *with*

1. *Internal signals* $z_j(t) = w_j(t)$.
2. *Unknown external disturbance signals* $v_{z_j}(t) = v_{w_j}(t)$.
3. *Unknown external disturbance signals* $v_{s_j}(t) = 0$.
4. *Known external excitation signals* $u_j(t) = r_k(t)$ *for all* $j = k$.
5. *External output signals* $y_j(t) = y_j(t)$.
6. *Unknown measurement noise signals* $v_{y_j}(t) = C_{jj}(q)v_{w_j}(t) + v_{y_j}(t)$.
7. *Subsystem internal input dynamics* $T_j^{zs}(q) = I$.
8. *Subsystem external input dynamics* $T_j^{zu}(q) = R_{jj}(q)$.
9. *Subsystem internal output dynamics* $T_j^{ys}(q) = C_{jj}(q)$.
10. *Subsystem external output dynamics* $T_j^{yu}(q) = C_{jj}(q)R_{jj}(q) + D_{jj}(q)$.
11. *Interconnection dynamics* $L_{ji}(q) = G_{ji}(q)$ *for* $i \in \mathcal{N}_j$ *and* $L_{ji}(q) = 0$ *for* $i \notin \mathcal{N}_j$.

Proof: From the module representation (3.3) with $R_{ji}(q) = 0$, $C_{ji}(q) = 0$, and $D_{ji}(q) = 0$ for $i \neq j$, selecting

$$s_j(t) := \sum_{i \in \mathcal{N}_j} G_{ji}(q)w_j(t),$$

which describes the interconnections of an interaction-oriented model (3.6) with 3. and 11. Substituting this expression for $s_j(t)$ into (3.3a) and substituting (3.3a) into (3.3b) leads to

$$\begin{aligned} w_j(t) &= s_j(t) + R_{jj}(q)u_j(t) + v_{w_j}(t), \\ y_j(t) &= C_{jj}(q)s_j(t) + \big(C_{jj}(q)R_{jj}(q) + D_{jj}(q)\big)u_j(t) + C_{jj}(q)v_{w_j}(t) + v_{y_j}(t), \end{aligned}$$

which describes the subsystems of an interaction-oriented model (3.5) with 1.-2 and 4.-10. ■

Proposition 3.13 shows that the input and output signals of the module representation and the interaction-oriented model are equal. As mentioned before, the

dynamic modules are captured by the interconnections in the interaction-oriented model, while the input and output dynamics of the module representation is captured by the subsystem dynamics in the interaction-oriented model. The external output dynamics described by $T_j^{ys}(q)$ and $T_j^{yu}(q)$ include a scaled version of the internal dynamics described by $T_j^{zs}(q)$ and $T_j^{zs}(q)$. Similar, the measurement noise includes a scaled version of the external disturbance signal. This is because the external output signal in the module representation explicitly depends on the internal signal $w(t)$, which becomes the internal output signal of the subsystems in the interaction-oriented model.

Figure 3.8 shows the transformation from the module representation to the interaction-oriented model. Figure 3.8a shows the module representation. First, the vertex of $w_1(t)$ is split into two vertices (summation points) to separate the result of the (internal) interconnections from the external input dynamics. This introduces a new latent variable $s_1(t)$. Second, the paths from the external input signals $r_1(t)$ and $v_{w_1}(t)$ to the output signal $y_1(t)$ are separated from their paths to the internal signal $w_1(t)$, leading to Figure 3.8b. Third, the network of Figure 3.8b is related to the interaction-oriented model described by (3.5) and (3.6) and the dynamic blocks and the signals are renamed accordingly, as shown in Figure 3.8c. Finally, all dynamics from $u_1(t)$ and the new latent variable $s_1(t)$ to $z_1(t)$ and $y_1(t)$ are captured by two-input two-output blocks, resulting in the interaction-oriented model shown in Figure 3.8d.

3.4 Discussion

The interaction-oriented model is a subsystem structure that is often used for the control of dynamic networks. On the other hand, the module representation is a signal structure that is popular in the identification of dynamic networks. In Section 3.3, two mappings from the interaction-oriented model to the module representation and one mapping in the reverse direction have been made. The existence of these mappings proves several important connections.

First of all, the mappings imply that every subsystem structure fitting the interaction-oriented model and every signal structure fitting the module representation can be transformed into one another. Using these mappings, results for one representation can be transformed into the other one. Observe that this mapping also transforms the graphical representation and the corresponding topological information.

Second, the mappings between the interaction-oriented model and the module representation connect the network control field with the network identification

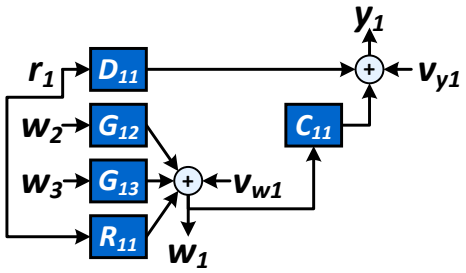

(a) Module representation.

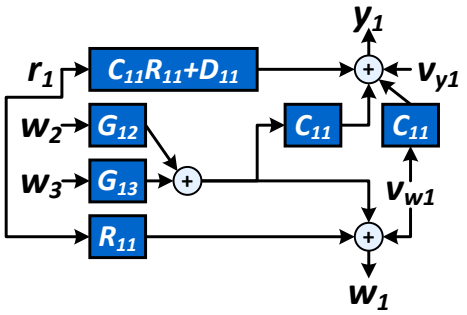

(b) Separated internal and external influences.

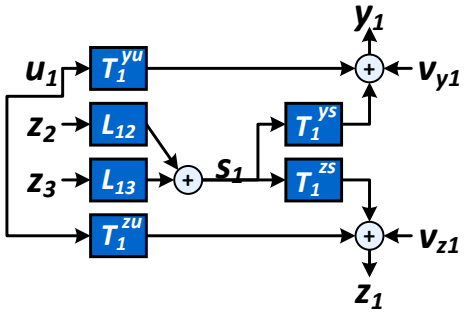

(c) Combined transfer functions.

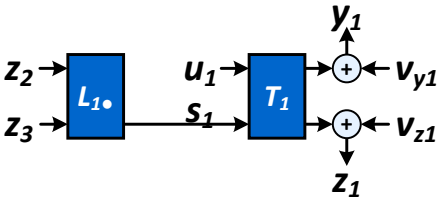

(d) Interaction-oriented model.

Figure 3.8: Module representation transformed into an interaction-oriented model by separating the internal and external influences on $w_1(t)$, where $L_{1\bullet}$ indicates the first row of $L(q)$.

domain. The control theory developed for interaction-oriented models can be mapped to module representations and the network identification theory developed for module representations can be mapped to interaction-oriented models. This means that there is no need to separately develop control theory for module representations or identification theory for interaction-oriented models, because they can use the available theory from the other domain.

Third, the two mappings from the interaction-oriented model into the module representation lead to module representations with shared dynamics in the dynamical objects. The elimination of $s(t)$ in Proposition 3.11 shows that all $G_{ji}(q)$ have common dynamics $T_j^{zs}(q)$ for all i with $L_{ji}(q) \neq 0$. A similar mechanism is present in $C_{ji}(q)$. The elimination of $z(t)$ in Proposition 3.12 shows that all $G_{ji}(q)$ and all $R_{ji}(q)$ have common dynamics $T_i^{zs}(q)$ and $T_i^{zu}(q)$, respectively, for all j with $L_{ji}(q) \neq 0$. In addition, $G_{ji}(q)$ and $R_{ji}(q)$ have common dynamics $L_{ji}(q)$ for all j, i. Even though this is allowed in signal structures according

to their definition, it is useful to take these shared dynamics into account in the parameterisation in the identification procedure to achieve minimum variance. Furthermore, identifiability analysis for module representations typically builds on the assumption that the modules do not share information (Weerts et al., 2018b).

Fourth, the mapping from the module representation to the interaction-oriented model also shows some shared dynamics between SISO transfer functions, but they are captured by the same MIMO subsystem. So, there are no shared dynamics between subsystems or interconnections, which satisfies the definition of a subsystem representation.

3.5 Conclusion

Linear dynamic network models can include different amounts of detailed information on the topology and manifest signals. Four different network structures have been presented, which represent the network at different levels of detail. A translation has been made between network structures that represent dynamics in the vertices and network structures that represent dynamics in the edges. Some of the relations between the network structure are well-studied in the literature. The relation between the signal structure and the subsystem structure is further investigated by studying the module representation and the interaction-oriented model. There exist mappings between the interaction-oriented model and the module representation, which directly connect the network control field with the network identification domain. As a result, the network identification domain can keep focusing on the module representation.

The relation between the complete computational structure and the signal structure deserves more attention and therefore, this is further studied in Chapter 4. In addition, the mechanisms of adding information to the network model or eliminating information from the network model are important for analysing networks. The consequences of this zooming mechanism are elaborated on in Chapter 4.

4 | Representations of linear dynamic networks

This chapter is a slightly extended version of

E.M.M. Kivits and P.M.J. Van den Hof. On representations of linear dynamic networks. *IFAC-PapersOnLine*, 51(15):838–843, 2018. Proceedings of the 18th IFAC Symposium on System Identification (SYSID).

Linear dynamic networks are typically described in either a state-space form or a module representation. The question is addressed under which conditions these representations are equivalent and can be transformed into one another. Hidden states and especially shared hidden states have a central position in this analysis. A consequence for identification is that multiple-input multiple-output (MIMO) parameterised modules may be necessary in order to appropriately take care of shared hidden states. Further, the construction of subnetworks in a linear dynamic network resulting in a module representation is illustrated. The module dynamic network allows to zoom in/out on/of the network to include/ exclude more detailed structural information. Zooming in and out is described by realisation and multi-path immersion, respectively.

4.1 Introduction

Linear dynamic networks are interconnections of linear dynamic systems. The attention for dynamic networks is growing, because in current day's technology, systems are increasing in complexity and size and an increasing number of systems is being interconnected. The interest in identification, control and reduction of dynamic networks is spreading over a diversity of scientific fields such as social

science, finance, computer science, bio-informatics, biology and engineering. As a result, a variety of representations of dynamic networks is developed and the question arises how these representations are related to each other.

In one part of the literature, state-space forms are used as a basis of dynamic network descriptions. State-space forms are typically related to first-principles modelling and can be very much appealing in this sense. State-space descriptions can be depicted in several ways. Often only the structure of the network is drawn in a directed or undirected graph, where the nodes are the states of the system, see e.g. Materassi and Salapaka (2015) and their references.

Sometimes, the edges of the graph are weighted with the corresponding elements of the system matrices (Chang et al., 2014), which gives some insight into the relations between the inputs, states and outputs. The weights can also be dynamic transfer functions, which closely relates to the dynamical structure function (Gonçalves et al., 2007) and the module representation (Van den Hof et al., 2013).

A dynamic network formulation in an identification context has been introduced by Van den Hof et al. (2013). Dynamic networks are considered in a node and link structure, including noise disturbances, excitation signals and sensor noises (Dankers et al., 2015). The network is based on scalar transfer function links (modules) between node signals.

Some different representations of dynamic networks are presented in literature (Yeung et al., 2010, 2011a; Chetty and Warnick, 2015; Warnick, 2015). They characterise the structure of dynamic networks on different levels. The emphasis is on the difference between the dynamical structure function and the module representation, while the relation to state-space forms is given less attention.

In terms of identification in dynamic networks, the following problems have been addressed so far: the identification of a single module (Van den Hof et al., 2013; Materassi and Salapaka, 2015; Dankers et al., 2016); the identification of all modules (Risuleo et al., 2017); the identification of the structure or topology (Materassi and Innocenti, 2010); and the identifiability of the network (Weerts et al., 2018b).

The main question in this chapter is: can a network in state-space form always be converted into a module representation without losing any information and vice versa? To answer this question, algorithms are developed to transform one network representation into the other. The focus is on discrete time systems, although the results are applicable to continuous time systems as well.

The chapter is organised as follows. Section 4.2 defines the module dynamic network and the state-space dynamic network. The relations between these two representations are described in Section 4.3. Section 4.4 extends to more general

networks. Section 4.5 describes the division of a network into subnetworks. Section 4.6 contains the discussion and Section 4.7 presents the conclusion. The proofs of the lemmas and propositions are included in the appendix following this chapter.

4.2 Representations of dynamic networks

4.2.1 Module dynamic networks

A module representation of dynamic networks as considered in this chapter is based on Van den Hof et al. (2013). A dynamic network is the interconnection of L nodes $w_j(t)$, $j = 1, \ldots, L$, and K known external excitation signals $r_k(t)$, $k = 1, \ldots, K$. Each node signal is equal to

$$w_j(t) = \sum_{i=1}^{L} G_{ji}(q) w_i(t) + \sum_{k=1}^{K} R_{jk}(q) r_k(t), \tag{4.1}$$

where $G_{ji}(q)$ and $R_{jk}(q)$ are proper rational transfer functions with q^{-1} the delay operator meaning $q^{-1}w_j(t) = w_j(t-1)$. As a further generalisation of the setup of Van den Hof et al. (2013), the signals $w_j(t)$ and $r_k(t)$ can be vector-valued in which case the related transfer functions become matrices of appropriate dimensions; additionally self-loops are allowed, i.e. $G_{ii}(q)$ is not necessarily 0.

Typically, node signals are affected by unknown disturbance signals. In this chapter, unknown inputs act similar to known inputs and therefore, disturbances are initially omitted for simplicity and considered in Section 4.4.

The expressions for the node signals (4.1) can be combined in a matrix equation describing the network as

$$w(t) = Gw(t) + Rr(t), \tag{4.2}$$

$$w(t) = (I - G)^{-1} Rr(t), \tag{4.3}$$

with matrices G and R composed of elements $G_{ji}(q)$ and $R_{jk}(q)$, respectively, and where $w(t) = \begin{bmatrix} w_1(t) & w_2(t) & \ldots & w_L(t) \end{bmatrix}^\top$ and $r(t) = \begin{bmatrix} r_1(t) & r_2(t) & \ldots & r_K(t) \end{bmatrix}^\top$. All minors of $I - G(\infty)$ should be nonzero in order to achieve a well-posed network. Equation (4.2) is a dynamical structure function as introduced by Gonçalves et al. (2007). Figure 4.1 shows a single building block of a module dynamic network.

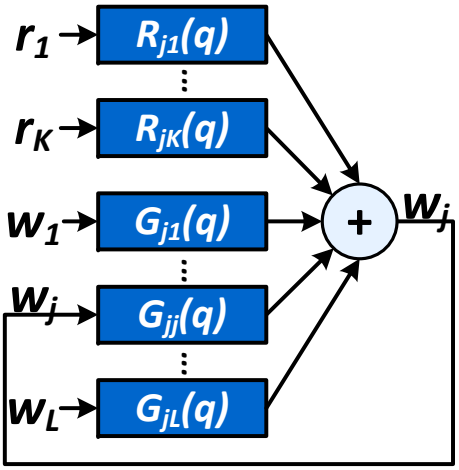

Figure 4.1: A single node of a module dynamic network.

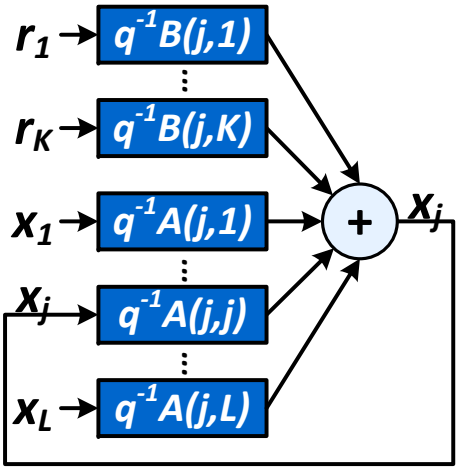

Figure 4.2: A single node of an SS dynamic network.

Definition 4.1 (Module dynamic network). *A module dynamic network is defined by the pair* (G, R) *describing a map* $r(t) \longrightarrow w(t)$ *according to* (4.3).

Definition 4.2 (Equal and equivalent networks). *Consider the well-posed networks* $\mathcal{N}_1$ *and* $\mathcal{N}_2$ *defined by the pairs* (G_1, R_1) *and* (G_2, R_2)*, respectively. The networks* $\mathcal{N}_1$ *and* $\mathcal{N}_2$ *are*

1. *equal if* $(G_1, R_1) = (G_2, R_2)$.
2. *equivalent if* $(I - G_1)^{-1}R_1 = (I - G_2)^{-1}R_2$.

A particular property of the module representations in literature is that they only allow for single-input single-output (SISO) modules and exclude self-loops. This choice has been made to avoid identifiability problems as implied by the following lemma:

Lemma 4.3 (Self-loops). *A module dynamic network with self-loops can always equivalently be written as a module dynamic network without self-loops.*

Proof: The proof is provided in Appendix 4.A. ■

In this chapter, self-loops are allowed in module dynamic networks in order to be able to link with state-space dynamic networks as described in the next section.

Network properties that depend on the structure or topology are referred to as structural or generic network properties. One such property is the *generic McMillan degree* (Karcanias et al., 2005).

Definition 4.4 (Generic McMillan degree). *Let a system be represented by a coefficient vector $\theta \in \mathbb{R}^{n_\theta}$. The generic McMillan degree of the system is the McMillan degree of the system for almost all θ, i.e. for all $\theta \in \mathbb{R}^{n_\theta}$ except for a set of measure* 0*.*

Lemma 4.5 (Generic McMillan degree). *The generic McMillan degree of a network is equal to the sum of the generic McMillan degrees of all modules in the network.*

Proof: The proof is provided in Appendix 4.B. ■

Example 4.6 (Generic McMillan degree). *Consider the electrical circuit of Example 2.9, where the relation between the voltage drop V and the current flow I is generically described by* (2.20a)*:*

$$\left(1 + (R_C + R_L)C\frac{d}{dt} + CL\frac{d^2}{dt^2}\right)V = \left(R_L + L\frac{d}{dt}\right)\left(1 + R_C C\frac{d}{dt}\right)I,$$

which has McMillan degree 2. In the special case that $R_L R_C C = L$, this relation reduces to (2.20b)*:*

$$\left(1 + R_L C\frac{d}{dt}\right)V = R_L\left(1 + R_C C\frac{d}{dt}\right)I,$$

which has McMillan degree 1. Hence, the generic McMillan degree of the electrical circuit of Example 2.9 is 2, because the McMillan degree is 2 for almost all combinations of R_L, R_C, C, and L (except for $R_L R_C C = L$).

4.2.2 State-space (SS) dynamic networks

In some research areas the behaviour of a dynamic network is mathematically described in a state-space form as

$$x(t+1) = Ax(t) + Br(t), \tag{4.4}$$

with $A \in \mathbb{R}^{L\times L}$ with elements $A(i,j) = a_{ij}$, $i,j = 1,2,\ldots,L$; $B \in \mathbb{R}^{L\times K}$ with elements $B(i,j) = b_{ij}$, $i = 1,2,\ldots,L$, $j = 1,2,\ldots,K$; and where $x(t)$ is the state

variable and $r(t)$ is a known external excitation signal. A state-space description can also be depicted as a module dynamic network. Figure 4.2 shows a single building block of a state-space dynamic network.

Definition 4.7 (State-space (SS) dynamic network). *A state-space (SS) dynamic network is a module dynamic network, as defined in Definition 4.1, with the additional properties that*

1. *Every state variable $x_j(t)$ is a node signal $w_j(t)$.*
2. *Every element in G has the form $G_{ji}(q) = q^{-1}A(j,i)$.*
3. *Every element in R has the form $R_{jk}(q) = q^{-1}B(j,k)$.*

In general, SS dynamic networks contain self-loops, because $A(i,i) \neq 0$. These diagonal elements of A represent the relation from $x_i(t)$ to $x_i(t+1)$.

4.3 Relations between module and SS dynamic networks

4.3.1 Abstraction of state-space dynamic networks

One of the major expansions of module dynamic networks compared to SS dynamic networks is that in module dynamic networks the states are grouped into a single module, while in SS dynamic networks the network is split into its core elements with modules that only have (weighted) delays. A natural step to go from SS dynamic networks to general module dynamic networks is by grouping states, that is, by removing state variables as node signals and thereby increasing the order of the dynamic terms in the modules of the network. This process is referred to as *abstraction*(Woodbury et al., 2017).

Definition 4.8 (Abstraction). *Consider the networks $\mathcal{N}_1$ and $\mathcal{N}_2$ defined by the pairs (G_1, R_1) and (G_2, R_2), respectively. $\mathcal{N}_1$ is an* abstraction *of $\mathcal{N}_2$ with respect to nodes $w_\alpha(t)$ if $(I - G_1)^{-1}R_1 = \left[(I - G_2)^{-1}R_2\right]_{w_\alpha}$, where $[T]_{w_\alpha}$ means T without the rows corresponding to nodes $w_\alpha(t)$.*

Abstracted node signals are still present in the network, but are hidden in the modules and therefore referred to as *hidden states*. Hidden states present in multiple modules are said to be shared by these modules and therefore referred to as *shared hidden states* (Warnick, 2015).

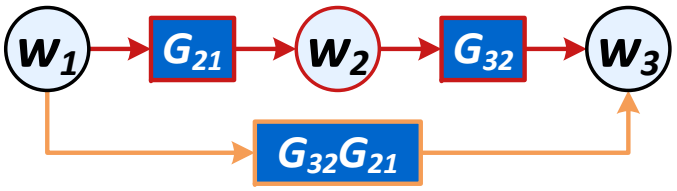

Figure 4.3: The path through w_2 is lifted by deleting the red paths and adding the orange path.

Abstraction is performed by eliminating $w_\alpha(t)$ from the node equations and this procedure and result are non-unique, since various node equations can be used for this (Weerts et al., 2020). If the node equation of $w_\alpha(t)$ itself is used as an explicit expression for $w_\alpha(t)$, this approach is referred to as *immersion* and has been worked out by Dankers et al. (2016) for module dynamic networks without self-loops and with only SISO modules, and is equivalent to vertex elimination. The immersion of several nodes has a unique result, regardless of the order in which the nodes are eliminated. This immersion process is generalised to dynamic networks with self-loops in the following algorithm and is equivalent to the Kron reduction (Dörfler and Bullo, 2013).

Algorithm 4.9 (Immersion). *An abstraction of a module dynamic network with respect to node $w_\alpha(t)$ is obtained through immersion by taking the following steps:*

1. *Substitute the node equation of $w_\alpha(t)$ into the other node equations.*
2. *Delete the node equation of $w_\alpha(t)$ from the network.*

Graphically, immersion is performed by lifting the paths through $w_\alpha(t)$ and deleting the isolated $w_\alpha(t)$.

Definition 4.10 (Lifting a path). Lifting the paths through $w_\alpha(t)$ *means that new paths are created by combining all paths entering $w_\alpha(t)$ with all paths leaving $w_\alpha(t)$.*

Example 4.11 (Lifting path). *Consider a network with three nodes w_1, w_2, and w_3 and two paths $w_1 \to w_2$ with weight G_{21} and $w_2 \to w_3$ with weight G_{32}. Lifting the path through w_2 means that the paths $w_1 \to w_2$ and $w_2 \to w_3$ are deleted and the path $w_1 \to w_3$ with weight $G_{32}G_{21}$ is added,*

as shown in Figure 4.3.

In general, this procedure of lifting paths can be performed in two ways. In the first approach, every single path through $w_\alpha(t)$ results in a new module and therefore, this approach is referred to as *single-path immersion*.

For a particular node, *local inputs* are all nodes and inputs that have direct paths towards this node and *local outputs* are all nodes that have direct paths from this node.

Algorithm 4.12 (Single-path immersion). *An abstraction of a module dynamic network with respect to node $w_\alpha(t)$ is graphically obtained through* single-path immersion *by taking the following steps:*

1. *Lift the paths from each local input, through $w_\alpha(t)$, to each local output.*
2. *Delete the isolated $w_\alpha(t)$ from the network.*

A part of the network that is present in multiple paths in the original dynamic network appears in multiple modules arising from single-path immersion. Due to this, shared hidden states are introduced and the network structure changes.

In a second approach of lifting the paths through $w_\alpha(t)$, all paths through $w_\alpha(t)$ together result in a new module and therefore, this approach is referred to as *multi-path immersion*.

Algorithm 4.13 (Multi-path immersion). *An abstraction of a module dynamic network is graphically obtained through* multi-path immersion *by Algorithm 4.12 with the modification that in step (1) the paths from all local inputs, through $w_\alpha(t)$, to all local outputs are lifted together to create one (multivariate) module.*

Algorithm 4.13 allows for MIMO modules and therefore only one module arises during multi-path immersion and hence, no shared hidden states are introduced. The main advantage of this approach is that multi-path immersion can be seen as *zooming out* of the network and excluding some detailed structural information.

Example 4.14 (Single-path immersion). *Consider a dynamic network with*

state-space description

$$\begin{bmatrix} x_1(t+1) \\ x_2(t+1) \\ x_3(t+1) \end{bmatrix} = \begin{bmatrix} 0 & 0 & a_{13} \\ a_{21} & 0 & a_{23} \\ 0 & 0 & 0 \end{bmatrix} \begin{bmatrix} x_1(t) \\ x_2(t) \\ x_3(t) \end{bmatrix} + \begin{bmatrix} 0 \\ 0 \\ b_{31} \end{bmatrix} r_1(t).$$

Its SS dynamic network is shown in Figure 4.4a with

$$G_{13} = q^{-1}a_{13},\ G_{21} = q^{-1}a_{21},\ G_{23} = q^{-1}a_{23},\ R_{31} = q^{-1}b_{31},$$

and with nodes $w_i = x_i$. Suppose that w_3 is abstracted from the network by single-path immersion. The abstraction is shown in Figure 4.4b and described by

$$\begin{bmatrix} w_1(t) \\ w_2(t) \end{bmatrix} = \begin{bmatrix} 0 & 0 \\ G_{21} & 0 \end{bmatrix} \begin{bmatrix} w_1(t) \\ w_2(t) \end{bmatrix} + \begin{bmatrix} \hat{R}_{11} \\ \hat{R}_{21} \end{bmatrix} r_1(t),$$

with

$$\hat{R}_{11} = q^{-2}a_{13}b_{31}, \qquad \hat{R}_{21} = q^{-2}a_{23}b_{31}.$$

The dynamics of $R_{31} = q^{-1}b_{31}$ appears in both modules and hence, w_3 has become a shared hidden state.

Example 4.15 (Multi-path immersion). *Consider the SS dynamic network of Example 4.14 and suppose that w_3 is abstracted from the network by multi-path immersion. The abstraction is shown in Figure 4.4c and described by*

$$\begin{bmatrix} w_1(t) \\ w_2(t) \end{bmatrix} = \begin{bmatrix} 0 & 0 \\ G_{21} & 0 \end{bmatrix} \begin{bmatrix} w_1(t) \\ w_2(t) \end{bmatrix} + \hat{R}_1 r_1(t),$$

with

$$\hat{R}_1 = \begin{pmatrix} q^{-2}a_{13}b_{31} \\ q^{-2}a_{23}b_{31} \end{pmatrix}.$$

Only one module results from immersion and hence, w_3 has not become a shared hidden state.

4.3.2 Realisation of module dynamic networks

The major difference between module dynamic networks and SS dynamic networks is that in SS dynamic networks the modules are one-dimensional state-space descriptions, while in module dynamic networks the modules contain higher-order

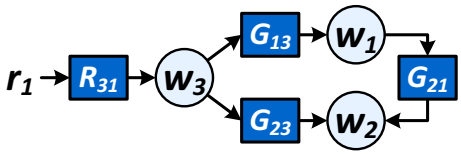

(a) The SS dynamic network of Example 4.14 and 4.15.

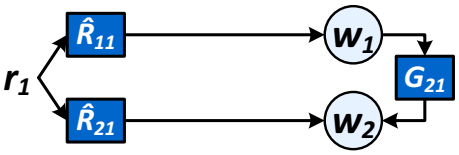

(b) The abstraction of $w_3(t)$ in (a) by single-path immersion.

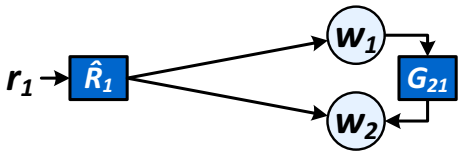

(c) The abstraction of $w_3(t)$ in (a) by multi-path immersion.

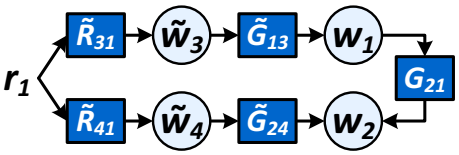

(d) A realisation of the module dynamic network in (b).

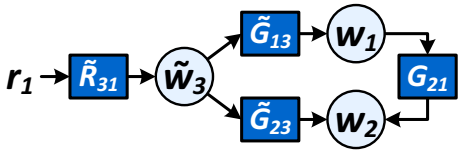

(e) A realisation of the module dynamic network in (c).

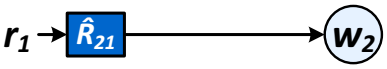

(f) The abstraction of w_1 in (b), corresponding to Example 4.21.

Figure 4.4: An SS dynamic network, three abstractions of it and realisations of two of the abstractions.

dynamics which have many possible state-space realisations. A natural step to go from a general module dynamic network to an SS dynamic network is by introducing nodes, that is, by turning state variables that correspond to a particular module into node signals and thereby decreasing the order of the dynamic terms in the modules of the network. The process of transforming a general module dynamic network into an SS dynamic network is called *realisation*.

Algorithm 4.16 (Realisation). *A realisation (SS dynamic network) of a module dynamic network is obtained by taking the following steps:*

1. *Select a module $M_\alpha(q)$.*
2. *Replace $M_\alpha(q)$ by a state-space realisation of it.*
3. *Turn all state variables into node signals and find the new modules in accordance with Definition 4.7.*

4. Repeat the procedure to realise all modules.

It is well-known that realisation is a non-unique process and therefore, the (number of) node signals added to the network depends on the state-space realisation. A minimum number of node signals is added if minimal state-space realisations are substituted into the modules. When using an observable canonical form, the outputs of the module are state variables in the new network. Realisation can be seen as zooming in on the network and including more detailed structural information.

Instead of finding realisations of all modules (to obtain an SS dynamic network), one can choose to find realisations of only some modules and instead of turning all state variables into node signals, one can choose to introduce only one or some nodes.

Example 4.17 (Realisation with shared hidden states). *Consider the module dynamic network of Figure 4.4b with*

$$\hat{R}_{11} = q^{-2}\alpha_1, \qquad \hat{R}_{21} = q^{-2}\alpha_2, \qquad G_{21} = q^{-1}\alpha_3.$$

A realisation (SS dynamic network) is found through Algorithm 4.16. It is shown in Figure 4.4d and described by

$$\begin{bmatrix} w_1(t) \\ w_2(t) \\ \tilde{w}_3(t) \\ \tilde{w}_4(t) \end{bmatrix} = \begin{bmatrix} 0 & 0 & \tilde{G}_{13} & 0 \\ G_{21} & 0 & 0 & 0 \\ 0 & 0 & 0 & 0 \\ 0 & 0 & 0 & 0 \end{bmatrix} \begin{bmatrix} w_1(t) \\ w_2(t) \\ \tilde{w}_3(t) \\ \tilde{w}_4(t) \end{bmatrix} + \begin{bmatrix} 0 \\ 0 \\ \tilde{R}_{31} \\ \tilde{R}_{41} \end{bmatrix} r_1(t),$$

with

$$\tilde{G}_{13} = q^{-1}\beta_1, \quad \tilde{G}_{24} = q^{-1}\beta_2, \quad \tilde{R}_{31} = q^{-1}\beta_3, \quad \tilde{R}_{41} = q^{-1}\beta_4,$$

where $\beta_1\beta_3 = \alpha_1$ and $\beta_2\beta_4 = \alpha_2$. This SS dynamic network has a different structure than the underlying SS dynamic network shown in Figure 4.4a, because of the shared hidden state in $\hat{R}_{11}$ and $\hat{R}_{21}$.

Example 4.18 (Realisation without shared hidden states). *Consider the module dynamic network of Figure 4.4c with*

$$\hat{R}_1 = \begin{pmatrix} q^{-2}\alpha_1 \\ q^{-2}\alpha_2 \end{pmatrix}, \qquad G_{21} = q^{-1}\alpha_3.$$

A realisation (SS dynamic network) is found through Algorithm 4.16. It is shown in Figure 4.4e and described by

$$\begin{bmatrix} w_1(t) \\ w_2(t) \\ \tilde{w}_3(t) \end{bmatrix} = \begin{bmatrix} 0 & 0 & \tilde{G}_{13} \\ G_{21} & 0 & \tilde{G}_{23} \\ 0 & 0 & 0 \end{bmatrix} \begin{bmatrix} w_1(t) \\ w_2(t) \\ \tilde{w}_3(t) \end{bmatrix} + \begin{bmatrix} 0 \\ 0 \\ \tilde{R}_{31} \end{bmatrix} r_1(t),$$

with

$$\tilde{G}_{13} = q^{-1}\beta_1, \qquad \tilde{G}_{23} = q^{-1}\beta_2, \qquad \tilde{R}_{31} = q^{-1}\beta_3,$$

where $\beta_1\beta_3 = \alpha_1$ and $\beta_2\beta_3 = \alpha_2$. This SS dynamic network has the same structure as the underlying SS dynamic network shown in Figure 4.4a.

4.3.3 Equivalence between module and SS dynamic networks

Now it is clear how to transform SS dynamic networks into general module dynamic networks and vice versa and that they are equivalent if the node signals remain invariant.

Proposition 4.19 (From SS to module dynamic network). *An SS dynamic network with minimal state-space dimension n can be transformed by abstraction into a general module dynamic network with generic McMillan degree $\geq n$, where equality holds if and only if the abstraction generates no shared hidden states.*

Proof: The proof is provided in Appendix 4.C. ■

Single-path immersion does not lead to shared hidden states if it is equivalent to multi-path immersion. The local network structure already reveals whether shared hidden states are generated by abstraction.

Proposition 4.20 (Shared hidden states).

(a) Single-path immersion of a single node leads to a shared hidden state if and only if this node has multiple local inputs or multiple local outputs.

(b) Single-path immersion of multiple nodes leads to shared hidden states if and only if at least one of the following holds:

- *The nodes jointly have multiple local inputs and at least one of the nodes has multiple local inputs.*

- *The nodes jointly have multiple local outputs and at least one of the nodes has multiple local outputs.*

(c) Multi-path immersion never leads to shared hidden states.

Proof: The proof is provided in Appendix 4.D. ■

Point (b) of Proposition 4.20 implies that the introduction of a shared hidden state can sometimes be nullified by removing an additional node from the network.

Example 4.21 (Nullified shared hidden state). *Consider the abstraction of Example 4.14 shown in Figure 4.4b. Suppose that w_1 is also removed from the network by immersion. Then $\hat{R}_{11}$, $\hat{R}_{21}$ and G_{21} are combined in one module, without shared hidden states. This module dynamic network is shown in Figure 4.4f and described by*

$$w_2(t) = \tilde{R}_2 1 r_1(t),$$

with

$$R_{21} = G_{21}\hat{R}_{11} + \hat{R}_{21} = q^{-3}a_{21}a_{13}b_{31} + q^{-2}a_{23}b_{31}.$$

The reverse transformation of abstraction is the realisation of a module dynamic network into an SS dynamic network. In this process, shared hidden states are not taken into account, because their existence is unknown.

Proposition 4.22 (From module to SS dynamic network). *A module dynamic network with generic McMillan degree n can be transformed into an equivalent SS dynamic network with state-space dimension n by realisation through Algorithm 4.16 using minimal state-space realisations.*

Proof: The proof is provided in Appendix 4.E. ■

The resulting SS dynamic network is not unique due to the freedom in creating minimal realisations of single modules. Further, shared hidden states represent the same node signal but are realised as different node signals. Sometimes the modelling procedure prevents for shared hidden states.

4.4 More general networks

4.4.1 Networks with disturbances

Dynamic networks as discussed in this chapter were only considered to have known input signals (4.2). However, the node signals of the network can also be influenced by unknown disturbance signals. Typically, these disturbance signals are modelled as realisations of stationary stochastic processes. The network is described in matrix form by

$$w(t) = Gw(t) + Rr(t) + He(t), \tag{4.5}$$

where $He(t)$ represents the disturbance signals with H monic, stable, with a stable inverse, and composed of the elements $H_{jp}(q)$, $p = 1, \ldots, P \leq L$ and with $e(t) = \begin{bmatrix} e_1(t) & e_2(t) & \ldots & e_P(t) \end{bmatrix}^\top$ a stationary white noise signal.

From (4.5) it can be seen that $e(t)$ and H have a similar role as $r(t)$ and R, respectively, and therefore, $e(t)$ and H can be considered likewise. Further, H is not part of the physics: it is just a modelling choice used for describing the unknown disturbance signals. This means that the realisations and hidden states of these modules are of less interest.

4.4.2 Networks with general measurements

The node signals of the dynamic networks discussed in this chapter were directly measured, but this is not always possible. The measurements can also be linear combinations of node signals and excitation signals and can be subject to additional sensor noise. The c measurements are then written in matrix form as

$$\tilde{w}(t) = Cw(t) + Dr(t) + s(t), \tag{4.6}$$

with $C \in \mathbb{R}^{c \times L}$ with elements $C(i, j) = c_{ij}$, $i = 1, 2, \ldots, c$, $j = 1, 2, \ldots, L$; $D \in \mathbb{R}^{c \times K}$ with elements $D(i, j) = d_{ij}$ $i = 1, 2, \ldots, c$, $j = 1, 2, \ldots, K$; and where $s(t)$ is the sensor noise.

Algorithm 4.23 (Handling general measurements). *A module dynamic network with measurements of the form* (4.6) *can be transformed into a module dynamic network with directly measured nodes by taking the following steps:*

1. *Add node signals to the network that are directly measured, i.e. equal*

to $\tilde{w}_j(t)$, $j = 1, \cdots, c$.

2. *Add the corresponding modules, containing gains of the form* $C(j,i)$, $D(j,k)$, *and* 1.

The resulting network contains unmeasured node signals $w_j(t)$, which can be removed from the network by abstraction, and measured node signals $\tilde{w}_j(t)$, which depend on the unmeasured node signals via static terms. Using abstraction, it is always possible to remove all unmeasured node signals from a module dynamic network with measurements.

4.5 Constructing subnetworks

Dynamic networks often consist of subsystems interacting with each other, where each subsystem has its own dynamics. From this point of view, a dynamic network can be seen as the interconnection of subnetworks, where a subnetwork consists of several modules and at least one node. A network can be partitioned into subnetworks by drawing boxes around certain areas in the network and grouping the interior of a box into a new module. The boxes should be non-overlapping, their terminals should be connected to inputs (r) or nodes (w) and each box should include all nodes between the modules in the box.

This method is equivalent to abstracting all nodes in the box by multi-path immersion and analogous to zooming out of the network, that is, viewing the network at a higher level, where the network consists of fewer modules and nodes.

Example 4.24 (Subnetworks). *Consider the module dynamic network of Figure 4.5a, where the red and orange box indicate subnetworks. The interiors of the red and the orange box are captured in the new modules* $\hat{R}_G$ *and* $\hat{G}_6$*, respectively, as shown in Figure 4.5b. This is the same as abstracting* w_1 *and* w_2 *in the red box and* w_5 *in the orange box by multi-path immersion.*

4.6 Discussion

Lemma 4.3 implies that module dynamic networks with self-loops in general are never a unique representation and thus cannot uniquely be identified from measurement data. This is not true for SS dynamic networks, because their

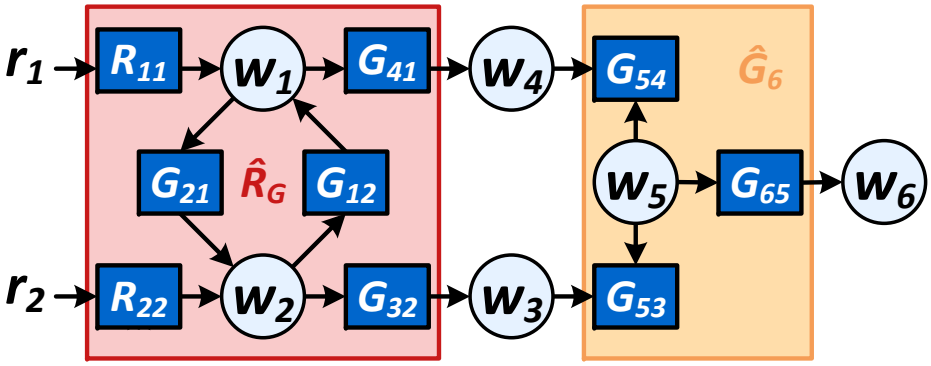

(a) The original dynamic network.

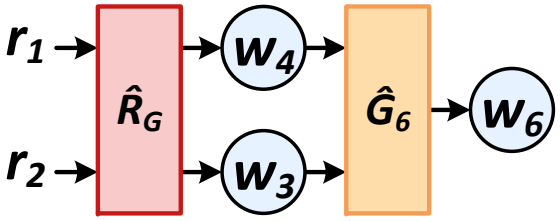

(b) The abstraction.

Figure 4.5: A module dynamic network with two subnetworks (the red and the orange box) and its abstraction.

modules have a specific structure. The identifiability problem can be solved by eliminating self-loops from the network, but this can introduce shared hidden states.

In the current literature, identification is often applied in a module dynamic network without self-loops and restricted to SISO modules. This implies that if there is a (physical) state-space form underneath the module dynamic network, shared hidden states can be present that will not be recognised as such, when all modules are independently parameterised as SISO modules. In order to appropriately deal with this situation (and arrive at minimum variance results for estimated models) the handling of MIMO parameterised modules would be necessary. From an identification perspective, this is the primal lesson to be learnt from the analysis in this chapter.

The network structure cannot completely be identified through its modules if a dynamic network contains hidden states. Only the network structure that manifests itself in transfer functions between inputs and node signals can be identified. The remaining structure is hidden in the modules and shared hidden states will remain

undetected.

4.7 Conclusion

A module dynamic network has been formalised as a model for describing dynamic networks. This concept has been extended by allowing self-loops and MIMO modules. As a result, the module dynamic network incorporates state-space forms as a special case.

A module dynamic network allows to zoom in/out on/of the network to include/exclude more detailed structural information. Zooming in/out is represented by an increased/decreased number of node signals and a decreased/increased order of the module dynamics. Zooming in takes place by realisation (replacing modules by state-space realisations), which in construction is non-unique. Zooming out takes place by multi-path immersion (removing measured node signals from the network), in which the loss of structural information by the introduction of shared hidden states is avoided.

The main question in this chapter was: can a state-space form always be converted into a module representation without losing any information and vice versa? The answer to this question is: yes, provided that MIMO modules are allowed in the module dynamic networks.

Appendix

4.A Proof of Lemma 4.3

Consider a module dynamic network as defined by Definition 4.1. Such network can be written as (4.2). The self-loops of this network are represented by the modules $G_{ii}(q)$, $i = 1, \cdots, L$, which can be found on the diagonal of G. The transfer function matrix G can be decomposed in two parts: a diagonal one containing only the self-loops, denoted by G_d, and one containing the remaining terms (with zeros on its diagonal), denoted by G_{nd}. The module dynamic network with self-loops is then written as

$$\begin{aligned} w(t) &= Gw(t) + Rr(t), \\ &= G_d w(t) + G_{nd} w(t) + Rr(t), \\ &= (I - G_d)^{-1} \left[G_{nd} w(t) + Rr(t) \right], \\ &= \hat{G} w(t) + \hat{R} r(t). \end{aligned} \tag{4.7}$$

The latter is again a module dynamic network, with transfer function matrices $\hat{G}$ and $\hat{R}$. From G_d being diagonal, it follows that $(I - G_d)^{-1}$ is diagonal as well. Combining this with the fact that G_{nd} has a zero diagonal gives that $\hat{G} = (I - G_d)^{-1} G_{nd}$ has a zero diagonal and thus the module dynamic network represented by (4.7) has no self-loops.

4.B Proof of Lemma 4.5

From the definition of the generic McMillan degree it follows that the generic McMillan degree of a module prevents for pole-zero cancellation within this module and that the generic McMillan degree of a network prevents for pole-zero cancellation in the overall network description. As a consequence, pole-zero

cancellations do not occur when any two (or more) modules in the network are merged and the generic McMillan degree of the resulting module is equal to the sum of the generic McMillan degrees of the merged modules. The overall transfer function of the network is obtained by merging all modules and hence, the generic McMillan degree of the network is equal to the sum of the generic McMillan degrees of all modules in the network.

4.C Proof of Proposition 4.19

Consider an state-space (SS) dynamic network, as defined in Definition 4.7, with minimal state-space dimension n. If unmeasured node signals are removed by single-path immersion, the resulting module dynamic network has generic McMillan degree $\geq n$.

Equality holds if the module dynamic network has no shared hidden states, because then each hidden state in the module dynamic network represents an unmeasured node signal of the underlying SS dynamic network.

If the module dynamic network has shared hidden states, multiple hidden states in the modules represent the same unmeasured node signal of the original SS dynamic network and the generic McMillan degree of the module dynamic network is larger than n.

If the unmeasured node signals are removed from the SS dynamic network by multi-path immersion, shared hidden states never occur and the resulting module dynamic network always has a generic McMillan degree equal to n.

4.D Proof of Proposition 4.20

(a) Consider a node with multiple local inputs and one local output. The paths from each local input, through the node, to the local output have an overlapping part, namely the part from the node to the local output. If this node is removed from the network by single-path immersion, the node (and the module between the node and the local output) is merged in all modules from each local input to the local output. Since the node is present in all these modules, it has become a shared hidden state.

A similar reasoning holds for a node with multiple local outputs. If a node has only one local input and one local output, single-path immersion results in only one module (without a shared hidden state).

(b) If a node (denoted as node 1) with multiple local inputs is removed from the network by single-path immersion, then a shared hidden state is introduced, see Proposition 4.20a. However, if all local inputs but one are nodes that also will be removed from the network, the introduction of the shared hidden state will be nullified if the local input to node 1 is the only local input to all nodes that also will be removed from the network. Hence, the nodes jointly have one local input and although node 1 has multiple local inputs, no shared hidden state is introduced. In other words, if a node has multiple local inputs, single-path immersion only introduces a shared hidden state if all nodes that will be removed from the network jointly have multiple local inputs.

A similar reasoning holds for a node with multiple local outputs. If no node has multiple local inputs or multiple local outputs, the nodes can subsequently be removed from the network by single-path immersion and, by Proposition 4.20a, no shared hidden states are introduced.

(c) If a node is removed from the network by multi-path immersion, all paths through the node are combined in one module. Thus the node becomes a hidden state in only one module and will therefore never be shared. If multiple nodes are removed, the nodes can be removed sequentially and no node becomes a shared hidden state.

4.E Proof of Proposition 4.22

Consider a module dynamic network, as defined in Definition 4.7, with generic McMillan degree n. Realisation through Algorithm 4.16 adds a minimum number of node signals to the network if every module is substituted by a minimal state-space realisation of it. When minimal state-space realisations are substituted into the modules, the dimension of the state-space realisation is equal to the generic McMillan degree in every module. As a result, the state-space dimension of the resulting SS dynamic network is equal to the generic McMillan degree of the module dynamic network, which is n.

5 | Diffusively coupled linear network models

Physical linear systems are typically described by second-order vector differential equations, which naturally follow from first-principles modelling. The question that is addressed is: what network model is suitable for describing the interconnections of physical linear systems for identification purposes. A linear network model is developed that is able to incorporate the specific characteristics of the symmetric nature of physical components. The application of this new network model to various physical linear networks is illustrated and their analogies are shown. It follows that this network model describes physical linear systems that are passive, dissipative and stable. Further, the use of this network model to other types of networks is discussed.

5.1 Introduction

Dynamic networks are gaining popularity among a wide range of scientific disciplines, because systems are becoming more complicated and larger. Some examples of these interconnected dynamic systems are the brain, models describing the spread rate of infectious diseases, models describing social interactions, electricity networks, and multiagent systems (Ren et al., 2005; Boccaletti et al., 2006; Mesbahi and Egerstedt, 2010). The class of dynamic networks that will receive our attention are physical networks, such as electrical circuits, mechanical and hydraulic systems, and biological and chemical processes.

Physical networks are often represented by a vector differential equation of maximum second order, which follows naturally from first-principles modelling through the laws of nature. Two well-known examples of physical networks are electrical resistor-inductor-capacitor circuits and mechanical mass-spring-damper

systems. For identification purposes, the second-order vector differential equations can be converted into a state-space form, after which matrix transformations (Friswell et al., 1999; Lopes dos Santos et al., 2015) or eigenvalue decompositions (Fritzen, 1986; Luş et al., 2003) are applied to estimate the model parameters. However, these methods typically do not have any guarantees on the statistical accuracy of the estimates and lack a consistency analysis. Physical networks can also be modelled by classical black-box models, for example, in the form of monic polynomial models, which can be identified using prediction error identification methods (Ljung and Glad, 1994; Ljung, 1999). Again, the network structure in the model is generally lost.

By representing a dynamic network as an interconnection structure of dynamic transfer function modules (Gonçalves and Warnick, 2008; Van den Hof et al., 2013), a framework for system identification in dynamic networks has been developed by Van den Hof et al. (2013), by extending classical closed-loop prediction error methods. In this framework, dynamic networks are considered to consist of directed interconnections of dynamic modules that can be of any dynamic order. However, the symmetric nature of physical components leads to diffusive couplings (Cheng et al., 2017; Cheng and Scherpen, 2021), which are characterised by undirected dynamic interconnections between node signals.

The overall objective of this research is to develop a comprehensive theory for the identification of individual interconnections in physical linear networks, where the dynamic order of these couplings is not restricted and where possibly correlated disturbances are present. Before moving towards identification in physical linear networks, an appropriate network model structure needs to be selected or developed. This network model should be such that the particular network characteristics can be incorporated in an effective manner.

In this chapter, a network model for the identification of physical linear networks is developed. The advantages of different representations are studied in Section 5.2. A physical perspective on the developed network model is given in Section 5.3. In Section 5.4, the application of the network model to various physical domains is illustrated. Section 5.5 describes other type of networks that can be described by the developed network model and finally, Section 5.6 concludes the chapter.

We consider the following notation throughout the chapter: A polynomial matrix $A(z^{-1})$ in complex indeterminate z^{-1}, consists of matrices A_ℓ and (j,k)th polynomial elements $a_{jk}(z^{-1})$ such that $A(z^{-1}) = \sum_{\ell=0}^{n_a} A_\ell z^{-\ell}$ and $a_{jk}(z^{-1}) = \sum_{\ell=0}^{n_a} a_{jk,\ell} z^{-\ell}$. Hence, the (j,k)th element of the matrix A_ℓ is denoted by $a_{jk,\ell}$. Physical components are indicated in sans serif font: A or a. A $p \times m$ rational function matrix $F(z)$ is proper if $\lim_{z\to\infty} F(z) = c \in \mathbb{R}^{p\times m}$; it is strictly proper

if $c = 0$, and monic if $p = m$ and c is the identity matrix. $F(z)$ is stable if all its poles are within the unit circle $|z| < 1$. Further, $D(z^{-1}) = \mathrm{diag}(A(z^{-1}))$ with $A(z^{-1}) \in \mathbb{R}^{m\times m}$ is a diagonal polynomial matrix $D(z^{-1}) \in \mathbb{R}^{m\times m}$ containing the diagonal of $A(z^{-1})$; $D(z^{-1}) = \mathrm{diag}(A(z^{-1}))$ with $A(z^{-1}) \in \mathbb{R}^{m\times 1}$ is a diagonal polynomial matrix $D(z^{-1}) \in \mathbb{R}^{m\times m}$ with diagonal elements $d_{ii}(z^{-1}) = a_{i1}(z^{-1})$; and $D(z^{-1}) = \mathrm{rowsum}(A(z^{-1}))$ with $A(z^{-1}) \in \mathbb{R}^{m\times m}$ is a column vector $D(z^{-1}) \in \mathbb{R}^{m\times 1}$ with elements $d_{i1}(z^{-1}) = \sum_{j=1}^{m} a_{ij}(z^{-1})$. The identity matrix is denoted by I.

5.2 Diffusively coupled linear network

5.2.1 Electrical circuit

Physical linear systems are often described by second-order vector differential equations. They can be considered to consist of L interconnected node signals $w_j(t)$, $j = 1, \ldots, L$, of which the behaviour is described according to

$$\mathsf{M}_{j0}\ddot{w}_j(t) + \mathsf{D}_{j0}\dot{w}_j(t) + \sum_{k\in\mathcal{N}_j} \mathsf{D}_{jk}[\dot{w}_j(t) - \dot{w}_k(t)] + \mathsf{K}_{j0}w_j(t) + \sum_{k\in\mathcal{N}_j} \mathsf{K}_{jk}[w_j(t) - w_k(t)] = u_j(t), \quad (5.1)$$

where $\mathsf{M}_{j0} \geq 0$, $\mathsf{D}_{jk} \geq 0$, $\mathsf{K}_{jk} \geq 0$, $\mathsf{D}_{jk} = 0$, $\mathsf{K}_{jk} = 0$, $\mathcal{N}_j$ is the set of indices of node signals $w_k(t)$, $k \neq j$, with connections to node signal $w_j(t)$, $u_j(t)$ are the external input signals and $\dot{w}_j(t)$ and $\ddot{w}_j(t)$ are the first and second-order derivatives of the node signals $w_j(t)$, respectively.

In physical linear systems, interconnections between node signals depend on both of these node signals. To be more precise, the couplings of node signal $w_i(t)$ with node signal $w_k(t)$ depend on $w_i(t) - w_k(t)$, which emerges in (5.1) by the terms $[\dot{w}_i(t) - \dot{w}_k(t)]$ and $[w_i(t) - w_k(t)]$. This type of coupling is referred to as a *diffusive coupling*. In addition, all connections are symmetric, meaning that the strength of the connection seen from node signal $w_i(t)$ is equal to the strength of the connection (in opposite direction) seen from node signal $w_k(t)$, which emerge in (5.1) from the symmetric relations $\mathsf{D}_{jk} = \mathsf{D}_{kj}$ and $\mathsf{K}_{jk} = \mathsf{K}_{kj}$, $j, k = 1, 2, \ldots, L$.

Further, a network is allowed to have higher-dimensional node signals $w_j(t)$, but without loss of generality, we will restrict our attention to scalar-valued node signals $w_j(t)$.

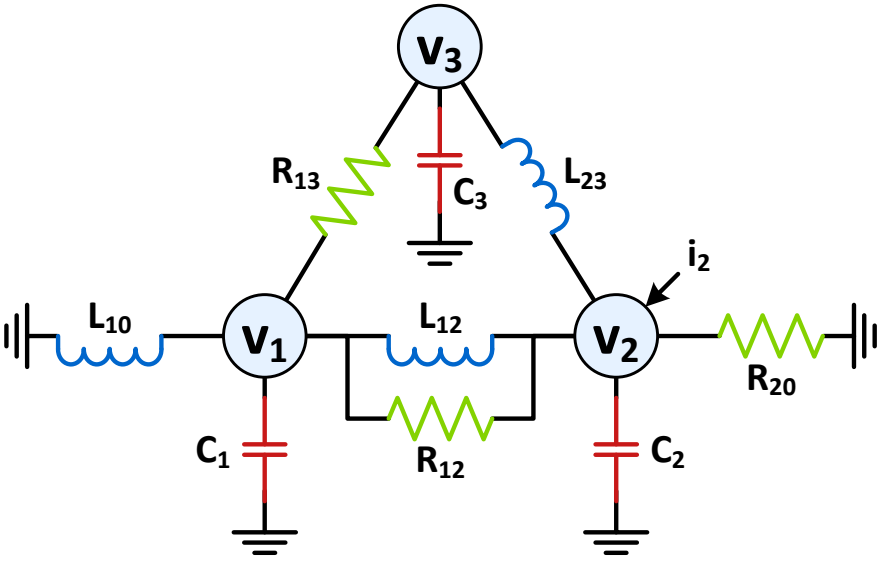

Figure 5.1: An electrical circuit with capacitors (C_j), resistors (R_{jk}), inductors (L_{jk}), current injection (i_j), and electric potentials (v_j).

An example of a physical linear system with diffusive couplings is an electrical circuit. Electrical circuits consist of interconnected capacitors, resistors, and inductors, where voltage or current sources can be present. The electrical circuit shown in Figure 5.1 consists of three nodes that are interconnected through resistors R_{jk} and inductors L_{jk} with $k \neq 0$ and are connected to the ground (or earth) with capacitors C_j, resistors R_{j0}, and inductors L_{j0}. Further, each node can be subject to an external current injection $u_j(t) := i_j(t)$ and the electric potentials at the nodes are the signals of interest and therefore the measurable node signals: $w_j(t) := v_j(t)$. The couplings are diffusive, because capacitors, resistors, and inductors are symmetric components. The behaviour of the circuit is derived by using the constitutive laws of the components and by applying Kirchhoff's current and voltage laws, leading to a second-order vector differential equation (5.1) with $\mathsf{M}_{j0} = C_j$, $\mathsf{D}_{j0} = R_{j0}^{-1}$, $\mathsf{K}_{j0} = Z_{j0}^{-1}$, $\mathsf{D}_{jk} = R_{jk}^{-1}$, and $\mathsf{K}_{jk} = L_{jk}^{-1}$, $j, k = 1, 2, \ldots, L$.

5.2.2 Higher order network

A physical network, such as the electrical circuit described in Section 5.2.1, is typically of second order, while all node signals are collected in $w(t)$. In this section, the theory will be extended to include higher-order dynamics. One reason for doing so is to be able to describe networks that explain only a subset of the

node signals. These networks can be constructed by removing node signals from the network through a Gaussian elimination procedure that is referred to as Kron reduction (Dörfler and Bullo, 2013; Dörfler et al., 2018) or immersion (Dankers et al., 2016). The elimination of node signals will generally lead to higher-order dynamics between the remaining node signals.

Definition 5.1 (Diffusively coupled linear network). *A* diffusively coupled linear network *is a network consisting of L node signals $w_1(t), \ldots, w_L(t)$ interconnected through diffusive couplings and with possibly connections of node signals to a ground. The behaviour of the node signals $w_j(t)$, $j = 1, \ldots, L$, is described by*

$$\sum_{\ell=0}^{n_x} \mathsf{x}_{jj,\ell} w_j^{(\ell)}(t) + \sum_{k \in \mathcal{N}_j} \sum_{\ell=0}^{n_y} \mathsf{y}_{jk,\ell} [w_j^{(\ell)}(t) - w_k^{(\ell)}(t)] = u_j(t), \qquad (5.2)$$

with n_x and n_y the order of the dynamics in the network, with real-valued coefficients $\mathsf{x}_{jj,\ell} \geq 0$, $\mathsf{y}_{jk,\ell} \geq 0$, $\mathsf{y}_{jk,\ell} = \mathsf{y}_{kj,\ell}$, with $\mathcal{N}_j$ is the set of indices of node signals $w_k(t)$, $k \neq j$, with connections to node signal $w_j(t)$, where $w_j^{(\ell)}(t)$ is the ℓ-th derivative of $w_j(t)$, and where $u_j(t)$ is the external signal entering the j-th node.

The graphical interpretation of the coefficients is as follows: x_{jj,n_x} represent the buffers, that is the components intrinsically related to the node signals $w_j(t)$; $\mathsf{x}_{jj,\ell}$ with $\ell \neq n_x$ represent the components connecting the node signals $w_j(t)$ to the ground (or reference); and $\mathsf{y}_{jk,\ell}$ represent the components in the diffusive couplings between the node signals $w_j(t)$ and $w_k(t)$. The ground is characterised by $w_{ground}(t) = 0$ for all time t and therefore can be seen as a node with an infinite buffer, see also Dörfler and Bullo (2013).

Graphically, diffusively coupled linear networks can be represented by an undirected graph, where every undirected interconnection actually represents a symmetric bi-directional interconnection. A graphical representation of a diffusively coupled linear network is shown in Figure 5.2. The network dynamics is represented by the blue boxes containing the polynomials $x_{jj}(p) = \sum_{\ell=0}^{n_x} \mathsf{x}_{jj,\ell} p^\ell$ and $y_{jk}(p) = \sum_{\ell=0}^{n_y} \mathsf{y}_{jk,\ell} p^\ell$, with differential operator p meaning $pw(t) = \frac{d}{dt} w(t)$, and the node signals are represented by the blue circles, which sum the diffusive couplings and the external signals. For example, $w_5(t) = \mathsf{x}_{55}\big(w_5(t) - 0\big) + \mathsf{y}_{45}\big(w_5(t) - w_4(t)\big) + u_5(t)$.

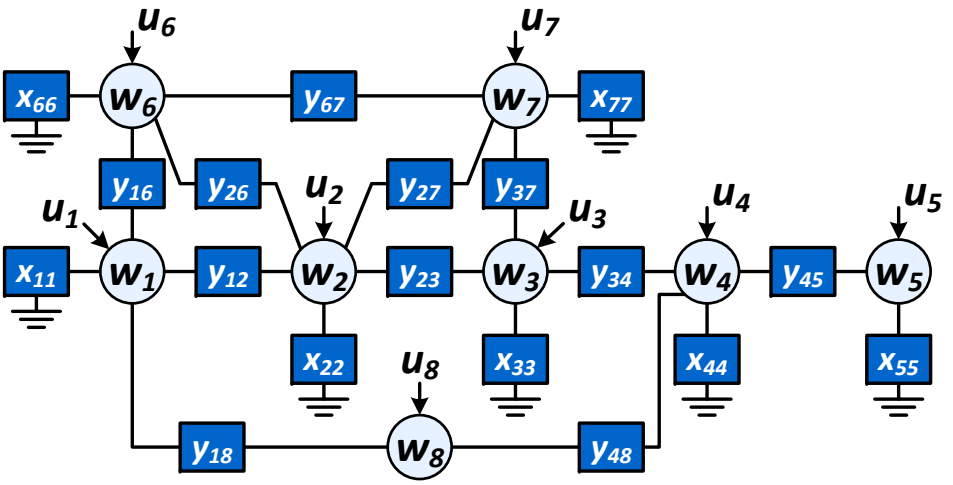

Figure 5.2: A diffusively coupled linear network as defined in Definition 5.1, with node signals $w_j(t)$, input signals $u_j(t)$, and dynamics between the node signals (y_{jk}) and to the ground (x_{jj}).

Proposition 5.2 (Diffusively coupled linear network). *A diffusively coupled linear network* (5.2) *can be described in matrix form as*

$$X(p)w(t) + Y(p)w(t) = u(t), \tag{5.3}$$

with diagonal $X(p)$ and Laplacian $Y(p)$ polynomial matrices in the differential operator p meaning $pw(t) = \frac{d}{dt}w(t)$ and composed of elements

$$x_{jk}(p) = \begin{cases} \sum_{\ell=0}^{n_x} \mathsf{x}_{jj,\ell} p^\ell, & \text{if } k = j \\ 0, & \text{otherwise} \end{cases} \tag{5.4a}$$

$$y_{jk}(p) = \begin{cases} \sum_{m \in \mathcal{N}_j} \sum_{\ell=0}^{n_y} \mathsf{y}_{jm,\ell} p^\ell, & \text{if } k = j \\ -\sum_{\ell=0}^{n_y} \mathsf{y}_{jk,\ell} p^\ell, & \text{if } k \in \mathcal{N}_j \\ 0, & \text{otherwise.} \end{cases} \tag{5.4b}$$

Proof: The expressions for the node signals (5.2) can be stacked for $w_1(t), \ldots, w_L(t)$ and combined in a matrix equation. ■

Every matrix X_ℓ composed of elements $x_{jj,\ell} := \mathsf{x}_{jj,\ell}$ is diagonal and every matrix Y_ℓ composed of elements $y_{jj,\ell} := \sum_{k \in \mathcal{N}_j} \mathsf{y}_{jk,\ell}$ and $y_{jk,\ell} := -\mathsf{y}_{jk,\ell}$ for

$k \neq j$ is Laplacian[1]. The Laplacian matrices Y_ℓ represent an undirected graph of a specific physical component (i.e. of a symmetric diffusive coupling of a specific order).

The diffusively coupled network (5.3) is assumed to be connected, which means that there is a path between every pair of nodes[2]. In addition, the network is assumed to have at least one connection to the ground, implying the well-posedness of the network. These two assumptions, together with the semi-positiveness of the component values, induce stability of the network by the stability of $\big(X(p) + Y(p)\big)^{-1}$.

5.2.3 A diagonal and hollow system representation

The module representation is often used for system identification in dynamic networks using prediction error methods. There is much literature available on various identification questions about dynamic networks in this framework. In order to connect with this system identification framework, a slightly different, but equivalent, network description will be used.

Proposition 5.3 (Diffusively coupled linear network). *A diffusively coupled linear network as in Proposition 5.2 with $X(p)$ diagonal and $Y(p)$ Laplacian, can equivalently be described by*

$$Q(p)w(t) = P(p)w(t) + u(t), \tag{5.5}$$

with diagonal polynomial matrix $Q(p)$ and symmetric, hollow polynomial matrix $P(p)$ defined by

$$Q(p) := X(p) + diag\big(Y(p)\big), \tag{5.6a}$$
$$P(p) := -Y(p) + diag\big(Y(p)\big), \tag{5.6b}$$

with $diag\big(Y(p)\big)$ the diagonal of $Y(p)$.

Proof: The definitions of $Q(p)$ and $P(p)$ show that $u(t) = \big(Q(p) - P(p)\big)w(t) = \big(X(p) + Y(p)\big)w(t)$. ■

[1] A Laplacian matrix is a symmetric matrix with nonpositive off-diagonal elements and with nonnegative diagonal elements that are equal to the negative sum of all other elements in the same row (or column) (Mesbahi and Egerstedt, 2010), see also Chapter 2 for the Laplacian of a polynomial matrix.

[2] The network is connected if its Laplacian matrix has a positive second-smallest eigenvalue (Mesbahi and Egerstedt, 2010; Dörfler and Bullo, 2013).

The diagonal elements of $P(p)$ are zero ($p_{jj}(p) = 0$) and the off-diagonal elements of $P(p)$ are equal to $p_{jk}(p) = -y_{jk}(p)$ for $k \neq j$. These polynomial elements $p_{jk}(p)$ contain the dynamics of all components in the interconnection between the node signals $w_j(t)$ and $w_k(t)$.

The off-diagonal elements of $Q(p)$ are zero ($q_{jk}(p) = 0$ for $k \neq j$) and the diagonal elements of $Q(p)$ are equal to $q_{jj}(p) = x_{jj}(p) + y_{jj}(p)$. These polynomial elements $q_{jj}(p)$ contain the dynamics of all components that are related to (or connected to) the node signal $w_j(t)$.

There exists a bijective relationship between the polynomial matrices $\big(X(p), Y(p)\big)$ and $\big(P(p), Q(p)\big)$, because of their particular structure. The polynomial matrices $X(p)$ and $Y(p)$ are obtained from $P(p)$ and $Q(p)$ as

$$X(p) = Q(p) - \operatorname{diag}\big(\operatorname{rowsum}\big(P(p)\big)\big), \tag{5.7a}$$

$$Y(p) = -P(p) + \operatorname{diag}\big(\operatorname{rowsum}\big(P(p)\big)\big), \tag{5.7b}$$

with $\operatorname{diag}(\cdot)$ a diagonal, square matrix and with $\operatorname{rowsum}\big(P(p)\big)$ a column vector with the $(i, 1)$th element equal to the sum of all elements in the ith row of $P(p)$.

5.2.4 A symmetric system representation

Polynomial models constitute a popular framework for system identification using prediction error methods. There is much literature available on various identification questions about systems in this framework. For example, autoregressive with exogeneous input (ARX) and autoregressive-moving average with exogeneous input (ARMAX) model structures are well-studied in the prediction error identification framework (Ljung, 1999; Hannan and Deistler, 2012). By Proposition 5.3, the diffusively coupled linear model as presented above, is closely related to these polynomial models. In order to connect with this system identification framework, we will formulate an equivalent network description and provide some additional details.

First of all, the node signals in the network might be affected by a user-applied excitation signal and subject to a disturbance signal. This needs to be included in the network description (5.5), which is achieved by splitting the external signal as

$$u(t) := B(p)r(t) + v(t), \tag{5.8}$$

where the known excitation signals $r(t)$ enter the network through dynamics described by polynomial matrix $B(p)$ and where the unknown disturbance signals acting on the network are modeled by $v(t)$.

In addition, not all node signals might be measured. This needs to be included in the network description, which is achieved by adding a measurement equation as

$$y(t) := C(p)w(t), \tag{5.9}$$

where the internal node signals are observed from the environment through dynamics described by polynomial matrix $C(p)$. This polynomial matrix $C(p)$ can be used to change the quantity of the measured signals. For example, if the node signal $w(t)$ is a position, while the velocity is measured, then this is captured by (5.9) through $C(p) = p$.

Proposition 5.4 (Diffusively coupled linear network). *A diffusively coupled linear network as in Proposition 5.2 or in Proposition 5.3 with external signal $u(t)$ described by* (5.8) *and measured signals $y(t)$ described by* (5.9)*, can equivalently be described by*

$$A(p)w(t) = B(p)r(t) + v(t), \qquad y(t) = C(p)w(t), \tag{5.10}$$

with

$$A(p) = X(p) + Y(p) = Q(p) - P(p) \tag{5.11}$$

and with

1. $A(p) = \sum_{k=0}^{n_a} A_k p^k \in \mathbb{R}^{L\times L}[p]$, *with* $a_{jk}(p) = a_{kj}(p), \forall k, j$ *and* $A^{-1}(p)$ *stable.*
2. $B(p) \in \mathbb{R}^{L\times K}[p]$.
3. $C(p) \in \mathbb{R}^{c\times L}[p]$.

Proof: The definitions of $A(p)$ and $u(t)$ show that $A(p)w(t) = B(p)r(t) + F(p)e(t) = u(t) = \big(X(p) + Y(p)\big)w(t) = \big(Q(p) - P(p)\big)w(t)$. ■

There exists a bijective relationship between the polynomial $A(p)$ and the polynomials $\big(X(p), Y(p)\big)$ and $\big(P(p), Q(p)\big)$. The polynomials $X(p)$, $Y(p)$, $Q(p)$, and $P(p)$ are obtained from $A(p)$ as

$$X(p) = \operatorname{diag}\big(\operatorname{rowsum}\big(A(p)\big)\big), \qquad Y(p) = A(p) - X(p) \tag{5.12a}$$

$$Q(p) = \operatorname{diag}\big(A(p)\big), \qquad P(p) = Q(p) - A(p). \tag{5.12b}$$

Figure 5.3 shows an overview of these three representations and the relations between them. There exist bijective mappings between all three representations, because of the particular structure of the polynomial matrices. This means that if one representation is given, the other two can always be obtained.

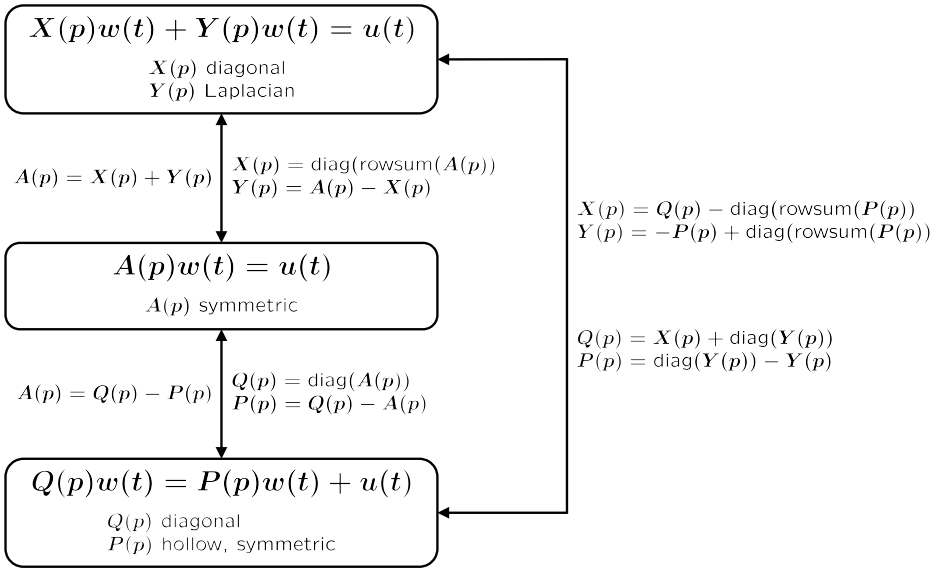

Figure 5.3: Overview of the relations between the three polynomial representations for diffusively coupled linear networks (5.3), (5.5), and (5.10) as presented in (5.11) and (5.12).

The diffusive character of the model is now represented by the symmetry of $A(p)$, where the polynomial elements $a_{jk}(p)$ characterise the dynamics in the link between node signals $w_j(t)$ and $w_k(t)$. The considered networks lead to polynomial models[3] with the particular properties that $A(p)$ is symmetric and nonmonic. Observe that $B(p)$ and $C(p)$ are nonmonic as well, but often they are chosen to be binary, diagonal, and known, implying that each excitation signal directly enters the network at a distinct node and that each measured signal is directly extracted from a distinct internal node signal.

The mapping from the external input signals $r(t)$ and $v(t)$ to the measured output signal $y(t)$ of (5.10) is given by

$$y(t) = T_{yr}(p)r(t) + \bar{v}(t), \tag{5.13}$$

with

$$T_{yr}(p) = C(p)A^{-1}(p)B(p), \qquad \bar{v}(t) = C(p)A^{-1}(p)v(t). \tag{5.14}$$

[3]Polynomial models are linear time-invariant dynamic models of the form $A(p)y(t) = E^{-1}(p)B(p)u(t) + v(t)$, where $A(p)$, $B(p)$, and $C(p)$ are polynomials in p that are all monic except for $B(p)$ (Ljung, 1999; Hannan and Deistler, 2012).

Observe that for binary $B(p)$ and $C(p)$, a subset of rows and columns of $A^{-1}(p)$ constitutes $T_{yr}(p)$.

5.3 A physical perspective

5.3.1 Introduction

It is well-known that there are many similarities among various physical domains (Paynter, 1961; Ljung and Glad, 1994; Borutzky, 2010, 2011; van der Schaft and Jeltsema, 2014). These processes include electrical resistor-inductor-capacitor circuits, mechanical mass-spring-damper systems and their analogous rotational system consisting of inertias, springs, and dampers, hydraulic processes in which vessels are interconnected with each other, thermodynamic systems, and chemical processes. In this section, we discuss how these physical linear networks can be represented by the diffusively coupled linear network model (5.10).

The behaviour of physical systems and networks is often described by using energy preservation and power balance relations (Paynter, 1961). These descriptions are generally based on two types of variables, effort and flow,which together are measures of energy and power. These variables originate from bond-graph models (Paynter, 1961) and are used in this section to explain how physical processes from various domains can be expressed by diffusively coupled linear networks (5.10).

5.3.2 Tetrahedron of state

The effort variable $e(t)$ and the flow variable $f(t)$ represent a generalised force and a generalised velocity, respectively. Their product results in power

$$P(t) = e^{\top}(t)f(t), \tag{5.15}$$

and hence, the energy is given by

$$E(t) = \int P(t)dt = \int e^{\top}(t)f(t)dt. \tag{5.16}$$

In association with the effort (generalised force) and flow (generalised velocity), define the generalised momentum $p(t)$ and the generalised displacement $q(t)$, respectively, according to the relations

$$e(t) = \frac{d}{dt}p(t), \qquad \text{or} \qquad p(t) = \int e(t)dt, \tag{5.17a}$$

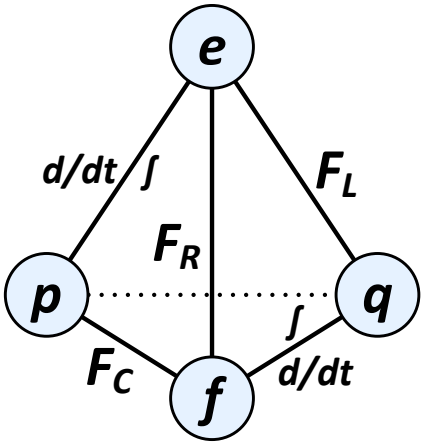

Figure 5.4: The *tetrahedron of state* illustrating the relations between the effort (e), the flow (f), the generalised momentum (p), and the generalised displacement (q) given by (5.17) and (5.18), with d/dt and $\int$ the derivative and integrator operators, respectively.

$$f(t) = \frac{d}{dt}q(t), \qquad \text{or} \qquad q(t) = \int f(t)dt. \tag{5.17b}$$

The four variables $(e(t), f(t), p(t), q(t))$ are the *variables of state* with which the dynamical and energetic conditions of physical systems can be described. The relations between these four variables are visualised by the *tetrahedron of state* (Paynter, 1961), which is shown in Figure 5.4. This figure shows the relations (5.17) and the following three additional characteristic relations, which are static by definition:

$$F_R\big(e(t), f(t)\big) = 0, \qquad F_C\big(q(t), e(t)\big) = 0, \qquad F_L\big(p(t), f(t)\big) = 0, \tag{5.18}$$

where $F_R(\cdot)$, $F_C(\cdot)$, and $F_L(\cdot)$ are generalised resistive, generalised capacitive, and generalised inertive functions. In general, these relations can be nonlinear. For linear time-invariant (LTI) systems, these relations are static and given by

$$e(t) = Rf(t), \qquad q(t) = Ce(t), \qquad p(t) = Lf(t), \tag{5.19}$$

with constant resistance R, capacitance C, and inertance L, respectively.

The three characteristic relations (5.18) are closely related to power and energy. Moreover, in the linear case, the generalised power loss, the generalised potential energy, and the generalised kinetic energy are, respectively, given by

$$P_\ell(t) = f^\top(t)Rf(t) = e^\top(t)R^{-1}e(t), \tag{5.20a}$$

$$E_p(t) = \frac{1}{2}e^\top(t)Ce(t) = \frac{1}{2}q^\top(t)C^{-1}q(t), \tag{5.20b}$$

$$E_k(t) = \frac{1}{2}f^\top(t)Lf(t) = \frac{1}{2}p^\top(t)L^{-1}p(t). \tag{5.20c}$$

Together these lead to the power balance of the system, which is given by

$$\frac{d}{dt}\big(E_p(t) + E_k(t)\big) + P_\ell(t) = P_s(t), \tag{5.21}$$

where $P_s(t)$ is the power supplied to the system from all energy sources. The total stored energy is represented by the *Hamiltonian*

$$H\big(q(t), p(t)\big) = E_p(t) + E_k(t) = \frac{1}{2}q^\top(t)C^{-1}q(t) + \frac{1}{2}p^\top(t)L^{-1}p(t). \tag{5.22}$$

5.3.3 Diffusively coupled linear network model

Interconnections are made via junctions, of which two types are considered. An effort junction is characterised by

$$\sum_i^k f_i(t) = 0, \qquad e_1(t) = e_2(t) = \ldots = e_k(t), \tag{5.23}$$

and it is a generalisation of Kirchhoff's loop law. A flow junction is characterised by

$$\sum_i^k e_i(t) = 0, \qquad f_1(t) = f_2(t) = \ldots = f_k(t), \tag{5.24}$$

and it is a generalisation of Kirchhoff's node law. Consider multidimensional state vectors $e(t)$, $f(t)$, $p(t)$, and $q(t)$ consisting of elements $e_{i1}(t) = e_i(t)$, $f_{i1}(t) = f_i(t)$, $p_{i1}(t) = p_i(t)$, and $q_{i1}(t) = q_i(t)$, respectively.

Describing a network based on its effort junctions results in a diffusively coupled network representation in terms of the flows (or generalised velocities) $f(t)$ and generalised momenta $p(t)$. On the other hand, a network that is described based on its flow junctions results in a diffusively coupled network representation in terms of its efforts (or generalised forces) $e(t)$ and generalised displacements $q(t)$. These results are formalised in the following two analogous propositions.

Proposition 5.5 (Diffusively coupled linear network). *Consider a physical linear network that is modelled with the variables of state* $(e(t), f(t), p(t), q(t))$ *satisfying* (5.17) *and* (5.19). *Based on a descrip-*

tion of its effort junctions, this network can be represented by a diffusively coupled linear network as

$$C\frac{d^2}{dt^2}p(t) + R^{-1}\frac{d}{dt}p(t) + L^{-1}p(t) = f_s(t), \tag{5.25}$$

that is (5.10) *with*

1. $w(t) = p(t)$*, the generalised momenta.*
2. $r(t) = f_s(t)$*, the flow coming from sources.*
3. $y(t) = e(t)$*, the effort.*
4. $A(p) = Cp^2 + R^{-1}p + L^{-1}$*, with* p *the differential operator.*
5. $B(p) = I$*.*
6. $C(p) = pI$*, with* p *the differential operator.*

Proof: Using (5.17) and (5.19), an effort junction can be characterised by

$$\sum_i f_i(t) = \frac{d}{dt}q(t) + R^{-1}e(t) + L^{-1}p(t) - f_s(t),$$

$$0 = C\frac{d^2}{dt^2}p(t) + R^{-1}\frac{d}{dt}p(t) + L^{-1}p(t) - f_s(t),$$

with $f_s(t)$ the flow coming from sources. ■

Proposition 5.6 (Diffusively coupled linear network). *Consider a physical linear network that is modelled with the variables of state* $(e(t), f(t), p(t), q(t))$ *satisfying* (5.17) *and* (5.19)*. Based on a description of its flow junctions, this network can be represented by a diffusively coupled linear network as*

$$L\frac{d^2}{dt^2}q(t) + R\frac{d}{dt}q(t) + C^{-1}q(t) = e_s(t), \tag{5.26}$$

that is (5.10) *with*

1. $w(t) = q(t)$*, the generalised displacements.*
2. $r(t) = e_s(t)$*, the effort coming from sources.*
3. $y(t) = f(t)$*, the flow.*

4. $A(p) = Lp^2 + Rp + C^{-1}$, *with* p *the differential operator.*
5. $B(p) = I$.
6. $C(p) = pI$, *with* p *the differential operator.*

Proof: Using (5.17) and (5.19), a flow junction can be characterised by

$$\sum_i e_i(t) = \frac{d}{dt}p(t) + Rf(t) + C^{-1}q(t) - e_s(t),$$

$$0 = L\frac{d^2}{dt^2}q(t) + R\frac{d}{dt}q(t) + C^{-1}q(t) - e_s(t),$$

with $e_s(t)$ the effort coming from sources. ■

In the diffusively coupled network of Proposition 5.5, the network is excited by generalised velocities and the generalised momenta are observed from the environment. In contrast, in the diffusively coupled network of Proposition 5.6, the network is excited by generalised forces and the generalised displacements are observed from the environment. This means that the diffusively coupled network model depends on the choice of junction on which the description is based, or equivalently, on the state variables that are interested and chosen as outputs (and inputs). In other words, the experiment is co-determining the model.

In both diffusively coupled network models (5.25) and (5.26), the nodes are interconnected with generalised capacitive, resistive, and inductive components. Components of the same types also connect the nodes to the ground node or relate the node to a reference node. These components are intrinsically related to the nodes and the buffers in which energy can be stored. The ground can be seen as a node where the node signal is zero at all times. The components interconnect node signals without posing any causality, which means that there is no predetermined direction of information flow in the network.

The diffusively coupled network of Proposition 5.5 is based on the generalised Kirchhoff's loop law and therefore, this model describes the relations of physical elements that are interconnected in parallel between junctions. In contrast, the diffusively coupled network of Proposition 5.6 is based on the generalisation of Kirchhoff's node law and therefore, this model describes the relations of physical elements that are interconnected in series between junctions. From Proposition 5.5 and 5.6 it follows that the role of the resistance R, capacitance C, and inertance L is opposite in both representations.

The matrices C, $G := R^{-1}$, and $Z := L^{-1}$ in (5.25) as well as the matrices L, R, and $Y := C^{-1}$ in (5.26) consist of a diagonal matrix plus a Laplacian matrix,

that is, all these matrices are constructed as $X = X_d + X_{\mathcal{L}}$ with X_d diagonal and $X_{\mathcal{L}}$ Laplacian (see also (5.11)). The diagonal matrix represents the components intrinsically related to the nodes with X_{dii} the value of the component intrinsically related to node $w_i(t)$, while the Laplacian matrix represents the components in the interconnections with $-[X_{\mathcal{L}}]_{ij}$, $i \neq j$, the value of the component between node $w_i(t)$ and $w_j(t)$. In addition, the matrices C, R, and L contain generalised capacitances, resistances, and inertances, respectively. The matrices $Y := C^{-1}$, $G := R^{-1}$, $Z := L^{-1}$ contain the inverses of the capacitances, resistances, and inductances, respectively, meaning that $Y_{ij} = c^{-1}$ with c a generalised capacitance and with G_{ij} and Z_{ij} *mutatis mutandis*.

The topology of the network can be interpreted as follows: In a network that is described based on the effort junction as in Proposition 5.5, nodes are interconnected through parallel interconnected components. In this network, a resistive connection between the ith and jth nodes is missing if $G_{ij} = 0$ implying that $R_{ij} = \infty$, which represents an open connection. Then there can still be capacitive or inertive (parallel) connections between the ith and jth nodes. On the other hand, in a network that is described based on the flow junction (5.26), nodes are interconnected through series interconnections of components. Hence, the interconnection between two nodes is a series interconnection of (possibly) a capacitive, resistive, and inertive component. A resistive connection between the ith and jth nodes is missing if $R_{ij} = 0$, which represents a shortcut connection. Then there can still be capacitive or inertive (series) components in the connection between the ith and jth nodes.

5.3.4 Dissipativity and stability

For both diffusively coupled linear networks (5.25) and (5.26), the total amount of stored energy is given by the Hamiltonian (5.22). These representations (5.25) and (5.26) can be expressed in terms of the Hamiltonian (as a port-Hamiltonian system) as

$$\frac{d}{dt}\begin{bmatrix} q(t) \\ p(t) \end{bmatrix} = \begin{bmatrix} 0 & I \\ -I & -R \end{bmatrix} \nabla H + \begin{bmatrix} 0 \\ I \end{bmatrix} e_s(t), \qquad y(t) = \begin{bmatrix} I & 0 \end{bmatrix} \nabla H, \tag{5.27a}$$

$$\frac{d}{dt}\begin{bmatrix} q(t) \\ p(t) \end{bmatrix} = \begin{bmatrix} -R & -I \\ I & 0 \end{bmatrix} \nabla H + \begin{bmatrix} I \\ 0 \end{bmatrix} f_s(t), \qquad y(t) = \begin{bmatrix} 0 & I \end{bmatrix} \nabla H, \tag{5.27b}$$

respectively, with $\nabla H = \left[\frac{\partial}{\partial q}^\top H\big(q(t), p(t)\big) \quad \frac{\partial}{\partial p}^\top H\big(q(t), p(t)\big) \right]^\top$.

Definition 5.7 (Dissipativity (Willems, 1972)). *A system with a supply rate $s(t)$ is said to be* dissipative *if there exists a nonnegative real function $S(x) : \mathcal{X} \to \mathbb{R}_+$, called the* storage function*, such that, for all $t \geq 0$,*

$$\frac{d}{dt} S\big(x(t)\big) \leq s(t). \tag{5.28}$$

Definition 5.8 (Passivity (Byrnes et al., 1991)). *A system is said to be* passive *if it is dissipative with respect to the supply rate $s(t) = r^\top(t)y(t)$ and the storage function $S(x)$ satisfies $S(0) = 0$.*

It is well-known that port-Hamiltonian systems are passive and therefore, also dissipative and stable (Willems, 1972; Byrnes et al., 1991; Khalil, 2014), where stability was defined in Definition 2.6.

Proposition 5.9 (Passive, dissipative, and stable). *The diffusively coupled linear networks* (5.25) *and* (5.26) *with $C \succeq 0$, $R \succeq 0$, and $L \succeq 0$ are passive, dissipative, and stable.*

Proof: Take the supply function $s(t) = r^\top(t)y(t)$ and as the storage function the Hamiltonian (5.22). Then

$$\frac{d}{dt} H\big(q(t), p(t)\big) = \nabla^\top H \begin{bmatrix} q(t) \\ p(t) \end{bmatrix}.$$

Express the diffusively coupled linear networks (5.25) and (5.26) by (5.27), which leads to

$$\begin{aligned} \frac{d}{dt} H\big(q(t), p(t)\big) &= -p^\top(t) L^{-1} R L^{-1} p(t) + r^\top(t) y(t) \leq r^\top(t) y(t), \\ \frac{d}{dt} H\big(q(t), p(t)\big) &= -q^\top(t) C^{-1} R C^{-1} q(t) + r^\top(t) y(t) \leq r^\top(t) y(t), \end{aligned}$$

respectively, where the inequality holds because $L^{-1}RL^{-1} \succeq 0$ and $L^{-1}RL^{-1} \succeq 0$, because $C \succeq 0$, $R \succeq 0$, and $L \succeq 0$. Stability follows from the fact that the Hamiltonian storage function is a Lyapunov function (Willems, 1972). ∎

Remark 5.10 (Stability). *Here we use the notion of stability to indicate bounded-input bounded-output (BIBO) stability. In the proof of Proposition 5.9, Lyapunov stability is proven. Lyapunov stability implies (BIBO) stability (Willems, 1972).*

Eliminating node signals from the network model results in higher-order representation. This process only changes the network representation, not the network itself. Hence, dissipativity and stability are preserved under the elimination of node signals. This raises the question of whether general higher-order diffusively coupled linear networks are also dissipative and stable. Before going into this, consider the following lemma.

Lemma 5.11 (Positive semi-definite). *If all components that are present in the network have a positive value, then all* $A_i \geq 0$ *in* $A(p)$ *in* (5.10).

Proof: Each A_i is symmetric and thus has real eigenvalues. Each A_i is constructed as the sum of a diagonal matrix plus a Laplacian matrix (5.11). The diagonal matrix has nonnegative elements if all components in the network have a positive value. Hence, the diagonal matrix is positive semi-definite. If all components in the network have a positive value, then the Laplacian matrix is positive semi-definite by definition (Mesbahi and Egerstedt, 2010). The sum of two positive semi-definite matrices is positive semi-definite. ■

To prove whether diffusively coupled linear networks are dissipative and stable, a supply rate and a storage function have to be found. The supply rate can again be chosen to be $s(t) = r^\top(t)y(t)$, which is also needed for passivity. The storage function can be chosen to be the Hamiltonian function, which can, for example, be derived once the network is represented in port-Hamiltonian form. Then dissipativity can be proven along the same line of reasoning as in Proposition 5.9, in which the result of Lemma 5.11 can be applied. Our expectation is that general higher-order diffusively coupled linear networks are dissipative and stable. Determining the storage function or Hamiltonian function for general diffusively coupled linear networks is saved for future research, because no results have been found in the literature yet and it is currently beyond the scope of this thesis.

5.4 Analogies among various physical domains

As mentioned, physical processes from various domains can be described by the variables of state $(e(t), f(t), p(t), q(t))$. In this section, it is explained what the diffusively coupled network model looks like for specific physical processes, including electrical resistor-inductor-capacitor circuits, mechanical mass-spring-damper systems, mechanical rotational systems, hydraulic processes, thermodynamic systems, and chemical processes.

Table 5.1 shows an overview of the variables of state and the generalised capacitive, resistive, and inertive components for these domains. The analogies

Table 5.1: The variables of state and the generalised components for various physical processes (Breedveld, 1982; Ljung and Glad, 1994; Borutzky, 2011).

(a) The variables of state $(e(t), f(t), p(t), q(t))$.

	$e(t)$	$f(t)$	$p(t)$	$q(t)$
Electromagnetic	Voltage	Current	Flux linkage	Charge
Mechanical translational	Force	Velocity	Momentum	Displacement
Mechanical rotational	Torque	Angular velocity	Angular momentum	Angular displacement
Hydraulic (pneumatic)	Pressure	Volume flow rate	Fluid momentum	Volume
Thermodynamic	Temperature	Entropy flow rate		Entropy
Chemical	Chemical potential	Molar flow		Molar mass

(b) The generalised capacitive, resistive, and inertive components.

	Capacitive	Resistive	Inertive
Electromagnetic	Capacitor	Resistor	Inductor
Mechanical translational	Spring	Damper	Body or mass
Mechanical rotational	Torsion	Friction	Axis
Hydraulic (pneumatic)	Tank	Pipe or hose	Water wheel
Thermodynamic	Heater or cooler	Barrier (conductivity)	
Chemical	Substance (amount)	Substance (resistance time)	

among the different fields become clear from the relations to the generalised variables and components. The components yield static relations among the variables of state, which are combined to form the second-order vector differential equations that lead to the diffusively coupled linear network representations (5.25) and (5.26). Thermodynamic systems and chemical processes naturally do not have a generalised displacement state and no generalised inertive component (Breedveld, 1982).

Electrical circuits with capacitors, resistors, and inductors are described by the diffusively coupled linear network model as

$$C\ddot{\varphi}(t) + G\dot{\varphi}(t) + Z\varphi(t) = i(t), \qquad \text{or} \qquad L\ddot{q}(t) + R\dot{q}(t) + Yq(t) = v(t) \quad (5.29)$$

with signals $\varphi(t)$ the flux linkage, $i(t)$ the injected current, $q(t)$ the charge, and $v(t)$ the injected voltage; with matrices C, R, and L containing the capacitances, resistances, and inductances, respectively; and with matrices Y, G, and Z containing the inverses of the capacitances, resistances, and inductances, respectively, meaning that $G_{ij} = R_{ij}^{-1}$ for $i \neq j$ and Y_{ij} and Z_{ij} are found *mutatis mutandis*.

Mechanical translational systems consist of masses interconnected with each other through dampers and springs. Dampers and springs can also connect the mass to the ground (or wall). The positions of the masses are selected as the node signals and external forces can be applied to the masses. These mechanical mass-spring-damper systems are typically described as

$$M\ddot{x}(t) + D\dot{x}(t) + Kx(t) = f(t), \quad (5.30)$$

which is of the form (5.26) with $x(t)$ the positions of the masses; $f(t)$ the external forces applied to the masses; M is a diagonal matrix containing the masses at the nodes; D contains the damper coefficients of the dampers; and K contains the spring coefficients. Of course, a mechanical translational system can also be described by a diffusively coupled linear network of the form (5.25), but the representation (5.30) is most commonly used.

Mechanical rotational systems are very similar to mechanical translational systems, where the masses are replaced by axes. For rotational mechanical systems, the node signals are the angular positions of the axes and the network is driven by external torques.

Hydraulic processes can be described by a diffusively coupled linear network model (5.26) or (5.25), with C the capacitance of valves that are interconnected through (narrowed) tubes with resistance R and water wheels with inertance L. The ground node can be seen as an infinitely large valve (like the ocean). Pneumatic processes are similar to hydraulic processes, with the difference that air travels instead of fluid.

Thermodynamic processes can only be described by a diffusively coupled network of the form (5.26), because there is no generalised momentum. Moreover, they can be described by first-order relations between the effort (temperature) and flow (entropy rate). Thermodynamic processes can approximately be represented by a space with heat capacitance C interconnected through barriers with thermal conductivity G (the inverse of the thermal resistivity), such as walls. The first-order diffusively coupled network model describing these thermodynamic systems

is given by

$$C_T\dot{T}(t) + GT(t) = q(t), \tag{5.31}$$

with $T(t)$ the temperatures of the spaces; $q(t)$ the external entropy flow rate of the injected entropy; C is a diagonal matrix containing the thermal capacitances; and G contains the thermal conductivity. The reference node can be seen as in infinitely large space (like the universe). The reference temperature can also be taken constant instead of zero, which means that the temperatures at the nodes are relative temperatures with respect to the reference temperature.

Figure 5.5-5.8 show four examples of physical networks that are typically described by a diffusively coupled network model of the form (5.26), because the nodes are interconnected through parallel interconnected components. Figure 5.5 and 5.6 show analogous networks from the electromagnetic and mechanical domains. Figure 5.7 shows a hydraulic system without inertive components and Figure 5.8 shows a thermodynamic system.

As a result of the fact that all these physical processes can be described by a diffusively coupled linear network model (5.10), this network model can also describe networks in which multiple physical processes from different fields are combined. Various physical processes can be interconnected through power conversion components, such as transformers, motors, generators, and pumps (also think of gear boxes, electrostats, and loudspeakers).

When multiple physical processes from different domains are combined in a single network, the overall network description becomes a combination of the network descriptions of the individual physical processes. Flow-junction-based (5.26) and effort-junction-based (5.25) diffusively coupled network models from the same physical domain can be combined as well. Processes are linked to each other through the power conversion components, which describe a linear relation between the node signals $w(t)$ of the different physical processes. As a result, the network description can contain node signals and input signals of multiple physical quantities.

5.5 Other diffusively coupled networks

5.5.1 Multiagent networks

The main objective in multiagent systems is cooperative control, which can be split into formation and nonformation control problems. The necessity for agents to share information for coordination, requires agents to cooperate in order to achieve a mutual agreement. This means that the coordination data for each agent

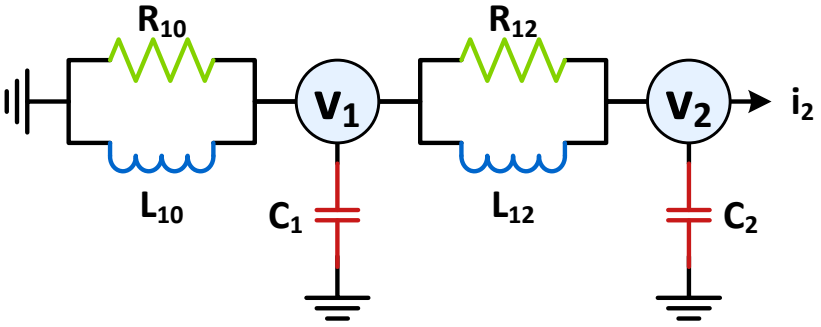

Figure 5.5: An electrical circuit with capacitances C_i, resistances R_{ik}, inductances L_{ik}, electric potentials $v_i(t)$ and external current $i_2(t)$.

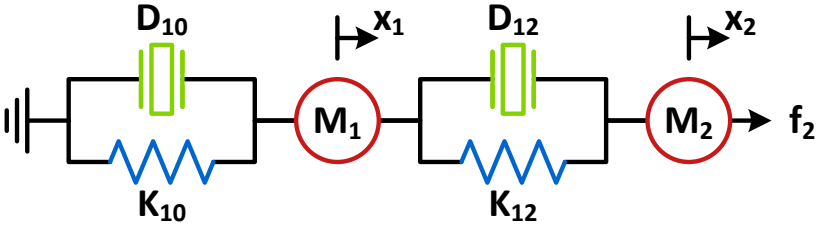

Figure 5.6: A mechanical system with masses M_i, damper coefficients D_{ik}, spring coefficients K_{ik}, positions $x_i(t)$ and external force $f_2(t)$.

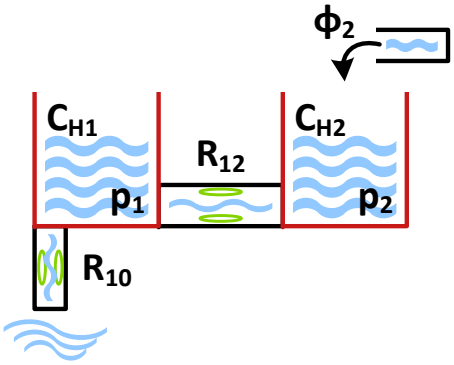

Figure 5.7: A hydraulic system with valve capacitances C_{H_i}, pipe resistances R_{ik}, pressures $p_i(t)$ and external volume flow rate $\phi_2(t)$.

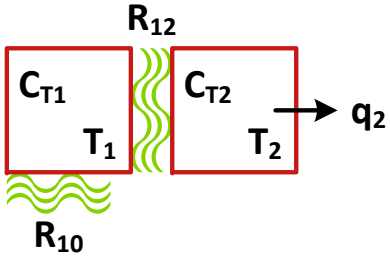

Figure 5.8: A thermodynamic system with thermal capacitances C_{T_i}, thermal resistivity R_{ik}, temperatures $T_i(t)$ and entropy flow rate $q_2(t)$.

need to converge to a common value. This problem is referred to as a *consensus* or *agreement* problem (Ren et al., 2005).

Networks of multiagent systems are often visualised by directed or undirected graphs with the agents at the nodes. The behaviour of the agents can be modelled by any modelling technique; often state-space models are used. The communication between the agents takes place according to a (continuous-time) consensus protocol (Ren et al., 2005; Mesbahi and Egerstedt, 2010):

$$\dot{x}_i(t) = -\sum_{j \in \mathcal{N}_j(t)} a_{ij}(t)\big(x_i(t) - x_j(t)\big), \tag{5.32}$$

where $x_i(t)$ is the state of agent i, $\mathcal{N}_j(t)$ represents the set of agents who can communicate to agent i at time t, and $a_{ij}(t)$ is the time-varying weighting factor of the communication from agent j to agent i. Often, $a_{ij}(t) > 0\ \forall t$. Observe that (5.32) describes a time-varying diffusive coupling as the strength of the communication depends on the difference between the states $x_i(t)$ and $x_j(t)$.

The consensus protocol of the complete graph can be written in matrix form as

$$\dot{x}(t) = -L(t)x(t), \tag{5.33}$$

where $L(t)$ is the time-varying graph-Laplacian and $x(t)$ is a vectorised version of $x_i(t)$. If $a_{ij}(t) = a_{ji}(t)\ \forall i, j$, then the communication protocol is symmetric. If $a_{ij}(t) = a_{ij}\ \forall t$, the communication protocol is time invariant and (5.33) describes a diffusively coupled linear network. Multiagent networks can also have external inputs, which are added to the right-hand side of (5.32) and (5.33) (Talukdar et al., 2020).

5.5.2 Kuramoto model

There are many processes and actions that rely on precise timing, occurring in biological, chemical, physical, and social systems. These actions take place as a result of synchronisation of the individual actions in a population. Some everyday examples one can think of are musicians in an orchestra or the audience applauding. The most successful model of these rhythmic actions was developed by Kuramoto (1975) by analysing coupled phase oscillators. This model is also applied to neural information processing in the brain, laser networks, chemical reactions, and power networks (Acebrón et al., 2005; Boccaletti et al., 2006; Mesbahi and Egerstedt, 2010; Guo et al., 2021).

The Kuramoto model captures the dynamics of coupled phase oscillators by

$$\dot{\theta}_i(t) = \omega_i + \sum_{j \in \mathcal{N}_j} K_{ij} \sin(\theta_j(t) - \theta_i(t)), \tag{5.34}$$

where $\theta_i(t)$ and ω_i are the angular position and the natural frequency of the ith oscillator, respectively, $\mathcal{N}_j$ represents the set of oscillators that is connected to the ith oscillator, and K_{ij} is the strength of the coupling. This model can be interpreted as each oscillator trying to run independently, while the couplings try to synchronise it with the others. It describes a nonlinear time-varying diffusive coupling, because the strength of the coupling depends on a nonlinear (sinusoidal) function of the difference between the angular positions of the oscillators. Often $K_{ij}(t) > 0 \; \forall t$ and if $K_{ij}(t) = K_{ji}(t)$, $\forall i, j$, then the couplings are symmetric. Sometimes, the dynamics of synchronisation systems is linearised around an operating point, leading to a linear second-order vector differential equation (Talukdar et al., 2020).

5.6 Conclusion

The diffusively coupled linear network model (5.10) has been introduced to describe physical linear networks of any order. This multivariable polynomial model has particular structural properties to incorporate the symmetric nature of the physical components and the linear diffusive couplings. Graphically, diffusively coupled linear networks are represented by undirected graphs. Various physical linear networks can be described by this network model in two analogous representations. Even interconnections of physical networks from different domains can be captured by the diffusively coupled network model. It has been shown that physical linear networks that are described by the diffusively coupled linear network model are passive, dissipative, and stable. Some other diffusively coupled networks are shown as well.

In the remaining research, the diffusively coupled linear network model (5.10) will be used to describe physical linear networks for identification purposes, because it is capable of incorporating the structural properties of physical linear networks, including the symmetry of the components and the diffusive couplings. The next step in this research will be to use this diffusively coupled linear network model for identification purposes.

Part II

Identification of physical linear networks

6 | Linear dynamic network identification tools

Many identification tools are available in the literature, but which ones are attractive and supportive for identification in diffusively coupled linear networks? Diffusively coupled linear networks are modelled by polynomial models with specific structural properties. These characteristics need to be incorporated into the identification procedure. The first candidate identification framework includes prediction error methods for linear polynomial models, because the modelling framework is close to that of diffusively coupled linear networks. The second candidate includes prediction error methods for dynamic networks, because they incorporate the interconnection structure. In addition, the weighted null-space fitting (WNSF) algorithm is discussed, because it is a computationally attractive algorithm for solving the (often) nonconvex optimisation problems resulting from prediction error methods.

6.1 Introduction

Diffusively coupled linear networks can describe various physical processes, among which are electrical circuits, chemical processes, and mechanical and hydraulic systems, as explained in Chapter 5. These networks possess the characteristic property that interconnections are based on the difference of signals instead of causal directions of information flow. Therefore, diffusively coupled networks are graphically represented by undirected graphs. Mathematically, they are described by polynomial models with specific structural properties to capture the symmetric interconnections.

These mathematical models can be obtained from the laws of nature or from experimental data. The process of obtaining mathematical models from data is

referred to as system identification. The main challenges in data-driven modelling of physical linear networks are to exploit the interconnection structure and the specific structural conditions in the system identification method as much as possible.

The two classical approaches for system identification are subspace identification methods (Verhaegen and Verdult, 2012) and prediction error identification methods (Ljung, 1999). Subspace identification concerns the identification of state-space representations from experimental data, while prediction error identification methods identify polynomial models from experimental data. For the latter, conditions for convergence and consistency are discussed, as are algorithms for computing the estimates (Ljung, 1999; Hannan and Deistler, 2012). System identification can also be performed in the frequency domain (Pintelon and Schoukens, 2012), for example, by the local polynomial method. These methods all identify systems in an open-loop configuration. The extension to closed-loop system identification is addressed by Ljung (1999), Van den Hof (1998), and Forssell and Ljung (1999).

Van den Hof et al. (2013) generalise closed-loop identification to more complex interconnections of linear dynamic systems. These dynamic networks describe measured signals of interest (node signals) that are interconnected through linear dynamic transfer function modules. Various identification questions are being studied, among which are full network identification methods (Weerts et al., 2016) and related algorithms (Galrinho et al., 2019; Fonken et al., 2022). These network identification questions are considered in a discrete-time prediction error framework.

The overall objective of this research is to develop a comprehensive theory for the identification of diffusively coupled linear networks. This includes three main network identification purposes: identification of the complete network dynamics, identification of subnetwork dynamics, and identification of the interconnection structure. In order to develop the necessary identification tools, the identification tools from the literature that are useful for the identification of diffusively coupled linear networks are reviewed.

Several identification tools are available in the literature. Both time and frequency domain identification methods and identifiability results are interesting, because diffusively coupled linear networks are also described by polynomial models (with specific structural properties). Network identification methods and algorithms in the module representation exploit the interconnection structure of dynamic networks and therefore, are interesting for the identification of diffusively coupled linear networks. Subspace identification methods are not selected, because it is more difficult to incorporate the structural properties of diffusively

coupled linear networks in state-space models and because there are no statistical guarantees for subspace identification.

In this chapter, identification tools from the literature are discussed. The selected tools are most promising for the identification of diffusively coupled linear networks and they are used as a basis in the remaining part of this thesis. Identification tools for dynamic networks have typically been developed for discrete-time systems. In order to fully exploit these tools, we consider only discrete-time network representations with delay operator q^{-1} meaning $q^{-1}w(t) = w(t-1)$. In Section 6.2, identification methods and identifiability aspects for scalar and multivariable polynomial models in the time domain are discussed. Section 6.3 includes a full network identification method and an algorithm for the module representation. Finally, Section 6.4 concludes the chapter.

6.2 Polynomial models

6.2.1 Introduction

Consider the polynomial model as described in Definition 2.20 of Section 2.4.4, where we discussed that this model is popular for describing dynamic systems, especially for identification purposes with prediction error identification methods (Ljung, 1999; Hannan and Deistler, 2012). As diffusively coupled linear networks are described by polynomial models (with particular structural properties), the identification theory for unstructured polynomial models will be helpful in the identification of diffusively coupled linear networks. In this section, prediction error identification methods and the identifiability of these (unstructured) polynomial models are summarised.

6.2.2 Matrix-fraction descriptions

In this section, some concepts regarding polynomial representations and some properties of polynomial matrices are introduced. First, unimodular matrices are introduced and then, matrix-fraction descriptions (MFDs) are discussed, including the concepts of relative primeness and greatest common divisors. For more information on unimodular matrices, see Polderman and Willems (1998, Chapter 2), and for more information on MFDs, see Kailath (1980, Chapter 6).

A polynomial matrix is said to be *nonsingular* if its determinant is nonzero. A special class of nonsingular polynomial matrices are unimodular polynomial matrices.

Definition 6.1 (Unimodular polynomial matrix (Polderman and Willems, 1998)). *The polynomial matrix $U(\xi) \in \mathbb{R}^{p\times p}[\xi]$ is said to be a* unimodular polynomial matrix *if the following equivalent statements hold:*

1. *There exists a polynomial matrix $V(\xi) \in \mathbb{R}^{p\times p}[\xi]$ such that*

$$V(\xi)U(\xi) = I.$$

2. $\det\big(U(\xi)\big) = c \in \mathbb{R}$, *with* $c \neq 0$.

Observe that $V(\xi)$ in Definition 6.1 is also a unimodular polynomial matrix. This means that a polynomial matrix is unimodular if its inverse is a polynomial matrix too.

Now it is clear what unimodular polynomial matrices are, let us move to the MFDs. An MFD of a rational matrix is the ratio of two polynomial matrices. A rational matrix can be written as a right matrix-fraction description (RMFD) or as a left matrix-fraction description (LMFD).

Definition 6.2 (RMFD). *A rational matrix $T(q) \in \mathbb{R}^{p\times m}(q)$ is written as an RMFD as*

$$T(q) = N_R(q^{-1})D_R^{-1}(q^{-1}), \tag{6.1}$$

with polynomial matrices $N_R(q^{-1}) \in \mathbb{R}^{p\times m}[q^{-1}]$ and $D_R(q^{-1}) \in \mathbb{R}^{m\times m}[q^{-1}]$.

Definition 6.3 (LMFD). *A rational matrix $T(q) \in \mathbb{R}^{p\times m}(q)$ is written as an LMFD as*

$$T(q) = D_L^{-1}(q^{-1})N_L(q^{-1}) \tag{6.2}$$

with polynomial matrices $D_L(q^{-1}) \in \mathbb{R}^{p\times p}[q^{-1}]$ and $N_L(q^{-1}) \in \mathbb{R}^{p\times m}[q^{-1}]$.

Observe that the RMFD and the LMFDs have a duality. As LMFDs are more common in system identification, the remainder of this section only describes LMFDs. Dual results hold for RMFDs.

The LMFD in (6.2) can equivalently be written as

$$T(q) = \bar{D}_L^{-1}(q^{-1})\bar{N}_L(q^{-1}), \tag{6.3}$$

with

$$\bar{D}_L(q^{-1}) = W^{-1}(q^{-1})D_L(q^{-1}), \qquad \bar{N}_L(q^{-1}) = W^{-1}(q^{-1})N_L(q^{-1}), \tag{6.4}$$

where the nonsingular polynomial matrix $W(q^{-1}) \in \mathbb{R}^{p\times p}[q^{-1}]$ is a *left divisor* of $D_L(q^{-1})$ and $N_L(q^{-1})$. The LMFD with the minimum degree is found by extracting a *greatest common left divisor* of $D_L(q^{-1})$ and $N_L(q^{-1})$. Then the only left divisors $W(q^{-1})$ of $D_L(q^{-1})$ and $N_L(q^{-1})$ that remain are the ones that have a determinant with zero degree and hence, are unimodular. This unimodularity of greatest common left divisors is a special property and therefore, captured by the following concept:

Definition 6.4 (Left coprime). *Two polynomial matrices $D_L(q^{-1}) \in \mathbb{R}^{p\times p}[q^{-1}]$ and $N_L(q^{-1}) \in \mathbb{R}^{p\times m}[q^{-1}]$ are said to be* relative left prime *or* left coprime *if they only have unimodular greatest common left divisors.*

The properties of LMFDs and left coprime polynomial matrices lead to the following equivalent statements for left coprime polynomial matrices:

Proposition 6.5 (Left coprime). *The two polynomial matrices $D_L(q^{-1})$ and $N_L(q^{-1})$ are left coprime if and only if the following equivalent statements hold:*

1. *All greatest common left divisors of $D_L(q^{-1})$ and $N_L(q^{-1})$ are unimodular.*
2. *All greatest common left divisors of $D_L(q^{-1})$ and $N_L(q^{-1})$ are nonsingular and can only differ by a unimodular (right) factor.*
3. *There exists polynomial matrices $X(q^{-1}) \in \mathbb{R}^{p\times p}[q^{-1}]$ and $Y(q^{-1}) \in \mathbb{R}^{m\times m}[q^{-1}]$ such that $D_L(q^{-1})X(q^{-1}) + N_L(q^{-1})Y(q^{-1}) = I$.*
4. *$\begin{bmatrix} D_L(z) & N_L(z) \end{bmatrix}$ has full row rank for all values of z.*
5. *$\begin{bmatrix} D_L(q^{-1}) & N_L(q^{-1}) \end{bmatrix}$ is irreducible, i.e. it has no common factors.*

As a result, left coprimeness can be determined by calculating the row rank of $\begin{bmatrix} D_L(z) & N_L(z) \end{bmatrix}$.

To conclude, the properties of a minimum-degree LMFD are summarised as follows: If the LMFD as defined in Definition 6.3 has a minimum degree, it has the following properties:

1. The polynomial matrices $D_L(q^{-1})$ and $N_L(q^{-1})$ are left coprime.
2. It has only unimodular greatest common left divisors $W(q^{-1})$.

3. It is irreducible, because the LMFD $D_L^{-1}(q^{-1})N_L(q^{-1})$ is irreducible if $D_L(q^{-1})$ and $N_L(q^{-1})$ are left coprime.

4. It is nonunique, because if the LMFD $D_L^{-1}(q^{-1})N_L(q^{-1})$ is irreducible, then so is the LMFD $\left[W(q^{-1})D_L(q^{-1})\right]^{-1}\left[W(q^{-1})N_L(q^{-1})\right]$ for any unimodular $W(q^{-1})$.

6.2.3 Prediction error methods

As discussed in Section 1.5.1, system identification aims to build a mathematical model of a dynamical system on the basis of experimental data. The best possible model is selected from the candidate models through an identification criterion (Eykhoff, 1974; Ljung, 1999; Pintelon and Schoukens, 2012). In prediction error methods, the selection criterion minimises a prediction error, which is thoroughly chosen by the user. In the prediction error framework, quasi-stationary signals are defined as summations of a stationary stochastic process and a bounded deterministic signal (Ljung, 1999).

The experimental data are generated by the data generating system $\mathcal{S}$. For open-loop system identification, the data generating system is typically described by

$$y(t) = G^0(q)u(t) + v(t), \tag{6.5}$$

where $G^0(q)$ is the dynamical system and $y(t)$, $u(t)$, and $v(t)$ are the measured output signal, known input signal, and unknown disturbance signal, respectively. The dynamical system $G^0(q)$ is described by a rational transfer function matrix. The experimental data $\{y(t), u(t)\}_{t=1}^N$ consist of the signals $y(t)$ and $u(t)$ at time instances $t = 1, 2, \ldots, N$. The data signals $u(t)$ and $y(t)$ are assumed to be quasi-stationary (Ljung, 1999) and the unknown disturbance signal $v(t)$ is assumed to be a stationary stochastic process.

In order to evaluate the predictor later on in the prediction error identification analysis, the unknown disturbance signal $v(t)$ needs to be modelled, for example, by filtered white noise

$$v(t) = H^0(q)e(t), \tag{6.6}$$

with $e(t)$ a white noise signal with bounded moments and with $H^0(q)$ a rational transfer function matrix that is *monic*, where monic means that $\lim_{z\to\infty} H^0(z) = I$, with I the identity matrix.

The model structure $\mathcal{M}$ describes a class of all candidate models of the form (6.5) and (6.6) by parameterising the system and noise model as

$$\mathcal{M} = \{M(q, \theta), \theta \in \Theta\}, \tag{6.7}$$

where $\Theta \subset \mathbb{R}^d$ describes the considered parameter space and with particular models

$$M(\theta) = \{G(q,\theta), H(q,\theta)\}, \tag{6.8}$$

where $G(q,\theta)$ and $H(q,\theta)$ satisfy the same assumptions as $G^0(q)$ and $H^0(q)$, for all $\theta \in \Theta$, respectively.

The identification criterion is often chosen to be a (weighted) least-squares criterion

$$\hat{\theta}_N = \arg\min_{\theta\in\Theta} \frac{1}{N} \sum_{t=1}^{N} \varepsilon^\top(t,\theta) W \varepsilon(t,\theta), \tag{6.9}$$

which aims to minimise the power of some error $\varepsilon(t,\theta)$ that is weighted with $W \succ 0$.

In prediction error identification methods, the error $\varepsilon(t,\theta)$ is carefully derived by first predicting the measured output signal. The one-step-ahead predictor is defined as the conditional expectation

$$\hat{y}(t|t-1) := \mathbb{E}\{y(t)|\, y^{t-1}, u^{t-1}\}, \tag{6.10}$$

where $y^{t-1} = \{y(1), y(2), \ldots, y(t-1)\}$ and $u^{t-1} = \{u(1), u(2), \ldots, u(t-1)\}$. This definition of the predictor results in

$$\hat{y}(t|t-1) = H^{-1}(q)G(q)u(t) + \big(I - H^{-1}(q)\big)y(t), \tag{6.11}$$

which can be written as

$$\hat{y}(t|t-1,\theta) = W(q)z(t), \tag{6.12}$$

with the stable predictor filter $W(q)$ and the data vector $z(t)$ given by

$$W(q) = \begin{bmatrix} H^{-1}(q)G(q) & I - H^{-1}(q) \end{bmatrix}, \qquad z(t) = \begin{bmatrix} u(t) \\ y(t) \end{bmatrix}. \tag{6.13}$$

Using the model structure $\mathcal{M}$ (6.7), the parameterised one-step-ahead predictor becomes

$$\hat{y}(t|t-1,\theta) = H^{-1}(q,\theta)G(q,\theta)u(t) + \big(I - H^{-1}(q,\theta)\big)y(t). \tag{6.14}$$

The prediction error is then defined as the difference between the actually measured output signals and the predicted output signals, i.e.

$$\varepsilon(t,\theta) := y(t) - \hat{y}(t|t-1,\theta), \tag{6.15}$$

which is given by

$$\varepsilon(t,\theta) := H^{-1}(q,\theta)\big(y(t) - G(q,\theta)u(t)\big). \tag{6.16}$$

This is the error that is used in the identification criterion (6.9) in prediction error identification methods.

6.2.4 Data informativity

Data informativity concerns the information content that is present in the data set. The data set is denoted by $Z^N := \{z(t)\}_{t=1}^{t=N}$, meaning all values of $z(t)$ at time $t = 1, 2, \ldots, N$. The data set should contain sufficient information to be able to distinguish between different models in the model structure. Therefore, a data set is called *informative* if it is capable of distinguishing between different models.

Definition 6.6 (Data informativity (Ljung, 1999)). *A quasi-stationary data set $Z^N := \{z(t)\}_{t=1}^{t=N}$ is informative enough with respect to the model set $\mathcal{M}$ (with a one-step-ahead predictor as in* (6.12)*) if, for any two predictor filters $W_1(q)$ and $W_2(q)$,*

$$\bar{\mathbb{E}}\{\big(W_1(q) - W_2(q)\big)z(t)\}^2 = 0 \tag{6.17}$$

implies that $W_1(e^{i\omega}) = W_2(e^{i\omega})$ for almost all ω.

The excluded ω are in a set of Lebesgue measure zero in $\mathbb{R}$.

Proposition 6.7 (Data informativity (Ljung, 1999)). *A quasi-stationary data set $Z^N := \{z(t)\}_{t=1}^{t=N}$ is informative enough with respect to the model set consisting of all LTI models if $\Phi_z(\omega) \succ 0$ for almost all ω, with $\Phi_z(\omega)$ the spectrum matrix of $z(t)$.*

6.2.5 Identifiability

Identifiability concerns the uniqueness of a system representation in a parameterised model set (or model structure). Using the concepts of a system $\mathcal{S}$ and a model structure $\mathcal{M}$, the identifiability concept can be formalised.

Definition 6.8 (Global identifiability at $\theta^\star$ (Ljung, 1999)). *A model structure $\mathcal{M}$ is* globally identifiable *at $\theta^\star$ if*

$$M(\theta) = M(\theta^\star), \quad \theta \in \Theta, \quad \Longrightarrow \quad \theta = \theta^\star, \tag{6.18}$$

Definition 6.9 (Global identifiability (Ljung, 1999)). *A model structure $\mathcal{M}$ is* globally identifiable *if it is globally identifiable at almost all $\theta^\star \in \Theta$.*

The excluded $\theta^\star$ are in a set of Lebesgue measure zero in $\mathbb{R}^d$.

Proposition 6.10 (Global identifiability (Ljung, 1999)). *Consider the model structure $\mathcal{M}$ corresponding to the SISO system*

$$A(q^{-1})y(t) = \frac{B(q^{-1})}{F(q^{-1})}u(t) + \frac{C(q^{-1})}{D(q^{-1})}e(t), \tag{6.19}$$

with θ being the coefficients of the polynomials $A(q^{-1})$, $B(q^{-1})$, $C(q^{-1})$, $D(q^{-1})$ and $F(q^{-1})$, which are all monic except for $B(q^{-1})$ and which have degrees n_a, n_b, n_c, n_d, and n_f, respectively. The model structure $\mathcal{M}$ is globally identifiable at $\theta^\star$ if and only if all of the following conditions hold:

1. *There is no common factor between all $z^{n_a}A(z,\theta^\star)$, $z^{n_b}B(z,\theta^\star)$, and $z^{n_c}C(z,\theta^\star)$.*
2. *There is no common factor between $z^{n_b}B(z,\theta^\star)$ and $z^{n_f}F(z,\theta^\star)$.*
3. *There is no common factor between $z^{n_c}C(z,\theta^\star)$ and $z^{n_d}D(z,\theta^\star)$.*
4. *If $n_a \geq 1$, then there must be no common factor between $z^{n_f}F(z,\theta^\star)$ and $z^{n_d}D(z,\theta^\star)$.*
5. *If $n_d \geq 1$, then there must be no common factor between $z^{n_a}A(z,\theta^\star)$ and $z^{n_b}B(z,\theta^\star)$.*
6. *If $n_f \geq 1$, then there must be no common factor between $z^{n_a}A(z,\theta^\star)$ and $z^{n_c}C(z,\theta^\star)$.*

For a generally chosen model set with $\Theta \in \mathbb{R}^d$, the conditions in Proposition 6.10 are only violated for a small selection of $\theta^\star$, i.e. for $\theta^\star$ in a set of Lebesgue measure zero in $\mathbb{R}^d$. Therefore, the model structure given in Proposition 6.10 is said to be globally identifiable and Proposition 6.10 can be formulated as follows (Ljung, 1999).

Consider the SISO system description $\mathcal{S}$ in

$$A^0(q^{-1})y(t) = \frac{B^0(q^{-1})}{F^0(q^{-1})}u(t) + \frac{C^0(q^{-1})}{D^0(q^{-1})}e(t), \tag{6.20}$$

with true polynomial orders n_a^0, n_b^0, n_c^0, n_d^0, and n_f^0. Consider the model structure $\mathcal{M}$ of Proposition 6.10. Then $\mathcal{S} \in \mathcal{M}$ (i.e. the system lies in the model set) and corresponds to a globally identifiable θ-value if and only if all of the following conditions hold (Ljung, 1999, Theorem 4.2):

1. $\min(n_a - n_a^0, n_b - n_b^0, n_c - n_c^0) = 0$.

2. $\min(n_b - n_b^0, n_f - n_f^0) = 0$.
3. $\min(n_c - n_c^0, n_d - n_d^0) = 0$.
4. If $n_a \geq 1$, then also $\min(n_f - n_f^0, n_d - n_d^0) = 0$.
5. If $n_d \geq 1$, then also $\min(n_a - n_a^0, n_b - n_b^0) = 0$.
6. If $n_f \geq 1$, then also $\min(n_a - n_a^0, n_c - n_c^0) = 0$.

If the system lies in the model set, θ^0 is often used to indicate the θ-value for the system, that is, $\mathcal{S} = M^0 := M(\theta^0)$.

6.2.6 Identifiability of multivariable systems

The above results on global identifiability can also be formulated for multivariable systems (Ljung, 1999, Appendix 4A).

Let us first introduce some notions for a polynomial matrix $X(q^{-1}) \in \mathbb{R}^{p\times m}[q^{-1}]$. Let the polynomial elements $x_{ij}(q^{-1})$ have degree $n_{x_{ij}}$, let $n_{x_j} = \max\left(n_{x_{ij}}\right), \forall i$, and let the degree of the polynomial matrix $X(q^{-1})$ be $n_x = \max\left(n_{x_{ij}}\right), \forall i, j$. Correspondingly, let us define the diagonal polynomial matrix $Z_x(z) = \operatorname{diag}\left(z^{n_{x_1}}, \ldots, z^{n_{x_m}}\right)$.

Proposition 6.11 (Global identifiability of multivariable systems (Ljung, 1999)). *Consider the model structure $\mathcal{M}$ corresponding to the multivariable system*

$$A(q^{-1})y(t) = B^{-1}(q^{-1})F(q^{-1})u(t) + C^{-1}(q^{-1})D(q^{-1})e(t), \qquad (6.21)$$

with θ being the coefficients of the polynomials $A(q^{-1})$, $B(q^{-1})$, $C(q^{-1})$, $D(q^{-1})$ and $F(q^{-1})$, which are all monic except for $B(q^{-1})$, and which have polynomial degrees n_a, n_b, n_c, n_d, and n_f, respectively. The model structure $\mathcal{M}$ is globally identifiable at $\theta^\star$ if and only if all of the following conditions hold:

1. *All $A(z,\theta^\star)Z_a(z)$, $B(z,\theta^\star)Z_b(z)$, and $C(z,\theta^\star)Z_c(z)$ are left coprime.*
2. *$B(z,\theta^\star)Z_b(z)$ and $F(z,\theta^\star)Z_f(z)$ are left coprime.*
3. *$C(z,\theta^\star)Z_c(z)$ and $D(z,\theta^\star)Z_d(z)$ are left coprime.*
4. *If $n_a \geq 1$, then also $D(z,\theta^\star)Z_d(z)$ and $F(z,\theta^\star)Z_f(z)$ are left coprime.*

5. *If* $n_d \geq 1$, *then also* $A(z, \theta^\star)Z_a(z)$ *and* $B(z, \theta^\star)Z_b(z)$ *are left coprime.*

6. *If* $n_f \geq 1$, *then also* $A(z, \theta^\star)Z_a(z)$ *and* $C(z, \theta^\star)Z_c(z)$ *are left coprime.*

Similar as before, for a generally chosen model set with $\Theta \in \mathbb{R}^d$, the conditions in Proposition 6.11 are only violated for a small selection of $\theta^\star$. The model structure given in Proposition 6.11 is said to be globally identifiable (Ljung, 1999).

Hannan and Deistler (2012) analyse identifiability for a specific class of autoregressive-moving average with exogeneous input (ARMAX) systems. They consider generalised multivariable systems with $F(q^{-1}) = I$ and $D(q^{-1}) = I$ and particularly, without restrictions on any of the parameters. This means that they consider multivariable ARMAX systems in which $A(q^{-1}, \theta)$ and $C(q^{-1}, \theta)$ are not necessarily monic, which leads to different conditions for identifiability. Moreover, the conditions for identifiability are mainly based on the absence of transfer function elements instead of on the parameters. As initially no assumptions on the parameters are made and the identifiability conditions are based on the structure of the system, the identifiability of these model structures is sometimes referred to as *structural identifiability*.

Proposition 6.12 (Identifiability of multivariable ARMAX systems (Hannan and Deistler, 2012)). *Consider the model structure* $\mathcal{M}$ *corresponding to the multivariable ARMAX system*

$$A(q^{-1})y(t) = B(q^{-1})u(t) + C(q^{-1})e(t), \tag{6.22}$$

with θ *being the coefficients of the polynomials* $A(q^{-1}) \in \mathbb{R}^{p\times p}[q^{-1}]$, $B(q^{-1}) \in \mathbb{R}^{p\times m}[q^{-1}]$, *and* $C(q^{-1}) \in \mathbb{R}^{p\times p}[q^{-1}]$, *and with* $\det(A_0) \neq 0$, *with* $A_0 := \lim_{z\to\infty} A(z)$. *Define the polynomial matrix*

$$D(q^{-1}, \theta) := \begin{bmatrix} A(q^{-1}, \theta) & B(q^{-1}, \theta) & C(q^{-1}, \theta) \end{bmatrix}$$

and let $d_i(q^{-1}, \theta)$ *be the matrix consisting of those columns of* $D(q^{-1}, \theta)$, *where we have a zero prescribed in the* i*th row. This class is identifiable if all of the following conditions hold:*

1. *In every row of* $D(q^{-1}, \theta)$ *there are at least* $p - 1$ *elements prescribed to be zero.*

2. $d_i(q^{-1}, \theta)$ *is assumed to have rank* $p - 1$ *(as a polynomial matrix, i.e.,* $d_i(z, \theta)$ *has rank* $p - 1$ *for all but a finite number of* z*'s).*

3. *Every row of $D(q^{-1}, \theta)$ is relatively prime (i.e., there is no common polynomial factor of degree greater than zero).*

4. *The diagonal elements of $A_0(\theta)$ are equal to 1.*

Conditions 1 and 2 of Proposition 6.12 are strictly structural conditions on the absence of transfer functions. Condition 3 of Proposition 6.12 is equivalent to Condition 1 of Proposition 6.11. Even though the diagonal elements of $A_0(\theta)$ are scaled to 1, there are no restrictions on the off-diagonal elements of $A_0(\theta)$ in Proposition 6.12. This means that these ARMAX models are not restricted to being monic.

6.3 Module representations

6.3.1 Introduction

Consider the module representation as described in Section 2.4.8, where we discussed that many questions related to network identification have been studied in the literature for this dynamic network model. One of these questions is related to identifiability in dynamic networks, which is different from identifiability in general systems as formulated in Section 6.2.

In general, network identification with prediction error methods leads to nonconvex optimisation problems, which are numerically difficult to solve and may take much computation time, especially for large networks. Therefore, smart algorithms need to be developed to be able to perform network identification in foreseeable time. One such algorithm is WNSF (Galrinho et al., 2019), which takes three (weighted) least-squares steps to solve a nonconvex network optimisation problem in an optimal way. This algorithm has been extended with additional least-squares steps to incorporate the estimation of an unknown disturbance topology (Fonken et al., 2022). The WNSF algorithm is summarised in Section 6.3.4, and further explored in Chapter 8.

6.3.2 Network identifiability

In Section 6.2.5 and 6.2.6, global identifiability for scalar and multivariable systems has been discussed. In this section, results for global identifiability of dynamic networks in the module representation are formulated (Weerts et al., 2018b). Similar to identifiability, the objective of network identifiability is to

distinguish different network models in a model set from each other on the basis of measured data. In contrast to global identifiability for (multivariable) systems is that global network identifiability is formulated for network models instead of for parameter vectors.

Consider a well-posed and stable module representation, as in Section 2.4.8, which is described by

$$w(t) = G(q)w(t) + R(q)r(t) + H(q)e(t), \tag{6.23}$$

where the covariance of the noise $e(t)$ is denoted by Λ. The response of the module representation (6.23) is given by

$$w(t) = T_{wr}(q)r(t) + \bar{v}(t), \qquad \bar{v}(t) := T_{we}(q)e(t), \tag{6.24}$$

with rational transfer function matrices $T_{wr}(q) = \big(I - G(q)\big)^{-1}R(q)$ and $T_{we}(q) = \big(I - G(q)\big)^{-1}H(q)$.

The network model corresponding to this module representation is defined by $M = \big(G(q), R(q), H(q), \Lambda\big)$ with $G(q) \in \mathbb{R}^{L\times L}(q)$ with all diagonal elements equal to zero and with all off-diagonal elements proper, $R(q) \in \mathbb{R}^{L\times K}(q)$ with all elements proper, $H(q) \in \mathbb{R}^{L\times L}(q)$ is monic and stable with a stable inverse, $\Lambda \in \mathbb{R}^{L\times L}$, the covariance of $e(t)$, that is positive definite, and the network is assumed to be well-posed and stable. The corresponding parameterised network model set is denoted by $\mathcal{M} := \{M(q,\theta), \theta \in \Theta\}$ and consists of particular parameterised models

$$M(q,\theta) := \{G(q,\theta), R(q,\theta), H(q,\theta), \Lambda(\theta)\}, \tag{6.25}$$

where $G(q,\theta)$, $R(q,\theta)$, $H(q,\theta)$, and $\Lambda(\theta)$ satisfy for all $\theta \in \Theta$ the same assumptions as $G(q)$, $R(q)$, $H(q)$, and Λ, respectively.

The second-order statistical properties of the measured data set $\{w(t), r(t)\}$ can be represented by the cross- and autocorrelation functions and spectral densities of these signals. They can be further utilised to obtain $T_{wr}(e^{i\omega})$ and $\Phi_{\bar{v}}(\omega)$. The relation with the parameterised model $M(\theta)$ is given by

$$T_{wr}(q,\theta) := \big(I - G(q,\theta)\big)^{-1}R(q,\theta), \tag{6.26a}$$

$$T_{we}(q,\theta) := \big(I - G(q,\theta)\big)^{-1}H(q,\theta), \tag{6.26b}$$

$$\Phi_{\bar{v}}(\omega,\theta) = T_{we}(e^{i\omega},\theta)\Lambda(\theta)T_{we}^{*}(e^{i\omega},\theta), \tag{6.26c}$$

where $(\cdot)^*$ indicates the complex conjugate transpose and $(\cdot)^{-*} = \big((\cdot)^{-1}\big)^*$, i.e. $(\cdot)^{-*}$ is the $(\cdot)^*$ of its inverse. A standard open-loop identification of (6.24) in case $r(t)$ and $\bar{v}(t)$ are uncorrelated can typically lead to consistent estimation of $T_{wr}(q)$ and $\Phi_{\bar{v}}(\omega)$. Using these relations, global network identifiability is defined in accordance with Definition 6.8 as follows:

Definition 6.13 (Global network identifiability at $M(\theta^*)$ (Weerts et al., 2018b)). *The network model set $\mathcal{M}$ is* globally network identifiable *at $M(\theta^\star)$ if for all $M(\theta) \in \mathcal{M}$*

$$\left.\begin{aligned} T_{wr}(q,\theta) &= T_{wr}(q,\theta^\star) \\ \Phi_{\bar{v}}(\omega,\theta) &= \Phi_{\bar{v}}(\omega,\theta^\star) \end{aligned}\right\} \Rightarrow M(\theta) = M(\theta^\star). \tag{6.27}$$

Definition 6.14 (Global network identifiability (Weerts et al., 2018b)). *A model structure $\mathcal{M}$ is* globally network identifiable *if it is globally network identifiable at all $M(\theta^\star) \in \mathcal{M}$.*

Remark 6.15 (Generic network identifiability). *Global identifiability is defined for almost all $\theta^* \in \Theta$ in Definition 6.9, while global network identifiability is defined for all $M(\theta^*) \in \mathcal{M}$ in Definition 6.14. Globally network identifiable at* almost *all $M(\theta^\star) \in \mathcal{M}$ is referred to as* generic network identifiability *(Hendrickx et al., 2019).*

A transfer function module $G_{ij}(q)$ possesses a direct feedthrough term if it satisfies $G_{ij}^{\infty} := \lim_{z\to\infty} G_{ij}(z) \neq 0$. A dynamic network has an algebraic loop if there exists a loop (i.e. a path that starts and ends at the same vertex) that has a nonzero direct feedthrough term. The direct feedthrough term of a path is the product of the direct feedthrough terms of the subsequent modules. In the constant term of the noise spectrum, that is $\Phi_{\bar{v}}(0)$, the direct feedthrough terms are multiplied with the covariance matrix of the noise Λ, which makes it impossible to separate the direct feedthrough terms from Λ.

If there are no direct feedthrough terms present in the network, i.e. if $G^{\infty,\theta} := \lim_{z\to\infty} G(z,\theta) = 0$ for all $\theta \in \Theta$, then

$$\left.\begin{aligned} T_{wr}(q,\theta) &= T_{wr}(q,\theta^\star) \\ \Phi_{\bar{v}}(\omega,\theta) &= \Phi_{\bar{v}}(\omega,\theta^\star) \end{aligned}\right\} \Rightarrow \begin{cases} T_{wr}(q,\theta) = T_{wr}(q,\theta^\star) \\ T_{we}(q,\theta) = T_{we}(q,\theta^\star) \\ \Lambda(\theta) = \Lambda(\theta^\star), \end{cases} \tag{6.28}$$

such that (6.27) in Definition 6.13 is equivalently formulated as

$$\left.\begin{aligned} T_{wr}(q,\theta) &= T_{wr}(q,\theta^\star) \\ T_{we}(q,\theta) &= T_{we}(q,\theta^\star) \end{aligned}\right\} \Rightarrow \begin{cases} G(q,\theta) = G(q,\theta^\star) \\ R(q,\theta) = R(q,\theta^\star) \\ H(q,\theta) = H(q,\theta^\star). \end{cases} \tag{6.29}$$

The spectral factorisation of $\Phi_{\bar{v}}(\omega)$ into a unique Λ and $T_{we}(q)$ that is stable, stably invertible, and monic is a result of Youla (1961).

If there are direct feedthrough terms present in the network and moreover, if there are algebraic loops present in the network, additional restrictions on the model set are necessary to force a unique recovery of the direct feedthrough terms and Λ. These conditions are specified in Weerts et al. (2018b, Proposition 3) and include two restrictions. The first restriction comprises that the number of parameterised direct feedthrough terms in $G(q,\theta)$ and $R(q,\theta)$ should be at most K (the number of known external excitation signals. The second restriction is a condition on the rank of a particular part of the transfer function $T_{wr}(q,\theta)$ related to parameterised rows in $G^{\infty}(\theta)$ and nonparameterised columns $R^{\infty}(\theta)$. If the additional restrictions are satisfied, then again the implication (6.28) holds, such that again (6.27) in Definition 6.13 is equivalently formulated as (6.29). As a result, conditions for global network identifiability of $\mathcal{M}$ (at $M(\theta^{\star})$) are formulated (Weerts et al., 2018b, Theorem 2).

6.3.3 Joint-direct method

The Joint-direct method is a prediction error identification method for consistently identifying all dynamics in a dynamic network that is formulated in the module representation. To take algebraic loops into account, a specific predictor is formulated that exploits external excitation signals (Weerts et al., 2016). The main idea of this method is that additional external excitation signals are used to identify the direct feedthrough terms, while excitation by disturbances is maximally utilised to identify the remaining dynamics. In the remainder of this section, we summarise the Joint-direct method (Weerts et al., 2016).

Consider a well-posed module representation as described in Section 2.4.8, which may contain algebraic loops, in which all node signals $w(t)$ are measured, in which some known external excitation signals $r(t)$ are present, where the noise covariance matrix $\Lambda \succ 0$ is diagonal, and where $\Phi_v(\omega)$ may be nondiagonal and has full rank. Let G^{∞} denote the direct feedthrough terms, i.e. $G^{\infty} = \lim_{z\to\infty} G(z)$. Remember that a dynamic network has an algebraic loop if there exists a loop that has a nonzero direct feedthrough term.

The Joint-direct method is a prediction-error identification method for dynamic networks. The network predictor is defined as the conditional expectation

$$\hat{w}(t|t-1) := \mathbb{E}\{w(t)|\, w^{t-1}, r^{t}\}, \tag{6.30}$$

where the delayed value $w^{t-1} = \{w(1), w(2), \ldots, w(t-1)\}$ and $r^{t} = \{r(1), r(2), \ldots, r(t)\}$. For the module representation (6.23), this definition of the network predictor leads to

$$\hat{w}(t|t-1) = W_w(q)w(t) + W_r(q)r(t), \tag{6.31}$$

with predictor filters

$$W_w(q) = \Big(I - (I - G^\infty)^{-1} H^{-1}(q)\big(I - G(q)\big)\Big), \tag{6.32a}$$

$$W_r(q) = (I - G^\infty)^{-1} H^{-1}(q) R(q). \tag{6.32b}$$

Observe that $\lim_{z\to\infty} W_w(z) = \Big(I - (I - G^\infty)^{-1} I (I - G^\infty\Big) = I - I = 0$ and therefore $W_w(q)$ is strictly proper, which is consistent with the use of only the past of $w(t)$ in (6.30).

The innovation related to the network predictor is defined as

$$\hat{e}(t) := w(t) - \hat{w}(t|t-1), \tag{6.33}$$

which results in a scaled version of the driving noise process $e(t)$:

$$\hat{e}(t) = (I - G^\infty)^{-1} e(t). \tag{6.34}$$

The scaling creates correlation over the (white noise) innovation signals.

The parameterised network model set $\mathcal{M}$ leads to the parameterised network predictor

$$\hat{w}(t|t-1;\theta) = W_w(q,\theta) w(t) + W_r(q,\theta) r(t), \tag{6.35}$$

with $\theta \in \Theta$ and with filters

$$W_w(q,\theta) = \Big(I - \big(I - G^\infty(\theta)\big)^{-1} H^{-1}(q,\theta)\big(I - G(q,\theta)\big)\Big), \tag{6.36a}$$

$$W_r(q,\theta) = \big(I - G^\infty(\theta)\big)^{-1} H^{-1}(q,\theta) R(q,\theta), \tag{6.36b}$$

and to the parameterised prediction error, that is defined as $\hat{\varepsilon}(t,\theta) := w(t) - \hat{w}(t|t-1;\theta)$,

$$\hat{\varepsilon}(t,\theta) = \big(I - G^\infty(\theta)\big)^{-1} \varepsilon(t,\theta), \tag{6.37}$$

with residual

$$\varepsilon(t,\theta) = H^{-1}(q,\theta)\Big(\big(I - G(q,\theta)\big) w(t) - R(q,\theta) r(t)\Big). \tag{6.38}$$

For the true parameter vector θ^0, the parameterised prediction error $\hat{\varepsilon}(t,\theta^0)$ reduces to the innovation $\hat{e}(t)$ and θ^0, $\varepsilon(t,\theta^0)$ reduces to the driving noise process $e(t)$.

The identification is performed by optimising a weighted least-squares criterion

$$\hat{\theta}_N = \arg\min_{\theta\in\Theta} \frac{1}{N}\sum_{t=1}^{N} \hat{\varepsilon}^\top(t,\theta) S^{-1} \hat{\varepsilon}(t,\theta), \tag{6.39}$$

where the weighting matrix $S \succ 0$ is chosen by the user and ideally equal to the covariance matrix of the noise.

Now conditions for consistency of the resulting estimate $M(\hat{\theta}_N)$ are formulated.

Proposition 6.16 (Consistent estimate (Weerts et al., 2016)). *The estimated model $M(\hat{\theta}_N)$ is a consistent estimate if the following three conditions are satisfied:*

1. *The network system is contained in the model set $\mathcal{M}$, meaning that $\exists\, \theta^0 \in \Theta$ such that $G(q,\theta^0) = G(q)$, $R(q,\theta^0) = R(q)$, and $H(q,\theta^0) = H(q)$.*
2. *The data are informative with respect to the model set $\mathcal{M}$, meaning that $\bar{\mathbb{E}}\{\hat{\varepsilon}(q,\theta_1) - \hat{\varepsilon}(q,\theta_2)\}^\top S^{-1} \bar{\mathbb{E}}\{\hat{\varepsilon}(q,\theta_1) - \hat{\varepsilon}(q,\theta_2)\} = 0$ implies that $\hat{W}_w(e^{i\omega},\theta_1) = \hat{W}_w(e^{i\omega},\theta_2)$ and $\hat{W}_r(e^{i\omega},\theta_1) = \hat{W}_r(e^{i\omega},\theta_2)$ for almost all ω and for any two $\theta_1, \theta_2 \in \Theta$.*
3. *The network model set $\mathcal{M}$ is globally network identifiable, meaning that for any two $\theta_1, \theta_2 \in \Theta$, $W_w(q,\theta_1) = W_w(q,\theta_2)$ and $W_r(q,\theta_1) = W_r(q,\theta_2)$ together imply $M(q,\theta_1) = M(q,\theta_2)$.*

Physical linear networks very often contain static elements, which cause direct feedthrough terms and algebraic loops in the relations between the signals of interest. Therefore, it is crucial to be able to incorporate these terms into the identification procedure. The Joint-direct method is the only network identification method that allows for algebraic loops in the network and incorporates them in the identification procedure. This makes the Join-direct method interesting for network identification of physical linear networks.

6.3.4 Weighted null-space fitting

Identification in dynamic networks often takes place through prediction error methods, such as the joint-direct method presented in Section 6.3.3. One major drawback of these methods is that the optimisation is nonconvex if the prediction error is not affine in the parameters. As a result, the optimisation may lead to local

optima instead of the global optimum. As an alternative, the WNSF algorithm has been developed, which consists of multiple (weighted) least-squares steps (Galrinho et al., 2019). First, an intermediate high-order model is estimated using least-squares. Then a maximum-likelihood model reduction step is applied using weighted least-squares. As the optimal weighting in the second step depends on the parameters, an additional weighted least-squares step is needed to achieve asymptotic efficiency. Additional iterations are possible in the third step to improve the estimate for a finite sample size. Due to the several convex steps, this method has attractive computational properties. Another advantage of this algorithm is that the dynamics and the noise model are estimated simultaneously.

WNSF has first been developed for scalar polynomial models (Galrinho et al., 2019) and was related to sequential least-squares, which is a multistep algorithm for identification of module representations with a specific structure (Weerts et al., 2018a). WNSF has also been extended to general module representations (Fonken et al., 2020), including the estimation of the noise topology (Fonken et al., 2022). In the latter situation, the role of the intermediate high-order model has been revised to estimate the residuals instead of the network dynamics, in accordance with Dankers (2019). In this section, the WNSF algorithm for scalar polynomial models with a BJ model structure is presented (Galrinho et al., 2019).

Consider the (scalar) polynomial system as presented in Section 2.4.4

$$y(t) = G^0(q)u(t) + H^0(q)e(t), \tag{6.40}$$

with stochastic signals $u(t)$ and $e(t)$, with stable and rational transfer functions $G^0(q)$ and $H^0(q)$, with $H^0(q)$ stably invertible, and with a BJ structure according to

$$G^0(q) = \frac{L^0(q^{-1})}{F^0(q^{-1})} = \frac{\ell_1 q^{-1} + \cdots + \ell_{m_\ell} q^{-m_\ell}}{1 + f_1 q^{-1} + \cdots + f_{m_f} q^{-m_f}} \tag{6.41a}$$

$$H^0(q) = \frac{C^0(q^{-1})}{D^0(q^{-1})} = \frac{1 + c_1 q^{-1} + \cdots + c_{m_c} q^{-m_c}}{1 + d_1 q^{-1} + \cdots + d_{m_d} q^{-m_d}}, \tag{6.41b}$$

where $F^0(q^{-1})$ and $L^0(q^{-1})$ as well as $C^0(q^{-1})$ and $D^0(q^{-1})$ do not have common factors.

The corresponding parameterised model set $\mathcal{M} := \{M(q,\theta), \theta \in \Theta\}$ consists of models

$$M(\theta) = \{L(q^{-1},\theta), F(q^{-1},\theta), C(q^{-1},\theta), D(q^{-1},\theta)\}, \tag{6.42}$$

with θ being the coefficients of the polynomials $F(q^{-1},\theta)$, $L(q^{-1},\theta)$, $C(q^{-1},\theta)$, and $D(q^{-1},\theta)$, respectively, and where $F(q^{-1},\theta)$, $L(q^{-1},\theta)$, $C(q^{-1},\theta)$, and

$D(q^{-1},\theta)$ satisfy for all $\theta \in \Theta$ the same assumptions as $F^0(q^{-1})$, $L^0(q^{-1})$, $C^0(q^{-1})$, and $D^0(q^{-1})$, respectively. Let the true system be denoted by $\mathcal{S} = M^0 := M(\theta^0)$.

Step 1 The true system $\mathcal{S}$ can alternatively be written as

$$A^0(q)y(t) = B^0(q)u(t) + e(t), \tag{6.43}$$

where the transfer functions

$$A^0(q) := \frac{1}{H^0(q)}, \qquad B^0(q) = \frac{G^0(q)}{H^0(q)}, \tag{6.44}$$

are stable. Hence, an ARX model

$$A(q,\eta^n)y(t) = B(q,\eta^n)u(t) + e(t), \tag{6.45}$$

with η^n being the parameters of the polynomials $A(q,\eta^n) = 1 + \sum_{k=1}^{n} a_k q^{-k}$ and $B(q,\eta^n) = \sum_{k=1}^{n} b_k q^{-k}$, that is

$$\eta^n = \begin{bmatrix} a_1 & a_2 & \cdots & a_n & b_1 & b_2 & \cdots & b_n \end{bmatrix}, \tag{6.46}$$

with η^{n0} the true parameter values, approximates (6.43) arbitrarily well if the model order n is chosen large enough.

The ARX model (6.45) can be rewritten in a linear regressor form as

$$y(t) = \left(\phi^n(t)\right)^\top \eta^n + e(t), \tag{6.47}$$

with

$$\phi^n(t) = \begin{bmatrix} -y(t-1) \\ -y(t-2) \\ \vdots \\ -y(t-n) \\ u(t-1) \\ u(t-2) \\ \vdots \\ u(t-n) \end{bmatrix}. \tag{6.48}$$

Now η^n is estimated from (6.47) through least-squares as

$$\hat{\eta}^n_N = \left(R^n_N\right)^{-1} r^n_N, \tag{6.49}$$

with

$$R^n_N = \frac{1}{N}\sum_{t=n+1}^{N} \phi^n(t)\left(\phi^n(t)\right)^\top, \qquad r^n_N = \frac{1}{N}\sum_{t=n+1}^{N} \phi^n(t)y(t). \tag{6.50}$$

Step 2 The high-order ARX model is used to identify the original model (6.42). The relations (6.41), and (6.44) can be rewritten as

$$C^0(q)A^0(q) - D^0(q) = 0, \qquad F^0(q)B^0(q) - L^0(q)A^0(q) = 0, \tag{6.51}$$

or in regression form as

$$\eta^{\infty 0} - Q_n(\eta_0^\infty)\theta^0 = 0, \tag{6.52}$$

with $\eta^{\infty 0}$ the true parameter values of the infinitely high order ARX model (6.45) exactly describing the true system (6.43).

Now θ is estimated from (6.52) through least-squares as

$$\hat{\theta}_N^{ls} = \left(Q_n^\top(\hat{\eta}_N^n)Q_n(\hat{\eta}_N^n)\right)^{-1}Q_n^\top(\hat{\eta}_N^n)\hat{\eta}_N^n, \tag{6.53}$$

where $\eta^{\infty 0}$ is substituted by its nth order estimate $\hat{\eta}_N^n$ obtained in Step 1 (6.49).

Step 3 In Step 2, the residuals of Step 1 have not been taken into account. This can be done by replacing $A^0(q)$ and $B^0(q)$ in (6.51) by their estimates $A(q, \hat{\eta}_N^n)$ and $B(q, \hat{\eta}_N^n)$, leading to

$$C^0(q)A(q,\hat{\eta}_N^n) - D^0(q) = C^0(q)\big(A(q,\hat{\eta}_N^n) - A^0(q)\big), \tag{6.54a}$$

$$\begin{aligned} F^0(q)B(q,\hat{\eta}_N^n) - L^0(q)A(q,\hat{\eta}_N^n) = \\ F^0(q)\big(B(q,\hat{\eta}_N^n) - B^0(q)\big) - L^0(q)\big(A(q,\hat{\eta}_N^n) - A^0(q)\big), \end{aligned} \tag{6.54b}$$

or in regression form

$$\hat{\eta}_N^n - Q_n(\hat{\eta}_N^n)\theta^0 = T_n(\theta^0)(\hat{\eta}_N^n - \eta^{\infty 0}), \tag{6.55}$$

on the basis of which θ is estimated through weighted least-squares as

$$\hat{\theta}_N^{wls} = \left(Q_n^\top(\hat{\eta}_N^n)W_n(\hat{\theta}_N^{ls})Q_n(\hat{\eta}_N^n)\right)^{-1}Q_n^\top(\hat{\eta}_N^n)W_n(\hat{\theta}_N^{ls})\hat{\eta}_N^n, \tag{6.56}$$

where again $\eta^{\infty 0}$ is replaced by its nth order estimate $\hat{\eta}_N^n$ obtained in Step 1 (6.49), where θ^0 substituted its estimate $\hat{\theta}_N^{ls}$ obtained in Step 2 (6.53), and with weighting matrix

$$W_n(\hat{\theta}_N^{ls}) = \left(T_n(\hat{\theta}_N^{ls})\left(R_N^n\right)^{-1}T_n^\top(\hat{\theta}_N^{ls})\right)^{-1}. \tag{6.57}$$

6.4 Conclusion

Several identification tools from two identification frameworks have been discussed that seem to be attractive for identification in diffusively coupled linear

networks. First, ingredients from the identification of polynomial models have been considered. These models are identified through prediction error methods in the time domain. Data informativity and identifiability aspects have been discussed. For multivariable systems, MFDs and relative primeness play a crucial role in identifiability. These ingredients are used to formulate data informativity and network identifiability conditions for the identification of physical linear networks.

Second, identification tools from the network identification framework have been discussed. In this context, linear dynamic networks that are described in the module representation are considered. The joint-direct method can incorporate algebraic loops in the identification procedure, which is again a prediction error method, but with a newly defined predictor. This predictor is used to formulate a prediction error identification method for the identification of physical linear networks. Finally, the WNSF algorithm has been presented, which is a multistep convex (and therefore computationally attractive) algorithm for solving the nonconvex optimisation problem resulting from prediction error methods. This algorithm is adapted to the structure of physical linear networks to perform the identification of these networks.

7 | Identification through a dynamic network approach

This chapter is a revised and extended version of

E.M.M. Kivits and P.M.J. Van den Hof. A dynamic network approach to identification of physical systems. In *Proceedings of the 58th IEEE Conference on Decision and Control (CDC)*, pages 4533–4538, 2019.

System identification problems utilizing a prediction error approach are typically considered in an input/output setting, where a directional cause-effect relationship is presumed and transfer functions are used to estimate the causal relationships. In more complex interconnection structures, as e.g. appearing in dynamic networks, the cause-effect relationships can be encoded by a directed graph. Physical dynamic networks are most commonly described by diffusive couplings between node signals, implying that cause-effect relationships between node signals are symmetric and therefore can be represented by an undirected graph. This chapter shows how (prediction error) identification methods developed for linear dynamic networks can be configured to identify components in (undirected) physical networks with known topology.

7.1 Introduction

Physical networks are only one example of dynamic networks, which are interconnections of dynamic units. Dynamic networks receive increasing attention from a variety of scientific fields, since systems are growing in complexity and

size. Other examples of dynamic networks are biological and chemical processes, neural networks, consensus networks, synchronisation, social interactions, the Internet, the stock market, and multiagent systems (Ren et al., 2005; Boccaletti et al., 2006; Mesbahi and Egerstedt, 2010).

By representing a dynamic network as an interconnection structure of dynamic transfer function modules (Gonçalves et al., 2007; Van den Hof et al., 2013), a framework for system identification in dynamic networks has been developed by Van den Hof et al. (2013), by extending classical closed-loop prediction error methods. Other developments focus on topology estimation (Materassi and Innocenti, 2010; Chiuso and Pillonetto, 2012), full network identification (Weerts et al., 2018c), local module identification (Materassi and Salapaka, 2015; Dankers et al., 2016; Ramaswamy and Van den Hof, 2021), and network identifiability (Weerts et al., 2018b; van Waarde et al., 2018; Gevers et al., 2019). In this framework, dynamic networks are considered to consist of directed interconnections of dynamic modules that can be of any dynamic order. In contrast, physical systems are typically considered as undirected dynamic interconnections between node signals, where the interconnections represent diffusive couplings (Cheng et al., 2017) and the model is typically described by a vector difference equation of maximum second order. The most well-known example is a mechanical mass-spring-damper system, with the positions of masses as node (state) signals and the dynamics being described by a second-order vector difference equation. Identification of these physical models can be done by converting the model into a state-space form, after which matrix transformations (Friswell et al., 1999; Lopes dos Santos et al., 2015) or eigenvalue decompositions (Fritzen, 1986; Luş et al., 2003) are applied to estimate the model parameters. However, during these operations, the network structure in the model is generally lost.

The overall objective of this research is to develop a comprehensive theory for the identification of individual interconnections (modules) in physical (undirected) networks, where the order of the individual modules is not restricted and possibly correlated disturbances can be present. The objective includes questions like which nodes to measure (sense) and which nodes to excite (actuate) in order to identify a particular (local) module in the network or to identify the full dynamics and topology of the network. In addition, the consistency and minimum variance properties of estimates have to be specified. In this way, the (prediction error) identification theory for directed networks is extended to undirected networks.

This chapter includes the first steps towards achieving the above-mentioned objective, by addressing the question of how current identification methods can be made applicable to undirected networks. The physical networks that will be considered in this chapter are defined in Section 7.2. Currently, extensive tools are under development for choosing which nodes to measure and/or excite for

identifying a local module in directed networks. In order to use the insights into the identification in directed networks also for physical/undirected networks, the relationship between physical networks and directed networks needs to be clear. This relationship is described in Section 7.3. Next, insights into the identification in directed networks are applied to these networks for estimating the dynamics of the full network (Section 7.4). Some first results are presented for addressing the local identification problem (Section 7.5). An alternative formulation for both full and local network identification is given in Section 7.6 . Finally, Section 7.7 concludes the chapter.

7.2 Physical network

7.2.1 Network model

Physical systems are often described by second-order vector differential equations. They can be considered to consist of L interconnected node signals $w_j(t)$, $j = 1, \ldots, L$, of which the behaviour is described according to

$$M_j \ddot{w}_j(t) + D_{j0}\dot{w}_j(t) + \sum_{k \in \mathcal{N}_j} D_{jk}\big(\dot{w}_j(t) - \dot{w}_k(t)\big) + K_{j0} w_j(t) + \sum_{k \in \mathcal{N}_j} K_{jk}\big(w_j(t) - w_k(t)\big) = u_j(t), \quad (7.1)$$

where $M_j \geq 0$, $D_{jk} \geq 0$, $K_{jk} \geq 0$, $D_{jj} = 0$, $K_{jj} = 0$, $\mathcal{N}_j$ is the set of indices of node signals $w_k(t)$ $k \neq j$ with connections to node signals $w_j(t)$, $u_j(t)$ are the external input signals, and $\dot{w}_j(t)$ and $\ddot{w}_j(t)$ are the first and second-order derivatives of the node signals $w_j(t)$, respectively.

In physical systems, all connections are symmetric, meaning that the strength of the connection from node signal $w_i(t)$ to node signal $w_k(t)$ is equal to the strength of the connection (in opposite direction) from node signal $w_k(t)$ to node signal $w_i(t)$. This means that the interconnections of the nodes are diffusive couplings, which emerge in (7.1) from the symmetric connections: $D_{jk} = D_{kj}$ and $K_{jk} = K_{kj}$ $\forall j, k$.

An example of a physical system with diffusive couplings is the mass-spring-damper system shown in Figure 7.1, in which masses M_j are interconnected through dampers D_{jk} and springs K_{jk} with $k \neq 0$ and are connected to the earth with dampers D_{j0} and springs K_{j0}. The positions of the masses are the signals of interest and therefore chosen to be the node signals: $w_j(t) := x_j(t)$. The couplings between the masses are diffusive, because springs and dampers are

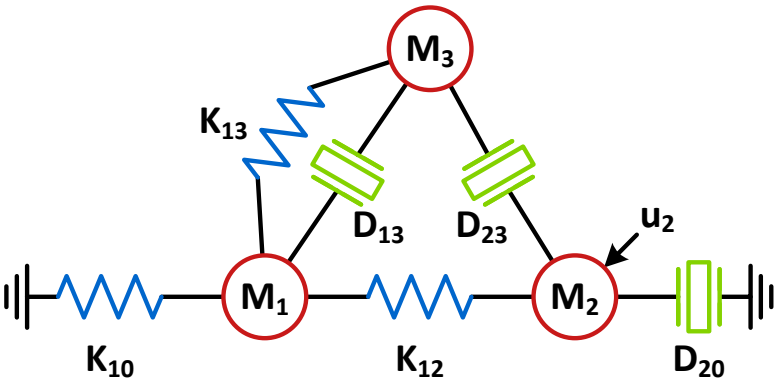

Figure 7.1: A network of masses (M_j), dampers (D_{jk}), and springs (K_{jk}).

symmetric components. Further, a network as shown in Figure 7.1 would require at least a two-dimensional position vector $w_j(t)$, but without loss of generality, we will restrict our attention to scalar-valued node signals $w_j(t)$.

7.2.2 Higher-order network

A physical system, such as the mass-spring-damper system in Section 7.2, is typically of second order when all node signals are collected in $w(t)$. The theory can easily be extended to higher-order terms, which is useful in, for example, immersion as explained in Section 7.5.2.

Definition 7.1 (Physical network). *A physical network is a network consisting of L node signals $w_1(t), \ldots, w_L(t)$ interconnected through diffusive couplings and with possibly connections of nodes to a ground node. The behaviour of the node signals $w_j(t)$, $j = 1, \ldots, L$, is described by*

$$\sum_{\ell=0}^{n_X} \mathsf{x}_{jj,\ell} w_j^{(\ell)}(t) + \sum_{k \in \mathcal{N}_j} \sum_{\ell=0}^{n_Y} \mathsf{y}_{jk,\ell} [w_j^{(\ell)}(t) - w_k^{(\ell)}(t)] = u_j(t), \qquad (7.2)$$

with n_X and n_Y the order of the dynamics in the network, with real-valued coefficients $\mathsf{x}_{jj,\ell} \geq 0$, $\mathsf{y}_{jk,\ell} \geq 0$, $\mathsf{y}_{jk,\ell} = \mathsf{y}_{kj,\ell}$, where $w_j^{(\ell)}(t)$ is the ℓ-th derivative of $w_j(t)$, and where $u_j(t)$ is the external signal entering the j-th node.

The graphical interpretation of the coefficients is as follows: $\mathsf{x}_{jj,n}$ represent the components intrinsically related to the nodes w_j; $\mathsf{x}_{jj,\ell}$ with $\ell \neq n$ represent

the components connecting the node w_j to the ground node (or earth); and $\mathsf{y}_{jk,\ell}$ represent the components in the diffusive couplings between the nodes $w_j(t)$ and $w_k(t)$. Further, every matrix X_ℓ composed of elements $x_{jj,\ell} := \mathsf{x}_{jj,\ell}$ is diagonal and every matrix Y_ℓ composed of elements $y_{jj,\ell} := \sum_{k\in\mathcal{N}_j} \mathsf{y}_{jk,\ell}$ and $y_{jk,\ell} := -\mathsf{y}_{jk,\ell}$ for $k \neq j$ is Laplacian[1] representing an undirected graph of a specific physical component (i.e. the diffusive couplings of a specific order).

7.2.3 Discretisation

For the purpose of identification in a discrete-time setting, the continuous-time network is converted to an equivalent discrete-time network.

Proposition 7.2 (Discrete time). *By using the approximation*

$$\frac{dw(t)}{dt} = \frac{w(t_d T_s) - w((t_d-1)T_s)}{T_s}, \tag{7.3}$$

the continuous time physical network (7.2) *can be approximated in discrete time by*

$$\sum_{\ell=0}^{n_X} \bar{\mathsf{x}}_{jj,\ell} q^{-\ell} w_j(t_d) + \sum_{k\in\mathcal{N}_j} \sum_{\ell=0}^{n_Y} \bar{\mathsf{y}}_{jk,\ell} q^{-\ell} [w_j(t_d) - w_k(t_d)] = u_j(t_d), \tag{7.4}$$

with q^{-1} the shift operator, meaning $q^{-1}w_j(t_d) = w_j(t_d-1)$, and with matrices

$$\bar{\mathsf{x}}_{jj,\ell} = (-1)^\ell \textstyle\sum_{i=\ell}^{n_X} \binom{i}{\ell} T_s^{-i} \mathsf{x}_{jj,i}, \tag{7.5a}$$

$$\bar{\mathsf{y}}_{jk,\ell} = (-1)^\ell \textstyle\sum_{i=\ell}^{n_Y} \binom{i}{\ell} T_s^{-i} \mathsf{y}_{jk,i}, \tag{7.5b}$$

where $\binom{i}{\ell}$ is a binomial coefficient and where T_s is the time interval defined by $t := t_d T_s$.

Proof: Equation (7.2) is discretised by a similar approach as by Ramos et al. (2013) by using a backward shift (7.3). ■

In the sequel, t is used for t_d. The expressions for the node signals (7.4) can be combined in a matrix equation describing the network as

$$\bar{X}(q^{-1})w(t) + \bar{Y}(q^{-1})w(t) = u(t), \tag{7.6}$$

[1] A Laplacian matrix is a symmetric matrix with nonpositive off-diagonal elements and with nonnegative diagonal elements that are equal to the negative sum of all other elements in the same row (or column) (Mesbahi and Egerstedt, 2010).

with $\bar{X}(q^{-1})$ and $\bar{Y}(q^{-1})$ polynomial matrices in the shift operator q^{-1} and composed of elements

$$\bar{X}_{jk}(q^{-1}) = \begin{cases} \sum_{\ell=0}^{n_X} \bar{\mathrm{x}}_{jj,\ell} q^{-\ell}, & \text{if } k = j \\ 0, & \text{otherwise} \end{cases} \tag{7.7a}$$

$$\bar{Y}_{jk}(q^{-1}) = \begin{cases} \sum_{m \in \mathcal{N}_j} \sum_{\ell=0}^{n_Y} \bar{\mathrm{y}}_{jm,\ell} q^{-\ell}, & \text{if } k = j \\ -\sum_{\ell=0}^{n_Y} \bar{\mathrm{y}}_{jk,\ell} q^{-\ell}, & \text{if } k \in \mathcal{N}_j \\ 0, & \text{otherwise.} \end{cases} \tag{7.7b}$$

Note that $\bar{X}(q^{-1})$ is diagonal and $\bar{Y}(q^{-1})$ is Laplacian, implying that the structural properties of (7.2) are maintained in (7.6)-(7.7).

7.2.4 Identification set-up

In order to connect with the system identification framework formulated for dynamic networks, we will use a slightly different, but equivalent, network description for identification purposes.

Proposition 7.3 (Physical network). *A physical network* (7.6) *with* $\bar{X}(q^{-1})$ *diagonal and* $\bar{Y}(q^{-1})$ *Laplacian, can uniquely be described by*

$$Q(q^{-1})w(t) = P(q^{-1})w(t) + u(t), \tag{7.8}$$

with diagonal polynomial matrix $Q(q^{-1}) := \bar{X}(q^{-1}) + diag\big(\bar{Y}(q^{-1})\big)$ *and hollow and symmetric polynomial matrix* $P(q^{-1}) := -\bar{Y}(q^{-1}) + diag\big(\bar{Y}(q^{-1})\big)$, *with* $diag\big(\bar{Y}(q^{-1})\big)$ *the diagonal of* $\bar{Y}(q^{-1})$.

Proof: The definitions of $Q(q^{-1})$ and $P(q^{-1})$ show that $u(t) = \big(Q(q^{-1}) - P(q^{-1})\big)w(t) = \big(\bar{X}(q^{-1}) + \bar{Y}(q^{-1})\big)w(t)$. ■

Note that there exists a one-to-one relationship between $\big(\bar{X}(q^{-1}), \bar{Y}(q^{-1})\big)$ and $\big(P(q^{-1}), Q(q^{-1})\big)$.

In the identification setting that will be considered, the node signals might be affected by a user-applied excitation signal and subject to a disturbance signal. This is achieved by splitting the input signal as $u(t) := Br(t) + F(q)e(t)$ with B a known binary and diagonal matrix, $F(q)$ a rational matrix, $r(t)$ a known excitation signal, and $e(t)$ a stationary white noise process. Applying this partitioning to (7.8) gives the following identification set-up:

Definition 7.4 (Identification set-up). *The physical network that will be considered during identification is defined as*

$$Q(q^{-1})w(t) = P(q^{-1})w(t) + Br(t) + F(q)e(t), \tag{7.9}$$

with

1. $Q(q^{-1}) \in \mathcal{Q} := \{Q \in \mathbb{R}^{L\times L}[q^{-1}] \mid q_{ij}(q^{-1}) = 0 \text{ for } i \neq j\}$.
2. $P(q^{-1}) \in \mathcal{P} := \{P \in \mathbb{R}^{L\times L}[q^{-1}] \mid p_{ij}(q^{-1}) = p_{ji}(q^{-1}),\ p_{ii}(q^{-1}) = 0\ \forall i, j\}$.
3. $B \in \mathcal{B} := \{B \in \mathbb{R}^{L\times L} \mid b_{ij} = 0 \text{ for } i \neq j,\ b_{ii} \in \{0, 1\}\ \forall i\}$.
4. $F(q) \in \mathcal{F} := \{F \in \mathbb{R}^{L\times L}(q) \mid F \text{ monic, stable, and stably invertible}\}$.

Further, the network is assumed to be well-posed and stable, implying that $\left(Q(q^{-1}) - P(q^{-1})\right)^{-1}$ *exists and is proper and stable.*

In order to address the questions formulated in Section 7.1, we will now show how this network description can be written as a so-called module representation, which is typically used in prediction error identification (Van den Hof et al., 2013).

7.3 Module representation

A commonly used description of dynamic networks is the module representation (Van den Hof et al., 2013), in which a network is considered to be the interconnection of modules through measured node signals. Every node signal $w_j(t)$ is described by

$$w_j(t) = \sum_{k\in\mathcal{N}_j} G_{jk}(q)w_k(t) + R_{jj}(q)r_j(t) + \sum_{p=1}^{L} H_{jp}(q)e_p(t), \tag{7.10}$$

where $G_{jk}(q)$, $R_{jj}(q)$ and $H_{jp}(q)$ are proper rational transfer functions, $r_j(t)$ are known external excitation signals, and $e_p(t)$ are white noises. The module representation does not allow for self-loops, implying that $G_{jj}(q) = 0$. The expressions for the node signals (7.10) can be combined in a matrix equation describing the network as

$$w(t) = G(q)w(t) + R(q)r(t) + H(q)e(t), \tag{7.11}$$

with matrices $G(q)$, $R(q)$, and $H(q)$ composed of elements $G_{jk}(q)$, $R_{jj}(q)$, and $H_{jp}(q)$, respectively, and where $w(t)$, $r(t)$, and $e(t)$ are vectorised versions of

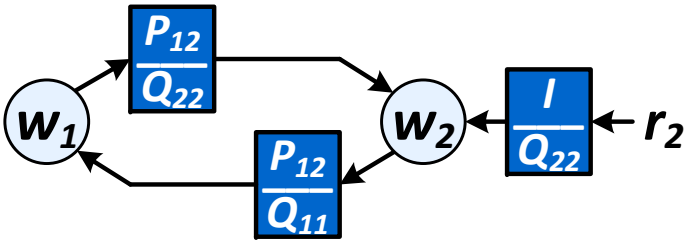

Figure 7.2: Module representation of a physical network.

$w_j(t)$, $r_j(t)$, and $e_p(t)$, respectively. Note that $G(q)$ is hollow, $R(q)$ is diagonal, and $H(q) \in \mathcal{F}$. In addition, $\big(I - G(q)\big)^{-1}$ must be stable to ensure network stability and $I - G(q)$ must be proper and full rank to ensure the well-posedness of the network.

The relationship between the module representation and physical networks is as follows:

Definition 7.5 (Equivalent network models). *A physical network* (7.9) *and a module representation* (7.11) *are called equivalent if the following equalities hold:*

$$G(q) = Q^{-1}(q^{-1})P(q^{-1}), \tag{7.12a}$$
$$R(q) = Q^{-1}(q^{-1})B, \tag{7.12b}$$
$$H(q) = Q^{-1}(q^{-1})Q_0F(q), \tag{7.12c}$$

with $Q_0 = \lim_{z\to\infty} Q(z)$.

As a result, physical networks lead to module representations that satisfy the following particular symmetric properties: in the factorisations (7.12), $G_{jk}(q)$ and $G_{kj}(q)$ have the same numerator for all j, k; $G_{jk}(q)$ and $R_{jj}(q)$ have the same denominator for all k; $G_{jk}(q)$ and $H_{jj}(q)$ have the same denominator for all k if $C(q)$ is polynomial.

The structure of $G(q)$ and $R(q)$ for a physical network with two nodes is illustrated by Figure 7.2. It shows that the modules $G_{12}(q) = \frac{p_{12}(q^{-1})}{q_{11}(q^{-1})}$ and $G_{21}(q) = \frac{p_{12}(q^{-1})}{q_{22}(q^{-1})}$ between $w_1(t)$ and $w_2(t)$ have the same numerator related to their interconnection and a different denominator related to the node they enter. It can also be seen that both paths entering node $w_2(t)$ indeed have the same denominator. Since $G_{12}(q)$ and $G_{21}(q)$ have the same numerator, they will either

be both present or both absent, which is in accordance with the fact that they represent a single physical interconnection.

Furthermore, the connections to the earth are only present in the denominators, because they are only present in $Q(q^{-1})$. This means that they do not have an effect on the topology in the module representation, although they are part of the topology in the physical network.

Next, the relationship between the module representation and physical networks is specified further, leading to a unique mapping between the models.

Lemma 7.6 (left matrix-fraction description (LMFD)). *Consider two left coprime matrices $Q(q^{-1}) \in \mathcal{Q}$ and $P(q^{-1}) \in \mathcal{P}$. Given the LMFD $Q(q^{-1})^{-1}P(q^{-1})$, $Q(q^{-1})$ and $P(q^{-1})$ are unique up to a scalar factor.*

Proof: According to Kailath (1980), the LMFD of any two polynomial and left coprime matrices is unique up to a unimodular matrix multiplication. In order to preserve the diagonality of $Q(q^{-1})$ and symmetry of $P(q^{-1})$, the unimodular matrix is restricted to be diagonal with equal elements. ■

Using Lemma 7.6, the following result for equivalent network models is formulated.

Proposition 7.7 (Unique equivalent network models). *Given a module representation* (7.11) *with*

1. $G(q) \in \mathcal{G} := \{G \in \mathbb{R}^{L\times L}(q) \mid \exists Q \in \mathcal{Q}, P \in \mathcal{P}$ *that satisfy* $G = Q^{-1}P$ *with* Q, P *left coprime*$\}$.
2. $R(q) \in \mathcal{R} := \{R \in \mathbb{R}^{L\times L}(q) \mid \exists Q \in \mathcal{Q}, B \in \mathcal{B}$ *that satisfy* $R = Q^{-1}B\}$.
3. $H(q) \in \mathcal{F}$.

There exists a unique equivalent network model (7.9) *with* $\big(Q(q^{-1}), P(q^{-1}), B, F(q)\big) \in \mathcal{Q}\times\mathcal{P}\times\mathcal{B}\times\mathcal{F}$ *if the following conditions are satisfied:*

1. *$Q(q^{-1})$ and $P(q^{-1})$ are left coprime.*
2. *B is nonzero.*

Proof: According to Lemma 7.6, the LMFD (7.12a) is unique up to a scalar factor if $Q(q^{-1})$ and $P(q^{-1})$ are left coprime. If, in addition, B is nonzero, this scalar factor is fixed to 1 in order to preserve binarity in B. $F(q) \in \mathcal{F}$ is uniquely obtained from (7.12c). ■

7.4 Full network identification

The module representation of a physical network can now be used to identify a dynamic network on the basis of measured data. The main difference with a general prediction error network identification problem (Weerts et al., 2018c), is that the symmetric structure of the interconnections has to be accommodated. This symmetry can simply be encoded in the parameterised model set that will be used for identification. This identification can be directed towards identifying particular dynamic modules while the topology of the network is given (it is known which nodes are interconnected) or towards identifying a full network in which all interconnections are being identified.

Definition 7.8 (Data generating network). *Consider a data generating network* $\mathcal{S}$ (7.9)*, defined according to*

$$Q^0(q^{-1})w(t) = P^0(q^{-1})w(t) + B^0 r(t) + F^0(q)e(t), \tag{7.13}$$

with $Q^0(q^{-1}) \in \mathcal{Q}$*,* $P^0(q^{-1}) \in \mathcal{P}$*,* $B^0 \in \mathcal{B}$*,* $F^0(q) \in \mathcal{F}$*, external excitations* $r(t)$ *being uncorrelated with white noise process* $e(t)$ *with bounded moments of order higher than* 4^a*.*

[a] This is the typical assumption for consistency of prediction error estimation (Ljung, 1999).

Definition 7.9 (Network model structure). *A network model structure used for identifying* (7.13) *is defined as a set of parameterised matrices*

$$\mathcal{M} := \{Q(q^{-1}, \theta), P(q^{-1}, \theta), B, F(q, \theta), \theta \in \Theta\}, \tag{7.14}$$

with $Q(q^{-1}, \theta) \in \mathcal{Q}$*,* $P(q^{-1}, \theta) \in \mathcal{P}$*,* $F(q, \theta) \in \mathcal{F}$*, and with known* $B = B^0$*.*

Since $Q(q^{-1}, \theta)$ is not monic, special attention is required for the identification set-up. We denote the parameterised residual $\varepsilon(t, \theta)$ as

$$\begin{aligned}\varepsilon(t, \theta) := \big(Q_0(\theta) - P_0(\theta)\big)^{-1} F^{-1}(q, \theta) \left[Q(q^{-1}, \theta) - P(q^{-1}, \theta)\right] w(t) \\ - \big(Q_0(\theta) - P_0(\theta)\big)^{-1} F^{-1}(q, \theta) B r(t).\end{aligned} \tag{7.15}$$

Theorem 7.10 (Joint-direct method). *Consider a network that has generated data according to* (7.13) *with* $F^0(q) := F^0(q^{-1})$ *polynomial and an "ARMAX" network model structure according to* (7.14) *with* $F(q, \theta) :=$

$F(q^{-1}, \theta)$ being polynomial. The joint-direct method with identification criterion

$$\hat{\theta}_N = \arg\min_{\theta \in \Theta} \frac{1}{N} \sum_{t=1}^{N} \varepsilon^\top(t, \theta) \varepsilon(t, \theta), \tag{7.16}$$

with $\varepsilon(t, \theta)$ given by (7.15)*, results in consistent estimates of the transfer functions $G(q, \hat{\theta}_N)$, $R(q, \hat{\theta}_N)$, and $H(q, \hat{\theta}_N)$ determined by*

$$G(q, \hat{\theta}_N) = Q^{-1}(q^{-1}, \hat{\theta}_N) P(q^{-1}, \hat{\theta}_N), \tag{7.17a}$$

$$R(q, \hat{\theta}_N) = Q^{-1}(q^{-1}, \hat{\theta}_N) B, \tag{7.17b}$$

$$H(q, \hat{\theta}_N) = Q^{-1}(q^{-1}, \hat{\theta}_N) Q_0(\hat{\theta}_N) F(q^{-1}, \hat{\theta}_N), \tag{7.17c}$$

provided that all of the following conditions hold:

1. *The data generating network $\mathcal{S}$ is in the model set $\mathcal{M}$.*
2. *The data are sufficiently informative (Weerts et al., 2016).*
3. *The model set $\mathcal{M}$ is globally network identifiable at $\mathcal{S}$ (Weerts et al., 2018b).*

If in addition, there exists at least one external excitation signal $r(t)$ (i.e. $B^0 \neq 0$), and Q^0, P^0 are left coprime, then the consistency result also applies to the polynomials $Q(q^{-1}, \hat{\theta}_N)$, $P(q^{-1}, \hat{\theta}_N)$, $F(q^{-1}, \hat{\theta}_N)$.

Proof: If $F^0(q) := F^0(q^{-1})$ and $F(q, \theta) := F(q^{-1}, \theta)$ are polynomial, the network model structure is "ARMAX" and the identification problem is similar to the joint-direct identification method of Weerts et al. (2016), for the particular situation that P^0 and $P(q^{-1}, \theta)$ are symmetric. Consistency of the polynomial terms follows from Proposition 7.7. ■

Remark 7.11 (Properness). *The estimated module dynamics is proper but not necessarily strictly proper. This has consequences for the conditions under which the network is identifiable. In the presence of algebraic loops, additional conditions on the presence of excitation signals need to be satisfied for achieving network identifiability (Weerts et al., 2018b, 2016).*

Proposition 7.12 (Linear regression). *Consider a network that has generated data according to* (7.13) *with $F^0(q) := I$, $B^0 \neq 0$, $Q_0^0 = I$, $P_0^0 = 0$, and an "ARX" network model structure according to* (7.14)*, that is $F(q, \theta) := I$,*

with $\mathcal{S} \in \mathcal{M}$. Under the conditions of Theorem 7.10, the polynomials $P(q^{-1})$ and $Q(q^{-1})$ are consistently estimated through a linear regression according to

$$\hat{\theta}_N = \left[\frac{1}{N}\sum_t \varphi(t)\varphi^\top(t)\right]^{-1}\left[\frac{1}{N}\sum_t \varphi(t)Br(t)\right], \tag{7.18}$$

with $\varphi(t)$ defined as

$$\varphi^\top(t) = \begin{bmatrix}\varphi^\top_{Q_0}(t) & \cdots & \varphi^\top_{Q_{n_Q}}(t) & \varphi^\top_{P_0}(t) & \cdots & \varphi^\top_{P_{n_P}}(t)\end{bmatrix}, \tag{7.19}$$

with

$$\varphi^\top_{Q_i}(t) = \begin{bmatrix} q^{-i}w_1(t) & & \\ & \cdots & \\ & & q^{-i}w_L(t)\end{bmatrix},$$

$$\varphi^\top_{P_i}(t) = -\left(\begin{bmatrix} Z_{0,L-1} \\ q^{-i}W_{2,L}(t) \\ q^{-i}d_{L-1}(w_1(t))\end{bmatrix}\begin{bmatrix} Z_{1,L-2} \\ q^{-i}W_{3,L}(t) \\ q^{-i}d_{L-2}(w_2(t))\end{bmatrix}\cdots\begin{bmatrix} Z_{L-2,1} \\ q^{-i}W_{L,L}(t) \\ q^{-i}d_1(w_{L-1}(t))\end{bmatrix}\right),$$

where $Z_{j,k}$ is a matrix of size $j \times k$ with all elements equal to 0*,*

$$W_{j,L}(t) = \begin{bmatrix} w_j(t) & \cdots & w_L(t)\end{bmatrix}, \tag{7.20}$$

and

$$d_i\big(w_j(t)\big) = \begin{bmatrix} w_j(t) & & \\ & \ddots & \\ & & w_j(t)\end{bmatrix}, \tag{7.21}$$

which is a square (and diagonal) matrix of dimension $i \times i$ with $i = L - j$.

Proof: The proof is provided in Appendix 7.A. ■

The symmetry in $P(q^{-1}, \theta)$ is included in the parameterisation and therefore, the resulting optimisation problem is unconstrained. That is, the identification procedure of the network results in an unconstrained least squares optimisation problem in which the structure of $P(q^{-1}, \theta)$ is taken into account.

7.5 Local network identification

7.5.1 Problem definition

The local identification problem in networks is in general formulated as the objective of identifying a single module in the network (Van den Hof et al., 2013; Materassi and Salapaka, 2015; Dankers et al., 2016; Ramaswamy and Van den Hof, 2021). However, due to the symmetry in the symmetric couplings in the networks considered in this chapter, it is attractive to formulate the local identification problem slightly differently.

Definition 7.13 (Local identification problem). *The local identification problem concerns the identification of a single coupling between two nodes in the physical network.*

A single coupling in the physical network is described by two modules in the module representation, meaning that the objective is to identify two modules simultaneously. For the nodes w_j and w_k, these modules are $G_{jk}(q) = q_{jj}^{-1}(q^{-1})p_{jk}(q^{-1})$ and $G_{kj}(q) = q_{kk}^{-1}(q^{-1})p_{kj}(q^{-1})$, which contain the full information on how the nodes w_j and w_k interact with each other. Due to the symmetry in $P(q^{-1})$, $p_{jk}(q^{-1}) = p_{kj}(q^{-1})$ and hence, this identification problem concerns the identification of three polynomials: $q_{jj}(q^{-1})$, $q_{kk}(q^{-1})$, and $p_{jk}(q^{-1})$. In order to take account of the symmetric properties of physical network interconnections, the currently available methods for local module identification need to be reconsidered.

7.5.2 Immersion

In order to decide which of the node signals need to be taken into account for the identification of a local module, the procedure introduced by Dankers et al. (2016) suggests to remove (immerse) node signals from the network, while adapting the dynamic modules such that the retained node signals are kept invariant. If node signals can be removed (immersed) while the target module remains invariant, the immersed node signals can be discarded in the identification. The results for target module invariance under immersion are described by Dankers et al. (2016). Applying these results to the two modules $G_{jk}(q)$ and $G_{kj}(q)$ simultaneously, leads to the following conditions on the graph of the network:

1. Every loop around $w_j(t)$ and every loop around $w_k(t)$ needs to pass through a retained node.

2. Every parallel path[2] from $w_j(t)$ to $w_k(t)$ and every parallel path from $w_k(t)$ to $w_j(t)$ needs to pass through a retained node.

Because of the symmetric properties of a physical network, these conditions lead to the following result:

Proposition 7.14 (Immersion in physical network). *Immersion in module representations of physical networks keeps two modules $G_{jk}(q)$ and $G_{kj}(q)$ invariant if $w_j(t)$ and $w_k(t)$ and all their neighbour nodes are retained.*

Proof: Since $P(q^{-1})$ is symmetric, all nodes are bilaterally connected. Therefore, all loops around $w_j(t)$ and all loops around $w_k(t)$ contain a retained node if and only if all neighbour nodes of $w_j(t)$ and all neighbour nodes of $w_k(t)$ are retained, respectively. As a consequence, all parallel paths from $w_j(t)$ to $w_k(t)$ and from $w_k(t)$ to $w_j(t)$ contain a retained node as well. ■

This proposition shows that for the identification of a single coupling between two nodes $w_j(t)$ and $w_k(t)$, all nodes that are not neighbours of $w_j(t)$ and $w_k(t)$ can be immersed from the network.

Remark 7.15. *Note that immersion of nodes can lead to higher-order dynamics in the modules after immersion. This order increase can simply be accommodated in the module representation of physical networks, i.e. the modules do not need to be restricted to second-order dynamics.*

Remark 7.16. *By using immersion, nodes are removed from the network and the identification problem can be solved locally, meaning that not all nodes are needed and not all dynamics in the network needs to be modelled in order to identify the dynamics of a specific coupling in the network.*

7.5.3 Identification set-up

After immersion, the system representation is as follows:

$$\begin{bmatrix} w_j(t) \\ w_k(t) \\ w_{\mathcal{D}}(t) \end{bmatrix} = \begin{bmatrix} 0 & G_{jk}(q) & G_{j\mathcal{D}}(q) \\ G_{kj}(q) & 0 & G_{k\mathcal{D}}(q) \\ \breve{G}_{\mathcal{D}j}(q) & \breve{G}_{\mathcal{D}k}(q) & \breve{G}_{\mathcal{D}\mathcal{D}}(q) \end{bmatrix} \begin{bmatrix} w_j(t) \\ w_k(t) \\ w_{\mathcal{D}}(t) \end{bmatrix} + \breve{R}(q)r(t) + \breve{H}(q)e(t), \tag{7.22}$$

[2] A parallel path from $w_j(t)$ to $w_k(t)$ is a path from $w_j(t)$ to $w_k(t)$ that does not pass through $G_{kj}(q)$.

where $w_{\mathcal{D}}(t)$ is the set of node signals that are being retained, i.e. the neighbour node signals of $w_j(t)$ and $w_k(t)$. Following the local identification approaches of Ramaswamy and Van den Hof (2021) and Weerts et al. (2016), (7.22) are used for locally identifying the two modules $G_{jk}(q)$ and $G_{kj}(q)$. The output signals of this local identification problem are $w_y(t) = \begin{bmatrix} w_j(t) & w_k(t) \end{bmatrix}^\top$ and the input signals are $w_m(t) = \begin{bmatrix} w_y^\top(t) & w_{\mathcal{D}}^\top(t) \end{bmatrix}^\top$ and $\tilde{r}(t) = \begin{bmatrix} r_j(t) & r_k(t) \end{bmatrix}^\top$. This means that the first two rows of (7.22) will be estimated. In order to do so, the disturbances affecting $w_{\mathcal{D}}(t)$ have to be uncorrelated with the disturbances affecting $w_j(t)$ and $w_k(t)$, but the disturbances affecting $w_j(t)$ and $w_k(t)$ can be mutually correlated, as well as the disturbances affecting $w_{\mathcal{D}}(t)$. This identification set-up has the parameterised residual

$$\begin{aligned}\varepsilon(t,\theta) = \left(\tilde{Q}_0(\theta) - \tilde{P}_0(\theta)\right)^{-1} \tilde{F}^{-1}(q,\theta) \left[\tilde{Q}(q^{-1},\theta) w_y(t) - \tilde{P}(q^{-1},\theta) w_m(t)\right] \\ - \left(\tilde{Q}_0(\theta) - \tilde{P}_0(\theta)\right)^{-1} \tilde{F}^{-1}(q,\theta) \tilde{B} \tilde{r}(t), \quad (7.23)\end{aligned}$$

with

$$\tilde{Q}(q^{-1},\theta) = \begin{bmatrix} q_{jj}(q^{-1},\theta) & \\ & q_{kk}(q^{-1},\theta) \end{bmatrix}, \quad (7.24a)$$

$$\tilde{P}(q^{-1},\theta) = \begin{bmatrix} 0 & p_{jk}(q^{-1},\theta) & p_{j\mathcal{D}}(q^{-1},\theta) \\ p_{kj}(q^{-1},\theta) & 0 & p_{k\mathcal{D}}(q^{-1},\theta) \end{bmatrix}, \quad (7.24b)$$

$$\tilde{B} = \begin{bmatrix} b_{jj} & \\ & b_{kk} \end{bmatrix}, \quad (7.24c)$$

$$\tilde{F}(q,\theta) = \begin{bmatrix} F_{jj}(q,\theta) & F_{jk}(q,\theta) \\ F_{kj}(q,\theta) & F_{kk}(q,\theta) \end{bmatrix}. \quad (7.24d)$$

The results of Ramaswamy and Van den Hof (2021) and Weerts et al. (2016) for single module identification can now be used to formulate conditions for consistent estimation of the two modules $G_{jk}(q)$ and $G_{kj}(q)$ simultaneously. If in the original network, the disturbances affecting $w_{\mathcal{D}}(t)$ are uncorrelated to the disturbances affecting $w_j(t)$ and $w_k(t)$, then the identification set-up described above will lead to consistent estimates $G_{jk}(q,\hat{\theta}_N)$ and $G_{kj}(q,\hat{\theta}_N)$ under the usual conditions on data informativity (sufficient excitation), as formalised by Ramaswamy and Van den Hof (2021).

Once $G_{jk}(q)$ and $G_{kj}(q)$ have been identified consistently, the physical components in the network model (7.2) can be retrieved from the estimated model $\left(\tilde{Q}(q^{-1}), \tilde{P}(q^{-1}), \tilde{B}, \tilde{F}(q)\right)$.

7.6 Alternative formulation

The presented results for both full network identification and local network identification are based on network description (7.9). Alternatively, (7.6) can be used instead, leading to similar results. In particular, for full network identification, the linear regression formulated in Proposition 7.12 can similarly be formulated with a corresponding new regressor $\varphi(t)$.

Proposition 7.17 (Alternative linear regression). *Consider a network that has generated data according to $\bar{\mathcal{S}}$:*

$$\bar{X}^0(q^{-1})w(t) + \bar{Y}^0(q^{-1})w(t) = B^0 r(t) + F^0(q)e(t), \tag{7.25}$$

with $\bar{X}^0(q^{-1}) \in \mathcal{Q}$, $\bar{Y}^0(q^{-1}) \in \mathcal{Y} := \{\bar{Y} \in \mathbb{R}^{L\times L}[q^{-1}] \mid \bar{y}_{ij}(q^{-1}) = \bar{y}_{ji}(q^{-1}), \bar{y}_{ii}(q^{-1}) = \sum_i \bar{y}_{ij}(q^{-1})\ \forall i, j\}$, $\bar{X}_0^0 + \bar{Y}_0^0 = I$, $B^0 \in \mathcal{B}$, $B^0 \neq 0$, $F^0(q) := I$, and an "ARX" network model structure according to

$$\bar{\mathcal{M}} := \{\bar{X}(q^{-1}, \theta), \bar{Y}(q^{-1}, \theta), B, F(q, \theta), \theta \in \Theta\}, \tag{7.26}$$

with $\bar{X}(q^{-1}, \theta) \in \mathcal{Q}$, $\bar{Y}(q^{-1}, \theta) \in \mathcal{Y}$, with known $B = B^0$, $F(q, \theta) := I$, and with $\bar{\mathcal{S}} \in \bar{\mathcal{M}}$. Under the conditions of Theorem 7.10 (with $\bar{\mathcal{S}}$ and $\bar{\mathcal{M}}$ instead of $\mathcal{S}$ and $\mathcal{M}$, respectively), the physical components represented by the polynomials $\bar{X}(q^{-1})$ and $\bar{Y}(q^{-1})$ are consistently estimated through a linear regression according to (7.18) *with $\varphi(t)$ defined as*

$$\varphi^\top(t) = \begin{bmatrix} \varphi^\top_{\bar{X}_0}(t) & \cdots & \varphi^\top_{\bar{X}_{n_x}}(t) & \varphi^\top_{\bar{Y}_0}(t) & \cdots & \varphi^\top_{\bar{Y}_{n_y}}(t) \end{bmatrix}, \tag{7.27}$$

with

$$\varphi^\top_{\bar{X}_i}(t) = \begin{bmatrix} q^{-i}w_1(t) & & \\ & \ddots & \\ & & q^{-i}w_L(t) \end{bmatrix},$$

$$\varphi^\top_{\bar{Y}_i}(t) = \left(\begin{bmatrix} Z_{0,L-1} \\ q^{-i}V_{2,L}(t) \\ -q^{-i}d\big(V_{2,L}(t)\big) \end{bmatrix} \begin{bmatrix} Z_{1,L-2} \\ q^{-i}V_{3,L}(t) \\ -q^{-i}d\big(V_{3,L}(t)\big) \end{bmatrix} \cdots \begin{bmatrix} Z_{L-2,1} \\ q^{-i}V_{L,L}(t) \\ -q^{-i}d\big(V_{L,L}(t)\big) \end{bmatrix} \right),$$

where $Z_{j,k}$ is a matrix of size $j \times k$ with all elements equal to 0 *and where*

$$V_{j,L}(t) = \begin{bmatrix} w_j(t) - w_{j-1}(t) & \cdots & w_L(t) - w_{j-1}(t) \end{bmatrix} \tag{7.28}$$

and $d\big(V_{j,L}(t)\big) = diag\big(V_{j,L}(t)\big)$.

Proof: The proof is provided in Appendix 7.B. ■

In Proposition 7.12, the node signals are directly visible in the regressor, see, for example, $W_{j,L}(t)$(7.20) and $d_i\big(w_j(t)\big)$ (7.21), while in Proposition 7.17, the diffusive couplings are directly visible in the regressor as the differences of node signals are visible in $V_{j,L}(t)$ (7.28) and $d\big(V_{j,L}(t)\big)$. In addition, observe that $\varphi_{Q_i}^\top(t)$ In Proposition 7.12 and $\varphi_{\bar{X}_i}^\top(t)$ In Proposition 7.17 are the same. To make the structure of the regressors more clearly visible, consider the following example:

Example 7.18 (Regressors). *Consider a network with four node signals, that is $L = 4$. The regressors $\varphi_{Q_i}^\top(t)$ and $\varphi_{P_i}^\top(t)$ in Proposition 7.12 are given by (for notational convenience, the argument $t - i$ of the node signals is omitted)*

$$\varphi_{Q_i}^\top(t) = \begin{bmatrix} w_1 & & & \\ & w_2 & & \\ & & w_3 & \\ & & & w_4 \end{bmatrix},$$

$$\varphi_{P_i}^\top(t) = \left[\begin{array}{ccc|cc|c} w_2 & w_3 & w_4 & 0 & 0 & 0 \\ \hline w_1 & & & w_3 & w_4 & 0 \\ & w_1 & & w_2 & & w_4 \\ & & w_1 & & w_2 & w_3 \end{array}\right].$$

The regressors $\varphi_{\bar{X}_i}^\top(t)$ and $\varphi_{\bar{Y}_i}^\top(t)$ in Proposition 7.17 are given by (for notational convenience, the argument $t - i$ of the node signals is omitted)

$$\varphi_{\bar{X}_i}^\top(t) = \begin{bmatrix} w_1 & & & \\ & w_2 & & \\ & & w_3 & \\ & & & w_4 \end{bmatrix},$$

$$\varphi_{\bar{Y}_i}^\top(t) = \left[\begin{array}{ccc|cc|c} w_2 - w_1 & w_3 - w_1 & w_4 - w_1 & 0 & 0 & 0 \\ \hline w_1 - w_2 & & & w_3 - w_2 & w_4 - w_2 & 0 \\ & w_1 - w_3 & & w_2 - w_3 & & w_4 - w_3 \\ & & w_1 - w_4 & & w_2 - w_4 & w_3 - w_4 \end{array}\right].$$

Observe that in Example 7.18 indeed $\varphi_{Q_i}^\top(t)$ and $\varphi_{\bar{X}_i}^\top(t)$ are the same and that $\varphi_{P_i}^\top(t)$ and $\varphi_{\bar{Y}_i}^\top(t)$ are very similar. The difference is that $\varphi_{P_i}^\top(t)$ shows node signals, while $\varphi_{\bar{Y}_i}^\top(t)$ shows differences of node signals. This is due to the hollow structure of P_i and the Laplacian structure of $\bar{Y}_i$, respectively. Hence, $\varphi_{\bar{Y}_i}^\top(t)$ clearly shows

the diffusive couplings through the differences of node signals being incorporated into the regression vector.

7.7 Conclusion

The undirected network description of physical networks has been extended by allowing for higher-order diffusive couplings. Undirected network descriptions of physical systems with diffusive couplings can be represented as directed dynamic networks with particular structural properties. This allows for effective identification of the global and local properties of the physical network.

The directed dynamic network representation of physical networks typically leads to modules with direct feedthrough terms, resulting in algebraic loops in the network. Additional excitation signals are required to account for algebraic loops. In addition, the identifiability analysis is based on independently parameterised modules, while the modules in the directed network representation of physical networks have common parameters. The structural properties of physical networks lead to too strict identifiability conditions and expensive experiments for identification in the module framework.

Therefore, it is more attractive to preserve the polynomial representation of physical networks, in which the structural properties of physical networks are simply incorporated by symmetry. These polynomial representations are typically nonmonic and therefore, the identification theory for monic polynomial models has to be extended. The next step in this research is to accomplish this extension and to develop an identification method for full and local network identification of physical networks in the polynomial representation.

Appendix

7.A Proof of Proposition 7.12

If $F^0(q) := I$ and $F(q,\theta)\big(Q_0(\theta) - P_0(\theta)\big) = I$, the network model structure is "ARX" and the residual $\varepsilon(t,\theta)$ is affine in the parameters θ, meaning that it can be written as

$$\varphi^\top(t)\theta - Br(t) = \left[Q(q^{-1},\theta) - P(q^{-1},\theta)\right] w(t) - Br(t), \tag{7.29}$$

$$= \left[\sum_{i=0}^{n_Q} Q_i(\theta) q^{-i} - \sum_{i=0}^{n_P} P_i(\theta) q^{-i}\right] w(t) - Br(t), \tag{7.30}$$

where the structure of $Q(q^{-1},\theta)$ and $P(q^{-1},\theta)$ is retained in $Q_i(\theta)$ and $P_i(\theta)$, respectively, and with parameter vector

$$\theta = \begin{pmatrix}\theta_{Q_0}^\top & \cdots & \theta_{Q_{n_Q}}^\top & \theta_{P_0}^\top & \cdots & \theta_{P_{n_P}}^\top\end{pmatrix}^\top, \tag{7.31}$$

with $\theta_{Q_i} = \begin{bmatrix} q_{i,1} & \cdots & q_{i,L}\end{bmatrix}^\top$, $\theta_{P_i} = \begin{bmatrix} p_{i,1} & \cdots & p_{i,L(L-1)/2}\end{bmatrix}^\top$, where these parameter vectors parameterise the matrices according to

$$Q_i(\theta) = \begin{pmatrix} q_{i,1} & & & & \\ & q_{i,2} & & & \\ & & \ddots & & \\ & & & & q_{i,L}\end{pmatrix}, \tag{7.32a}$$

$$P_i(\theta) = \begin{pmatrix} 0 & p_{i,1} & p_{i,2} & \cdots & p_{i,L-1} \\ \star & 0 & p_{i,L} & \cdots & p_{i,2L-3} \\ \star & \star & 0 & \ddots & \vdots \\ \star & \star & \star & 0 & p_{i,L(L-1)/2} \\ \star & \star & \star & \star & 0\end{pmatrix}, \tag{7.32b}$$

where the elements $\star$ follow from the symmetry.

7.B Proof of Proposition 7.17

If $F^0(q) := I$ and $F(q,\theta)\big(\bar{X}_0(\theta) + \bar{Y}_0(\theta)\big) = I$, the network model structure is "ARX" and the residual $\varepsilon(t,\theta)$ (7.15) is affine in the parameters θ (remember that $\bar{X}(q^{-1}) + \bar{Y}(q^{-1}) = Q(q^{-1}) - P(q^{-1})$), meaning that it can be written as

$$\varphi^\top(t)\theta - Br(t) = \left[\bar{X}(q^{-1},\theta) + \bar{Y}(q^{-1},\theta)\right] w(t) - Br(t), \tag{7.33}$$

$$= \left[\sum_{i=0}^{n_X} \bar{X}_i(\theta) q^{-i} + \sum_{i=0}^{n_Y} \bar{Y}_i(\theta) q^{-i}\right] w(t) - Br(t), \tag{7.34}$$

where the structure of $\bar{X}(q^{-1},\theta)$ and $\bar{Y}(q^{-1},\theta)$ is retained in $\bar{X}_i(\theta)$ and $\bar{Y}_i(\theta)$, respectively, and with parameter vector

$$\theta = \begin{bmatrix} \theta_{\bar{X}_0}^\top & \cdots & \theta_{\bar{X}_{n_X}}^\top & \theta_{\bar{Y}_0}^\top & \cdots & \theta_{\bar{Y}_{n_Y}}^\top \end{bmatrix}^\top, \tag{7.35}$$

with $\theta_{\bar{X}_i} = \begin{bmatrix} \bar{x}_{i,1} & \cdots & \bar{x}_{i,L} \end{bmatrix}^\top$, $\theta_{\bar{Y}_i} = \begin{bmatrix} \bar{y}_{i,1} \cdots \bar{y}_{i,L(L-1)/2} \end{bmatrix}^\top$, where these parameter vectors parameterise the matrices according to

$$\bar{X}_i(\theta) = \begin{pmatrix} \bar{x}_{i,1} & & & \\ & \bar{x}_{i,2} & & \\ & & \ddots & \\ & & & \bar{x}_{i,L} \end{pmatrix}, \tag{7.36a}$$

$$\bar{Y}_i(\theta) = \begin{pmatrix} \star & \bar{y}_{i,1} & \bar{y}_{i,2} & \cdots & \bar{y}_{i,L-1} \\ \star & \star & \bar{y}_{i,L} & \cdots & \bar{y}_{i,2L-3} \\ \star & \star & \star & \ddots & \vdots \\ \star & \star & \star & \star & \bar{y}_{i,L(L-1)/2} \\ \star & \star & \star & \star & \star \end{pmatrix}, \tag{7.36b}$$

where the elements $\star$ follow from the Laplacian structure.

8 | Identification through structured polynomial models

This chapter is equivalent to

E.M.M. Kivits and P.M.J. Van den Hof. Identification of diffusively coupled linear networks through structured polynomial models. In *IEEE Transactions on Automatic Control*, vol. 68, no. 6, pages 3513-3528, 2023.

Physical dynamic networks most commonly consist of interconnections of physical components that can be described by diffusive couplings. These diffusive couplings imply that the cause-effect relationships in the interconnections are symmetric and therefore physical dynamic networks can be represented by undirected graphs. This chapter shows how prediction error identification methods developed for linear time-invariant systems in polynomial form can be configured to consistently identify the parameters and the interconnection structure of diffusively coupled networks. Further, a multistep least squares convex optimisation algorithm is developed to solve the nonconvex optimisation problem that results from the identification method.

8.1 Introduction

8.1.1 Dynamic Networks

Physical networks can describe many physical processes from different domains, such as mechanical, magnetic, electrical, hydraulic, acoustic, thermal, and chem-

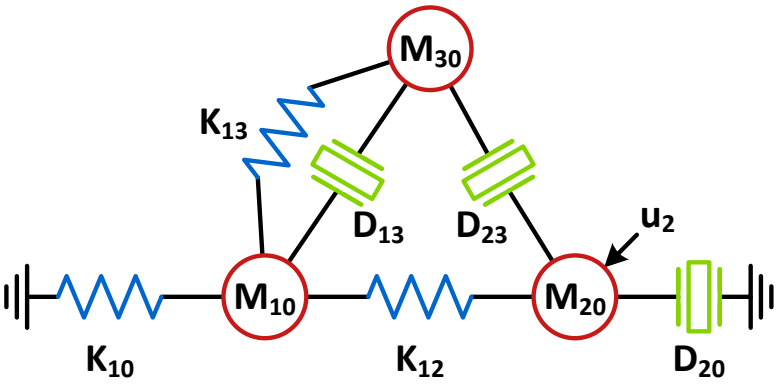

Figure 8.1: A network of masses (M_{j0}), dampers (D_{jk}) and springs (K_{jk}).

ical processes. Their dynamic behaviour is typically described by undirected dynamic interconnections between nodes, where the interconnections represent diffusive couplings (Cheng et al., 2017; Dörfler and Bullo, 2013; Dörfler et al., 2018). A corresponding representation can be considered to consist of L interconnected node signals $w_j(t)$, $j = 1, \ldots, L$, of which the behaviour is described according to a second-order vector differential equation:

$$\mathsf{M}_{j0}\ddot{w}_j(t) + \mathsf{D}_{j0}\dot{w}_j(t) + \sum_{k\in\mathcal{N}_j} \mathsf{D}_{jk}[\dot{w}_j(t) - \dot{w}_k(t)] + \mathsf{K}_{j0}w_j(t) + \sum_{k\in\mathcal{N}_j} \mathsf{K}_{jk}[w_j(t) - w_k(t)] = \underbrace{r_j(t) + v_j(t)}_{u_j(t)}, \quad (8.1)$$

with real-valued coefficients $\mathsf{M}_{j0} \geq 0$, $\mathsf{D}_{jk} \geq 0$, $\mathsf{K}_{jk} \geq 0$, $\mathsf{D}_{jj} = 0$; $\mathsf{K}_{jj} = 0$; $\mathcal{N}_j$ the set of indices of node signals $w_k(t)$, $k \neq j$, with connections to node signals $w_j(t)$; $u_j(t)$ the external signals composed of measured excitation signals $r_j(t)$ and unmeasured disturbances $v_j(t)$; and with $\dot{w}_j(t)$ and $\ddot{w}_j(t)$ the first and second-order derivative of the node signals $w_j(t)$, respectively. The diffusive type of coupling induces the symmetry constraints $\mathsf{D}_{jk} = \mathsf{D}_{kj}$ and $\mathsf{K}_{jk} = \mathsf{K}_{kj}$ $\forall j, k$.

An obvious physical example of such a network is the mass-spring-damper system shown in Figure 8.1, in which masses M_{j0} are interconnected through dampers D_{jk} and springs K_{jk} with $k \neq 0$ and are connected to the ground with dampers D_{j0} and springs K_{j0}. The positions $w_j(t)$ of the masses M_{j0} are the signals that are considered to be the node signals[1]. The couplings between the

[1]Note that a system as the one shown in Figure 8.1 would require at least a two-dimensional position vector $w_j(t)$, but for notational convenience and without loss of generality, we will restrict our attention to scalar-valued node signals $w_j(t)$.

masses are diffusive, because springs and dampers are symmetric components.

The considered type of networks occurs in many other applications, such as RLC circuits, power grids, and climate control systems.

8.1.2 Network identification

In this chapter, we address the problem of identifying the physical components in the network on the basis of measured node signals $w(t)$ and possibly external excitation signals $r(t)$. We develop a general framework for identifying such networks. Currently available methods for solving this problem can be classified into different categories. Black-box prediction error identification methods (Ljung, 1999) can be used to model the transfer functions from measured $r_j(t)$ signals to node signals $w_j(t)$, leading to a nontrivial second step in which the estimated models need to be converted to the structure representation of the physical network for arriving at estimated component values. Moreover, this modelling procedure and the required conversion would become essentially dependent on the particular location of the external signals $r_j(t)$. In a second category, black-box state-space models can be estimated from which the model parameters can be derived by applying matrix transformations (Friswell et al., 1999; Lopes dos Santos et al., 2015; Ramos et al., 2013) or eigenvalue decompositions (Fritzen, 1986; Luş et al., 2003). However, these methods typically do not have any guarantees on the statistical accuracy of the estimates and lack a consistency analysis. In another approach, state-space models with tailor-made physical parameterisations can be employed in a prediction error/maximum likelihood setting, typically leading to the situation that the network parameters appear nonlinearly in the state-space model, resulting in highly nonconvex optimisation problems to solve (The Mathworks, Inc., 2021).

In this chapter, we follow an approach that starts with the network representation of the model, while we maintain and exploit the network structure during the identification procedure.

Dynamic networks are currently a topic of research in different areas, while exploiting different network representations. Often, state-space models are used, possibly involving diffusive couplings, e.g. in model reduction (Cheng and Scherpen, 2021), estimating network connectivity (Timme, 2007), multiagent consensus-type algorithms (Nabi-Abdolyousefi and Mesbahi, 2012), and subspace identification (Haber and Verhaegen, 2014). A different model setting is used by Gonçalves et al. (2007), where transfer functions are being used to represent the dynamic interactions between node signals, exploited further by Materassi and Salapaka (2012); van Waarde et al. (2021) for topology identification and by Van den Hof et al. (2013) for prediction error identification of the network dynamics

(modules). In the realistic situation where not all states of a network can be measured, the transfer function approach appears attractive for identifying the network, but at the same time it is less fit for representing the physical diffusive types of couplings that would need to be included. As a result, an identification framework that can effectively exploit the physical structure of diffusive couplings, while identifying the dynamics on the basis of selected measurements, is still missing.

8.1.3 Research objective and contribution

The overall objective of this research is to develop a comprehensive theory for the identification of the physical component in diffusively coupled linear networks, where the order of the dynamics is not restricted and possibly correlated disturbances can be present. The objective includes questions like which nodes to measure (sense) and which nodes to excite (actuate) in order to identify particular local dynamics in the network or to identify the full dynamics and topology of the network. In addition, the consistency and minimum variance properties of estimates have to be specified. In this chapter, we focus on the problem of identifying the full dynamics and topology of diffusively coupled linear networks.

We will develop a prediction error framework for identifying the components in a diffusively coupled network of linear time-invariant systems, by fully adhering to the structure of the underlying constitutive model equations. We develop a polynomial representation of diffusively coupled networks, that is special due to its non-monicity and symmetric structure. For this representation, the standard (prediction error) identification algorithms cannot be applied directly. A dedicated prediction error identification method is developed that exploits the structured polynomial representation of the network and allows for handling dynamics of any finite order representing the interconnections and therefore, also allows for identifying the topology of the network. New conditions for identifiability and consistent estimation of the network components are derived. While the developed prediction error method in general relies on nonconvex optimisation, which is poorly scalable to large dimensions, an alternative multistep algorithm is presented, following the recent developments in the so-called weighted null-space fitting (WNSF) algorithm (Galrinho et al., 2019). This algorithm is adapted to accommodate the particular structured models that are considered by involving constrained optimisations rather than unconstrained ones.

This chapter builds further on the preliminary work presented in Chapter 7, in which the first results on the polynomial representation are presented in the scope of particular linear regression schemes. These results are extended to the general situation of rational noise models, including detailed identifiability and consistency results as well as the implementation of an adapted WNSF algorithm.

After specifying the notation of our networks in continuous- and discrete-time in Section 8.2, the set-up for identification of the full network dynamics is described in Section 8.3. In order to be able to consistently identify the network dynamics, data informativity and network identifiability conditions need to be satisfied. These conditions are formulated in Section 8.4 as well as the results for consistent identification of the networks. Section 8.5 contains the multistep algorithm for consistently identifying the network dynamics and Section 8.6 consists of a simulation example that illustrates and supports these results. Section 8.7 contains some extensions, after which conclusions are formulated in Section 8.8.

We consider the following notation throughout the chapter: A polynomial matrix $A(z^{-1})$ in complex indeterminate z^{-1}, consists of matrices A_ℓ and (j,k)th polynomial elements $a_{jk}(z^{-1})$ such that $A(z^{-1}) = \sum_{\ell=0}^{n_a} A_\ell z^{-\ell}$ and $a_{jk}(z^{-1}) = \sum_{\ell=0}^{n_a} a_{jk,\ell} z^{-\ell}$. Hence, the (j,k)th element of the matrix A_ℓ is denoted by $a_{jk,\ell}$. Physical components are indicated in sans serif font: A or a. A $p \times m$ rational function matrix $F(z)$ is proper if $\lim_{z\to\infty} F(z) = c \in \mathbb{R}^{p\times m}$; it is strictly proper if $c = 0$, and monic if $p = m$ and c is the identity matrix. $F(z)$ is stable if all its poles are within the unit circle $|z| < 1$. As a signal framework we adopt the prediction error framework of Ljung (1999), where quasi-stationary signals are defined as summations of a stationary stochastic process and a bounded deterministic signal, and $\bar{\mathbb{E}} := \lim_{N\to\infty} \frac{1}{N} \sum_{t=1}^{N} \mathbb{E}$, with $\mathbb{E}$ the expectation operator.

8.2 Physical network

8.2.1 Higher-order network

A physical network as described in the previous section is typically of second order, where all node signals are collected in $w(t)$. Network models that explain only a selection of the node signals can be constructed by removing nodes from the network through a Gaussian elimination procedure that is referred to as Kron reduction (Dörfler and Bullo, 2013; Dörfler et al., 2018) or immersion (Dankers et al., 2016), which will generally lead to higher-order dynamics between the remaining node signals. In order to accommodate this, we will include higher-order terms in our model.

Definition 8.1 (Physical network). *A physical network is a network consisting of L node signals $w_1(t), \ldots, w_L(t)$ interconnected through diffusive couplings and with at least one connection of a node to the ground node.*

The behaviour of the node signals $w_j(t)$, $j = 1, \ldots, L$, is described by

$$\sum_{\ell=0}^{n_x} \mathsf{x}_{jj,\ell} w_j^{(\ell)}(t) + \sum_{k \in \mathcal{N}_j} \sum_{\ell=0}^{n_y} \mathsf{y}_{jk,\ell} [w_j^{(\ell)}(t) - w_k^{(\ell)}(t)] = u_j(t), \qquad (8.2)$$

with n_x and n_y the order of the dynamics in the network, with real-valued coefficients $\mathsf{x}_{jj,\ell} \geq 0$, $\mathsf{y}_{jk,\ell} \geq 0$, $\mathsf{y}_{jk,\ell} = \mathsf{y}_{kj,\ell}$, where $w_j^{(\ell)}(t)$ is the ℓth derivative of $w_j(t)$ and where $u_j(t)$ is the external signal entering the jth node. The network is assumed to be connected, which means that there is a path between every pair of nodes[a].

[a] The network is connected if its Laplacian matrix (i.e. the degree matrix minus the adjacency matrix) has a positive second smallest eigenvalue (Dörfler and Bullo, 2013).

The graphical interpretation of the coefficients is as follows: $\mathsf{x}_{jj,n}$ represent the buffers, that is, the components intrinsically related to the nodes $w_j(t)$; $\mathsf{x}_{jj,\ell}$ with $\ell \neq n$ represent the components connecting the node $w_j(t)$ to the ground node; and $\mathsf{y}_{jk,\ell}$ represent the components in the diffusive couplings between the nodes $w_j(t)$ and $w_k(t)$. The ground node is characterised by $w_{ground}(t) = 0$ and therefore can be seen as a node with an infinite buffer; see also Dörfler and Bullo (2013).

A graphical representation of a physical network is shown in Figure 8.2. The network dynamics is represented by the blue boxes containing the polynomials $x_{jj} = \sum_{\ell=0}^{n_x} \mathsf{x}_{jj,\ell} p^\ell$ and $y_{jk} = \sum_{\ell=0}^{n_y} \mathsf{y}_{jk,\ell} p^\ell$, with p the differential operator d/dt, and the node signals are represented by the blue circles, which sum the diffusive couplings and the external signals. For example, $w_5(t) = \mathsf{x}_{55}\big(w_5(t) - 0\big) + \mathsf{y}_{45}\big(w_5(t) - w_4(t)\big) + u_5(t)$.

Furthermore, every matrix X_ℓ composed of elements $x_{jj,\ell} := \mathsf{x}_{jj,\ell}$ is diagonal and every matrix Y_ℓ composed of elements $y_{jj,\ell} := \sum_{k \in \mathcal{N}_j} \mathsf{y}_{jk,\ell}$ and $y_{jk,\ell} := -\mathsf{y}_{jk,\ell}$ for $k \neq j$ is Laplacian[2] representing an undirected graph of a specific physical component, i.e., the diffusive couplings of a specific order.

8.2.2 Discretisation

In order to fully exploit the results of network identification that typically have been developed for discrete-time systems, the continuous-time network is converted

[2] A Laplacian matrix is a symmetric matrix with nonpositive off-diagonal elements and with nonnegative diagonal elements that are equal to the negative sum of all other elements in the same row (or column) (Mesbahi and Egerstedt, 2010).

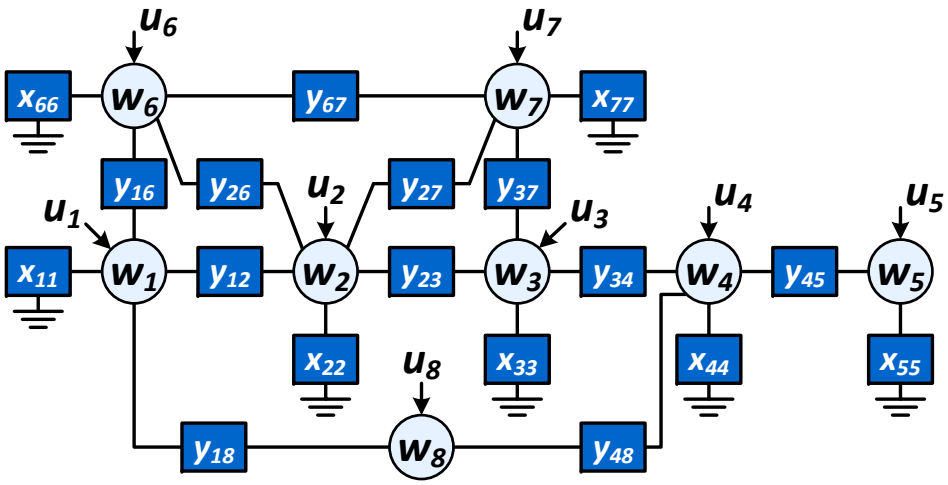

Figure 8.2: A physical network as defined in Definition 8.1, with node signals $w_j(t)$, input signals $u_j(t)$, and dynamics between the nodes ($y_{jk}(q^{-1})$) and to the ground node ($x_{jj}(q^{-1})$).

into an equivalent discrete-time form. Out of the group of discretisation methods that commute with series, parallel, and feedback connections of systems (Mori et al., 1987) we select the backward difference method. This method is relatively simple, results in a causal network representation, and describes a unique bijective mapping between the continuous-time and discrete-time model, by substituting

$$\left.\frac{dw(t)}{dt}\right|_{t=t_d} = \frac{w(t_d) - w(t_{d-1})}{T_s}, \tag{8.3}$$

with discrete-time sequence $t_d = dT_s$, $d = 0, 1, \ldots$ and time interval T_s. Using (8.3), the continuous-time diffusively coupled network (8.2) can be approximated in discrete time by

$$\sum_{\ell=0}^{n_x} \bar{\mathsf{x}}_{jj,\ell} q^{-\ell} w_j(t_d) + \sum_{k \in \mathcal{N}_j} \sum_{\ell=0}^{n_y} \bar{\mathsf{y}}_{jk,\ell} q^{-\ell} [w_j(t_d) - w_k(t_d)] = u_j(t_d), \tag{8.4}$$

with q^{-1} the shift operator meaning $q^{-1} w_j(t_d) = w_j(t_{d-1})$ and with

$$\bar{\mathsf{x}}_{jj,\ell} = (-1)^\ell \textstyle\sum_{i=\ell}^{n_x} \binom{i}{\ell} T_s^{-i} \mathsf{x}_{jj,i}, \tag{8.5a}$$

$$\bar{\mathsf{y}}_{jk,\ell} = (-1)^\ell \textstyle\sum_{i=\ell}^{n_y} \binom{i}{\ell} T_s^{-i} \mathsf{y}_{jk,i}, \tag{8.5b}$$

where $\binom{i}{\ell}$ is a binomial coefficient. In the sequel, $(t-i)$ is used for $t_{d-i} = t_d - iT_s$. The expressions for the node signals (8.4) can be combined in a matrix equation

describing the network as

$$\bar{X}(q^{-1})w(t) + \bar{Y}(q^{-1})w(t) = u(t), \tag{8.6}$$

with $\bar{X}(q^{-1})$ and $\bar{Y}(q^{-1})$ polynomial matrices in the shift operator q^{-1} and composed of elements

$$\bar{X}_{jk}(q^{-1}) = \begin{cases} \sum_{\ell=0}^{n_x} \bar{\mathrm{x}}_{jj,\ell} q^{-\ell}, & \text{if } k = j \\ 0, & \text{otherwise} \end{cases} \tag{8.7a}$$

$$\bar{Y}_{jk}(q^{-1}) = \begin{cases} \sum_{m \in \mathcal{N}_j} \sum_{\ell=0}^{n_y} \bar{\mathrm{y}}_{jm,\ell} q^{-\ell}, & \text{if } k = j \\ -\sum_{\ell=0}^{n_y} \bar{\mathrm{y}}_{jk,\ell} q^{-\ell}, & \text{if } k \in \mathcal{N}_j \\ 0, & \text{otherwise.} \end{cases} \tag{8.7b}$$

Observe that $\bar{X}(q^{-1})$ is diagonal and $\bar{Y}(q^{-1})$ is Laplacian, implying that the structural properties of (8.2) are maintained in (8.6)-(8.7). In the sequel, we will use the notation $A(q^{-1}) = \bar{X}(q^{-1}) + \bar{Y}(q^{-1})$ while $\bar{X}(q^{-1})$ and $\bar{Y}(q^{-1})$ can always be uniquely recovered from $A(q^{-1})$, because of their particular structure.

8.3 Identification set-up

As mentioned before, the objective of this chapter is to identify the full dynamics and topology of diffusively coupled networks. In this section, the identification setting is described, which includes the network model, the network predictor, the model set, and the identification criterion.

The node signals in the network might be affected by a user-applied excitation signal and subject to a disturbance signal. This needs to be included in the network description, which is achieved by splitting the external signal as

$$u(t) := B(q^{-1})r(t) + F(q)e(t), \tag{8.8}$$

where, the known excitation signals $r(t)$ enter the network through dynamics described by polynomial matrix $B(q^{-1})$ and where the unknown disturbance signals acting on the network are modelled as filtered white noise, i.e. $F(q)$ is a rational matrix and $e(t)$ is a vector-valued wide-sense stationary white noise process, i.e. $\mathbb{E}[e(t)e^\top(t-\tau)] = 0$ for $\tau \neq 0$.

Definition 8.2 (Network model). *The network that will be considered during identification is assumed to be connected, with at least one connection to the ground node; it consists of L node signals $w(t)$ and K excitation*

signals $r(t)$; and is defined as

$$A(q^{-1})w(t) = B(q^{-1})r(t) + F(q)e(t), \tag{8.9}$$

with

1. $A(q^{-1}) = \sum_{k=0}^{n_a} A_k q^{-k} \in \mathbb{R}^{L\times L}[q^{-1}]$, *with* $a_{jk}(q^{-1}) = a_{kj}(q^{-1})$, *for all* k, j, *and* $A^{-1}(q^{-1})$ *stable.*
2. $B(q^{-1}) \in \mathbb{R}^{L\times K}[q^{-1}]$.
3. $F(q) \in \mathcal{H} := \{F \in \mathbb{R}^{L\times L}(q) \mid F$ *monic, stable and tably invertible*$\}$.
4. $\Lambda \succ 0$ *the covariance matrix of the noise* $e(t)$.
5. $r(t)$ *is a deterministic and bounded sequence.*
6. $e(t)$ *is a zero-mean white noise process with bounded moments of an order larger than 4 (Ljung, 1999).*

Lemma 8.3. *In* (8.9) *it holds that* $\text{rank}(A_0) = L$.

Proof: The proof is provided in Appendix 8.A. ■

$\text{rank}(A_0) = L$ also implies that $A^{-1}(q^{-1})$ exists and is proper, which means that the network is well-posed. The network is also stable as $A^{-1}(q^{-1})$ is stable.

Often, $B(q^{-1})$ is chosen to be binary, diagonal, and known, which represents the assumption that each external excitation signal directly enters the network at a distinct node.

As a result, the considered networks lead to polynomial models[3] with the particular properties that $A(q^{-1})$ is symmetric and nonmonic. Moreover, if $F(q)$ is polynomial or even stronger if $F(q) = I$, the network (8.9) leads to an ARMAX-like or ARX-like[4] model structure, respectively.

Now that the network representation and its properties have been defined, the next step is to formulate the identification setting.

[3]Polynomial models are linear time-invariant dynamic models of the form $A(q^{-1})y(t) = E^{-1}(q^{-1})B(q^{-1})u(t) + D^{-1}(q^{-1})C(q^{-1})e(t)$, where $A(q^{-1})$, $B(q^{-1})$, $C(q^{-1})$, $D(q^{-1})$, and $E(q^{-1})$ are polynomials in q^{-1} that are all monic except for $B(q^{-1})$ (Ljung, 1999; Hannan and Deistler, 2012).

[4]The structure is formally only an ARMAX (autoregressive-moving average with exogenous variables) or ARX (autoregressive with exogenous variables) structure if the $A(q^{-1})$ polynomial is monic (Hannan and Deistler, 2012).

8.3.1 Network predictor

The objective is to identify the dynamics of the complete network. This estimation is performed using a prediction error method, which is the most common system identification method and it is applicable to networks (Van den Hof et al., 2013). In order to identify the network dynamics, all node signals $w(t)$ are predicted based on the measured signals that are available in the network. This leads to the following predictor.

Definition 8.4 (Network predictor). *In line with Weerts et al. (2016), the network predictor is defined as the conditional expectation*

$$\hat{w}(t|t-1) := \mathbb{E}\{w(t) \mid w^{t-1},\ r^t\}, \tag{8.10}$$

where w^{t-1} represents the past of $w(t)$, that is, $w(t-1), w(t-2), \ldots$ and r^t represents $r(t), r(t-1), \ldots$

Proposition 8.5 (Network predictor). *For a network model* (8.9)*, the one-step-ahead network predictor* (8.10) *is given by*

$$\hat{w}(t|t-1) = \left[I - A_0^{-1}F^{-1}(q)A(q^{-1})\right] w(t) + A_0^{-1}F^{-1}(q)B(q^{-1})r(t). \tag{8.11}$$

Proof: The proof is provided in Appendix 8.B. ■

Proposition 8.6 (Innovation). *The innovation corresponding to the network predictor* (8.11) *is*

$$\bar{e}(t) := w(t) - \hat{w}(t|t-1) = A_0^{-1}e(t), \tag{8.12}$$

which has covariance matrix $\bar{\Lambda} = A_0^{-1}\Lambda A_0^{-1}$.

Proof: This follows directly from subsequently substituting $\hat{w}(t|t-1)$ (8.11) and $w(t)$ (8.9) into (8.12). ■

The innovation is a scaled version of the driving noise process. As A_0 is not necessarily diagonal, the scaling may cause correlations among the noise channels, but the innovation signal $\bar{e}(t)$ remains a white noise process.

8.3.2 Model set and prediction error

The network models that will be considered during identification are gathered in the network model set.

Definition 8.7 (Network model set). *The model set is defined as a set of parameterised functions as*

$$\mathcal{M} := \{M(\theta),\ \theta \in \Theta\ \subset \mathbb{R}^d\}, \tag{8.13}$$

with $d \in \mathbb{N}$, with all particular models

$$M(\theta) := \left(A(q^{-1},\theta),\ B(q^{-1},\theta),\ F(q,\theta), \Lambda(\theta)\right) \tag{8.14}$$

satisfying the properties in Definition 8.2.

In this setting, θ contains all the unknown coefficients that appear in the entries of the model matrices $A(q^{-1})$, $B(q^{-1})$, $F(q)$, and Λ.

The experimental data that are available for identification are generated by the true system.

Definition 8.8 (Data generating system). *The data generating system $\mathcal{S}$ is denoted by the model*

$$M^0 := (A^0, B^0, F^0, \Lambda^0). \tag{8.15}$$

The true system is in the model set ($\mathcal{S} \in \mathcal{M}$) if $\exists \theta^0 \in \Theta$ such that $M(\theta^0) = M^0$, where θ^0 indicate the true parameters.

Using the parameterised network model set, the parameterised one-step-ahead network predictor is defined.

Definition 8.9 (Parameterised predictor). *The parameterised network predictor is defined in accordance with* (8.11) *as*

$$\hat{w}(t|t-1;\theta) = W(q,\theta)z(t), \tag{8.16}$$

with data $z(t) := \begin{bmatrix} w(t) \\ r(t) \end{bmatrix}$, *and predictor filter*

$$W(q,\theta) := \begin{bmatrix} I - W_w(q,\theta) & W_r(q,\theta) \end{bmatrix}, \tag{8.17}$$

where

$$W_w(q,\theta) = A_0^{-1}(\theta)F^{-1}(q,\theta)A(q^{-1},\theta), \tag{8.18a}$$

$$W_r(q,\theta) = A_0^{-1}(\theta)F^{-1}(q,\theta)B(q^{-1},\theta). \tag{8.18b}$$

The parameterised predictor leads to the prediction error.

Proposition 8.10 (Prediction error). *The prediction error corresponding to the parameterised predictor* (8.16) *is defined as*

$$\bar{\varepsilon}(t,\theta) := w(t) - \hat{w}(t|t-1;\theta), \tag{8.19}$$

which is obtained as

$$\begin{aligned}\bar{\varepsilon}(t,\theta) &= A_0^{-1}(\theta)F^{-1}(q,\theta)\left[A(q^{-1},\theta)w(t) - B(q^{-1},\theta)r(t)\right], &(8.20a)\\ &= W_w(q,\theta)w(t) - W_r(q,\theta)r(t), &(8.20b)\end{aligned}$$

which equals the innovation $\bar{e}(t)$ (8.12) *for* $\theta = \theta^0$.

Proof: The proof is provided in Appendix 8.C. ■

8.3.3 Identification criterion

In order to estimate the parameters, a weighted least squares identification criterion is applied:

$$\hat{\theta}_N = \arg\min_{\theta\in\Theta} V_N(\theta), \tag{8.21a}$$

$$V_N(\theta) := \frac{1}{N}\sum_{t=1}^{N} \bar{\varepsilon}^\top(t,\theta)S\bar{\varepsilon}(t,\theta), \tag{8.21b}$$

$$\bar{\Lambda}(\hat{\theta}_N) := \frac{1}{N}\sum_{t=1}^{N} \bar{\varepsilon}(t,\hat{\theta}_N)\bar{\varepsilon}^\top(t,\hat{\theta}_N), \tag{8.21c}$$

with weight $S \succ 0$ that has to be chosen by the user. It is a standard result in prediction error identification (Ljung, 1999, Theorem 8.2), that under uniform stability conditions on the parameterised model set, (8.21a) converges with probability 1 to

$$\theta^* := \arg\min_{\theta\in\Theta} \bar{V}(\theta), \tag{8.22a}$$

$$\text{with } \bar{V}(\theta) := \bar{\mathbb{E}}\left\{\bar{\varepsilon}^\top(t,\theta)S\bar{\varepsilon}(t,\theta)\right\}. \tag{8.22b}$$

8.4 Consistent identification

In order to consistently identify the network, the experimental data need to satisfy certain conditions. These conditions are referred to as data informativity conditions. In addition, the network itself needs to satisfy certain conditions so that it can be uniquely recovered. These conditions are referred to as network identifiability conditions. This section describes these conditions, after which the results for consistent network identification can be formulated.

The network (8.9) can be represented as

$$w(t) = T_{wr}(q)r(t) + \bar{v}(t), \quad \bar{v}(t) = T_{w\bar{e}}(q)\bar{e}(t), \tag{8.23}$$

where $\bar{e}(t)$ is the innovation (8.12) and

$$T_{wr}(q) = A^{-1}(q^{-1})B(q^{-1}), \tag{8.24a}$$
$$T_{w\bar{e}}(q) = A^{-1}(q^{-1})F(q)A_0. \tag{8.24b}$$

For estimating a network model, prediction error identification methods typically use the second-order statistical properties of the measured data, which are represented by the spectral densities of $w(t)$ and $r(t)$. As $r(t)$ is measured, but $\bar{e}(t)$ is not, the second-order properties of $w(t)$ are generated by the transfer function $T_{wr}(q)$ and spectral density

$$\Phi_{\bar{v}}(\omega) := \mathcal{F}\left\{\mathbb{E}\left[\bar{v}(t)\bar{v}^\top(t-\tau)\right]\right\}, \tag{8.25a}$$
$$= T_{w\bar{e}}(e^{i\omega})\bar{\Lambda}T^*_{w\bar{e}}(e^{i\omega}), \tag{8.25b}$$

with $\mathcal{F}$ the discrete-time Fourier transform and $(\cdot)^*$ the complex conjugate transpose. Observe that the spectral factorisation in (8.25b) is unique, as $T_{w\bar{e}}(q) \in \mathcal{H}$ and $\bar{\Lambda} \succ 0$ (Youla, 1961).

8.4.1 Data informativity

The data are called informative if they contain sufficient information to uniquely recover the predictor filter $W(q, \theta)$ from the second-order statistical properties of the data $z(t)$. This can be formalised in line with Ljung (1999) as follows:

Definition 8.11 (Data informativity). *A quasi-stationary data sequence* $\{z(t)\}$ *is called informative with respect to the model set* $\mathcal{M}$ (8.13) *if for any*

two $\theta_1, \theta_2 \in \Theta$

$$\bar{\mathbb{E}}\left\{\|[W(q,\theta_1) - W(q,\theta_2)]z(t)\|^2\right\} = 0 \Rightarrow \{W(e^{i\omega},\theta_1) = W(e^{i\omega},\theta_2)\} \tag{8.26}$$

for almost all ω.

Applying this definition to physical networks leads to the following conditions for data informativity:

Proposition 8.12 (Data informativity). *The quasi-stationary data sequence* $z(t)$ *is informative with respect to the model set* $\mathcal{M}$ *if* $\Phi_z(\omega) \succ 0$ *for a sufficiently high number of frequencies*[a]. *In the situation* $K \geq 1$, *this is guaranteed by* $\Phi_r(\omega) \succ 0$ *for a sufficiently high number of frequencies.*

[a] The number of frequencies for which $\Phi_z(\omega) \succ 0$ is required, is dependent on the number of parameters in $\mathcal{M}$.

Proof: The proof is provided in Appendix 8.D. ■

The condition that $\Phi_r(\omega) \succ 0$ for a sufficiently high number of frequencies seems to be a general condition. However, observe that the dimensions of $\Phi_r(\omega)$ depend on the number of excitation signals $r(t)$, denoted by K, which is specified in the model set. Thus, all excitation signals $r(t)$ that are present (according to the model set), need to be persistently exciting. This is because each additional excitation signal $r_j(t)$ also introduces new polynomials $b_{kj}(q^{-1})$ that need to be identified.

Informativity of $z(t)$ implies that $W(q)$ can uniquely be recovered from data, which by (8.18) and (8.24) implies that the pair $(T_{wr}(q), \Phi_{\bar{v}}(\omega))$ can uniquely be recovered from data.

8.4.2 Network identifiability

The concept of network identifiability has been defined for general linear dynamic networks by Weerts et al. (2018b) as follows:

Definition 8.13 (Network identifiability). *The network model set* $\mathcal{M}$ (8.13) *is globally network identifiable from* $z(t)$ *if the parameterised model* $M(\theta)$ *can uniquely be recovered from* $T_{wr}(q,\theta)$ *and* $\Phi_{\bar{v}}(\omega,\theta)$, *that is, if for all*

models $M(\theta_1), M(\theta_2) \in \mathcal{M}$

$$\left.\begin{aligned} T_{wr}(q,\theta_1) &= T_{wr}(q,\theta_2) \\ \Phi_{\bar{v}}(\omega,\theta_1) &= \Phi_{\bar{v}}(\omega,\theta_2) \end{aligned}\right\} \Rightarrow M(\theta_1) = M(\theta_2). \tag{8.27}$$

Whereas the original definition has been applied to network models with all transfer function elements, here we apply it to our choice of models (8.14), where through the particular parameterisation of the polynomials $A(q,\theta)$ and $B(q,\theta)$, equality of models implies equality of the physical parameters in these polynomial matrices. Before formulating the conditions for the identifiability of our particular networks, a result on left matrix-fraction descriptions (LMFDs) is presented.

Lemma 8.14 (LMFD). *Consider a network model set* $\mathcal{M}$ (8.13)*. Given the LMFD* $A(q^{-1})^{-1}B(q^{-1})$*,* $A(q^{-1})$ *and* $B(q^{-1})$ *are unique within* $\mathcal{M}$ *up to a scalar factor if the following conditions are satisfied:*[a]

1. $A(q^{-1})$ *and* $B(q^{-1})$ *are left coprime in* $\mathcal{M}$*.*
2. *Within* $\mathcal{M}$*, at least one of the matrices in the set* $\{A_k, k = 0, \cdots n_a; B_\ell, \ell = 0, \cdots n_b\}$ *is diagonal and full rank.*

[a] This lemma is slightly different formulated than by Kivits and Van den Hof (2023b).

Proof: According to Kailath (1980), the LMFD of any two polynomial and left coprime matrices is unique up to a premultiplication with a unimodular matrix. To preserve the diagonality of A_k or B_ℓ, the unimodular matrix is restricted to be diagonal. To preserve the symmetry of $A(q^{-1})$, this diagonal matrix is further restricted to have equal elements. ■

In general polynomial models, like ARMAX (Deistler, 1983), $A(q^{-1})$ is monic and therefore $A_0 = I$ is diagonal. Then the LMFD $A(q^{-1})^{-1}B(q^{-1})$ is unique, as the conditions of Lemma 8.14 are satisfied and scaling with a scalar factor is not possible anymore, since the diagonal elements of A_0 are equal to 1. Hence, both Condition 2. in Lemma 8.14 and the scaling factor freedom are a result of the fact that $A(q^{-1})$ is not necessarily monic.

Now the conditions for global network identifiability can be formulated.

Proposition 8.15 (Network identifiability). *A network model set* $\mathcal{M}$ (8.13) *is globally network identifiable from* $z(t)$ *if the following conditions are satisfied:*[a]

1. $A(q^{-1})$ *and* $B(q^{-1})$ *are left coprime in* $\mathcal{M}$*.*

2. *Within $\mathcal{M}$, at least one of the matrices in the set $\{A_k, k = 0, \cdots n_a; B_\ell, \ell = 0, \cdots n_b\}$ is diagonal and full rank.*

3. *At least one excitation signal $r_j(t)$ is present: $K \geq 1$.*

4. *There is at least one constraint on the parameters of $A(q^{-1}, \theta_a)$ and $B(q^{-1}, \theta_b)$ of the form $\tilde{\Gamma}\tilde{\theta} = \gamma \neq 0$, with $\tilde{\theta} := \begin{bmatrix} \theta_a^\top & \theta_b^\top \end{bmatrix}^\top$.*

[a] This proposition is slightly different formulated than by Kivits and Van den Hof (2023b).

Proof: Condition 3. implies that $T_{wr}(q, \theta)$ is nonzero. According to Lemma 8.14, Conditions 1. and 2. imply that $A(q^{-1}, \theta)$ and $B(q^{-1}, \theta)$ are found up to a scalar factor α. $T_{w\bar{e}}(q, \theta)$ and $\bar{\Lambda}(\theta)$ are uniquely recovered from $\Phi_{\bar{v}}(\omega, \theta)$ as $T_{w\bar{e}}(q) \in \mathcal{H}$ and $\bar{\Lambda} \succ 0$ (Youla, 1961). Together with the fact that $A(q^{-1}, \theta)$ is found up to a scalar factor α, $T_{w\bar{e}}(q, \theta)$ gives a unique $F(q, \theta)$, and $\bar{\Lambda}(\theta)$ gives $\Lambda(\theta)$ up to a scalar factor α^2. Finally, Condition 4. implies that the parameters cannot be scaled anymore and therefore α is fixed. ■

The coprimeness of $A(q^{-1})$ and $B(q^{-1})$ ensures that $A(q^{-1})$ and $B(q^{-1})$ have no common factors. This condition is also necessary for the global identifiability of typical polynomial model structures (Ljung, 1999, Theorem 4.1). The parameter α is a scaling factor that is introduced by the nonmonicity of $A(q^{-1})$. The scaling factor needs to be fixed by additional constraints induced by Conditions 2. and 4. in Proposition 8.15. The parameter constraint in Condition 4. of Proposition 8.15 can, for example, be

1. One nonzero element in $B(q^{-1}, \theta)$ is known, i.e. one excitation signal enters a node through known dynamics.

2. One nonzero parameter is known.

3. The fraction of two nonzero parameters is known.

4. The sum of some nonzero parameters is known.

Remark 8.16. *In general, dynamic network conditions for global network identifiability typically include algebraic conditions verifying the rank of particular transfer functions from external signals to internal node signals (Weerts et al., 2018b). For the generic version of network identifiability, this entails a related graph-based check on vertex disjoint paths in the network model (Hendrickx et al., 2019; Cheng et al., 2022). In contrast to these conditions, the current conditions in Proposition 8.15 are very simple and*

require only a single excitation signal $r(t)$ to be present in the network. This is induced by the structural properties of the diffusive couplings between the nodes, reflected by the fact that the polynomial matrix $A(q^{-1})$ is restricted to being symmetric.

8.4.3 Consistency

Now, we can formulate the consistency result as follows:

Theorem 8.17 (Consistency). *Consider a data generating system $\mathcal{S}$ as defined in Definition 8.8 and a model set $\mathcal{M}$ in which the predictor filter* (8.17) *is uniformly stable. Then $M(\hat{\theta}_N)$ is a consistent estimate of M^0 if the following conditions hold:*

1. *The true system is in the model set ($\mathcal{S} \in \mathcal{M}$).*
2. *The data are informative with respect to the model set.*
3. *The model set is globally network identifiable.*

Proof: The proof is provided in Appendix 8.E ■

Observe that any weight $S \succ 0$ leads to consistent estimates, but that minimum variance is only achieved for $S = \bar{\Lambda}^{-1}$.

Now it has been proven that diffusively coupled networks can be identified consistently, the next step is to formulate algorithms for obtaining these estimates.

8.5 A multistep algorithm

The parameterised prediction error (8.20a) is not affine in the parameters θ. Only in the very special situation where $F(q, \theta) = I$ and $A_0(\theta) = I$, the structure of (8.20a) is affine. This situation causes the optimisation problem (8.21a) to be nonconvex. Especially for networks with many nodes, this results in high computational complexity and the occurrence of local optima. One approach to reduce the problem is to solve multiple multiple-input single-output (MISO) problems instead of one large multiple-input multiple-output (MIMO) problem (Van den Hof et al., 2013; Dankers et al., 2016; Gevers et al., 2018). However, since the dynamics is coupled (that is, $A(q^{-1})$ is symmetric and therefore its elements are not independently parameterised), a decomposition into MISO problems cannot be made without loss of accuracy.

In this section, as an alternative, a multistep algorithm is developed, where in each step a quadratic problem is solved using a linear regression scheme. With that, the developed method contains steps that are similar to sequential least squares (SLS) (Weerts et al., 2018a), weighted null-space fitting (WNSF) (Galrinho et al., 2019), and the multistep least squares method of Fonken et al. (2022), but particularly tuned to the network model structure of the current chapter.

In Step 1, an unstructured nonparametric ARX model is estimated from the data. This ARX model is reduced to a structured parametric ARMAX network model in Step 2, which is improved in Step 3. Once the network dynamics has been estimated, the noise model is found in Step 4 and the discrete-time components are extracted in Step 5. Finally, the components are mapped back to the continuous-time domain in Step 6. The particular difference between our method and the aforementioned methods is that the structure of the parameterised objects in Steps 2 and 3 is different and that the optimisation problem in Step 2 is a constrained optimisation problem. Furthermore, Steps 4, 5, and 6 have been added.

As only quadratic problems are solved, the optimisations are convex and have unique solutions. In this way, the formulated algorithm achieves a consistent parameter estimation with minimum variance and limited computation complexity. This makes the algorithm also applicable to networks with many nodes.

For the development of the algorithm, we will restrict attention to the situation of an ARMAX-like model structure, where we consider a data generating system $\mathcal{S} = (A^0, B^0, F^0, \Lambda^0)$ with $F^0(q) := C^0(q^{-1})$ being a monic polynomial, leading to the network equation

$$A^0(q^{-1})w(t) = B^0(q^{-1})r(t) + C^0(q^{-1})e(t), \tag{8.28}$$

which would have an ARMAX structure if $A^0(q^{-1})$ would be monic. Multiplying both sides of (8.28) with $[C^0(q^{-1})A_0^0]^{-1}$ leads to

$$\breve{A}^0(q^{-1})w(t) = \breve{B}^0(q^{-1})r(t) + \bar{e}(t), \tag{8.29}$$

where $\breve{A}^0(q^{-1})$ is monic, $\bar{e}(t)$ is the innovation (8.12), and

$$\breve{A}^0(q^{-1}) = [\bar{C}^0(q^{-1})]^{-1}A^0(q^{-1}), \tag{8.30a}$$
$$\breve{B}^0(q^{-1}) = [\bar{C}^0(q^{-1})]^{-1}B^0(q^{-1}), \tag{8.30b}$$
$$\bar{C}^0(q^{-1}) = C^0(q^{-1})A_0^0. \tag{8.30c}$$

Now consider the model structure $A(q^{-1}, \theta_a)$, $B(q^{-1}, \theta_b)$, and $\bar{C}(q^{-1}, \eta_c, \theta_a)$, as models of $A^0(q^{-1})$, $B^0(q^{-1})$, and $\bar{C}^0(q^{-1})$, respectively, with $\bar{C}(q^{-1}, \eta_c, \theta_a) =$

$C(q^{-1}, \theta_c)A_0(\theta_a)$, and with $\vartheta := \begin{bmatrix}\theta_a^\top & \theta_b^\top & \eta_c^\top\end{bmatrix}^\top$.As $C(q^{-1})$ is monic and A_0 is constant, $\bar{C}_0 = A_0$ and therefore parameterised as such. All other matrices $\bar{C}_\ell$ are independently parameterised with parameters η_c. The exact parameterisation is given in Appendix 8.F.

Step 1: Estimating the nonparametric ARX model

As a first step, we are going to estimate a nonparametric ARX model for (8.29), by parameterising the infinite series expansions $\breve{A}^0(q^{-1})$ and $\breve{B}^0(q^{-1})$ by high-order polynomial (finite) expansions $\breve{A}(q^{-1}, \zeta^n)$ and $\breve{B}(q^{-1}, \zeta^n)$, according to

$$\bar{\varepsilon}_A(t, \zeta^n) = \breve{A}(q^{-1}, \zeta^n)w(t) - \breve{B}(q^{-1}, \zeta^n)r(t), \tag{8.31a}$$

$$= w(t) - [\varphi^n(t)]^\top \zeta^n, \tag{8.31b}$$

with n the finite order of the polynomials, which is typically chosen to be high. The parameter vector ζ^n and the matrix $[\varphi^n(t)]^\top$ are given in Appendix 8.G. The nonparametric ARX model (8.29) is then estimated by estimating its parameters ζ^n. As this step serves to make an initial estimate of the network, the network structure is not taken into account. Further, consistency of this step is only achieved if the order n tends to infinity as a function of the data length N at an appropriate rate, according to Ljung and Wahlberg (1992). However, the bias will be negligibly small if the order n is chosen sufficiently large. The least-squares estimate of ζ^n is found by

$$\hat{\zeta}_N^n = \left[\frac{1}{N}\sum_{t=n+1}^{N} \varphi^n(t)[\varphi^n(t)]^\top\right]^{-1}\left[\frac{1}{N}\sum_{t=n+1}^{N} \varphi^n(t)w(t)\right]. \tag{8.32}$$

Under conditions of consistent estimation, and so if n and N approach infinity, $\bar{\varepsilon}_A(t, \hat{\zeta}_N^n)$ will be an accurate estimate of the innovation $\bar{e}(t)$. The covariance of the innovation is estimated as the covariance of the residual as

$$\bar{\Lambda}(\hat{\zeta}_N^n) = \frac{1}{N}\sum_{t=n+1}^{N} \bar{\varepsilon}_A(t, \hat{\zeta}_N^n)\bar{\varepsilon}_A^\top(t, \hat{\zeta}_N^n), \tag{8.33}$$

with residual (8.31a) evaluated at $\hat{\zeta}_N^n$. The covariance of the parameter estimation error $\epsilon(t, \hat{\zeta}_N^n) := \hat{\zeta}_N^n - \zeta^{n0}$ with ζ^{n0} the actual coefficients of the expansions in (8.29), is estimated by

$$P(\hat{\zeta}_N^n) = \left[\frac{1}{N}\sum_{t=n+1}^{N} \varphi^n(t)\bar{\Lambda}^{-1}(\hat{\zeta}_N^n)[\varphi^n(t)]^\top\right]^{-1}. \tag{8.34}$$

Remark 8.18. *As each row in* (8.31b) *is independently parameterised, the parameters ζ^n can be estimated for each row independently, resulting in L MISO problems instead of one MIMO problem. This is attractive for networks with many nodes.*

Step 2: Reducing to the structured network model

The high-order ARX model is used to identify the structured network model through the relations (8.30a) and (8.30b). In this step, the structural properties of $A^0(q^{-1})$ are incorporated and the parameter constraint is taken into account to fix the scaling parameter and obtain a unique solution.

The relations (8.30a) and (8.30b) are equivalently written as

$$A^0(q^{-1}) - \bar{C}^0(q^{-1})\breve{A}^0(q^{-1}) = 0, \tag{8.35a}$$

$$B^0(q^{-1}) - \bar{C}^0(q^{-1})\breve{B}^0(q^{-1}) = 0. \tag{8.35b}$$

Then from (8.35) we can extract:

$$-Q(\zeta^{n0})\vartheta^0 = 0, \tag{8.36}$$

where ϑ^0 represents the coefficients of the actual underlying system described by $A^0(q^{-1})$, $B^0(q^{-1})$, and $\bar{C}^0(q^{-1})$ (8.28) and where the nonparametric ARX representation $\breve{A}^0(q^{-1})$ and $\breve{B}^0(q^{-1})$ of the system is incorporated into $Q(\zeta^{n0})$. The specific structure of $Q(\zeta^{n0})$ is provided in Appendix 8.H. The polynomial terms in (8.35) are considered up to time lag n, and the row dimension of $Q(\zeta^{n0})$ is equal to $\dim(\zeta^{n0})$.

On the basis of the estimated nonparametric ARX model parameters $\hat{\zeta}_N^n$, an initial least-squares[5] estimate of ϑ^0 is obtained by the linear constrained optimisation problem

$$\hat{\vartheta}_N^{(0)} = \min_{\vartheta} \quad \vartheta^\top Q^\top(\hat{\zeta}_N^n)Q(\hat{\zeta}_N^n)\vartheta \tag{8.37a}$$

$$\text{subject to} \quad \Gamma\vartheta = \gamma, \tag{8.37b}$$

where the constraint (8.37b) results from Condition 4. in Proposition 8.15. The optimisation problem can be solved using the Lagrangian and the Karush–Kuhn–Tucker conditions (Chong and Żak, 2008), giving

$$\begin{bmatrix} \hat{\vartheta}_N^{(0)} \\ \hat{\lambda}_N^{(0)} \end{bmatrix} = \begin{bmatrix} Q^\top(\hat{\zeta}_N^n)Q(\hat{\zeta}_N^n) & \Gamma^\top \\ \Gamma & 0 \end{bmatrix}^{-1} \begin{bmatrix} 0 \\ \gamma \end{bmatrix}, \tag{8.38}$$

[5]Weighted least-squares can be used as well (see Step 3) with weighting matrix $W(\hat{\zeta}_N^n) = P^{-1}(\hat{\zeta}_N^n)$ (Galrinho, 2016).

where $\hat{\lambda}_N^{(0)}$ are the estimated Lagrange multipliers. The covariance of the residuals is updated according to (initially for $k = 0$):

$$\bar{\Lambda}(\hat{\vartheta}_N^{(k)}) = \frac{1}{N}\sum_{t=n+1}^{N} \bar{\varepsilon}(t, \hat{\vartheta}_N^{(k)})\bar{\varepsilon}^\top(t, \hat{\vartheta}_N^{(k)}), \tag{8.39}$$

with residual

$$\bar{\varepsilon}(t, \hat{\vartheta}_N^{(k)}) = \bar{C}^{-1}(q^{-1}, \hat{\vartheta}_N^{(k)}) \left[A(q^{-1}, \hat{\vartheta}_N^{(k)})w(t) - B(q^{-1}, \hat{\vartheta}_N^{(k)})r(t)\right]. \tag{8.40}$$

Step 3: Improving the structured network model

This step aims to correct for the residuals in (8.36) that are not accounted for in (8.38), due to the fact that only a high-order approximation of the nonparametric ARX model is used.

Substituting $\breve{A}(q^{-1}, \hat{\zeta}_N^n)$ and $\breve{B}(q^{-1}, \hat{\zeta}_N^n)$ for $\breve{A}^0(q^{-1})$ and $\breve{B}^0(q^{-1})$, respectively, into (8.35) gives

$$\begin{aligned} A^0(q^{-1}) - \bar{C}^0(q^{-1})\breve{A}^0(q^{-1}) = \\ \bar{C}^0(q^{-1})[\breve{A}(q^{-1}, \hat{\zeta}_N^n) - \breve{A}^0(q^{-1})], \end{aligned} \tag{8.41a}$$

$$\begin{aligned} B^0(q^{-1}) - \bar{C}^0(q^{-1})\breve{B}^0(q^{-1}) = \\ \bar{C}^0(q^{-1})[\breve{B}(q^{-1}, \hat{\zeta}_N^n) - \breve{B}^0(q^{-1})], \end{aligned} \tag{8.41b}$$

which are equivalently written as (by using (8.36))

$$-Q(\hat{\zeta}_N^n)\vartheta^0 = T(\vartheta^0)(\hat{\zeta}_N^n - \zeta^{no}), \tag{8.42}$$

where the matrix $T(\vartheta^0)$ is given in Appendix 8.H. The estimate of ϑ^0 with minimum variance is obtained by solving a weighted least-squares problem, where the weighting matrix is given by the inverse covariance matrix of the right-hand side expression in (8.42). As this term depends on ϑ this problem is solved iteratively by

$$\hat{\vartheta}_N^{(k)} = \min_{\vartheta} \quad \vartheta^\top Q^\top(\hat{\zeta}_N^n)W(\hat{\vartheta}_N^{(k-1)})Q(\hat{\zeta}_N^n)\vartheta \tag{8.43a}$$

$$\text{subject to} \quad \Gamma\vartheta = \gamma, \tag{8.43b}$$

where the weighting matrix $W(\hat{\vartheta}_N^{(k-1)})$ is iteratively updated for $k = 1, 2, \cdots$ according to

$$W(\hat{\vartheta}_N^{(k-1)}) = T^{-\top}(\hat{\vartheta}_N^{(k-1)})P^{-1}(\hat{\vartheta}_N^{(k-1)})T^{-1}(\hat{\vartheta}_N^{(k-1)}), \tag{8.44}$$

where $P(\hat{\vartheta}_N^{(k-1)})$ is updated according to

$$P^{-1}(\hat{\vartheta}_N^{(k-1)}) = \frac{1}{N}\sum_{t=n+1}^{N} \varphi^n(t)\bar{\Lambda}^{-1}(\hat{\vartheta}_N^{(k-1)})[\varphi^n(t)]^\top. \tag{8.45}$$

Similar to Step 2, this optimisation problem can be solved through

$$\begin{bmatrix} \hat{\vartheta}_N^{(k)} \\ \hat{\lambda}_N^{(k)} \end{bmatrix} = \begin{bmatrix} Q^\top(\hat{\zeta}_N^n)W(\hat{\vartheta}_N^{(k-1)})Q(\hat{\zeta}_N^n) & \Gamma^\top \\ \Gamma & 0 \end{bmatrix}^{-1} \begin{bmatrix} 0 \\ \gamma \end{bmatrix}, \tag{8.46}$$

where $\hat{\lambda}_N^{(k)}$ are the estimated Lagrange multipliers. Finally, the covariance of the residuals is updated according to (8.39).

Remark 8.19. *Although this step is asymptotically efficient, iterating may improve the estimate for finite data length N. The cost*

$$V_N(\hat{\vartheta}_N^{(k)}) = \frac{1}{N}\det\sum_{t=1}^{N} \bar{\varepsilon}(t,\hat{\vartheta}_N^{(k)})\bar{\varepsilon}^\top(t,\hat{\vartheta}_N^{(k)}) \tag{8.47}$$

is evaluated at each iteration to decide whether the parameter estimation has improved. However, as (8.47) *is not affine in the parameters, an improved cost may still result in deteriorated parameter estimates. The cost* (8.47) *is used as it is independent of* $\Lambda(\theta)$ *and under Gaussian assumptions, minimising* (8.47) *results in the minimum variance of the estimates if* $\Lambda(\theta)$ *is independently parameterised from* $A(q^{-1},\theta)$*,* $B(q^{-1},\theta)$*, and* $C(q^{-1},\theta)$*. In this situation, the asymptotic (minimum) variance resulting from* (8.22b) *is equal to the asymptotic variance of the maximum likelihood estimator (Ljung, 1999).*

Step 4: Obtaining the noise model

Having estimated $A^0(q^{-1})$, $B^0(q^{-1})$, and $\bar{C}^0(q^{-1})$, the noise model represented by $C^0(q^{-1})$ and Λ^0 can be recovered. On the basis of (8.30c), the estimate of $C^0(q^{-1})$ is constructed as

$$C(q^{-1},\hat{\theta}_N^{(k)}) = \bar{C}(q^{-1},\hat{\vartheta}_N^k)A_0^{-1}(\hat{\vartheta}_N^k). \tag{8.48}$$

Further, as $\Lambda^0 = A_0^0\bar{\Lambda}^0A_0^0$, the estimate of Λ^0 is given by

$$\Lambda(\hat{\theta}_N^{(k)}) = A_0(\hat{\vartheta}_N^{(k)})\bar{\Lambda}(\hat{\vartheta}_N^{(k)})A_0(\hat{\vartheta}_N^{(k)}). \tag{8.49}$$

Step 5: Estimating the discrete-time components

With the estimate of $A^0(q^{-1})$ from Step 3, the dynamics of the discrete-time network has been estimated. The components, represented by $\bar{X}(q^{-1})$ and $\bar{Y}(q^{-1})$, are obtained through the inverse mapping of $A(q^{-1}) = \bar{X}(q^{-1}) + \bar{Y}(q^{-1})$, with $\bar{X}(q^{-1})$ diagonal and $\bar{Y}(q^{-1})$ Laplacian, given by

$$\bar{x}_{jk,\ell} = \begin{cases} 0 & \text{if } j \neq k \\ a_{jj,\ell} + \sum_{i \neq j} a_{ij,\ell}, & \text{if } j = k \end{cases} \tag{8.50a}$$

$$\bar{y}_{jk,\ell} = \begin{cases} a_{jk,\ell}, & \text{if } j \neq k \\ -\sum_{i \neq j} a_{ij,\ell}, & \text{if } j = k. \end{cases} \tag{8.50b}$$

Step 6: Estimating the continuous-time components

The continuous-time representation $X(p), Y(p), \bar{B}(p)$ can be obtained from the estimated discrete-time model from Steps 5 and 3 through the inverse mapping of (8.5), given by

$$x_{jk,\ell} = (-T_s)^\ell \sum_{i=\ell}^{n_a} \binom{i}{\ell} \bar{x}_{jk,i}, \tag{8.51a}$$

$$y_{jk,\ell} = (-T_s)^\ell \sum_{i=\ell}^{n_a} \binom{i}{\ell} \bar{y}_{jk,i}, \tag{8.51b}$$

$$\bar{b}_{jj,\ell} = (-T_s)^\ell \sum_{i=\ell}^{n_b} \binom{i}{\ell} b_{jj,i}. \tag{8.51c}$$

The complete algorithm

The above steps describe the procedure for identifying the physical components of a diffusively coupled linear network with an ARMAX-like model structure. This procedure leads to the following algorithm:

Algorithm 8.20 (ARMAX-like model structure). *Consider a data generating system $\mathcal{S}$ with $F^0(q) := C^0(q^{-1})$ a monic polynomial and a network model set $\mathcal{M}$ (8.13) with $F(q,\theta) := C(q^{-1},\theta)$ a monic polynomial. Then $M(\hat{\theta}_N)$, a consistent estimate of M^0, is obtained through the following steps:*

1. *Estimate the nonparametric ARX model (8.29) by least squares (8.32) to obtain $\hat{\zeta}_N^n$.*
2. *Reduce the nonparametric ARX model to a parametric model (8.9) by weighted least-squares (8.38) to obtain $\hat{\vartheta}_N^{(0)}$.*

3. *Improve the parametric model* (8.9) *by weighted least-squares* (8.38) *to obtain* $\hat{\vartheta}_N^{(k)}$ *for* $k = 1, 2, \ldots$.
4. *Obtain the noise model by calculating* (8.48) *and* (8.49) *to obtain* $C(q^{-1}, \hat{\theta}_N^{(k)})$ *and* $\Lambda(\hat{\theta}_N^{(k)})$.
5. *Obtain the discrete-time component values through* (8.50) *to estimate* $\bar{X}(q^{-1})$ *and* $\bar{Y}(q^{-1})$.
6. *Obtain the continuous-time parametric model through* (8.51) *to estimate* $X(p)$, $Y(p)$, *and* $\bar{B}(p)$.

Consistency and minimum variance of the estimates obtained with Algorithm 8.20 follow from the similarity with WNSF and its proof, under technical conditions on the rates with which n and N tend to infinity (Galrinho et al., 2019). The main difference is that $A(q^{-1}, \theta)$ is nonmonic and symmetrically parameterised, resulting in a different structure in (8.36). In particular, the structure in $Q(\zeta^n)$ and $T(\vartheta^0)$ is different and the optimisation problem (8.37) is constrained. For consistency, $Q(\hat{\zeta}_N^n)$ needs to have full column rank, which can be shown to be satisfied if the identifiability conditions in Proposition 8.15 are satisfied. Consistency in Step 4, 5, and 6 follows naturally.

Remark 8.21 (Orders). *In order to perform Algorithm 8.20, the measured data* $\{z(t)\}$ *are needed; the order* n *of the ARX model needs to be chosen; and the true orders* n_a, n_b, *and* n_c *of* $A(q^{-1})$, $B(q^{-1})$, *and* $C(q^{-1})$, *respectively, need to be known.*

Remark 8.22 (Simplification to an ARX-like model structure). *If the noise is not filtered, that is,* $F(q) := C(q^{-1}) = I$, *the network has an ARX-like model structure and the ARX model* (8.29) *can exactly describe the diffusively coupled network, where* $\breve{A}(q^{-1})$ *and* $\breve{B}(q^{-1})$ *are of the same order as* $A(q^{-1})$ *and* $B(q^{-1})$, *respectively. Algorithm 8.20 improves in the sense that Step 1 is consistent for sufficiently large data length N and therefore, no additional estimation error is made in Step 2, which makes Step 3 superfluous.*

Remark 8.23 (Simplification to an ARX model structure). *If* $A_0 = I$ *in addition to unfiltered noise (*$F(q) := C(q^{-1}) = I$*), the network has an ARX model structure. In this case, the network can consistently be identified in a single step by incorporating the symmetric structure into Step 1 of*

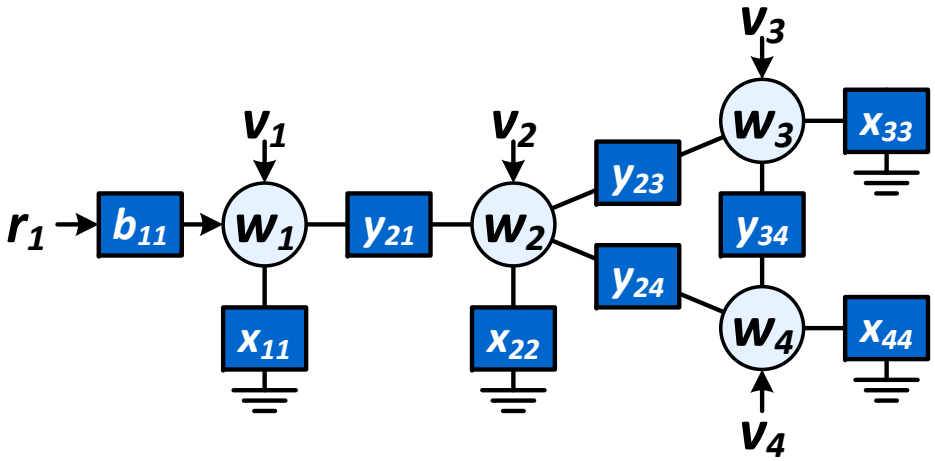

Figure 8.3: The continuous-time network model with interconnection dynamics described by the polynomials $y_{jk}(p)$, dynamics to the ground described by the polynomial $x_{jj}(p)$, and static excitation filter b_{11}.

> *Algorithm 8.20 and by choosing the order of $\breve{A}(q^{-1})$ and $\breve{B}(q^{-1})$ equivalent to the order of $A(q^{-1})$ and $B(q^{-1})$, respectively. The resulting identification procedure has been described in Chapter 7.*

8.6 Simulation example

This section contains a simulation example that serves to illustrate the theory and to show that indeed, the topology and the physical components of a network can be identified using a single excitation signal only. The identification is performed with the algorithm presented above.

8.6.1 Experimental set-up

Consider the continuous-time diffusively coupled network (8.2) consisting of four one-dimensional nodes, with an external signal $u(t) = B_0 r(t) + v(t)$, described by

$$(X_0 + Y_0)w(t) + (X_1 + Y_1)\frac{d}{dt}w(t) + X_2\frac{d^2}{dt^2}w(t) = B_0 r(t) + v(t), \qquad (8.52)$$

where $r(t)$ is one-dimensional and known, and B_0 has dimension 4×1 and has only the first element nonzero. Figure 8.3 shows the structure of this network, where it can be seen that the excitation signal $r(t) = r_1(t)$ enters the network only at node $w_1(t)$. One can think of this network as a mechanical mass-spring-damper network as explained in Section 8.2, where X_0 and Y_0 contain the spring constants, X_1 and Y_1 contain the damper coefficients, X_2 contains the masses, the node signals $w(t)$ represent the positions of the masses, and the excitation signal $r(t)$ is a force. One can also think of this network as an electrical circuit with nodes that are interconnected through capacitors, resistors, and inductors (in parallel). The matrices X_0 and Y_0 contain the capacitances, X_1 and Y_1 contain the conductance values of the resistors, X_2 contain the inverses of the inductances, the node signals $w(t)$ represent the electric potentials of the interconnection points, and the excitation signal $r(t)$ is the derivative of a current flow.

The discrete-time representation is obtained by applying the discretisation method described in Section 8.2.2 with the sampling frequency $f_s = 100$ Hz. In addition, the disturbance $v(t)$ acting on the network is modelled in discrete time as white noise filtered by a first-order filter. This results in the discrete-time network model (8.9)

$$[A_0 + A_1 q^{-1} + A_2 q^{-2}]w(t) = B_0 r(t) + [I + C_1 q^{-1}]e(t), \tag{8.53}$$

with $A_i = \bar{X}_i + \bar{Y}_i$ and $A_i, \bar{Y}_i$ symmetric and $\bar{X}_i$ diagonal for $i = 0, 1, 2$. The network topology is assumed to be unknown, as reflected by the fact that in the model there are parameterised second-order connections between all pairs of nodes. As $A_2 = \bar{X}_2$ is diagonal, identifiability Condition 2. in Proposition 8.15 is satisfied. The location where $r(t)$ enters and the first nonzero parameter of B_0 are assumed to be known, which imply that B_0 is fixed and not parameterised. This guarantees that identifiability Condition 4. in Proposition 8.15 is satisfied.

The symmetric structure of $Y(p)$ is taken into account in the parameterisation of the continuous-time model. The continuous-time model matrices (8.52) are parameterised as

$$X_0 = \begin{bmatrix} \theta_1^c & 0 & 0 & 0 \\ 0 & \theta_4^c & 0 & 0 \\ 0 & 0 & \theta_7^c & 0 \\ 0 & 0 & 0 & \theta_{10}^c \end{bmatrix}, \qquad X_1 = \begin{bmatrix} \theta_2^c & 0 & 0 & 0 \\ 0 & \theta_5^c & 0 & 0 \\ 0 & 0 & \theta_8^c & 0 \\ 0 & 0 & 0 & \theta_{11}^c \end{bmatrix}, \tag{8.54}$$

$$X_2 = \begin{bmatrix} \theta_3^c & 0 & 0 & 0 \\ 0 & \theta_6^c & 0 & 0 \\ 0 & 0 & \theta_9^c & 0 \\ 0 & 0 & 0 & \theta_{12}^c \end{bmatrix}, \tag{8.55}$$

$$Y_0 = \begin{bmatrix} \star & \theta^c_{13} & \theta^c_{15} & \theta^c_{17} \\ \theta^c_{13} & \star & \theta^c_{19} & \theta^c_{21} \\ \theta^c_{15} & \theta^c_{19} & \star & \theta^c_{23} \\ \theta^c_{17} & \theta^c_{21} & \theta^c_{23} & \star \end{bmatrix}, \qquad Y_1 = \begin{bmatrix} \star & \theta^c_{14} & \theta^c_{16} & \theta^c_{18} \\ \theta^c_{14} & \star & \theta^c_{20} & \theta^c_{22} \\ \theta^c_{16} & \theta^c_{20} & \star & \theta^c_{24} \\ \theta^c_{18} & \theta^c_{22} & \theta^c_{24} & \star \end{bmatrix}, \tag{8.56}$$

where the elements $\star$ follow from the Laplacian structure. Observe that $\theta^c_i \geq 0$ for $i = 1, \ldots, 12$ and $\theta^c_i \leq 0$ for $i = 13, \ldots, 24$ as all components have positive values; see Section 8.2.1. The exact true parameter values, represented by θ^{c0} are given in Table 8.1.

The external excitation signal $r_1(t)$ is an independent white noise process with mean 0 and variance $\sigma_r^2 = 1$. All nodes are subject to disturbances $e_i(t)$, which are independent white noise processes (uncorrelated with $r_1(t)$) with mean 0 and variance $\sigma_e^2 = 10^{-4}$. In Step 2 of the algorithm, the possibility to apply the weighting $W(\hat{\zeta}^n_N) = P^{-1}(\hat{\zeta}^n_N)$ is exploited. In Step 3 of the algorithm, at most 50 iterations are allowed to improve the result of Step 2.

Experiment 1 serves to show that the parameters can consistently be identified with a single excitation signal only. In order to do so, the identification is performed for different orders n of the ARX model in Step 1 and different data lengths N, such that they increase at an appropriate rate, guaranteeing that n^4/N decreases for increasing n and N (Galrinho et al., 2019). The chosen values n, N and the rate n^4/N are given in Table 8.2. For each experimental set, 20 Monte-Carlo simulations are performed, where in each run new excitation and noise signals are generated.

Experiment 2 serves to identify the parameters and topology with a single excitation signal only and to show that using more excitation signals at different nodes improves the results. In order to show this, two sets of experiments are performed, one set with a single excitation signal ($K = 1$) entering at node $w_1(t)$ and one set with three excitation signals ($K = 3$) entering the network at node $w_1(t)$, $w_2(t)$, and $w_3(t)$. In the former case, B_0 is a 4×1 unit vector that is fully known and in the latter case, B_0 is a 4×3 selection matrix with $b_{11,0} = 1$; with parameterised elements $b_{22,0} = \theta^c_{24}$ and $b_{33,0} = \theta^c_{25}$ with true values $\theta^{c0}_{24} = 1$ and $\theta^{c0}_{25} = 1$; and with all other elements equal to 0. The order of the ARX model in Step 1 of the algorithm is $n = 5$ and the number of samples generated for each data set is $N = 10,000$. Both experimental sets consist of 100 Monte-Carlo simulations, where in each run new excitation and noise signals are generated.

8.6.2 Simulation results

The simulation results of Experiment 1 are shown in Figure 8.4. This figure shows a Boxplot of the relative mean squared error (RMSE) of the continuous-time model

Table 8.1: The true parameter values of $X(p)$ and $Y(p)$ and the mean and standard deviation (SD) of their estimates for both sets ($K = 1$ and $K = 3$) of Experiment 2.

Parameter	θ^c_1	θ^c_2	θ^c_3	θ^c_4	θ^c_5	θ^c_6	θ^c_7	θ^c_8
True value	1	0	1×10^{-2}	1	0	2×10^{-2}	1	0
$K = 1$ Mean	1.0136	-5.6440×10^{-4}	9.9999×10^{-3}	1.0171	-7.3562×10^{-4}	2.0054×10^{-2}	1.0221	-1.6503×10^{-3}
$K = 1$ SD	3.6467×10^{-2}	2.0287×10^{-3}	2.3009×10^{-6}	9.5878×10^{-2}	6.1179×10^{-3}	1.3032×10^{-4}	1.4998×10^{-1}	8.2037×10^{-3}
$K = 3$ Mean	1.0012	-7.7029×10^{-5}	1.0000×10^{-2}	1.0032	-2.0946×10^{-4}	2.0001×10^{-2}	-1.0085	-5.6775×10^{-4}
$K = 3$ SD	4.7774×10^{-3}	2.8210×10^{-4}	1.2971×10^{-6}	8.2831×10^{-3}	4.9076×10^{-4}	1.3605×10^{-5}	1.5390×10^{-2}	1.1072×10^{-3}

Parameter	θ^c_9	θ^c_{10}	θ^c_{11}	θ^c_{12}	θ^c_{13}	θ^c_{14}	θ^c_{15}	θ^c_{16}
True value	5×10^{-2}	10	0	7×10^{-2}	-4	-3×10^{-1}	0	0
$K = 1$ Mean	4.9848×10^{-2}	9.9676	1.4936×10^{-3}	6.9868×10^{-2}	–4.0061	-3.0078×10^{-1}	6.2954×10^{-3}	2.1455×10^{-4}
$K = 1$ SD	8.5376×10^{-4}	1.5783×10^{-1}	8.0059×10^{-3}	6.6951×10^{-4}	5.4752×10^{-2}	1.8156×10^{-3}	6.6368×10^{-2}	6.6894×10^{-4}
$K = 3$ Mean	4.9992×10^{-2}	1.003×10^{1}	-1.8345×10^{-4}	7.008×10^{-2}	-3.9998	-3.0003×10^{-1}	4.2531×10^{-4}	-2.4708×10^{-5}
$K = 3$ SD	4.8096×10^{-5}	3.0088×10^{-2}	1.8316×10^{-3}	7.9796×10^{-5}	2.8000×10^{-3}	1.9475×10^{-4}	3.0851×10^{-3}	1.1680×10^{-4}

Parameter	θ^c_{17}	θ^c_{18}	θ^c_{19}	θ^c_{20}	θ^c_{21}	θ^c_{22}	θ^c_{23}	θ^c_{24}
True value	0	0	0	-4×10^{-1}	-8	0	-9	-6×10^{-1}
$K = 1$ Mean	8.9935×10^{-3}	-1.0261×10^{-4}	1.3912×10^{-2}	-4.0102×10^{-1}	-8.0188	-3.3463×10^{-4}	-8.9442	-5.9889×10^{-1}
$K = 1$ SD	3.8590×10^{-2}	6.2002×10^{-4}	1.6645×10^{-1}	9.1170×10^{-3}	1.1026×10^{-1}	3.9220×10^{-3}	1.5367×10^{-1}	1.2576×10^{-2}
$K = 3$ Mean	5.2077×10^{-4}	-2.0221×10^{-5}	2.1762×10^{-3}	-4.0005×10^{-1}	-8.0012	-5.8232×10^{-5}	-8.9958	-6.0024×10^{-1}
$K = 3$ SD	3.4376×10^{-3}	1.6190×10^{-4}	6.1368×10^{-3}	3.9797×10^{-4}	7.6248×10^{-3}	2.8442×10^{-4}	1.3217×10^{-2}	9.3302×10^{-4}

Table 8.2: The order n of the ARX fit, the data length N, and the rate n^4/N for each set of Experiment 1.

Set	1	2	3	4	5	6	7	8	9	10
n	3	4	5	6	7	8	9	10	11	12
N	96	320	834	1852	3694	6827	11930	20000	32536	51841
n^4/N	0.85	0.80	0.75	0.70	0.65	0.60	0.55	0.50	0.45	0.40

parameters, where the RMSE is determined as

$$\text{RMSE} = \frac{\|\theta^{c0} - \hat{\theta}^c_N\|_2^2}{\|\theta^{c0}\|_2^2}, \tag{8.57}$$

where θ^c contains the parameters of $X(p)$ and $Y(p)$. From Figure 8.4 it can be seen that the RMSE decreases if both n and N increase, such that the rate n^4/N decreases. This observation supports the statement that consistent identification is achieved if the order of the ARX model n tends to infinity as a function of the data length N at an appropriate rate (Galrinho et al., 2019).

The simulation results of Experiment 2 are shown in Figures 8.5-8.8 and Table 8.1.

Figure 8.5 and 8.6 show a Boxplot of the relative parameter estimation errors for $K = 1$ and $K = 3$, respectively, for parameters for which their underlying true value is unequal to 0. For the other parameters, the mean values are provided in Figures 8.7 and 8.8. From Figures 8.5 and 8.6, it can be seen that the median of the relative errors is around 0 for all parameters, which means that the medians of the estimated parameter values are close to the true values. This supports the statement that the parameters can be identified with a single excitation signal only. However, Figure 8.5 also shows that for the experiment with a single excitation signal ($K = 1$), 50% of the relative parameter errors are within a range of 10% deviation. This is quite a large deviation. From Figure 8.6, it can be seen that this range reduces to 2% deviation if the number of excitation signals is increased to three ($K = 3$). Increasing the number of excitation signals improves the signal-to-noise ratio, which has a clear effect on the variance of the estimated parameters.

Table 8.1 contains the mean and standard deviation of the estimated model parameters. The experiment with three external excitation signals has two additional parameters θ^c_{25} and θ^c_{26}, which have true values 1 and which are estimated with mean 1.000 and 9.9983×10^{-1}, respectively, and standard deviation 6.6505×10^{-4} and 9.2690×10^{-4}, respectively. Although the estimates are quite accurate, small biases can still occur because of the finite values of n and N. For all parameters, this bias is within a bound of 1 standard deviation.

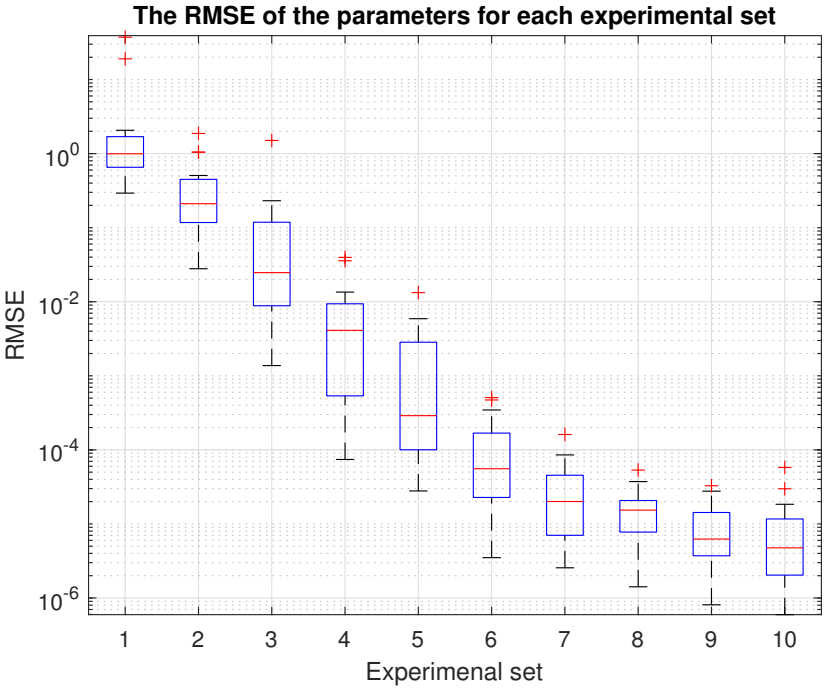

Figure 8.4: Boxplot of the relative mean squared error (RMSE) (8.57) of the parameters of $X(p)$ and $Y(p)$ for each experimental set.

Figure 8.7 and 8.8 show the true values and the mean estimated values of the parameters, focusing on those parameters whose true values are equal to 0. For $K = 1$ it would be hard to identify the correct topology of the network, i.e. estimate which parameters are unequal to 0, on the basis of the estimated mean values only. Note that for example, the zero parameter θ^c_{19} has a mean value that is higher than the nonzero parameter θ^c_3. For $K = 3$ this situation improves drastically.

8.7 Discussion

In this section, three extensions of the presented theory are discussed. First, the connection with dynamic networks is made. Second, networks with unmeasured nodes are considered. Third, parameter constraints are discussed.

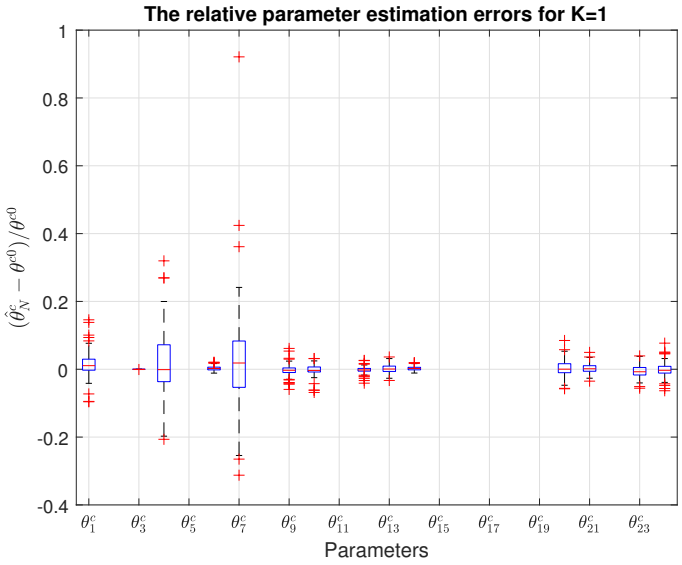

Figure 8.5: Boxplot of the relative estimation errors of the parameters of $X(p)$ and $Y(p)$ for the experimental set with a single excitation signal ($K = 1$), for parameters with a nonzero true value.

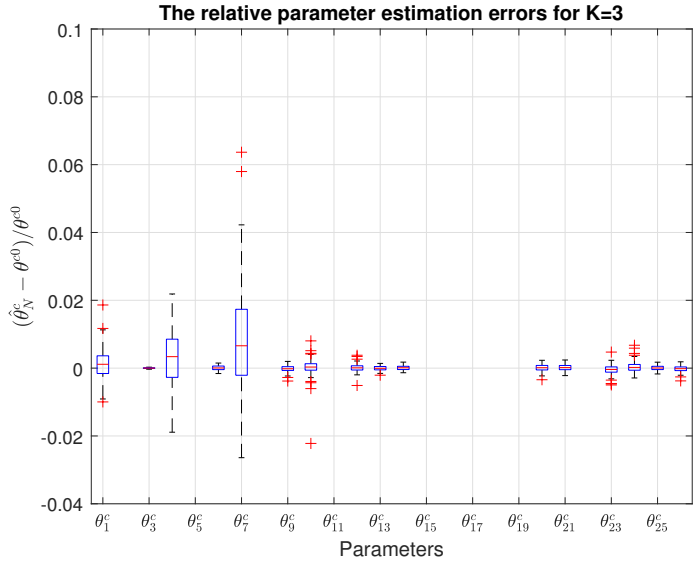

Figure 8.6: Boxplot of the relative estimation errors of the parameters of $X(p)$, $Y(p)$ and $B(p)$ for the experimental set with three excitation signals ($K = 3$), for parameters with a nonzero true value.

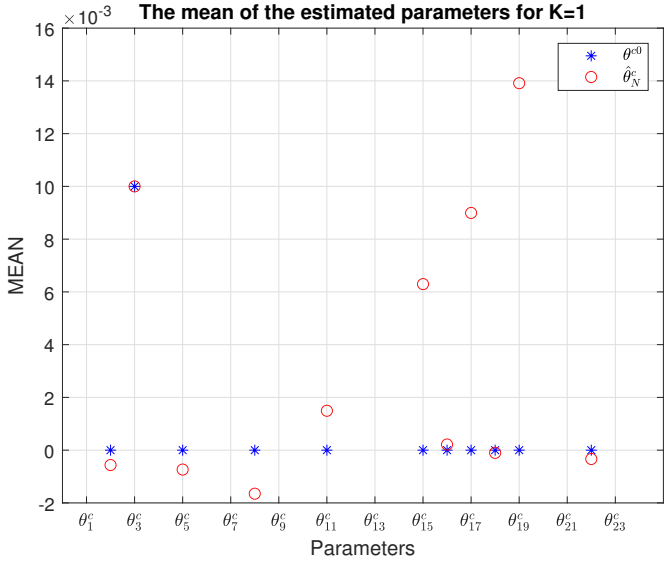

Figure 8.7: The true parameter values (blue) and the mean of the estimated parameter values (red) of $X(p)$ and $Y(p)$ for the experimental set with a single excitation signal ($K = 1$), focusing on parameters with a true value of 0.

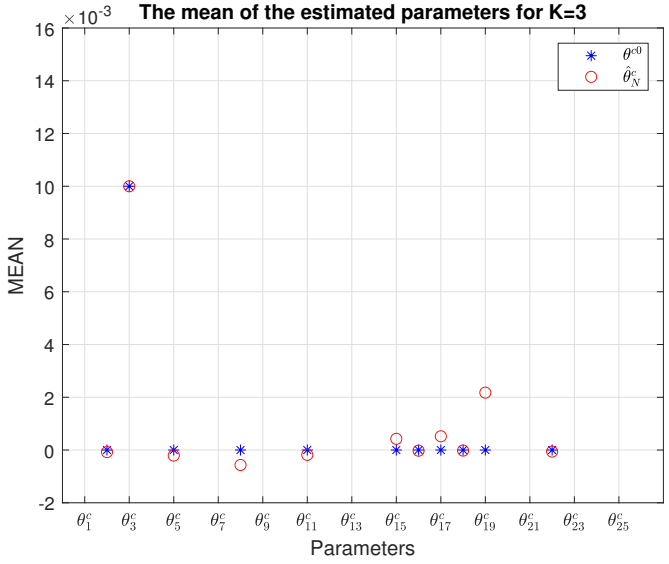

Figure 8.8: The true parameter values (blue) and the mean of the estimated parameter values (red) of $X(p)$, $Y(p)$ and $B(p)$ for the experimental set with three excitation signals ($K = 3$), focusing on parameters with a true value of 0.

8.7.1 Dynamic networks

A commonly used description of dynamic networks is the module representation (Van den Hof et al., 2013), in which a network is considered to be the interconnection of directed transfer functions (modules) through measured node signals as

$$w(t) = G(q)w(t) + R(q)r(t) + H(q)\tilde{e}(t), \tag{8.58}$$

with white noise process $\tilde{e}(t)$ and with proper rational transfer function matrices $G(q)$, $R(q)$, and $H(q) \in \mathcal{H}$, where the matrix entries $G_{jk}(q)$, $R_{jk}(q)$, and $H_{jk}(q)$ describe the dynamics in the paths from $w_k(t)$, $r_k(t)$, and $\tilde{e}_k(t)$ to $w_j(t)$, respectively. A diffusively coupled network (8.9) can be described as a module representation with the following particular symmetrical properties: (see Chapter 7)

1. The transfer functions $G_{jk}(q)$ and $G_{kj}(q)$ have the same numerator for all j, k.
2. The transfer functions $G_{jk}(q)$ and $R_{jm}(q)$ have the same denominator for all k, m.
3. The transfer functions $G_{jk}(q)$ and $H_{jm}(q)$ have the same denominator for all k, m if $F(q)$ is polynomial.

Moreover, conditions for a unique mapping between a module representation and a diffusively coupled network are formulated in Chapter 7.

The structure of $G(q)$ and $R(q)$ corresponding to a diffusively coupled network with three nodes is illustrated by Figure 8.9. It shows that the modules $G_{jk}(q) = -a_{jj}^{-1}(q^{-1})a_{jk}(q^{-1})$ and $G_{kj}(q) = -a_{kk}^{-1}(q^{-1})a_{jk}(q^{-1})$ have the same numerator $(a_{jk}(q^{-1}))$ and all transfer functions in the paths towards a specific node $w_j(t)$ have the same denominator $(a_{jj}(q^{-1}))$. Since $G_{jk}(q)$ and $G_{kj}(q)$ have the same numerator, they will either be both present or both absent, which is in accordance with the fact that they represent a single diffusively coupled interconnection. In addition, the connections to the ground node are only present in the denominators, because they are only present in $a_{jj}(q^{-1})$. This means that they do not have an effect on the topology in the module representation, although they are part of the topology in the diffusively coupled network.

8.7.2 Partial measurements

Throughout this chapter, we assumed that all node signals are measured, which is a situation to which the identification method that we presented is particularly

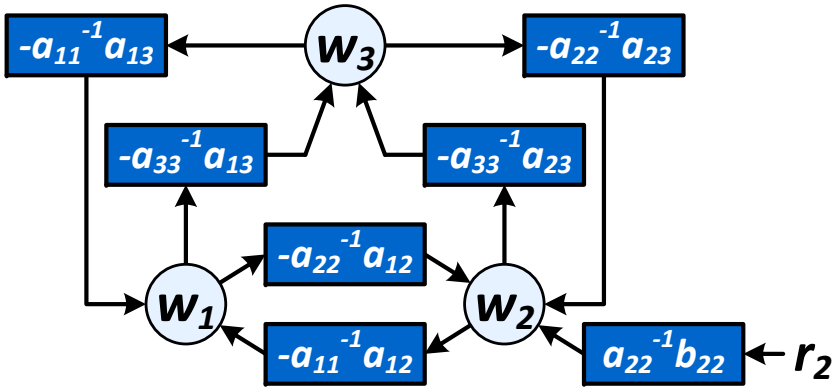

Figure 8.9: A module representation of a diffusively coupled network with three nodes.

tuned. From the literature, it is known (Friswell et al., 1999; Lopes dos Santos et al., 2015) that network identifiability can be achieved if all nodes are measured and one node is excited, or if all nodes are excited and one node is measured. The former situation is covered in this chapter, see Proposition 8.15, as the latter situation seems less common and leads to higher experimental costs. In this latter situation, a different identification method would be required, further exploiting the role of the different excitation signals, leading to a so-called indirect method of identification.

For the situation where only a subset of nodes is measured and/or excited, general identifiability conditions are not yet known, but some particular situations are considered by Bazanella et al. (2019) for the case of directed networks.

For estimating only a particular component or a particular connection in the network, the identifiability conditions will be less severe. In the partial measurement situation, unmeasured node signals can be removed from the representation by Gaussian elimination, which is equivalent to Kron reduction (Dörfler and Bullo, 2013) and immersion (Dankers et al., 2016), which has been effectively applied in the local module identification problem of directed networks; see e.g. Dankers et al. (2016). Related results for the situation of undirected networks will be reported in a follow-up chapter.

8.7.3 Parameter constraints

Physical networks that consist of interconnected physical components, such as mass-spring-damper systems and RLC circuits, are known to have positive real-

valued component values in the continuous-time representation (8.2). This also leads to coefficients with known signs in the corresponding discrete-time representation. In both the consistency proof and the presented algorithm, these sign constraints are not taken into account. They can be taken into account in the algorithm by adding inequality constraints of the form $\Gamma_u \vartheta < 0$ to the optimisation problems (8.37) and (8.43). A priori known parameter values can easily be taken into account by the equality constraint $\Gamma\vartheta = \gamma$ in the optimisation problems (8.37) and (8.43). Known (continuous-time) component values can be taken into account as well, by splitting ϑ as $\vartheta = \vartheta_u + \vartheta_k$, where ϑ_u and ϑ_k represent the unknown and known part of ϑ, respectively. Then the linear form $-Q(\zeta^n)\vartheta = 0$ leads to $-Q(\zeta^n)\vartheta_u + \gamma_k(\zeta^n, \vartheta_k) = 0$, where $\gamma_k(\zeta^n, \vartheta_k) := -Q(\zeta^n)\vartheta_k$ is known.

8.8 Conclusion

Undirected networks of diffusively coupled systems can be represented by polynomial representations with particular structural properties. This has enabled the development of an effective prediction error identification method for identifying the physical components and the topology of the network. Conditions for consistent parameter estimates have been formulated for the situation where all network nodes are measured, showing that only a single excitation signal is needed for consistency. The identification is performed through a multistep algorithm that relies on convex optimisations and is a reworked version of the recently introduced weighted null-space fitting method, adapted to the situation of the structured network models. The results of identifying the topology and parameters of a network are illustrated in a Monte Carlo simulation example. It shows that, while consistency is guaranteed for a single excitation signal, the variance of parameter estimates improves considerably when increasing the number of excitations.

Appendix

8.A Proof of Lemma 8.3

$A_0 = \bar{X}_0 + \bar{Y}_0$, with diagonal $\bar{X}_0 = \sum_{i=1}^{n_a} T_s^{-i} X_i$ and Laplacian $\bar{Y}_0 = \sum_{i=1}^{n_a} T_s^{-i} Y_i$, following from (8.5a) with $n_x = n_a$ and (8.5b) with $n_y = n_a$, respectively. Since $\bar{Y}_0$ is Laplacian, the sum of each row is equal to 0, that is, $\bar{Y}_0 \mathbf{1} = 0$, with $\mathbf{1} = \begin{bmatrix} 1 & 1 & \dots & 1 \end{bmatrix}^\top \in \mathbb{R}^L$ (Mesbahi and Egerstedt, 2010). Because the network is connected, $\bar{Y}_0$ has one-dimensional kernel $\ker(\bar{Y}_0) = \operatorname{span}(\mathbf{1})$ (Dörfler and Bullo, 2013). Since the network has at least one connection to the ground node, $\exists j, \ell$ such that $x_{jj,\ell} > 0$, implying that $\bar{x}_{jj,0} > 0$ and thus $\bar{X}_0 \succeq 0$. The vectors that span the kernel of $\bar{X}_0$ will have at least one zero element, implying that $\ker(\bar{Y}_0) \not\subset \ker(\bar{X}_0)$. Because both $\bar{Y}_0 \succeq 0$ and $\bar{X}_0 \succeq 0$, $\ker(A_0) = \ker(\bar{Y}_0 + \bar{X}_0) = \ker(\bar{Y}_0) \cap \ker(\bar{X}_0) = \emptyset$ and hence, $\operatorname{rank}(A_0) = L$.

8.B Proof of Proposition 8.5

The network (8.9) can be described by

$$A(q^{-1})w(t) = B(q^{-1})r(t) + F(q)e(t) = B(q^{-1})r(t) + F(q)A_0A_0^{-1}e(t). \quad (8.59)$$

Premultiplying with $A_0^{-1}F^{-1}(q)$ gives

$$A_0^{-1}F^{-1}(q)A(q^{-1})w(t) = A_0^{-1}F^{-1}(q)B(q^{-1})r(t) + A_0^{-1}e(t). \quad (8.60)$$

Adding $w(t)$ to both sides of the equality and rewriting gives

$$w(t) = \left[I - A_0^{-1}F^{-1}(q)A(q^{-1})\right] w(t) + A_0^{-1}F^{-1}(q)B(q^{-1})r(t) + A_0^{-1}e(t) \quad (8.61)$$

where the factor A_0^{-1} makes the filter $\left[I - A_0^{-1}F^{-1}(q)A(q^{-1})\right]$ strictly proper and where $A_0^{-1}F^{-1}(q)B(q^{-1})$ is proper. The one-step-ahead network predictor (8.11) follows directly by applying its definition (8.10) to (8.61).

8.C Proof of Proposition 8.10

The expression for the parameterised prediction error (8.20a) directly follows from its definition (8.19) and the network predictor (8.16). Expressing the parameterised prediction error (8.20a) in terms of $r(t)$ and $e(t)$ yields

$$\bar{\varepsilon}(t,\theta) = W_{\bar{\varepsilon}r}(q,\theta)r(t) + W_{\bar{\varepsilon}e}(q,\theta)e(t) + (A_0^0)^{-1}e(t), \tag{8.62}$$

with

$$W_{\bar{\varepsilon}r}(q,\theta) = A_0^{-1}(\theta)F^{-1}(q,\theta)\left[A(q^{-1},\theta)\big(A^0(q^{-1})\big)^{-1}B^0(q^{-1}) - B(q^{-1},\theta)\right], \tag{8.63a}$$

$$W_{\bar{\varepsilon}e}(q,\theta) = A_0^{-1}(\theta)F^{-1}(q,\theta)A(q^{-1},\theta)\big(A^0(q^{-1})\big)^{-1}F^0(q) - (A_0^0)^{-1}. \tag{8.63b}$$

The latter two terms in (8.62) are uncorrelated since $e(t)$ is white noise and $W_{\bar{\varepsilon}e}(q,\theta)$ is strictly proper. If the true system is in the model set, the prediction error for the true system is equal to the innovation (8.12):

$$\bar{\varepsilon}(t,\theta^0) = (A_0^0)^{-1}e(t) = \bar{e}(t). \tag{8.64}$$

8.D Proof of Proposition 8.12

The premise of implication (8.26) is satisfied if and only if

$$\Delta_W(q,\theta) := W(q,\theta_1) - W(q,\theta_2) = 0. \tag{8.65}$$

Applying Parseval's theorem gives

$$\frac{1}{2\pi}\int_{-\pi}^{\pi}\Delta_W(e^{i\omega},\theta)\Phi_z(\omega)\Delta_W^{\top}(e^{-i\omega},\theta)d\omega = 0. \tag{8.66}$$

This implies $\Delta_W(q,\theta) = 0$ only if $\Phi_z(\omega) \succ 0$ for a sufficiently high number of frequencies. In the situation $K \geq 1$, $w(t)$ depends on $r(t)$ and substituting the open-loop response (8.9) for $w(t)$ gives

$$z(t) = J(q)\kappa(t). \tag{8.67}$$

with

$$J(q) = \begin{bmatrix} A^{-1}F & A^{-1}B \\ 0 & I \end{bmatrix}, \qquad \kappa(t) = \begin{bmatrix} e(t) \\ r(t) \end{bmatrix}. \tag{8.68}$$

As $J(q)$ has always full rank, $\Phi_z(\omega) \succ 0$ if and only if $\Phi_\kappa(\omega) \succ 0$. As $e(t)$ and $r(t)$ are assumed to be uncorrelated and $E\{e(t)\} = 0$, we have that $\Phi_{re} = \Phi_{er} = 0$ and

$$\Phi_\kappa = \begin{bmatrix} \Phi_r & \Phi_{re} \\ \Phi_{er} & \Phi_e \end{bmatrix} = \begin{bmatrix} \Phi_r & 0 \\ 0 & \Lambda \end{bmatrix}. \tag{8.69}$$

Then $\Phi_\kappa(\omega) \succ 0$ if and only if $\Lambda \succ 0$ (which is assumed) and $\Phi_r(\omega) \succ 0$. The condition $\Phi_z(\omega) \succ 0$ reduces to $\Phi_r(\omega) \succ 0$.

8.E Proof of Theorem 8.17

The proof consists of three steps. First, convergence of $V_N(\theta)$ to $\bar{V}(\theta)$ for $N \to \infty$ follows directly from applying Ljung (1999, Theorem 2B.1) and the fact that $S \succ 0$ as the conditions for convergence are satisfied by the network model set. Second, by Condition 1., θ^0 is a minimum of $\bar{V}(\theta)$, which can be seen as follows. As $r(t)$ and $e(t)$ are uncorrelated and $W_{\bar{\varepsilon}e}(q, \theta)$ is strictly proper, the power of any cross term between the three terms in the prediction error (8.62) is zero, so the power of each term can be minimised individually. As a result, $W_{\bar{\varepsilon}r}(q, \theta^0) = 0$ and $W_{\bar{\varepsilon}e}(q, \theta^0) = 0$ and thus the cost function reaches its minimum value when the prediction error is equal to the innovation as in (8.12). Third, following the result of Ljung (1999, Theorem 8.3), under Condition 2., this minimum of $\bar{V}(\theta)$ at θ^0 provides a unique predictor filter $W(q, \theta)$ and therefore also a unique pair $(T_{wr}(q), \Phi_{\bar{v}}(\omega))$. With Condition 3. this implies that the resulting model $M(\theta) = M(\theta^0)$ is unique. Therefore, $M(\hat{\theta}_N)$ converges to $M(\theta^0)$ with probability 1.

8.F Parameters of the structured network

Remember that a polynomial matrix $A(q^{-1})$ as its (i, j)th element has $a_{ij}(q^{-1}) = \sum_{\ell=0}^{n_a} a_{jk,\ell} q^{-\ell}$. The model structure $A(q^{-1}, \theta_a)$, $B(q^{-1}, \theta_b)$, $C(q^{-1}, \theta_c)$ of the network model (8.28) is parameterised in terms of the parameters θ_a, θ_b, and η_c, where $\bar{C}(q^{-1}, \eta_c, \theta_a) = C(q^{-1}, \theta_c) A_0(\theta_a)$, having its constant term parameterised by θ_a and its dynamic terms by parameters θ_c. $A(q^{-1})$ is parameterised symmetrically. The parameter vectors θ_a, θ_b, θ_c, and η_c are given by

$$\theta_a = \begin{bmatrix} \theta_{a_1} \\ \theta_{a_2} \\ \vdots \\ \theta_{a_L} \end{bmatrix}, \quad \theta_{a_i} = \begin{bmatrix} \theta_{a_{ii}} \\ \theta_{a_{ii1}} \\ \vdots \\ \theta_{a_{iL}} \end{bmatrix}, \quad \theta_{a_{ij}} = \begin{bmatrix} a_{ij,0} \\ a_{ij,1} \\ \vdots \\ a_{ij,n_a} \end{bmatrix}, \tag{8.70a}$$

$$\theta_b = \begin{bmatrix} \theta_{b_1} \\ \theta_{b_2} \\ \vdots \\ \theta_{b_L} \end{bmatrix}, \quad \theta_{b_i} = \begin{bmatrix} \theta_{b_{i1}} \\ \theta_{b_{i2}} \\ \vdots \\ \theta_{b_{iK}} \end{bmatrix}, \quad \theta_{b_{ij}} = \begin{bmatrix} b_{ij,0} \\ b_{ij,1} \\ \vdots \\ b_{ij,n_b} \end{bmatrix}, \tag{8.70b}$$

$$\theta_c = \begin{bmatrix} \theta_{c_1} \\ \theta_{c_2} \\ \vdots \\ \theta_{c_L} \end{bmatrix}, \quad \theta_{c_i} = \begin{bmatrix} \theta_{c_{i1}} \\ \theta_{c_{i2}} \\ \vdots \\ \theta_{c_{iL}} \end{bmatrix}, \quad \theta_{c_{ij}} = \begin{bmatrix} c_{ij,1} \\ c_{ij,2} \\ \vdots \\ c_{ij,n_c} \end{bmatrix}, \tag{8.70c}$$

$$\eta_c = \begin{bmatrix} \eta_{c_1} \\ \eta_{c_2} \\ \vdots \\ \eta_{c_L} \end{bmatrix}, \quad \eta_{c_i} = \begin{bmatrix} \eta_{c_{i1}} \\ \eta_{c_{i2}} \\ \vdots \\ \eta_{c_{iL}} \end{bmatrix}, \quad \eta_{c_{ij}} = \begin{bmatrix} \bar{c}_{ij,1} \\ \bar{c}_{ij,2} \\ \vdots \\ \bar{c}_{ij,n_c} \end{bmatrix}. \tag{8.70d}$$

8.G ARX parameterisation and regressor

The model structure $\breve{A}(q^{-1}, \zeta_a^n)$ and $\breve{B}(q^{-1}, \zeta_b^n)$ of the nonparametric ARX model (8.29) is parameterised in terms of the parameters ζ^n. The parameter vector $\zeta^n := \left[[\zeta_a^n]^\top \quad [\zeta_b^n]^\top \right]^\top$ is given by

$$\zeta_a^n = \begin{bmatrix} \zeta_{a_1}^n \\ \zeta_{a_2}^n \\ \vdots \\ \zeta_{a_L}^n \end{bmatrix}, \quad \zeta_{a_i}^n = \begin{bmatrix} \zeta_{a_{i1}}^n \\ \zeta_{a_{i2}}^n \\ \vdots \\ \zeta_{a_{iL}}^n \end{bmatrix}, \quad \zeta_{a_{ij}}^n = \begin{bmatrix} \breve{a}_{ij,1} \\ \breve{a}_{ij,2} \\ \vdots \\ \breve{a}_{ij,n} \end{bmatrix}, \tag{8.71a}$$

$$\zeta_b^n = \begin{bmatrix} \zeta_{b_1}^n \\ \zeta_{b_2}^n \\ \vdots \\ \zeta_{b_L}^n \end{bmatrix}, \quad \zeta_{b_i}^n = \begin{bmatrix} \zeta_{b_{i1}}^n \\ \zeta_{b_{i2}}^n \\ \vdots \\ \zeta_{b_{iK}}^n \end{bmatrix}, \quad \zeta_{b_{ij}}^n = \begin{bmatrix} \breve{b}_{ij,0} \\ \breve{b}_{ij,1} \\ \vdots \\ \breve{b}_{ij,n} \end{bmatrix}. \tag{8.71b}$$

The regressor $[\varphi^n(t)]^\top$ in (8.31b) is given by $[\varphi^n(t)]^\top = \left[-[\varphi_w^n(t)]^\top \quad [\varphi_r^n(t)]^\top \right]$ with

$$[\varphi_w^n(t)]^\top = \left[[\varphi_{w_1}^n(t)]^\top \quad [\varphi_{w_2}^n(t)]^\top \quad \cdots \quad [\varphi_{w_L}^n(t)]^\top \right], \tag{8.72a}$$

$$[\varphi_{w_i}^n(t)]^\top = \left[w_i(t-1) \quad w_i(t-2) \quad \cdots \quad w_i(t-n) \right], \tag{8.72b}$$

$$[\varphi_r^n(t)]^\top = \left[[\varphi_{r_1}^n(t)]^\top \quad [\varphi_{r_2}^n(t)]^\top \quad \cdots \quad [\varphi_{r_K}^n(t)]^\top \right], \tag{8.72c}$$

$$[\varphi_{r_i}^n(t)]^\top = \left[r_i(t) \quad r_i(t-1) \quad r_i(t-2) \quad \cdots \quad r_i(t-n) \right]. \tag{8.72d}$$

8.H Matrices $Q(\zeta^{n0})$ and $T(\vartheta^0)$

In order to construct $Q(\zeta^{n0})$ and $T(\vartheta^0)$, we first define some other matrices.

8.H.1 Zero and identity

Let $0_{i,j}$ denote a matrix of dimension $i \times j$ with all its elements equal to 0. Let $I_{i,j}$ denote an identity matrix of dimension $i \times j$, where $I_{i,j} = \begin{bmatrix} I_{i,i} & 0_{i,j-i} \end{bmatrix}$ for $i \leq j$ and $I_{i,j} = \begin{bmatrix} I_{j,j} & 0_{j,i-j} \end{bmatrix}^\top$ for $i \geq j$. Let $I_{k(i,j)}$ denote a block diagonal matrix of k blocks of $I_{i,j}$ and let $I_{\ell(k(i,j))}$ denote a block diagonal matrix of ℓ blocks of $I_{k(i,j)}$.

8.H.2 Matrix Π

Define the matrices

$$\Pi_i^a := \begin{bmatrix} \zeta_{a_{i1}^n} & 0_{n,n_a} \\ \vdots & \vdots \\ \zeta_{a_{i(i-1)}^n} & 0_{n,n_a} \\ \zeta_{a_{ii}^n} & -I_{n,n_a} \\ \zeta_{a_{i(i+1)}^n} & 0_{n,n_a} \\ \vdots & \vdots \\ \zeta_{a_{iL}^n} & 0_{n,n_a} \end{bmatrix}, \qquad \Pi_i^b := \begin{bmatrix} \zeta_{b_{i1}^n} & 0_{n+1,n_a} \\ \zeta_{b_{i2}^n} & 0_{n+1,n_a} \\ \vdots & \vdots \\ \zeta_{b_{iK}^n} & 0_{n+1,n_a} \end{bmatrix}, \tag{8.73}$$

and observe that Π_i^a has dimensions $Ln \times (n_a + 1)$ and that Π_i^b has dimensions $K(n+1) \times (n_a + 1)$.

For $x \in \{a, b\}$, define the block matrix

$$\bar{\Pi}_L^x := \begin{bmatrix} Z_{0,L}^x & Z_{1,L-1}^x & \cdots & Z_{L-1,1}^x \\ R(\Pi_1^x, \Pi_L^x) & R(\Pi_2^x, \Pi_L^x) & \cdots & R(\Pi_L^x, \Pi_L^x) \\ S_{L-1}(\Pi_1^x) & S_{L-2}(\Pi_2^x) & \cdots & S_{L-L}(\Pi_L^x) \end{bmatrix}, \tag{8.74}$$

with $Z_{i,j}^a$ an $i \times j$ block matrix with blocks $0_{Ln,(n_a+1)}$ and with $Z_{i,j}^b$ an $i \times j$ block matrix with blocks $0_{K(n+1),(n_a+1)}$ (that is, $Z_{i,j}^a := 0_{iLn,j(n_a+1)}$ and $Z_{i,j}^b := 0_{iK(n+1),j(n_a+1)}$), with

$$R(\Pi_i^x, \Pi_j^x) := \begin{bmatrix} \Pi_i^x & \Pi_{i+1}^x & \cdots & \Pi_j^x \end{bmatrix}, \quad \text{for } i \leq j, \tag{8.75}$$

and with

$$S_i(\Pi_j^x) := \begin{bmatrix} Z_{i,1}^x & D_i(\Pi_j^x) \end{bmatrix}, \tag{8.76}$$

with $D_i(\Pi_j^x)$ a block diagonal matrix consisting of i blocks of Π_j^x. Observe that $\bar{\Pi}_L^a$ has dimensions $L^2 n \times \frac{1}{2}L(L+1)(n_a+1)$ and $\bar{\Pi}_L^b$ has dimensions $LK(n+1) \times \frac{1}{2}L(L+1)(n_a+1)$.

8.H.3 Toeplitz matrix

Let $\mathcal{T}_{i,j}(x)$ denote a Toeplitz matrix of dimension $i \times j$ (with $i \geq j$) given by

$$\mathcal{T}_{i,j}(x) := \mathcal{T}_{i,j}\left(\begin{bmatrix} x_0 & x_1 & \cdots & x_{i-1} \end{bmatrix} \right) = \begin{bmatrix} x_0 & & & 0 \\ \vdots & \ddots & & \\ x_{j-1} & \cdots & & x_0 \\ \vdots & \ddots & & \vdots \\ x_{i-1} & \cdots & & x_{i-j-1} \end{bmatrix}. \tag{8.77}$$

Define the following Toeplitz matrices of dimension $k \times \ell$:

$$\mathcal{T}_{k,\ell}(\breve{a}_{ij}) := \mathcal{T}_{k,\ell}(\begin{bmatrix} \breve{a}_{ij,0} & \breve{a}_{ij,1} & \cdots & \breve{a}_{ij,k} \end{bmatrix}), \tag{8.78a}$$

$$\mathcal{T}_{k,\ell}(\breve{b}_{ij}) := \mathcal{T}_{k,\ell}(\begin{bmatrix} 0 & \breve{b}_{ij,0} & \breve{b}_{ij,1} & \cdots & \breve{b}_{ij,k} \end{bmatrix}), \tag{8.78b}$$

$$\mathcal{T}_{k,\ell}(\bar{c}_{ij}) := \mathcal{T}_{k,\ell}(\begin{bmatrix} a_{ij,0} & \bar{c}_{ij,1} & \cdots & \bar{c}_{ij,k} \end{bmatrix}), \tag{8.78c}$$

Note that for $\breve{a}_{ij}$ it is known that $\breve{a}_{ij,0} = 1$ for $i = j$ and $\breve{a}_{ij,0} = 0$ for $i \neq j$; and note that for $\bar{c}_{ij}$ it is known that $\bar{c}_{ij,0} = a_{ij,0} = a_{ji,0}$ and $\bar{c}_{ij,k} = 0$ for $k > n_c$.

Define the following block matrices

$$\bar{\mathcal{T}}_{k,\ell}(\breve{A}) := \begin{bmatrix} \mathcal{T}_{k,\ell}(\breve{a}_{11}) & \cdots & \mathcal{T}_{k,\ell}(\breve{a}_{L1}) \\ \vdots & & \vdots \\ \mathcal{T}_{k,\ell}(\breve{a}_{1L}) & \cdots & \mathcal{T}_{k,\ell}(\breve{a}_{LL}) \end{bmatrix}, \tag{8.79a}$$

$$\bar{\mathcal{T}}_{k,\ell}(\breve{B}) := \begin{bmatrix} \mathcal{T}_{k,\ell}(\breve{b}_{11}) & \cdots & \mathcal{T}_{k,\ell}(\breve{b}_{L1}) \\ \vdots & & \vdots \\ \mathcal{T}_{k,\ell}(\breve{b}_{1K}) & \cdots & \mathcal{T}_{k,\ell}(\breve{b}_{LK}) \end{bmatrix}, \tag{8.79b}$$

where $\bar{\mathcal{T}}_{k,\ell}(\breve{A})$ has dimensions $Lk \times L\ell$ and $\bar{\mathcal{T}}_{k,\ell}(\breve{B})$ has dimensions $Kk \times L\ell$.

For $x \in \{a, b\}$, let $\bar{\mathcal{T}}_{m(k,\ell)}(\breve{X})$ denote a block diagonal matrix consisting of m blocks of $\bar{\mathcal{T}}_{k,\ell}(\breve{X})$. Observe that $\bar{\mathcal{T}}_{n,n_c}(\breve{A})$ has dimension $Ln \times Ln_c$ and that $\bar{\mathcal{T}}_{n+1,n_c}(\breve{B})$ has dimension $K(n+1) \times Ln_c$.

Let $\mathcal{T}_{m(k,\ell)}(\bar{c}_{ij})$ denote a block diagonal matrix consisting of m blocks of $\mathcal{T}_{k,\ell}(\bar{c}_{ij})$. Observe that $\mathcal{T}_{L(n,n)}(\bar{c}_{ij})$ is an $Ln \times Ln$ block diagonal matrix consisting of L blocks of $\mathcal{T}_{n,n}(\bar{c}_{ij})$ and that $\mathcal{T}_{K(n+1,n+1)}(\bar{c}_{ij})$ is an $K(n+1) \times K(n+1)$ block diagonal matrix consisting of K blocks of $\mathcal{T}_{n+1,n+1}(\bar{c}_{ij})$. Finally, define

$$T_{m(k,\ell)}(\bar{C}) := \begin{bmatrix} \mathcal{T}_{m(k,\ell)}(\bar{c}_{11}) & \cdots & \mathcal{T}_{m(k,\ell)}(\bar{c}_{1L}) \\ \vdots & & \vdots \\ \mathcal{T}_{m(k,\ell)}(\bar{c}_{L1}) & \cdots & \mathcal{T}_{m(k,\ell)}(\bar{c}_{LL}) \end{bmatrix}. \tag{8.80}$$

8.H.4 Matrix $Q(\zeta^{n0})$

With the matrices defined above, we can now describe the matrix $Q(\zeta^{n0})$ in (8.36) by

$$Q(\zeta^{n0}) = \begin{bmatrix} \bar{\Pi}_L^a & 0 & \bar{\mathcal{T}}_{L(n,n_c)}(\breve{A}^0) \\ \bar{\Pi}_L^b & -I_{L(K(n+1,n_b))} & \bar{\mathcal{T}}_{L(n+1,n_c)}(\breve{B}^0) \end{bmatrix}, \tag{8.81}$$

which has dimensions $\left[L^2 n + LK(n+1)\right] \times \left[\frac{1}{2}L(L+1)(n_a+1) + LK(n_b+1) + L^2 n_c\right]$.

8.H.5 Matrix $T(\vartheta^0)$

With the matrices defined above, we can now describe the matrix $T(\vartheta^0)$ in (8.42) by

$$T(\vartheta^0) = \begin{bmatrix} -T_{L(n,n)}(\bar{C}^0) & 0 \\ 0 & -T_{K(n+1,n+1)}(\bar{C}^0) \end{bmatrix}, \tag{8.82}$$

which has dimensions $\left[L^2 n + LK(n+1)\right] \times \left[L^2 n + LK(n+1)\right]$.

9 | Subnetwork identification

This chapter adds Section 9.9 and 9.10 to the work that is equivalent to

E.M.M. Kivits and P.M.J. Van den Hof. Local identification in diffusively coupled linear networks. In *Proceedings of the 61st IEEE Conference on Decision and Control (CDC)*, pages 874-879, 2022.

Physical dynamic networks most commonly consist of interconnections of physical components that can be described by diffusive couplings. Diffusive couplings imply symmetric cause-effect relationships in the interconnections and therefore diffusively coupled networks can be represented by undirected graphs. This chapter shows how local dynamics of (undirected) diffusively coupled networks can be identified on the basis of local signals only. Sensors and actuators are allocated to guarantee consistent identification. An algorithm is developed for identifying the local dynamics.

9.1 Introduction

Physical networks can describe a diversity of physical processes from various domains, such as electrical, mechanical, hydraulic, thermal, and chemical processes. Their dynamic behaviour is typically described by undirected dynamic interconnections between node signals, where the interconnections represent diffusive couplings (Cheng et al., 2017; Dörfler and Bullo, 2013). The network is typically described by a vector differential equation of maximum second order. Some famous examples of physical networks are electrical resistor-inductor-capacitor circuits and mechanical mass-spring-damper systems.

In the literature, there are several methods available for identifying the physical components in the network on the basis of measured signals. Black-box prediction error identification methods (Ljung, 1999) can model the transfer functions from measured excitation signals to node signals. These models need to be converted to the structure of the physical network for estimating the component values, which is nontrivial. Moreover, this modelling procedure depends on the particular location of the external signals. Second, black-box state-space models can be estimated from which the model parameters can be derived by applying matrix transformations (Friswell et al., 1999; Lopes dos Santos et al., 2015; Ramos et al., 2013) or eigenvalue decompositions (Fritzen, 1986; Luş et al., 2003). However, these methods typically do not have any guarantees on the statistical accuracy of the estimates. State-space models of first-order diffusively coupled networks are considered by van Waarde et al. (2018). Third, physical networks can be considered to be directed dynamic networks with specific structural properties (Chapter 7). Dynamic networks can be modelled as directed interconnections of transfer function modules (Gonçalves and Warnick, 2008; Van den Hof et al., 2013) for which an identification framework has been developed by Van den Hof et al. (2013). However, the network structure in the model is generally lost. Information on the global network structure of undirected graphs can be provided by spectral network identification (Mauroy and Hendrickx, 2017).

Instead of identifying the full network dynamics, one can also aim for identifying only a part of the network, such that more simple experiments can be used to obtain a particular component. This is often referred to as 'local', 'single module', or 'subnetwork' identification, for which several methods have been developed for dynamic networks (Gevers et al., 2018; Materassi and Salapaka, 2020; Ramaswamy and Van den Hof, 2021). Again, the structural properties of undirected network models cannot easily be accounted for in these identification procedures for directed dynamic networks.

This chapter builds further on the preliminary work presented in Chapter 8, in which the identification of the full diffusively coupled network dynamics is discussed, including detailed identifiability and consistency results as well as the implementation into a convex multistep algorithm. This chapter addresses the problem of identifying a particular (local) dynamics in the diffusively coupled network. The order of the dynamics is not restricted and possibly correlated disturbances can be present. The question that is addressed is: Which nodes to measure (sense) and which nodes to excite (actuate) in order to identify the dynamics of a local interconnection in the network? An identification procedure is developed that is shown to lead to consistent estimates thereof.

The networks that will be considered in this chapter are defined in Section 9.2. The identification problem is specified in Section 9.3. Section 9.4 and Section 9.5

describe how to remove unmeasured nodes from the network, without affecting the target component. Section 9.6 describes the identification procedure, including experiment design and conditions for consistent estimates. Section 9.7 discusses some algorithmic aspects. Section 9.8 shows a simulation example of local identification. In Section 9.9, the null-space fitting algorithm in the final step of the identification procedure is described. Section 9.10 contains an alternative local identification problem. Finally, Section 9.11 concludes the chapter. For simplicity, we restrict to representations in the discrete-time domain. This chapter is equivalent to Kivits and Van den Hof (2022) with Section 9.9 and 9.10 added to it.

We consider the following notation throughout the chapter: A polynomial matrix $A(q^{-1})$ consists of matrices A_ℓ and (j,k)th polynomial elements $a_{jk}(q^{-1})$ such that $A(q^{-1}) = \sum_{\ell=0}^{n_a} A_\ell q^{-\ell}$ and $a_{jk}(q^{-1}) = \sum_{\ell=0}^{n_a} a_{jk,\ell} q^{-\ell}$. Hence, the (j,k)th element of the matrix A_ℓ is denoted by $a_{jk,\ell}$. Further, let $A_{\mathcal{J}\bullet}(q^{-1})$ indicate all jth rows of $A(q^{-1})$ for which $j \in \mathcal{J}$.

9.2 Diffusively coupled networks

Diffusively coupled networks are linear dynamic networks in which the interaction between the nodes depends on the difference between the node signals. Such an interaction implies a symmetric coupling between the nodes. The nodes can also be a coupled with the zero node, referred to as the ground node. The networks that will be considered in this chapter are defined in accordance with Chapter 8 as follows:

Definition 9.1 (Network model). *The network that will be considered consists of L node signals $w(t)$, K known excitation signals $r(t)$, and L unknown disturbance signals $v(t)$ and is defined as*

$$A(q^{-1})w(t) = B(q^{-1})r(t) + v(t), \tag{9.1}$$

with q^{-1} the delay operator, i.e. $q^{-1}w(t) = w(t-1)$; with $v(t)$ modelled as filtered white noise, i.e. $v(t) = F(q)e(t)$ with $e(t)$ a vector-valued wide-sense stationary white noise process, i.e. $\mathbb{E}[e(t)e^\top(t-\tau)] = 0$ for $\tau \neq 0$; and with

1. *$A(q^{-1}) = \sum_{k=0}^{n_a} A_k q^{-k} \in \mathbb{R}^{L\times L}[q^{-1}]$, with $A^{-1}(q^{-1})$ stable; $\mathrm{rank}(A_0) = L$; and $a_{jk}(q^{-1}) = a_{kj}(q^{-1})\ \forall k, j$.*
2. *$B(q^{-1}) \in \mathbb{R}^{L\times K}[q^{-1}]$.*

3. $F(q) \in \mathbb{R}^{L\times L}(q)$, *monic, stable, and stably invertible.*

4. $\Lambda \succ 0$ *the covariance matrix of the noise* $e(t)$.

The diffusive character of the model is represented by the symmetry property of $A(q^{-1})$. It is assumed that the network is connected, which means that there is a path between every pair of nodes[1]. If the network has at least one connection to the ground node, then the network is well-posed, which means that $A^{-1}(q^{-1})$ exists and is proper. Stability of the network is induced by the stability of $A^{-1}(q^{-1})$.

Both $A(q^{-1})$ and $B(q^{-1})$ are nonmonic polynomial matrices. In the symmetric $A(q^{-1})$, the polynomial $a_{ij}(q^{-1})$ characterises the dynamics in the link between node signals $w_i(t)$ and $w_j(t)$. Often, $B(q^{-1})$ is chosen to be a submatrix of the identity matrix, implying that each external excitation signal directly enters the network at a distinct node. If $F(q)$ is polynomial or even stronger if $F(q) = I$, the network (9.1) leads to an ARMAX-like or ARX-like[2] model structure, respectively.

A diffusively coupled network induces an undirected graph, where the vertices (nodes) represent the node signals and the links (interconnections) represent the symmetric couplings. Figure 9.1 shows a diffusively coupled network with the dynamics captured by the boxes containing the polynomials $a_{ij}(q^{-1})$ and $b_{ij}(q^{-1})$ and with the nodes represented by the circles, which sum the diffusive couplings and the external signals.

9.3 Identification problem

In view of the symmetric couplings in the considered networks, the local identification problem is formulated as follows:

Definition 9.2 (Local identification problem). *The local identification problem concerns the identification of a single* coupling *between two nodes in the network on the basis of selected measured signals* $w(t)$ *and* $r(t)$.

A single coupling in the network contains the full information on how two nodes interact with each other. For the nodes $w_i(t)$ and $w_j(t)$, this coupling is

[1] The network is connected if its Laplacian matrix (i.e. the degree matrix minus the adjacency matrix) has a positive second-smallest eigenvalue (Fiedler, 1973).

[2] The structure is formally only an ARMAX (autoregressive-moving average with exogenous variables) or ARX (autoregressive with exogenous variables) structure if the $A(q^{-1})$ polynomial is monic (Hannan and Deistler, 2012).

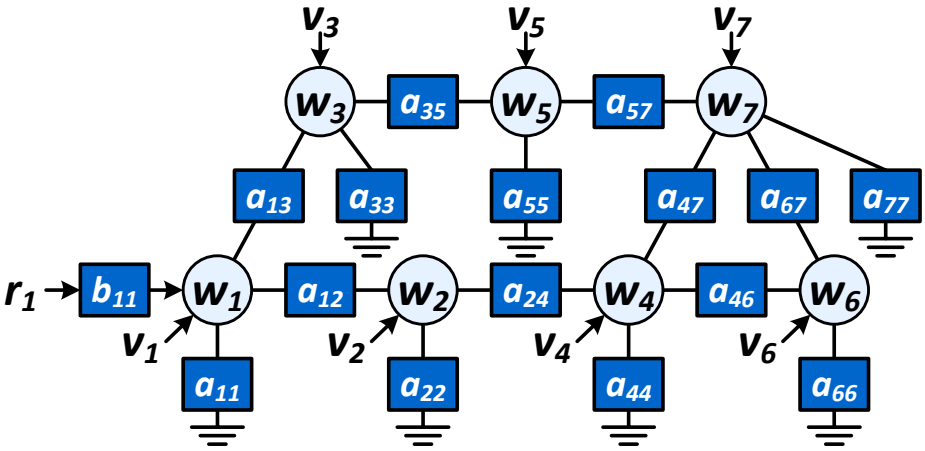

Figure 9.1: Diffusively coupled network as defined in Definition 9.1, with nodes $w_j(t)$, excitations $r_j(t)$, disturbances $v_j(t)$, network dynamics $a_{jk}(q^{-1})$, and input dynamics $b_{jk}(q^{-1})$.

described by the polynomials $a_{ii}(q^{-1})$, $a_{ij}(q^{-1}) = a_{ji}(q^{-1})$, and $a_{jj}(q^{-1})$. One could interpret this identification problem as the identification of the *subnetwork* described by the nodes $w_i(t)$ and $w_j(t)$. For solving this identification problem, it is assumed to be known which nodes are the neighbour nodes of the subnetwork.

9.4 Immersion

The identification of a subnetwork is preferably based on partial measurement of the network. This means that only a selected set of node signals is measured. One way to deal with unmeasured node signals is by eliminating them from the representation. In the literature, this Gaussian elimination is referred to as Kron reduction (Dörfler and Bullo, 2013) or immersion (Dankers et al., 2016). In this section, this reduction procedure is adapted to polynomial representations in order to preserve the network model structure.

For the purpose of immersion, consider a network as defined in Definition 9.1, with the node signals partitioned into two groups: the signals that will be immersed $w_{\mathcal{Z}}(t)$ and the signals that will be preserved $w_{\mathcal{Y}}(t)$. Define the sets $\mathcal{Z} := \{\ell \mid w_\ell(t) \in w_{\mathcal{Z}}(t)\}$ and $\mathcal{Y} := \{\ell \mid w_\ell \notin w_{\mathcal{Z}}\}$. The external signal $v(t)$ is partitioned accordingly, as well as the network matrices $A(q^{-1})$ and $B(q^{-1})$. This

partitioning leads to the equivalent network description

$$\begin{bmatrix} A_{\mathcal{Y}\mathcal{Y}}(q^{-1}) & A_{\mathcal{Y}\mathcal{Z}}(q^{-1}) \\ A_{\mathcal{Z}\mathcal{Y}}(q^{-1}) & A_{\mathcal{Z}\mathcal{Z}}(q^{-1}) \end{bmatrix} \begin{bmatrix} w_{\mathcal{Y}}(t) \\ w_{\mathcal{Z}}(t) \end{bmatrix} = \begin{bmatrix} B_{\mathcal{Y}\bullet}(q^{-1}) \\ B_{\mathcal{Z}\bullet}(q^{-1}) \end{bmatrix} r(t) + \begin{bmatrix} v_{\mathcal{Y}}(t) \\ v_{\mathcal{Z}}(t) \end{bmatrix}. \tag{9.2}$$

Proposition 9.3 (Immersion in diffusively coupled networks). *Consider the network in* (9.2)*. Removing the nodes $w_{\mathcal{Z}}(t)$ through a Gaussian elimination procedure results in the* immersed *network representation*

$$\breve{A}(q^{-1})\breve{w}(t) = \breve{B}(q^{-1})r(t) + \breve{v}(t), \tag{9.3}$$

with $\breve{w}(t) = w_{\mathcal{Y}}(t)$, $\breve{A}(q^{-1})$ symmetric, and (omitting arguments q^{-1}, t)

$$\breve{A}(q^{-1}) = d_{\mathcal{Z}\mathcal{Z}}A_{\mathcal{Y}\mathcal{Y}} - d_{\mathcal{Z}\mathcal{Z}}A_{\mathcal{Y}\mathcal{Z}}A_{\mathcal{Z}\mathcal{Z}}^{-1}A_{\mathcal{Z}\mathcal{Y}}, \tag{9.4a}$$

$$\breve{B}(q^{-1}) = d_{\mathcal{Z}\mathcal{Z}}B_{\mathcal{Y}\bullet} - d_{\mathcal{Z}\mathcal{Z}}A_{\mathcal{Y}\mathcal{Z}}A_{\mathcal{Z}\mathcal{Z}}^{-1}B_{\mathcal{Z}\bullet}, \tag{9.4b}$$

$$\breve{v}(t) = d_{\mathcal{Z}\mathcal{Z}}v_{\mathcal{Y}} - d_{\mathcal{Z}\mathcal{Z}}A_{\mathcal{Y}\mathcal{Z}}A_{\mathcal{Z}\mathcal{Z}}^{-1}v_{\mathcal{Z}}, \tag{9.4c}$$

$$d_{\mathcal{Z}\mathcal{Z}}(q^{-1}) := \frac{det(A_{\mathcal{Z}\mathcal{Z}})}{gcd\left(det(A_{\mathcal{Z}\mathcal{Z}}), adj(A_{\mathcal{Z}\mathcal{Z}})\right)}, \tag{9.4d}$$

where $det(A_{\mathcal{Z}\mathcal{Z}})$ and $adj(A_{\mathcal{Z}\mathcal{Z}})$ are the determinant and the adjugate of the polynomial matrix $A_{\mathcal{Z}\mathcal{Z}}(q^{-1})$, respectively, and $gcd(x, Y)$ is the greatest common divisor of scalar x and all scalar elements of matrix Y.

Proof: This follows from Gaussian elimination of $w_{\mathcal{Z}}(t)$ and the fact that $\breve{A}(q^{-1})$ is a symmetric polynomial matrix. As $A_{\mathcal{Z}\mathcal{Z}}^{-1}(q^{-1})$ is rational, an additional scaling with the monic scalar polynomial $d_{\mathcal{Z}\mathcal{Z}}(q^{-1})$ is needed in order to make the representation polynomial again. ■

The immersed network represents the dynamical relations between a selected subset of nodes in the network. It plays a crucial role in the identification of local network properties that is based on a selected set of (local) node measurements.

9.5 Invariant local dynamics

As mentioned in Section 9.3, the objective is to identify a subnetwork described by the nodes $w_i(t)$ and $w_j(t)$. Let this subnetwork be described by node signals $w_{\mathcal{J}}(t)$ and dynamics $A_{\mathcal{J}\mathcal{J}}(q^{-1})$, where we define the set $\mathcal{J} := \{\ell \mid w_\ell(t) \in w_{\mathcal{J}}(t)\}$. From (9.4a), it follows that the dynamics of $A_{\mathcal{Y}\mathcal{Y}}(q^{-1})$ is preserved after immersion, up to the scalar polynomial factor $d_{\mathcal{Z}\mathcal{Z}}(q^{-1})$, if the signals $w_{\mathcal{Y}}(t)$ are

preserved such that $A_{\mathcal{YZ}}(q^{-1}) = 0$. This can simply be done by preserving the nodes $w_{\mathcal{J}}(t)$ and all their neighbour nodes and immersing all remaining nodes.

In line with this reasoning, we partition the node signals into three groups: the signals of interest $w_{\mathcal{J}}(t)$, their neighbour signals $w_{\mathcal{D}}(t)$, and the remaining signals $w_{\mathcal{Z}}(t)$. Define the set $\mathcal{D} := \{\ell \mid w_\ell(t) \in w_{\mathcal{D}}(t)\}$. The external signal $v(t)$ is partitioned accordingly, as well as the network matrices $A(q^{-1})$, $B(q^{-1})$, and $F(q)$. We assume that the disturbance signals $v_{\mathcal{J}}(t)$ are uncorrelated to the other disturbances in the network ($v_{\mathcal{D}}(t)$ and $v_{\mathcal{Z}}(t)$). This partitioning leads to the network description

$$\begin{bmatrix} A_{\mathcal{JJ}}(q^{-1}) & A_{\mathcal{JD}}(q^{-1}) & 0 \\ A_{\mathcal{DJ}}(q^{-1}) & A_{\mathcal{DD}}(q^{-1}) & A_{\mathcal{DZ}}(q^{-1}) \\ 0 & A_{\mathcal{ZD}}(q^{-1}) & A_{\mathcal{ZZ}}(q^{-1}) \end{bmatrix} \begin{bmatrix} w_{\mathcal{J}}(t) \\ w_{\mathcal{D}}(t) \\ w_{\mathcal{Z}}(t) \end{bmatrix} = \begin{bmatrix} B_{\mathcal{J}\bullet}(q^{-1}) \\ B_{\mathcal{D}\bullet}(q^{-1}) \\ B_{\mathcal{Z}\bullet}(q^{-1}) \end{bmatrix} r(t) + \begin{bmatrix} v_{\mathcal{J}}(t) \\ v_{\mathcal{D}}(t) \\ v_{\mathcal{Z}}(t) \end{bmatrix}, \quad (9.5)$$

where $A_{\mathcal{JZ}}(q^{-1}) = 0 = A^\top_{\mathcal{ZJ}}(q^{-1})$, as the node signals $w_{\mathcal{J}}(t)$ are not directly connected to the node signals $w_{\mathcal{Z}}(t)$.

Immersing the node signals $w_{\mathcal{Z}}(t)$ leads to

$$\begin{bmatrix} \breve{A}_{\mathcal{JJ}}(q^{-1}) & \breve{A}_{\mathcal{JD}}(q^{-1}) \\ \breve{A}_{\mathcal{DJ}}(q^{-1}) & \breve{A}_{\mathcal{DD}}(q^{-1}) \end{bmatrix} \begin{bmatrix} w_{\mathcal{J}}(t) \\ w_{\mathcal{D}}(t) \end{bmatrix} = \begin{bmatrix} \breve{B}_{\mathcal{J}\bullet}(q^{-1}) \\ \breve{B}_{\mathcal{D}\bullet}(q^{-1}) \end{bmatrix} r(t) + \begin{bmatrix} \breve{F}_{\mathcal{JJ}}(q) & 0 \\ 0 & \breve{F}_{\mathcal{DD}}(q) \end{bmatrix} \begin{bmatrix} e_{\mathcal{J}}(t) \\ \breve{e}_{\mathcal{D}}(t) \end{bmatrix}, \quad (9.6)$$

that is, $\breve{A}(q^{-1})\breve{w}(t) = \breve{B}(q^{-1})r(t) + \breve{F}(q)\breve{e}(t)$, with (omitting arguments q^{-1}, q, t)

$$\breve{A}_{\mathcal{JJ}} = d_{\mathcal{ZZ}} A_{\mathcal{JJ}}, \qquad \breve{A}_{\mathcal{JD}} = d_{\mathcal{ZZ}} A_{\mathcal{JD}}, \quad (9.7a)$$

$$\breve{A}_{\mathcal{DJ}} = d_{\mathcal{ZZ}} A_{\mathcal{DJ}}, \qquad \breve{B}_{\mathcal{J}\bullet} = d_{\mathcal{ZZ}} B_{\mathcal{J}\bullet}, \quad (9.7b)$$

$$\breve{A}_{\mathcal{DD}} = d_{\mathcal{ZZ}} A_{\mathcal{DD}} - d_{\mathcal{ZZ}} A_{\mathcal{DZ}} A^{-1}_{\mathcal{ZZ}} A_{\mathcal{ZD}}, \quad (9.7c)$$

$$\breve{B}_{\mathcal{D}\bullet} = d_{\mathcal{ZZ}} B_{\mathcal{D}\bullet} - d_{\mathcal{ZZ}} A_{\mathcal{DZ}} A^{-1}_{\mathcal{ZZ}} B_{\mathcal{Z}\bullet}, \quad (9.7d)$$

$$\breve{F}_{\mathcal{JJ}} = d_{\mathcal{ZZ}} F_{\mathcal{JJ}}, \quad (9.7e)$$

$$\breve{F}_{\mathcal{DD}} \breve{e}_{\mathcal{D}} = \left(d_{\mathcal{ZZ}} F_{\mathcal{DD}} - d_{\mathcal{ZZ}} A_{\mathcal{DZ}} A^{-1}_{\mathcal{ZZ}} F_{\mathcal{ZD}} \right) e_{\mathcal{D}}(t) + \left(d_{\mathcal{ZZ}} F_{\mathcal{DZ}} - d_{\mathcal{ZZ}} A_{\mathcal{DZ}} A^{-1}_{\mathcal{ZZ}} F_{\mathcal{ZZ}} \right) e_{\mathcal{Z}}(t), \quad (9.7f)$$

with $\breve{F}_{\mathcal{DD}}(q)$ a monic, stable, and stably invertible transfer function matrix and with $\breve{e}_{\mathcal{D}}(t)$ white noise.

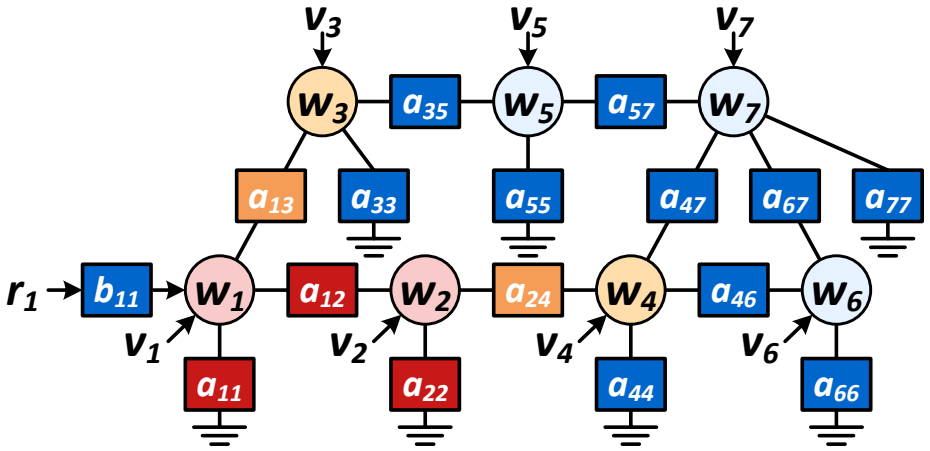

Figure 9.2: Diffusively coupled network with a target subnetwork indicated in red, with its neighbour dynamics and nodes indicated in orange.

Proposition 9.4 (Invariant local dynamics). *Immersion for diffusively coupled networks, as described in Proposition 9.3, applied to the network* (9.5) *resulting in* (9.6)*, gives for* $\ell \in \mathcal{J}$*:*

$$\breve{a}_{\ell\ell}^{-1}(q^{-1})\breve{A}_{\ell\bullet}(q^{-1}) = a_{\ell\ell}^{-1}(q^{-1})A_{\ell\bullet}(q^{-1}), \tag{9.8a}$$
$$\breve{a}_{\ell\ell}^{-1}(q^{-1})\breve{B}_{\ell\bullet}(q^{-1}) = a_{\ell\ell}^{-1}(q^{-1})B_{\ell\bullet}(q^{-1}), \tag{9.8b}$$
$$\breve{a}_{\ell\ell}^{-1}(q^{-1})\breve{F}_{\ell\bullet}(q) = a_{\ell\ell}^{-1}(q^{-1})F_{\ell\bullet}(q). \tag{9.8c}$$

Proof: For $\ell \in \mathcal{J}$ it holds that

$$\begin{aligned}
\breve{a}_{\ell\ell}^{-1}(q^{-1})\breve{A}_{\ell\bullet}(q^{-1}) &= a_{\ell\ell}^{-1}(q^{-1})d_{\mathcal{Z}\mathcal{Z}}^{-1}(q^{-1})d_{\mathcal{Z}\mathcal{Z}}(q^{-1})A_{\ell\bullet}(q^{-1}) \\
&= a_{\ell\ell}^{-1}(q^{-1})A_{\ell\bullet}(q^{-1}), \\
\breve{a}_{\ell\ell}^{-1}(q^{-1})\breve{B}_{\ell\bullet}(q^{-1}) &= a_{\ell\ell}^{-1}(q^{-1})d_{\mathcal{Z}\mathcal{Z}}^{-1}(q^{-1})d_{\mathcal{Z}\mathcal{Z}}(q^{-1})B_{\ell\bullet}(q^{-1}) \\
&= a_{\ell\ell}^{-1}(q^{-1})B_{\ell\bullet}(q^{-1}), \\
\breve{a}_{\ell\ell}^{-1}(q^{-1})\breve{F}_{\ell\bullet}(q) &= a_{\ell\ell}^{-1}(q^{-1})d_{\mathcal{Z}\mathcal{Z}}^{-1}(q^{-1})d_{\mathcal{Z}\mathcal{Z}}(q^{-1})F_{\ell\bullet}(q) \\
&= a_{\ell\ell}^{-1}(q^{-1})F_{\ell\bullet}(q).
\end{aligned}$$

■

The result of Proposition 9.4 is that the local identification problem of identifying a subnetwork really becomes a local problem in the sense that (9.6) can be used to identify $A_{\mathcal{J}\mathcal{J}}(q^{-1})$ on the basis of the signals of interest $w_{\mathcal{J}}(t)$ and their

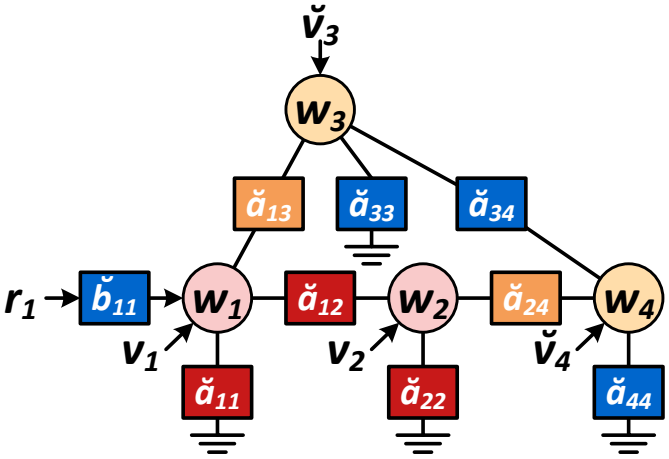

Figure 9.3: Immersed network representation corresponding to the diffusively coupled network in Figure 9.2, with the target subnetwork indicated in red.

neighbour node signals $w_{\mathcal{D}}(t)$ only and that all other node signals $w_{\mathcal{Z}}(t)$ can be discarded.

Figure 9.2 shows a diffusively coupled network with in red the subnetwork described by the node signals $w_{\mathcal{J}}(t) = \begin{bmatrix} w_1(t) & w_2(t) \end{bmatrix}^\top$ and in orange the neighbour dynamics and node signals $w_{\mathcal{D}}(t) = \begin{bmatrix} w_3(t) & w_4(t) \end{bmatrix}^\top$. Immersing the remaining node signals from the network, results in the immersed network representation shown in Figure 9.3, where $\breve{a}_{ij}$ and $\breve{b}_{11}$ are related to a_{ik} and b_{11} according to the relations in (9.7).

Remark 9.5 (Module representation). *The result of Proposition 9.4 is a specific version of the condition on parallel paths and loops around the output as defined by Dankers et al. (2016). To see this, observe that all loops around $w_j(t)$ contain a measured node signal if and only if all neighbour nodes of $w_j(t)$ are measured and consequently, all parallel paths from $w_i(t)$ to $w_j(t)$ contain a measured node signal as well; see Chapter 7.*

9.6 Identification procedure

9.6.1 Identifying the immersed network

For identifying the complete immersed network, a predictor model is set up based on the parameterised model set

$$\breve{\mathcal{M}} := \big(\breve{A}(q^{-1},\eta), \breve{B}(q^{-1},\eta), \breve{F}(q,\eta), \breve{\Lambda}(\eta), \eta \in \Pi\big), \tag{9.9}$$

where η contains all unknown coefficients that appear in the entries of the model matrices $\breve{A}$, $\breve{B}$, $\breve{F}$, and $\breve{\Lambda}$ and where $\Pi \subset \mathbb{R}^d$ with $d \in \mathbb{N}$. The corresponding data generating network is denoted by $\breve{\mathcal{S}} := \{\breve{A}^0(q^{-1}), \breve{B}^0(q^{-1}), \breve{F}^0(q), \breve{\Lambda}^0\}$. Define the one-step-ahead predictor of $\breve{w}(t)$ in line with Chapter 8 as

$$\hat{\breve{w}}(t|t-1) = \mathbb{E}\{\breve{w}(t) \mid \breve{w}^{t-1},\ r^t\}, \tag{9.10}$$

where $\breve{w}^\ell$ and r^ℓ refer to signal samples $\breve{w}(\tau)$ and $r(\tau)$, respectively, for all $\tau \leq \ell$. The resulting prediction error becomes (omitting arguments q^{-1}, q)

$$\breve{\varepsilon}(t,\eta) = \breve{w}(t) - \hat{\breve{w}}(t|t-1;\eta), \tag{9.11a}$$

$$= \breve{A}_0^{-1}(\eta)\breve{F}^{-1}(\eta)\left[\breve{A}(\eta)\breve{w}(t) - \breve{B}(\eta)r(t)\right]. \tag{9.11b}$$

The parameters of the immersed network are estimated through the least-squares identification criterion

$$\hat{\eta}_N = \arg\min_{\eta\in\Pi} \frac{1}{N}\sum_{t=1}^{N} \breve{\varepsilon}^\top(t,\eta)\Lambda\breve{\varepsilon}(t,\eta) \tag{9.12}$$

with $\Lambda \succ 0$. Under some mild conditions[3] this criterion converges with probability 1 to

$$\eta^* := \arg\min_{\eta\in\Pi} \lim_{N\to\infty} \sum_{t=1}^{N} \mathbb{E}\left\{\breve{\varepsilon}^\top(t,\eta)\Lambda\breve{\varepsilon}(t,\eta)\right\}. \tag{9.13}$$

Proposition 9.6 (Consistent full identification). *The parameter estimate $\hat{\eta}_N$ provides a consistent estimate of the system $\breve{\mathcal{S}}$ if the following conditions hold.*[a]

1. *The true system is in the model set: $\breve{\mathcal{S}} \subset \breve{\mathcal{M}}$.*

[3] The standard conditions for convergence of predictor error estimates include the condition that the white noise process $e(t)$ has bounded moments of an order larger than 4 (Ljung, 1999).

2. *At least one excitation signal is present:* $K \geq 1$.

3. $\Phi_r(\omega) \succ 0$ *for a sufficiently high number of frequencies.*

4. $\breve{A}(q^{-1}, \eta)$ *and* $\breve{B}(q^{-1}, \eta)$ *are left coprime in* $\breve{\mathcal{M}}$.

5. *There exists a permutation matrix* P *such that within* $\breve{\mathcal{M}}$, $\begin{bmatrix} \breve{A}_0(\eta) & \breve{A}_1(\eta) & \cdots & \breve{A}_{n_a}(\eta) & \breve{B}_0(\eta) & \breve{B}_1(\eta) & \cdots & \breve{B}_{n_b}(\eta) \end{bmatrix} P = \begin{bmatrix} D(\eta) & R(\eta) \end{bmatrix}$ *with* $D(\eta)$ *square, diagonal, and full rank.*

6. *There is at least one parameter constraint on the parameters of* $\breve{A}(q^{-1}, \eta_A)$ *and* $\breve{B}(q^{-1}, \eta_B)$ *of the form* $\Gamma\bar{\eta} = \gamma \neq 0$, *with* $\bar{\eta} := \begin{bmatrix} \eta_A^\top & \eta_B^\top \end{bmatrix}^\top$.

[a] This proposition is slightly different formulated than by Kivits and Van den Hof (2023a).

Proof: A consistent estimate is obtained if the model is uniquely recovered from the data. Condition 1 is necessary for this. Condition 3 ensures that the transfer functions from $r(t)$ and $\bar{e}(t) := A_0^{-1} e(t)$ to $\breve{w}(t)$ (i.e. $T_{wr}(q, \eta)$ and $T_{w\bar{e}}(q, \eta)$) can uniquely be recovered from data (Chapter 8). Condition 2 implies that $T_{wr}(q, \eta)$ is nonzero. From $T_{wr}(q, \eta)$, Condition 4 ensures that $\breve{A}(q^{-1}, \eta)$ and $\breve{B}(q^{-1}, \eta)$ are found up to a premultiplication with a unimodular matrix. To satisfy Condition 5, this unimodular matrix is restricted to being diagonal. To preserve the symmetry of $\breve{A}(q^{-1}, \eta)$, this diagonal matrix is further restricted to having equal elements. Condition 6 fixes the remaining scaling factor. As $\breve{A}(q^{-1}, \eta)$ is uniquely found, $T_{w\bar{e}}(q, \eta)$ gives unique $\breve{F}(q, \eta)$ and $\breve{\Lambda}(\eta)$ (Chapter 8). ■

For Condition 6, it is possible to choose a custom constraint, leading to a scaled immersed network representation.

9.6.2 Identifying the target subnetwork

Once the complete immersed network representation (9.6) is identified, the target subnetwork can be estimated. The correct scaling is obtained through a parameter constraint on the target subnetwork. An additional identification step is needed for this, because this dynamics is only present in the identified immersed network with a scaled polynomial factor that needs to be removed. The relations in (9.7) lead to

$$\tilde{A}_{\mathcal{J}\bullet}(q^{-1}) = \alpha d_{\mathcal{Z}\mathcal{Z}}(q^{-1}) A_{\mathcal{J}\bullet}(q^{-1}), \tag{9.14a}$$

$$\tilde{B}_{\mathcal{J}\bullet}(q^{-1}) = \alpha d_{\mathcal{Z}\mathcal{Z}}(q^{-1}) B_{\mathcal{J}\bullet}(q^{-1}), \tag{9.14b}$$

with $\tilde{A}_{\mathcal{J}\bullet}(q^{-1}) := \alpha \breve{A}_{\mathcal{J}\bullet}(q^{-1})$, $\tilde{B}_{\mathcal{J}\bullet}(q^{-1}) := \alpha \breve{B}_{\mathcal{J}\bullet}(q^{-1})$, and unknown scaling factor $\alpha \in \mathbb{R}_+$.

Proposition 9.7 (Consistent local identification). *If a nonzero polynomial element $a_{ij}(q^{-1})$ or $b_{ij}(q^{-1})$ of $A_{\mathcal{J}\bullet}(q^{-1})$ or $B_{\mathcal{J}\bullet}(q^{-1})$, respectively, is known, a consistent estimate of the true $A^0_{\mathcal{J}\bullet}(q^{-1})$ and $B^0_{\mathcal{J}\bullet}(q^{-1})$ is obtained through* (9.14).

Proof: From Proposition 9.6, the true $\tilde{A}^0_{\mathcal{J}\bullet}(q^{-1})$ and $\tilde{B}^0_{\mathcal{J}\bullet}(q^{-1})$ have been estimated consistently with a custom parameter constraint on η. Using a known $a_{ij}(q^{-1})$ or $b_{ij}(q^{-1})$, polynomial factor $\alpha d_{\mathcal{Z}\mathcal{Z}}(q^{-1})$ can be extracted from (9.14). Then, (9.14) leads to consistent estimates of the true $A^0_{\mathcal{J}\bullet}(q^{-1})$ and $B^0_{\mathcal{J}\bullet}(q^{-1})$. ■

The constraint that a nonzero polynomial element $a_{ij}(q^{-1})$ or $b_{ij}(q^{-1})$ needs to be known, means that a single interconnection in the network is known or that an excitation signal enters the network through known dynamics (e.g. $b_{ij}(q^{-1}) = 1$), respectively. The identification meant in Proposition 9.7 is performed through a null-space fitting as explained in Section 9.9. If only one of the parameters of $A_{\mathcal{J}\bullet}(q^{-1})$ or $B_{\mathcal{J}\bullet}(q^{-1})$ is constraint (similar to the constraint in Condition 6 of Proposition 9.6), a consistent estimate of the target subnetwork is obtained through the same null-space fitting with fewer parameter constraints; see again Section 9.9. If this constraint is not satisfied, the target subnetwork can be identified up to a scaling factor that remains unknown.

Remark 9.8 (MIMO identification). *The difference with a general MIMO identification lies in the nonmonicity and symmetry of $A(q^{-1})$ and in the interpretation of the model that leads to the selection of the necessary node signals.*

9.7 Algorithmic aspects

For performing the identification of the immersed network, we adopt the multistep algorithm for full network identification presented in Chapter 8 for systems with a polynomial noise model, i.e. $F(q) = C(q^{-1})$ polynomial. The prime steps of this algorithm are: 1) estimate a nonstructured high-order ARX model; 2) reduce this model to a structured network model through a weighted null-space fitting (WNSF); 3) improve the structured network model through a WNSF; 4) obtain the noise model.

While in (9.4) the matrix expressions are forced to become polynomial by premultiplying with the common polynomial factor $d_{\mathcal{Z}\mathcal{Z}}(q^{-1})$, this causes many

polynomial terms in (9.4) to have common factors. As this can lead to undesired effects in our identification algorithm because of cancelling terms, we adopt a different route for arriving at a polynomial model. We remove $d_{\mathcal{Z}\mathcal{Z}}(q^{-1})$ from (9.4) and approximate the rational term $A^{-1}_{\mathcal{Z}\mathcal{Z}}(q^{-1})$ by a symmetric polynomial matrix. If the order of this polynomial matrix is chosen sufficiently high, $A^{-1}_{\mathcal{Z}\mathcal{Z}}(q^{-1})$ is approximated sufficiently well. The order of $\breve{A}(q^{-1})$ can be controlled and no terms will cancel out. In addition, the target subnetwork appears directly in the immersed network representation. Because of these advantages, we continue with this alternative approach. Observe that if $B_{\mathcal{Z}\bullet}(q^{-1}) = 0$, then $A^{-1}_{\mathcal{Z}\mathcal{Z}}(q^{-1})$ only appears in $\breve{A}_{\mathcal{D}\mathcal{D}}(q^{-1})$ and $\breve{A}_{\mathcal{D}\mathcal{D}}(q^{-1})$ can be approximated by a symmetric polynomial matrix instead. The identification procedure simplifies in the sense that Condition 6 in Proposition 9.6 directly applies to the target subnetwork and that the subnetwork can be extracted from the immersed network representation, without an additional identification step. This means that Proposition 9.6 guarantees a consistent estimate of the target subnetwork.

9.8 Simulation example

This simulation example serves to illustrate that indeed a subnetwork can be identified from a single excitation signal and by measuring the nodes of interest and their neighbour nodes only.

9.8.1 Simulation set-up

Consider the network (9.1) consisting of seven scalar nodes, with a single excitation signal directly entering the network at node $w_1(t)$ and with a polynomial noise model $F(q) = C(q^{-1})$. This network is shown in Figure 9.1, where $b_{11} = 1$. The objective is to identify the coupling between the nodes $w_1(t)$ and $w_2(t)$ indicated in red in Figure 9.2. Hence, $w_{\mathcal{J}}(t) = \begin{bmatrix} w_1(t) & w_2(t) \end{bmatrix}^\top$ and thus $w_{\mathcal{D}}(t) = \begin{bmatrix} w_3(t) & w_4(t) \end{bmatrix}^\top$. The corresponding immersed network representation is shown in Figure 9.3, where $\breve{b}_{11} = 1$.

The exact parameter values are

$$A_0 = \begin{bmatrix} 80 & -40 & -20 & 0 & 0 & 0 & 0 \\ -40 & 80 & 0 & -10 & 0 & 0 & 0 \\ -20 & 0 & 50 & 0 & -5 & 0 & 0 \\ 0 & -10 & 0 & 35 & 0 & -5 & -5 \\ 0 & 0 & -5 & 0 & 15 & 0 & -5 \\ 0 & 0 & 0 & -5 & 0 & 25 & -20 \\ 0 & 0 & 0 & -5 & -5 & -20 & 30 \end{bmatrix}, \tag{9.15a}$$

$$A_1 = \begin{bmatrix} -60 & 30 & 0 & 0 & 0 & 0 & 0 \\ 30 & -60 & 0 & 0 & 0 & 0 & 0 \\ 0 & 0 & -40 & 0 & 0 & 0 & 0 \\ 0 & 0 & 0 & -40 & 0 & 0 & 0 \\ 0 & 0 & 0 & 0 & 0 & 0 & 0 \\ 0 & 0 & 0 & 0 & 0 & -20 & 20 \\ 0 & 0 & 0 & 0 & 0 & 20 & -20 \end{bmatrix}, \tag{9.15b}$$

$$A_2 = \operatorname{diag}(\begin{bmatrix} 20 & 20 & 20 & 20 & 0 & 0 & 0 \end{bmatrix}), \tag{9.15c}$$

$$B_0 = \begin{bmatrix} 1 \\ 0 \\ 0 \\ 0 \\ 0 \\ 0 \\ 0 \end{bmatrix}, \quad C_1 = 10^{-2} \begin{bmatrix} 2 & 9 & 6 & 3 & 8 & 4 & 1 \\ 3 & 6 & 1 & 7 & 1 & 6 & 7 \\ 9 & 6 & 5 & 7 & 6 & 3 & 6 \\ 7 & 9 & 4 & 6 & 6 & 3 & 7 \\ 3 & 6 & 4 & 9 & 9 & 5 & 8 \\ 7 & 8 & 6 & 6 & 5 & 6 & 5 \\ 8 & 2 & 9 & 5 & 2 & 4 & 4 \end{bmatrix}. \tag{9.15d}$$

The external excitation signal $r_1(t)$ is an independent white noise process with mean 0 and variance $\sigma_r^2 = 1$. All nodes are subject to disturbances $e_\ell(t)$, which are independent white noise processes (uncorrelated with $r_1(t)$) with mean 0 and variance $\sigma_e^2 = 10^{-2}$. The experiments consist of 100 Monte-Carlo simulations, where in each run, new excitation and noise signals are generated. The number of samples generated for each data set is $N = 10\,000$.

In the immersed network representation, $\breve{A}_{\mathcal{D}\mathcal{D}}(q^{-1})$ is approximated by a second-order polynomial matrix. The full immersed network is identified through the algorithm in Chapter 8, where in Step 1, the order of the ARX model approximation is chosen to be 10. The network topology of the immersed network is assumed to be unknown, meaning that all connections between nodes are parameterised. However, it is assumed to be known that $\breve{A}_2(\theta)$ is diagonal and that $\breve{A}_k(\theta) = 0$, $\forall k \geq 3$, such that Condition 5 in Proposition 9.6 is satisfied. The knowledge that the excitation signal enters the network directly at node $w_1(t)$ induces that $\breve{B}$ is the 4×1 unit vector, such that Condition 6 in Proposition 9.6 is satisfied.

Table 9.1: True parameters values of $A_{\mathcal{J}\bullet}(q^{-1}, \theta)$ and the mean and standard deviation (SD) of their estimates.

Parameter	θ_1	θ_2	θ_3	θ_4	θ_5	θ_6
True value	80	-60	20	-40	30	0
Mean	79.4219	-59.7437	20.1294	-39.0483	29.3419	0
SD	0.6564	0.3255	0.1626	1.1800	0.7409	0
Parameter	θ_7	θ_8	θ_9	θ_{10}	θ_{11}	θ_{12}
True value	-20	0	0	0	0	0
Mean	-19.7780	-0.0534	0	-0.1235	0.0339	0
SD	0.3821	0.1623	0	0.2261	0.1078	0
Parameter	θ_{13}	θ_{14}	θ_{15}	θ_{16}	θ_{17}	θ_{18}
True value	80	-60	20	0	0	0
Mean	78.0318	-58.6126	19.6240	-0.0104	-0.0957	0
SD	2.1832	1.6962	0.4578	0.6798	0.4375	0
Parameter	θ_{19}	θ_{20}	θ_{21}			
True value	-10	0	0			
Mean	-9.6627	-0.0820	0			
SD	0.3790	0.1841	0			

The target subnetwork $A_{\mathcal{J}\bullet}(q^{-1})$ is extracted from the immersed network, where the symmetric structure of $A(q^{-1})$ is incorporated into the parametrisation. The target subnetwork (the first two rows of (9.15a)-(9.15c)) is parameterised as

$$A_{\mathcal{J}\bullet,0}(\theta) = \begin{bmatrix} \theta_1 & \theta_4 & \theta_7 & \theta_{10} & 0 & 0 & 0 \\ \theta_4 & \theta_{13} & \theta_{16} & \theta_{19} & 0 & 0 & 0 \end{bmatrix}, \tag{9.16a}$$

$$A_{\mathcal{J}\bullet,1}(\theta) = \begin{bmatrix} \theta_2 & \theta_5 & \theta_8 & \theta_{11} & 0 & 0 & 0 \\ \theta_5 & \theta_{14} & \theta_{17} & \theta_{20} & 0 & 0 & 0 \end{bmatrix}, \tag{9.16b}$$

$$A_{\mathcal{J}\bullet,2}(\theta) = \begin{bmatrix} \theta_3 & \theta_6 & \theta_9 & \theta_{12} & 0 & 0 & 0 \\ \theta_6 & \theta_{15} & \theta_{18} & \theta_{21} & 0 & 0 & 0 \end{bmatrix}. \tag{9.16c}$$

Table 9.1 shows the true parameter values of $A_{\mathcal{J}\bullet}(q^{-1}, \theta)$. The assumption that $\breve{A}_2$ is diagonal implies the constraints $\theta_6 = \theta_9 = \theta_{12} = \theta_{18} = \theta_{21} = 0$.

9.8.2 Simulation results

The simulation results are shown in Table 9.1 and Figure 9.4. Table 9.1 shows the mean and standard deviation of the estimated parameters of $A_{\mathcal{J}\bullet}(q^{-1}, \theta)$. It can

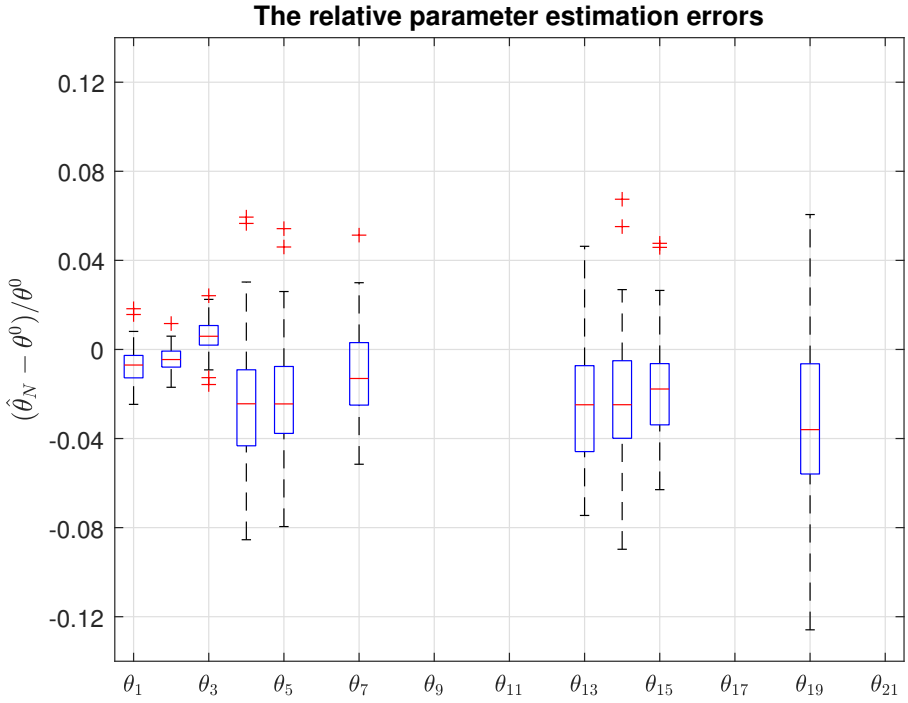

Figure 9.4: Boxplot of the relative parameter estimation errors of the parameters of $A_{\mathcal{J}\bullet}(q^{-1}, \theta)$ (9.16), for parameters with a nonzero true value.

be seen that the constraints $\theta_6 = \theta_9 = \theta_{12} = \theta_{18} = \theta_{21} = 0$ are incorporated, as these parameters are estimated without bias and variance. The other parameters are estimated with a bias that is within a bound of 1 standard deviation. This bias is less than 3.5% deviation for θ_{19} and within 2.5% deviation for all other (nonzero) parameters. The bias is caused by the limited order of the ARX approximation in Step 1 of the algorithm. Figure 9.4 shows the relative estimation errors of the parameters of $A_{\mathcal{J}\bullet}(q^{-1}, \theta)$ that have a nonzero true value. The bias is visible through the nonzero median.

To conclude, the subnetwork described by the nodes $w_1(t)$ and $w_2(t)$ has been identified by measuring only four node signals ($w_1(t)$, $w_2(t)$, $w_3(t)$, and $w_4(t)$) and with a single excitation signal ($r_1(t)$) only. The dynamics between the target subnetwork and its neighbour nodes has been identified as well. The variance can be reduced further by adding external excitation signals $r(t)$ to the experiment.

9.9 Null-space fitting

This section is additional to the work presented by Kivits and Van den Hof (2022). As mentioned, the constraint in Proposition 9.7 can be replaced by a more relaxed constraint on a single parameter instead of on a single polynomial element. Before presenting the algorithm for consistent identification of the target dynamics from the (scaled) immersed network, consider the following manipulations of (9.14).

Equation (9.14a) gives

$$[A^0_{\mathcal{J}\mathcal{J}}(q^{-1})]^{-1}\tilde{A}^0_{\mathcal{J}\mathcal{J}}(q^{-1}) = \alpha d^0_{\mathcal{Z}\mathcal{Z}}(q^{-1})I, \tag{9.17}$$

with I an identity matrix of appropriate size and $A^0_{\mathcal{J}\mathcal{J}}(q^{-1})$ square. Substituting (9.17) into (9.14) gives

$$A^0_{\mathcal{J}\mathcal{J}}(q^{-1})\tilde{A}^0_{\mathcal{J}\mathcal{D}}(q^{-1}) - \tilde{A}^0_{\mathcal{J}\mathcal{J}}(q^{-1})A^0_{\mathcal{J}\mathcal{D}}(q^{-1}) = 0, \tag{9.18a}$$

$$A^0_{\mathcal{J}\mathcal{J}}(q^{-1})\tilde{B}^0_{\mathcal{J}\bullet}(q^{-1}) - \tilde{A}^0_{\mathcal{J}\mathcal{J}}(q^{-1})B^0_{\mathcal{J}\bullet}(q^{-1}) = 0, \tag{9.18b}$$

which is independent of $\alpha d^0_{\mathcal{Z}\mathcal{Z}}(q^{-1})$ and from which we can extract

$$-Q(\eta^0)\bar{\theta}^0 = 0, \tag{9.19}$$

where $\tilde{A}^0_{\mathcal{J}\mathcal{J}}(q^{-1})$, $\tilde{A}^0_{\mathcal{J}\mathcal{D}}(q^{-1})$, and $\tilde{B}^0_{\mathcal{J}\bullet}(q^{-1})$ are incorporated into $Q(\eta^0)$, and where $\bar{\theta}^0$ represents the actual underlying system described by $A^0_{\mathcal{J}\mathcal{J}}(q^{-1})$, $A^0_{\mathcal{J}\mathcal{D}}(q^{-1})$, and $B^0_{\mathcal{J}\bullet}(q^{-1})$. The parameter vectors η and $\bar{\theta}$ and the matrix $Q(\eta)$ are given in Appendix 9.A and 9.B, respectively.

If a single polynomial element is known, then all parameters of this polynomial are known and thus constraint. If only a single parameter is known, then only this particular parameter is constrained. Linear constraints on the parameters $\bar{\theta}$ of $A_{\mathcal{J}\mathcal{J}}(q^{-1},\bar{\theta})$, $A_{\mathcal{J}\mathcal{D}}(q^{-1},\bar{\theta})$, and $B_{\mathcal{J}\bullet}(q^{-1},\bar{\theta})$ are formulated as

$$\Gamma\bar{\theta} = \gamma \neq 0, \tag{9.20}$$

with Γ full row rank. The least-squares estimate of $\bar{\theta}$ is obtained from (9.19) and (9.20) by the linear constraint optimisation problem (Chapter 8)

$$\begin{aligned} \hat{\bar{\theta}}_N = \min_{\bar{\theta}} \quad & \bar{\theta}^\top Q^\top(\hat{\eta}_N)Q(\hat{\eta}_N)\bar{\theta} \\ \text{subject to} \quad & \Gamma\bar{\theta} = \gamma, \end{aligned} \tag{9.21}$$

which can be solved using the Lagrangian and the Karush–Kuhn–Tucker conditions, leading to

$$\begin{bmatrix} \hat{\bar{\theta}}_N \\ \hat{\lambda}_N \end{bmatrix} = \begin{bmatrix} Q^\top(\hat{\eta}_N)Q(\hat{\eta}_N) & \Gamma^\top \\ \Gamma & 0 \end{bmatrix}^{-1} \begin{bmatrix} 0 \\ \gamma \end{bmatrix}, \tag{9.22}$$

where $\hat{\lambda}_N$ are the estimated Lagrange multipliers.

Using the resulting constraint least-squares optimisation problem (9.21), Proposition 9.7 is reformulated as follows:

Proposition 9.9 (Consistent local identification). *If there is at least one linear parameter constraint on the parameters of $A_{\mathcal{J}\bullet}(q^{-1}, \theta_A)$ or $B_{\mathcal{J}\bullet}(q^{-1}, \theta_B)$ of the form $\Gamma\bar{\theta} = \gamma \neq 0$, with Γ full row rank and with $\bar{\theta} := \begin{bmatrix}\theta_A^\top & \theta_B^\top\end{bmatrix}^\top$, then a consistent estimate of the true $A^0_{\mathcal{J}\bullet}(q^{-1})$ and $B^0_{\mathcal{J}\bullet}(q^{-1})$ is obtained through the constraint least-squares optimisation problem* (9.21) *as* (9.22)*.*

Proof: From Proposition 9.6, the true $\tilde{A}^0_{\mathcal{J}\bullet}(q^{-1})$ and $\tilde{B}^0_{\mathcal{J}\bullet}(q^{-1})$ have been estimated consistently with a custom parameter constraint on η. Then (9.21) leads to consistent estimates of the true $A^0_{\mathcal{J}\bullet}(q^{-1})$ and $B^0_{\mathcal{J}\bullet}(q^{-1})$ (Chapter 8). ■

9.10 Alternative local identification

In this chapter, the focus lies on the local identification problem of identifying a single *coupling* between two nodes, as formulated in Definition 9.2. The target dynamics is captured by the subnetwork of the corresponding nodes. The smallest possible subnetwork only consists of the single polynomial $a_{ii}(q^{-1})$, which represents the connection of $w_i(t)$ to the ground node. The presented identification procedure for consistent estimation of a subnetwork has the bonus of also obtaining a consistent estimate of the neighbour dynamics of the subnetwork, captured by the polynomials $a_{ij}(q^{-1}) \neq 0$.

A different identification problem that can also be considered is the identification of a single *interaction* between two nodes. The interaction between the nodes $w_i(t)$ and $w_j(t)$ is described by the polynomial $a_{ij}(q^{-1}) = a_{ji}(q^{-1})$. These dynamics can be identified by identifying the subnetwork corresponding to the nodes $w_i(t)$ and $w_j(t)$, corresponding to the identification of the *coupling* between the nodes $w_i(t)$ and $w_j(t)$. However, it is also possible to identify only one of the polynomials $a_{ij}(q^{-1})$ and $a_{ji}(q^{-1})$, instead of both of them. Then an additional node can be immersed, leading to an immersed network with fewer nodes and, thus, a smaller identification problem. Identification of the subnetwork corresponding to $w_i(t)$ (or $w_j(t)$) only, results in a consistent estimate of $a_{ij}(q^{-1})$ (or $a_{ji}(q^{-1})$), because this polynomial contains neighbour dynamics.

Remark 9.10 (Module representation). *Methods for local identification in dynamic networks have been developed for the module representation (Gevers et al., 2018; Materassi and Salapaka, 2020; Ramaswamy and Van den Hof, 2021). The objective is to identify a single transfer function module from one node signal to another. The conditions for consistent local identification contain extensive requirements on the number and location of excitation signals and the selection of measurement signals.*
In contrast, the local identification method proposed in this chapter requires only a single excitation signal that can be located at any node and a very simple selection of measurement signals. This simplification is caused by the symmetry in the network model, which restricts the networks dynamics sufficiently to achieve identifiability with only a singel excitation signal. The simple selection of measurement signals also results from the static relations in the network dynamics.

9.11 Conclusion

A method and an algorithm for identifying a subnetwork in a diffusively coupled linear network have been presented. For this local identification problem, it is sufficient to measure only the node signals of interest and their neighbour node signals, while all other node signals can be discarded. Only a single excitation signal is required. The identification is performed by identifying the complete immersed network representation from which the target subnetwork is identified using a single parameter constraint.

Appendix

9.A Parameter vectors $\bar{\theta}$ and η

The target dynamics of the physical network (9.5) is parameterised in terms of $\bar{\theta} := \begin{bmatrix}\theta_{A_J}^\top & \theta_{A_D}^\top & \theta_B^\top\end{bmatrix}^\top$, with the parameter vectors of the polynomial matrices $A_{\mathcal{J}\mathcal{J}}(q^{-1}, \theta_{A_J})$, $A_{\mathcal{J}\mathcal{D}}(q^{-1}, \theta_{A_D})$, and $B_{J\bullet}(q^{-1}, \theta_B)$, respectively, given by

$$\theta_{A_J} = \begin{bmatrix}\theta_{a_{J1}}\\ \theta_{a_{J2}}\\ \vdots\\ \theta_{a_{JJ}}\end{bmatrix}, \qquad \theta_{a_{Ji}} = \begin{bmatrix}\theta_{a_{ii}}\\ \theta_{a_{ii\mathbf{1}}}\\ \vdots\\ \theta_{a_{iJ}}\end{bmatrix}, \qquad \theta_{a_{ij}} = \begin{bmatrix}a_{0,ij}\\ a_{1,ij}\\ \vdots\\ a_{n_A,ij}\end{bmatrix}, \tag{9.23a}$$

$$\theta_{A_D} = \begin{bmatrix}\theta_{a_{D1}}\\ \theta_{a_{D2}}\\ \vdots\\ \theta_{a_{DJ}}\end{bmatrix}, \qquad \theta_{a_{Di}} = \begin{bmatrix}\theta_{a_{i\boldsymbol{J1}}}\\ \theta_{a_{i\boldsymbol{J2}}}\\ \vdots\\ \theta_{a_{iD}}\end{bmatrix}, \qquad \theta_{a_{ij}} = \begin{bmatrix}a_{0,ij}\\ a_{1,ij}\\ \vdots\\ a_{n_A,ij}\end{bmatrix}, \tag{9.23b}$$

$$\theta_B = \begin{bmatrix}\theta_{b_1}\\ \theta_{b_2}\\ \vdots\\ \theta_{b_J}\end{bmatrix}, \qquad \theta_{b_i} = \begin{bmatrix}\theta_{b_{i1}}\\ \theta_{b_{i2}}\\ \vdots\\ \theta_{b_{iK}}\end{bmatrix}, \qquad \theta_{b_{ij}} = \begin{bmatrix}b_{0,ij}\\ b_{1,ij}\\ \vdots\\ b_{n_B,ij}\end{bmatrix}. \tag{9.23c}$$

Observe that $A(q^{-1})$ is parameterised symmetrically.

The immersed physical network model (9.6) is parameterised in terms of η. The parameter vectors of the polynomials $\breve{a}_{ij}(q^{-1}, \eta_{a_{ij}})$ and $\breve{b}_{ij}(q^{-1}, \eta_{b_{ij}})$ are respectively given by

$$\eta_{a_{ij}} = \begin{bmatrix}a_{0,ij}\\ a_{1,ij}\\ \vdots\\ a_{n_{\breve{A}},ij}\end{bmatrix}, \ j \geq i, \qquad \eta_{b_{ij}} = \begin{bmatrix}b_{0,ij}\\ b_{1,ij}\\ \vdots\\ b_{n_{\breve{B}},ij}\end{bmatrix}, \tag{9.24}$$

and as $\breve{A}(q^{-1})$ is symmetric, $\eta_{a_{ij}} = \eta_{a_{ji}}$ for $j \leq i$.

9.B Matrix $Q(\eta)$

In order to construct $Q(\eta)$, we first define some other matrices. Let $0_{i,j}$ denote a matrix of dimension $i \times j$ with all its elements equal to 0.

Let $\mathcal{T}_{i,j}(x)$ denote a Toeplitz matrix of dimension $i \times j$ (with $i \geq j$) given by

$$\mathcal{T}_{i,j}(x) := \mathcal{T}_{i,j}\left(\begin{bmatrix} x_0 & x_1 & \cdots & x_{i-1} \end{bmatrix}\right) = \begin{bmatrix} x_0 & & 0 \\ \vdots & \ddots & \\ x_{j-1} & \cdots & x_0 \\ \vdots & \ddots & \vdots \\ x_{i-1} & \cdots & x_{i-j-1} \end{bmatrix}. \tag{9.25}$$

Define the following block matrices

$$\Pi_i^a := \begin{bmatrix} \mathcal{T}_{k,n_A^+}(\tilde{a}_{i(J+1)}) \\ \vdots \\ \mathcal{T}_{k,n_A^+}(\tilde{a}_{iS}) \end{bmatrix}, \qquad \Pi_i^b := \begin{bmatrix} \mathcal{T}_{\ell,n_A^+}(\tilde{b}_{i1}) \\ \vdots \\ \mathcal{T}_{\ell,n_A^+}(\tilde{b}_{iK}) \end{bmatrix}, \tag{9.26}$$

of dimensions $Dk \times (n_A + 1)$ and $K\ell \times (n_A + 1)$, respectively, with $n_A^+ := n_A + 1$, $n_B^+ := n_B + 1$, $k := (n_A + n_{\tilde{A}} + 1)$, and $\ell := (n_A + n_{\tilde{B}} + 1)$.

For $x \in \{a, b\}$, define the block matrix

$$\bar{\Pi}_J^x := \begin{bmatrix} Z_{0,J}^x & Z_{1,J-1}^x & \cdots & Z_{J-1,1}^x \\ R(\Pi_1^x, \Pi_J^x) & R(\Pi_2^x, \Pi_J^x) & \cdots & R(\Pi_J^x, \Pi_J^x) \\ S_{J-1}(\Pi_1^x) & S_{J-2}(\Pi_2^x) & \cdots & S_{J-J}(\Pi_J^x) \end{bmatrix}, \tag{9.27}$$

with $Z_{i,j}^a$ an $i \times j$ block matrix with blocks $0_{Dk,(n_A+1)}$ and with $Z_{i,j}^b$ an $i \times j$ block matrix with blocks $0_{K\ell,(n_A+1)}$ (that is $Z_{i,j}^a := 0_{iDk,j(n_A+1)}$ and $Z_{i,j}^b := 0_{iK\ell,j(n_A+1)}$), with

$$R(\Pi_i^x, \Pi_j^x) := \begin{bmatrix} \Pi_i^x & \Pi_{i+1}^x & \cdots & \Pi_j^x \end{bmatrix}, \quad \text{for } i \leq j, \tag{9.28}$$

and with

$$S_i(\Pi_j^x) := \begin{bmatrix} Z_{i,1}^x & T_i(\Pi_j^x) \end{bmatrix} \tag{9.29}$$

with $T_i(\Pi_j^x)$ a block diagonal matrix consisting of i blocks of Π_j^x. Observe that $\bar{\Pi}_J^a$ has dimensions $JDk \times \frac{1}{2}J(J+1)(n_A+1)$ and $\bar{\Pi}_L^b$ has dimensions $JK\ell \times \frac{1}{2}J(J+1)(n_A+1)$.

Define $\bar{T}_{u,k,v}$ as an $J\times J$ block matrix with its (i, j)-th block equal to $T_{u,k,v}(\tilde{a}_{ij})$, where $T_{u,k,v}(\tilde{a}_{ij})$ is a block diagonal matrix consisting of u blocks of $\mathcal{T}_{k,v}(\tilde{a}_{ij})$.

With the matrices defined above, we can now describe the matrix $Q(\eta)$ in (9.19) by

$$Q(\eta) = \begin{bmatrix} \bar{\Pi}_J^a & \bar{T}_{D,k,n_A^+} & 0_{JDk,JKn_B^+} \\ \bar{\Pi}_J^b & 0_{JK\ell,JDn_A^+} & \bar{T}_{K,k,n_B^+} \end{bmatrix}, \tag{9.30}$$

which has dimensions $\big[J(Dk + K\ell)\big] \times J\big[(\frac{1}{2}(J + 1) + D)(n_A + 1) + K(n_B + 1)\big]$.

10 | Identifiability with partial instrumentation

This chapter adds Remark 10.18 to the work that is equivalent to

E.M.M. Kivits and P.M.J. Van den Hof. Identifiability of diffusively coupled linear networks with partial instrumentation. *Preprints of the 22nd IFAC World Congress*, 2706-2711, July 2023.

This chapter presents identifiability conditions for identifying the complete dynamics of diffusively coupled linear networks. These conditions are derived by exploiting the uniqueness of the nonmonic polynomial network description, given the locations of the actuators and sensors. The analysis is performed under a more relaxed instrumentation setup than the typical restriction to a full set of sensors (full measurement) or a full set of actuators (full excitation). This leads to more general identifiability conditions, including more flexible instrumentation requirements.

10.1 Introduction

In recent years, large-scale interconnected systems are receiving increasingly more attention. Diffusively coupled linear networks model interconnected systems with symmetric cause-effect relationships in the links. Examples are physical linear networks, which can describe many processes from different domains, such as electrical circuits, mechanical systems, and chemical and biological processes.

In the literature, there are several methods available for identifying the complete dynamics of diffusively coupled networks from data. For example, black-box

state-space models can be estimated from which the model parameters can be derived using eigenvalue decompositions (Friswell et al., 1999; Luş et al., 2003). De Angelis et al. (2002) concluded that the model parameters of a second-order model can be extracted from an (identified) state-space model if all nodes contain either a sensor or an actuator with at least one colocated sensor–actuator pair. Mukhopadhyay et al. (2014) made the same observation and further analysed instrumentation conditions and identifiability issues for shear-type systems. These methods are restricted to second-order models and typically do not consider disturbances. They also do not have any guarantees on the statistical accuracy of the estimates and lack a consistency analysis.

Van Waarde et al. (2018) considered undirected state-space models, which can be seen as first-order diffusively coupled linear networks with the states as nodes. Their identifiability analysis based on Markov parameters resulted in a specific subset of nodes that is required to have a colocated sensor-actuator pair. For higher-order diffusively coupled linear networks, the Markov parameters become more complex, which hinders the analysis.

Diffusively coupled networks can also be modelled as directed dynamic networks with specific structural properties (Chapter 7). These networks can be modelled as interconnections of transfer function modules (Gonçalves and Warnick, 2008; Van den Hof et al., 2013), for which an identification framework has been developed by Van den Hof et al. (2013). In this framework, the identifiability of the complete dynamics or a subset of the dynamics is analysed under partial instrumentation conditions (Bazanella et al., 2019; Cheng et al., 2023; Shi et al., 2023). However, the specific network model structure is generally lost, resulting in conservative conditions.

Hannan and Deistler (2012) analysed the identifiability of polynomial models. These models have the typical assumption of monicity and therefore do not fit the diffusively coupled linear network model, where monicity does not hold.

In this chapter, we follow the modelling approach of Chapter 8, who discuss the identification of the full diffusively coupled network dynamics in the case of full measurement, including detailed identifiability and consistency results. The objective of this chapter is to derive conditions for the identifiability of the full diffusively coupled network dynamics in the case that only some nodes are excited and only some node signals are measured. We do this by reviewing the identifiability results for the full measurement case, which are based on nonmonic matrix-fraction descriptions (MFDs) (Chapter 8 and Chapter 9), combining it with the dual situation of the full excitation case, and then formulating the conditions for the generalised case, involving MFDs with three polynomials.

The networks that will be considered are defined in Section 10.2. Section 10.3

defines identifiability. Section 10.4 recaps the identifiability conditions for full measurement and Section 10.5 describes the dual conditions for full excitation. Section 10.6 presents the main result: identifiability conditions for partial instrumentation. Finally, section 10.7 concludes the chapter. For simplicity, we restrict to representations in the discrete-time domain. This chapter is equivalent to Kivits and Van den Hof (2023a) with Remark 10.18 added to it.

We consider the following notation throughout the chapter: A polynomial matrix $A(q^{-1})$ consists of matrices A_ℓ and (j,k)th polynomial elements $a_{jk}(q^{-1})$ such that $A(q^{-1}) = \sum_{\ell=0}^{n_a} A_\ell q^{-\ell}$ and $a_{jk}(q^{-1}) = \sum_{\ell=0}^{n_a} a_{jk,\ell} q^{-\ell}$. Hence, the (j,k)th element of the matrix A_ℓ is denoted by $a_{jk,\ell}$. Let $A_{C\mathcal{Z}}(q^{-1})$, $A_{C\bullet}(q^{-1})$, and $A_{\bullet\mathcal{Z}}(q^{-1})$ indicate all $a_{jk}(q^{-1})$, $a_{jm}(q^{-1})$, and $a_{mk}(q^{-1})$ with $j \in C$ and $k \in \mathcal{Z}$, respectively. Let $det(A)$ and $adj(A)$ denote the determinant and adjugate of $A(q^{-1})$, respectively.

10.2 Diffusively coupled network

10.2.1 Diffusive couplings

Diffusive couplings describe an interaction that depends on the difference between the signals of interest (or nodes). The nodes can also have diffusive couplings with a zero node (or ground node). In line with Chapter 8, the behaviour of each node signal $w_j(t)$ can be described by

$$\sum_{\ell=0}^{n_x} \mathsf{x}_{jj,\ell} w_j^{(\ell)}(t) + \sum_{k\in\mathcal{N}_j} \sum_{\ell=0}^{n_y} \mathsf{y}_{jk,\ell} \left[w_j^{(\ell)}(t) - w_k^{(\ell)}(t) \right] = u_j(t), \tag{10.1}$$

with n_x and n_y the order of the dynamics in the network; with $\mathcal{N}_j$ the set of indices of all neighbour nodes of $w_j(t)$; with real-valued coefficients $\mathsf{x}_{jj,\ell} \geq 0$ and $\mathsf{y}_{jk,\ell} = \mathsf{y}_{kj,\ell} \geq 0$; where $w^{(\ell)}(t)$ is the ℓth derivative of $w_j(t)$; and where $u_j(t)$ is the external signal entering the jth node. Combining the expressions (10.1) in a matrix equation gives

$$X(p)w(t) + Y(p)w(t) = u(t), \tag{10.2}$$

with differential operator p, i.e. $p^\ell w(t) = w^{(\ell)}(t)$; with diagonal polynomial matrix $X(p)$, with $x_{jj}(p) = \sum_{\ell=0}^{n_x} \mathsf{x}_{jj,\ell} p^\ell$, containing the components intrinsically related to the nodes (e.g. in the couplings with the zero node); with Laplacian[1]

[1] A Laplacian matrix is a symmetric matrix with nonpositive off-diagonal elements and with nonnegative diagonal elements that are equal to the negative sum of all other elements in the same row (or column) (Mesbahi and Egerstedt, 2010).

polynomial matrix $Y(p)$, with $y_{jk}(p) = -\sum_{\ell=0}^{n_y} \mathsf{y}_{jk,\ell} p^\ell$ if $k \in \mathcal{N}_j$ and $y_{jk}(p) = 0$ if $k \notin \{\mathcal{N}_j, j\}$, containing the components in the diffusive couplings between the nodes.

Examples of diffusively coupled networks are physical networks, such as electrical circuits, which are characterised by their symmetric components that imply diffusive couplings. For example, a resistor describes the relation between the current and the difference in electric potential on each side of the resistor. A physical network typically exhibits second-order dynamics between all node signals. Generalising to include higher-order dynamics is particularly useful for describing a selection of (measured) node signals by removing the other (unmeasured) node signals through a Gaussian elimination procedure (called immersion or Kron reduction (Dankers et al., 2016; Dörfler and Bullo, 2013)).

To exploit the network identification results that have been developed for discrete-time systems, a backward difference method (describing a bijective mapping) is used to approximate (10.2) by the equivalent form

$$\bar{X}(q^{-1})w(t) + \bar{Y}(q^{-1})w(t) = u(t), \tag{10.3}$$

with delay operator q^{-1}, i.e. $q^{-1}w(t) = w(t-1)$, and with $\bar{X}(q^{-1})$ and $\bar{Y}(q^{-1})$ having the same structural properties as $X(p)$ and $Y(p)$, respectively. In the sequel, we will use $A(q^{-1}) = \bar{X}(q^{-1}) + \bar{Y}(q^{-1})$, from which $\bar{X}(q^{-1})$ and $\bar{Y}(q^{-1})$ can uniquely be recovered due to their structure.

10.2.2 Network model

As explained in Section 10.2.1, diffusively coupled networks exhibit a symmetric interaction between nodes. We define these networks in line with Chapter 8.

Definition 10.1 (Diffusively coupled linear network model). *A* diffusively coupled linear network model *consists of L internal node signals $w_j(t)$, $j = 1, \dots, L$; $K \leq L$ known excitation signals $r_j(t)$, $j = 1, \dots, K$; L unknown disturbance signals $v_j(t)$, $j = 1, \dots, L$; and $c \leq L$ measured signals $y_j(t)$, $j = 1, \dots, c$ and is defined as*

$$A(q^{-1})w(t) = B(q^{-1})r(t) + v(t), \quad y(t) = C(q^{-1})w(t), \tag{10.4}$$

with $w(t)$, $r(t)$, $v(t)$, and $y(t)$ vectorised versions of $w_j(t)$, $r_j(t)$, $v_j(t)$, and $y_j(t)$, respectively; with $v(t)$ modelled as filtered white noise, i.e. $v(t) = F(q)e(t)$ with $e(t)$ a vector-valued white noise process; and with

1. *$A(q^{-1}) = \sum_{k=0}^{n_a} A_k q^{-k} \in \mathbb{R}^{L \times L}[q^{-1}]$, with $A^{-1}(q^{-1})$ stable;*

rank$(A_0) = L$; *and* $a_{jk}(q^{-1}) = a_{kj}(q^{-1})\ \forall k, j$.

2. $B(q^{-1}) = \begin{bmatrix}\tilde{B}^\top(q^{-1}) & 0\end{bmatrix}^\top \in \mathbb{R}^{L\times K}[q^{-1}]$, *with* $\tilde{B}(q^{-1}) \in \mathbb{R}^{K\times K}[q^{-1}]$; *and* $\tilde{b}_{jk}(q^{-1}) = 0,\ \forall j,\ j \neq k$.

3. $C(q^{-1}) = \begin{bmatrix}0 & \bar{C}(q^{-1})\end{bmatrix} \in \mathbb{R}^{c\times L}[q^{-1}]$, *with* $\bar{C}(q^{-1}) \in \mathbb{R}^{c\times c}[q^{-1}]$; *rank*$(\bar{C}_0) = c$; *and* $\bar{c}_{jk}(q^{-1}) = 0,\ \forall j,\ j \neq k$.

4. $F(q) \in \mathbb{R}^{L\times L}(q)$, *monic, stable, and stably invertible.*

5. $\Lambda \succ 0$ *the covariance matrix of the noise* $e(t)$.

Assumption 10.2 (Connected and well-posed). *It is assumed that the network* (10.4) *is:*

1. *Connected: Every pair of nodes yields a path*[a].

2. *Well-posed:* $A^{-1}(q^{-1})$ *exists and is proper.*

[a]The network is connected if its Laplacian matrix (i.e. the degree matrix minus the adjacency matrix) has a positive second-smallest eigenvalue (Fiedler, 1973).

The polynomial matrices $A(q^{-1})$, $B(q^{-1})$, and $C(q^{-1})$ are nonmonic. Stability of the network is induced by the stability of $A^{-1}(q^{-1})$. The diffusive character of the model is represented by the symmetry of $A(q^{-1})$. The polynomial $a_{jk}(q^{-1})$ characterises the dynamics in the link between node signals $w_j(t)$ and $w_k(t)$. Due to the diagonal structure in $B(q^{-1})$ and $C(q^{-1})$, the first K nodes are excited and the last c node signals are measured. Often, $B(q^{-1})$ and $C(q^{-1})$ are chosen to be binary, implying that each excitation signal directly enters the network at a distinct node and that each measured signal is directly extracted from distinct internal node signals. If $F(q)$ is polynomial or even stronger if $F(q) = I$, the network (10.4) leads to an ARMAX-like or ARX-like[2] model structure, respectively.

The input-output mapping of (10.4) is given by

$$y(t) = T_{yr}(q)r(t) + \bar{v}(t), \quad \bar{v}(t) = T_{ye}(q)e(t), \tag{10.5}$$

with

$$T_{yr}(q) = C(q^{-1})A^{-1}(q^{-1})B(q^{-1}), \tag{10.6a}$$

[2]The structure is formally only an ARMAX (autoregressive-moving average with exogenous variables) or ARX (autoregressive with exogenous variables) structure if the $A(q^{-1})$ polynomial is monic (Hannan and Deistler, 2012).

$$T_{ye}(q) = C(q^{-1})A^{-1}(q^{-1})F(q), \tag{10.6b}$$

$$\Phi_{\bar{v}}(\omega) = T_{ye}(e^{i\omega})\Lambda T_{ye}^{*}(e^{i\omega}), \tag{10.6c}$$

with $(\cdot)^*$ the complex conjugate transpose. A standard open-loop identification of (10.5) can typically lead to consistent estimation of $T_{yr}(q)$ and $\Phi_{\bar{v}}(\omega)$. Observe that for binary $B(q^{-1})$ and $C(q^{-1})$, (10.6a) leads to a subset of rows and columns of $A^{-1}(q^{-1})$ that constitute $T_{yr}(q)$.

10.3 Identifiability

Identifiability concerns the ability to distinguish between different models in a network model set, given the locations of the external signals in the network. Therefore, identifiability can be analysed by exploiting the uniqueness of network models.

Definition 10.3 (Equivalent network models). *The two network models* $M_1 = \left(A_1(q^{-1}), B_1(q^{-1}), C_1(q^{-1}), F_1(q), \Lambda_1\right)$ *and* $M_2 = \left(A_2(q^{-1}), B_2(q^{-1}), C_2(q^{-1}), F_2(q), \Lambda_2\right)$ *are* equivalent *if*

$$T_{yr,1}(q) = T_{yr,2}(q) \;\; \textit{and} \;\; \Phi_{\bar{v},1}(\omega) = \Phi_{\bar{v},2}(\omega). \tag{10.7}$$

This concept of equivalent network models implies that two network models can model the same measured data (y, r), because both models will have the same transfer function $T_{yr}(q)$ and power spectrum $\Phi_{\bar{v}}(\omega)$. Exploiting the spectral factorisation of $\Phi_{\bar{v}}(\omega)$ (10.6c) leads to an equivalent network model with a simplified noise model. This result is analogous to Shi et al. (2023, Theorem 1).

Proposition 10.4 (Noise model). *Any network model*

$$M = \left(A(q^{-1}), B(q^{-1}), C(q^{-1}), F(q), \Lambda\right) \tag{10.8}$$

admits an equivalent network model

$$\tilde{M} \triangleq \left(A(q^{-1}), B(q^{-1}), C(q^{-1}), \begin{bmatrix} 0 & \tilde{F}^{*}(q) \end{bmatrix}^{*}, \tilde{\Lambda}\right), \tag{10.9}$$

where $\tilde{F}(q) \in \mathbb{R}^{c\times c}(q)$ *is monic, stable, and stably invertible and* $\tilde{\Lambda} \in \mathbb{R}^{c\times c} \succ 0$.

Proof: The proof is provided in Appendix 10.A. ∎

As $T_{yr}(q)$ and $\Phi_{\bar{v}}(\omega)$ only reflect the properties of the measured nodes, there is freedom in transforming the unmeasured internal signals and in modelling the

disturbances affecting the measured signals. In $\tilde{M}$, all unmeasured node signals are disturbance-free. Hence, there are multiple models M (with different noise processes) that admit the same equivalent model $\tilde{M}$. As $\tilde{M}$ admits a simpler noise model, it is more attractive for the identifiability analysis.

Before defining the model set corresponding to the models $\tilde{M}$, let us take a deeper look at the power spectrum $\Phi_{\bar{v}}(\omega)$. As $T_{y\tilde{e}}(q) = C(q^{-1})A^{-1}(q^{-1})\begin{bmatrix}0 & \tilde{F}^*(q)\end{bmatrix}^*$ is not monic, the spectral factorisation of $\Phi_{\bar{v}}(\omega)$ into $T_{y\tilde{e}}(e^{i\omega})$ and $\tilde{\Lambda}$ is not unique. However, the spectral factorisation of $\Phi_{\bar{v}}(\omega)$ can be made unique by properly scaling $T_{y\tilde{e}}(e^{i\omega})$ and $\tilde{\Lambda}$.

Proposition 10.5 (Spectral factorisation). *The power spectrum $\Phi_{\bar{v}}(\omega)$ admits a unique* spectral factorisation *into $T_{y\breve{e}}(e^{i\omega})$ and $\breve{\Lambda}$, where $T_{y\breve{e}}(q) = \bar{C}(q^{-1})\bar{A}^{-1}(q^{-1})\breve{F}(q)$ is monic, with $\breve{F}(q) = \tilde{F}(q)\bar{A}_0\bar{C}_0^{-1}$, and $\breve{\Lambda} = \bar{C}_0\bar{A}_0^{-1}\tilde{\Lambda}\bar{A}_0^{-1}\bar{C}_0^{\top} \succ 0$.*

Proof: Redefine the noise model $\bar{v}(t) = \tilde{F}(q)\tilde{e}(t)$ as $\bar{v}(t) = \breve{F}(q)\breve{e}(t)$ with $\breve{F}(q) = \tilde{F}(q)\bar{A}_0\bar{C}_0^{-1}$ and with $\breve{\Lambda} \succ 0$ the covariance of $\breve{e}(t)$. Then $\Phi_{\bar{v}}(\omega) = T_{y\breve{e}}(e^{i\omega})\breve{\Lambda}T_{y\breve{e}}^*(e^{i\omega})$, which admits a unique spectral factorisation into $T_{y\breve{e}}(e^{i\omega})$ and $\breve{\Lambda}$ as $T_{y\breve{e}}(q)$ is monic, stable, and stably invertible and $\breve{\Lambda} \succ 0$ (Youla, 1961). ■

Now, let us define the model set of the models (10.9).

Definition 10.6 (Network model set). *The* network model set $\tilde{\mathcal{M}}$ *is defined as a set of parameterised functions as*

$$\tilde{\mathcal{M}} := \{\tilde{M}(\theta),\ \theta \in \Theta \subset \mathbb{R}^d\}, \tag{10.10}$$

with $d \in \mathbb{N}$ and with all particular models

$$\tilde{M}(\theta) := \left(A(q^{-1},\theta),\ B(q^{-1},\theta),\ C(q^{-1},\theta),\ \begin{bmatrix}0 & \tilde{F}^*(q,\theta)\end{bmatrix}^*,\ \tilde{\Lambda}(\theta)\right) \tag{10.11}$$

satisfying the properties in Definition 10.1 and Assumption 10.2, where Property 4 of Definition 10.1 is replaced by

(4) $\tilde{F}(q) \in \mathbb{R}^{c\times c}(q)$, monic, stable, and stably invertible.

Here, θ contains all the unknown coefficients that appear in the entries of the model matrices $A(q^{-1})$, $B(q^{-1})$, $C(q^{-1})$, $\tilde{F}(q)$, and $\tilde{\Lambda}$.

Since the network models that will be considered and the corresponding network model set have been defined, we can now continue with the identifiability

analysis. Let us adopt the concept of network identifiability from Weerts et al. (2018b).

Definition 10.7 (Global network identifiability). *The network model set $\tilde{\mathcal{M}}$ is* globally network identifiable *from data $z(t) := \{y(t), r(t)\}$ if the parameterised model $\tilde{M}(\theta)$ can uniquely be recovered from $T_{yr}(q,\theta)$ and $\Phi_{\bar{v}}(\omega,\theta)$, that is, if for all models $\tilde{M}(\theta_1), \tilde{M}(\theta_2) \in \tilde{\mathcal{M}}$*

$$\left.\begin{aligned} T_{yr}(q,\theta_1) &= T_{yr}(q,\theta_2) \\ \Phi_{\bar{v}}(\omega,\theta_1) &= \Phi_{\bar{v}}(\omega,\theta_2) \end{aligned}\right\} \implies \tilde{M}(\theta_1) = \tilde{M}(\theta_2). \tag{10.12}$$

Using the result of Proposition 10.5 on the power spectral factorisation of $\Phi_{\bar{v}}(\omega)$, we have the following identifiability result:

Proposition 10.8 (Global network identifiability). *For a network model set $\tilde{\mathcal{M}}$, implication* (10.12) *can equivalently be formulated as*

$$\left.\begin{aligned} T_{yr}(q,\theta_1) &= T_{yr}(q,\theta_2) \\ T_{y\check{e}}(q,\theta_1) &= T_{y\check{e}}(q,\theta_2) \\ \check{\Lambda}(\theta_1) &= \check{\Lambda}(\theta_2) \end{aligned}\right\} \implies \tilde{M}(\theta_1) = \tilde{M}(\theta_2). \tag{10.13}$$

Proof: From Proposition 10.5, $T_{y\check{e}}(q)$ and $\check{\Lambda}$ are uniquely determined by $\Phi_{\bar{v}}(\omega)$ and therefore, $\Phi_{\bar{v}}(\omega,\theta)$ in (10.12) can be replaced by $T_{y\check{e}}(q,\theta)$ and $\check{\Lambda}(\theta)$. ■

10.4 Full measurement

Consider a network as defined in Definition 10.1, where all node signals are directly measured. This is the most common instrumentation setting for identification in dynamic networks. Let us recap the corresponding identifiability conditions of Chapter 8 and Chapter 9.

Assumption 10.9 (Full measurement). *Assume $C(q^{-1}) = I$.*

Observe that in this case $\tilde{F} = F$ and thus $\tilde{M} = M$. The identifiability analysis is based on the uniqueness of the network model. Therefore, we present a result on the left MFD (LMFD), before formulating the identifiability conditions for our particular network models.

Lemma 10.10 (LMFD). *Consider a network model set $\tilde{\mathcal{M}}$ satisfying Assumption 10.9. Given the* LMFD $A(q^{-1})^{-1}B(q^{-1})$, $A(q^{-1})$ *and* $B(q^{-1})$ *are unique within $\tilde{\mathcal{M}}$ up to a scalar factor if the following conditions are satisfied:*

1. *$A(q^{-1})$ and $B(q^{-1})$ are left coprime in $\tilde{\mathcal{M}}$.*
2. *There exists a permutation matrix P_b such that within $\tilde{\mathcal{M}}$, $\begin{bmatrix} A_0 & A_1 & \cdots & A_{n_a} & B_0 & B_1 & \cdots & B_{n_b} \end{bmatrix} P_b = \begin{bmatrix} D_b & R_b \end{bmatrix}$ with D_b square, diagonal, and full rank.*

Proof: According to Kailath (1980), the LMFD of any two polynomial and left coprime matrices is unique up to a premultiplication with a unimodular matrix. To satisfy Condition 2, the unimodular matrix is restricted to being diagonal. As $A(q^{-1})$ is symmetric, this diagonal matrix is further restricted to having equal elements. ■

In general polynomial models, like ARMAX (Deistler, 1983), $A(q^{-1})$ is monic, i.e. $A_0 = I$. Then the LMFD $A(q^{-1})^{-1}B(q^{-1})$ is unique, as the conditions of Lemma 10.10 are satisfied and scaling with a scalar factor is not possible anymore. Hence, both Condition 2 in Lemma 10.10 and the scaling factor freedom are a result of the fact that $A(q^{-1})$ is not necessarily monic.

Now the conditions for global network identifiability can be formulated.

Proposition 10.11 (Identifiability full measurement). *A network model set $\tilde{\mathcal{M}}$ satisfying Assumption 10.9 is* globally network identifiable *from $z(t)$ if the following conditions are satisfied:*

1. *$A(q^{-1})$ and $B(q^{-1})$ are left coprime in $\tilde{\mathcal{M}}$.*
2. *There exists a permutation matrix P_b such that within $\tilde{\mathcal{M}}$, $\begin{bmatrix} A_0 & A_1 & \cdots & A_{n_a} & B_0 & B_1 & \cdots & B_{n_b} \end{bmatrix} P_b = \begin{bmatrix} D_b & R_b \end{bmatrix}$ with D_b square, diagonal, and full rank.*
3. *At least one excitation signal $r_j(t)$, $j = 1, \ldots, K$, is present: $K \geq 1$.*
4. *There is at least one constraint on the parameters of $A(q^{-1}, \theta_a)$ and $B(q^{-1}, \theta_c)$ of the form $\Gamma\theta_{ab} = \gamma \neq 0$, with Γ full row rank and with $\theta_{ab} := \begin{bmatrix} \theta_a^\top & \theta_b^\top \end{bmatrix}^\top$.*

Proof: Condition 3 implies that $T_{yr}(q, \theta)$ is nonzero. According to Lemma 10.10, Condition 1 and 2 imply that $A(q^{-1}, \theta)$ and $B(q^{-1}, \theta)$ are unique up to a scalar factor α. According to Proposition 10.5, $T_{y\breve{e}}(q, \theta)$ and $\breve{\Lambda}(\theta)$ are uniquely

recovered from $\Phi_{\bar{v}}(\omega, \theta)$. Together with the fact that $A(q^{-1}, \theta)$ is unique up to a scalar factor α, $T_{y\breve{e}}(q, \theta)$ gives a unique $\tilde{F}(q, \theta)$, and $\breve{\Lambda}(\theta)$ gives $\tilde{\Lambda}(\theta)$ up to a scalar factor α^2. Finally, Condition 4 implies that α is unique. ■

10.5 Full excitation

Consider a network as defined in Definition 10.1, where now all node signals are directly excited. This is the dual instrumentation setting compared to the full measurement setup in Section 10.4. In this section, we present the identifiability conditions for networks with full excitation.

Assumption 10.12 (Full excitation). *Assume* $B(q^{-1}) = I$.

Again, the identifiability analysis is based on the uniqueness of the network model. Here, we present a result on the right MFD (RMFD), before formulating the identifiability conditions for our particular network models.

Lemma 10.13 (RMFD). *Consider a network model set* $\tilde{\mathcal{M}}$ *satisfying Assumptions 10.12. Given the* RMFD $C(q^{-1},)A(q^{-1},)^{-1}$, $C(q^{-1})$ *and* $A(q^{-1})$ *are unique within* $\tilde{\mathcal{M}}$ *up to a scalar factor if the following conditions are satisfied:*

1. $A(q^{-1})$ *and* $C(q^{-1})$ *are right coprime in* $\tilde{\mathcal{M}}$.
2. *There exists a permutation matrix* P_c *such that within* $\tilde{\mathcal{M}}$, $\begin{bmatrix} A_0 & A_1 & \cdots & A_{n_a} & C_0 & C_1 & \cdots & C_{n_c} \end{bmatrix} P_c = \begin{bmatrix} D_c & R_c \end{bmatrix}$ *with* D_c *square, diagonal, and full rank.*

Proof: According to Kailath (1980), the RMFD of any two polynomial and right coprime matrices is unique up to a postmultiplication with a unimodular matrix. To satisfy Condition 2, the unimodular matrix is restricted to being diagonal. As $A(q^{-1})$ is symmetric, this diagonal matrix is further restricted to having equal elements. ■

Similar to Section 10.4, a monic $A(q^{-1})$ implies that the RMFD $C(q^{-1})A(q^{-1})^{-1}$ is unique, as the conditions of Lemma 10.13 are satisfied and scaling with a scalar factor is not possible anymore. Hence, again, Condition 2 in Lemma 10.13 and the scaling factor freedom are a result of the fact that $A(q^{-1})$ is not necessarily monic.

Now the conditions for global network identifiability can be formulated.

Proposition 10.14 (Identifiability full excitation). *A network model set $\tilde{\mathcal{M}}$ satisfying Assumption 10.12 is* globally network identifiable *from $z(t)$ if the following conditions are satisfied:*

1. *$A(q^{-1})$ and $C(q^{-1})$ are right coprime in $\tilde{\mathcal{M}}$.*
2. *There exists a permutation matrix P_c such that within $\tilde{\mathcal{M}}$, $\begin{bmatrix} A_0 & A_1 & \cdots & A_{n_a} & C_0 & C_1 & \cdots & C_{n_c} \end{bmatrix} P_c = \begin{bmatrix} D_c & R_c \end{bmatrix}$ with D_c square, diagonal, and full rank.*
3. *At least one measured signal $y_j(t)$, $j = 1, \ldots, c$, is present: $c \geq 1$.*
4. *There is at least one constraint on the parameters of $A(q^{-1}, \theta_a)$ and $C(q^{-1}, \theta_c)$ of the form $\Gamma\theta_{ac} = \gamma \neq 0$, with Γ full row rank and with $\theta_{ac} := \begin{bmatrix} \theta_a^\top & \theta_c^\top \end{bmatrix}^\top$.*

Proof: The proof is fully dual to the proof of Proposition 10.11. ■

10.6 Partial instrumentation

10.6.1 Network model analysis

This section contains the main results, which are the identifiability conditions for networks with partial instrumentation. Consider a network as defined in Definition 10.1, where now all node signals are either measured or excited and at least one node signal is both measured and excited:

Assumption 10.15 (Partial instrumentation). *Assume $K + c \geq L + 1$.*

As before, the analysis is based on the uniqueness of the network model. We present a result on the MFD, before formulating the identifiability conditions for our particular network models.

Lemma 10.16 (MFD). *For a network model set $\tilde{\mathcal{M}}$ satisfying Assumptions 10.15, the* MFD *$C(q^{-1})A(q^{-1})^{-1}B(q^{-1},)$, gives unique $C(q^{-1})$, $A(q^{-1})$, and $B(q^{-1})$ within $\tilde{\mathcal{M}}$ if the following conditions are satisfied:*

1. *$A(q^{-1})$ and $B(q^{-1})$ are left coprime in $\tilde{\mathcal{M}}$.*
2. *$A(q^{-1})$ and $C(q^{-1})$ are right coprime in $\tilde{\mathcal{M}}$.*

3. *There exists a permutation matrix P_b such that within $\tilde{\mathcal{M}}$, $\begin{bmatrix} A_0 & A_1 & \cdots & A_{n_a} & B_0 & B_1 & \cdots & B_{n_b} \end{bmatrix} P_b = \begin{bmatrix} D_b & R_b \end{bmatrix}$ with D_b square, diagonal, and full rank.*

4. *There exists a permutation matrix P_c such that within $\tilde{\mathcal{M}}$, $\begin{bmatrix} A_0 & A_1 & \cdots & A_{n_a} & C_0 & C_1 & \cdots & C_{n_c} \end{bmatrix} P_c = \begin{bmatrix} D_c & R_c \end{bmatrix}$ with D_c square, diagonal, and full rank.*

5. *For each $k = 1, 2, \ldots, L$, there is a nonzero linear equality constraint on the parameters related to node $w_k(t)$, i.e. on $a_{\ell k}(q^{-1}, \theta)$, $b_{kk}(q^{-1}, \theta)$, or $c_{kk}(q^{-1}, \theta)$. These L constraints are on L different polynomials.*

6. *There is at least one extra constraint on the parameters of $A(q^{-1}, \theta_a)$, $B(q^{-1}, \theta_b)$, and $C(q^{-1}, \theta_c)$ of the form $\Gamma\theta_{abc} = \gamma \neq 0$, with Γ full row rank and with $\theta_{abc} := \begin{bmatrix} \theta_a^\top & \theta_b^\top & \theta_c^\top \end{bmatrix}^\top$.*

Proof: The proof is provided in Appendix 10.B. ■

Condition 5 and 6 of Lemma 10.16 can, for example, be satisfied by binary $B(q^{-1})$ and $C(q^{-1})$, implying that nodes are directly excited and measured, respectively. Condition 6 of Lemma 10.16 is similar to Condition 4 of Propositions 10.11 and 10.14.

Now the main results of this paper are formulated, which are the conditions for global network identifiability for diffusively coupled networks with partial instrumentation.

Theorem 10.17 (Identifiability partial instrumentation). *A network model set $\tilde{\mathcal{M}}$ satisfying Assumption 10.15 is* globally network identifiable *from $z(t)$ if the conditions in Lemma 10.16 are satisfied.*

Proof: Assumption 10.15 implies that $K \geq 1$ and $c \geq 1$ and thus $T_{yr}(q, \theta)$ is nonzero. Lemma 10.16 implies that $A(q^{-1}, \theta)$, $B(q^{-1}, \theta)$, and $C(q^{-1}, \theta)$ are uniquely found from $T_{yr}(q, \theta)$. According to Proposition 10.5, $T_{y\check{e}}(q, \theta)$ and $\check{\Lambda}(\theta)$ are uniquely recovered from $\Phi_{\bar{v}}(\omega, \theta)$. Together with the fact that $A(q^{-1}, \theta)$ and $C(q^{-1}, \theta)$ are unique, $T_{y\check{e}}(q, \theta)$ gives a unique $\tilde{F}(q, \theta)$, and $\check{\Lambda}(\theta)$ gives a unique $\tilde{\Lambda}(\theta)$. ■

$A(q^{-1}, \theta)$, $B(q^{-1}, \theta)$, and $C(q^{-1}, \theta)$ are uniquely determined from $T_{yr}(q, \theta)$, where the required constraints can be imposed on actuators and sensors locations only. $\Phi_{\bar{v}}(\omega, \theta)$ is used to determine $\tilde{F}(q, \theta)$ and $\tilde{\Lambda}(\theta)$. Extracting information from $\Phi_{\bar{v}}(\omega, \theta)$ on $A(q^{-1}, \theta)$ and $C(q^{-1}, \theta)$ is limited by the non-monicity of these

polynomials. In the special case of a known $C(q^{-1})$ and a polynomial $F(q,\theta)$, $T_{y\check{e}}(q^{-1},\theta)$ can lead to $A(q^{-1},\theta)$ under L additional constraints on the network *dynamics* $A(q^{-1},\theta)$.

10.6.2 Transfer function analysis

The role of the partial instrumentation condition in Assumption 10.15, can also be understood from analysing $T_{yr}(q)$ in (10.6a), which shows that the input dynamics in $B(q^{-1})$ and the output dynamics in $C(q^{-1})$ have an equivalent influence on $T_{yr}(q)$. For simplicity, we restrict to binary B and C in this section. An equivalent analysis is presented by De Angelis et al. (2002) for identifying disturbance-free second-order models from first-order state-space models.

For full instrumentation, $B = I$ and $C = I$. Then $T_{yr}(q^{-1}) = A^{-1}(q^{-1})$ and $A(q^{-1})$ can directly be obtained from $T_{yr}(q^{-1})$. For full measurement, $C = I$ and at least one excitation signal is required, e.g. at $w_i(t)$. Then $T_{yr}(q^{-1}) = (A^{-1})_{\bullet i}(q^{-1})$, i.e. the ith column of $A^{-1}(q^{-1})$. Due to symmetry, the ith row of $A^{-1}(q^{-1})$ is also known. For full excitation, $B = I$ and at least one measured signal is required, e.g. $w_i(t)$. Then $T_{yr}(q^{-1}) = (A^{-1})_{i\bullet}(q^{-1})$, i.e. the ith row of $A^{-1}(q^{-1})$. Due to symmetry, the ith column of $A^{-1}(q^{-1})$ is also known. It might seem surprising that knowing only the ith row and column of $A^{-1}(q^{-1})$ is sufficient for uniquely determining $A(q^{-1})$, but this is due to the symmetry and the other conditions in Propositions 10.11 and 10.14. Observe the equivalent influence of excitations and measurements on the identifiability of $A(q^{-1})$.

Partial instrumentation requires at least one node signal to be both excited and measured, e.g. $w_i(t)$. Then $K + c = L + 1$, $B = \begin{bmatrix} I_K & 0 \end{bmatrix}^\top$, and $C = \begin{bmatrix} 0 & I_c \end{bmatrix}$, with I_j the identity matrix of size $j \times j$. Then $T_{yr}(q^{-1}) = [A^{-1}]_{C\mathcal{K}}(q^{-1})$, i.e. all $[a^{-1}]_{jk}(q^{-1})$, with $j \in C \triangleq \{j \mid L{+}1{-}c \leq j \leq L\}$ and $k \in \mathcal{K} \triangleq \{j \mid 1 \leq j \leq K\}$. Due to symmetry, all $[a^{-1}]_{kj}(q^{-1})$, with $j \in C$ and $k \in \mathcal{K}$ are also known. As $C \cap \mathcal{K} = \{i\}$, the complete ith row and ith column of $A^{-1}(q^{-1})$ are known, which is sufficient for uniquely determining $A(q^{-1})$. In other words, it is possible to transform the partial instrumentation case (satisfying Assumption 10.15) to the full measurement or full excitation case if at least one node signal is both excited and measured.

Remark 10.18 (Module representation). *In the literature, the identifiability of the complete dynamics or a subset of the dynamics is analysed for module representations with partial instrumentation conditions (Bazanella et al., 2019; Cheng et al., 2023; Shi et al., 2023). These analyses lead to conditions on the rank of the overall input-output transfer function, which*

can be translated into graphical conditions in terms of vertex-disjoint paths, disconnecting sets, and (pseudo-/anti-)tree coverings. These conditions imply requirements for the number and locations of external excitation signals and node signal measurements.
In contrast, very simple and more relaxed identifiability conditions are presented in this chapter for the identification of diffusively coupled networks with partial instrumentation. This simplification is due to the symmetry that is present in the network model, which restricts the network dynamics sufficiently to achieve identifiability with only very simple requirements on instrumentation locations.

10.7 Conclusion

Identifiability conditions for identifying the complete dynamics of diffusively coupled linear networks have been formulated. Analysing the uniqueness of the network description leads to more flexible instrumentation requirements than requiring to measure all node signals or to excite all node signals. For identifiability, it is sufficient to either measure or excite each node signal and to both measure and excite (at least) one node signal.

Appendix

10.A Proof of Proposition 10.4

Omit the arguments q, q^{-1}, ω, and $e^{i\omega}$ for notational simplicity. The behaviour of the measured signals $y(t)$ is described in an immersed network model, which is obtained by eliminating the unmeasured signals (through immersion or Kron reduction (Dankers et al., 2016; Dörfler and Bullo, 2013)). Partition the internal signals as $w(t) = \begin{bmatrix} w_{\mathcal{Z}}^\top(t) & w_C^\top(t) \end{bmatrix}^\top$, such that $y(t) = \bar{C} w_C(t)$. Partition A, B, and F accordingly and define

$$\begin{aligned} \bar{A} &\triangleq d_{\mathcal{Z}\mathcal{Z}} \left(A_{CC} - A_{C\mathcal{Z}} A_{\mathcal{Z}\mathcal{Z}}^{-1} A_{\mathcal{Z}C} \right), \\ \bar{B} &\triangleq d_{\mathcal{Z}\mathcal{Z}} \left(B_{C\bullet} - A_{C\mathcal{Z}} A_{\mathcal{Z}\mathcal{Z}}^{-1} B_{\mathcal{Z}\bullet} \right), \\ \bar{F} &\triangleq d_{\mathcal{Z}\mathcal{Z}} \left(F_{C\bullet} - A_{C\mathcal{Z}} A_{\mathcal{Z}\mathcal{Z}}^{-1} F_{\mathcal{Z}\bullet} \right), \\ d_{\mathcal{Z}\mathcal{Z}} &\triangleq \frac{det(A_{\mathcal{Z}\mathcal{Z}})}{gcd\left(det(A_{\mathcal{Z}\mathcal{Z}}), adj(A_{\mathcal{Z}\mathcal{Z}})\right)}, \end{aligned}$$

so that $\bar{A}$ and $\bar{B}$ are polynomial (Chapter 9). The immersed network model is now given by

$$\bar{A} w_C(t) = \bar{B} r(t) + \bar{F} e(t), \quad y(t) = \bar{C} w_C(t),$$

which has input-output mapping

$$y(t) = \bar{C} \bar{A}^{-1} \bar{B} r(t) + \bar{C} \bar{A}^{-1} \bar{F} e(t).$$

Together with (10.5), (10.6b), and (10.6c) this gives

$$\Phi_{\tilde{v}} = C A^{-1} F \Lambda F^* A^{-*} C^* = \bar{C} \bar{A}^{-1} \bar{F} \Lambda \bar{F}^* \bar{A}^{-*} \bar{C}^*,$$

where $C = \bar{C} \begin{bmatrix} 0 & I \end{bmatrix}$ and $\bar{A}^{-1} = d_{\mathcal{Z}\mathcal{Z}}^{-1} \begin{bmatrix} 0 & I \end{bmatrix} A^{-1} \begin{bmatrix} 0 & I \end{bmatrix}^\top$, i.e.

$$\bar{C} \bar{A}^{-1} = d_{\mathcal{Z}\mathcal{Z}}^{-1} C A^{-1} \begin{bmatrix} 0 \\ I \end{bmatrix}.$$

Further, $\bar{F}\Lambda\bar{F}^*$ can be refactorised as $d_{\mathcal{Z}\mathcal{Z}}\tilde{F}\tilde{\Lambda}\tilde{F}^* d^*_{\mathcal{Z}\mathcal{Z}}$ (Gevers et al., 2019), where $\tilde{F}$ and $\tilde{\Lambda}$ satisfy the properties of this proposition. This leads to

$$\Phi_{\bar{v}} = CA^{-1}\begin{bmatrix}0\\ \tilde{F}\end{bmatrix}\tilde{\Lambda}\begin{bmatrix}0 & \tilde{F}^*\end{bmatrix}A^{-*}C^*.$$

Hence, the input-output mapping

$$y(t) = CA^{-1}Br(t) + CA^{-1}\begin{bmatrix}0\\ \tilde{F}\end{bmatrix}\tilde{e}(t),$$

where noise signal $\tilde{e}(t)$ has covariance matrix $\tilde{\Lambda}$, leads to the same T_{yr} and $\Phi_{\bar{v}}$ as in (10.6a) and (10.6c), respectively.

10.B Proof of Lemma 10.16

According to Kailath (1980), any matrix-fraction description (MFD) satisfying Conditions 1 and 2 is unique up to multiplication with unimodular matrices, i.e.

$$C(q^{-1},\theta_1)A^{-1}(q^{-1},\theta_1)B(q^{-1},\theta_1) = C(q^{-1},\theta_2)A^{-1}(q^{-1},\theta_2)B(q^{-1},\theta_2),$$

for all $\theta_1, \theta_2 \in \Theta$, with

$$\begin{aligned}
C(q^{-1},\theta_2) &\triangleq C(q^{-1},\theta_1)Z(q^{-1}),\\
A(q^{-1},\theta_2) &\triangleq R(q^{-1})A(q^{-1},\theta_1)Z(q^{-1}),\\
B(q^{-1},\theta_2) &\triangleq R(q^{-1})B(q^{-1},\theta_1),
\end{aligned}$$

and with unimodular matrices $R(q^{-1})$ and $Z(q^{-1})$. Conditions 3 and 4, respectively, imply that $R(q^{-1}) =: R$ and $Z(q^{-1}) =: Z$ are diagonal (and thus static). To satisfy Assumption 10.2 in $A(q^{-1},\theta_2) = RA(q^{-1},\theta_1)Z$, the elements of R and Z need to satisfy

$$r_{11}^{-1}z_{11} = r_{22}^{-1}z_{22} = \ldots = r_{LL}^{-1}z_{LL}.$$

Condition 5 fixes r_{kk} or z_{kk}, $k = 1, 2, \ldots, L$. Finally, Condition 6 fixes the ratios $r_{kk}^{-1}z_{kk}$, resulting in $R = I$ and $Z = I$.

Part III

Extension of physical linear networks

11 | Mixed linear dynamic networks

Diffusively coupled linear networks consist of symmetric interconnections and therefore, can be represented by undirected graphs. On the other hand, digital controllers and nonsymmetric physical components, such as diodes, can only be represented by directed graphs. These directed dynamics need to be incorporated into the modelling framework, consistency analysis, and identification procedure. This chapter presents two types of mixed linear dynamic networks that contain both undirected and directed interconnections between node signals, for which dynamic network models (in polynomial and rational form) are derived. In addition, conditions for consistent identification of all dynamics in the network are formulated and directions for identification algorithms are developed.

11.1 Introduction

Diffusively coupled linear networks can model a variety of physical processes. The symmetric cause-effect relationships in the interactions can be represented by undirected graphs. On the other hand, digital controllers explicitly describe input-output relationships and therefore, can only be represented by directed graphs. The same holds for nonsymmetric physical components, such as diodes or one-way check valves. This chapter investigates how mixed dynamic networks, containing both undirected and directed interconnections, can be modelled and identified.

In the foregoing chapters, a comprehensive theory has been developed for the modelling and identification of diffusively coupled linear networks. These networks are modelled by a new polynomial framework that is able to include the characteristic symmetric property of the network (Chapter 5). This model is

the basis for prediction error identification methods that are able to incorporate the characteristics into the identification procedure for identifying the full dynamics and topology of the network (Chapter 8) or for identifying a particular dynamics in the network (Chapter 9) and under different experimental conditions (Chapter 10). However, the consequences of including nonsymmetric couplings in this framework are not clear yet.

In the literature, directed dynamic networks are modelled by interconnections through dynamic transfer function modules (Gonçalves et al., 2007; Van den Hof et al., 2013), for which a prediction error identification framework has been developed (Van den Hof et al., 2013). Many identification questions have been addressed, including topology estimation (Materassi and Innocenti, 2010; van Waarde et al., 2021), full network identification (Weerts et al., 2018c), local module identification (Materassi and Salapaka, 2015; Dankers et al., 2016; Ramaswamy and Van den Hof, 2021), and network identifiability (Weerts et al., 2018b; Gevers et al., 2019). Further, Dreef et al. (2022) analysed identifiability of networks that contain fixed dynamics, such as known controllers. However, this framework is less attractive for including symmetric diffusive couplings, because their structural properties are more difficult to incorporate into the modelling and identification procedure and cannot be accounted for in the analysis (Chapter 7).

The objective of this chapter is to identify individual interconnections in mixed dynamic networks that contain both undirected as well as directed linear dynamic interactions. This includes determining an attractive modelling framework and selecting the node signals that need to be measured (sensed) and/or need to be excited (actuated) in order to identify the full dynamics or a particular (local) dynamics in the network. In addition, the consistency and minimum variance properties of the estimates have to be specified and algorithms for performing the identification have to be developed and implemented. These objectives are achieved by extending the theory for modelling and (prediction error) identification of diffusively coupled linear networks to include directed dynamics.

This chapter includes the modelling frameworks and the theoretical identification results that lead towards achieving the above-mentioned objectives. The mixed networks that will be considered are defined in Section 11.2. Section 11.3 describes the mixed network model for diffusively coupled linear networks with additional directed dynamics between the nodes. Conditions for consistent identification of these networks, in particular, including conditions for data informativity and network identifiability, are presented in Section 11.4. Section 11.5 describes two mixed network models for diffusively coupled linear networks that are interconnected with directed linear dynamic networks. Conditions for data informativity, network identifiability, and consistent identification are presented in Section 11.6 and Section 11.7. Further insights and open questions are discussed

in Section 11.8, after which Section 11.9 concludes the chapter.

We consider the following notation throughout the chapter: A polynomial matrix $A(z^{-1})$ in complex indeterminate z^{-1}, consists of matrices A_ℓ and (j,k)th polynomial elements $a_{jk}(z^{-1})$ such that $A(z^{-1}) = \sum_{\ell=0}^{n_a} A_\ell z^{-\ell}$ and $a_{jk}(z^{-1}) = \sum_{\ell=0}^{n_a} a_{jk,\ell} z^{-\ell}$. Hence, the (j,k)th element of the matrix A_ℓ is denoted by $a_{jk,\ell}$ and $\lim_{z\to\infty} A(z) = A_0$. A $p\times m$ rational function matrix $F(z)$ consists of elements $F_{jk}(z)$ and is proper if $F^\infty := \lim_{z\to\infty} F(z) = c \in \mathbb{R}^{p\times m}$; it is strictly proper if $F^\infty = 0$, and monic if $p = m$ and $F^\infty = I$, the identity matrix. $F(z)$ is stable if all its poles are within the unit circle $|z| < 1$. A matrix is called *hollow* if all elements on the diagonal are zero.

11.2 Linear dynamic networks

11.2.1 Diffusively coupled linear networks

Diffusively coupled linear networks can describe various physical processes, such as electrical circuits, mechanical rotational and translational systems, chemical reactions, hydraulic systems, and biological systems. These networks are characterised by symmetric cause-effect relationships in the interactions between the node signals, which are a result of the symmetric nature of the physical components that are present in the interconnections. Diffusively coupled linear networks are modelled in the polynomial framework of Chapter 8.

Definition 11.1 (Diffusively coupled network model (Definition 8.2)). *A diffusively coupled linear network consists of L node signals $w(t)$ and K excitation signals $r(t)$ and is defined as*

$$A(q^{-1})w(t) = B(q^{-1})r(t) + F(q)e(t), \tag{11.1}$$

with q^{-1} the shift operator meaning $q^{-1}w(t) = w(t-1)$ and with

1. *$A(q^{-1}) \in \mathbb{R}^{L\times L}[q^{-1}]$, with $a_{jk}(q^{-1}) = a_{kj}(q^{-1}), \forall k,j$ and $A^{-1}(q^{-1})$ stable.*
2. *$B(q^{-1}) \in \mathbb{R}^{L\times K}[q^{-1}]$.*
3. *$F(q) \in \mathcal{H} := \{F \in \mathbb{R}^{L\times L}(q) \mid F$ monic, stable and stably invertible$\}$.*
4. *$\Lambda \succ 0$ the covariance matrix of the noise $e(t)$.*
5. *$r(t)$ is a deterministic and bounded sequence.*

6. *$e(t)$ is a zero-mean white noise process with bounded moments of an order larger than 4 (Ljung, 1999).*

This network is assumed to be connected (there is a path between every pair of nodes), with at least one connection to the ground node[a].

[a]The network is connected if its Laplacian matrix (i.e. the degree matrix minus the adjacency matrix) has a positive second-smallest eigenvalue (Dörfler and Bullo, 2013). If the network is connected, it has at least one connection to the ground node if $\text{rank}\big(A(q^{-1})\big) = L$ (Chapter 2).

$A(q^{-1})$ is a symmetric and nonmonic polynomial matrix, which can always uniquely be decomposed into a diagonal polynomial matrix $Q(q^{-1}) := \text{diag}\big(A(q^{-1})\big)$ and a hollow and symmetric polynomial matrix $P(q^{-1}) := Q(q^{-1}) - A(q^{-1})$ (Chapter 5).

11.2.2 Module representations

Directed dynamic networks are modelled as interconnections of transfer functions. This can be seen as a generalisation of the closed-loop system to a more complex interconnection structure of linear dynamic systems. The module representation of Van den Hof et al. (2013) describes measured signals of interest (node signals) that are interconnected through linear dynamic transfer function modules. We adopt this framework for modelling directed dynamic networks.

Definition 11.2 (Module representation (Van den Hof et al., 2013)). *A module representation consists of L node signals $w(t)$ and K excitation signals $r(t)$ and is defined as*

$$w(t) = G(q)w(t) + R(q)r(t) + H(q)e(t), \tag{11.2}$$

with q^{-1} the shift operator meaning $q^{-1}w(t) = w(t-1)$ and with

1. *$G(q) \in \mathbb{R}^{L\times L}(q)$ consisting of proper elements $G_{ij}(q)$ with $G_{jj}(q) = 0$.*
2. *$R(q) \in \mathbb{R}^{L\times K}(q)$ consisting of proper and stable elements $R_{ij}(q)$.*
3. *$H(q) \in \mathcal{H}$.*
4. *$\Lambda \succ 0$ the covariance matrix of the noise $e(t)$.*
5. *$r(t)$ is a deterministic and bounded sequence.*

6. *$e(t)$ is a zero-mean white noise process with bounded moments of an order larger than 4 (Ljung, 1999).*

This network is assumed to be well-posed and stable[a].

[a] The network is stable if $\left(I - G^0(q)\right)^{-1}$ only consists of stable transfer functions. The network is well-posed if all principal minors of $\lim_{z\to\infty}\left(I - G^0(z)\right)$ are nonzero (Dankers, 2014).

11.2.3 Mixed dynamic networks

Undirected networks can describe diffusive interconnections of physical components that are characterised by symmetric behaviour. However, there also exist components with diffusive nonsymmetric behaviour, such as a generic chamber-valve, which is more likely to have fluid flow in one direction than in the other direction, i.e. the resistance in one direction is different from the resistance in the other (similar to a conventional diode). There also exist components with nondiffusive (directed) behaviour, such as ideal diodes and one-way check valves, which can be seen as components with zero resistance in one direction and infinite resistance in the other direction. Another example of a directed interconnection is the interaction of two robots of which one can communicate to the other, but not the other way around. In addition, digital controllers describe cause-effect relations from input signals to output signals. If these directed dynamics are inserted into undirected diffusively coupled linear networks, they ruin the symmetric structure of the network model. Therefore, the directed behaviour needs to be accounted for in the identification procedure, as it needs to be compensated by additional properties to preserve the identifiability of the network dynamics.

Instead of only adding a few directed interconnections to undirected networks, even more complex combinations of undirected and directed interconnections might be present in dynamic networks. To this end, we define mixed linear dynamic networks as follows:

Definition 11.3 (Mixed linear dynamic network). *A* mixed linear dynamic network *is a linear dynamic network that contains both undirected and directed connections between the nodes.*

Two main cases of mixed linear dynamic networks will be considered in this chapter.

Definition 11.4 (Case 1). *A* mixed linear dynamic network *is an undirected network with additional directed links between the nodes.*

Definition 11.5 (Case 2). *A* mixed linear dynamic network *consists of an undirected diffusively coupled linear network and a directed linear dynamic network that are interconnected with each other through directed links between the nodes.*

The mixed dynamic networks in Case 1. are (undirected) diffusively coupled linear networks with additional (input-output) controllers or nonsymmetric components. Consequently, the behaviour of the additional directed couplings may be described by polynomials or by transfer function modules. Both situations have different implications for modelling the mixed network. In addition, controllers are typically known, while nonsymmetric physical components are often unknown. Whether or not the dynamics are known has an effect on the identification procedure, in particular on the identifiability conditions.

An example of such a mixed dynamic network is shown in Figure 11.1, where two node signals are interconnected through an undirected coupling (indicated in black) and where a directed connection is added from node signal $w_2(t)$ to node signal $w_1(t)$ (indicated in red).

The mixed dynamic networks in Case 2. are partially undirected and partially directed interconnected. The undirected part can be described by the polynomial framework, while the directed part can be described by the module representation. It is possible to translate these mixed networks into the polynomial framework or into the module representation. Similar to the mixed networks in Case 1., an additional distinction can be made between networks with additional known or unknown dynamics.

An example of such a mixed dynamic network is shown in Figure 11.2, where two node signals are interconnected through an undirected coupling and where two additional nodes are added with directed connections between them. The interconnection between the two networks is established through directed connections (indicated in red).

The interconnection between the undirected network and the directed network can also be established through undirected interconnections. However, in this modelling procedure, we choose to collect all node signals with undirected couplings in the undirected part and all remaining node signals in the directed part. In this way, the symmetric nature of the undirected linear diffusive couplings can be maximally exploited.

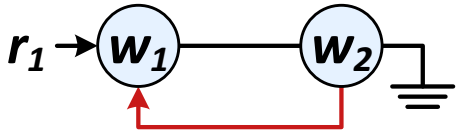

Figure 11.1: A mixed dynamic network in Case 1. consisting of an undirected diffusive coupling (black) and a directed link (red) between the node signals $w_1(t)$ and $w_2(t)$ and with the external excitation signal $r_1(t)$.

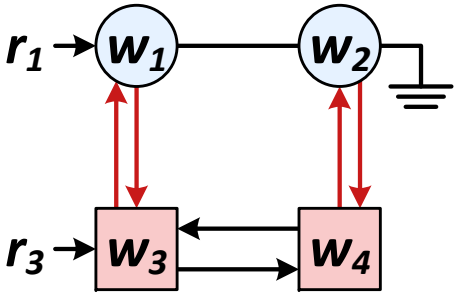

Figure 11.2: A mixed dynamic network in Case 2. in which an undirected diffusively coupled network with node signals $w_1(t)$ and $w_2(t)$ (blue circles) is connected through directed links (red arrows) to a directed dynamic network with node signals $w_3(t)$ and $w_4(t)$ (red squares) and with the external excitation signals $r_1(t)$ and $r_3(t)$.

11.2.4 Cases of mixed dynamic networks

Two cases for mixed dynamic networks have been defined in Definition 11.4 and 11.5. In this section, we discuss what types of mixed dynamic networks are included and excluded by these definitions and how these mixed dynamic networks can be extended to other situations.

To analyse the mixed dynamic networks, we divide the nodes of the mixed dynamic network into two sets: one set containing the nodes with undirected couplings, referred to as *undirected nodes*, and indicated with the subscript u; and one set containing the nodes without undirected couplings (and thus with only directed interconnections), referred to as *directed nodes*, and indicated with the subscript d. In this way, the node signals of a mixed dynamic network can always be uniquely separated into two sets of nodes. Consider, for example, the mixed network shown in Figure 11.2, where $w_1(t)$ and $w_2(t)$ have an undirected interconnection and $w_3(t)$ and $w_4(t)$ have only directed interconnections. It also implies that the interconnections between the sets can only be directed, otherwise the nodes are incorrectly divided into the two sets. As mentioned before, this choice has been made to maximally exploit the symmetric nature of the linear diffusive couplings. In addition, we split these sets further, such that each set of nodes represents a connected network (that is, a single network and not two or more distinct networks). Figure 11.3 shows four examples of mixed dynamic

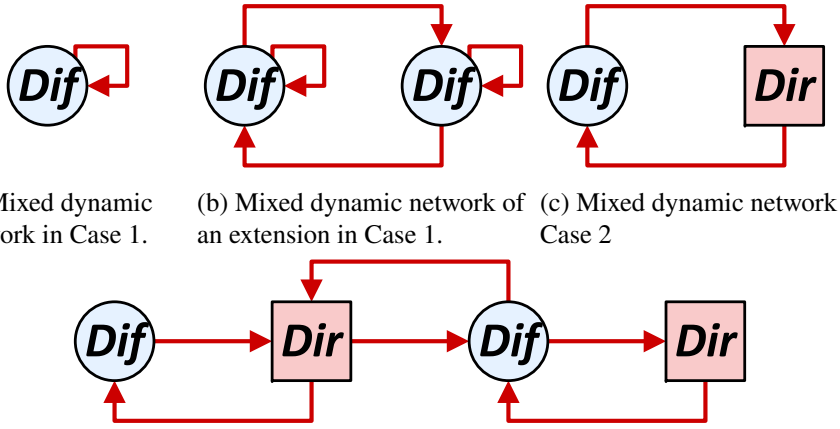

(a) Mixed dynamic network in Case 1.

(b) Mixed dynamic network of an extension in Case 1.

(c) Mixed dynamic network of Case 2

(d) Mixed dynamic network of an extension in Case 2.

Figure 11.3: An overview of several cases of mixed dynamic networks, with sets of undirected nodes (blue circles), sets of directed nodes (red squares), and directed interconnections (red arrows) between the sets of nodes.

networks, which will be discussed further.

Following this classification of nodes in mixed dynamic networks, the most simple mixed dynamic network is the one in Case 1., as defined in Definition 11.4, where one set of undirected nodes can have some additional directed interconnections. This mixed dynamic network is graphically depicted in Figure 11.3a. An extension to this case is the case where multiple sets of undirected nodes are interconnected through directed connections. In this case, the mixed dynamic network with all directed interactions removed, is an undirected network that is not connected and thus consists of multiple distinct undirected networks. Such mixed dynamic network with two sets of undirected nodes is graphically depicted in Figure 11.3b.

Another class of mixed dynamic networks is the one in Case 2., as defined in Definition 11.5, where one set of undirected nodes is interconnected with one set of directed nodes. Again, we consider two sets of nodes of which each represents a single distinct network. This mixed dynamic network is graphically depicted in Figure 11.3c. An extension to this case is the situation in which multiple sets of undirected nodes and multiple sets of directed nodes are interconnected through directed connections. If these interconnections are removed from the mixed dynamic network, the remaining network consists of multiple distinct undirected networks and directed networks. An example of such mixed dynamic network is graphically depicted in Figure 11.3d.

More advanced mixed dynamic networks consist of combinations of the extended versions in Case 1. and 2. In this chapter, we focus on mixed dynamic networks in Case 1. or 2. Implications for extended cases of mixed dynamic network are elaborated on in the discussion in Section 11.8.

11.3 Case 1: Modelling

11.3.1 General model

Consider a diffusively coupled linear network (11.1) to which directed links are added. These directed links can represent the dynamics of nonsymmetric components or digital controllers. The behaviour of the node signals $w_j(t)$, $j = 1, \ldots, L$, of these mixed dynamic networks is described by

$$\sum_{i \in \{j, \mathcal{N}_j^u\}} a_{ji}(q^{-1}) w_i(t) = \sum_{k=1}^{K} b_{jk}(q^{-1}) r_k(t) + \sum_{i \in \mathcal{N}_j^d} G_{ji}(q) w_i(t) + \sum_{i=1}^{L} F_{ji}(q) e_i(t), \quad (11.3)$$

where $\mathcal{N}_j^u$ and $\mathcal{N}_j^d$ are the set of indices of $w_k(t)$, $k \neq j$, with undirected couplings with node signals $w_j(t)$ and with directed connections towards node signals $w_j(t)$, respectively, and where $G_{ij}(q)$ models the (possibly rational) directed dynamics in the link from node signal $w_j(t)$ to node signal $w_i(t)$. It is assumed that $G_{ii}(q) = 0$, so that there are no self-loops.

The behaviour of all node signals can be combined in a matrix equation describing the mixed network as

$$A(q^{-1}) w(t) = B(q^{-1}) r(t) + G(q) w(t) + F(q) e(t), \quad (11.4)$$

where $A(q^{-1})$ is a symmetric polynomial matrix, $B(q^{-1})$ is a polynomial matrix, $G(q)$ is a hollow rational matrix with proper elements, and $F(q)$ is a rational matrix that is monic and stable and has a stable inverse.

Remark 11.6 (Well-posed and stable). *The network is well-posed and stable if* $\left(A(q^{-1}) - G(q)\right)^{-1}$ *exists and is proper and stable (Dankers, 2014).*

11.3.2 Polynomial model

Consider the most general situation in which the dynamics in the directed links are modelled by rational functions. Then the model (11.4) is indeed not polynomial anymore and hence, it has to be rewritten to fit into the polynomial modelling framework. This is achieved by an approach that is similar to the approach for rewriting the network in the second step of immersion (Chapter 9). First, $G(q)$ is factorised, such that

$$G(q) = D_G^{-1}(q^{-1})N_G(q^{-1}), \tag{11.5}$$

with $D_G(q^{-1})$ diagonal and full rank and with the notational rule that $D_{G_{ii}}(q^{-1}) := 1$ if $G_{ij} = 0$ for all j. Then, (11.4) is multiplied with $det\big(D_G(q^{-1})\big)$, where the common factors of $det\big(D_G(q^{-1})\big)$ and $N_G(q^{-1})$ are taken out. To be precise, define the monic polynomial

$$d_G(q^{-1}) := \frac{det\big(D_G(q^{-1})\big)}{gcd\big(det\big(D_G(q^{-1})\big), adj\big(D_G(q^{-1})\big)\big)}, \tag{11.6}$$

with $gcd(x, Y)$ the greatest common divisor of scalar x and all scalar elements of matrix Y.

Proposition 11.7 (Mixed dynamic network model). *Every mixed dynamic network* (11.4) *can be described by*

$$\big(\breve{A}(q^{-1}) - \breve{G}(q^{-1})\big)w(t) = \breve{B}(q^{-1})r(t) + \breve{F}(q)e(t), \tag{11.7}$$

with

$$\breve{A}(q^{-1}) = d_G(q^{-1})A(q^{-1}), \tag{11.8a}$$
$$\breve{B}(q^{-1}) = d_G(q^{-1})B(q^{-1}), \tag{11.8b}$$
$$\breve{F}(q) = d_G(q^{-1})F(q), \tag{11.8c}$$
$$\breve{G}(q^{-1}) = d_G(q^{-1})D_G^{-1}(q^{-1})N_G(q^{-1}), \tag{11.8d}$$

with $\big(A(q^{-1}), B(q^{-1}), F(q^{-1}), \Lambda\big)$ *satisfying Definition 11.1, with* $D_G^{-1}(q^{-1})$ *and* $N_G(q^{-1})$ *as in* (11.5)*, and with* $G(q)$ *a hollow rational matrix with proper elements.*

Proof: Consider the mixed dynamic network model in (11.4). Subtract $G(q)w(t)$ from both sides of the equation, premultiply both sides of the equation with $d_G(q^{-1})$ (11.6), and substitute (11.5) for $G(q)$. ■

In the mixed dynamic network model of Proposition 11.7, $\breve{A}(q^{-1})$ is a symmetric polynomial matrix and $\breve{G}(q^{-1})$ is a nonsymmetric polynomial mat-

rix. Further, $\breve{A}(q^{-1})$, $\breve{B}(q^{-1})$, $\breve{G}(q^{-1})$ (and $N_G(q^{-1})$), and $\breve{F}(q)$ adopt the zero structure of $A(q^{-1})$, $B(q^{-1})$, $G(q)$, and $F(q)$, respectively. This also means that the polynomials $\breve{g}_{ii}(q^{-1}) = 0$, $\forall i$, because the transfer functions $G_{ii}(q) = 0$, $\forall i$, meaning that there are no directed self-loops. All transfer functions $G_{ij}(q) := \frac{g_{ij}^N(q^{-1})}{g_{ij}^D(q^{-1})}$ can be modelled with monic denominator polynomials $g_{ij}^D(q^{-1})$. Then properness of the transfer functions $G_{ij}(q)$, $\forall i, j$, implies that $N_G(q^{-1})$ and $d_G(q^{-1})D_G^{-1}(q^{-1}) = adj\big(G(q)\big)$ are proper and therefore, all polynomials $\breve{g}_{ij}(q^{-1})$, $\forall i, j$, are proper. The directed dynamics destroy the symmetric nature of the network, as the internal network dynamics is described by $\big(\breve{A}(q^{-1}) - \breve{G}(q^{-1})\big)$, which is not symmetric anymore. The polynomial model (11.7) will be used for identification of the mixed dynamic network.

Proposition 11.8 (Well-posed and stable). *The network* (11.7) *is well-posed and stable if* $\big(A(q^{-1}) - G(q)\big)^{-1}(q)$ *exists and is proper and stable.*

Proof: From (11.8a), (11.8d), and (11.11) it follows that:

$$\breve{A}(q^{-1}) - \breve{G}(q^{-1}) = d_G(q^{-1})\big(A(q^{-1}) - G(q)\big),$$

with $d_G(q^{-1})$ a monic polynomial. So, if $\big(A(q^{-1}) - G(q)\big)^{-1}$ exists and is proper and stable, then this also holds for $\big(\breve{A}(q^{-1}) - \breve{G}(q^{-1})\big)^{-1}$. If $\big(\breve{A}(q^{-1}) - \breve{G}(q^{-1})\big)^{-1}$ exists and is proper and stable, then the network is well-posed according to Remark 11.6. ■

The network (11.7) has input-output relations between the signals that can be described by

$$\begin{aligned} w(t) &= \big(\breve{A}(q^{-1}) - \breve{G}(q^{-1})\big)^{-1}\left[\breve{B}(q^{-1})r(t) + \breve{F}(q)e(t)\right], && \text{(11.9a)}\\ &= \big(A(q^{-1}) - G(q)\big)^{-1}B(q^{-1})r(t) + \big(A(q^{-1}) - G(q)\big)^{-1}F(q)e(t), && \text{(11.9b)}\\ &= T_{wr}(q)r(t) + T_{we}(q)e(t), && \text{(11.9c)} \end{aligned}$$

where (11.9b) follows from (11.9a) by substituting (11.8) into (11.9a).

If the directed dynamics are modelled by polynomials instead of rational functions, the network model (11.4) remains polynomial and does not have to be rewritten.

Proposition 11.9 (Polynomial directed dynamics). *If the directed dynamics are polynomial, then* (11.7) *reduces to*

$$\big(A(q^{-1}) - G(q^{-1})\big)w(t) = B(q^{-1})r(t) + F(q)e(t), \qquad (11.10)$$

where $G(q^{-1})$ is a nonsymmetric polynomial matrix describing the directed dynamics.

Proof: If $G(q)$ is polynomial, then $D_G(q^{-1}) = I$, $N_G(q^{-1}) = G(q^{-1})$, and $d_G(q^{-1}) = 1$. Substituting this into (11.8) gives $\breve{A}(q^{-1}) = A(q^{-1})$, $\breve{B}(q^{-1}) = B(q^{-1})$, $\breve{F}(q) = F(q)$, and $\breve{G}(q^{-1}) = G(q^{-1})$. Substituting this into (11.7) results in (11.10). ■

The implication of Proposition 11.9 is that (11.7) is a generalised model for both polynomial and rational directed dynamics.

In the next section, we will develop theory for the identification of the mixed dynamic networks (11.7). Before moving on, consider the special role that known directed dynamics have in the mixed dynamic networks (11.4) in Case 1. If the directed dynamics are known, they do not have to be identified and therefore, they play a different role in the mixed network model.

Remark 11.10 (Known directed dynamics). *If the dynamics in the directed links are known, they act like input dynamics, even though they are coming from elsewhere in the network. In this situation, the directed dynamics do not really change the structure of the undirected polynomial network model. The mixed dynamic network can be modelled as* (11.4) *with $G(q)$ known.*

The situation of known directed dynamics can be seen as a special case of polynomial and rational directed dynamics. The model (11.7) is a general model that captures the situations of rational directed dynamics, polynomial directed dynamics, and known directed dynamics and therefore, it is used in the identification analysis.

11.4 Case 1: Identification

11.4.1 Identification setup

This chapter involves the full network identification of mixed dynamic networks. In this section, this problem is dealt with in the polynomial framework, where the model (11.7) will be used for identification. The identification problem that will be considered in this section is defined as follows:

Definition 11.11 (Mixed identification problem). *The full network identification problem for mixed dynamic networks concerns the identification*

of all dynamics in the network.

Additionally, some parts of the topology might be identified as well. If the topology is assumed to be unknown, it can be retrieved from the identification. However, some parts of the topology might be assumed to be known in order to perform the identification procedure.

In the particular identification of mixed dynamic networks in Case 1., the directed dynamics are assumed to be unknown and will be identified as well. The topology of the undirected part, captured by $A(q^{-1})$, is assumed to be unknown and will be identified. The topology of the directed part, captured by $G(q)$, will later be assumed to be known and incorporated into the identification procedure.

Consider the network model (11.7). For ease of notation, define

$$\breve{\Upsilon}(q^{-1}) := \breve{A}(q^{-1}) - \breve{G}(q^{-1}), \tag{11.11}$$

with polynomial elements $\breve{\Upsilon}_{ij}(q^{-1}) = \breve{\upsilon}_{ij}(q^{-1})$ and with $\lim_{z\to} \breve{\Upsilon}(z) = \breve{\Upsilon}_0$.

For solving the mixed identification problem of Definition 11.11, a similar approach is applied as for full network identification of diffusively coupled linear networks (Chapter 8), because the mixed dynamic network is modelled in a similar polynomial framework. The difference is that $\breve{\Upsilon}(q^{-1})$ is not completely symmetric.

First, a predictor model is set up based on the parameterised model set

$$\mathcal{M} := \{M(\theta), \theta \in \Theta \subset \mathbb{R}^d\} \tag{11.12}$$

with $d \in \mathbb{N}$ and with particular models

$$M(\theta) := \big(A(q^{-1}, \theta), B(q^{-1}, \theta), F(q, \theta), G(q^{-1}, \theta), \Lambda(\theta)\big), \tag{11.13}$$

where θ contains all unknown coefficients that appear in the entries of the model matrices $A(q^{-1})$, $B(q^{-1})$, $F(q)$, $G(q^{-1})$, and Λ. The data generating network is denoted by $\mathcal{S} := \big(A^0, B^0, F^0, G^0, \Lambda^0\big)$. The true system lies in the model set if $\mathcal{S} = M(\theta^0)$, where $\theta^0 \in \Theta$ indicate the true parameter values.

In addition, consider the model set

$$\breve{\mathcal{M}} := \{\breve{M}(\eta), \eta \in \Pi \subset \mathbb{R}^d\} \tag{11.14}$$

with $d \in \mathbb{N}$ and with particular models

$$\breve{M}(\eta) := \big(\breve{A}(q^{-1}, \eta), \breve{B}(q^{-1}, \eta), \breve{F}(q, \eta), \breve{G}(q^{-1}, \eta), \breve{\Lambda}(\eta)\big), \tag{11.15}$$

where η contains all unknown coefficients that appear in the entries of the model matrices $\breve{A}(q^{-1})$, $\breve{B}(q^{-1})$, $\breve{F}(q)$, $\breve{G}(q^{-1})$, and $\breve{\Lambda}$, with $\Lambda(\theta) = \breve{\Lambda}(\eta)$. The corresponding data generating network is denoted by $\breve{\mathcal{S}} := \left(\breve{A}^0, \breve{B}^0, \breve{F}^0, \breve{G}^0, \breve{\Lambda}^0\right)$. The true system lies in the model set if $\breve{\mathcal{S}} = \breve{\mathcal{M}}(\eta^0)$, where $\eta^0 \in \Pi$ indicate the true parameter values.

The network predictor is defined as in Definition 8.4 and leads to

$$\hat{w}(t|t-1) = \left[I - \breve{\Upsilon}_0^{-1}\breve{F}^{-1}(q)\breve{\Upsilon}(q^{-1})\right] w(t) + \breve{\Upsilon}_0^{-1}\breve{F}^{-1}(q)\breve{B}(q^{-1})r(t). \quad (11.16)$$

Along the same line of reasoning as in Proposition 8.10, the parameterised predictor leads to the prediction error, which is defined as

$$\breve{\varepsilon}(t,\eta) := w(t) - \hat{w}(t|t-1;\eta), \quad (11.17)$$

and obtained as

$$\breve{\varepsilon}(t,\eta) = W_w(q,\eta)w(t) - W_r(q,\eta)r(t), \quad (11.18)$$

with predictor filters

$$W_w(q,\eta) = \breve{\Upsilon}_0^{-1}(\eta)\breve{F}^{-1}(q,\eta)\breve{\Upsilon}(q^{-1},\eta), \quad (11.19a)$$

$$W_r(q,\eta) = \breve{\Upsilon}_0^{-1}(\eta)\breve{F}^{-1}(q,\eta)\breve{B}(q^{-1},\eta). \quad (11.19b)$$

The parameters are estimated through the least-squares identification criterion

$$\hat{\eta}_N = \arg\min_{\eta\in\Pi} \frac{1}{N}\sum_{t=1}^{N} \breve{\varepsilon}^\top(t,\eta)\breve{\Lambda}\breve{\varepsilon}(t,\eta) \quad (11.20)$$

with $\breve{\Lambda} \succ 0$. Under mild conditions[1] this criterion converges with a probability of 1 to

$$\eta^* := \arg\min_{\eta\in\Pi} \lim_{N\to\infty} \sum_{t=1}^{N} \mathbb{E}\left\{\breve{\varepsilon}^\top(t,\eta)\breve{\Lambda}\breve{\varepsilon}(t,\eta)\right\}. \quad (11.21)$$

In order to identify the mixed dynamic network (11.4), first the mixed dynamic network model in polynomial form (11.7) will be identified from the data, after which the identified polynomial network model is used to obtain the original mixed network model.

In the next sections, the consistent identification of the mixed network model is analysed by considering data informativity and network identifiability. This leads to sufficient conditions for which a consistent estimate of the data generating mixed dynamic network $\mathcal{S}$ can be found.

[1]The standard conditions for convergence of predictor error estimates include the condition that the white noise process $e(t)$ has bounded moments of an order larger than 4 (Ljung, 1999).

11.4.2 Data informativity

The data $z(t)$ are called *informative* if they contain sufficient information to uniquely recover the predictor filter $W(q,\eta)$ from second-order statistical properties of the data $z(t)$. This is formalised in line with Ljung (1999) as follows:

Definition 11.12 (Data informativity (Ljung, 1999)). *A quasi-stationary data sequence* $\{z(t)\}$ *is called* informative with respect to the model set $\breve{\mathcal{M}}$ (11.14) *if for any two* $\eta_1, \eta_2 \in \Pi$

$$\bar{\mathbb{E}}\left\{\|[W(q,\eta_1) - W(q,\eta_2)]z(t)\|^2\right\} = 0 \Rightarrow \{W(e^{i\omega},\eta_1) = W(e^{i\omega},\eta_2)\} \tag{11.22}$$

for almost all ω.

Conditions for data informativity are derived along the same line of reasoning as in Proposition 8.12. A crucial role is reserved for the relation $z(t) = J(q)\kappa(t)$ (8.67), with signals $z(t) := \begin{bmatrix} w^\top(t) & r^\top(t) \end{bmatrix}^\top$ and $\kappa(t) := \begin{bmatrix} e^\top(t) & r^\top(t) \end{bmatrix}^\top$ (8.68).

Applying Definition 11.12 to mixed dynamic networks, leads to the following conditions for data informativity:

Proposition 11.13 (Data informativity). *The quasi-stationary data sequence* $\{z(t)\}$ *is* informative with respect to the model set $\breve{\mathcal{M}}$ (11.12) *if* $\Phi_z(\omega) \succ 0$ *for a sufficiently high number of frequencies. In the situation* $K \geq 1$*, this is guaranteed by* $\Phi_r(\omega) \succ 0$ *for a sufficiently high number of frequencies.*

Proof: The proof is provided in Appendix 11.A. ■

The implication of Proposition 11.13 is that the additional directed links captured by $G(q)$ do not change the data informativity conditions that hold for diffusively coupled linear networks, as formulated in Proposition 8.12. This means that the directed links can be identified for free, which is due to the fact that no node signals are added to the network and that the node signals that are present in the network already have to be sufficiently excited.

11.4.3 Network identifiability

The concept of network identifiability has been defined for general linear dynamic networks by Weerts et al. (2018b) as follows (see also Definition 8.13):

Definition 11.14 (Network identifiability (Weerts et al., 2018b)). *The network model set $\mathcal{M}$ is* globally network identifiable *from $z(t)$ if the parameterised model $M(\theta)$ can uniquely be recovered from $T_{wr}(q,\theta)$ and $\Phi_{\bar{v}}(\omega,\theta)$, with $\bar{v}(t) := T_{we}(q)e(t)$. That is, if for all models $M(\theta_1), M(\theta_2) \in \mathcal{M}$*

$$\left.\begin{aligned} T_{wr}(q,\theta_1) &= T_{wr}(q,\theta_2) \\ \Phi_{\bar{v}}(\omega,\theta_1) &= \Phi_{\bar{v}}(\omega,\theta_2) \end{aligned}\right\} \Rightarrow M(\theta_1) = M(\theta_2). \tag{11.23}$$

Conditions for network identifiability are derived along the same line of reasoning as in Propositions 8.15 and 10.11. The first step includes the left matrix-fraction description (LMFD) to recover $\breve{A}(q^{-1})$, $\breve{B}(q^{-1})$, and $\breve{G}(q^{-1})$ from $T_{wr}(q)$. Second, $\breve{A}(q^{-1})$, $\breve{B}(q^{-1})$, and $\breve{G}(q^{-1})$ are used to estimate $A(q^{-1})$, $B(q^{-1})$, and $G(q)$. Finally, $F(q)$ and Λ are found from $\Phi_{\bar{v}}(\omega)$ using a spectral factorisation (Youla, 1961).

Lemma 11.15 (LMFD). *Consider a network model set $\breve{\mathcal{M}}$ (11.14). Given the* LMFD $\breve{\Upsilon}^{-1}(q^{-1})\breve{B}(q^{-1})$ *with $\breve{\Upsilon}(q^{-1})$ as in* (11.11)*, the polynomial matrices $\breve{A}(q^{-1})$, $\breve{G}(q^{-1})$, and $\breve{B}(q^{-1})$ are unique within $\breve{\mathcal{M}}$ up to a scalar factor if the following conditions are satisfied:*

1. *The polynomials $\breve{\Upsilon}(q^{-1})$ and $\breve{B}(q^{-1})$ are left coprime in $\breve{\mathcal{M}}$.*
2. *There exists a permutation matrix P such that within $\breve{\mathcal{M}}$, $\begin{bmatrix}\breve{\Upsilon}_0 & \breve{\Upsilon}_1 & \cdots & \breve{\Upsilon}_{n_{\breve{v}}} & \breve{B}_0 & \breve{B}_1 & \cdots & \breve{B}_{n_{\breve{b}}}\end{bmatrix} P = \begin{bmatrix}\breve{D} & \breve{R}\end{bmatrix}$ with $\breve{D}$ square, diagonal, and full rank.*
3. *The zero structure of $\breve{G}(q^{-1})$ is known in $\breve{\mathcal{M}}$.*
4. *If $\breve{g}_{ij}(q^{-1}) \neq 0$, then $\breve{g}_{ji}(q^{-1}) = 0$, $\forall i, j = 1, 2, \ldots, L$, within $\breve{\mathcal{M}}$.*

Proof: The proof is provided in Appendix 11.B. ■

The conditions of Lemma 11.15 can be translated into conditions on the original mixed network model set $\mathcal{M}$, leading to the following lemma:

Lemma 11.16 (LMFD). *The conditions of Lemma 11.15 are satisfied if the following conditions are satisfied:*

1. *Condition 1. of Lemma 11.15 is satisfied if the polynomials $\begin{bmatrix}A(q^{-1}) & N_G(q^{-1})\end{bmatrix}$ and $B(q^{-1})$ are left coprime within $\mathcal{M}$* (11.12)*.*
2. *Let $\Upsilon(q^{-1}) := \begin{pmatrix}A(q^{-1}) - N_G(q^{-1})\end{pmatrix}$. Condition 2. of Lemma 11.15 is satisfied if there exists a permutation matrix P such that within*

$\mathcal{M}$, $\begin{bmatrix} \Upsilon_0 & \Upsilon_1 & \cdots & \Upsilon_{n_v} & B_0 & B_1 & \cdots & B_{n_b} \end{bmatrix} P = \begin{bmatrix} D & R \end{bmatrix}$ *with* D *square, diagonal, and full rank.*

3. *The zero structure of* $G(q)$ *is known in* $\mathcal{M}$.

4. *If* $G_{ij}(q) \neq 0$, *then* $G_{ji}(q) = 0$, $\forall i, j = 1, 2, \ldots, L$, *within* $\mathcal{M}$.

Proof: The proof is provided in Appendix 11.C. ■

Condition 3. implies that the locations of the directed links are known. In other words, the topology of the directed part of the network is assumed to be known for identifiability purposes, while the topology of the undirected part of the network is still allowed to be unknown. Lemma 11.16 provides conditions under which $\breve{A}(q^{-1})$, $\breve{B}(q^{-1})$, and $\breve{G}(q^{-1})$ can be estimated up to a scalar factor from $T_{wr}(q)$. Next, we prove that $A(q^{-1})$, $B(q^{-1})$, and $G(q^{-1})$ can be obtained from scaled versions of $\breve{A}(q^{-1})$, $\breve{B}(q^{-1})$, and $\breve{G}(q^{-1})$. The relations (11.8a), (11.8b), and (11.8d) lead to

$$\tilde{A}(q^{-1}) = \alpha d_G(q^{-1}) A(q^{-1}), \tag{11.24a}$$

$$\tilde{B}(q^{-1}) = \alpha d_G(q^{-1}) B(q^{-1}), \tag{11.24b}$$

$$\tilde{G}(q^{-1}) = \alpha d_G(q^{-1}) G(q), \tag{11.24c}$$

with $\tilde{A}(q^{-1}) := \alpha \breve{A}(q^{-1})$, $\tilde{B}(q^{-1}) := \alpha \breve{B}(q^{-1})$, and $\tilde{G}(q^{-1}) := \alpha \breve{G}(q^{-1})$, the scalar scaled versions of $\breve{A}(q^{-1})$, $\breve{B}(q^{-1})$, and $\breve{G}(q^{-1})$, respectively, and with scaling factor $\alpha \in \mathbb{R}_+$.

Lemma 11.17 (Uniqueness of $A(q^{-1})$, $B(q^{-1})$, and $G(q)$). *If there is at least one linear constraint on the coefficients of* $A(q^{-1}, \theta_A)$ *and* $B(q^{-1}, \theta_B)$ *of the form* $\Gamma \bar{\theta} = \gamma \neq 0$, *with* Γ *full row rank and with* $\bar{\theta}^\top := \begin{bmatrix} \theta_A^\top & \theta_B^\top \end{bmatrix}$, *then* $A(q^{-1})$, $B(q^{-1})$, *and* $G(q)$ *are uniquely obtained from* $\tilde{A}(q^{-1})$, $\tilde{B}(q^{-1})$, *and* $\tilde{G}(q)$ *through* (11.24).

Proof: Because $A(q^{-1})$ and $B(q^{-1})$ are left coprime, the polynomial $d_G(q^{-1})$ is the greatest monic common divisor of the polynomial matrices $\tilde{A}(q^{-1})$ and $\tilde{B}(q^{-1})$, which can be found uniquely (Kailath, 1980). The scalar factor α is fixed with the parameter constraint, leading to unique $A(q^{-1})$, $B(q^{-1})$, and $G(q)$. ■

Computing the greatest monic common divisor $d_G(q^{-1})$ of the polynomial matrices $\tilde{A}(q^{-1})$ and $\tilde{B}(q^{-1})$ leads to a nonconvex optimisation problem for which many algorithms are available in the literature, see, for example, Fazzi et al. (2019) and their references.

The problem reduces to a convex optimisation problem consisting of two steps if a nonzero polynomial element $a_{ij}(q^{-1})$ or $b_{ij}(q^{-1})$ of $A(q^{-1})$ or $B(q^{-1})$ is known, which means that a single interconnection in the network is known or that an excitation signal enters the network through known dynamics (e.g. $b_{ij}(q^{-1}) = 1$), respectively. In this case, the first step of the optimisation includes the estimation of the polynomial factor $\alpha d_G(q^{-1})$ from the polynomial relation in (11.24a) or (11.24b) corresponding to the known polynomial. This optimisation problem is convex and thus leads to a consistent result. Second, the estimated polynomial factor is substituted into (11.24a), (11.24b), and (11.24c) to formulate new linear regressions for estimating $A(q^{-1})$, $B(q^{-1})$, and $G(q)$, respectively. The resulting optimisation problems are again convex, leading to consistent estimates of $A(q^{-1})$, $B(q^{-1})$, and $G(q)$.

Lemmas 11.15, 11.16, and 11.17 are combined to obtain the following identifiability result:

Proposition 11.18 (Identifiability). *A network model set $\mathcal{M}$ is* globally network identifiable *from $z(t)$ if the following conditions are satisfied:*

1. $\begin{bmatrix} A(q^{-1}) & N_G(q^{-1}) \end{bmatrix}$ *and* $B(q^{-1})$ *are left coprime within* $\mathcal{M}$.
2. *Let* $\Upsilon(q^{-1}) := \begin{pmatrix} A(q^{-1}) - N_G(q^{-1}) \end{pmatrix}$. *There exists a permutation matrix P such that within* $\mathcal{M}$, $\begin{bmatrix} \Upsilon_0 & \Upsilon_1 & \cdots & \Upsilon_{n_\upsilon} & B_0 & B_1 & \cdots & B_{n_b} \end{bmatrix} P = \begin{bmatrix} D & R \end{bmatrix}$ *with D square, diagonal, and full rank.*
3. *The zero structure of $G(q)$ is known in* $\mathcal{M}$.
4. *If $G_{ij}(q) \neq 0$, then $G_{ji}(q) = 0$, $\forall i, j = 1, 2, \ldots, L$, within* $\mathcal{M}$.
5. *At least one excitation signal $r_j(t)$, $j = 1, \ldots, K$, is present: $K \geq 1$.*
6. *There is at least one constraint on the parameters of $A(q^{-1}, \theta_A)$ and $B(q^{-1}, \theta_B)$ of the form $\Gamma\bar{\theta} = \gamma \neq 0$, with Γ full row rank and with $\bar{\theta}^\top := \begin{bmatrix} \theta_A^\top & \theta_B^\top \end{bmatrix}$.*

Proof: The proof is provided in Appendix 11.D. ■

If the directed dynamics are polynomial: $G(q) = G(q^{-1})$, then these dynamics can also be used to find unique $A(q^{-1})$, $B(q^{-1})$, and $G(q)$ from $\tilde{A}(q^{-1})$, $\tilde{B}(q^{-1})$, and $\tilde{G}(q)$.

Proposition 11.19 (Identifiability for polynomial directed dynamics). *If the directed dynamics are polynomial: $G(q) = G(q^{-1})$, then Condition 6.*

of Proposition 11.18 can be replaced by

6. *There is at least one constraint on the parameters of* $A(q^{-1}, \theta_A)$, $B(q^{-1}, \theta_B)$, *and* $G(q^{-1}, \theta_G)$ *of the form* $\Gamma\bar{\theta} = \gamma \neq 0$, *with* Γ *full row rank and with* $\bar{\theta} := \begin{bmatrix} \theta_A^\top & \theta_B^\top & \theta_G^\top \end{bmatrix}^\top$.

Proof: If the directed dynamics are polynomial, then $d_G(q^{-1}) = 1$, see Propositions 11.9, and (11.24c) changes to $\tilde{G}(q^{-1}) = \alpha G(q^{-1})$. Then Lemma 11.17 only needs to fix the scaling factor α in (11.24). ■

The parameter constraint in Condition 6. of Proposition 11.19 means, for example, that: one parameter, a fraction of two parameters, or the sum of some nonzero parameters is known; one excitation signal enters a node through (partially) known dynamics; the directed dynamics in one link are (partially) known. The first one relates to the undirected dynamics in the network, while the second one relates to the dynamics through which an external excitation signal enters the network, and the third one relates to the directed dynamics in the network.

Remark 11.20 (Identifiability for known directed dynamics). *If the directed dynamics* $G(q)$ *are known, then Condition 3. of Proposition 11.18 is satisfied and Conditions 4. and 6. of Proposition 11.18 drop, because* (11.24c) *leads to unique* $\alpha d_G(q^{-1})$ *(with* $d_g(q^{-1})$ *known from* $G(q)$*) and* $\breve{A}(q^{-1})$ *can uniquely be determined from* $\breve{\Upsilon}(q^{-1})$.

11.4.4 Consistency

Now, the consistency result is formulated as follows:

Theorem 11.21 (Consistency). *Consider a data generating network* $\mathcal{S}$ *and a model set* $\mathcal{M}$ (11.12). *Then* $M(\hat{\theta}_N)$ *is a consistent estimate of* $\mathcal{S}$ *if the following conditions hold:*

1. *The true system is in the model set (*$\mathcal{S} \in \mathcal{M}$*).*
2. *The data are informative with respect to the model set.*
3. *The model set is globally network identifiable.*

Proof: The proof is provided in Appendix 11.E. ■

11.4.5 Algorithm

In order to consistently identify the mixed dynamic network model set $\mathcal{M}$ (11.12), multiple identification steps have to be performed. First, the polynomial network representation (11.7) has to be identified. This can be achieved by an adapted version of the multistep least-squares algorithm presented in Section 8.5. The adaptation that has to be made, is that the partially asymmetric structure of $\breve{\Upsilon}(q^{-1})$ has to be incorporated. Once the polynomial representation of the mixed dynamic network (11.7) is identified, it can be used to identify the original mixed dynamic network (11.4). This is achieved by an additional step, as indicated by Lemma 11.17. In general, this leads to a nonconvex optimisation problem, which can be formulated as, for example, a separable least-squares problem or a bilinear optimisation problem. Several algorithms have been developed for solving the nonconvex optimisation problem, which leads to local optima (Fazzi et al., 2019; Golub and Pereyra, 1973). Obtaining the global optimum cannot be guaranteed due to the nonconvex nature of the optimisation problem.

The mixed dynamic networks in Case 1. can be identified once the proposed algorithm is implemented. This includes the identification of the full dynamics and, with that, the identification of the topology of the undirected part. The topology of the directed part is included in the identification procedure and assumed to be known for identifiability purposes. In Section 11.8.1, relaxation of the topological conditions on the directed part, and particular on identifiability Condition 4., (Proposition 11.18) is discussed. Most of the steps in the algorithm are convex least-squares steps that are the same or similar to the steps for full identification of diffusively coupled linear networks, as discussed in Chapter 8. The critical part of the algorithm is the nonconvex optimisation step for determining $A(q^{-1})$, $B(q^{-1})$, and $G(q)$ from $\breve{A}(q^{-1})$, $\breve{B}(q^{-1})$, and $\breve{G}(q^{-1})$; see Lemma 11.17. As this optimisation is nonconvex, it may lead to local optima instead of the global optimum. Additional research is required to understand the consequences of this and to determine a proper approach (possibly applying weighted null-space fitting (WNSF) to make the optimisation convex).

11.5 Case 2: Modelling

11.5.1 Introduction

In Case 2., we consider a mixed dynamic network that consists of an undirected and a directed network that are interconnected with each other through directed links between the nodes. As mentioned before, the node signals in the undirected

part are referred to as *undirected node signals* and related signals are indicated with the subscript u, while the node signals in the directed part are referred to as *directed node signals* and related signals are indicated with the subscript d. This separation into two sets of node signals will lead to two different types of modelling equations for the two different sets.

11.5.2 Directed node signals

The behaviour of the directed node signals $w_j(t)$, $j = 1, \ldots, L$, is described by

$$w_j(t) = \sum_{i \in \mathcal{N}_j^d} G_{ji}(q) w_i(t) + \sum_{k=1}^{K} R_{jk}(q) r_k(t) + \sum_{i \in \mathcal{N}_j^u} W_{ji}(q) w_i(t) + \sum_{i=1}^{L} H_{ji}(q) e_i(t), \quad (11.25)$$

where $\mathcal{N}_j^d$ is the set of indices of directed node signals $w_k(t)$, $k \neq j$, with connections to node signal $w_j(t)$; $\mathcal{N}_j^u$ is the set of indices of undirected node signals $w_k(t)$, $k \neq j$, with connections to node signal $w_j(t)$; $W_{ji}(q)$ are proper rational transfer functions that describe the directed interconnection from the undirected node signals to the directed node signals.

The behaviour of all directed node signals can be combined in a matrix equation as

$$w_d(t) = G(q) w_d(t) + W_{du}(q) w_u(t) + R(q) r_d(t) + H(q) e_d(t), \quad (11.26)$$

where $w_d(t)$ are the directed node signals, $w_u(t)$ are the undirected node signals, and $r_d(t)$ and $e_d(t)$ are the external excitation and noise signals acting on $w_d(t)$, respectively. The expression (11.26) is just a module representation (11.2), where the undirected node signals $w_u(t)$ enter the model as external input signals through dynamics $W_{du}(q)$.

11.5.3 Undirected node signals

The behaviour of the undirected node signals $w_j(t)$, $j = 1, \ldots, L$, is described by

$$x_{jj}(q^{-1}) w_j(t) + \sum_{k \in \mathcal{N}_j^u} y_{jk}(q^{-1}) \big[w_j(t) - w_k(t) \big] =$$

$$\sum_{k=1}^{K} b_{jk}(q^{-1})r_k(t) + \sum_{i\in\mathcal{N}_j^d} W_{ji}(q)w_i(t) + \sum_{i=1}^{L} F_{ji}(q)e_i(t), \quad (11.27)$$

where $\mathcal{N}_j^u$ is the set of indices of undirected node signals $w_k(t)$, $k \neq j$, with connections to node signal $w_j(t)$; $\mathcal{N}_j^d$ is the set of indices of directed node signals $w_k(t)$, $k \neq j$, with connections to node signal $w_j(t)$; $W_{ji}(q)$ are proper rational transfer functions that describe the directed interconnection from the directed node signals to the undirected node signals.

The behaviour of all undirected node signals can be combined in a matrix equation as

$$A(q^{-1})w_u(t) = B(q^{-1})r_u(t) + W_{ud}(q)w_d(t) + F(q)e_u(t). \quad (11.28)$$

where $w_u(t)$ are the undirected node signals, $w_d(t)$ are the directed node signals, and $r_u(t)$ and $e_u(t)$ are the external excitation and noise signals acting on $w_u(t)$, respectively. The expression (11.28) is (almost) an undirected network model (11.1), where the directed node signals $w_d(t)$ enter the model as external input signals through dynamics $W_{ud}(q)$. The only difference with the diffusively coupled network model (11.1) is that $W_{ud}(q)$ is allowed to be rational.

11.5.4 Mixed dynamic network

The mixed network can now be derived by combining (11.26) and (11.28), leading to

$$\begin{bmatrix} I & 0 \\ 0 & A(q^{-1}) \end{bmatrix} \begin{bmatrix} w_d(t) \\ w_u(t) \end{bmatrix} = \begin{bmatrix} G(q) & W_{du}(q) \\ W_{ud}(q) & 0 \end{bmatrix} \begin{bmatrix} w_d(t) \\ w_u(t) \end{bmatrix} + \begin{bmatrix} R(q) & 0 \\ 0 & B(q^{-1}) \end{bmatrix} r(t) + \begin{bmatrix} H(q) & 0 \\ 0 & F(q) \end{bmatrix} e(t), \quad (11.29)$$

where $W_{du}(q)$ and $W_{ud}(q)$ are generally not square. Define

$$\breve{J}(q) := \begin{bmatrix} I - G(q) & -W_{du}(q) \\ -W_{ud}(q) & A(q^{-1}) \end{bmatrix} \quad (11.30)$$

then the input-output relations between the signals can be described by

$$w(t) = \breve{J}^{-1}(q) \begin{bmatrix} R(q) & 0 \\ 0 & B(q^{-1}) \end{bmatrix} r(t) + \breve{J}^{-1}(q) \begin{bmatrix} H(q) & 0 \\ 0 & F(q) \end{bmatrix} e(t), \quad (11.31a)$$

$$= T_{wr}(q)r(t) + T_{we}(q)e(t), \quad (11.31b)$$

with $\breve{J}(q)$ as in (11.30).

Proposition 11.22 (Well-posedness). *The network* (11.29) *is well-posed if all principal minors of* $\lim_{z\to\infty} \breve{J}(z)$ *are nonzero.*

Proof: The proof follows from applying Dankers (2014, Proposition 2.14) to the network (11.29). ■

The well-posedness of the network implies that $\breve{J}(q)$ has full rank.

The network model (11.29) contains both rational matrices ($G(q)$, $W_{du}(q)$, $W_{ud}(q)$, $R(q)$) and polynomial matrices ($A(q^{-1})$, $B(q^{-1})$) and therefore, it is not written in polynomial form (11.1). It does not satisfy the properties of the module representation (11.2) either, because of $A(q^{-1})$ on the left-hand side (which could be brought to the right-hand side, but then dynamics of several interconnections (or modules) get mixed).

The objective is to consistently identify the complete dynamics of the mixed dynamic network. To achieve this objective, identification theory from the polynomial framework for diffusively coupled networks and from the module representation for directed interconnected networks is used. In order to analyse the mixed dynamic network for this purpose, we consider two situations:

a. The network (11.29) is written in polynomial form (11.1).

b. The network (11.29) is written in the module representation (11.2).

11.5.5 Mixed dynamic network in polynomial form

In order to model the mixed network in polynomial form, the directed part (11.26) needs to be rewritten into a polynomial form. This is done by splitting the transfer functions into numerator and denominator polynomials. Consider the monic and diagonal polynomial denominator matrix $D_d(q^{-1})$ and polynomial numerator matrices $G^N(q^{-1})$, $W_{du}^N(q^{-1})$, and $R^N(q^{-1})$ such that

$$\begin{bmatrix} G(q) & W_{du}(q) & R(q) \end{bmatrix} = D_d^{-1}(q^{-1}) \begin{bmatrix} G^N(q^{-1}) & W_{du}^N(q^{-1}) & R^N(q^{-1}) \end{bmatrix}. \tag{11.32}$$

Observe that the numerator matrices $G^N(q^{-1})$, $W_{du}^N(q^{-1})$, and $R^N(q^{-1})$ adopt the zero structure of $G(q)$, $W_{du}(q)$, and $R(q)$, respectively. Substituting the matrix-fraction description (11.32) into (11.26) leads to a polynomial model of the directed part:

$$\begin{aligned} \big(D_d(q^{-1}) - G^N(q^{-1})\big) w_d(t) - W_{du}^N(q^{-1}) w_u(t) = \\ R^N(q^{-1}) r_d(t) + D_d(q^{-1}) H(q) e_d(t). \end{aligned} \tag{11.33}$$

As $D_d(q^{-1})$ is diagonal and $G^N(q^{-1})$ is hollow, they can uniquely be found from the polynomial matrix $\big(D_d(q^{-1}) - G^N(q^{-1})\big)$.

The undirected part (11.28) is only modelled by a polynomial network model (11.1) if $W_{ud}(q)$ is restricted to be polynomial. However, in general, $W_{ud}(q)$ is rational and therefore, it needs to be rewritten into a polynomial form. This is done similarly as before, by splitting $W_{ud}(q)$ into a numerator polynomial matrix $W^N_{ud}(q^{-1})$ and a monic and diagonal denominator polynomial matrix $D_u(q^{-1})$, such that

$$W_{ud}(q) = D_u^{-1}(q^{-1})W^N_{ud}(q^{-1}), \tag{11.34}$$

where $W^N_{ud}(q^{-1})$ adopts the zero structure of $W_{ud}(q)$. In order to make the expression (11.28) polynomial, we need to premultiply the whole expression with

$$d(q^{-1}) := \frac{det\big(D_u(q^{-1})\big)}{gcd\big(det\big(D_u(q^{-1})\big), adj\big(D_u(q^{-1})\big)\big)}, \tag{11.35}$$

with $gcd(x, Y)$ the greatest common divisor of scalar x and all scalar elements of matrix Y. This leads to a polynomial model of the undirected part:

$$\begin{aligned} d(q^{-1})A(q^{-1})w_u(t) - d(q^{-1})D_u^{-1}(q^{-1})W^N_{ud}(q^{-1})w_d(t) = \\ d(q^{-1})B(q^{-1})r_u(t) + d(q^{-1})F(q^{-1})e_u(t). \end{aligned} \tag{11.36}$$

Now, the polynomial descriptions of the directed part (11.33) and the undirected part (11.36) can be combined to describe the mixed network in a polynomial form as

$$\begin{aligned} \begin{bmatrix} D_d(q^{-1}) - G^N(q^{-1}) & -W^N_{du}(q^{-1}) \\ -d(q^{-1})D_u^{-1}(q^{-1})W^N_{ud}(q^{-1}) & d(q^{-1})A(q^{-1}) \end{bmatrix} \begin{bmatrix} w_d(t) \\ w_u(t) \end{bmatrix} = \\ \begin{bmatrix} R^N(q^{-1}) & 0 \\ 0 & d(q^{-1})B(q^{-1}) \end{bmatrix} \begin{bmatrix} r_d(t) \\ r_u(t) \end{bmatrix} + \\ \begin{bmatrix} D_d(q^{-1})H(q) & 0 \\ 0 & d(q^{-1})F(q) \end{bmatrix} \begin{bmatrix} e_d(t) \\ e_u(t) \end{bmatrix}. \end{aligned} \tag{11.37}$$

This leads to the following representation of the mixed dynamic network in polynomial form:

Proposition 11.23 (Mixed dynamic network model in polynomial form). *Every mixed dynamic network* (11.29) *can be described by*

$$A_m(q^{-1})w(t) = B_m(q^{-1})r(t) + F_m(q)e(t), \tag{11.38}$$

with

$$A_m(q^{-1}) = \begin{bmatrix} A_{m11}(q^{-1}) & A_{m12}(q^{-1}) \\ A_{m21}(q^{-1}) & A_{m22}(q^{-1}) \end{bmatrix} = \begin{bmatrix} D_d(q^{-1}) - G^N(q^{-1}) & -W_{du}^N(q^{-1}) \\ -d(q^{-1})D_u^{-1}(q^{-1})W_{ud}^N(q^{-1}) & d(q^{-1})A(q^{-1}) \end{bmatrix}, \tag{11.39a}$$

$$B_m(q^{-1}) = \begin{bmatrix} B_{m11}(q^{-1}) & B_{m12}(q^{-1}) \\ B_{m21}(q^{-1}) & B_{m22}(q^{-1}) \end{bmatrix} = \begin{bmatrix} R^N(q^{-1}) & 0 \\ 0 & d(q^{-1})B(q^{-1}) \end{bmatrix}, \tag{11.39b}$$

$$F_m(q) = \begin{bmatrix} F_{m11}(q) & F_{m12}(q) \\ F_{m21}(q) & F_{m22}(q) \end{bmatrix} = \begin{bmatrix} D_d(q^{-1})H(q) & 0 \\ 0 & d(q^{-1})F(q) \end{bmatrix}, \tag{11.39c}$$

$$\Lambda_m = \begin{bmatrix} \Lambda_d & 0 \\ 0 & \Lambda_u \end{bmatrix}, \tag{11.39d}$$

with $\big(A(q^{-1}), B(q^{-1}), F(q^{-1}), \Lambda_u\big)$ *satisfying Definition 11.1, with* $\big(G(q), R(q), H(q), \Lambda_d\big)$ *satisfying Definition 11.2, and with* $W_{du}(q)$ *and* $W_{ud}(q)$ *being rational matrices.*

Proof: Consider the mixed dynamic network model in (11.29). Substitute (11.32) and (11.34), premultiply both sides of the equation with

$$\begin{bmatrix} D_d(q^{-1}) & 0 \\ 0 & d(q^{-1}) \end{bmatrix}$$

with $d(q^{-1})$ given by (11.37), and subtract

$$\begin{bmatrix} G^N(q^{-1}) & W_{du}^N(q^{-1}) \\ d(q^{-1})D_u^{-1}(q^{-1})W_{ud}^N(q^{-1}) & 0 \end{bmatrix} \begin{bmatrix} w_d(t) \\ w_j(t) \end{bmatrix}$$

from both sides of the equation. This results in (11.37). ■

As a result of Proposition 11.23, $B_m(q^{-1})$, $F_m(q)$, and Λ_m are block diagonal and $F_m(q)$ is monic, stable, and stably invertible, because $H(q)$ (11.26) and $F(q)$ (11.28) are monic, stable, and stably invertible and $D_d(q^{-1})$ and $d(q^{-1})$ are both monic.

The network is assumed to be well-posed and stable, implying that $A_m^{-1}(q^{-1})$ exists and is proper and stable. As explained before, the well-posedness of the mixed dynamic network is satisfied if Proposition 11.22 is satisfied, where this proposition implies that all principle minors of $\lim_{z\to\infty} A_m(z)$ are nonzero.

11.5.6 Mixed dynamic network in the module representation

In order to model the mixed network in the module representation, the undirected part (11.28) needs to be rewritten into the module representation. This is done by using the method described in Chapter 7[2]. Define

$$Q(q^{-1}) := \operatorname{diag}\big(A(q^{-1})\big), \qquad P(q^{-1}) := Q(q^{-1}) - A(q^{-1}), \tag{11.40}$$

where $Q(q^{-1})$ is a diagonal polynomial matrix and $P(q^{-1})$ is a hollow and symmetric polynomial matrix. Let $P(q^{-1})$ and $Q(q^{-1})$ as in (11.40) and apply Definition (7.5), which relates module representations with $G(q)$, $R(g)$ and $H(q)$ to diffusively coupled network models with $P(q^{-1})$, $Qq^{-1})$, $B(q^{-1})$, and $F(q^{-1})$, to the mixed dynamic network model (11.28). This leads to

$$w_u(t) = G_u(q)w_u(t) + \tilde{W}_{ud}(q)w_d(t) + R_u(q)r_u(t) + H_u(q)\tilde{e}_u(t), \tag{11.41}$$

with $\tilde{e}_u(t) = Q_0^{-1}e_u(t)$, $Q_0 = \lim_{z\to\infty} Q(z)$, and

$$G_u(q) = Q^{-1}(q^{-1})P(q^{-1}), \tag{11.42a}$$
$$\tilde{W}_{ud}(q) = Q^{-1}(q^{-1})W_{ud}(q), \tag{11.42b}$$
$$R_u(q) = Q^{-1}(q^{-1})B(q^{-1}), \tag{11.42c}$$
$$H_u(q) = Q^{-1}(q^{-1})F(q)Q_0. \tag{11.42d}$$

Due to the structure of $Q(q^{-1})$ and $P(q^{-1})$, the module representation (11.41) satisfies the structural properties explained in Chapter 7.

Now, the module representation of the directed part (11.26) and the undirected part (11.41) can be combined to describe the mixed network in a module representation as

$$\begin{bmatrix} w_d(t) \\ w_u(t) \end{bmatrix} = \begin{bmatrix} G(q) & -W_{du}(q) \\ -\tilde{W}_{ud}(q) & G_u(q) \end{bmatrix} \begin{bmatrix} w_d(t) \\ w_u(t) \end{bmatrix} + \begin{bmatrix} R(q) & 0 \\ 0 & R_u(q) \end{bmatrix} \begin{bmatrix} r_d(t) \\ r_u(t) \end{bmatrix} + \begin{bmatrix} H(q) & 0 \\ 0 & H_u(q) \end{bmatrix} \begin{bmatrix} e_d(t) \\ \tilde{e}_u(t) \end{bmatrix}. \tag{11.43}$$

This leads to the following description of the mixed dynamic network in the module representation:

[2]The difference with the method in Chapter 7 is that the noise model is made monic in a slightly different way to simplify the relation between $e_u(t)$ and $\tilde{e}_u(t)$.

Proposition 11.24 (Mixed dynamic network model in module representation). *Every mixed dynamic network* (11.29) *can be described by*

$$w(t) = G_m(q)w(t) + R_m(q)r(t) + H_m(q)\tilde{e}(t), \tag{11.44}$$

with $\tilde{e}(t) = \begin{bmatrix} e_d^\top(t) & \tilde{e}_u^\top(t) \end{bmatrix}^\top$ *and*

$$G_m(q) = \begin{bmatrix} G_{m11}(q) & G_{m12}(q) \\ G_{m21}(q) & G_{m22}(q) \end{bmatrix} = \begin{bmatrix} G(q) & -W_{du}(q) \\ -\tilde{W}_{ud}(q) & G_u(q) \end{bmatrix}, \tag{11.45a}$$

$$R_m(q) = \begin{bmatrix} R_{m11}(q) & R_{m12}(q) \\ R_{m21}(q) & R_{m22}(q) \end{bmatrix} = \begin{bmatrix} R(q) & 0 \\ 0 & R_u(q) \end{bmatrix}, \tag{11.45b}$$

$$H_m(q) = \begin{bmatrix} H_{m11}(q) & H_{m12}(q) \\ H_{m21}(q) & H_{m22}(q) \end{bmatrix} = \begin{bmatrix} H(q) & 0 \\ 0 & H_u(q) \end{bmatrix}, \tag{11.45c}$$

$$\tilde{\Lambda}_m = \begin{bmatrix} \Lambda_d & 0 \\ 0 & \tilde{\Lambda}_u \end{bmatrix}, \tag{11.45d}$$

with $\tilde{\Lambda}_u = Q_0^{-1}\Lambda_u Q_0^{-1}$, *with* $\left(A(q^{-1}), B(q^{-1}), F(q^{-1}), \Lambda_u\right)$ *satisfying Definition 11.1, with* $\left(G(q), R(q), H(q), \Lambda_d\right)$ *satisfying Definition 11.2, and with* $W_{du}(q)$ *and* $W_{ud}(q)$ *being rational matrices.*

Proof: Consider the mixed dynamic network model in (11.29). Substitute $A(q^{-1}) = Q(q^{-1}) - P(q^{-1})$ with $P(q^{-1})$ and $Q(q^{-1})$ as in (11.40), add

$$\begin{bmatrix} 0 & 0 \\ 0 & P(q^{-1})w_u(t) \end{bmatrix}$$

to both sides of (11.29), premultiply both sides with

$$\begin{bmatrix} I & 0 \\ 0 & Q^{-1}(q^{-1}) \end{bmatrix},$$

and rewrite the noise model $H(q)e_u(t)$ as $H_u(q)\tilde{e}_u(t)$. This results in (11.43). ■

As a result of Proposition 11.24, $G_m(q)$, $G(q)$, and $G_u(q)$ are hollow and $R_m(q)$, $H_m(q)$, and $\tilde{\Lambda}_m$ are block diagonal. Further, $H_m(q)$ is monic, stable, and stably invertible. In addition, the mixed dynamic network model in module representation (11.44) contains some structural restrictions in terms of symmetry, which are similar to the ones described in Chapter 7. Observe that the transfer functions $G_{f_{jk}}(q)$ and $G_{f_{kj}}(q)$ have the same numerator; the transfer functions $G_{f_{jk}}(q)$ and $\tilde{W}_{ud_{j\ell}}(q)$ have the same denominator if $W_{ud}(q)$ is polynomial; $G_{f_{jk}}(q)$ and $R_{f_{j\ell}}(q)$ have the same denominator; $G_{f_{jk}}(q)$ and $H_{f_{j\ell}}(q)$ have the same denominator if $F(q)$ is polynomial.

11.6 Case 2: Identification in polynomial form

11.6.1 Identification setup

This chapter involves the full network identification of mixed dynamic networks. In this section, this problem is dealt with in the polynomial framework, which means that the model (11.38) will be used for identification. The identification problem that will be considered in this section is defined as before, see Definition 11.11, and concerns the identification of all dynamics in the network. In this case, the topology of the complete network can be identified as well.

This means that both the directed and undirected dynamics are assumed to be unknown and will be identified, as well as the topology of the complete network. The only topological aspect that is assumed to be known, is the separation of the node signals into a set of directed node signals and a set of undirected node signals. Both the directed part and the undirected part are assumed to be *connected*, meaning that the mixed dynamic network consists of a single undirected network and a single directed network that are interconnected with each other.

Consider the polynomial representation of the mixed dynamic network model (11.38). For solving the mixed identification problem formulated above, a similar approach is applied as for full network identification of diffusively coupled linear networks (Chapter 8), because the mixed dynamic network is modelled in a similar polynomial framework. The difference is that a major part of the network dynamics captured by $A_m(q^{-1})$ in (11.38) is not symmetric.

First, a predictor model is set up based on the parameterised model set

$$\mathcal{M} := \{M(\theta), \theta \in \Theta \subset \mathbb{R}^d\} \tag{11.46}$$

with $d \in \mathbb{N}$ and with particular models

$$M(\theta) := \big(A(q^{-1},\theta), B(q^{-1},\theta), F(q,\theta), G(q,\theta), R(q,\theta), H(q,\theta), W_{du}(q,\theta), W_{ud}(q,\theta), \Lambda_u(\theta), \Lambda_d(\theta)\big), \tag{11.47}$$

where θ contains all unknown coefficients that appear in the entries of the model matrices $A(q^{-1})$, $B(q^{-1})$, $F(q)$, $G(q^{-1})$, $R(q)$, $H(q)$, $W_{du}(q)$, $W_{ud}(q)$, and Λ. The data generating network is denoted by $\mathcal{S} := \big(A^0, B^0, F^0, G^0, R^0, H^0, W^0_{du}, W^0_{ud}, \Lambda^0_u, \Lambda^0_d\big)$. The true system lies in the model set if $\mathcal{S} = M(\theta^0)$, where $\theta^0 \in \Theta$ indicate the true parameter values.

In addition, consider the model set

$$\mathcal{M}_{mu} := \{M_{mu}(\eta), \eta \in \Pi \subset \mathbb{R}^d\} \tag{11.48}$$

with $d \in \mathbb{N}$ and with particular models

$$M_{mu}(\eta) := \big(A_m(q^{-1},\eta), B_m(q^{-1},\eta), F_m(q,\eta), \Lambda_m(\eta)\big), \tag{11.49}$$

where η contains all unknown coefficients that appear in the entries of the model matrices $A_m(q^{-1})$, $B_m(q^{-1})$, $F_m(q)$, and Λ_m, with Λ_m the covariance of $e(t)$ given by

$$\Lambda_m = \begin{bmatrix} \Lambda_d & 0 \\ 0 & \Lambda_u \end{bmatrix}. \tag{11.50}$$

The data generating network is denoted by $\mathcal{S}_{mu} := \big(A_m^0, B_m^0, F_m^0, \Lambda_m^0\big)$. The true system lies in the model set if $\mathcal{S}_{mu} = M_{mu}(\eta^0)$, where $\eta^0 \in \Pi$ indicate the true parameter values.

The network predictor is defined as in Definition 8.4 and leads to

$$\hat{w}(t|t-1) = \left[I - A_{m0}^{-1}F_m^{-1}(q)A_m(q^{-1})\right] w(t) + A_{m0}^{-1}F_m^{-1}(q)B_m(q^{-1})r(t), \tag{11.51}$$

with $A_{m0} := \lim_{z\to\infty} A_m(z)$. Along the same lines of reasoning as for Case 1. presented in Section 11.4.1, the parameterised predictor leads to the prediction error $\breve{e}(t,\eta)$ (11.17) resulting in

$$\breve{\varepsilon}(t,\eta) = W_w(q,\eta)w(t) - W_r(q,\eta)r(t), \tag{11.52}$$

with predictor filters

$$W_w(q,\eta) = A_{m0}^{-1}(\eta)F_m^{-1}(q,\eta)A_m(q^{-1},\eta), \tag{11.53a}$$

$$W_r(q,\eta) = A_{m0}^{-1}(\eta)F_m^{-1}(q,\eta)B_m(q^{-1},\eta). \tag{11.53b}$$

Again, the parameters are estimated through the least-squares identification criterion (11.20) with prediction error (11.52).

In order to identify the mixed dynamic network (11.29), first the mixed dynamic network model in polynomial form (11.38) will be identified from the data, after which the identified polynomial network model is used to obtain the original mixed network model.

In the next sections, the consistent identification of the mixed network model is analysed by considering data informativity and network identifiability. This leads to conditions for which a consistent estimate of the data generating mixed dynamic network $\mathcal{S}$ can be found.

11.6.2 Data informativity

Conditions for data informativity are again derived along the same line of reasoning as in Proposition 8.12, where a crucial role is reserved for the relation $z(t) =$

$J(q)\kappa(t)$ (8.67). We find the following conditions for data informativity for the mixed dynamic network model (11.29) or, equivalently, (11.38):

Proposition 11.25 (Data informativity). *The quasi-stationary data sequence $z(t)$ is* informative with respect to the model set $\mathcal{M}$ (11.46) *if $\Phi_z(\omega) \succ 0$ for a sufficiently high number of frequencies. In the situation $K \geq 1$, this is guaranteed by $\Phi_r(\omega) \succ 0$ for a sufficiently high number of frequencies.*

Proof: The proof is provided in Appendix 11.F. ■

The implication of Proposition 11.25 is that all node signals in the mixed dynamic network have to be sufficiently excited. The difference with Proposition 11.13 is that now the directed node signals also have to be sufficiently excited, while in Case 1., which is considered in Proposition 11.13, there are no node signals with only directed interconnections present in the mixed network. The final condition ($\Phi_r(\omega) \succ 0$ for a sufficiently high number of frequencies) is the same in both situations, because it is assumed that all node signals in the network are excited by disturbances.

11.6.3 Network identifiability

Conditions for network identifiability are derived along the same line of reasoning as in Proposition 8.15. The first step includes the unique recovery of the LMFD $A_m^{-1}B_m(q^{-1})$ from $T_{wr}(q)$. Second, $A_m(q^{-1})$ and $B_m(q^{-1})$ are used to recover the network dynamics $A(q^{-1})$, $B(q^{-1})$, $G(q)$, $R(q)$, $W_{du}(q)$ and $W_{ud}(q)$. Finally, the noise model described by $H(q)$, $F(q)$, Λ_u, and Λ_d is uniquely recovered from $\Phi_{\bar{v}}(\omega)$.

In the undirected part of the mixed dynamic network, direct feedthrough terms and algebraic loops are allowed to be present. For the directed part in the mixed dynamic network, we make the following assumption on properness:

Assumption 11.26 (Properness). *Consider the network model set* (11.47). *Assume that $G(q)$ is proper and that $W_{du}(q)$ and $W_{ud}(q)$ are strictly proper.*

This means that it is possible that there are direct feedthrough terms in the directed part of the network. However, the interconnection dynamics between the directed and the undirected parts of the network has no direct feedthrough term and therefore, there cannot be algebraic loops in these interconnections.

Before moving to the LMFDs, consider the following result:

Lemma 11.27 (Left coprime). *The polynomials $A_m(q^{-1})$ and $B_m(q^{-1})$ are left coprime within $\mathcal{M}_{mu}$ if $A(q^{-1})$ and $B(q^{-1})$ are left coprime within $\mathcal{M}$.*

Proof: The proof is provided in Appendix 11.G. ■

Now, the following result on the LMFD is formulated:

Lemma 11.28 (LMFD). *Consider the network model set $\mathcal{M}$* (11.47) *satisfying Assumption 11.26 and with $A_m(q^{-1})$ and $B_m(q^{-1})$ given by* (11.39a) *and* (11.39b)*, respectively. Given the* LMFD $A_m^{-1}(q^{-1})B_m(q^{-1})$*, then within $\mathcal{M}$, the polynomial matrices $A_m(q^{-1})$ and $B_m(q^{-1})$ are unique up to a scalar factor for $A_{m22}(q^{-1})$ and $B_{m22}(q^{-1})$, if the following conditions are satisfied:*

1. *The polynomials $A(q^{-1})$ and $B(q^{-1})$ are left coprime in $\mathcal{M}$.*
2. *There exists a permutation matrix P such that within $\mathcal{M}$, $\begin{bmatrix} A_0 & A_1 & \cdots & A_{n_a} & B_0 & B_1 & \cdots & B_{n_b} \end{bmatrix} P = \begin{bmatrix} D & R \end{bmatrix}$ with D square, diagonal, and full rank.*
3. *There are no algebraic loops in $G(q)$.*

Proof: The proof is provided in Appendix 11.H. ■

The algebraic loops in $A(q^{-1})$ are accounted for by the symmetry that is present in $A(q^{-1})$. This is not possible for the algebraic loops that are present in $G(q)$.

Remark 11.29 (LMFD proper interconnection dynamics). *If $W_{du}(q)$ and $W_{ud}(q)$ are proper (not necessarily strictly proper), then it is unclear which conditions need to be satisfied to guarantee that the polynomial matrices $A_m(q^{-1})$ and $B_m(q^{-1})$ are unique within $\mathcal{M}$ up to a scalar factor. Condition 1. of Lemma 11.28 again implies that $A_m(q^{-1})$ and $B_m(q^{-1})$ are left coprime and according to Kailath (1980) are unique up to a premultiplication with a unimodular matrix $U(q^{-1})$. With proper $G(q)$, $W_{du}(q)$, and $W_{ud}(q)$, it follows that:*

$$A_{m0} := \lim_{z\to\infty} A_m(z) = \begin{bmatrix} I - G_0^N & -W_{fr0}^N \\ -W_{rf0}^N & A_0 \end{bmatrix},$$

because $d(q^{-1})$, $D_u(q^{-1})$, and $D_d(q^{-1})$ are monic, with $A_0 := \lim_{z\to\infty} A(z)$, $W_{fr0}^N := \lim_{z\to\infty} W_{ud}^N(z)$, $W_{rf0}^N := \lim_{z\to\infty} W_{du}^N(z)$, and

$G_0^N := \lim_{z\to\infty} G^N(z)$. It is unclear under what conditions $U(q^{-1})A_{m0}$ has the same structural properties as A_{m0}. The expectation is that Condition 2. of Lemma 11.28 has to hold and that there has to be a condition like Condition 3. of Lemma 11.28 that has to hold for $G(q)$, $W_{du}(q)$, and $W_{ud}(q)$ together.

The result of Lemma 11.28 directly leads to unique $G(q)$, $R(q)$, and $W_{du}(q)$ as follows: As $D_d(q^{-1})$ is diagonal and $G^N(q^{-1})$ has zero elements on the diagonal, $D_d(q^{-1})$ and $G^N(q^{-1})$ can directly be determined from $A_m(q^{-1})$. Polynomials $W_{du}^N(q^{-1})$ and $R^N(q^{-1})$ can directly be extracted from $A_m(q^{-1})$ and $B_m(q^{-1})$, respectively. This leads to $G(q)$, $R(q)$, and $W_{du}(q)$ through the relation in (11.32).

Next, we prove that $A(q^{-1})$, $B(q^{-1})$, and $W_{ud}(q^{-1})$ can be obtained from scaled versions of $A_m(q^{-1})$ and $B_m(q^{-1})$. From $A_m(q^{-1})$ (11.39a) and $B_m(q^{-1})$ (11.39b), the following relations hold:

$$\tilde{A}_{m21}(q^{-1}) = \alpha d(q^{-1})W_{ud}(q), \tag{11.54a}$$

$$\tilde{A}_{m22}(q^{-1}) = \alpha d(q^{-1})A(q^{-1}), \tag{11.54b}$$

$$\tilde{B}_{m22}(q^{-1}) = \alpha d(q^{-1})B(q^{-1}), \tag{11.54c}$$

with $\tilde{A}_{m21}(q^{-1}) := \alpha A_{m21}(q^{-1})$, $\tilde{A}_{m22}(q^{-1}) := \alpha A_{m22}(q^{-1})$, $\tilde{B}_{m22}(q^{-1}) := \alpha B_{m22}(q^{-1})$, the scalar scaled versions of $A_{m21}(q^{-1})$, $A_{m22}(q^{-1})$, and $B_{m22}(q^{-1})$, respectively, and with scaling factor $\alpha \in \mathbb{R}_+$.

Lemma 11.30 (Uniqueness of $A(q^{-1})$, $B(q^{-1})$, and $W_{ud}(q)$). *If there is at least one linear constraint on the coefficients of $A(q^{-1}, \theta_A)$ and $B(q^{-1}, \theta_B)$ of the form $\Gamma\bar{\theta} = \gamma \neq 0$, with Γ full row rank and with $\bar{\theta}^\top := \begin{bmatrix}\theta_A^\top & \theta_B^\top\end{bmatrix}$, then $A(q^{-1})$, $B(q^{-1})$, and $W_{ud}(q)$ are uniquely obtained from $\tilde{A}_{m21}(q^{-1})$, $\tilde{A}_{m22}(q^{-1})$, and $\tilde{B}_{m22}(q^{-1})$ through* (11.54).

Proof: Because $A(q^{-1})$ and $B(q^{-1})$ are left coprime, the polynomial $d(q^{-1})$ is the greatest monic common divisor of the polynomial matrices $\tilde{A}_{m22}(q^{-1})$ and $\tilde{B}_{m22}(q^{-1})$, which can be found uniquely (Kailath, 1980). The scalar factor α is fixed with the parameter constraint, leading to unique $A(q^{-1})$, $B(q^{-1})$, and $W_{ud}(q)$. ■

Lemma 11.30 is similar to Lemma 11.17 and therefore the solution is obtained in a similar fashion. Again, the problem reduces to a convex optimisation problem if a nonzero polynomial element $a_{ij}(q^{-1})$ or $b_{ij}(q^{-1})$ of $A(q^{-1})$ or $B(q^{-1})$ is known, which is, for example, satisfied if an excitation signal enters the network through known dynamics (e.g. $b_{ij}(q^{-1}) = 1$).

The LMFD results of Lemmas 11.28 and 11.30 are combined to obtain the following identifiability result:

Proposition 11.31 (Identifiability). *A network model set $\mathcal{M}$* (11.46) *satisfying Assumption 11.26 is* globally network identifiable *from $z(t)$ if the following conditions are satisfied:*

1. *The polynomials $A(q^{-1})$ and $B(q^{-1})$ are left coprime in $\mathcal{M}$.*
2. *There exists a permutation matrix P such that within $\mathcal{M}$, $\begin{bmatrix} A_0 & A_1 & \cdots & A_{n_a} & B_0 & B_1 & \cdots & B_{n_b} \end{bmatrix} P = \begin{bmatrix} D & R \end{bmatrix}$ with D square, diagonal, and full rank.*
3. *There are no algebraic loops in $G(q)$.*
4. *At least one excitation signal $r_j(t)$, $j = 1, \ldots, K$, is present: $K \geq 1$.*
5. *There is at least one linear constraint on the coefficients of $A(q^{-1}, \theta_A)$ and $B(q^{-1}, \theta_B)$ of the form $\Gamma\bar{\theta} = \gamma \neq 0$, with Γ full row rank and with $\bar{\theta}^\top := \begin{bmatrix} \theta_A^\top & \theta_B^\top \end{bmatrix}$.*

Proof: The proof is provided in Appendix 11.I. ■

If $G(q)$ is strictly proper, then $G(q)$ does not have algebraic loops and Condition 3. in Proposition 11.31 (and Lemma 11.28) is always satisfied; see also Weerts et al. (2018b, Proposition 1). If $G(q)$ does have algebraic loops, then Condition 3. in Proposition 11.31 (and Lemma 11.28) can be replaced by the conditions of Weerts et al. (2018b, Proposition 3), which restricts the number of parameterised elements in each row of $\begin{bmatrix} G^\infty(\theta) & R^\infty(\theta) \end{bmatrix}$, with $G^\infty := \lim_{z\to\infty} G(z)$ and $R^\infty := \lim_{z\to\infty} R(z)$, to the number of excitation signals $r_d(t)$ that are present and it restricts the rank of each row of the rational matrix $\left(I - G^\infty(\theta)\right)^{-1} R^\infty(\theta)$ containing only the parameterised elements of $G^\infty(\theta)$ and the fixed (nonparameterised) elements of $R^\infty(\theta)$.

If $W_{ud}(q)$ is polynomial, then these dynamics can also be used to find a unique $A(q^{-1})$, $B(q^{-1})$, and $W_{ud}(q^{-1})$ from $A_m(q^{-1})$ and $B_m(q^{-1})$, as formulated next.

Proposition 11.32 (Identifiability for partially polynomial interconnection dynamics). *If $W_{ud}(q)$ is polynomial, then Condition 5. of Proposition 11.31 can be replaced by*

5. *There is at least one constraint on the parameters of $A(q^{-1}, \theta_A)$, $B(q^{-1}, \theta_B)$, and $W_{ud}(q^{-1}, \theta_W)$ of the form $\Gamma\bar{\theta} = \gamma \neq 0$, with Γ full row rank and with $\bar{\theta}^\top := \begin{bmatrix} \theta_A^\top & \theta_B^\top & \theta_W^\top \end{bmatrix}^\top$.*

Proof: If $W_{ud}(q)$ is polynomial, then $d(q^{-1}) = 1$ and (11.54a) changes to $\tilde{W}_{ud}(q^{-1}) = \alpha W_{ud}(q^{-1})$. Then Lemma 11.30 only needs to fix the scaling factor α in (11.54). ■

11.6.4 Consistency

Now, the consistency result is formulated as follows:

Theorem 11.33 (Consistency). *Consider a data generating network $\mathcal{S}$ and a model set $\mathcal{M}$ (11.46). Then $M(\hat{\theta}_N)$ is a consistent estimate of $\mathcal{S}$ if the following conditions hold:*

1. *The true system is in the model set ($\mathcal{S} \in \mathcal{M}$).*
2. *The data are informative with respect to the model set.*
3. *The model set is globally network identifiable.*

Proof: The proof is provided in Appendix 11.J. ■

11.6.5 Algorithm

In order to consistently identify the mixed dynamic network model set $\mathcal{M}$ (11.46), multiple identification steps have to be performed. First, the polynomial network representation (11.38) has to be identified. This can be achieved by an adapted version of the multistep least-squares algorithm presented in Section 8.5. The adaptation that has to be made, is that the partially asymmetric structure of $A_m(q^{-1})$ needs to be incorporated into the parameterisation of the model set. Once the polynomial form of the mixed dynamic network (11.38) is identified, it is used to identify the original mixed network matrices (11.29). In order to do so, an additional step is needed, as indicated by Lemma 11.30. In general, this leads to a nonconvex optimisation problem, for which several algorithms have been developed (Fazzi et al., 2019).

The mixed dynamic networks in Case 2. that are represented in polynomial form (11.38) can be identified once the proposed algorithm is implemented. This includes the identification of all dynamics and the complete topology. The conditions for identifiability are the same as the ones for full network identification of purely diffusively coupled networks, with an additional condition on the absence of algebraic loops in the directed part ($G(q)$). Most of the steps in the algorithm are convex least-squares steps that are the same or similar to the steps for mixed

dynamic networks in Case 1. Similar to Case 1., the critical part of the algorithm is the nonconvex optimisation step for determining $A(q^{-1})$, $B(q^{-1})$, and $W_{ud}(q)$ from $\breve{A}(q^{-1})$, $\breve{B}(q^{-1})$, and $\breve{W}_{ud}(q^{-1})$; see Lemma 11.30. As this optimisation is nonconvex, it may lead to local optima instead of the global optimum. Additional research is required to understand the consequences of this and to determine a proper approach (possibly including WNSF to make it convex).

11.7 Case 2: Identification in module representation

11.7.1 Identification setup

This chapter involves the full network identification of mixed dynamic networks. In this section, this problem is dealt with in the module representation, which means that the model (11.44) will be used for identification. The identification problem that will be considered in this section is equal to the one considered in Section 11.6, see Definition 11.11, and concerns the identification of all dynamics in the network and, optionally, the topology of the complete network.

Consider the module representation of the mixed dynamic network model (11.44). For solving the mixed identification problem formulated above, the approach for full network identification of module representations of Weerts et al. (2016) is applied, because the mixed dynamic network is modelled in the same framework and contains direct feedthrough terms and algebraic loops. After the model (11.44) is identified, the original mixed dynamic network model matrices (11.29) are obtained.

Because we consider the same mixed dynamic network as in Section 11.6, we use the same set of parameterised functions (11.46) with particular models (11.47). In addition, we define the model set

$$\mathcal{M}_{md} := \{M_{md}(\eta), \eta \in \Pi \subset \mathbb{R}^d\} \tag{11.55}$$

with $d \in \mathbb{N}$ and with particular models

$$M_{md}(\eta) := \big(G_m(q,\eta), R_m(q,\eta), H_m(q,\eta), \Lambda_m(\eta)\big), \tag{11.56}$$

where η contains all unknown coefficients that appear in the entries of the model matrices $G_m(q^{-1})$, $R_m(q^{-1})$, $H_m(q)$, and Λ_m, with Λ_m the covariance of $\tilde{e}(t)$ given by

$$\Lambda_m = \begin{bmatrix} \Lambda_d & 0 \\ 0 & \tilde{\Lambda}_u \end{bmatrix}, \tag{11.57}$$

with $\tilde{\Lambda}_u$ the covariance matrix of $\tilde{e}_u(t)$, where $e_d(t)$ and $\tilde{e}_u(t)$ are uncorrelated. The data generating network is denoted by $\mathcal{S}_{md} := \left(G_m^0, R_m^0, H_m^0, \Lambda_m^0\right)$. The true system lies in the model set if $\mathcal{S}_{md} = M_{md}(\eta^0)$, where $\eta^0 \in \Pi$ indicate the true parameter values.

The network predictor is defined in line with Weerts et al. (2016) as before, see Definition 8.4, and leads to

$$\hat{w}(t|t-1) = \left[I - \left(I - G_m^\infty\right)^{-1} H_m^{-1}(q)\left(I - G_m(q)\right)\right] w(t) + \left(I - G_m^\infty\right)^{-1} H_m^{-1}(q) R_m(q) r(t), \quad (11.58)$$

with $G_m^\infty := \lim_{z\to\infty} G_m(z)$. The parameterised predictor leads to the prediction error $\breve{e}(t,\eta)$ (11.17) resulting in

$$\breve{\varepsilon}(t,\eta) = W_w(q,\eta)w(t) - W_r(q,\eta)r(t), \quad (11.59)$$

with predictor filters

$$W_w(q,\eta) = \left(I - G_m^\infty(\eta)\right)^{-1} H_m^{-1}(q,\eta)\left(I - G_m(q,\eta)\right), \quad (11.60a)$$

$$W_r(q,\eta) = \left(I - G_m^\infty(\eta)\right)^{-1} H_m^{-1}(q,\eta) R_m(q^{-1},\eta). \quad (11.60b)$$

Again, the parameters are estimated through the least-squares identification criterion (11.20) with prediction error (11.59).

In the next sections, the consistent identification of the mixed network model is analysed by considering network identifiability. Data informativity conditions have already been derived in Section 11.6.2. The following analysis leads to conditions for which a consistent estimate of the data generating mixed dynamic network $\mathcal{S}$ can be found.

11.7.2 Network identifiability

Conditions for network identifiability are derived by first applying the identifiability results of Weerts et al. (2018b, Proposition 3), because there will be algebraic loops present in the network, due to the nonmonicity of $A(q^{-1})$. Next, the identifiability results of Weerts et al. (2018b, Theorem 2) are applied, which will lead to conservative results, because parameter dependencies will not be taken into account. This is because the currently available results from the literature (Weerts et al., 2018b) are all based on independently parameterisations.

Even though the results will be conservative by definition, they are relevant for several reasons. They give the opportunity to view and analyse mixed dynamic networks from a module representation perspective. This gives insight

into consistency results in comparison with module representations without any undirected interconnections. In the future, the results can be improved by studying how parameter dependencies can be taken into account.

Before presenting the identifiability result, the two matrices $\breve{T}^{\infty}_{wr_i}(\eta)$ and $\breve{T}_i(q,\eta)$ are defined in line with Weerts et al. (2018b).

First, suppose that the ith row of $G^{\infty}_m(\eta)$ has $\bar{\wedge}_i$ parameterised entries. Define the permutation matrix $\bar{\bigwedge}_i$ such that all parameterised entries in the ith row of $\left(I - G^{\infty}_m(\eta)\right)\bar{\bigwedge}_i$ are gathered on the left-hand side. Similar, suppose that the ith row of $R^{\infty}_m(\eta)$ has $\bar{\vee}_i$ parameterised entries. Define the permutation matrix $\bar{\bigvee}_i$ such that all parameterised entries in the ith row of $R^{\infty}_m(\eta)\bar{\bigvee}_i$ are gathered on the right-hand side. Now the matrix $\breve{T}^{\infty}_{wr_i}(\eta)$ is constructed as a submatrix of $T^{\infty}_{wr}(\eta) = \left(I - G^{\infty}_m(\eta)\right)^{-1} R^{\infty}_m(\eta)$ by taking the rows that correspond to the parameterised columns of $G^{\infty}_m(\eta)$ and the columns that correspond to the nonparameterised columns of $R^{\infty}_m(\eta)$. That is,

$$\breve{T}^{\infty}_{wr_i}(\eta) := \begin{bmatrix} I_{\bar{\wedge}_i} & 0 \end{bmatrix} \bar{\bigwedge}_i^{-1} \left(I - G^{\infty}_m(\eta)\right)^{-1} R^{\infty}_m(\eta) \bar{\bigvee}_i \begin{bmatrix} I_{K-\bar{\vee}_i} \\ 0 \end{bmatrix}. \tag{11.61}$$

Second, suppose that the ith row of $G_m(q,\eta)$ has $\wedge_i$ parameterised entries. Define the permutation matrix $\bigwedge_i$ such that all parameterised entries in the ith row of $\left(I - G_m(q,\eta)\right)\bigwedge_i$ are gathered on the left-hand side. Similar, suppose that the ith row of $\begin{bmatrix} R_m(q,\eta) & H_m(q,\eta) \end{bmatrix}$ has $\vee_i$ parameterised entries. Define the permutation matrix $\bigvee_i$ such that all parameterised entries in the ith row of $\begin{bmatrix} R_m(q,\eta) & H_m(q,\eta) \end{bmatrix}\bigvee_i$ are gathered on the right-hand side. Now, the matrix $\breve{T}_i(q,\eta)$ is constructed as a submatrix of $T(q,\eta) = \left(I - G_m(q,\eta)\right)^{-1} \begin{bmatrix} R_m(q,\eta) & H_m(q,\eta) \end{bmatrix}$ by taking the rows that correspond to the parameterised columns of $G_m(q,\eta)$ and the columns that correspond to the nonparameterised columns of $\begin{bmatrix} R_m(q,\eta) & H_m(q,\eta) \end{bmatrix}$. That is,

$$\breve{T}_i(q,\eta) := \begin{bmatrix} I_{\wedge_i} & 0 \end{bmatrix} \bigwedge_i^{-1} \left(I - G_m(q,\eta)\right)^{-1} \begin{bmatrix} R_m(q,\eta) & H_m(q,\eta) \end{bmatrix} \bigvee_i \begin{bmatrix} I_{K+L-\vee_i} \\ 0 \end{bmatrix}. \tag{11.62}$$

The identifiability result for the model set $\mathcal{M}_{md}$ (11.55) is now formulated as follows:

Lemma 11.34 (Identifiability of $\mathcal{M}_{md}$). *A network model set $\mathcal{M}_{md}$ (11.55) is* globally network identifiable *if and only if the following conditions are satisfied:*

1. *Each row of $\begin{bmatrix} G^{\infty}_m(\eta) & R^{\infty}_m(\eta) \end{bmatrix}$ has at most K parameterised entries.*

2. *For each i,* $\breve{T}^{\infty}_{wr_i}(\eta)$ (11.61) *has full row rank for all* $\eta \in \Pi$.
3. *Every parameterised entry in the model* $\{M_{md}(\eta), \eta \in \Pi\}$ *covers the set of all proper rational transfer functions.*
4. *All parameterised transfer functions in the model* $M_{md}(\eta)$ *are parameterised independently (i.e. there are no common parameters).*
5. *Each row of* $\begin{bmatrix} G_m(q,\eta) & R_m(q,\eta) & H_m(q,\eta) \end{bmatrix}$ *has at most* $K + L$ *parameterised entries.*
6. *For each i,* $\breve{T}_i(q,\eta)$ (11.62) *has full row rank for all* $\eta \in \Pi$.

Proof: This follows directly by applying Weerts et al. (2018b, Proposition 3) and Weerts et al. (2018b, Theorem 2) to mixed dynamic network model in module representation (11.44). ■

Condition 4. of Lemma 11.34 states that all parameterised transfer functions need to be independently parameterised. However, from the relations in (11.42) it is clear that there are common parameters between the transfer functions in the model $M_{md}(\eta)$. The equivalence between these parameters is thus ignored in the identification analysis. However, it can be incorporated into the identification procedure by including a linear parameter constraint in the optimisation problem (11.21). The constraint can be included in the cost function, leading to a convex least-squares optimisation problem. Including the constraint will keep the estimated parameters consistent and improve their variance. It only requires a dedicated optimisation problem implementation.

Once the network model set $\mathcal{M}_{md}$ (11.55) is identified, it is used to identify the original network model set $\mathcal{M}$ (11.46). The rational matrices $G(q)$, $W_{du}(q)$, $R(q)$, and $H(q)$ can directly be extracted from $G_m(q)$, $R_m(q)$, and $H_m(q)$. The rational matrices $G_u(q)$, $\tilde{W}_{ud}(q)$, $R_u(q)$, and $H_u(q)$ can also directly be extracted from $G_m(q)$, $R_m(q)$, and $H_m(q)$ and are used to identify $A(q^{-1})$, $W_{ud}(q)$, $B(q^{-1})$, and $F(q)$. For doing so, consider first the following result on the LMFD (11.42a):

Lemma 11.35 (LMFD). *Consider a network model set* $\mathcal{M}$ (11.46)*. Given the* LMFD $G_u(q) = Q^{-1}(q^{-1})P(q^{-1})$ *as in* (11.42a) *with* $Q(q^{-1})$ *diagonal and* $P(q^{-1})$ *hollow and symmetric, the polynomial matrix* $A(q^{-1}) = Q(q^{-1}) - P(q^{-1})$ *is unique within* $\mathcal{M}$ *up to a scalar factor.*

Proof: The proof is provided in Appendix 11.K. ■

Due to their characteristic structure, $Q(q^{-1})$ and $P(q^{-1})$ do not have to be left coprime.

The LMFD $G_u(q) = Q^{-1}(q^{-1})P(q^{-1})$ can be calculated through a WNSF (Galrinho et al., 2019) in which the structure of $Q(q^{-1})$ and $P(q^{-1})$ can be incorporated. WNSF includes multiple least-squares steps (and thus convex optimisations) that lead to a consistent result.

Using this result on the LMFD, identifiability conditions for the original network model set $\mathcal{M}$ (11.46) are derived.

Proposition 11.36 (Identifiability). *A network model set $\mathcal{M}$* (11.46) *is* globally network identifiable *from $z(t)$ if the following conditions are satisfied:*

1. *Each row of $\begin{bmatrix} G_m^\infty(\eta) & R_m^\infty(\eta) \end{bmatrix}$ has at most K parameterised entries.*
2. *For each i, $\breve{T}_{wr_i}^\infty(\eta)$* (11.61) *has full row rank for all $\eta \in \Pi$.*
3. *Every parameterised entry in the model $\{M_{md}(\eta), \eta \in \Pi\}$ covers the set of all proper rational transfer functions.*
4. *All parameterised transfer functions in the model $M_{md}(\eta)$ are parameterised independently (i.e. there are no common parameters).*
5. *Each row of $\begin{bmatrix} G_m(q,\eta) & R_m(q,\eta) & H_m(q,\eta) \end{bmatrix}$ has at most $K + L$ parameterised entries.*
6. *For each i, $\breve{T}_i(q,\eta)$* (11.62) *has full row rank for all $\eta \in \Pi$.*
7. *There is at least one constraint on the parameters of $A(q^{-1},\theta_a)$ and $B(q^{-1},\theta_b)$ of the form $\Gamma\theta_{ab} = \gamma \neq 0$, with Γ full row rank and with $\theta_{ab} := \begin{bmatrix} \theta_a^\top & \theta_b^\top \end{bmatrix}^\top$.*

Proof: The proof is provided in Appendix 11.L. ■

Conditions 1.-6. of Proposition 11.36 are the same as the conditions of Proposition 11.34 and are used to identify the module representation of the mixed dynamic network model. This leads to a unique representation of the directed part in the original mixed dynamic network model (11.29), while the undirected part is unique up to a scalar factor. Condition 7. fixes the scaling factor and ensures the uniqueness of the undirected part in (11.29).

If $W_{ud}(q)$ is polynomial, then the parameters of $W_{ud}(q^{-1},\theta_w)$ can be included in the constraint in Condition 7. of Proposition 11.36, leading to the same parameter constraint as in Proposition 11.32.

11.7.3 Consistency

Now, the consistency result is formulated as follows:

Theorem 11.37 (Consistency). *Consider a data generating network $\mathcal{S}$ and a model set $\mathcal{M}$ (11.46). Then $M(\hat{\theta}_N)$ is a consistent estimate of $\mathcal{S}$ if the following conditions hold:*

1. *The true system is in the model set ($\mathcal{S} \in \mathcal{M}$).*
2. *The data are informative with respect to the model set.*
3. *The model set is globally network identifiable.*

Proof: The proof is provided in Appendix 11.M. ■

11.7.4 Algorithm

In order to consistently identify the network model set $\mathcal{M}$ (11.46), multiple identification steps have to be performed. First, the module representation (11.44) has to be identified. The parameters of this model are estimated through the least-squares identification criterion (11.20); see also Weerts et al. (2016). This optimisation problem is not convex due to the fact that the parameterised prediction error (11.59), with filters (11.60), is not affine in the parameters. Using a WNSF (Galrinho et al., 2019), this optimisation problem can be solved using several convex steps; see also Section 8.5. Once the module representation of the mixed dynamic network (11.44) is identified, it is used to identify the original mixed dynamic network (11.29). Again, a WNSF can be used to calculate the LMFD of Lemma 11.35.

The mixed dynamic networks in Case 2. in module representation can be identified once the proposed algorithm is implemented. This includes the identification of the full dynamics and, with that, the topology of the network. Note, however, that some topological aspects of the directed part of the network are assumed to be known as the number of parameterised transfer functions is limited by the identifiability conditions in Proposition 11.36. Additional research is needed to adapt the identifiability conditions to the case of dependent parameterisations. Then fewer parameters have to be identified and therefore, it is expected that the identifiability conditions in Proposition 11.36, and in particular Conditions 1.-2. and 4.-6., relax. All steps in the identification algorithm are convex least-squares steps due to the extensive application of WNSF.

11.8 Discussion

11.8.1 Extended cases of mixed dynamic networks

In this chapter, several mixed dynamic networks are considered, which contain both undirected and directed interconnections between node signals. This chapter focused on the mixed dynamic networks defined in Definition 11.4 and 11.5, which consist either of a single distinct undirected network with additional directed interconnections, or directed interconnections between a single distinct undirected network and a single distinct directed network. In Section 11.2.4, the generality of these mixed dynamic networks is discussed, including extensions to these cases.

For the mixed dynamic network satisfying Definition 11.4, it is assumed that the undirected part represents a connected graph, meaning that there is a path between every pair of nodes, even if all directed links are removed from the network. Consider the extended version that is also discussed in Section 11.2.4, where this condition is relaxed, such that some nodes are only interconnected through a directed interconnection. Then the mixed dynamic network consists of several distinct undirected networks that are interconnected with each other through directed links (and still additional directed links may be present between undirected nodes). In this situation, the identifiability conditions of Proposition 11.18 slightly change, in the sense that instead of a single parameter constraint, there has to be a single parameter constraint for each distinct undirected network and each distinct undirected network has to be excited by an external excitation signal.

Example 11.38 (Extension in Case 1). *Consider the mixed dynamic network shown in Figure 11.4, which has an undirected coupling between node $w_1(t)$ and node $w_2(t)$, a directed connection from node $w_2(t)$ to node $w_3(t)$, and an undirected coupling between node $w_3(t)$ and node $w_4(t)$. For identifiability, there has to be a parameter constraint on the dynamics of $A(q^{-1})$ and $B(q^{-1})$ related to node $w_1(t)$ and node $w_2(t)$ and a second parameter constraint on the dynamics of $A(q^{-1})$ and $B(q^{-1})$ related to node $w_3(t)$ and node $w_4(t)$. There should be two external excitation signals present, one located at node $w_1(t)$ or node $w_2(t)$ and one located at node $w_3(t)$ or node $w_4(t)$.*

11.8.2 Relaxation of single directed connection in Case 1

Further, for identifiability in Case 1., it is assumed that there is only one directed interconnection between a pair of nodes, so either from node $w_j(t)$ to node $w_k(t)$

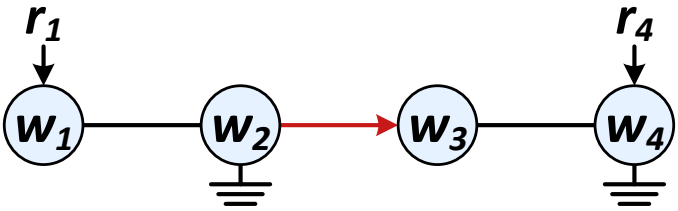

Figure 11.4: A mixed dynamic network, consisting of two diffusively coupled networks interconnected with a directed link (red arrow), and with the external excitation signals $r_1(t)$ and $r_4(t)$.

or the other way around, but not both; see Proposition 11.18. There are some special situations in which this assumption may be violated, while the mixed dynamic network is still identifiable.

This is, for example, the case when it is known that the jth node has no connection to the ground node and directed interconnections ($G_{jk}(q)$ and $G_{kj}(q)$) with only the kth node. Then $\breve{\Upsilon}(q^{-1})$ directly leads to polynomial elements $\breve{a}_{j\ell}(q^{-1})$, $\ell \in \{1,\ldots,L\} \setminus \{k\}$. As the jth node has no connection to the ground node, $\breve{a}_{jj}(q^{-1}) = -\sum_{\ell\neq j} \breve{a}_{j\ell}(q^{-1})$, from which $\breve{a}_{jk}(q^{-1})$ can be found. This case can be extended to the case where, in addition, the kth node has only directed connections with node ℓ such that either $G_{\ell k}(q) = 0$ or $G_{k\ell}(q) = 0$, because the corresponding deviation of $\breve{a}_{k\ell}(q^{-1})$ or $\breve{a}_{\ell k}(q^{-1})$, respectively, can be identified from the ℓth node and subsequently be subtracted from $\breve{a}_{jj}(q^{-1})$.

Another exception can be made if the directed dynamics are known. The topological conditions that need to hold for the directed connections only hold for the unknown dynamics in these interconnections. If the directed dynamics in the interconnection are known, they can be excluded from the reasoning. So are, for example, directed connections that are known to be zero, because they are known to be absent.

To summarise, Condition 4. of Proposition 11.18 can be relaxed as follows:

Proposition 11.39 (Identifiability Condition 4. for Case 1). *Condition 4. of Proposition 11.18 can be replaced by the condition that within $\mathcal{M}$, for each $G_{ij}(q) \neq 0$, $i, j = 1, 2, \ldots, L$, either one of the following conditions is satisfied:*

1. *$G_{ji}(q) = 0$ within $\mathcal{M}$.*
2. *$w_i(t)$ has no connection to the ground node and within $\mathcal{M}$, $G_{ik}(q) = 0$ for all $k \neq j$ for which $G_{ki}(q) \neq 0$.*

3. *$w_j(t)$ has no connection to the ground node and within $\mathcal{M}$, $G_{kj}(q) = 0$ for all $k \neq i$ for which $G_{jk}(q) \neq 0$.*

Proof: The proof is provided in Appendix 11.N. ■

11.8.3 Identifiability conditions

For Case 1. and 2., where the mixed dynamic network is represented in polynomial form, the identifiability results ask for at least one nonzero parameter constraint; see Propositions 11.18 and 11.31. This constraint is used to identify the dynamics related to the undirected nodes; see Lemmas 11.17 and 11.30. This constraint is equivalent to the one in Condition 7. of Proposition 11.36 and the one for full network identifiability in diffusively coupled linear networks; see Proposition 8.15. It has been proven in Propositions 11.19 and 11.32 that if the directed dynamics entering the undirected nodes are described by polynomials, then the constraint can include their parameters.

The mixed dynamic network in Case 2., described by Definition 11.5, is modelled in either the polynomial form or the module representation. Propositions 11.31 and 11.36 list the conditions for global network identifiability of the network model set $\mathcal{M}$ (11.46) in these modelling frameworks, respectively. These propositions show that the identifiability conditions are very different from each other. In the polynomial form, the identifiability conditions stated in Proposition 11.31 contain one algebraic constraint; two topological constraints, one on the undirected part and one on the directed part; the requirement of only a single excitation signal; and one parameter constraint. In the module representation, the identifiability conditions in Proposition 11.36 also include the parameter constraint, while the other conditions are mainly on the number of parameterised entries and the rank of the transfer function matrices. These conditions lead to requirements on the number and locations of excitation signals, which can be demanding. Observe that in this case, independent parameterisations of all transfer functions is required. A more extensive study on the identifiability conditions in Propositions 11.31 and 11.36 can lead to a better understanding of the similarities, differences, and relations between them; see also Remark 8.16.

In some situations, it might be more attractive to let the undirected node signals be modelled in the polynomial framework and the directed node signals be modelled in the module representation, as in the mixed dynamic network model (11.29) and use this network model for identifiability analysis and consistent identification. In this model, each part of the network is modelled in its most advantageous form, which might also lead to the most relaxed identifiability

conditions and the most accurate identification results. However, no identifiability analysis for this situation is yet available.

11.8.4 Correlated noise

In the mixed dynamic network model in Case 2. (11.29) it is assumed that the noise acting on the directed part of the network $e_d(t)$ and the noise acting on the undirected part of the network $e_u(t)$ are uncorrelated. If this is not the case, then the mixed dynamic network model can be modelled with a noise model $F_m(q)$ and a noise covariance matrix Λ_m that are not block diagonal, but full matrices with full rank, with $F_m(q)$ still being monic, stable, and stably invertible, and with $\Lambda_m \succ 0$ (implying $\tilde{\Lambda}_m \succ 0$). In this case, the noise model consisting of $F_m(q)$ and Λ_m is still identifiable under the presented identifiability conditions for the polynomial form in Proposition 11.31 and for the module representation in Proposition 11.36.

11.8.5 Future research

In this chapter, theoretical conditions for consistent identification of mixed linear dynamic networks with both undirected and directed dynamics are presented. When such a network satisfies these conditions, it can be consistently identified. In order to do so, the algorithms for the identification procedures described in Section 11.4.5, Section 11.6.5, and Section 11.7.4 need to be formalised and implemented.

One of the next steps in this research is to extend the results for Case 1. and Case 2. to their extensions discussed in Section 11.2.4 and 11.8.1 and to even more complex mixed linear dynamic networks.

The directed dynamics that are added to undirected linear networks, especially in Case 1., are often digital controllers. These controllers might be known and therefore, one of the next steps is to include known dynamics in the identification procedure. This will relax the identifiability conditions as, for example, explained in Remark 11.10 and Dreef et al. (2022).

Furthermore, the next step in this research is to consider the identification of a single interconnection, a single interaction, or a subnetwork. In the literature this is referred to as ‘local’, ‘single module’, or ‘subnetwork’ identification, where the concept of immersion (the elimination of irrelevant signals) plays a crucial role. Of course, the subnetwork identification results for polynomial models (Chapter 9) can be applied to the network models in Propositions 11.7 and 11.23, and the local

identification results for module representations (Gevers et al., 2018; Materassi and Salapaka, 2020; Ramaswamy and Van den Hof, 2021) can be applied to the network models in Proposition 11.24. The exact implications due to the specific structural properties of these network models need to be analysed.

11.9 Conclusion

Mixed dynamic network contain both undirected and directed interconnections between the node signals. Two general cases of mixed dynamic networks have been modelled and reformulated in either the polynomial framework or the module representation. For all three mixed dynamic network models that are presented in this chapter, conditions for consistent parameter estimation of all dynamics in the network have been formulated. The resulting conditions for consistency are closely related to the ones for full network identification in diffusively coupled linear networks (Chapter 8) and for full network identification in the module representation (Weerts et al., 2018b). Directions for developments of identification algorithms have been proposed as well. Their formalisation and implementation are subject for future research.

Appendix

11.A Proof of Proposition 11.13

The proof follows the proof of Proposition 8.12, with the difference that the presence of the directed dynamics $G(q)$ changes the rational matrix $J(q)$ in (8.68) to

$$J(q) = \begin{bmatrix} \big(A(q^{-1}) - G(q)\big)^{-1} F(q) & \big(A(q^{-1}) - G(q)\big)^{-1} B(q^{-1}) \\ 0 & I \end{bmatrix}.$$

Due to well-posedness of the network, $\big(A(q^{-1}) - G(q)\big)$ has full rank. This is true regardless of whether $G(q)$ is rational or polynomial. This means that $J(q)$ will always have full rank. Hence, again $\Phi_z(\omega) \succ 0$ if and only if $\Phi_\kappa(\omega) \succ 0$. As $e(t)$ and $r(t)$ are assumed to be uncorrelated and $E\{e(t)\} = 0$, $\Phi_\kappa(\omega) \succ 0$ if and only if $\breve{\Lambda} \succ 0$ (which follows from $\Lambda \succ 0$, which is assumed) and $\Phi_r(\omega) \succ 0$. The condition $\Phi_z(\omega) \succ 0$ reduces to $\Phi_r(\omega) \succ 0$.

11.B Proof of Lemma 11.15

According to Kailath (1980), the left matrix-fraction description (LMFD) of any two polynomial and left coprime matrices is unique up to a premultiplication with a unimodular matrix. To satisfy Condition 2., the unimodular matrix is restricted to be diagonal. Let $\bar{A}(q^{-1})$ denote the symmetric part of $\breve{\Upsilon}(q^{-1})$ and be consisting of elements

$$\bar{a}_{ij}(q^{-1}) = \begin{cases} \breve{a}_{ij}(q^{-1}), & \text{if } \breve{v}_{ij}(q^{-1}) = \breve{v}_{ji}(q^{-1}), \\ 0, & \text{otherwise.} \end{cases}$$

This $\bar{A}(q^{-1})$ represents a connected network consisting of all node interactions that do not have directed connections (in either direction). To preserve the symmetry

of $\bar{A}(q^{-1})$, the diagonal premultiplication matrix is further restricted to have equal elements, resulting in unique $\breve{\Upsilon}(q^{-1})$ and $\breve{B}(q^{-1})$ up to a scalar factor. As the zero structure of $\breve{G}(q^{-1})$ is known, $\breve{g}_{ji} = 0$ if $\breve{g}_{ij} \neq 0$, and $\breve{A}(q^{-1})$ is symmetric, the elements of $\breve{A}(q^{-1})$ are found as

$$\breve{a}_{ij}(q^{-1}) = \begin{cases} \breve{\upsilon}_{ij}(q^{-1}), & \text{if } \breve{g}_{ij} = 0, \\ \breve{\upsilon}_{ji}(q^{-1}), & \text{if } \breve{g}_{ij} \neq 0. \end{cases}$$

Finally, $\breve{G}(q^{-1}) = \breve{A}(q^{-1}) - \breve{\Upsilon}(q^{-1})$ and thus, $\breve{A}(q^{-1})$ and $\breve{G}(q^{-1})$ can uniquely be determined from $\breve{\Upsilon}(q^{-1})$. As $\breve{\Upsilon}(q^{-1})$ is unique up to a scalar factor, so are $\breve{A}(q^{-1})$ and $\breve{G}(q^{-1})$.

11.C Proof of Lemma 11.16

Condition 1. implies Condition 1. of Lemma 11.15, because if $A(q^{-1})$ and $B(q^{-1})$ are left coprime within $\mathcal{M}$, then $d_G(q^{-1})$ is exactly the common factor between $\breve{A}(q^{-1})$ and $\breve{B}(q^{-1})$ within $\breve{\mathcal{M}}$. The polynomial $d_G(q^{-1})$ is constructed such that all common factors of $D_G(q^{-1})$ and $N_G(q^{-1})$ are taken out, such that there are no common terms created in $G(q^{-1})$. Therefore, if $N_G(q^{-1})$ and $B(q^{-1})$ are left coprime within $\mathcal{M}$, then also $\breve{G}(q^{-1})$ and $\breve{B}(q^{-1})$ are left coprime within $\breve{\mathcal{M}}$.

Condition 2.-4. imply Condition 2.-4. of Lemma 11.15, because $\breve{A}(q^{-1})$, $\breve{G}(q^{-1})$, and $\breve{B}(q^{-1})$ adopt the zero structure of $A(q^{-1})$, $N_G(q^{-1})$, and $B(q^{-1})$, respectively, where the zero structure of $N_G(q^{-1})$ is the same as the one of $G(q)$.

11.D Proof of Proposition 11.18

Condition 5. implies that $T_{wr}(q, \theta)$ is nonzero. According to Lemma 11.15, Condition 1.-4. imply that $\breve{A}(q^{-1}, \eta)$, $\breve{B}(q^{-1}, \eta)$, and $\breve{G}(q^{-1}, \eta)$ are unique up to a scalar factor $\alpha \in \mathbb{R}_+$. According to Lemma 11.17, Condition 6. implies that $A(q^{-1}, \theta)$, $B(q^{-1}, \theta)$, and $G(q, \theta)$ are uniquely found from $\alpha\breve{A}(q^{-1}, \eta)$, $\alpha\breve{B}(q^{-1}, \eta)$, and $\alpha\breve{G}(q^{-1}, \eta)$. It also implies that $\alpha d_G(q^{-1}, \eta)$ is uniquely determined and as $d_G(q^{-1}, \eta)$ is monic, α is found as well. As $A(q^{-1}, \theta)$ is uniquely found, $\Phi_{\bar{v}}(\omega, \theta)$ gives unique $F(q, \theta)$ and $\Lambda(\theta)$; see Proposition 8.15.

11.E Proof of Theorem 11.21

Condition 1. ensures that θ^0 is a minimum of the criterion (11.20), because the predictor filters (11.19) can be rewritten as

$$W_w(q,\theta) = \big(A_0(\theta) - G^\infty(q,\theta)\big)^{-1} F^{-1}(q,\theta)\big(A(q^{-1},\theta) - G(q,\theta)\big),$$
$$W_r(q,\theta) = \big(A_0(\theta) - G^\infty(q,\theta)\big)^{-1} F^{-1}(q,\theta) B(q^{-1},\theta),$$

with $A_0 := \lim_{z\leftarrow\infty} A(z)$ and $G^\infty := \lim_{z\to\infty} G(z)$. According to Proposition 11.13, Condition 2. ensures that $T_{wr}(q,\theta)$ and $\Phi_{\bar{v}}(\omega,\theta)$ can uniquely be recovered from data (Chapter 8). Finally, according to Proposition 11.18, Condition 3. implies that the parameterised model $M(\theta)$ can uniquely be recovered from $T_{wr}(q,\theta)$ and $\Phi_{\bar{v}}(\omega,\theta)$.

11.F Proof of Proposition 11.25

For the mixed dynamic network model (11.29), the input-output relations between the signals can be described by (11.31a):

$$w(t) = \breve{J}^{-1}(q)\begin{bmatrix} R(q) & 0 \\ 0 & B(q^{-1}) \end{bmatrix} r(t) + \breve{J}^{-1}(q)\begin{bmatrix} H(q) & 0 \\ 0 & F(q) \end{bmatrix} e(t),$$

with $\breve{J}(q)$ as in (11.30).

The proof of Proposition 11.25 follows the proof of Proposition 8.12, with the difference that the rational matrix $J(q)$ in (8.68) is changed to

$$J(q) = \begin{bmatrix} \breve{J}^{-1}(q)\begin{bmatrix} H(q) & 0 \\ 0 & F(q) \end{bmatrix} & \breve{J}^{-1}(q)\begin{bmatrix} R(q) & 0 \\ 0 & B(q^{-1}) \end{bmatrix} \\ 0 & I \end{bmatrix}$$

According to Proposition 11.22, well-posedness of the network implies that $\breve{J}(q)$ has full rank. This means that $J(q)$ will also have full rank. Hence, again $\Phi_z(\omega) \succ 0$ if and only if $\Phi_\kappa(\omega) \succ 0$. As $e(t)$ and $r(t)$ are assumed to be uncorrelated and $E\{e(t)\} = 0$, $\Phi_\kappa(\omega) \succ 0$ if and only if $\Lambda_m \succ 0$ (which follows from $\Lambda_d \succ 0$ and $\Lambda_u \succ 0$, which is assumed) and $\Phi_r(\omega) \succ 0$. The condition $\Phi_z(\omega) \succ 0$ reduces to $\Phi_r(\omega) \succ 0$.

11.G Proof of Lemma 11.27

If $A(q^{-1})$ and $B(q^{-1})$ are left coprime within $\mathcal{M}$, then $d(q^{-1})$ is exactly the common factor between $A_{m22}(q^{-1})$ and $B_{m22}(q^{-1})$ within $\mathcal{M}$. The polynomial

$d(q^{-1})$ is constructed such that all common factors of $D_u(q^{-1})$ and $W_{ud}^N(q^{-1})$ are taken out, such that there are no common terms created in $A_{m21}(q^{-1})$. Therefore, if $W_{ud}^N(q^{-1})$ and $B(q^{-1})$ are left coprime, then also $A_{m21}(q^{-1})$ and $B_{m22}(q^{-1})$ are left coprime within $\breve{\mathcal{M}}$. Similar, $D_d(q^{-1})$ is constructed such that $D_d(q^{-1})$ and $\begin{bmatrix} G^N(q^{-1}) & W_{du}^N(q^{-1}) & R^N(q^{-1}) \end{bmatrix}$ are left coprime within $\mathcal{M}$. Hence, there are no common terms created in $\begin{bmatrix} A_{m11}(q^{-1}) & A_{m21}(q^{-1}) \end{bmatrix}$ and $B_{m11}(q^{-1})$ and therefore, $\begin{bmatrix} A_{m11}(q^{-1}) & A_{m21}(q^{-1}) \end{bmatrix}$ and $B_{m11}(q^{-1})$ are left coprime within $\mathcal{M}$. Hence, $A_m(q^{-1})$ and $B_m(q^{-1})$ are left coprime.

11.H Proof of Lemma 11.28

From Lemma 11.27, Condition 1. implies that $A_m(q^{-1})$ and $B_m(q^{-1})$ are left coprime. According to Kailath (1980), the LMFD of any two polynomial and left coprime matrices is unique up to a premultiplication with a unimodular matrix $U(q^{-1}) := \begin{bmatrix} U_{11}(q^{-1}) & U_{12}(q^{-1}) \\ U_{21}(q^{-1}) & U_{22}(q^{-1}) \end{bmatrix}$. With proper $G(q)$ and strictly proper $W_{du}(q)$ and $W_{ud}(q)$, it follows from (11.39a) that

$$\lim_{z\to\infty} A_m(z) = \begin{bmatrix} I - G_0 & 0 \\ 0 & A_0 \end{bmatrix}.$$

To preserve this structure, $U_{12}(q^{-1}) = 0$ and $U_{21}(q^{-1}) = 0$. To satisfy Condition 2., $U_{22}(q^{-1})$ is restricted to be diagonal and to preserve symmetry (and connectivity) of $A(q^{-1})$, $U_{22}(q^{-1})$ is further restricted to have equal elements. To satisfy Condition 3., $U_{11}(q^{-1}) = I$ (Weerts et al., 2018b, Proposition 2).

11.I Proof of Proposition 11.31

Condition 4. implies that $T_{wr}(q, \theta)$ is nonzero. According to Lemma 11.28, Condition 1.-3. imply that $A_m(q^{-1}, \eta)$ and $B_m(q^{-1}, \eta)$ are unique within $\mathcal{M}$ up to a scalar factor $\alpha \in \mathbb{R}_+$ for $A_{m22}(q^{-1}, \eta)$ and $B_{m22}(q^{-1}, \eta)$. This leads directly to unique $G(q, \theta)$, $R(q, \theta)$, and $W_{du}(q, \theta)$. According to Lemma 11.30, Condition 5. implies that $A(q^{-1}, \theta)$, $B(q^{-1}, \theta)$, and $W_{ud}(q, \theta)$ are uniquely found from $\alpha A_{m21}(q^{-1}, \eta)$, $\alpha B_{m22}(q^{-1}, \eta)$, and $\alpha A_{m22}(q^{-1}, \eta)$. It also implies that $\alpha d(q^{-1}, \eta)$ is uniquely determined and as $d(q^{-1}, \eta)$ is monic, α is found as well. As $A(q^{-1}, \theta)$ is uniquely found, $\Phi_{\bar{v}}(\omega, \theta)$ gives unique $F(q, \theta)$, $\Lambda_u(\theta)$ and $\Lambda_d(\theta)$; see Proposition 8.15.

11.J Proof of Theorem 11.33

Condition 1. ensures that θ^0 is a minimum of the criterion (11.20), because the predictor filters (11.53) can be rewritten as

$$W_w(q,\theta) = \begin{bmatrix} H(q,\theta)\big(I - G^\infty(\theta)\big) & 0 \\ 0 & F(q,\theta)A_0(\theta) \end{bmatrix}^{-1} \begin{bmatrix} I - G(q,\theta) & -W_{du}(q,\theta) \\ -W_{ud}(q,\theta) & A(q^{-1},\theta) \end{bmatrix},$$

$$W_r(q,\theta) = \begin{bmatrix} H(q,\theta)\big(I - G^\infty(\theta)\big) & 0 \\ 0 & F(q,\theta)A_0(\theta) \end{bmatrix}^{-1} \begin{bmatrix} R(q,\theta) & 0 \\ 0 & B(q^{-1},\theta) \end{bmatrix},$$

with $A_0 := \lim_{z\leftarrow\infty} A(z)$ and $G^\infty := \lim_{z\to\infty} G(z)$. According to Proposition 11.25, Condition 2. ensures that $T_{wr}(q,\theta)$ and $\Phi_{\bar{v}}(\omega,\theta)$ can uniquely be recovered from data (Chapter 8). Finally, according to Proposition 11.31, Condition 3. implies that the parameterised model $M(\theta)$ can uniquely be recovered from $T_{wr}(q,\theta)$ and $\Phi_{\bar{v}}(\omega,\theta)$.

11.K Proof of Lemma 11.35

Due to the diagonality of $Q(q^{-1})$, the LFMD is unique up to a premultiplication with a diagonal polynomial matrix. To preserve symmetry and connectivity of $A(q^{-1})$ and $(P(q^{-1}))$, this diagonal matrix is further restricted to have equal elements. The remaining polynomial term is restricted to be constant to preserve the order of $A(q^{-1})$. As $Q(q^{-1})$ and $P(q^{-1})$ are unique up to a scalar factor, so is $A(q^{-1}) = Q(q^{-1}) - P(q^{-1})$.

11.L Proof of Proposition 11.36

According to Lemma 11.34, Condition 1.-6. imply that $G_m(q,\eta)$, $R_m(q,\eta)$, $H_m(q,\eta)$, and $\Lambda_m(\eta)$ are uniquely found, from which $G(q,\theta) = G_{m11}(q,\eta)$, $W_{du}(q,\theta) = -G_{m12}(q,\eta)$, $R(q,\theta) = R_{m11}(q,\eta)$, $H(q,\theta) = H_{m11}(q,\eta)$, and $\Lambda_d(\theta) = \Lambda_{m11}(\eta)$ are uniquely extracted. In addition, we determine $G_u(q,\eta) = G_{m22}(q,\eta)$, $\tilde{W}_{ud}(q,\eta) = G_{m21}(q,\eta)$, $R_u(q,\eta) = R_{m22}(q,\eta)$, and $H_u(q,\eta) = G_{m11}(q,\eta)$.

According to Lemma 11.35, $G_u(q,\eta)$ leads to $Q(q^{-1},\theta)$, $P(q^{-1},\theta)$ and $A(q^{-1},\theta)$ that are unique up to a scalar factor $\alpha \in \mathbb{R}_+$. Using (11.42), this leads to unique $F(q,\theta)$ and $B(q^{-1},\theta)$, $W_{ud}(q,\theta)$, and $\Lambda_u(\theta) = Q_0(\theta)\Lambda_{m22}(\eta)$ that are also unique up to this scalar factor α. Condition 7. fixes the scaling factor.

11.M Proof of Theorem 11.37

Condition 1. ensures that θ^0 is a minimum of the criterion (11.20), because the predictor filters (11.60) can be rewritten as

$$W_w(q,\theta) = \begin{bmatrix} H(q,\theta)\big(I - G^\infty(\theta)\big) & 0 \\ 0 & F(q,\theta)A_0(\theta) \end{bmatrix}^{-1} \begin{bmatrix} I - G(q,\theta) & -W_{du}(q,\theta) \\ -W_{ud}(q,\theta) & A(q^{-1},\theta) \end{bmatrix},$$

$$W_r(q,\theta) = \begin{bmatrix} H(q,\theta)\big(I - G^\infty(\theta)\big) & 0 \\ 0 & F(q,\theta)A_0(\theta) \end{bmatrix}^{-1} \begin{bmatrix} R(q,\theta) & 0 \\ 0 & B(q^{-1},\theta) \end{bmatrix},$$

with $A_0 := \lim_{z\leftarrow\infty} A(z)$ and $G^\infty := \lim_{z\to\infty} G(z)$. According to Proposition 11.25, Condition 2. ensures that $T_{wr}(q,\theta)$ and $\Phi_{\bar{v}}(\omega,\theta)$ can uniquely be recovered from data (Chapter 8). Finally, according to Proposition 11.36, Condition 3. implies that the parameterised model $M(\theta)$ can uniquely be recovered from $T_{wr}(q,\theta)$ and $\Phi_{\bar{v}}(\omega,\theta)$.

11.N Proof of Proposition 11.39

This proof consists of proving that each condition in Proposition 11.39 can replace Condition 4. of Proposition 11.18, that is Condition 4. of Lemma 11.16, which implies Condition 4. of Lemma 11.15, which is used to proof that $\breve{A}(q^{-1})$ and $\breve{G}(q^{-1})$ can uniquely be determined from $\breve{\Upsilon}(q^{-1})$, with $\breve{\Upsilon}(q^{-1}) = \breve{A}(q^{-1}) + \breve{G}(q^{-1})$.

First, remember that $\breve{G}(q^{-1})$ adopt the zero structure of $N_G(q^{-1})$, which is the same as the zero structure of $G(q)$. Hence, the conditions of Proposition 11.39 imply, respectively, that for the polynomial $\breve{g}_{ij}(q^{-1}) \neq 0$ either one of the following conditions is satisfied:

1. $\breve{g}_{ji}(q^{-1}) = 0$ within $\breve{\mathcal{M}}$.
2. $w_i(t)$ has no connection to the ground node and within $\breve{\mathcal{M}}$, $\breve{g}_{ik}(q^{-1}) = 0$ for all $k \neq j$ for which $\breve{g}_{ki}(q^{-1}) \neq 0$.
3. $w_j(t)$ has no connection to the ground node and within $\breve{\mathcal{M}}$, $\breve{g}_{kj}(q^{-1}) = 0$ for all $k \neq i$ for which $\breve{g}_{jk}(q^{-1}) \neq 0$.

Second, observe that $\breve{A}(q^{-1})$ consists of a Laplacian polynomial matrix plus a diagonal polynomial matrix, where the latter contains the dynamics of the connections to the ground. This means that if node $w_i(t)$ does not have a connection to the ground, then $\breve{a}_{ii}(q^{-1}) = \sum_{j=1,k\neq i}^{L} \breve{a}_{ij}(q^{-1}) = \sum_{j=1,k\neq i}^{L} \breve{a}_{ji}(q^{-1})$.

Condition 1. of Proposition 11.39 is equivalent to Condition 1. above and Condition 4. of Proposition 11.18. It holds that for $i, j = 1, 2, \ldots, L$:

1. $\breve{a}_{ij}(q^{-1}) = \breve{v}_{ij}(q^{-1})$, if $\breve{g}_{ij} = 0$.
2. $\breve{a}_{ij}(q^{-1}) = \breve{v}_{ji}(q^{-1})$, if $\breve{g}_{ij} \neq 0$.

Condition 2. of Proposition 11.39 is equivalent to Condition 2. above, for which it holds that $\breve{a}_{ii}(q^{-1}) = \sum_{k=1,k\neq i}^{L} \breve{a}_{ik}(q^{-1})$. As $\breve{v}_{ij}(q^{-1}) = \breve{a}_{ij}(q^{-1}) + \breve{g}_{ij}(q^{-1})$, $i, j = 1, 2, \ldots, L$, it holds that for the polynomial $\breve{g}_{ij}(q^{-1}) \neq 0$:

1. $\breve{a}_{ii}(q^{-1}) = \breve{v}_{ii}(q^{-1})$, because $w_i(t)$ has not connection to the ground node.
2. $\breve{a}_{ik}(q^{-1}) = \breve{v}_{ik}(q^{-1})$, if $\breve{g}_{ik} = 0$, $k = 1, 2, \ldots, L$.
3. $\breve{a}_{ik}(q^{-1}) = \breve{v}_{ki}(q^{-1})$, if $\breve{g}_{ik} \neq 0$ and $\breve{g}_{ki} = 0$, $k = 1, 2, \ldots, L$.
4. $\breve{a}_{ij}(q^{-1}) = \breve{a}_{ii}(q^{-1}) - \sum_{k=1,k\neq i,j}^{L} \breve{a}_{ik}(q^{-1})$.

from which we find all $\breve{a}_{ij}(q^{-1})$, $j = 1, 2, \ldots, L$. We can repeat this for all i to find $\breve{A}(q^{-1})$. Then $\breve{G}(q^{-1}) = \breve{A}(q^{-1}) - \breve{\Upsilon}(q^{-1})$ and thus, $\breve{A}(q^{-1})$ and $\breve{G}(q^{-1})$ can uniquely be determined from $\breve{\Upsilon}(q^{-1})$.

Similar, Condition 3. of Proposition 11.39 is equivalent to Condition 3. above, for which it holds that $\breve{a}_{jj}(q^{-1}) = \sum_{k=1,k\neq j}^{L} \breve{a}_{kj}(q^{-1})$. As $\breve{v}_{ij}(q^{-1}) = \breve{a}_{ij}(q^{-1}) + \breve{g}_{ij}(q^{-1})$, $i, j = 1, 2, \ldots, L$, it holds that for the polynomial $\breve{g}_{ij}(q^{-1}) \neq 0$:

1. $\breve{a}_{jj}(q^{-1}) = \breve{v}_{jj}(q^{-1})$, because $w_j(t)$ has not connection to the ground node.
2. $\breve{a}_{kj}(q^{-1}) = \breve{v}_{kj}(q^{-1})$, if $\breve{g}_{kj} = 0$, $k = 1, 2, \ldots, L$.
3. $\breve{a}_{kj}(q^{-1}) = \breve{v}_{jk}(q^{-1})$, if $\breve{g}_{kj} \neq 0$ and $\breve{g}_{jk} = 0$, $k = 1, 2, \ldots, L$.
4. $\breve{a}_{kj}(q^{-1}) = \breve{a}_{jj}(q^{-1}) - \sum_{k=1,k\neq i,j}^{L} \breve{a}_{kj}(q^{-1})$.

from which we find all $\breve{a}_{ij}(q^{-1})$, $i = 1, 2, \ldots, L$. We can repeat this for all j to find $\breve{A}(q^{-1})$. Then $\breve{G}(q^{-1}) = \breve{A}(q^{-1}) - \breve{\Upsilon}(q^{-1})$ and thus, $\breve{A}(q^{-1})$ and $\breve{G}(q^{-1})$ can uniquely be determined from $\breve{\Upsilon}(q^{-1})$.

12 | Conclusions and future research

Physical linear networks consist of interconnected systems that exist in the natural and physical world. Conclusions on the developed model structures and identification tools for parameter estimation in physical linear networks are discussed. In addition, directions for future research are suggested.

12.1 Conclusions

12.1.1 Research objective

Science helps us to understand the extremely complicated world. It enables us to predict future outcomes and even to influence them. We can contribute to this knowledge by studying the properties of systems. The enormous technological developments in the last decades led to larger and more complex systems. With this, it has become more valuable to analyse interconnections between systems as well. Physical linear networks consist of interconnected systems that exist in the natural and physical world. These networks occur every where around us and therefore, they are examined in many research areas. To study these networks, their behaviour has to be described. This is accomplished by creating a mathematical model by exploiting the laws of nature and by utilising experimental data. This resulted in the research objective of this thesis:

Develop model structures and identification tools for parameter estimation in physical linear networks.

The process of achieving this research objective comprises several topics. These topics led to the subquestions of this research. Each chapter contributed to one or more of these subquestions. These answers to the research questions

are discussed next, after which we reflect on how the research objective has been achieved.

12.1.2 Model structure

The model structure for identification of physical linear networks is extensively studied in Chapter 2-5. The selection of candidate models is one of the first steps in identification. The model structure for identification of physical linear networks has to be such that it captures the specific characteristics of physical components and that it incorporates the network topology.

In *Chapter 2*, twelve mathematical models from the literature are analysed. Based on the above-mentioned criteria and the generality of the network model, the polynomial model, module representation, and interaction-oriented model are selected as the most attractive ones for the modelling and identification of physical linear networks. From the examination of the mathematical models, it follows that dynamic networks can be represented on different structural levels, where each level includes different amounts of detailed information. The relations between these structures learn us how to include more detailed information in the network model and how to view a network model on a less detailed level by excluding detailed information.

In *Chapter 3*, the relations between network structures that represent dynamics in the vertices and network structures that represent dynamics in the edges show that these representations are closely related. Therefore, research domains using either one of the representations can also exploit theory that has been developed for the other representation. As a result, a wide range of theory is applicable to each research domain.

In addition, the mappings between the interaction-oriented model used in the network control field and the module representation used in the network identification domain imply that these models are strongly connected and therefore, the theory for one model can be mapped into the other model. This means that the control field and the identification domain are closely related and can use each other's results by applying these mappings.

In *Chapter 4*, the module dynamic network is introduced by extending the module representation by allowing for self-loops and multiple-input multiple-output (MIMO) modules. This new network model incorporates state-space forms as a special case and it allows for zooming in into and zooming out of the network. As a result, a state-space form can always be converted into a module representation without losing any information (and vice versa), provided that MIMO modules are allowed in the module dynamic networks.

In *Chapter 5*, the diffusively coupled linear network model is developed to describe various physical linear networks. This multivariable polynomial model is capable of incorporating the symmetric (undirected) nature of the physical components and the linear diffusive couplings, by particular structural properties. As a result, this new network model is used in the remaining research to describe physical linear networks for identification purposes.

12.1.3 Network identifiability

Network identifiability concerns the problem of distinguishing network models in a network model set. The aim is to find a network model in the model set that uniquely describes the data. If multiple solutions are available, it is not possible to make the connection between the estimated parameters and the coefficients of the physical components that are present in the physical network. The approach to deriving conditions for network identifiability is based on uniqueness of the matrix-fraction descriptions (MFDs), which describes a transfer function matrix in terms of a numerator and denominator polynomial matrix. To be precise, the transfer function matrix that describes the behaviour from excitation signals to measured signals is considered. For the diffusively coupled linear networks that we use, the denominator polynomial matrix has the particular structural properties that it is symmetric and nonmonic.

In *Chapter 8 and 9*, four sufficient conditions are presented for the identifiability of the network model for full network identification in the situation that all manifest signals are measured. These conditions include: left coprimeness of the numerator and denominator polynomial matrix; the presence of at least one excitation signal; a structural diagonality constraint on the numerator and denominator polynomial matrix; and a single parameter constraint. These conditions are a generalisation of the conditions that hold for MFDs with a monic and nonsymmetric polynomial denominator matrix, where monicity replaces the last two conditions and the symmetry property.

The *condition* on coprimeness and excitation are rather weak conditions that are easy to satisfy. The parameter constraint can, for example, be on the input dynamics, which are often known. Therefore, this condition is not restrictive either. This leaves the diagonality constraint as the most restrictive condition for network identifiability. This condition is still only sufficient, which means that even network models that do not satisfy this condition can be network identifiable.

In *Chapter 10*, the identifiability conditions are extended to the dual case in which all manifest signals are excited instead of measured. In addition, conditions for network identifiability in the case of partial instrumentation of the manifest

signals are derived from combining the full measurement and full excitation cases. The experimental conditions that have to be satisfied in the partial instrumentation case are that all manifest signals have to be either measured or excited and that at least one manifest signal has to be both measured and excited. This results in flexible instrumentation options for arriving at network identifiability.

In comparison with the module representation, the conditions that are sufficient for network identifiability for the diffusively coupled network model are very simple. This is because they do not include algebraic conditions verifying the rank of particular transfer functions from external signals to internal node signals or related graph-based checks on vertex-disjoint paths. This is entirely due to the structural properties of the diffusive couplings between the node signals, which is reflected by the symmetry in the polynomial matrix $A(q^{-1})$.

12.1.4 Full network identification

Full network identification includes the identification of all dynamics in the network and identification of the network topology. Two different approaches are taken to achieve this objective.

In *Chapter 7*, a physical linear network, which is characterised by undirected interconnections, is represented as a directed dynamic network by the module representation, for which many methods for full network identification are available in the literature. The resulting module representation has particular structural properties reflected in shared parameters among modules. In addition, all modules have direct feedthrough terms leading to algebraic loops. Therefore, the Joint-direct method is applied for consistent identification. In the identifiability analysis of this method it is not possible to incorporate dependent parameterisations among modules, which leads to very strong conditions: every manifest node signal is required to be measured àn̈d excited.

In *Chapter 8*, the newly developed polynomial model is used for describing physical linear networks, which is much better capable of incorporating the symmetric characteristics of the diffusive couplings. A prediction error identification method is used in which the one-step-ahead predictor uses both internal node signals and external excitation signals as prediction input signals, which is the same as in the Joint-direct method. This approach leads to consistent identification of all dynamics in the network.

Decisions on the topology can be made based on the identified dynamics: if some dynamics are (almost) zero, we may assume that they are actually not there. In addition, it is also possible to include knowledge on the presence or absence of interconnections in the identification procedure. Known dynamics, which do

not have to be identified anymore, can also be incorporated in the identification procedure.

The *resulting optimisation problem* is nonconvex. A multistep algorithm, consisting of multiple convex steps, is developed for solving the optimisation problem. This algorithm leads to the global optimum and therefore, consistent parameter estimates are obtained. In this way, the algorithm is also suitable for larger networks, which typically contain more parameters. This algorithm also allows for incorporating prior knowledge of the dynamics or topology of the network.

In *Chapter 10*, the experimental set-up for full network identifications is reconsidered and relaxed. In previous results, presented in Chapter 8, it is assumed that all manifest node signals are measured, leading to the requirement of a single excitation signal. In the most general situation, it is sufficient to either measure or excite each manifest node signal and to both measure and excite (at least) one manifest node signal. This enables a very flexible sensor and actuator allocation scheme, where sensors and actuators can be interchanged.

12.1.5 Subnetwork identification

In *subnetwork identification*, the objective is to identify only the dynamics (and possibly the topology) of a small part of the network. This problem is particularly relevant for large networks, where it might not be interesting to identify all dynamics, or where it is impossible to satisfy the instrumentation conditions. The subnetwork identification problem is different from local identification in directed dynamic networks. In directed dynamic networks, the target is typically a single transfer function from one node to another, described by a single module. In contrast, in physical linear networks, the target is the coupling between two (or more) nodes, described by a subnetwork. In this way, the symmetry property of the physical components is maximally exploited, as explained in Chapter 7 and 9.

Immersion is used to eliminate latent node signals from the network. In literature, the so-called *parallel-path and loop condition* has been derived to keep the target dynamics invariant in the module representation. In the most simple case, this leads to the condition that all output nodes of the target dynamics and all nodes with a direct path to the output nodes of the target dynamics (i.e. all in-neighbours of the output nodes) have to be measured. The *parallel-path and loop condition* for physical linear networks reduces to the very simple condition that only the nodes of the subnetwork and their neighbour nodes have to be measured to keep the subnetwork dynamics invariant. This is similar to the aforementioned condition for module representations, because in a physical network, each neighbour node

is by definition an in-neighbour. As a result, subnetwork identification really becomes a local identification problem in the sense that a subnetwork can be identified on the basis of the node signals of the subnetwork and their neighbour node signals, and that all other node signals can be discarded.

12.1.6 Directed interconnections

Directed dynamics can be present in physical linear networks as, for example, controllers or nonsymmetric components, such as diodes and one-way check valves. These directed dynamics can be included in diffusively coupled linear network models, leading to mixed dynamic networks that contain both undirected and directed interconnections. Several different mixed dynamic networks can be distinguished, which are composed of two basic mixed dynamic network structures. This means that understanding the two basic mixed dynamic networks also leads to insight into more complex mixed dynamic networks.

In *Chapter 11*, the two basic mixed dynamic networks are modelled. In addition, conditions for consistent identification of the full network are derived and algorithms for performing the identification are proposed. Both the undirected as well as the directed dynamics can be identified, along with parts of the topology (depending on the structure of the mixed dynamic network). Mixed dynamic networks can be modelled in the polynomial framework, which is more dedicated to undirected networks, or in the module representation, which is more dedicated to directed networks. In either case, the conditions for consistency are closely related to the ones for full network identification in that same framework for undirected networks or directed networks, respectively.

In *Chapter 7*, it is already shown that describing undirected interconnections in the module representation naturally leads to shared dynamics among the modules. It is not yet possible to incorporate dependent parameterisations in the consistency analysis of the module representation. This leads to conservative conditions for consistent identification of mixed dynamic networks. On the other hand, the polynomial framework is capable of describing both directed and undirected interconnections. In the analysis of consistent identification, the characteristic properties of undirected and directed interconnections can be accounted for. This makes the polynomial framework more attractive than the module representation for describing mixed dynamic networks.

12.1.7 Research results

The *model structure* that is most attractive for parameter estimation in physical linear networks is the polynomial diffusively coupled linear network model that we developed in Chapter 5. This model structure is capable of incorporating the characteristic symmetry property of the diffusive couplings that naturally emerges from the symmetric nature of physical components. It also represents the topology of the network in its polynomial matrices. This model structure can be used to describe various physical processes and other dynamic networks with undirected couplings.

The *identification tools* that we developed and used include multi-path and single-path immersion, data informativity conditions, network identifiability conditions, MFDs, experimental instrumentation conditions, one-step-ahead predictors, prediction-error identification methods, and (multi-step) least-squares algorithms. These tools support the identification of physical linear networks, which include the following objectives:

1. Identification of all dynamics of a physical linear network and, optionally, the network topology.

2. Identification of the dynamics of a subnetwork of a physical linear network and, optionally, the subnetwork topology.

3. Identification of all (undirected and directed) dynamics of a mixed dynamic network and, possibly, (some parts of) the network topology.

A priori knowledge on dynamics and topology can be incorporated in the corresponding identification procedures.

> **Research result.** *A symmetric, nonmonic polynomial model structure and a number of identification tools have been developed for physical linear networks and are used for identification of physical linear networks.*

So, are we done? In some sense yes and, as there is always room for improvement, some directions for future research are suggested in the following section.

12.2 Future research

12.2.1 Modelling

The *model structure* that we developed for the identification of physical linear networks is close to the physics, because it is able to incorporate the characteristic properties that emerge from natural and physical laws. Nevertheless, there remain some aspects of physical networks that cannot be accounted for with this model structure.

The *developed model structure* is able to describe a physical linear network with a single network model that remains the same for different experiments with the same type of input and output signals. However, for experiments with different physical quantities of input and output signals, the network model changes. This means that the developed model structure is co-determined by the chosen quantity for the external input signals and the internal node signals (which are candidate output signals). One direction for future research is to develop a model structure that is fully independent of the experimental setup, such that there is no separation of input and output signals and that multiple quantities can be chosen as node signals.

The *kernel representation* in the behavioural approach (see Definition 1.18 and 2.38) is capable of doing this and it is even closer to the physics than the developed polynomial model structure. This representation is also able to describe the physical linear network for different experiments and data sets. In this modelling framework, one can also investigate how to combine data sets from different experiments. This can, for example, be used to obtain network identifiability with data sets from different experiments when it is not possible to obtain network identifiability with a data set from a single experiment. In the behavioural approach, there is also theory available to separate the signals into input and output signals, which can, for example, be used for describing experiments with specific types of input and output signals (Willems, 1986a; Polderman and Willems, 1998), see also Section 2.4.10. The resulting representation is very similar to the model structure that is developed in this thesis.

Nonlinear components cannot be included in the model structure yet, only nonsymmetric linear behaviour can be accounted for by mixed dynamic networks. In addition, there are interconnection structures that are based on nonlinear physical laws, such as the ideal gas law. A direction for future research is to find a modelling framework that is able to incorporate these nonlinear dynamics and interconnections. In order to do so, one has to go back to the basics of modelling and, again, the behavioural approach is able to do so (Willems, 2007). A general

mathematical representation is expected to be more extensive than a linear one.

12.2.2 Identification

Ongoing developments

The *identification theory* that we developed for physical linear networks provides solutions to many identification problems. These results can be improved further and also extended to networks with less ideal circumstances. As the network identification theory for the module representation is still ahead of the identification theory for physical networks, it is advised to keep an eye on the developments in that research area and to convert those results to physical linear networks.

Full network identification

For *full network identification*, the multistep algorithm can be improved by using the high-order model of the first step to estimate the innovation instead of the parameters. This method is also able to take rank-reduced noise into account (Fonken et al., 2022). Many algorithms have been developed for the simplified ARX-like situation. The main difference between these algorithms lies in the parameterisation and consequently, in the formulation of the optimisation problem for minimising the cost function. The next step is to implement and compare these algorithms to see which one is the most attractive in terms of accuracy and computation time. The corresponding strategy can be adopted by the more advanced ARMAX-like situation.

Known dynamics can be incorporated in the identification procedure. However, physical linear networks exist in continuous-time, but are identified in discrete-time. This means that known component values have to be translated to the discrete-time parameters. In addition, the discrete-time model is an approximation of the continuous-time model and therefore, some information is lost during the discretisation, which leads to errors in the identification. The discretisation method can be improved, by using a higher-order approximation instead of the first-order backward shift that is currently used.

Continuous-time identification is an even more attractive approach, because then discretisation is not needed at all. For continuous-time identification, the frequency domain is preferred over the time domain, because no derivatives of signals have to be determined. With the local polynomial method (LPM), a non-parametric estimation of the frequency response function is obtained, which is in a second step used to find a parametric estimation of the network model (Schoukens

et al., 2009; Pintelon et al., 2010a,b; Gevers et al., 2011). Preliminary results on the implementation and simulation of continuous-time frequency-domain identification of diffusively coupled linear networks are under development (Liang, 2023). Here, LPM is used followed by a parametric identification step tailored to the diffusively coupled network structure to estimate the parameters of the full network or a subnetwork.

In *continuous-time modelling and identification* of physical networks, additional aspects are relevant. One of them is the intersample behaviour, which is typically band-limited for physical systems. Further, discretisation with the backward-shift method automatically results in an invertible A_0 for the discrete-time representation of a connected network. However, for the continuous-time representation, the A_0 of a connected network is not necessarily invertible, while the currently available identification analysis is strongly based on this property. Additional research is required to translate the identification analysis of discrete-time diffusively coupled linear network models to continuous-time.

Another *extension to full network identification* is to include the preservation of network properties, such as dissipativity, stability, and semipositive-definiteness of the polynomial matrices. For this, the first step is to prove that higher-order diffusively coupled linear networks are dissipative and stable. This has been proven for second-order models, but not yet for higher-order models, although it is believed to be true. Second, a way must be found to incorporate these properties in the identification procedure, such that the identified network model will always satisfy these properties.

Network identifiability

Including specific structural condition in the identifiability analysis has been studied by van Waarde et al. (2018) for first-order state-space models with known input and output matrices, which are a special case of the diffusively coupled linear network model developed in this thesis. The *identifiability conditions* are derived based on the Markov parameters and lead to partial instrumentation conditions, for full network and subnetwork identifiability. The instrumentation conditions are translated into graphical conditions based on an algorithm of Hogben (2010). It would be interesting to extend these results to higher-order diffusively coupled linear networks and compare them with the identifiability results derived in this thesis. The Markov parameters for the (discrete-time and the continuous-time) diffusively coupled network model have already been derived using theory of Holzel and Bernstein (2012). The next step is to proof that the network dynamics can uniquely be obtained from the Markov parameters. Further research is necessary to complete this proof.

Local network identification

For *subnetwork identification*, the full immersed network is considered to be identifiable. The main reason for this is that the direct feedthrough terms in the whole immersed network are needed to identify the subnetwork dynamics. However, only the target subnetwork is required to be consistently identified and therefore, only the subnetwork needs to be identifiable. Revising the identifiability conditions in this context, might lead to more relaxed identifiability conditions for subnetwork identification. As only the dynamics of the subnetwork is of interest, the other dynamics in the immersed network is latent and may be approximated as long as the subnetwork dynamics remains identifiable. To this end, the latent dynamics can be approximated with lower-order models or by nonparametric models. The latter can, for example, be achieved with kernel-based methods (Ramaswamy et al., 2021).

An *alternative local identification problem* concerns the identification of a single interaction between two nodes, described by the polynomial $a_{ij}(q^{-1}) = a_{ji}(q^{-1})$, $i \neq j$. This is different from the subnetwork identification problem, where the coupling between node signals is described by a subnetwork. For identifying a single interaction, three approaches can be distinguished. First, the subnetwork of $w_i(t)$ and $w_j(t)$ is identified, which includes the dynamics $a_{ij}(q^{-1})$ and $a_{ji}(q^{-1})$. Second, the subnetwork of only $w_i(t)$ is identified, where the polynomial $a_{ij}(q^{-1})$ is also identified, because it describes neighbouring dynamics. For the same reason, the identification of the subnetwork of only $w_j(t)$ leads to the polynomial $a_{ji}(q^{-1})$. In the latter two cases, an extra node can be immersed, leading to less dynamics that has to be identified. On the other hand, using less information also increases the variance of the estimates.

Variance

Analysing the variance of the estimates (or the deviation from the mean value) is especially interesting for local identification problems. All three proposed approaches will lead to consistent estimates, and therefore, a trade-off between computational costs, variance, and experimental costs has to be made. Related to this is the fact that it is currently unclear how helpful it is for identification to include known dynamics or use more excitation signals than necessary. While consistency can already be obtained without this extra information, the variance is expected to improve. However, an extensive analysis of the variance is still missing for the full network identification problem.

12.2.3 Extension

For *mixed dynamic networks* containing both undirected and directed dynamics, the modelling and identification results presented in this thesis are preliminary and can be further developed. The currently available results can be extended to more advanced combinations of mixed dynamic networks. The critical part in obtaining conditions for consistent identification lies in the identifiability analysis. Comparing the identifiability conditions in the polynomial framework and the module representation is necessary to improve the insight in the differences between these conditions and modelling frameworks. To apply the results to real-life set-ups, the proposed algorithms have to be implemented and simulation examples have to be created to illustrate the results.

12.2.4 Application

Applying the comprehensive modelling and identification theory that is developed in this thesis, to practice is hardly done yet. Some simulation examples are created to illustrate the results, but applying the developed algorithms to real-life set-ups is only under development. In practice, *testing and fault detection and diagnostics* seem to be the most relevant applications for identification in dynamic networks.

In-circuit testing of printed circuit board assemblys (PCBAs) is one application that has already been examined. A PCBA is a physical linear network that can be modelled in the diffusively coupled network model that has been developed in this thesis. It has been motivated that considering the PCBA as a physical linear network and incorporating the network structure into the identification procure, drastically reduces the experiment cost and improves the identification and test results (Meijer, 2021).

Fault detection and diagnostics in wafer scanners is another application that has been considered. A digital twin can be built in the modelling framework developed in this thesis. Subsequently, this digital twin can be used to generate faulty data to learn about faults that can occur in the wafer scanners. This data is used to develop fault detection and diagnostics algorithms (Nikitas, 2023). In these wafer scanners, physical components with undirected behaviour (such as bodies and screws) are combined with digital components with directed behaviour (such as controllers). Therefore, modelling and identification theory for mixed dynamic networks is important for achieving fault detection. In addition, model validation has a valuable role in this whole, because it supports in deciding whether a fault occurs in the network (Shi, 2023).

Pipelines and electric power networks are other evident application domains. These physical linear networks are naturally described by diffusively coupled linear

networks and therefore, they are very suitable for applying the theory developed in this thesis.

A *MATLAB app and toolbox* are under development for dynamic network identification to make all the developed theory accessible to (industrial) users (SYSDYNET, 2023). This app and toolbox features a user-friendly graphical interface for manipulating and analysing dynamic networks. It is currently being extended to include identification algorithms as well. It includes theory from data-driven modelling in the module representation and will be extended with the results of this thesis regarding modelling and identification of physical linear networks and mixed dynamic networks.

12.2.5 Reverse questions

As *theoretical researchers*, we, typically search for conditions to proof an objective can be obtained. In other words, we search for the circumstances that are necessary or sufficient for achieving a theoretically formulated goal. For example, we look for sufficient conditions for full network identifiability or for the locations for sensors and actuators to be able to identify a particular part of the network.

From the industry's point of view, a relevant question might be the exact reverse: considering given circumstances, what can be achieved? If the experimental set-up is limited to these sensor and actuator locations, which part of the network can still be identified? These *reverse questions* are less natural for us as theoretical researchers to ask, but might be equivalently important for industry. In answering these questions, the solutions to the original problems will of course help.

Acknowledgements

The academic journey of the past years has eventually led to this thesis and more importantly, contributed highly to my personal and professional development. The enormous growth I am still experiencing is supported by a reciprocity between this research trajectory and several environments in my personal live.

prof.dr.ir. Paul Van den Hof, thank you so much for starting this challenge with me. I am deeply grateful that you gave me this opportunity. You are always willing to think along and you made me feel comfortable in discussing anything with you. Your guidance and advice helpt me learning and improving many skills from critical thinking, writing papers, and checking programming code to traveling by plane and visiting conferences. You steer (and even brake) whenever you think it is necessary and at the same time you stimulate to come up with my own ideas. This led to research in which I could do what I like the most: describing behaviour with physics and mathematics.

prof.dr. Siep Weiland, your great enthusiasm for systems, control, and of course the beauty of mathematics persuade me to perform both my internship and graduation project with you, after you already introduced me to all aspects of systems and control during my Bachelor End Project. I am grateful for your mentorship and support during these projects and for directing me to Paul for continuing a research trajectory within the Control Systems group. Your passionate and interactive way of teaching is very inspiring to me.

Committee members prof.dr.ir. Tom Oomen, em.prof.dr.ir. Johan Schoukens, prof.dr.ir. Bart de Moor, prof.dr. Martin Enqvist, and dr.ir. Matthijs van Berkel, thank you for taking the time and effort to review this (large) thesis and for being part of the defence ceremony. Matthijs, your extensive comments and suggestions were helpful in improving this thesis.

Team members of the SYSDYNET project, and especially Shengling, Karthik, Tom, Mannes, and Stefanie, we had the fortunate advantage of being able to present and discuss research with each other during the Friday (and later on Thursday)

morning meetings. These discussions created insight in each others topics and problems at different levels of the project. I have learnt a lot from it and these meetings have been very valuable to me.

Job and Desen, supervising your master projects allowed me to practice with guiding and steering students. It has been nice to work with you.

Siep, Sofie, and Birgit, you knew how to utilize my strengths and you made the teaching tasks very enjoyable and valuable. It has been a great pleasure to teach with you.

Colleagues from the Control Systems group, we shared an enjoyable and social working atmosphere. Especially the last few years, you dragged me into the group and made me feel part of it, also during conferences. I really appreciate this.

Department of Electrical Engineering, I would like to express my gratitude for your financial support to this research trajectory.

Maarten, your coaching greatly supported the tremendous personal growth I have experienced during my studies up until the start of this research project. I also appreciate the guidance of other coaches during these years.

Hans, thank you for proceeding the coaching and helping me in continuing this enormous personal growth. You have already taught me a lot and I am sure there will be much more to come. Most importantly, you are a fantastic friend.

Mathijs, you are a fine friend too. We share the same obsession for judo, from teaching to refereeing, and you are an amazing role model to me.

Harald, Mathijs, Hans, and all other referee friends, you make judo tournaments a great place for friendship and fun. You create an environment where I truly feel part of, where I fully feel at ease, and which is ideal for improving all kind of abilities, such as multitasking, self-confidence, and social skills. This is the most wonderful thing one can offer!

Lianne and Peter, you encouraged me to teach (judo) again. It is bringing me a lot of pleasure and satisfaction. Besides becoming a better teacher, I am also becoming more confident.

Mam and Pap, thank you for teaching me very early on to push my boundaries and to pursue maximum performance. This mind set is helping me substantially. Sometimes, you try to protect me from myself when you feel like I am demanding to much of myself. I really appreciate your support over the years, especially when I run into a brick wall, and that you are so proud when I achieve my goals.

Johan, Thijs, and Daan, we are always have a great time together, which is being a major support and distraction to me.

Bibliography

J.A. Acebrón, L.L. Bonilla, C.J. Pérez Vicente, F. Ritort, and R. Spigler. The Kuramoto model: a simple paradigm for synchronization phenomena. *Reviews of Modern Physics*, 77(1):137–185, 2005.

J. Adebayo, T. Southwick, V. Chetty, E. Yeung, Y. Yuan, J. Gonçalves, J. Grose, J. Prince, G.B. Stan, and S. Warnick. Dynamical structure function identifiability conditions enabling signal structure reconstruction. In *Proceedings of the 51st IEEE Conference on Decision and Control (CDC)*, pages 4635–4641, 2012.

L. Aguirre, B. Barbosa, and A. Braga. Prediction and simulation errors in parameter estimation for nonlinear systems. *Mechanical Systems and Signal Processing*, 24:2855–2867, 11 2010.

J. Anderson, Y.-C. Chang, and A. Papachristodoulou. Model decomposition and reduction tools for large-scale networks in systems biology. *Automatica*, 47(6): 1165–1174, 2011. Special Issue on Systems Biology.

N. Balabanian and T.A. Bickart. *Electrical network theory*. John Wiley & Sons, Inc., New York, 1969. ISBN 978-0-471-04576-2.

A.S. Bazanella, M. Gevers, J.M. Hendrickx, and A. Parraga. Identifiability of dynamical networks: which nodes need be measured? In *Proceedings of the 56th IEEE Conference on Decision and Control (CDC)*, pages 5870–5875, 2017.

A.S. Bazanella, M. Gevers, and J.M. Hendrickx. Network identification with partial excitation and measurement. In *Proceedings of the 58th IEEE Conference on Decision and Control (CDC)*, pages 5500–5506, 2019.

S. Boccaletti, V. Latora, Y. Moreno, M. Chavez, and D.-U. Hwang. Complex networks: structure and dynamics. *Physics Reports*, 424(4):175–308, 2006.

X. Bombois, K. Colin, P.M.J. Van den Hof, and H. Hjalmarsson. On the informativity of direct identification experiments in dynamical networks. *Automatica*, 148:110742, 2023.

W. Borutzky. *Bond graph methodology: development and analysis of multidisciplinary dynamic system models*. Springer London, London, 2010. ISBN 978-1-84882-882-7.

W. Borutzky. *Bond graph modelling of engineering systems: theory, applications and software support*. Springer London, London, 2011. ISBN 978-1-4419-9368-7.

G. Bottegal, A. Chiuso, and P.M.J. Van den Hof. On dynamic network modeling of stationary multivariate processes. *IFAC-PapersOnLine*, 51(15):850–855, 2018. Proceedings of the 18th IFAC Symposium on System Identification (SYSID).

P.C. Breedveld. Thermodynamic bond graphs and the problem of thermal inertance. *Journal of the Franklin Institute*, 314(1):15–40, 1982.

F. Bullo. *Lectures on Network Systems*. Kindle Direct Publishing, 2022. ISBN 978-1-986425-64-3.

C.I. Byrnes, A. Isidori, and J.C. Willems. Passivity, feedback equivalence, and the global stabilization of minimum phase nonlinear systems. *IEEE Transactions on Automatic Control*, 36(11):1228–1240, 1991.

Y.H. Chang, J.W. Gray, and C.J. Tomlin. Exact reconstruction of gene regulatory networks using compressive sensing. *BMC Bioinformatics*, 15(1), 2014.

X. Cheng and J.M.A. Scherpen. Model reduction methods for complex network systems. *Annual Reviews of Control, Robotics, and Autonomous Systems*, 4: 425–453, 2021.

X. Cheng, Y. Kawano, and J.M.A. Scherpen. Reduction of second-order network systems with structure preservation. *IEEE Transactions on Automatic Control*, 62(10):5026–5038, 2017.

X. Cheng, S. Shi, and P.M.J. Van den Hof. Allocation of excitation signals for generic identifiability of linear dynamic networks. *IEEE Transactions on Automatic Control*, 67(2):692–705, 2022.

X. Cheng, S. Shi, I. Lestas, and P.M.J. Van den Hof. Identifiability in dynamic acyclic networks with partial excitations and measurements. *Provisionally accepted for publication in IEEE Transactions on Automatic Control*, 2023. ArXiv:2201.07548.

V. Chetty and S. Warnick. Network semantics of dynamical systems. In *Proceedings of the 54th IEEE Conference on Decision and Control (CDC)*, pages 1557–1562, 2015.

V. Chetty and S. Warnick. Meanings and applications of structure in networks of dynamic systems. In S. Roy and S.K. Das, editors, *Principles of cyber-physical systems: an interdisciplinary approach*, chapter 7, pages 162–206. Cambridge University Press, Cambridge, 2020.

A. Chiuso and G. Pillonetto. A Bayesian approach to sparse dynamic network identification. *Automatica*, 48(8):1553–1565, 2012.

E.K.P. Chong and S.H. Żak. *An introduction to optimization*. Wiley Interscience, third edition, 2008. ISBN 978-0-471-75800-6.

J. Coiffier. *Fundamentals of numerical weather prediction*. Cambridge University Press, 2011. ISBN 978-1-107-00103-9.

A. Dankers, P.M.J. Van den Hof, X. Bombois, and P.S.C. Heuberger. Errors-in-variables identification in dynamic networks - consistency results for an instrumental variable approach. *Automatica*, 62:39–50, 2015.

A. Dankers, P.M.J. Van den Hof, D. Materassi, and H.H.M. Weerts. Conditions for handling confounding variables in dynamic networks. *IFAC-PapersOnLine*, 50(1):3983–3988, 2017. Proceedings of the 20th IFAC World Congress.

A. Dankers, D. Westwick, and E. Jalilian. Pipeline monitoring using acoustic measurements and network system identification. Technical report, University of Calgary, 2021. Submitted to *IEEE Transactions on Instrumentation and Measurement*.

A.G. Dankers. *System identification in dynamic networks*. PhD thesis, Technische Universiteit Delft, 2014.

A.G. Dankers. Optimization method for obtaining estimates in a dynamic network. Technical note, 2019.

A.G. Dankers, P.M.J. Van den Hof, X. Bombois, and P.S.C. Heuberger. Identification of dynamic models in complex networks with prediction error methods: predictor input selection. *IEEE Transactions on Automatic Control*, 61(4): 937–952, 2016.

M. De Angelis, H. Luş, R. Betti, and R.W. Longman. Extracting physical parameters of mechanical models from identified state-space representations. *Journal of Applied Mechanics*, 69(5):617–625, 2002.

M. Deistler. The properties of the parameterization of ARMAX systems and their relevance for structural estimation and dynamic specification. *Econometrica*, 51(4):1187–1207, 1983.

M. Dimovska and D. Materassi. A control theoretic look at Granger causality: extending topology reconstruction to networks with direct feedthroughs. *IEEE Transactions on Automatic Control*, 66(2):699–713, 2021.

F. Dörfler and F. Bullo. Kron reduction of graphs with applications to electrical networks. *IEEE Transactions on Circuits and Systems I: Regular Papers*, 60 (1):150–163, 2013.

F. Dörfler, J.W. Simpson-Porco, and F. Bullo. Electrical networks and algebraic graph theory: models, properties, and applications. *Proceedings of the IEEE*, 106(5):977–1005, 2018.

H.J. Dreef, S. Shi, X. Cheng, M.C.F. Donkers, and P.M.J. Van den Hof. Excitation allocation for generic identifiability of linear dynamic networks with fixed modules. *IEEE Control Systems Letters*, 6:2587–2592, 2022.

G.E. Dullerud and R. D'Andrea. Distributed control of heterogeneous systems. *IEEE Transactions on Automatic Control*, 49(12):2113–2128, 2004.

N. Everitt, G. Bottegal, and H. Hjalmarsson. An empirical bayes approach to identification of modules in dynamic networks. *Automatica*, 91:144–151, 2018.

P. Eykhoff. *System identification: parameter and state estimation*. John Wiley & Sons, Ltd., London, 1974. ISBN 978-0-471-24980-1.

M. Fang, M. Galrinho, and H. Hjalmarsson. Recursive weighted null-space fitting method for identification of multivariate systems. *IFAC-PapersOnLine*, 54 (7):345–350, 2021. Proceedings of the 19th IFAC Symposium on System Identification (SYSID).

A. Fazzi, N. Guglielmi, and I. Markovsky. An ODE-based method for computing the approximate greatest common divisor of polynomials. *Numerical Algorithms*, 81(2):719–740, 2019.

M. Fiedler. Algebraic connectivity of graphs. *Czechoslovak Mathematical Journal*, 23(2):298–305, 1973.

S. Fonken, M. Ferizbegovic, and H. Hjalmarsson. Consistent identification of dynamic networks subject to white noise using weighted null-space fitting. *IFAC-PapersOnLine*, 53(2):46–51, 2020. Proceedings of the 21st IFAC World Congress.

S.J.M. Fonken, K. R. Ramaswamy, and P.M.J. Van den Hof. A scalable multi-step least squares method for network identification with unknown disturbance topology. *Automatica*, 41:110295, 2022.

U. Forssell and L. Ljung. Closed-loop identification revisited. *Automatica*, 35(7): 1215–1241, 1999.

K.J. Friston, J. Kahan, B. Biswal, and A. Razi. A DCM for resting state fMRI. *NeuroImage*, 94:396–407, 2014.

M.I. Friswell, S.D. Garvey, and J.E.T. Penny. Extracting second order systems from state space representations. *AIAA Journal*, 37(1):132–135, 1999.

C.-P. Fritzen. Identification of mass, damping, and stiffness matrices of mechanical systems. *Journal of Vibration, Acoustics, Stress, and Reliability in Design*, 108 (1):9–16, 1986.

M. Galrinho. *Least squares methods for system identification of structured models*. PhD thesis, KTH School of Electrical Engineering, 2016.

M. Galrinho, C.R. Rojas, and H. Hjalmarsson. Parametric identification using weighted null-space fitting. *IEEE Transactions on Automatic Control*, 64(7): 2798–2813, 2019.

General Radio. *Introduction to in-circuit testing*. GenRad, Inc., Concord, MA, 1984. URL `www.ietlabs.com/pdf/Handbooks/Introduction%20to%20In-Circuit%20Testing.pdf`.

M. Gevers and A.S. Bazanella. Identification in dynamic networks: identifiability and experiment design issues. In *Proceedings of the 54th IEEE Conference on Decision and Control (CDC)*, pages 4005–4010, 2015.

M. Gevers, R. Pintelon, and J. Schoukens. The local polynomial method for nonparametric system identification: improvements and experimentation. In *Proceedings of the 50th IEEE Conference on Decision and Control (CDC) and European Control Conference (ECC)*, pages 4302–4307, 2011.

M. Gevers, A.S. Bazanella, and G.V. da Silva. A practical method for the consistent identification of a module in a dynamical network. *IFAC-PapersOnLine*, 51 (15):862–867, 2018. Proceedings of the 18th IFAC Symposium on System Identification (SYSID).

M. Gevers, A.S. Bazanella, and G.A. Pimentel. Identifiability of dynamical networks with singular noise spectra. *IEEE Transactions on Automatic Control*, 64(6):2473–2479, 2019.

C. Godsil and G. Royle. *Algebraic graph theory*. Graduate Texts in Mathematics. Springer, New York, 2001. ISBN 978-0-387-95220-8.

G. Golo, A.J. van der Schaft, P.C. Breedveld, and B.M. Maschke. Hamiltonian formulation of bond graphs. In R. Johansson and A. Rantzer, editors, *Nonlinear and hybrid Systems in Automotive Control*, pages 351–372. Springer, London, 2003.

G.H. Golub and V. Pereyra. The differentiation of pseudo-inverses and nonlinear least squares problems whose variables separate. *SIAM Journal on Numerical Analysis*, 10(2):413–432, 1973.

J. Gonçalves and S. Warnick. Necessary and sufficient conditions for dynamical structure reconstruction of LTI networks. *IEEE Transactions on Automatic Control*, 53(7):1670–1674, 2008.

J. Gonçalves, R. Howes, and S. Warnick. Dynamical structure functions for the reverse engineering of LTI networks. In *Proceedings of the 46th IEEE Conference on Decision and Control (CDC)*, pages 1516–1522, 2007.

Y. Guo, D. Zhang, Z. Li, Q. Wang, and D. Yu. Overviews on the applications of the Kuramoto model in modern power system analysis. *International Journal of Electrical Power and Energy Systems*, 129:106804, 2021.

A. Haber and M. Verhaegen. Subspace identification of large-scale interconnected systems. *IEEE Transactions on Automatic Control*, 59(10):2754–2759, 2014.

E.J. Hannan and M. Deistler. *The statistical theory of linear systems*. Society for Industrial and Applied Mathematics (SIAM), Philadelphia, 2012. ISBN 978-1-611972-18-4.

D. Hayden, Y. Yuan, and J. Gonçalves. Network reconstruction from intrinsic noise: minimum-phase systems. In *Proceedings of the 2014 American Control Conference (ACC)*, pages 4391–4396, 2014.

D. Hayden, Y.H. Chang, J. Gonçalves, and C.J. Tomlin. Sparse network identifiability via compressed sensing. *Automatica*, 68:9–17, 2016.

D. Hayden, Y. Yuan, and J. Gonçalves. Network identifiability from intrinsic noise. *IEEE Transactions on Automatic Control*, 62(8):3717–3728, 2017.

J.M. Hendrickx, M. Gevers, and A.S. Bazanella. Identifiability of dynamical networks with partial node measurements. *IEEE Transactions on Automatic Control*, 64(6):2240–2253, 2019.

J.P. Hespanha. *Linear systems theory*. Princeton University Press, Princeton, second edition, 2023. ISBN 978-1-4008-9008-8.

L. Hogben. Minimum rank problems. *Linear Algebra and its Applications*, 432 (8):1961–1974, 2010.

M. S. Holzel and D. S. Bernstein. From polynomial matrices to markov parameters and back: theory and numerical algorithms. *Linear Algebra and its Applications*, 437(3):783–808, 2012.

S. Huang, G. Eichler, Y. Bar-Yamand, and D.E. Ingber. Cell fates as high-dimensional attractor states of a complex gene regulatory network. *Physical Review Letters*, 94:128701, 2005.

G. Innocenti and D. Materassi. Modeling the topology of a dynamical network via wiener filtering approach. *Automatica*, 48(5):936–946, 2012.

S. Jahandari and D. Materassi. Optimal selection of observations for identification of multiple modules in dynamic networks. *IEEE Transactions on Automatic Control*, 67(9):4703–4716, 2022a.

S. Jahandari and D. Materassi. Sufficient and necessary graphical conditions for MISO identification in networks with observational data. *IEEE Transactions on Automatic Control*, 67(11):5932–5947, 2022b.

M.B. Jones. Plant microclimate. In J. Coombs, D.O. Hall, S.P. Ljong, and J.M.O. Scurlock, editors, *Techniques in bioproductivity and photosynthesis*, Pergamon International Library of Science, Technology, Engineering and Social Studies, chapter 3, pages 26–40. Pergamon, second edition, 1985. ISBN 978-0-08-031999-5.

T. Kailath. *Linear systems*. Prentice-Hall, Englewood Cliffs, NJ, 1980. ISBN 978-0-13-536961-4.

R.E. Kalman. A new approach to linear filtering and prediction problems. *Journal of Basic Engineering*, 82(1):35–45, 1960.

N. Karcanias, E. Sagianos, and E. Milonidis. Structural identification: the computation of the generic McMillan degree. In *Proceedings of the 44th IEEE Conference on Decision and Control (CDC)*, pages 7222–7227, 2005.

H.K. Khalil. *Nonlinear systems: Pearson new international edition*. Pearson, Essex, third edition, 2014. ISBN 978-1-292-03921-3.

E.M.M. Kivits and P.M.J. Van den Hof. Local identification in diffusively coupled linear networks. In *Proceedings of the 61st IEEE Conference on Decision and Control (CDC)*, pages 874–879, 2022.

E.M.M. Kivits and P.M.J. Van den Hof. Identifiability of diffusively coupled linear networks with partial instrumentation. *IFAC-PapersOnLine*, 56(2):2395–2400, July 2023a. 22nd IFAC World Congress.

E.M.M. Kivits and P.M.J. Van den Hof. Identification of diffusively coupled linear networks through structured polynomial models. *IEEE Transactions on Automatic Control*, 68(6):3513–3528, 2023b.

D. Koller and N. Friedman. *Probabilistic graphical models: principles and techniques*. Adaptive computation and machine learning. MIT Press, Cambridge, MA, 2009. ISBN 978-0-262-01319-2.

G. Kron. *Tensor analysis of networks*. John Wiley & Sons, Inc., London, second edition, 1949.

Y. Kuramoto. Self-entrainment of a population of coupled non-linear oscillators. In H. Araki, editor, *International Symposium on Mathematical Problems in Theoretical Physics*, pages 420–422, 1975.

C. Langbort, R.S. Chandra, and R. D'Andrea. Distributed control design for systems interconnected over an arbitrary graph. *IEEE Transactions on Automatic Control*, 49(9):1502–1519, 2004.

A. Legat and J.M. Hendrickx. Local network identifiability with partial excitation and measurement. In *Proceedings of the 59th IEEE Conference on Decision and Control (CDC)*, pages 4342–4347, 2020.

Q. Li, X. Deng X., Liu, W. Sun, W. Li, J. Li, and Z. Liu. Autonomous smart grid fault detection. *IEEE Communications Standards Magazine*, 7(2):40–47, 2023.

D. Liang. Frequency domain identification in the dynamic network for in-circuit testing. Msc thesis, Technische Universiteit Eindhoven, December 2023. In preparation.

J. Linder and M. Enqvist. Identification and prediction in dynamic networks with unobservable nodes. *IFAC-PapersOnLine*, 50(1):10574–10579, 2017. Proceedings of the 20th IFAC World Congress.

L. Ljung. *System identification: theory for the user*. Prentice-Hall, Englewood Cliffs, NJ, second edition, 1999. ISBN 978-0-13-656695-2.

L. Ljung and T. Glad. *Modeling of dynamic systems*. Prentice-Hall, Englewood Cliffs, NJ, 1994. ISBN 978-0-13-597097-0.

L. Ljung and B. Wahlberg. Asymptotic properties of the least-squares method for estimating transfer functions and disturbance spectra. *Advances in Applied Probabilities*, 24(2):412–440, 1992.

P. Lopes dos Santos, J.A. Ramos, T. Azevedo-Perdicoúlis, and J.L. Martins de Carvalho. Deriving mechanical structures in physical coordinates from data-driven state-space realizations. In *Proceedings of the 2015 American Control Conference (ACC)*, pages 1107–1112, 2015.

H. Luş, M. De Angelis, R. Betti, and R.W. Longman. Constructing second-order models of mechanical systems from identified state space realizations part I: theoretical discussions. *Journal of Engineering Mechanics*, 129(5):477–488, 2003.

J. Lunze. *Feedback control of large-scale systems*. Series in Systems and Control Engineering. Prentice Hall International, 1992. ISBN 978-0-13-318353-5.

R.N. Mantegna. Hierarchical structure in financial markets. *The European Physical Journal B - Condensed Matter and Complex Systems*, 11(1):193–197, 1999.

I. Mareels. Sufficiency of excitation. *Systems & Control Letters*, 5(3):159–163, 1984.

I. Markovsky, J.C. Willems, S. Van Huffel, and B. De Moor. *Exact and approximate modeling of linear systems: a behavioral approach*. Number 11 in Monographs on Mathematical Modeling and Computation. Society for Industrial and Applied Mathematics (SIAM), Philadelphia, PA, 2006. ISBN 978-0-89871-603-0.

D. Materassi and G. Innocenti. Topological identification in networks of dynamical systems. *IEEE Transactions on Automatic Control*, 55(8):1860–1871, 2010.

D. Materassi and M.V. Salapaka. On the problem of reconstructing an unknown topology via locality properties of the Wiener filter. *IEEE Transactions on Automatic Control*, 57(7):1765–1777, 2012.

D. Materassi and M.V. Salapaka. Identification of network components in presence of unobserved nodes. In *Proceedings of the 54th IEEE Conference on Decision and Control (CDC)*, pages 1563–1568, 2015.

D. Materassi and M.V. Salapaka. Signal selection for estimation and identification in networks of dynamic systems: a graphical model approach. *IEEE Transactions on Automatic Control*, 65(10):4138–4153, 2020.

A. Mauroy and J. Hendrickx. Spectral identification of networks using sparse measurements. *SIAM Journal on Applied Dynamical Systems*, 16(1):479–513, 2017.

J. Meijer. Improvements for in-circuit testing using RLC network identification. Msc thesis, Technische Universiteit Eindhoven, November 2021.

M. Mesbahi and M. Egerstedt. *Graph theoretic methods in multiagent networks*. Princeton University Press, Princeton, NJ, 2010. ISBN 978-0-691-14061-2.

A. Mishra and R.A. de Callafon. Recursive estimation of three phase line admittance in electric power networks. *IFAC-PapersOnLine*, 53(2):34–39, 2020. Proceedings of the 21st IFAC World Congress.

T. Mori, P.N. Nikiforuk, M.M. Gupta, and N. Hori. A class of discrete time models for a continuous time system. In *Proceedings of the 1987 American Control Conference (ACC)*, pages 953–957, 1987.

D.A. Morrison. Genealogies: pedigrees and phylogenies are reticulating networks not just divergent trees. *Evolutionary Biology*, 43:456–473, 2016.

S. Mukhopadhyay, H. Luş, and R. Betti. Modal parameter based structural identification using input–output data: minimal instrumentation and global identifiability issues. *Mechanical Systems and Signal Processing*, 45(2):283–301, 2014.

S. Mukhopadhyay, H. Luş, and R. Betti. Structural identification with incomplete instrumentation and global identifiability requirements under base excitation. *Structural Control and Health Monitoring*, 22(7):1024–1047, 2015.

S. Mukhopadhyay, H. Luş, and R. Betti. Structural identification with incomplete output-only data and independence of measured information for shear-type systems. *Earthquake Engineering & Structural Dynamics*, 45(2):273–296, 2016.

M. Nabi-Abdolyousefi and M. Mesbahi. Network identification via node knockout. *IEEE Transactions on Automatic Control*, 57(12):3214–3219, 2012.

K. Nice. How cruise control systems work, 2021. URL `auto.howstuffworks.com/cruise-control.htm`.

D. Nikitas. Digital twin for diagnostics of wafer scanners. Msc thesis, Technische Universiteit Eindhoven, Oktober 2023.

Oxford University Press. Oxford learner's dictionary of academic english, 2023. URL `www.oxfordlearnersdictionaries.com/definition/academic/`.

H.M. Paynter. *Analysis and design of engineering systems*. M.I.T. Press, Cambridge, Mass, 1961.

J. Pearl. *Causality*. Cambridge University Press, Cambridge, 2000. ISBN 978-0-521-77362-8.

G. Pillonetto, F. Dinuzzo, T. Chen, G. De Nicolao, and L. Ljung. Kernel methods in system identification, machine learning and function estimation: a survey. *Automatica*, 50(3):657–682, 2014.

R. Pintelon and J. Schoukens. *System identification: a frequency domain approach*. John Wiley & Sons, Inc., Hoboken, NJ, second edition, 2012. ISBN 978-0-470-64037-1.

R. Pintelon, J. Schoukens, G. Vandersteen, and K. Barbé. Estimation of nonparametric noise and FRF models for multivariable systems part I: theory. *Mechanical Systems and Signal Processing*, 24(3):573–595, 2010a.

R. Pintelon, J. Schoukens, G. Vandersteen, and K. Barbé. Estimation of nonparametric noise and FRF models for multivariable systems part II: extensions, applications. *Mechanical Systems and Signal Processing*, 24(3):596–616, 2010b.

J.W. Polderman and J.C. Willems. *Introduction to mathematical systems theory, a behavioral approach*. Texts in Applied Mathematics. Springer, New York, 1998. ISBN 978-0-387-98266-3.

G. Prando, M. Zorzi, A. Bertoldo, M. Corbetta, M. Zorzi, and A. Chiuso. Sparse DCM for whole-brain effective connectivity from resting-state fMRI data. *NeuroImage*, 208:116367, 2020.

K. R. Ramaswamy and P.M.J. Van den Hof. A local direct method for module identification in dynamic networks with correlated noise. *IEEE Transactions on Automatic Control*, 66(11):3237–3252, 2021.

K. R. Ramaswamy, G. Bottegal, and P.M.J. Van den Hof. Local module identification in dynamic networks using regularized kernel-based methods. In *Proceedings of the 57th IEEE Conference on Decision and Control (CDC)*, pages 4713–4718, 2018.

K. R. Ramaswamy, P.M.J. Van den Hof, and A.G. Dankers. Generalized sensing and actuation schemes for local module identification in dynamic networks. In *Proceedings of the 58th IEEE Conference on Decision and Control (CDC)*, pages 5519–5524, 2019.

K. R. Ramaswamy, G. Bottegal, and P.M.J. Van den Hof. Learning linear modules in a dynamic network using regularized kernel-based methods. *Automatica*, 129:109591, 2021.

J. Ramos, G. Mercère, and O. Prot. Identifying second-order models of mechanical structures in physical coordinates: an orthogonal complement approach. In *Proceedings of the 12th European Control Conference (ECC)*, pages 3973–3978, 2013.

W. Ren, R.W. Beard, and E.M. Atkins. A survey of consensus problems in multi-agent coordination. In *Proceedings of the 2005 American Control Conference (ACC)*, pages 1859–1864, 2005.

R.S. Risuleo, G. Bottegal, and H. Hjalmarsson. Variational Bayes identification of acyclic dynamic networks. *IFAC-PapersOnLine*, 50(1):10556–10561, 2017. Proceedings of the 20th IFAC World Congress.

B. Roorda and C. Heij. Global total least squares modeling of multivariable time series. *IEEE Transactions on Automatic Control*, 40(1):50–63, 1995.

J. Schoukens, G. Vandersteen, K. Barbé, and R. Pintelon. Nonparametric preprocessing in system identification: a powerful tool. *European Journal of Control*, 15(3):260–274, 2009.

S. Shahrampour and V. M. Preciado. Topology identification of directed dynamical networks via power spectral analysis. *IEEE Transactions on Automatic Control*, 60(8):2260–2265, 2015.

S. Shi, G. Bottegal, and P.M.J. Van den Hof. Bayesian topology identification of linear dynamic networks. In *Proceedings of the 18th European Control Conference (ECC)*, pages 2814–2819, 2019.

S. Shi, X. Cheng, and P.M.J. Van den Hof. Single module identifiability in linear dynamic networks with partial excitation and measurement. *IEEE Transactions on Automatic Control*, 68(1):285–300, 2023.

Y. Shi. Fault detection and diagnoses using the dynamic network framework. Msc thesis, Technische Universiteit Eindhoven, October 2023.

T.R.V. Steentjes, M. Lazar, and P.M.J. Van den Hof. Scalable distributed H-2 controller synthesis for interconnected linear discrete-time systems. *IFAC-PapersOnLine*, 54(9):66–71, 2021. Proceedings of the 24th International Symposium on Mathematical Theory of Networks and Systems (MTNS).

L.E. Sucar. *Probabilistic graphical models: principles and applications*. Advances in computer vision and pattern recognition. Springer International Publishing, Cham, second edition, 2021. ISBN 978-3-030-61943-5.

SYSDYNET. *MATLAB app and toolbox for dynamic network identification, Version Beta 0.2.0*. Control Systems Group, Eindhoven University of Technology, 2023. URL `www.sysdynet.net`.

S. Talukdar, D. Deka, H. Doddi, D. Materassi, M. Chertkov, and M.V. Salapaka. Physics informed topology learning in networks of linear dynamical systems. *Automatica*, 112:108705, 2020.

The Mathworks, Inc. *MATLAB and system identification toolbox release 2021b*. Natick, MA, 2021. URL `www.mathworks.com/products/sysid`.

M. Timme. Revealing network connectivity from response dynamics. *Physical Review Letters*, 98, 2007.

R.S. Tsay. *Multivariate time series analysis: with R and financial applications*. John Wiley & Sons, Inc., Hoboken, NJ, 2013. ISBN 978-1-118-61790-8.

P.P.J. Van den Bosch. Models of physical processes. Lecture notes 5DD20, January 2009.

P.M.J. Van den Hof. Closed-loop issues in system identification. *Annual Reviews in Control*, 22:173–186, 1998.

P.M.J. Van den Hof and K. R. Ramaswamy. Path-based data-informativity conditions for single module identification in dynamic networks. In *Proceedings of the 59th IEEE Conference on Decision and Control (CDC)*, pages 4354–4359, 2020.

P.M.J. Van den Hof, A. Dankers, P.S.C. Heuberger, and X. Bombois. Identification of dynamic models in complex networks with prediction error methods-basic methods for consistent module estimates. *Automatica*, 49(10):2994–3006, 2013.

P.M.J. Van den Hof, K. R. Ramaswamy, and S.J.M. Fonken. Integrating data-informativity conditions in predictor models for single module identification in dynamic networks. *IFAC-PapersOnLine*, 56(2):2377–2382, July 2023. 22nd IFAC World Congress.

A.J. van der Schaft and D. Jeltsema. *Port-Hamiltonian systems theory: an introductory overview*. now Publishers Inc., Delft, 2014. ISBN 978-1-60198-786-0.

A.J. van der Schaft and B.M. Maschke. Port-Hamiltonian systems on graphs. *SIAM Journal on Control and Optimization*, 51(2):906–937, 2013.

H.J. van Waarde, P. Tesi, and M.K. Camlibel. Identifiability of undirected dynamical networks: a graph-theoretic approach. *IEEE Control Systems Letters*, 2(4): 683–688, 2018.

H.J. van Waarde, P. Tesi, and M.K. Camlibel. Necessary and sufficient topological conditions for identifiability of dynamical networks. *IEEE Transactions on Automatic Control*, 65(11):4525–4537, 2020.

H.J. van Waarde, P. Tesi, and M.K. Camlibel. Topology identification of heterogeneous networks: identifiability and reconstruction. *Automatica*, 123:109331, 2021.

M. Verhaegen and V. Verdult. *Filtering and system identification: a least squares approach*. Cambridge University Press, Cambridge, 2012. ISBN 978-1-107-40502-8.

S. Warnick. Shared hidden state and network representations of interconnected dynamical systems. In *Proceedings of the 53rd Allerton Conference on Communication, Control, and Computing*, pages 25–32, 2015.

H.H.M. Weerts, P.M.J. Van den Hof, and A.G. Dankers. Identification of dynamic networks operating in the presence of algebraic loops. In *Proceedings of the 55th IEEE Conference on Decision and Control (CDC)*, pages 4606–4611, 2016.

H.H.M. Weerts, M. Galrinho, G. Bottegal, H. Hjalmarsson, and P.M.J. Van den Hof. A sequential least squares algorithm for ARMAX dynamic network identification. *IFAC-PapersOnLine*, 51(15):844–849, 2018a. Proceedings of the 18th IFAC Symposium on System Identification (SYSID).

H.H.M. Weerts, P.M.J. Van den Hof, and A.G. Dankers. Identifiability of linear dynamic networks. *Automatica*, 89:247–258, 2018b.

H.H.M. Weerts, P.M.J. Van den Hof, and A.G. Dankers. Prediction error identification of linear dynamic networks with rank-reduced noise. *Automatica*, 98: 256–268, 2018c.

H.H.M. Weerts, J. Linder, M. Enqvist, and P.M.J. Van den Hof. Abstractions of linear dynamic networks for input selection in local module identification. *Automatica*, 117:108975, 2020.

J.C. Willems. Dissipative dynamical systems part I: general theory. *Archive for Rational Mechanics and Analysis*, 45:321–351, 1972.

J.C. Willems. From time series to linear system part I: finite dimensional linear time invariant systems. *Automatica*, 22(5):561–580, 1986a.

J.C. Willems. From time series to linear system part II: exact modelling. *Automatica*, 22(6):675–694, 1986b.

J.C. Willems. From time series to linear system part III: approximate modelling. *Automatica*, 23(1):87–115, 1987.

J.C. Willems. The behavioral approach to open and interconnected systems. *IEEE Control Systems*, 27(6):46–99, 2007.

J.C. Willems. Terminals and ports. *IEEE Circuits and Systems Magazine*, 10(4): 8–26, 2010.

J. Wittenburg. *Dynamics of systems of rigid bodies*. B.G. Teubner, Stuttgart, 1977. ISBN 978-3-519-02337-1.

N. Woodbury and S. Warnick. Abstractions and realizations of dynamic networks. In *2019 American Control Conference (ACC)*, pages 5167–5172, 2019.

N. Woodbury, A. Dankers, and S. Warnick. On the well-posedness of LTI networks. In *Proceedings of the 56th IEEE Conference on Decision and Control (CDC)*, pages 4813–4818, 2017.

N. Woodbury, A. Dankers, and S. Warnick. Dynamic networks: representations, abstractions, and well-posedness. In *Proceedings of the 57th IEEE Conference on Decision and Control (CDC)*, pages 4719–4724, 2018.

E. Yeung, J. Gonçalves, H. Sandberg, and S. Warnick. Representing structure in linear interconnected dynamical systems. In *Proceedings of the 49th IEEE Conference on Decision and Control (CDC)*, pages 6010–6015, 2010.

E. Yeung, J. Gonçalves, H. Sandberg, and S. Warnick. Mathematical relationships between representations of structure in linear interconnected dynamical systems. In *Proceedings of the 2011 American Control Conference (ACC)*, pages 4348–4353, 2011a.

E. Yeung, J. Gonçalves, H. Sandberg, and S. Warnick. The meaning of structure in interconnected dynamic systems, 2011b.

D. Youla. On the factorization of rational matrices. *IRE Transactions on Information Theory*, 7(3):172–189, 1961.

H.D. Young and R.A. Freedman. *Sears and Zemansky's university physics: with modern physics*. Addison-Wesley, San Francisco, CA, thirteenth edition, 2012. ISBN 978-0-321-76218-4. International edition.

Y. Yuan, G.B. Stan, S. Warnick, and J. Gonçalves. Robust dynamical network structure reconstruction. *Automatica*, 47(6):1230–1235, 2011. Special Issue on Systems Biology.

Y. Yuan, A. Rai, E. Yeung, G.B. Stan, S. Warnick, and J. Gonçalves. A minimal realization technique for the dynamical structure function of a class of LTI systems. *IEEE Transactions on Control of Network Systems*, 4(2):301–311, 2017.

Publiekssamenvatting

Modellering en identificatie van fysische lineaire netwerken

Netwerken zijn essentiële onderdelen van onze natuurlijke en fysieke wereld. Ze zijn overal om ons heen en zijn diep doorgedrongen in onze hedendaagse samenleving. *Fysische netwerken* bestaan uit onderling verbonden systemen uit de natuurlijke en fysieke wereld. Enkele voorbeelden van deze netwerken zijn: interacties in ecologische systemen; industriële procesinstallaties die chemicaliën produceren; pijpleidingen om vloeistoffen of gas over lange afstanden te transporteren; printplaten en chips; en robots die met elkaar communiceren.

In de afgelopen decennia hebben enorme technologische ontwikkelingen geleid tot grotere en complexere systemen, waardoor het waardevoller is geworden om netwerken te bestuderen en hun gedrag te begrijpen. Dit wordt gedaan door een wiskundige beschrijving te maken door gebruik te maken van de natuurwetten (modellering) en experimentele gegevens (identificatie). Ons doel is: *Het ontwikkelen van hulpmiddelen voor het modelleren en identificeren van fysische lineaire netwerken*.

In dit proefschrift richten we ons op fysische lineaire netwerken, die worden gekenmerkt door *symmetrische diffuse koppelingen*. Een diffuse koppeling is een relatie tussen signalen die gebaseerd is op het delen van informatie in plaats van op een vooraf gedefinieerde richting van de informatiestroom. Dit type koppeling is vanzelfsprekender voor fysische netwerken, terwijl ingangs-uitgangsrelaties vanzelfsprekender zijn voor digitale systemen, zoals regelaars. Fysische netwerken worden vaak verbonden met digitale regelaars, wat leidt tot gemengde netwerken.

Het uiteindelijke doel is om natuurwetten te combineren met gemeten signalen om zo de interne verbindingsstructuur van het netwerk, al het gedrag of een selectie van gedrag in het netwerk te bepalen. Hiervoor hebben we een geschikte vorm (model) voor het beschrijven van het netwerk nodig. Bestaande modellen voor het beschrijven van systemen zijn niet voldoende geschikt voor fysische

netwerken. Daarom ontwikkelen we een nieuw model dat zowel de karakteristieke eigenschappen van fysische systemen als de verbindingsstructuur van het netwerk kan integreren.

Dan ontwikkelen we identificatiehulpmiddelen en -algoritmes voor het bepalen van het gedrag (en interne verbindingsstructuur) in fysische lineaire netwerken, waarin we de structurele eigenschappen van fysische netwerken opnemen. De voorwaarden voor het uitvoeren van een consistente identificatie zijn zeer eenvoudig vergeleken met de voorwaarden die gelden voor netwerken met een ingangs-uitgangsvorm. Deze eenvoud is volledig te danken aan de structurele eigenschappen die maximaal kunnen worden benut. Daarnaast ontwikkelen we een algoritme voor het oplossen van het resulterende concave optimalisatieprobleem. Dit algoritme bestaat uit meerdere convexe stappen die leiden tot consistente resultaten, ook voor grote netwerken.

De vereiste experimentele opstelling voor het bepalen van het gedrag van een deelnetwerk is opnieuw zeer eenvoudig: Een enkel excitatiesignaal is voldoende en alleen de knooppuntsignalen van het deelnetwerk en de direct naastgelegen knooppuntsignalen dienen gemeten te worden. Alle andere knooppuntsignalen kunnen genegeerd worden, waardoor identificatie van een deelnetwerk zeer lokaal in het netwerk kan worden opgelost.

De analyse van de uniciteit van de netwerkbeschrijving resulteert in flexibele instrumentatievoorwaarden voor de experimentele opstelling. Voor het identificeren van het volledige netwerkgedrag is het voldoende om ieder knooppuntsignaal te meten of te exciteren en een knooppuntsignaal zowel te meten als te exciteren.

Tenslotte concentreren we ons op fysische lineaire netwerken die gerichte componenten, zoals digitale regelaars, bevatten. Het gerichte gedrag vernietigt de symmetrie-eigenschap van het netwerkmodel, wat wordt verwerkt in de identificatieprocedure door de voorwaarden en de procedure aan te passen.

We kunnen concluderen dat we een nieuw model hebben ontwikkeld voor het identificeren van fysische lineaire netwerken, met als voordeel dat de karakteristieke eigenschappen van fysische systemen en de verbindingsstructuur van het netwerk wordt geïntegreerd. Met de ontwikkelde modelvorm en identificatiehulpmiddelen kunnen ingenieurs onder eenvoudige voorwaarden en met goedkope experimenten het gedrag en de interne verbindingsstructuur van een fysisch lineair netwerk of deelnetwerk bepalen.

Index

About the author

Lizan Kivits received her B.Sc. degree in Electrical Engineering and her M.Sc. degree in Systems and Control with distinction (great appreciation) from Eindhoven University of Technology, Eindhoven, The Netherlands, in 2014 and 2017, respectively. Her M.Sc. thesis was entitled *Control relevant model reduction for disturbance decoupling* and was supervised by dr.ir. Ruben W.H. Merks and prof.dr. Siep Weiland.

In June 2017, she started as a researcher in the Control Systems research group at the Department of Electrical Engineering, Eindhoven University of Technology. Her research project was on *Modelling of dynamic networks* and under supervision of prof.dr.ir. Paul M.J. Van den Hof. As of July 2018, she continued as a Ph.D. researcher under supervision of prof.dr.ir. Paul M.J. Van den Hof. Her research was entitled *Modelling and identification of physical linear networks* and part of a project on data-driven modelling in dynamic networks.

Following graduate courses offered by the Dutch Institute of Systems and Control (DISC), she received the (DISC) certificate in 2023. She was a teaching assistent for the bachelor course *Mathematics II* (2019-2020) and the master courses *Modelling dynamics* and *Model reduction* (2020-2022).

Her research interests include first-principles modelling, data-driven modelling, and dynamic network identification.

Modelling and identification of physical linear networks

Lizan Kivits